NUREG/CR-6075
SAND93-1535
Supp. 1

The Probability of Containment Failure by Direct Containment Heating in Zion

Prepared by
M. M. Pilch, M. D. Allen, D. L. Knudson, D. W. Stamps, E. L. Tadios

Sandia National Laboratories
Operated by
Sandia Corporation

Prepared for
U.S. Nuclear Regulatory Commission

DISTRIBUTION OF THIS DOCUMENT IS UNLIMITED

AVAILABILITY NOTICE

Availability of Reference Materials Cited in NRC Publications

Most documents cited in NRC publications will be available from one of the following sources:

1. The NRC Public Document Room, 2120 L Street, NW., Lower Level, Washington, DC 20555-0001

2. The Superintendent of Documents, U.S. Government Printing Office, P. O. Box 37082, Washington, DC 20402-9328

3. The National Technical Information Service, Springfield, VA 22161-0002

Although the listing that follows represents the majority of documents cited in NRC publications, it is not intended to be exhaustive.

Referenced documents available for inspection and copying for a fee from the NRC Public Document Room include NRC correspondence and internal NRC memoranda; NRC bulletins, circulars, information notices, inspection and investigation notices; licensee event reports; vendor reports and correspondence; Commission papers; and applicant and licensee documents and correspondence.

The following documents in the NUREG series are available for purchase from the Government Printing Office: formal NRC staff and contractor reports, NRC-sponsored conference proceedings, international agreement reports, grantee reports, and NRC booklets and brochures. Also available are regulatory guides, NRC regulations in the *Code of Federal Regulations,* and *Nuclear Regulatory Commission Issuances.*

Documents available from the National Technical Information Service include NUREG-series reports and technical reports prepared by other Federal agencies and reports prepared by the Atomic Energy Commission, forerunner agency to the Nuclear Regulatory Commission.

Documents available from public and special technical libraries include all open literature items, such as books, journal articles, and transactions. *Federal Register* notices, Federal and State legislation, and congressional reports can usually be obtained from these libraries.

Documents such as theses, dissertations, foreign reports and translations, and non-NRC conference proceedings are available for purchase from the organization sponsoring the publication cited.

Single copies of NRC draft reports are available free, to the extent of supply, upon written request to the Office of Administration, Distribution and Mail Services Section, U.S. Nuclear Regulatory Commission, Washington, DC 20555-0001.

Copies of industry codes and standards used in a substantive manner in the NRC regulatory process are maintained at the NRC Library, Two White Flint North, 11545 Rockville Pike, Rockville, MD 20852-2738, for use by the public. Codes and standards are usually copyrighted and may be purchased from the originating organization or, if they are American National Standards, from the American National Standards Institute, 1430 Broadway, New York, NY 10018-3308.

DISCLAIMER NOTICE

This report was prepared as an account of work sponsored by an agency of the United States Government. Neither the United States Government nor any agency thereof, nor any of their employees, makes any warranty, expressed or implied, or assumes any legal liability or responsibility for any third party's use, or the results of such use, of any information, apparatus, product, or process disclosed in this report, or represents that its use by such third party would not infringe privately owned rights.

DISCLAIMER

Portions of this document may be illegible in electronic image products. Images are produced from the best available original document.

NUREG/CR–6075
SAND93–1535
Supp. 1

The Probability of Containment Failure by Direct Containment Heating in Zion

Manuscript Completed: July 1994
Date Published: December 1994

Prepared by
M. M. Pilch, M. D. Allen, D. L. Knudson,* D. W. Stamps, E. L. Tadios

Sandia National Laboratories
Albuquerque, NM 87185

Prepared for
Division of Systems Research
Office of Nuclear Regulatory Research
U.S. Nuclear Regulatory Commission
Washington, DC 20555–0001
NRC Job Code J6027

*Idaho National Engineering Laboratory
Idaho Falls, ID 83415

MASTER

DISTRIBUTION OF THIS DOCUMENT IS UNLIMITED

ABSTRACT

Supplement 1 of NUREG/CR-6075 brings to closure the DCH issue for the Zion plant. It includes the documentation of the peer review process for NUREG/CR-6075, the assessments of four new splinter scenarios defined in working group meetings, and modeling enhancements recommended by the working groups. In the four new scenarios, consistency of the initial conditions has been implemented by using insights from systems-level codes. SCDAP/RELAP5 was used to analyze three short-term station blackout cases with different leak rates. In all three cases, the hot leg or surge line failed well before the lower head and thus the primary system depressurized to a point where DCH was no longer considered a threat. However, these calculations were continued to lower head failure in order to gain insights that were useful in establishing the initial and boundary conditions. The most useful insights are that the RCS pressure is low at vessel breach, metallic blockages in the core region do not melt and relocate into the lower plenum, and melting of upper plenum steel is correlated with hot leg failure. The SCDAP/RELAP5 output was used as input to CONTAIN to assess the containment conditions at vessel breach. The containment-side conditions predicted by CONTAIN are similar to those originally specified in NUREG/CR-6075.

The methodology originally developed in NUREG/CR-6075 was used to analyze the new splinter scenarios. Some modeling enhancements in response to working group discussions were implemented for these analyses. The entrainment of preexisting hydrogen (in the atmosphere) into a burning jet was examined more carefully. In addition, the impact of DCH-induced deflagrations on DCH loads was quantified. A new computational tool--the two-cell equilibrium/Latin hypercube sampling (TCE/LHS) code--was developed for this effort to perform Monte Carlo sampling of the scenario distributions. The TCE/LHS code was benchmarked against the original Scenario I calculations in NUREG/CR-6075 performed using the ALPHA code, which is based on the method of discrete probability distributions (DPD). The results were in excellent agreement.

The analyses of the new scenarios showed no intersection of the load distributions and the containment fragility curves, and thus the containment failure probability was negligible for each scenario. These supplemental analyses complete closure of the DCH issue for Zion.

CONTENTS

Page

Abstract iii

Figures vi

Tables xiii

Acronyms xv

Acknowledgments xvii

Executive Summary xix

1.0 Introduction 1

2.0 Probabilistic Framework 4

3.0 Quantification of Initial Conditions 9

4.0 Quantification of the DCH Phenomenon 48

5.0 Quantification of Containment Fragility 63

6.0 Results and Sensitivities 71

7.0 Conclusions and Recommendations 81

Appendix A. Peer Review of NUREG/CR-6075 . . . . . A-1

Appendix B. Monte Carlo Framework B-1

Appendix C. A SCDAP/RELAP5 Analysis Supporting DCH Issue Resolution for the Zion PWR C-1

Appendix D. CONTAIN Calculations and Hydrogen Combustion Analyses D-1

Appendix E. Hydrogen Combustion During DCH Events E-1

LIST OF FIGURES

Figure | Page

2.1 The probabilistic framework for containment failure under Direct Containment Heating scenarios 7

2.2 Illustration of the probabilistic framework in terms of schematic depiction of its components 8

3.1 Splinter DCH scenarios used in NUREG/CR-6075 38

3.2 Splinter DCH scenarios reflecting working group recommendations 39

3.3 Zion nuclear power plant 40

3.4 Distribution for fraction of Zr oxidized (core-wide) in Scenarios V and VI 41

3.5 Crucible formation in a flooded RPV - Scenario V 42

3.6 Distribution for UO_2 release from the crucible in Scenario V 43

3.7 Distribution for molten UO_2 in the lower plenum at the time of vessel rupture for Scenario V 44

3.8 Crucible formation in wet core scenario with partial operator intervention - Scenario VI 45

3.9 Distribution for UO_2 release from the crucible in Scenario VI 46

3.10 Distribution for molten UO_2 in the lower plenum at the time of vessel rupture for Scenario VI 47

4.1 Validation of the two-cell equilibrium model against all experiments with compartmentalized geometry 60

4.2 Validation of the coherence ratio for Zion-like cavity designs for scenarios without coejected water 61

4.3 Validation of the hole ablation model 62

5.1 Zion fragility curve as presented in the Zion IPE 68

5.2 Zion fragility curve as developed by FAI for the Zion IPE 69

5.3 Comparison of the FAI-supplied Zion fragility curve with the approximation used in NUREG/CR-6075 70

LIST OF FIGURES (continued)

Figure		Page
6.1	Calculated distribution for the hole size	76
6.2	Calculated distribution for the coherence ratio	77
6.3	Calculated distribution for the containment temperature	78
6.4	Calculated distribution for the containment pressure	79
6.5	Scenario V with TMI-like containment conditions	80
B.1	DCH calculational process	B-4
B.2	Schematic of TCE driver logic	B-4
B.3	Benchmarking of the Monte Carlo method using TCE/LHS against the discrete probability distribution (DPD) method for Scenario I in NUREG/CR-6075	B-5
C.1	Zion reactor vessel nodalization with provisions for in-vessel natural circulation	C-37
C.2	Pressurizer coolant loop nodalization for the Zion PWR without provisions for hot leg countercurrent natural circulation	C-38
C.3	Pressurizer coolant loop nodalization for the Zion PWR with provisions for hot leg countercurrent natural circulation	C-39
C.4	Nodalization detail showing the surge line connection to the split hot legs	C-39
C.5	Cross section of the five channel core with assembly and channel relative power levels	C-40
C.6	Cross section of the five channel core with CRA (control rod assembly) locations	C-41
C.7	COUPLE mesh representing the lower reactor vessel head of the Zion PWR	C-42
C.8	Pressure in the reactor vessel lower head in Case 1	C-43
C.9	Reactor vessel collapsed liquid level in Case 1	C-43
C.10	Volume-averaged temperatures of selected ex-vessel structures in the pressurizer loop in Case 1	C-44

LIST OF FIGURES (continued)

Figure Page

C.11 Hot leg volume-averaged temperatures in Case 1 . . . . . C-44

C.12 Lower head debris depth (referenced to the bottom inside surface of the head) in Case 1 . . . . . C-45

C.13 Lower head maximum debris temperature in Case 1 . . . . . C-45

C.14 Mass of liquid in the reactor vessel in Case 1 . . . . . C-46

C.15 Total hydrogen generated in Case 1 . . . . . C-46

C.16 Total hydrogen vented to containment through the hot leg break in Case 1 . . . . C-47

C.17 Pressure in the reactor vessel lower head in Case 2 . . . . . C-47

C.18 Reactor vessel collapsed liquid level in Case 2 . . . . . C-48

C.19 Volume-averaged temperatures of selected ex-vessel structures in a non-pressurizer loop in Case 2 . . . . . C-48

C.20 Hot leg volume-averaged temperatures in Case 2 . . . . . C-49

C.21 Lower head debris depth (referenced to the bottom inside surface of the head) in Case 2 . . . . . C-49

C.22 Lower head maximum debris temperature in Case 2 . . . . . C-50

C.23 Mass of liquid in the reactor vessel in Case 2 . . . . . C-50

C.24 Total hydrogen generated in Case 2 . . . . . C-51

C.25 Total hydrogen vented to containment through the hot leg break in Case 2 . . . . C-51

C.26 Pressure in the reactor vessel lower head in Case 3 . . . . . C-52

C.27 Reactor vessel collapsed liquid level in Case 3 . . . . . C-52

C.28 Volume-averaged temperatures of selected structures in the pressurizer loop in Case 3 . . . . . C-53

C.29 Lower head debris depth (referenced to the bottom inside surface of the head) in Case 3 . . . . . C-53

LIST OF FIGURES (continued)

Figure | Page

C.30 Lower head maximum debris temperature in Case 3 . . . . . C-54

C.31 Mass of liquid in the reactor vessel in Case 3 . . . . . C-54

C.32 Total hydrogen generated in Case 3 . . . . . C-55

C.33 Total hydrogen vented to containment through the hot leg break in Case 3 . . . . C-55

D.1 Schematic of containment design and nodalizatin for Zion power plant D-16

D.2 Case 1: Hydrogen source flow rates D-17

D.3 Case 1: Steam source flow rates D-17

D.4 Case 1: Temperatures at source locations D-18

D.5 Case 2: Hydrogen source flow rates D-18

D.6 Case 2: Steam source flow rates D-19

D.7 Case 2: Temperatures at source locations D-19

D.8 Case 3: Hydrogen source flow rates D-20

D.9 Case 3: Steam source flow rates D-20

D.10 Case 3: Temperatures at source locations D-21

D.11 Case 1: Containment pressure D-21

D.12 Case 1: Cavity gas mole fractions D-22

D.13 Case 1: Cavity gas temperature D-22

D.14 Case 1: Steam generator room gas mole fractions D-23

D.15 Case 1: Steam generator room gas temperature D-23

D.16 Case 1: Annulus gas mole fractions D-24

D.17 Case 1: Annulus gas temperature D-24

D.18 Case 1: Dome gas mole fractions D-25

LIST OF FIGURES (continued)

Figure | Page

D.19 Case 1: Dome gas temperature D-25

D.20 Case 2: Containment pressure D-26

D.21 Case 2: Cavity gas mole fractions D-26

D.22 Case 2: Cavity gas temperature D-27

D.23 Case 2: Steam generator room gas mole fractions D-27

D.24 Case 2: Steam generator room gas temperature D-28

D.25 Case 2: Annulus gas mole fractions D-28

D.26 Case 2: Annulus gas temperature D-29

D.27 Case 2: Dome gas mole fractions D-29

D.28 Case 2: Dome gas temperature D-30

D.29 Case 3: Containment pressure D-30

D.30 Case 3: Cavity gas mole fractions D-31

D.31 Case 3: Cavity gas temperature D-31

D.32 Case 3: Steam generator room gas mole fractions D-32

D.33 Case 3: Steam generator room temperature D-32

D.34 Case 3: Annulus gas mole fractions D-33

D.35 Case 3: Annulus gas temperature D-33

D.36 Case 3: Dome gas mole fractions D-34

D.37 Case 3: Dome gas temperature D-34

D.38 Autoignition temperature data for hydrogen-steam jets D-35

D.39 Case 1: Jet hydrogen concentration and temperature of the gases released from the PORV D-35

LIST OF FIGURES (continued)

Figure | Page

D.40 Case 1: Jet hydrogen concentration and temperature of the gases released from the hot-leg break D-36

D.41 Case 2: Jet hydrogen concentration and temperature of the gases released from the PORV D-36

D.42 Case 2: Jet hydrogen concentration and temperature of the gases released from the RCP1 seal leak D-37

D.43 Case 2: Jet hydrogen concentration and temperature of the gases released from the RCP2 seal leak D-37

D.44 Case 2: Jet hydrogen concentration and temperature of the gases released from the RCP3 seal leak D-38

D.45 Case 2: Jet hydrogen concentration and temperature of the gases released from the RCP4 seal leak D-38

D.46 Case 2: Jet hydrogen concentration and temperature of the gases released from the hot-leg break D-39

D.47 Case 3: Jet hydrogen concentration and temperature of the gases released from the PORV D-39

D.48 Case 3: Jet hydrogen concentration and temperature of the gases released from the RCP1 seal leak D-40

D.49 Case 3: Jet hydrogen concentration and temperature of the gases released from the RCP2 seal leak D-40

D.50 Case 3: Jet hydrogen concentration and temperature of the gases released from the RCP3 seal leak D-41

D.51 Case 3: Jet hydrogen concentration and temperature of the gases released from the RCP4 seal leak D-41

D.52 Case 3: Jet hydrogen concentration and temperature of the gases released from the hot-leg break D-42

E.1 Hydrogen combustion during DCH events E-35

E.2 Temperature history in the triangular vent space above RCP 1A in the SNL/IET experiment E-36

LIST OF FIGURES (concluded)

Figure | Page

E.3 Jet combustion in the SNL/IET tests E-37

E.4 Development of jets during DCH events E-38

E.5 Stability criterion for round, free, buoyant jets E-39

E.6 Thermal stratification in the IET-11 experiment E-40

E.7 Hydrogen/air/steam flammability charts from Marshall (1986) and Kumar (1985) E-41

E.8 Validation of combustion completeness model E-42

E.9 SENKIN calculations for volumetric hydrogen combustion (X_{H2} = 0.048; X_{STM} = 0.38) E-43

E.10 Autoignition temperatures for hydrogen/air/steam mixtures E-44

E.11 Molecular mixing via jets in a confined volume E-45

LIST OF TABLES

Table		Page
3.1	Characterization of the Zion plant	33
3.2	Definition of probability levels	34
3.3	Summary of initial condition quantification	35
3.4	RCS gas temperature for Scenario VI	36
3.5	Comparison with working group recommendations	37
3.6	Comparison with prior work	37
4.1	Survey of DCH-relevant experiments	56
4.2	Applicability of the database to reactors	59
5.1	Fragility of the Zion containment	66
6.1	Summary of results	74
6.2	Sensitivity study using SCDAP/RELAP5 conditions at the time of melt relocation	75
C.1	SCDAP/RELAP5 model elevations relative to the lower reactor vessel head	C-26
C.2	Comparison of countercurrent flow parameters with values calculated by SCDAP/RELAP5	C-26
C.3	Zion UFSAR core inventory compared to the SCDAP/RELAP5 model	C-27
C.4	SCDAP core damage input	C-27
C.5	Time/flow area relationship for simulating RCP seal leaks	C-28
C.6	Zion UFSAR steady state parameters compared to values calculated by SCDAP/RELAP5	C-28
C.7	Case 1 sequence of events	C-29
C.8	DCH parameters at selected times in Case 1	C-30
C.9	Case 2 sequence of events	C-31

LIST OF TABLES (concluded)

Table		Page
C.10	DCH parameters at selected times in Case 2	C-33
C.11	Case 3 sequence of events	C-34
C.12	DCH parameters at selected times in Case 3	C-36
D.1	SCDAP/RELAP5 calculations sequence of events	D-11
D.2	Zion plant nodalization	D-15
D.3	Initial conditions	D-15
E.1	Inerting criteria for jet combustion	E-27
E.2	Comparison of jet entrainment using stoichiometric and hydrodynamic estimates	E-28
E.3	Potential for stratification of the atmosphere during DCH events	E-29
E.4	Composition stratification in SNL/IET-11	E-29
E.5	Assessment of deflagrations during DCH events	E-30
E.6	Assessment of volumetric combustion	E-31
E.7	Evaluation of forced mixing	E-32
E.8	Evaluation of mixing between the subcompartment and the dome	E-33
E.9	Evaluation of mixing in the dome due to a wall jet	E-34
E.10	Scaling implications of the mixing mechanisms	E-34

ACRONYMS/INITIALISMS

AC	Alternating current
ANL	Argonne National Laboratory
ANS	American Nuclear Society
CFP	Containment Failure Probability
CLCH	Convection Limited Containment Heating
COV	Coefficient of variation
CR	Causal Relation
CRA	Control rod assembly
DCH	Direct Containment Heating
DPD	Discrete Probability Distribution
ECCS	Emergency core cooling system
ERI	Energy Research, Inc.
GPM	Gallons per Minute
HPME	High-Pressure Melt Ejection
INEL	Idaho National Engineering Laboratory
IPE	Individual Plant Examination
LFL	Lower Flammability Limit
NPP	Nuclear Power Plant
NRC	Nuclear Regulatory Commission
PORV	Pilot-Operated Relief Valve
PRA	Probabilistic Risk Assessment
PWR	Pressurized Water Reactor
RCP	Reactor Coolant Pump
RCS	Reactor Coolant System
RPV	Reactor Pressure Vessel
SASM	Severe Accident Scaling Methodology
SBLOCA	Small Break Loss-of-Coolant Accident
SG	Steam generator
SNL	Sandia National Laboratories
SRV	Safety relief valve
TCE	Two-Cell Equilibrium
TPG	Technical Program Group
UCSB	University of California at Santa Barbara
UFSAR	Updated Final Safety Analysis Report

ACKNOWLEDGMENTS

Reaching consensus on a major severe accident issue as complex as Direct Containment Heating (DCH) was a formidable task that required input from a diverse team of individuals. The resolution process for the DCH issue evolved over time and involved a number of major efforts that should be acknowledged.

Much of the successful resolution of the DCH issue is the result of an extensive experimental program. The DCH experiments were reviewed as part of a Nuclear Regulatory Commission (NRC) sponsored effort known as the Severe Accident Scaling Methodology (SASM) Program that was chaired by Novak Zuber. As a result of SASM recommendations, the NRC-sponsored experimental programs were redirected toward performing integral counterpart experiments at two different physical scales at Sandia National Laboratories (SNL) and Argonne National Laboratory (ANL). These experiments included detailed (geometrically scaled) simulations of the Zion subcompartment structures and had initial conditions closely tied to postulated accident scenarios.

Guidance for the experiment programs was assigned by the NRC to a five-member DCH Experiment Technical Review Group (TRG) who were all members of the original SASM program. They included R.E. Henry, M. Ishii, F.J. Moody, B.R. Sehgal, and T.G. Theofanous. The DCH working group for the experimental program consisted of representatives of the sponsor (NRC), universities and industry (TRG), and the national laboratories (SNL and ANL), and met at periodic intervals to discuss new results and decide future directions.

NUREG/CR-6075 and the original version of NUREG/CR-6109 were reviewed by a panel of 13 experts representing national laboratories, universities, and industry. The peer reviewers identified two areas of unresolved concerns: initial conditions and model validity. Two working group meetings addressed these unresolved concerns. The first meeting, on initial conditions, included R.E. Henry, S. Levy, and M. Modarres. The second meeting, on model validity, included J. Sheppard, M. Ishii, S. Levy, F.J. Moody, and R.E. Henry. The authors would like to thank these reviewers for their guidance on NUREG/CR-6075 and its supplement.

Nestor Ortiz and John Kelly provided management support and guidance during the process of writing NUREG/CR-6075 and its supplement. In addition, the authors appreciate the extensive internal review by Sandia staff. The authors are particularly grateful to Mary Lou Garcia, who typed and compiled NUREG/CR-6075 and its supplement.

Susan Dingman and Jacquelin Pfarner developed and benchmarked the TCE/LHS code described in Appendix B that was used to calculate the containment failure probabilities for the new splinter scenarios. They received advice from Greg Wyss on how to implement the LHS code. Michael Bohn and Eric Klamerus reviewed Section 5 on containment fragility.

SCDAP/RELAP5 calculations in Appendix C were performed by Daryl Knudson with consultation from Chris Allison and management support from Ed Harvego. The CONTAIN calculations in Appendix D were performed by Eden Tadios and Doug Stamps with recommendations from Dave Williams and Richard Griffith.

This work was sponsored by the Accident Evaluation Branch of the Office of Research of the Nuclear Regulatory Commission. Input and valuable guidance were supplied by Farouk Eltawila, Charles Tinkler, and Richard Lee.

EXECUTIVE SUMMARY

In a light water reactor core melt accident, if the reactor pressure vessel (RPV) fails while the reactor coolant system (RCS) is at high pressure, the expulsion of molten core debris may pressurize the reactor containment building (RCB) beyond its failure pressure. A failure in the bottom head of the RPV, followed by melt expulsion and blowdown of the RCS, will entrain molten core debris in the high-velocity steam blowdown gas. This chain of events is called a high-pressure melt ejection (HPME). Four mechanisms may cause a rapid increase in pressure and temperature in the reactor containment: (1) blowdown of the RCS, (2) efficient debris-to-gas heat transfer, (3) exothermic metal/steam and metal/oxygen reactions, and (4) hydrogen combustion. These processes that lead to increased loads on the containment building are collectively referred to as direct containment heating (DCH). Understanding factors that enhance or mitigate DCH is necessary because the pressure load imposed on the RCB may lead to early failure of the containment.

NUREG/CR-6075, "The Probability of Containment Failure by Direct Containment Heating in Zion," has been written and was published with minor corrections. NUREG/CR-6075 assesses the probability of containment failure by DCH for the Zion Nuclear Power Plant. It underwent an extensive peer review by a panel of 13 experts representing national laboratories, universities, and industry. The reviewers provided written comments; the authors responded to the reviewers' comments; and finally, the reviewers wrote rebuttals to the authors' responses. From the peer review process, two areas of residual concern were identified: initial conditions and model validity. Two working group meetings were held to address these two unresolved issues; and as a result, the NRC requested SNL to prepare this supplement to NUREG/CR-6075 to document the peer review process, address residual concerns on initial conditions and model validity, and document modeling enhancements.

Four new splinter scenarios were defined in the working group meetings. The new scenarios either bound the scenarios in NUREG/CR-6075 or stress greater consistency in the conditions at vessel breach; thus, the new scenarios are intended to replace those in NUREG/CR-6075. Two high-pressure scenarios resulting from operator intervention were defined. One high pressure scenario is characterized by coejection of large quantities of water (75 mt) because of operator action to reflood the RCS, and the other is characterized by coejection of 10 mt of water. The expected melt composition is predominantly oxidic. Two

low-pressure scenarios were also defined. These are characterized by melts with a larger metallic component and small amounts of coejected water. The working group members stressed using insights from systems-level codes, specifically SCDAP/RELAP5 and CONTAIN, to ensure consistency of initial conditions in each scenario. The working group members also identified combustion of preexisting hydrogen in the containment atmosphere as an area requiring closer attention.

Idaho National Engineering Laboratory analyzed three short-term station blackout cases for Zion using SCDAP/RELAP5 to gain insights to ensure consistency of initial conditions. Three different leak rates were analyzed: (1) no leaks, (2) 250 gpm per pump, and (3) 480 gpm per pump. Failure of the hot leg or surge line that resulted in complete depressurization of the primary system was observed well before core relocation and lower head failure in all three cases. However, the calculations were continued until the lower head failed in order to gain insights about conditions at lower head failure. The SCDAP/RELAP5 analyses predict molten UO_2 masses at lower head failure that are similar to the original UO_2 melt mass distributions given in NUREG/CR-6075. SCDAP/RELAP5 analyses showed that only a small amount of metallic debris relocates to the lower plenum. Little or no melting of upper plenum steel was observed and there was very little relocation of metallic core blockages into the lower plenum. Temperatures sufficient to melt upper plenum steel will also lead to hot leg failure. These insights were used in developing the distributions for the four new scenarios defined in this supplement to NUREG/CR-6075. The melt masses and compositions predicted by SCDAP/RELAP5 are similar to those used in NUREG/CR-6075. In addition, these analyses showed that the only way that the RCS pressure could remain high is if the vessel was reflooded by operator intervention.

Outputs from the same three cases analyzed with SCDAP/RELAP5 were used as input to CONTAIN to gain insights about the containment initial conditions at vessel breach. The calculations indicated containment conditions (pressure and hydrogen concentration) similar to those used in NUREG/CR-6075.

Hydrogen combustion during DCH events was examined from a more detailed phenomenological perspective. The autoignition temperature was conservatively reduced from 1100 K to 950 K. In addition, a deflagration model was added to the two-cell equilibrium (TCE) model. These enhancements had negligible impact on the predicted containment load

distributions for scenarios with ~50 percent steam in the containment atmosphere. Deflagrations did augment DCH loads in a TMI-like scenario with essentially no steam in the containment atmosphere, but the increased loads were offset by the initially lower pressure in the containment. Entrainment of preexisting atmosphere was examined in response to working group suggestions to determine how much hydrogen in the atmosphere will burn in conjunction with the combustion of hot hydrogen laden jets venting from the subcompartments. We have examined entrainment into the jet from a hydrodynamic perspective and conclude that entrainment and combustion of atmospheric hydrogen within a jet is comparable to modeling based on a stoichiometric criterion. The stoichiometric criterion assumes that preexisting atmosphere (and hydrogen) is entrained into the jet to the extent necessary to burn all the hydrogen in the jet.

A new computational tool based on Monte Carlo sampling--the two-cell equilibrium/Latin hypercube sampling (TCE/LHS) code--was developed to sample the distributions developed for the four new splinter scenarios. It was used to propagate the distributions through the TCE model. TCE/LHS was benchmarked with excellent agreement against the original Scenario I calculations in NUREG/CR-6075 performed with the ALPHA code, which is based on discrete probability distributions (DPDs). TCE/LHS was used to calculate containment failure probabilities for the new scenarios. The load distributions did not intersect the containment fragility distributions, and thus the containment failure probability was negligible for each of the scenarios analyzed. These supplemental analyses complete closure of the DCH issue for Zion.

1.0 INTRODUCTION

In a light water reactor core melt accident, if the reactor pressure vessel (RPV) fails while the reactor coolant system (RCS) is at high pressure, the expulsion of molten core debris may pressurize the reactor containment building (RCB) beyond its failure pressure. A failure in the bottom head of the RPV, followed by melt expulsion and blowdown of the RCS, will entrain molten core debris in the high-velocity steam blowdown gas. This chain of events is called a high-pressure melt ejection (HPME). Four mechanisms may cause a rapid increase in pressure and temperature in the reactor containment: (1) blowdown of the RCS, (2) efficient debris-to-gas heat transfer, (3) exothermic metal/steam and metal/oxygen reactions, and (4) hydrogen combustion. These processes that lead to increased loads on the containment building are collectively referred to as direct containment heating (DCH). Understanding factors that enhance or mitigate DCH is necessary because the pressure load imposed on the RCB may lead to early failure of the containment.

Direct Containment Heating (DCH) is a prominent severe accident issue because of its potential for early containment failure. The Nuclear Regulatory Commission (NRC) has identified DCH as a major issue for resolution in the Revised Severe Accident Research Plan (NRC, 1992) and has sponsored a program at Sandia National Laboratories to resolve the DCH issue. The first step in this process was writing NUREG/CR-6075 (Pilch et al., 1994): "The Probability of Containment Failure by Direct Containment Heating in Zion." NUREG/CR-6075 assesses the probability of containment failure by DCH for the Zion Nuclear Power Plant (NPP). NUREG/CR-6075 was extensively reviewed by a panel of 15 experts representing national laboratories, universities, and industry. The review process included written comments by the peer reviewers, responses to the comments by the authors, and rebuttals by the reviewers (see Appendix A). Major issues that were identified as part of the peer review process, such as consistency of initial conditions and hydrogen combustion, are addressed in Supplement 1 of NUREG/CR-6075. Following the comment, response, and rebuttal process, two working group meetings of selected members of the original peer review group were held to resolve two residual concerns: initial conditions and model validity.

Supplement 1 to NUREG/CR-6075 focuses on closure of the DCH issue for the Zion plant. It contains the additional analyses that the working groups indicated were necessary to strengthen the original conclusions. The probabilistic framework for these analyses is described

in Section 2 of this report. The working groups suggested four new possible scenarios for analyses using the methodology in NUREG/CR-6075. The scenarios are described and justified in Section 3. Quantification of the DCH phenomenon with the TCE model is discussed in Section 4, and quantification of the Zion fragility is described in Section 5. The probabilistic synthesis is carried out using a Monte Carlo sampling method in the TCE/LHS code, which is described in Appendix B. Section 6 contains the results of the calculations for the splinter scenarios. The conclusions and recommendations are summarized in Section 7.

The working group members stressed consistency of the DCH initial conditions. They recommended using insights from core melt progression analyses performed by the Idaho National Engineering Laboratory (INEL) with SCDAP/RELAP5 for the Zion plant. Consistent with that recommendation INEL analyzed three short-term station blackout cases for the Zion plant with different leak rates: (1) no leaks, (2) a leak rate of 250 gpm per pump, and (3) a leak rate of 480 gpm per pump. Failure of the hot leg or surge line resulting in depressurization of the primary system was observed well before core relocation and lower head failure in all three cases. However, the calculations were continued until the lower head failed in order to gain insights about conditions at lower head failure, such as the melt mass and composition, reactor coolant system pressure, melting of upper plenum steel, and relocation of metallic core blockages into the lower plenum. These insights were applied in developing the distributions for the new scenarios defined in this supplement.

The NRC-sponsored experimental program has played a major role in developing an understanding of the key physical processes in DCH. The technical basis for these scaled experiments was developed by the Severe Accident Scaling Methodology Technical Program Group (SASM-TPG) (Zuber et al., 1992) and by Pilch et al. (1992). The extensive database from counterpart experiments by Sandia National Laboratories and Argonne National Laboratory has allowed the development and validation of simple analytical models for predicting the containment loads. In particular, the two-cell equilibrium (TCE) model is based on phenomenological insights from the experimental program and is used in the analyses presented here. The TCE model takes into account the coherence between the entrained debris and the RCS blowdown steam. Any noncoherence in the entrainment process limits the interactions that result in debris-to-gas heat transfer and in chemical reactions that produce hydrogen.

The methodology that has been developed in NUREG/CR-6075 and its supplement will be applied to the Surry plant in NUREG/CR-6109: "The Probability of Containment Failure by Direct Containment Heating in Surry." Extrapolation to other power plants is being addressed in another NUREG/CR report to be released soon.

1.1 References

NRC (December 1992). *Severe Accident Research Program Plan Update*, NUREG-1365, Rev. 1, U.S. Nuclear Regulatory Commission, Washington, DC.

Pilch, M.M., M.D. Allen, and J.L. Binder (1992). "Counterpart and Replicate DCH Experiments Conducted at Two Different Physical Scales: The SNL/IET-1, 1R and the ANL/IET-1R, 1RR Experiments," Letter Report to the NRC, Sandia National Laboratories, Albuquerque, NM.

Pilch, M.M., H. Yan, and T.G. Theofanous (1994). *"The Probability of Containment Failure by Direct Containment Heating in Zion,"* NUREG/CR-6075, SAND93-1535, Sandia National Laboratories, Albuquerque, NM.

Zuber, N., B. Boyack, A. Dukler, P. Griffith, J. Healzer, R. Henry, M. Ishii, J. Lehner, S. Levy, F. Moody, M. Pilch, B. Sehgal, B. Spencer, T. Theofanous, J. Valente, G. Wilson, and W. Wulff (1992). *An Integrated Structure and Scaling Methodology for Severe Accident Technical Issue Resolution*, Draft for Comment, NUREG/CR-5809, EGG-2659, EG&G Idaho, Inc., Idaho Falls, ID.

2.0 PROBABILISTIC FRAMEWORK

The basic understanding upon which this approach to resolving the DCH issue is based (and confirmed in repeated experiments) is that the intermediate (or steam generator) compartment traps most of the debris dispersed from the reactor cavity and that the thermal/chemical interactions during this dispersal process are limited by the incoherence in the steam blowdown and melt entrainment processes. To put it simply, for blowdowns that are sufficient to cause entrainment and significant thermal/chemical interactions, the entrainment time is short compared with the blowdown time so that the molten debris is exposed to only a small fraction of the steam from the primary system. Because this steam is the principal medium for carrying the melt energy and the hydrogen produced by steam/metal interactions to the main containment volume, this incoherence is a crucial mitigating factor. With this understanding, it is possible to reduce most of the complexity of the DCH phenomenon to a single parameter: the ratio of the melt entrainment time constant to the system blowdown time constant ($R_\tau = \tau_e/\tau_b$ in the TCE model). For simplicity, R_τ is referred to as a coherence ratio.

Besides these modeling factors, the DCH loads depend on parameters that characterize the system initial conditions; that is, primary system pressure, temperature and composition (i.e., hydrogen mole fraction), melt quantity and composition (zirconium and stainless steel mass fractions), initial containment pressure and composition (hydrogen mole fraction), and geometry (containment volume and the size of the breach). The key component of the framework, therefore, is the causal relation (CR1) between these parameters and the resulting containment pressure (and temperature) under the influence of the uncertainty in the coherence ratio, R_τ. Of these parameters, some are fixed, some vary only over a narrow range, and some are so uncertain that they can be approached only in a very bounding sense. The following features were considered in coming up with the final choice of a framework:

1. *Geometry.* The specific geometry is fixed for a given plant; however, the basic features are that there is an intermediate compartment between the cavity and the main containment volume and that the lower head fails in a local (rather than global) manner. In addition, the geometry is characterized by the free volume of the containment and the primary system volume.

2. *Containment Conditions.* Typically, high-pressure scenarios evolve with significant primary system venting prior to vessel breach (see Section 3); this venting increases the containment pressure to ~0.25 MPa with temperatures near saturation. This pressure will be lower if any of the active containment heat removal systems are operational. The containment atmosphere will also contain hydrogen at a concentration of a few mole percent. Preexisting hydrogen is limited by the quantity of zirconium available to react in the core, and thus there is a constrained relationship between preexisting hydrogen in the containment and the hydrogen produced by steam/zirconium reactions in the DCH event.

3. *Primary System Conditions.* We emphasize here the reasonable consistency between reactor coolant system (RCS) pressure (and temperature) and melt mass and composition. Model predictions indicate that DCH loadings are insensitive to the temperature of the primary system (see Appendix D, NUREG/CR-6075), and accident analyses indicate that the primary system pressure can be enveloped rather than predicted (Section 3). This leaves only the expelled melt parameters in need of quantification: melt quantity, composition, and temperature. These are the variables that drive the DCH process; however, they are highly uncertain. They depend on the complex interactions and the many scenario bifurcations in the core meltdown, relocation, and lower head failure processes and are hence in need of very careful quantification. This is done in Section 3.

The probabilistic framework can be structured in the manner illustrated in Figures 2.1 and 2.2. As shown in these figures, the initial melt parameters are to be quantified as independent probability density functions, representing modeling uncertainty in the parameters (variations from stochastic processes are assessed as insignificant relative to modeling uncertainty). These functions are formed into a joint probability density function and then combined with CR1, under the parameter distribution function that represents model uncertainty for the DCH processes, R_r, to obtain a probability density function for the peak containment pressure. This distribution function is combined with the set of containment fragility curves

(probabilistically distributed themselves[1]) to obtain a probability distribution of the containment failure frequency.[2]

The discrete probability distribution (DPD) method was used to propagate distributions through the probabilistic framework in NUREG/CR-6075. The ALPHA code, developed at the University of California at Santa Barbara (UCSB), was the software based on the DPD approach that was used in NUREG/CR-6075 to calculate containment failure probabilities. An alternative to using ALPHA was developed by Sandia for the present supplement document, with an eye towards continued use in future extrapolation efforts. Sandia has developed software to perform either traditional Monte Carlo sampling or stratified Monte Carlo sampling (Latin Hypercube Sampling, LHS). The software, called LHS (Appendix B) is user-friendly and has an established quality assurance pedigree, including code assessment and verification. Sandia chose to use a new numerical tool based on LHS to propagate distributions through the probabilistic framework. The resulting software is described more fully in Appendix B and benchmarked against existing ALPHA predictions.

---

[1] In the current assessments, only a single fragility curve is available, but the discussion here has been generalized to accommodate desired improvements in information.

[2] Note here the terminology that each fragility curve is expressed in terms of failure frequency, and this frequency expresses the statistically meaningful variations (based on actual experience) in containment strength due to variations in material and workmanship; that is, the fraction failed from a nominally similar population of structures subjected to the same load. On the other hand, the probability assigned to each fragility curve expresses a subjective degree of belief as to the appropriateness of it in meeting the intended task.

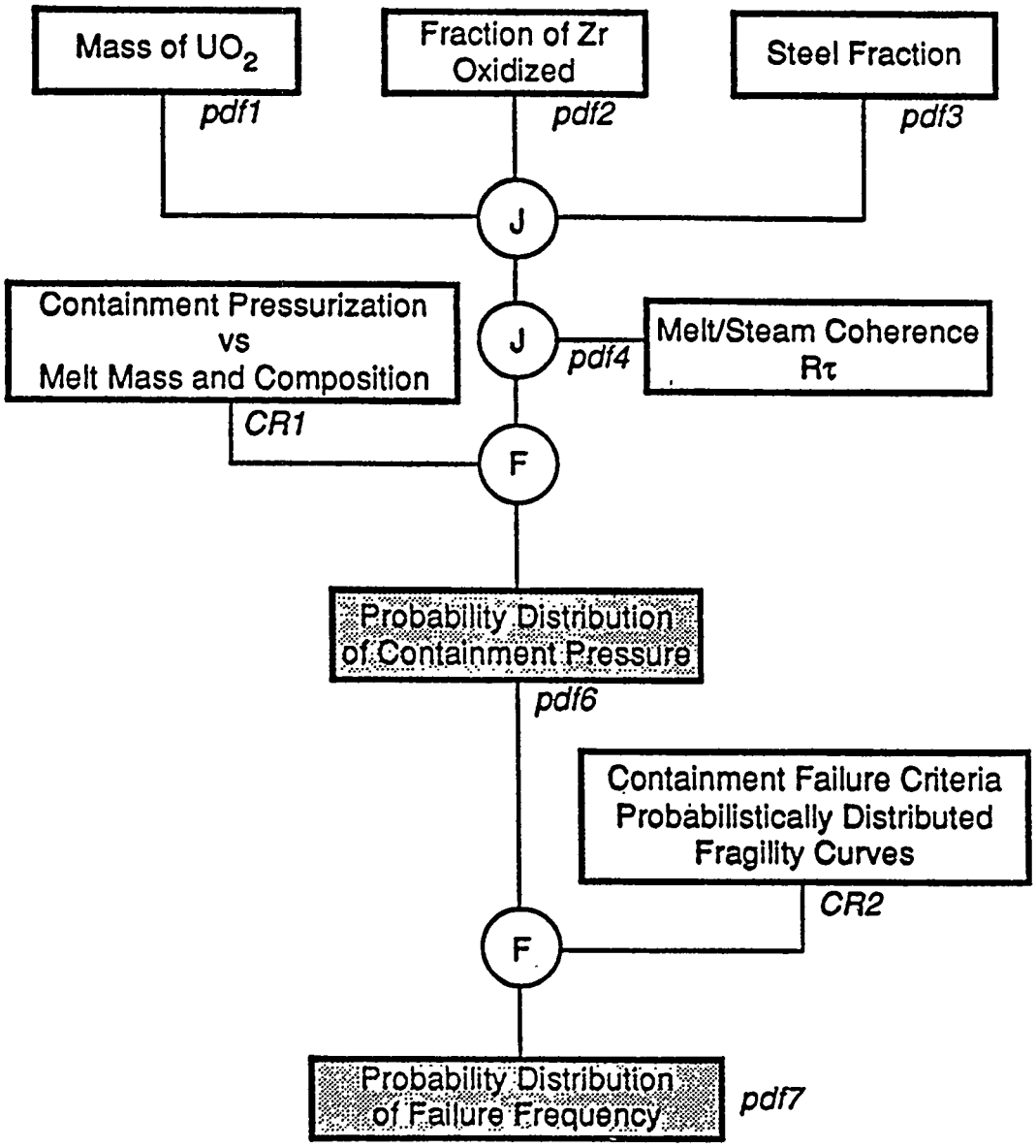

Figure 2.1. **The probabilistic framework for containment failure under Direct Containment Heating scenarios. The (J) and (F) are the "joint" and "function" operations, respectively, as described in the text.**

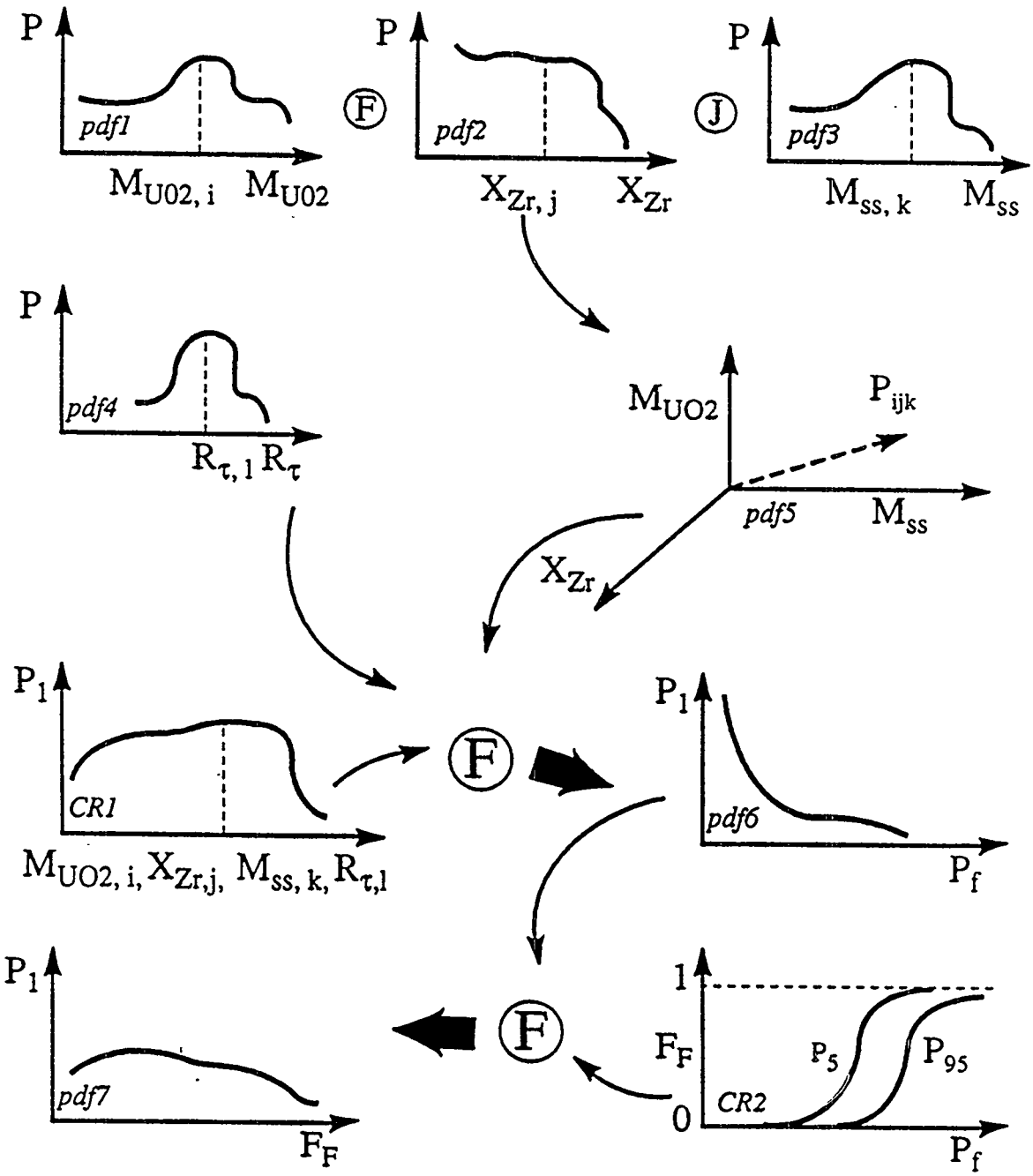

Figure 2.2. **Illustration of the probabilistic framework in terms of schematic depiction of its components.**

3.0 QUANTIFICATION OF INITIAL CONDITIONS

3.1 Introduction

DCH has traditionally been examined for a rather narrow range of hypothesized severe accident conditions: unmitigated station blackout at full system pressure, formation of a metallic blockage ceramic crust in the core that contains a large fraction of core in a molten state, sudden downward failure of this blockage and crust, resulting in a massive relocation of the melt into the lower plenum, failure of a penetration passing through the lower head of the reactor pressure vessel (RPV), rapid ablation of the resulting hole in the RPV from 5 to about 40 cm (Pilch and Tarbell, 1985), and high pressure melt ejection from the single hole followed by high-pressure steam blowdown. In attempts to address the DCH issue from either a systems point of view or an accident management point of view, intentional depressurization of the primary system has been examined (Hanson et al., 1990). Experiments have shown that the pressure must be very low (less than 1 MPa) to preclude the onset of dispersal from the cavity and to prevent the possibility of DCH (Tutu et al., 1988). Bounding calculations (Pilch and Tarbell, 1986) suggest that only 20 percent of the core (participating in DCH) could pose a threat for the containment. With this traditional understanding, containment- threatening loads from DCH can only be precluded if the RCS is almost fully depressurized. However, based on the understanding developed in NUREG/CR-6075 (Pilch et al. 1994), a substantial reduction of DCH is achieved without having to invoke nearly complete depressurization of the RCS.

Quantification of melt release conditions was developed by attempting to envelope the physically possible behavior in a comprehensive and systematic manner. This means that we needed to examine all reasonably conceivable severe accident scenarios, identify key aspects of their phenomenology and respective ranges of behavior, and establish the few scenarios that envelope the DCH challenge to the containment.

Peer reviewers raised the following questions (Appendix A) regarding the completeness of the splinter scenarios considered in NUREG/CR-6075:

1. Can full system pressure cases be ruled out?

2. Should operator intervention scenarios be analyzed?

3. Can dry core scenarios lead to melting and relocation of the metal (Zr) blockage from the core to the lower plenum?

Generally, the peer reviewers characterized initial condition quantifications in NUREG/CR-6075 as "optimistic." Specifically, they expressed concern that ~8 MPa RCS pressure might not be adequately bounding, that the melt mass distributions were too narrow, and that the melt composition did not contain sufficient metallics (Zr and steel). The reviewers also stressed that SCDAP/RELAP5 analyses be performed and used in a consistent manner in establishing initial conditions.

The NRC convened a working group to make recommendations on how to resolve these concerns. The group's minutes are included in Appendix A and summarized in Section 3.2, where additional splinter scenarios are defined. SCDAP/RELAP5 calculations were performed to provide confirmatory insight into the working group recommendations. These calculations are discussed in Appendix C and the relevant insights are summarized in Section 3.3. Quantifications for the new scenarios are presented in Sections 3.6 and 3.7.

3.2 Splinter Scenarios

Figure 3.1 depicts the four splinter scenarios analyzed in NUREG/CR-6075. The phenomenological complexity of severe accidents leads to the possibility of two major scenario bifurcations: one concerned with the quantity of melt that accumulates in the core region prior to its release and relocation into the lower plenum, and the other concerned with the mode and timing of lower head failure. The first bifurcation considers crucible formation/failure versus gradual relocation (no crucible) as the mechanism for melt relocation into the lower plenum. The second bifurcation considers a localized penetration failure of the lower head versus rupture.

Working group recommendations focused on four new splinter scenarios as shown in Figure 3.2. The intent was to place greater reliance on systems-level codes (SCDAP/RELAP5) in order to achieve better consistency between RCS pressure at vessel breach with melt mass and composition. Specifically, the working group emphasized that high RCS pressures are correlated with predominantly oxidic melts and that metallic melts are correlated with reduced RCS pressures. The working group minutes (Appendix A) refer to the new splinters as Scenarios II, IIa, IIb, and III; however, to avoid confusion with the scenarios already analyzed in

NUREG/CR-6075, we refer to the new splinters in this report as Scenarios V, VI, VII, and VIII. The new scenarios either bound the scenarios in NUREG/CR-6075 or stress greater consistency in the conditions at vessel breach; thus, the new scenarios are intended to replace those in NUREG/CR-6075. The rationale leading to these new splinter scenarios is discussed next.

The working group felt that there was no compelling need to further analyze scenarios with penetration failures. The INEL lower head failure analysis (Rempe et al., 1993) and the OECD-NEA-TMI-2 vessel investigation project (Stickler et al., 1993) both concluded that rupture was much more likely than a penetration-type failure. Marshall (1988) performed some scoping experiments on tube ejection. Specifically, he confirmed that binding caused by differential thermal expansion could prevent ejection of a penetration from the lower head (for the conditions and materials tested); however, ballooning of the lower head, which could induce ejection of a penetration as a precursor to rupture, was not modeled in these experiments. Fauske and Associates, Inc. (FAI) (Hammersley et al., 1993), under the sponsorship of the Electric Power Research Institute (EPRI), has examined melt penetration into in-core instrument guide tubes. Pressure-driven melt was observed to travel approximately 2 m, which is far enough to carry it well beyond the lower head. However, the melt mass is too small to threaten the integrity of the guide tube. These limited experiments confirm INEL and OECD conclusions that penetration-type failures are unlikely. NUREG/CR-6075 (Pilch et al., 1994) showed that a penetration failure followed by ablation of the lower head would produce a hole about the same size as would be expected for a local rupture of the lower head. Finally, work reported in NUREG/CR-6075 (Pilch et al., 1994) showed that predicted loads for rupture scenarios bound predicted loads for penetration failure scenarios; consequently, penetration failures need not be considered further in the supplement assessments for Zion or in any extrapolation activities.

Scenario VI is very similar to Scenario II in NUREG/CR-6075. Here, the working group wanted to emphasize the presence of water in the lower head. They recommended the addition of a new TMI-like scenario (Scenario V) characterized by reflooding and repressurization ($\sim$16 MPa) of the RCS as a result of operator actions. Scenarios V and VI were envisioned as having water in the core (at least covering the bottom) during much of the core melt progression; consequently, slumping core material would form a crucible which could fail only locally. The melt composition would be largely oxidic, with most unoxidized Zr permanently retained as a metal blockage in the core.

The working group then recommended consideration of scenarios in which core melting would proceed without water in the core region and largely without water in the lower plenum. It was their expectation that these scenarios would evolve to much lower RCS pressures at vessel failure for typical small break loss-of-coolant accidents (SBLOCAs). At the lower pressures, the possibility of melting upper plenum steel without also failing the hot leg becomes possible; thus, both scenarios VII and VIII augment the oxidic melt with large quantities of upper plenum steel. Scenario VIII is distinguished from Scenario VII in that the metal blockage is also assumed to remelt, allowing large quantities of unoxidized Zr to relocate to the lower plenum.

NUREG/CR-6075 (Scenarios III and IV) considered a gradual relocation that progressed under high pressure ($\sim$8 MPa) with complete melting of upper plenum steel. Working group discussions pointed out that these scenarios are overly conservative and that melting of upper plenum steel is strongly correlated with hot leg failure. In fact, a gradual relocation scenario has only been predicted in one MELPROG calculation for the Surry plant; and even here, hot leg failure was predicted before core relocation into the lower plenum. Should a gradual relocation scenario occur, working group members believed that it would look like Scenario VIII at the time of vessel failure.

SCDAP/RELAP5 calculations have been performed (based on working group recommendations) to confirm the basic features of Scenarios VII and VIII. Three cases were run with SCDAP/RELAP5 representing the full spectrum of expected SBLOCAs: no leaks, 250 gpm/pump, and 480 gpm/pump. Appendix C presents these calculations in detail, and the results are summarized in Section 3.3. The key conclusion, however, is that hot leg failure is predicted to occur before core relocation for all SBLOCAs leading to complete depressurization of the RCS before lower head failure. Consequently, Scenarios VII and VIII are not further analyzed in this report.

3.3 Summary of SCDAP/RELAP5 and CONTAIN Insights

The initial and boundary conditions for the new scenarios analyzed in this supplement are based on insights from SCDAP/RELAP5 and CONTAIN calculations. These system code calculations are used to justify the initial and boundary conditions for the dry core splinter scenarios discussed in Section 3.2. In this report, "dry core" implies that the RPV water level is below the bottom of the core so that the potential exists for metallic blockages to relocate to

the lower plenum. All of the cases analyzed produced "dry core" conditions. However, SCDAP/RELAP5 calculations did not predict any significant relocation of metallic blockages in any of the dry-core cases that were analyzed.

Three dry core cases were run with SCDAP/RELAP5 at different leak rates: (1) no leaks, (2) 250 gpm per pump leaks, and (3) 480 gpm per pump leaks. The results of these calculations are discussed in Appendix C. The goal of these calculations was to develop a better understanding of the melt mass, melt composition, and RCS pressure at the time of lower head failure for dry scenarios. In each case, hot leg failure was allowed to occur, if predicted during the calculation. This failure would lead to depressurization and complete accumulator discharge. The output from SCDAP/RELAP5 for these cases was used in CONTAIN to determine the containment conditions at the time of lower head failure. The flow of steam, water, hydrogen, and nitrogen into the containment was provided to Sandia by INEL for use in CONTAIN. The hydrogen flow into the containment was assessed to determine if the hydrogen would burn as it entered the containment. A number of important insights were obtained from these calculations.

First, the SCDAP/RELAP5 calculations indicated that hot leg failure occurred prior to melt relocation into the lower plenum in all cases. The failure resulted in depressurization and accumulator discharge. In all cases, the RCS pressure was at containment pressure at the time of lower head failure. Owing to the significant amount of time between hot leg failure and lower head failure, we conclude that the sequences, as calculated by SCDAP/RELAP5, will not result in a DCH threat. This supports the assessment in NUREG/CR-6075 that full system pressure scenarios can be excluded (except operator intervention accidents such as TMI-II). The SCDAP/RELAP5 calculations also confirm that the ~8 MPa bound in NUREG/CR-6075 is not only conservative, but perhaps excessively so unless the operator intervenes in the accident. This assumes, of course, that water injection does not arrest melt progression.

A second insight is related to the amount of metallic debris present in the melt in the lower plenum. We noted that the degree of upper plenum steel melting is limited in all cases and is strongly correlated with hot leg failure. The maximum amount of upper plenum steel that was predicted to melt was on the order of 3 mt. We also noted that lower plenum steel was assumed to melt in all cases, representing an additional 5 mt of steel. Hence, the amount of steel in the melt is limited to ~8 mt. This ~8 mt of steel can be compared with the original

25 mt analyzed in Scenarios III and IV in NUREG/CR-6075. We conclude that the analyses confirm the conservatism in the original steel mass distributions.

With respect to zirconium in the melt, SCDAP/RELAP5 indicates that very little zirconium is predicted to relocate into the lower plenum. The maximum amount of zirconium in the lower plenum melt is ~0.5 mt. This result implies that melt-out of the metallic blockage in the core region is not predicted, even in dry core scenarios. Again, the SCDAP/RELAP5 predictions confirm NUREG/CR-6075 assessments.

The reason for this behavior can be seen by a careful review of the calculations. In all cases, the melt that relocated into the lower plenum is predicted to quench, but not all of the available water is vaporized. This is likely due to displacement of water from the lower plenum as the melt relocates. The water eventually settles back into the lower plenum, but a stratified condition exists, i.e., the water overlies the debris residing on the lower head. Owing to inefficient heat transfer between the debris and the water, the water is vaporized slowly and, in all cases, water remains in the lower plenum at the time of lower head failure. The presence of water and its slow vaporization appears to be sufficient to prevent melt-out of the in-core blockages. Hence, we conclude that the amount of zirconium in the melt in the lower plenum is expected to be very limited.

A third insight is related to the amount of hydrogen generated. We observed that the amount of hydrogen generated in Cases 2 and 3 corresponds to ~40 to 60 percent zirconium oxidation. Our expectation is that the 60 percent level is a likely upper bound since much of the remaining zirconium is contained in metallic blockages that are difficult to oxidize. The distributions for Zr oxidation in NUREG/CR-6075 envelope the SCDAP/RELAP5 predictions.

The fourth insight is related to the amount of molten material at the time of lower head failure. We noted that the amount of oxide material that relocated into the lower plenum varies from approximately 77 mt to 104 mt for the three cases, but the amount of *molten* oxide varies from 55 mt to 66 mt. Hence, while the amount of oxide material in the lower plenum shows some variation, the amount of *molten* oxide at vessel breach is limited to a rather narrow range. The SCDAP/RELAP5 predictions (~60 mt oxide) are about 10 mt higher than the assessments in NUREG/CR-6075, with most of the difference attributed to a NUREG/CR-6075 assessment that the crucible cannot fail at the bottom and drain completely, whereas SCDAP/RELAP5

analyses assume failure of the crucible results in complete drainage of the molten contents. However, sensitivity studies have shown that DCH loads are very insensitive to oxide mass (see Appendix A, Responses H19 and H32, and Comments by Reviewer O).

The CONTAIN calculations were used to provide insights into the containment conditions at the time of lower head failure. The Zion containment was represented by four cells: one each for the cavity, steam generator compartments, annular region, and the dome. The SCDAP/RELAP5 predictions of the temperature and mass flow rates of water, steam, hydrogen, and nitrogen from the RCS were used as inputs to the CONTAIN calculations. Because of the complexity of the hydrogen combustion issues, CONTAIN was run with all burn models disabled. This allows the maximum accumulation of hydrogen at the time of RPV failure. Hydrogen combustion analyses were performed separately by examining sources from SCDAP/RELAP5 and CONTAIN predictions of the atmosphere composition in each cell to determine if hydrogen released prior to RPV failure would burn as it entered containment. Several insights were obtained from the CONTAIN calculations.

The CONTAIN calculations showed that the containment pressure at the time of lower head failure was in the range of 0.23 to 0.26 MPa for the three cases. These values are consistent with the ~0.25 MPa estimate used in NUREG/CR-6075. Condensation on internal structures and containment walls had a significant influence on the steam concentration in the containment atmosphere prior to vessel breach.

It was predicted that the gases would not accumulate in the steam generator compartments or in the containment annulus. This is consistent with gases released from relatively low release locations but the predictions were also influenced by the CONTAIN nodalization scheme and use of a lumped-parameter code.

During the time hydrogen was injected into the containment, the global mixtures were nonflammable for the three cases analyzed. In the dome, for example, the steam concentration varied between approximately 40 - 60 percent as the hydrogen was injected while the hydrogen concentration was typically below 5 percent.

Insights were obtained on non DCH-induced hydrogen combustion using both the SCDAP/RELAP5 and CONTAIN calculations. The SCDAP/RELAP5 predictions were analyzed

to determine what fraction, if any, of the hydrogen injected into the containment would be consumed as an autoigniting jet. Furthermore, since the scenarios analyzed were station blackout scenarios, the autoigniting jets were considered to be the only possible ignition source for deflagrations in the containment. Therefore, CONTAIN predictions of the source compartments were analyzed to determine if mixtures were flammable at the time the jets autoignited.

It was determined that the only possibility of jet autoignition would occur at the hot leg break in Cases 1 and 3, and these cases would depressurize so quickly that they would not be a DCH threat. Otherwise, the temperatures of the gases (~600 K) released from the power-operated relief valves (PORVs) were too low for autoignition for all cases, and the hydrogen concentration in the jet never exceeded ~5 percent and usually was zero. Likewise, gases released from the RCPs likely would not autoignite in all of the cases analyzed because hydrogen concentrations in the jets were very low (~5 - 15 percent) during periods of high gas temperatures. Thus, the hydrogen concentration in the containment just prior to vessel failure can be simply determined by summing all hydrogen released from the RCS.

For Case 1, it was estimated that between 35 - 40 percent of the total hydrogen released into the containment could have burned as an autoigniting jet. Conditions for autoigniting jets were not satisfied for Case 2. For Case 3, it was estimated that approximately 1 - 2 percent of the total hydrogen released into the containment could have burned as an autoigniting jet. These results are for three cases that had different leak rates for the reactor coolant pump seal but otherwise were the same. The large variation in the fraction of hydrogen that could have burned for the three cases illustrates that hydrogen is very scenario dependent.

Gases in the source compartments were not flammable during the time the jets were autoigniting for the three cases analyzed. The analyses accounted for the decrease in hydrogen that was consumed in the autoigniting jets. The containment pressure increase resulting from blowdown and autoignition of jets in Case 1 is ~0.03 MPa higher for a total pressure of ~0.30 MPa at the time (~2000 s) of jet combustion. This pressure is far from a containment-threatening load.

3.4 Characterization of the Zion Plant

Quantification of initial conditions for analyzing containment loads is based on the plant characteristics shown in Table 3.1. It is worth noting that approximately 30 percent of the core is within one fuel assembly distance to the edge of the core. This material, owing to its low decay power and high heat transfer to the core barrel, is difficult to melt, and it is an unlikely contributor to the core melt (in the lower plenum) at vessel breach. Although the core contains little steel, the upper and lower plenums contain large quantities of steel that might be added to the core melt, depending on the scenario. Here, we have restricted ourselves to relatively thin steel that has no substantial inertia to thermal loads that might be imposed on the structure. Based on a more careful examination of a TRAC deck for Zion, and in consultation with FAI (MAAP input deck), the quantity of meltable steel in the lower plenum has been revised from 15 mt (NUREG/CR-6075) to 10 mt.

Figure 3.3 depicts the Zion NPP. Debris ejected from the reactor pressure vessel first enters the reactor cavity, where high-pressure blowdown gases can disperse the debris into the containment by one of two possible paths. The first is an annular gap around the RPV, which would allow debris to disperse directly to the upper dome. This annular gap is partially filled with reflective insulation and is blocked by neutron shielding and the eight nozzles near the top of the RPV. The SNL/IET-11 (Blanchat et al., 1994) experiment showed that if gas can carry debris into the gap, then the insulation will melt and be swept clear of the gap. Such a situation cannot be precluded at Zion; consequently, this potential flow path is explicitly bounded in the evaluation of containment loads evaluations.

As shown in Figure 3.3, the major dispersal path (by virtue of its large flow area) is through a tunnel leading from under the RPV, which exists so that in-core instrument guide tubes can have access to the lower head. Debris dispersed from the cavity through this path will enter the lower compartmentalized regions of the containment. In particular, a significant amount of debris will enter the containment basement, which comprises only ~6 percent of the containment volume. The TCE model treats this subcompartment room as part of its basic formulation, but it is found that DCH interactions are dominated by the interaction with the blowdown gas rather than any gas initially in the subcompartment. Consequently, this room plays no real role in DCH except to confine debris to an insignificant portion of the containment

atmosphere. However, hydrogen produced in the cavity and basement during the DCH event will be pushed to the upper dome through vent paths by blowdown steam.

The seal table room sits over the cavity exit. Experiments have shown that some dispersed debris can reach the upper dome through the seal table room and through vents located above the reactor coolant pumps.

3.5 Definition of Probability Levels

Our approach here recognizes that, in the absence of experiments that are fully representative (scaled) *of the sequence* in question, it makes no sense to speak of "statistical expectation" or "relative frequency." Nor can there be any claim that our judgment of likelihood can be cast in terms of actual frequency. Moreover, variability (i.e., statistical variations for nominally similar conditions) would normally be dwarfed by uncertainties in the phenomena themselves. Thus we use probability as a tool to propagate judgmental degrees of belief through the probabilistic model, i.e., the numbers by themselves have no intrinsic meaning. That is, we use a physically based probability scale (Table 3.2) for the quantification of inputs and using the same scale we convert bottom-line results to a physical interpretation.

Empirically, it can be shown that the physical interpretation of the probability calculation is invariant relative to the numbers assigned to the judgmental degrees of belief, as long as the same geometrical progression is preserved. With our recommended assignments, the product of two "edge of spectrum" events ($P \sim 10^{-1}$) is 10^{-2}, which should be interpreted physically as an "upper bound." The interpretations in Table 3.2 might be given the alternate assignments: 1, 1/3, and 1/9. Once again, the product of two "edge of spectrum" events ($P \sim 1/3$) is 1/9, which should be interpreted physically as an "upper bound" with the new assignments. Therefore, the specific value of a judgmental degree of belief has no intrinsic meaning; it is only meaningful when measured against the physical assignment.

Our judgmental degree of belief for any process can be characterized as likely ($P \sim 1$), as unlikely ($P \sim 10^{-2}$), or as something in between ($P \sim 10^{-1}$). As a practical matter, we assign $P \sim 1$ to our best estimate and $P \sim 10^{-2}$ to our estimate of a reasonable upper bound (assuming we have a reasonable expectation that the upper bound is unlikely). Working group members concurred with this interpretation.

3.6 Scenario V - SBLOCA with Repressurization of the RCS by Operator Intervention

Scenario V represents a core melt accident that progresses with water still present in the lower portions of the core. Such conditions lead to formation of a crust within the core followed by a massive release of melt when the crust fails. Accumulation of core material on the lower head of the RPV causes the lower head to heat up, eventually to the point where its structural strength is so degraded it can no longer withstand the stresses induced in the lower head by elevated RCS pressures. Thus, creep rupture of the lower head is the expected failure mechanism. The distinguishing feature of Scenario V is that operator actions are assumed to refill the RPV with water and to fully repressurize the RCS. Analysis of DCH for a repressurized RCS is deemed conservative because we expect operators to depressurize the RCS in a core damage accident.

Table 3.3 summarizes the initial conditions for this scenario. Operator actions are assumed to repressurize the RCS to 16 MPa. Operator intervention refills the RPV with water (~75 mt) to the hot leg nozzles and quenches any steam remaining in the RCS to near saturation (~700 K). Recall that a noncondensible gas bubble prevented operators from refilling the entire RCS at TMI-II. The RPV lower head must be heated by accumulated core material to the point that steel loses its strength (~1000 K), which leads to rupture of the lower head. The initial hole diameter is ~0.40 m (Pilch et al., 1994) because of the likely presence of hot spots and because of stress concentrations associated with the existence and spacing of lower head penetrations. This rupture size is in accordance with working group recommendations (Appendix A). The final hole size (~0.46 m at the upper bound) is computed with the ablation model Eq. (4.2); however, ablation is not important for the large initial hole sizes associated with rupture of the lower head.

Oxidation of Zr occurs predominantly before significant core degradation, as demonstrated in various calculations. In earlier 2-D MELPROG calculations performed by Kelly et al. (1987), 80 percent of the Zr oxidation occurred prior to formation of a molten pool. SCDAP/RELAP5 calculations (Appendix C) performed specifically for this report confirm these early assessments and show that nearly 100 percent of the hydrogen is produced before core slump. Furthermore, most Zr will be permanently retained in core blockages, with any Zr remaining in the melt existing as a eutectic with the other (mainly oxidic) constituents. Little of this Zr is expected to oxidize during massive relocations. To first order then, Zr oxidation

is independent of the core melt progression that follows the main oxidation event; and since oxidation occurs predominantly before molten pool formation, existing systems-level computer codes are technically adequate to assess the range of possible oxidation.

Referring then to SCDAP/RELAP5 calculations (Knudson and Dobbe, 1993; Knudson, 1993, Appendix C), MELPROG/PWR-MOD1 calculations (Kelly et al., 1987), and CORMLT calculations (Denny and Sehgal, 1983), we find that the fraction of Zr oxidized ranges from 20 to 60 percent with a mean around 40 percent. Consistent with NUREG-1150 expert elicitations, the extremes of the distributions are considered unlikely ($P \sim 0.01$). The distribution is shown in Figure 3.4. The calculations cited were chosen because of their explicit treatment of recirculating flow patterns in the core.

Consistent with TMI-II, the potential release of molten material to the lower head is controlled by the formation of a hemispherical crucible that excludes only the outer assemblies of the core (Figure 3.5). The outer assemblies are generally not in a severely degraded state because the RPV is flooded. Asymmetries in crucible growth ensure that localized penetration of the outer assembly and the core barrel would most likely occur when the crucible has grown (on average) to the outer assembly.

The maximum volume of such a crucible is $\sim 7\ m^3$ and it would be filled with a predominantly oxidic melt with a density of $\sim 10{,}000\ kg/m^3$. This means that the crucible can hold a maximum of ~ 70 mt of molten material. The amount of melt released from the crucible is a function of where the crucible fails, with downward and sideward representing the two extremes. Recent studies by Schmidt and Humphries (1994), considering only conduction processes, suggest that bottom failure of a crucible is very unlikely. Natural convection patterns (which produce edge-peaked heat flux distributions) in the molten pool, should they develop, would only reinforce the prediction of side failure of the crucible. The MP-2 experiment (Gasser et al., 1994) tends to confirm that downward failure of an oxidic crust is unlikely, even in the absence of active cooling. To establish an upper bound ($P \sim 0.01$) on the UO_2 mass that relocates to the lower plenum, it was assumed that the crucible could fail at the bottom, releasing the entire ~ 70 mt of material to the lower plenum head.[3]

---

[3] As an upper bound, NUREG/CR-6075 assumed that 75 percent of the molten material bottled up in the crucible would relocate. The working group recommended that 100 percent relocation should be used as the upper bound.

To fix the composition a little more closely, we note that ~80 - 90 percent of 70 mt (0.85 x 70 ~ 60 mt) is UO_2. As a best estimate, and consistent with TMI-II observations and working group recommendations, side failure of the crucible is expected to release about half of the material (~35 mt total) to the lower head. Likewise, the best estimate on the amount of relocated UO_2 is ~30 mt. On this basis, the distribution for the amount of UO_2 released from the crucible can be constructed as in Figure 3.6.

It should be noted that the amount of UO_2 released from the crucible exceeds the amount of *molten* material available to participate in DCH at the time of vessel failure. First, not all material released from the TMI-II crucible reached the lower head. Some froze between the core former plates and the core barrel and some additional material froze on other structures as it drained into the lower plenum. Second, some molten material will quench and freeze as it flows through the water in the lower plenum. Calculations using the THIRMAL code (Rempe et al., 1993) suggest that as much as ~50 percent might freeze during this process if the water is subcooled. Experiments (Spencer et al., 1994) tend to confirm this number if the water is subcooled, but suggest that only ~10 percent will quench if the water is saturated. Third, some of the molten material accumulated on the lower head will form an upper crust resulting from heat transfer to the overlying water. Finally, some of the molten material will freeze as heat is transferred to the lower head causing the temperature to increase to levels where failure might be expected. While this was the case at TMI-II, the post accident examination revealed that rapid cooling of the lower head region occurred after these elevated temperatures were achieved.

The extent to which these solidified materials persist to vessel rupture is coupled to generation of decay heat within the debris and the time required to heat the vessel to rupture. SCDAP/RELAP5 calculations (Appendix C) indicate that ~20 - 25 mt of material are frozen on the lower head at the time of vessel breach. The SCDAP/RELAP5 calculations are themselves a lower bound since they do not account for water intrusion into the melt through cracks in the overlying crust or gaps along the vessel wall. These additional cooling mechanisms were identified as part of the TMI-II vessel investigation program (Stickler et al., 1993).

As a bound, we consider only melt freezing in the process of heating the lower head to rupture. Boucheron (referenced in Zuber et al., 1991) shows that ~10 - 15 mt of oxide will freeze (with decay heat coupling) in order to heat the lower head to a point where it loses its

strength and ruptures. With this in mind, we shift the UO_2 distribution in Figure 3.6 an additional 10 mt to the left. The distribution of *molten* UO_2 at the time of vessel breach is then given by Figure 3.7. The best estimate is then centered at 20 mt, with an upper bound of 50 mt. We emphasize the conservative nature of this distribution given the additional quenching mechanisms that have been ignored.

The amount of molten ZrO_2 in the melt is controlled by the amount of oxidation that occurs prior to core melt. The amount of molten ZrO_2 can be estimated from

$$M_{ZrO2} = \frac{M_{UO2}(melt)}{M_{UO2}(core)} M^0_{Zr} f_{Zr} \frac{123}{91} \quad . \tag{3.1}$$

This expression assumes that ZrO_2 is contained in the melt in the same fraction to which the core is degraded $M_{UO2}(degraded)/M_{UO2}(core)$ and that ZrO_2 relocates to the lower plenum in the same manner as the UO_2, that is, $M_{UO2}(melt)/M_{UO2}(degraded)$.

The relocation of Zr metal within the core plays a key role in the ultimate formation of core blockages. Upon melting, most of the Zr metal and $(U,Zr)O_2$ relocates downward until it freezes in cooler portions of the core, forming partial or complete blockages, depending on the amount of relocating material. The subsequent melting of UO_2 and ZrO_2 allow molten oxides (at least initially) to settle and refreeze on top of the metallic blockages. In this way, the accumulating melt forms a crucible on top of the metallic blockage. This picture is consistent with SCDAP/RELAP5 calculations. This separation of molten oxides from the blockage, which consists of unoxidized clad and dissolution products, ensures that little metal enters the melt, except possibly through some additional formation of $(U,Zr)O_2$ eutectics, dripping of Zr from fuel stubs above the degraded region, or when the crust fails. However, SCDAP/RELAP5 predicts only negligible additional formation of eutectics and dripping is not predicted even in scenarios in which the core is completely dry. As observed in TMI-II, the crust is expected to fail locally (from inhomogeneities in the crust and asymmetries in crucible growth), carrying only small quantities of metal from the blockage into the lower plenum. The flooded core scenario precludes melting out of the blockage. Thus, little or no Zr is expected in the melt.

To account for uncertainties in eutectic formation and crucible failure (and consistent with the working group recommendations), we assume that the molten Zr mass is proportional to the mass of molten UO_2. Thus, the amount of molten Zr can be computed from

$$M_{Zr} = 0.029\ M_{UO2}\ . \tag{3.2}$$

Consistent with working group recommendations, we assume that ~2 mt of Zr is associated with the upper bound of the UO_2 distribution, which we take as ~70 mt. The ~70 mt of UO_2 is actually associated with Scenario VI; so that for Scenario V, the amount of Zr associated with the upper limit of the UO_2 distribution (~50 mt) is 1.45 mt. In this way, Scenarios V and VI are both treated consistently. This formulation is equivalent to a hypostoichiometry of urania, which can be expressed as UO_{2-x}, where x~0.17.

In a wet core scenario such as this, the control rod material will be an initial contributor to the metal blockage in the core and the flooded core scenario precludes melting out of the blockage. Consequently, only trivial quantities (~0 mt) of control rod will be present in the melt at the time of vessel breach.

Melting of upper plenum steel is strongly correlated with failure of the surge line or hot leg nozzle at high system pressures (~8 MPa). Specifically, gas temperatures that are hot enough to melt upper plenum steel (~1700 K) are also hot enough to induce rupture (under pressure) of the hot leg or surge line. Upper plenum steel is a potential contributor to melt mass and composition only in those scenarios (Scenarios VII and VIII) that proceed to relatively low pressures at the time of vessel breach; and even then, SCDAP/RELAP5 predicts failure of the hot leg. In any case, melting of upper plenum steel cannot be important when operators reflood the RPV as they did in TMI-II. The small amount of steel initially in the core, like cladding and control rod material, is largely retained in core blockages, which cannot melt out in a flooded core scenario.

The melting of lower plenum steel by relocated core material is the only source of molten steel of potential importance in a DCH event. Only thin lower plenum steel (e.g., nozzles) that is submerged in the accumulating core material is assumed to melt. The quantity of submerged steel depends on the volume of core material in the lower plenum and can be computed from

$$M_s = M_{s,LP}\ \frac{\dfrac{M_{UO2}}{\rho_{UO2}} + \dfrac{M_{ZrO2}}{\rho_{ZrO2}} + \dfrac{10x10^3}{\rho_{UO2/ZrO2}} + \dfrac{M_{Zr}}{\rho_{Zr}} + \dfrac{M_{CRM}}{\rho_{CRM}}}{V_{LP}} \tag{3.3}$$

where the densities (kg/m^3) are ρ_{UO2} = 10400, ρ_{ZrO2} = 5900, $\rho_{UO2/ZrO2}$ = 9660, ρ_{Zr} = 6500, and ρ_{CRM} = 9250. Note that the quenched 10 mt must be taken into account because it is part of the volume of core material. We note that submerged nozzles at TMI-II did not all melt; consequently, Eq. (3.3) gives a conservative result.

Consideration of natural convection in volumetrically heated pools (Theofanous, 1988; Epstein and Fauske, 1989) indicates that the melt superheat cannot exceed ~200 K under steady state conditions. These assessments are also consistent with SCDAP/RELAP5 analyses. The UO_2/ZrO_2 eutectic melts at about 2800 K, so the maximum temperature on relocation is about 3000 K (~2900 K has been estimated for TMI-II), but some cooling on relocation is expected. Thus, we believe that a conservative bounding value of ~2800 K is appropriate for Scenario V.

MAAP calculations for the Zion plant indicate that the containment pressure at vessel breach is about ~0.25 MPa and the conditions are saturated (~380 K). CONTAIN calculations (Tutu et al., 1990) for the Zion plant produced 0.3 MPa at vessel breach. The most recent CONTAIN calculations (Appendix D), using sources from SCDAP/RELAP5 (Appendix C), show containment pressures in excess of ~0.25 MPa up to and through the period of accumulator discharge. As a result, ~0.25 MPa is chosen as representative for our purposes, which is consistent with NUREG/CR-6075 (Pilch et al., 1994). Appendix D in NUREG/CR-6075 (Pilch et al., 1994) concludes that DCH loads are insensitive to reasonable choices of initial containment pressure. The Zion containment is initially at atmospheric pressure, so approximately 0.1 MPa (400 K/314 K) ≈ 0.13 MPa of the pressure at vessel breach is air. Consequently, the initial steam concentration is ~48 percent.

The containment conditions discussed above assume that active containment cooling systems (i.e., fan coolers or sprays) are not operational. We note that fan coolers were operational at TMI-II and that containment conditions were P ~ 0.11 MPa, T ~ 326 K, X_{STM} ~0.035, and X_{H2} ~0.079. Thus, there was little steam in the containment. This situation will also be analyzed in Section 6.

The core-wide oxidation of Zr also controls the amount of preexisting hydrogen that can exist in the containment building at the time of vessel breach. The RCS retains very little of this hydrogen because it is produced early in the accident and most is vented to the containment. This is supported by earlier SCDAP/RELAP5 calculations (Knudson, 1993) where more than

90 percent of the H_2 was released to the containment. The most recent SCDAP/RELAP5 calculations performed for this report (Appendix C) indicate that essentially all the in-vesssel produced hydrogen will be released to the containment. Steam/H_2 sources from SCDAP/RELAP5 are sometimes very hot (Appendix D) and there is a possibility that hydrogen will burn as it enters the containment. However, recent CONTAIN assessments using SCDAP/RELAP5 sources suggest that this effect is minimal except in the event of a hot leg failure, which precludes a DCH event. Consequently, we assume that all hydrogen produced in-vessel will be released to containment, where it will not burn prior to vessel breach. The moles of preexisting hydrogen in the containment are given by:

$$N_{H2}\ (g \cdot mole) = \frac{2}{0.091} f_{Zr} M_{Zr}^{0}\ (core) \tag{3.4}$$

or alternatively, a concentration can be specified

$$X_{H2} = \frac{N_{H2}}{N_{ATM}^{0}} \ . \tag{3.5}$$

We note that at TMI-II there was ~7.9 percent H_2 in the atmosphere and essentially no steam. Since these conditions are in the flammable regime, we cannot guarantee that an ignition source (unless intentional) will burn off hydrogen prior to the DCH event if the flammability limits are exceeded.

3.7 Scenario VI - SBLOCA Under Wet Core Conditions

Table 3.3 also summarizes the initial conditions for Scenario VI. In the absence of any RCS leaks, SCDAP/RELAP5 (Appendix C) predicts hot leg failure long before bottom head failure. These cases fully depressurize and are of no interest to DCH. We then seek SBLOCAs of just the right size to depressurize sufficiently that natural circulation degrades to the point that surge line or hot leg failure is not assured. Such an intermediate state was not found. In fact, SCDAP/RELAP5 predicts hot leg failure before core relocation for the full spectrum of SBLOCAs; consequently, Scenario VI can only exist as the consequence of partial operator intervention. For the expected SBLOCAs, SCDAP/RELAP5 predicts depressurization to the ~4 MPa range. However, repressurization spikes due to accumulator injection or melt relocation could sometimes repressurize the RCS to ~8 MPa, which is consistent with NUREG/CR-6075 (Pilch et al., 1994) assessments. Thus, the ~8 MPa RCS pressure used in NUREG/CR-6075

is adequately bounding, particularly in light of SCDAP/RELAP5 predictions that the hot leg will fail before core relocation. Owing to the similarity in Scenarios V and VI, we emphasize only the differences in RCS temperature, melt mass, and composition, with all other parameters developed in a manner similar to Scenario V.

The RCS gas at the time of vessel breach clearly must be superheated. In conjunction with the pressure and volume, the moles of gas in the RCS can be computed with the RCS temperature, which can be estimated with the aid of Table 3.4 where the entire RCS is broken down into representative regions, with the approximate fraction of RCS free volume noted for each region. The gas temperatures in each region of the RCS are estimated from SCDAP/RELAP5 output (Appendix C). Given this assessment, a lower bound of ~ 1000 K is assigned to this scenario.

The potential release of molten material to the lower head is again controlled by the formation and failure of a crucible in the core region. Water occupies only the lowest regions of the core, so radial cooling of a growing crucible is reduced in this situation, and consistent with SCDAP/RELAP5 predictions, the crucible could take on the bounding shape of an upright cylinder as depicted in Figure 3.8. Again, the outer assemblies are largely excluded, although SCDAP/RELAP5 does predict some localized degradation of the outer assemblies.

In the extreme of this geometry, ~ 80 percent of the core can be contained in the crucible. The upper bound to the UO_2 distribution is then 0.8 x 100 mt ~ 80 mt if the crucible fails on the bottom. Again, the calculations of Schmidt and Humphries (1994) favor side failure before the crucible obtains these extreme proportions. As a best estimate we assume ~ 40 mt of UO_2 can be released. With this in mind, the distribution of UO_2 released from the crucible can be constructed as indicated in Figure 3.9. Again allowing (~ 10 mt) only for melt freezing in order to heat the lower head to rupture, the distribution of molten UO_2 at the time of vessel failure is given by Figure 3.10.

The fraction of Zr oxidized remains unchanged. This, in conjunction with the causal relations (Equations 3.1 - 3.4) developed in Section 3.6, defines the remaining melt constituents and atmosphere compositions.

CONTAIN calculations (Appendix D), using sources from SCDAP/RELAP5 (Appendix C), show containment pressures in excess of ~0.25 MPa during the period of accumulator discharge. Consistent with the coupled SCDAP/RELAP5 and CONTAIN calculations, we take P^0_{RCS} ~0.25 MPa and T^0_{RCS} ~400 K. The steam concentration in the containment is assumed to be ~50 percent.

3.8 Summary Melt Masses and Compositions

Because many of the melt constituents are correlated, it is useful to tabulate the lower bound, best estimate, and upper bound masses for a more direct comparison and to compare them with working group recommendations. This is done in Table 3.5. The lower and upper bounds are taken at the ~1 percent probability level. In addition, there is a natural curiosity to compare these quantifications with prior work. This is done in Table 3.6.

Consider first the comparison of Scenarios V and VI by composition. The ZrO_2 values are a function of both the UO_2 mass and the fraction of Zr oxidized. For this comparison, the three UO_2 masses are used in conjunction with the best estimate for the fraction of Zr oxidized. This ensures that lower and upper bounds to the ZrO_2 values are also at the ~1 percent probability level. This prescription is not unique. For instance, it is possible to use the best estimate for the UO_2 mass in conjunction with the lower, best estimate, and upper bound values for the fraction of Zr oxidized. This procedure, however, gives somewhat less ZrO_2 mass for the best estimate and upper bound value.

The current quantification meets or exceeds working group recommendations for both oxidic and metallic constituents in the melt. For consistency reasons, the amount of Zr in Scenario V is less than working group recommendations; however, this is compensated for with increased steel in the melt, again for consistency reasons.

At the outset, we should state that no potential comparisons are fully consistent with the plant and scenarios discussed in this report, so some compromise is necessary to make suitable comparisons. Prior summary efforts (i.e., NUREG-1150 and SASM) are therefore the most useful for comparison (see Table 3.6) since these activities employed panels of knowledgeable experts who were able to synthesize the experimental and analytical information available at the

time. Since the time of these summary efforts, new information has become available and these new data are reflected in our current quantifications.

Peer review comments on NUREG/CR-6075 (Appendix A) sometimes characterized the melt mass distributions as "optimistic." A comparison with Scenario II in NUREG/CR-6075 shows that both the best estimate and upper bound of the distribution of total mass for Scenarios V and VI are ~10 mt and ~30 mt higher, respectively. Thus, the current quantifications for oxide mass are broader than similar scenarios in NUREG/CR-6075. However, DCH loads are insensitive to oxide masses (see Appendix A, Responses H19 and H32, and Comments by Reviewer O). The broader distributions used here are due principally to the assumption that the crucible can drain entirely, whereas NUREG/CR-6075 argued that bottom failure of the crucible was not possible so that only 75 percent of the molten material could drain into the lower plenum.

NUREG-1150 was the first summary assessment of core melt progression parameters, which addressed only the core fraction that is molten and the fraction of cladding oxidized. NUREG-1150 assessments were largely based on MARCH, early MAAP, and preliminary MELPROG calculations. The distribution for molten core fraction in Scenario VI is in good agreement with the expert elicitation results in NUREG-1150.

SASM (Zuber et al., 1991) is the most recent of the summary assessments, and it was focused specifically on the DCH issue. The SASM recommendations for molten oxides are enveloped by the current quantifications; however, the metals are outside the current assessments. This is important because DCH loads are generally more sensitive to metal content than oxide content because of the increased potential to produce hydrogen, which can subsequently burn. Assessment of steel mass in the SASM effort was largely based on a MELPROG calculation (Kelly et al., 1987) of a station blackout accident in which significant upper plenum melting was predicted. Melting of upper plenum steel is strongly correlated with surge line or hot leg failure, which in fact was predicted in the MELPROG calculation. Specifically, gases hot enough to melt upper plenum steel are also hot enough to rupture the surge line or hot leg. This is also consistent with the current SCDAP/RELAP5 assessments. The large quantities of Zr and CRM in the SASM assessment are traceable to a MELPROG modeling assumption that crucible failure occurs as a massive event carrying most of the metallic

blockage into the lower plenum. Thus, the SASM assessment of metals in the melt is not consistent with our current understanding of core melt progression under wet core conditions.

Table 3.6 also summarizes the melt mass predicted by SCDAP/RELAP5 at the time of vessel failure. Current quantifications (Scenarios V and VI) for oxide mass are in general agreement with the system code predictions, which are interpreted as upper bounds because SCDAP/RELAP5 assumes complete drainage of the in-core molten pool. Note that the three SCDAP/RELAP5 entries in Table 3.6 represent upper bound numbers for the three cases analyzed in Appendix C. SCDAP/RELAP5 predicts essentially no Zr in the melt while our quantifications chose to bound the amount with ~2 mt. The amount of lower plenum steel predicted by SCDAP/RELAP5 is also in agreement with the current assessment. With the exception of the oxide mass, the SCDAP/RELAP5 predictions are also in reasonable agreement with NUREG/CR-6075 assessments, with SCDAP/RELAP5 predicting ~15 mt more oxide due to assumptions about complete drainage of the molten pool.

3.9 References

Blanchat, T.K., M.D. Allen, M.M. Pilch, and R.T. Nichols (April 1994). *Experiments to Investigate Direct Containment Heating Phenomena With Scaled Models of the Surry Nuclear Power Plant*, NUREG/CR-6152, SAND93-2519, Sandia National Laboratories, Albuquerque, NM.

Denny, V.E. and B.R. Sehgal (1983). "Analytical Prediction of Core Heatup/Liquefaction/Slumping," *Proceedings International Meeting on Light Water Reactor Severe Accident Evaluation*, Aug. 28-Sept. 1, Cambridge, MA.

Epstein, M. and H.K. Fauske (1989). "The Three Mile Island Unit 2 Core Relocation -- Heat Transfer Mechanisms," *Nuclear Technology*, Vol. 87, 1021.

Gasser, R.D., R.O. Gauntt, S.C. Bourcier, R.L. Schmidt, L.L. Humphries, and K.O. Reil (1994 draft). *Late Phase Melt Progression Experiment--MP-2, Results and Analysis*, NUREG/CR-6167, SAND93-3931, Sandia National Laboratories, Albuquerque, NM.

Hammersley, R.J., M. Merilo, and R.E. Henry (Jan. 26-29, 1993). "Experiments to Address Lower Plenum Response Under Severe Accident Conditions," Proceedings of the International Topical Meeting on Probabilistic Safety Assessment (PSA93), Clearwater Beach, FL.

Hanson, D.J. et al. (October 1990). *Depressurization as an Accident Management Strategy to Minimize the Consequence of DCH*, NUREG/CR-5447, U.S. Nuclear Regulatory Commission, Washington, DC.

Kelly, J.E., R.J. Henninger, and J.F. Dearing (January 1987). *MELPROG-PWT/MODI Analysis of a TMLB' Accident Sequence*, NUREG/CR-4742, SAND86-2175, Sandia National Laboratories, Albuquerque, NM.

Knudson, D.L. (April 1993). Transmittal of SCDAP/RELAP5/MOD3 Results for the Zion Power Station, Letter Report to NRC.

Knudson, D.L. and C.A. Dobbe (November 1993). *Assessment of the Potential for High Pressure Melt Ejection Resulting from a Surry Station Blackout Transient*, NUREG/CR-5949, EGG-2689, EG&G Idaho, Inc., Idaho Falls, ID.

Marshall, B.W. (1988). *Reactor Safety Research Semi-annual Report July-December 1987*, NUREG/CR-5039, SAND87-2411, Vol. 2, pp. 244, Sandia National Laboratories, Albuquerque, NM.

Pilch, M.M., H. Yan, and T.G. Theofanous (1994). *The Probability of Containment Failure by Direct Containment Heating in Zion*, NUREG/CR-6075, SAND93-1535, Sandia National Laboratories, Albuquerque, NM.

Pilch, M. and W.W. Tarbell (September 1985). *High Pressure Ejection of Melt from a Reactor Pressure Vessel: The Discharge Phase*, NUREG/CR-4383, SAND85-0012, Sandia National Laboratories, Albuquerque, NM.

Pilch, M. and W.W. Tarbell (July 1986). *Preliminary Calculations on Direct Heating of a Containment Atmosphere by Airborne Core Debris*, NUREG/CR-4455, SAND85-2439, Sandia National Laboratories, Albuquerque, NM.

Rempe, J.L., S.A. Chavez, G.L. Thinnes, C.M. Allison, G.E. Korth, R.J. Witt, J.J. Sienicki, S.K. Wang, L.A. Stickler, C.H. Heath, and S.D. Snow (Oct. 1993). *Light Water Reactor Lower Head Failure Analysis*, NUREG/CR-5642, EGG-2618, Idaho National Engineering Laboratory, Idaho Falls, ID.

Schmidt, R.L. and L.L. Humphries (1994). *Late Phase Melt Progression Scoping and Sensitivity Studies*, Draft, SAND92-2831, Sandia National Laboratories, Albuquerque, NM.

Spencer, B.W., K. Wang, C.A. Blomquist, L.M. McUmber, and J.P. Schneider (Feb. 1994). *Fragmentation and Quench Behavior of Corium Melt Streams in Water*, NUREG/CR-6133, ANL-93/32, Argonne National Laboratory, Argonne, IL.

Stickler, L.A., J.L. Rempe, S.A. Chavez, G.L. Thinnes, S.D. Snow, R.J. Witt, M.L. Corradini, and J.A. Koss (Oct. 1993). *Calculations to Estimate the Margin to Failure in the TMI-2 Vessel*, TMI V(93)EG01, Idaho National Engineering Laboratory; EG&G Idaho, Inc., Idaho Falls, ID.

Theofanous, T.G. (1988). "Some Considerations of Severe Accidents at Loviisa," Report Prepared for Imatron Voima 04, Helsinki, Finland.

Tutu, N.K., T. Ginsberg, and L. Fintrok (1988). "Low Pressure Cutoff for Melt Dispersal from Reactor Cavities," *Fourth Proceedings of Nuclear Thermal Hydraulics*, 29-37.

Tutu, N.K., C.K. Park, C.A. Grimshaw, and T. Ginsberg (January 1990). *Estimation of Containment Pressure Loading Due to Direct Containment Heating for the Zion Plant*, NUREG/CR-5282, BNL-NUREG-52181, Brookhaven National Laboratory, Upton, NY.

Zuber, N., B. Boyack, A. Dukler, P. Griffith, J. Healzer, R. Henry, M. Ishii, J. Lehner, S. Levy, F. Moody, M. Pilch, B. Sehgal, B. Spencer, T. Theofanous, J. Valente, G. Wilson, and W. Wulff (1991). *An Integrated Structure and Scaling Methodology for Severe Accident Technical Issue Resolution*, NUREG/CR-5809, EFF-2659, EG&G Idaho, Inc., Idaho Falls, ID.

3.10 Nomenclature

f_{Zr}	=	fraction of Zr oxidized core-wide
M_{CRM}	=	mass of control rod material in melt at vessel failure
M^0_{Zr}	=	mass of Zr initially in core
M_s	=	mass of steel in melt at vessel failure
$M_{s,LP}$	=	mass of steel in lower plenum
M_{UO2}	=	mass of UO_2 in melt at vessel failure
M_{Zr}	=	mass of Zr in melt at vessel failure
M_{ZrO2}	=	mass of ZrO_2 in melt at vessel failure
N^0_{ATM}	=	atmosphere moles in containment just prior to vessel failure
N_{H2}	=	mole of hydrogen produced from Zr oxidation
P^0_{RCS}	=	initial RCS pressure
T^0_{RCS}	=	initial RCS temperature
V_{LP}	=	volume of lower plenum
X_{H2}	=	hydrogen concentration in the containment atmosphere

Greek

ρ_{CRM} = mass density of control rod material

ρ_{UO2} = mass density of UO_2

$\rho_{UO2/ZrO2}$ = mass density of UO_2/ZrO_2 eutectic

ρ_{Zr} = mass density of Zr

ρ_{ZrO2} = mass density of ZrO_2

Table 3.1 Characterization of the Zion plant

Parameter	Value
Thermal power (MW)	3238
Core height (m)	3.66
Core diameter (m)	3.39
Number of fuel assemblies	193
Number of fuel assemblies at edge of core	64
Fuel assembly dimensions (m)	0.214
Number of in-core instruments	58
RCS volume (m^3)	353
Lower head ID (m)	4.2
Lower head thickness (m)	0.14
Core inventory (mt)	
UO_2	98.2
Zr	20.0
Steel	3.2
CRM	3.6
Thin upper plenum steel	20
Thin lower plenum steel	10
Lower plenum volume (m^3)	30
Containment volume (m^3)	76.9×10^3
Subcompartment volume (m^3)	4.83×10^3
Cavity volume (m^3)	190
Containment pressure (MPa)	0.1
Containment temperature (K)	316

Table 3.2 Definition of probability levels

Process Likelihood	Process Characteristics
~ 1	Behavior is within known trends - best estimate.
10^{-1}	Behavior is within known trends but obtainable only at the edge of spectrum parameter.
10^{-2}	Behavior cannot be positively excluded - upper bound.

Table 3.3 Summary of initial condition quantification

Parameter	SCENARIO	
	V	VI
RCS pressure (MPa)	16	8
RCS temperature (K)	700	1000
RPV water (mt)	75	10
RPV temperature (K)	1000	1000
Initial hole dia. (m)	0.4	0.4
Final hole dia. (m)	Eq. 4.3	Eq. 4.3
Fraction Zr oxidized	Fig. 3.4	Fig. 3.4
UO_2 mass (mt)	Fig. 3.7	Fig. 3.10
Zr mass (mt)	Eq. 3.2	Eq. 3.2
ZrO_2 mass (mt)	Eq. 3.1	Eq. 3.1
Steel mass (mt)	Eq. 3.3	Eq. 3.3
CRM mass (mt)	0.0	0.0
Melt temp. (K)	2800	2800
Fraction of Zr blockage relocated	0.0	0.0
Containment pressure (MPa)	0.25	0.25
Containment temperature (K)	400	400
Preexisting H_2	Eq. 3.4	Eq. 3.4
Autoignition temperature (K)	950	950
Melt fraction ejected into cavity	1.0	1.0
Ejected fraction dispersed from cavity	0.85	0.85
Fraction dispersed through gap	0.09	0.09
Fraction dispersed through seal table room and SG vents	0.05	0.05
Coherence ratio	Eq. 4.2	Eq. 4.2

Table 3.4 RCS gas temperature for Scenario VI

RCS Region	Volume Fraction	Temperature (K)
Core	0.10	2800
Upper plenum	0.20	1700
Hot leg	0.28	1700
Cold leg	0.28	650
Lower plenum and downcomer	0.14	650
RCS Avg. Temp. (K) = $\left[\sum \frac{f_{v,i}}{T_i}\right]^{-1}$		1037

Table 3.5 Comparison with working group recommendations

Parameter	Scenario V	Scenario V WG Recommendations	Scenario VI	Scenario VI WG Recommendations
UO_2 mass (mt)	0/20/50	-/20/40	0/30/70	-/30/50
ZrO_2 mass (mt)	0/2.2/5.5		0/3.3/7.7	
Zr mass (mt)	0/0.6/1.5	1/1/2	0/0.9/2.0	1/1/2
Steel mass (mt)	0.3/1.1/2.3	0	0.3/1.8/4.4	some
CRM mass (mt)	0		0	
Total melt mass (mt)	0.3/23.9/59.3		0.3/36.0/84.1	
Core fraction molten	0.002/0.19/0.47		0.002/0.29/0.67	
Fraction Zr oxidized	0.15/0.40/0.65	0.15/0.40/0.65	0.15/0.40/0.65	0.15/0.40/0.65

Table 3.6 Comparison with prior work

Parameter	Scenario V	Scenario VI	Scenario II NUREG/CR-6075	NUREG-1150	SASM NUREG/CR-5809	SCDAP/RELAP5 Case 1-2-3
UO_2 mass (mt)	0/20/50	0/30/70	0/15/40		32	43.3-52.8-44.4
ZrO_2 mass (mt)	0/2.2/5.5	0/3.3/7.7	0/1.6/4.3		5.9	11.2-13.4-12.3
Zr mass (mt)	0/0.6/1.5	0/0.9/2.0	0.7/1.2/1.7		8.5	0-0.5-0
Steel mass (mt)	0.3/1.1/2.3	0.3/1.8/4.4	1.4/2.7/3.8		11.9	4.8-8.2-5.0
CRM mass (mt)	0	0	4		2.3	0-3.3-2.2
Total melt mass (mt)	0.3/23.9/59.3	0.3/36.0/84.1	6.1/24.5/53.8		60.8	59.3-78.2-63.9
Core fraction molten	0.002/0.19/0.47	0.002/0.29/0.67	0.08/0.20/0.43	0/0.28/0.60	0.49	0.47-0.63-0.51
Fraction Zr oxidized	0.15/0.40/0.65	0.15/0.40/0.65	0.15/0.40/0.65	0.08/0.32/0.76	0.40	0.53-0.59-0.48

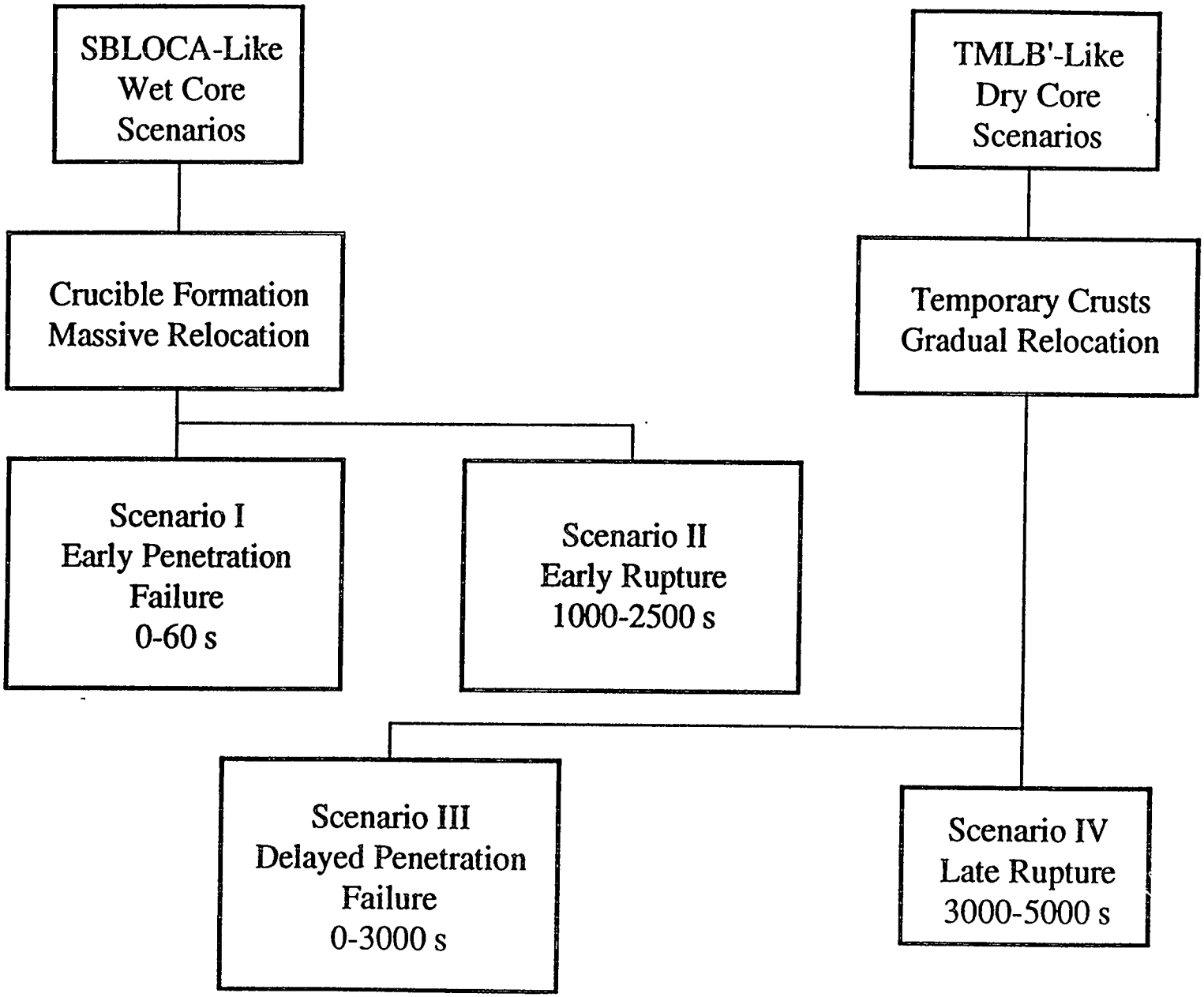

Figure 3.1. Splinter DCH scenarios used in NUREG/CR-6075.

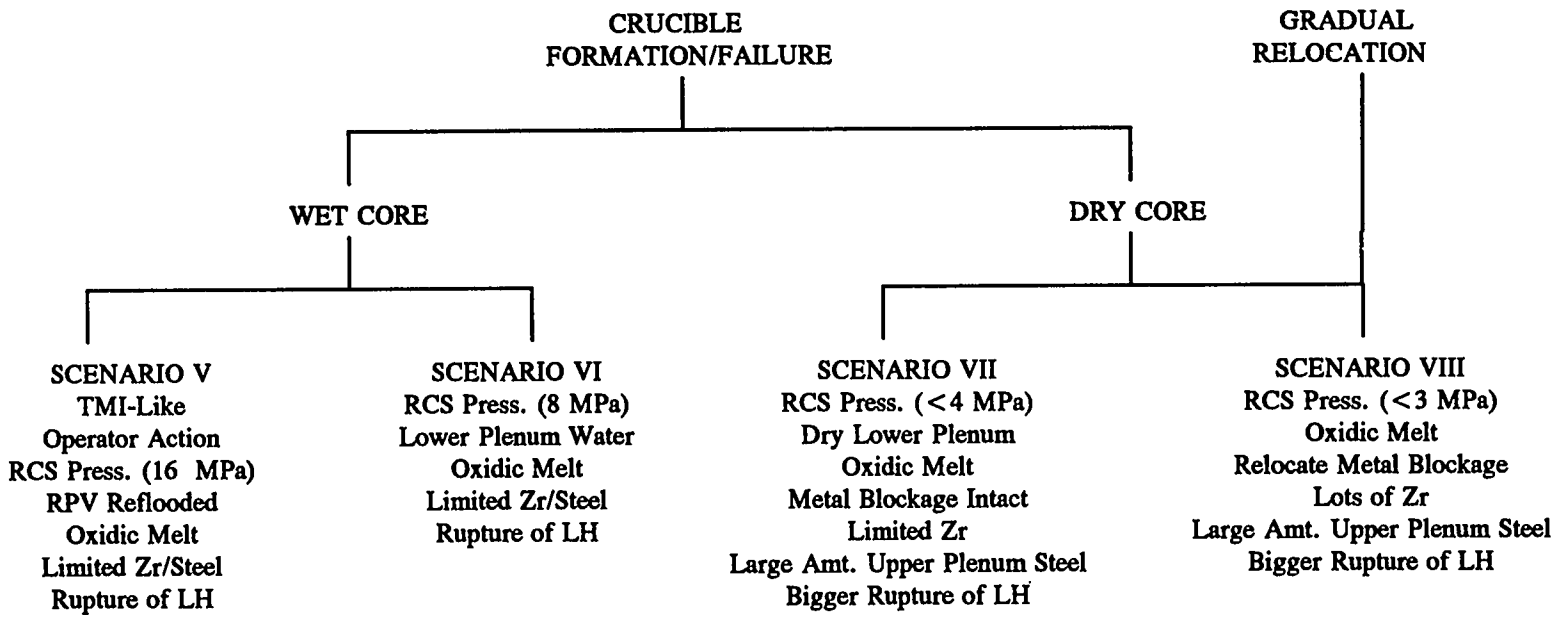

Figure 3.2. Splinter DCH scenarios reflecting working group recommendations.

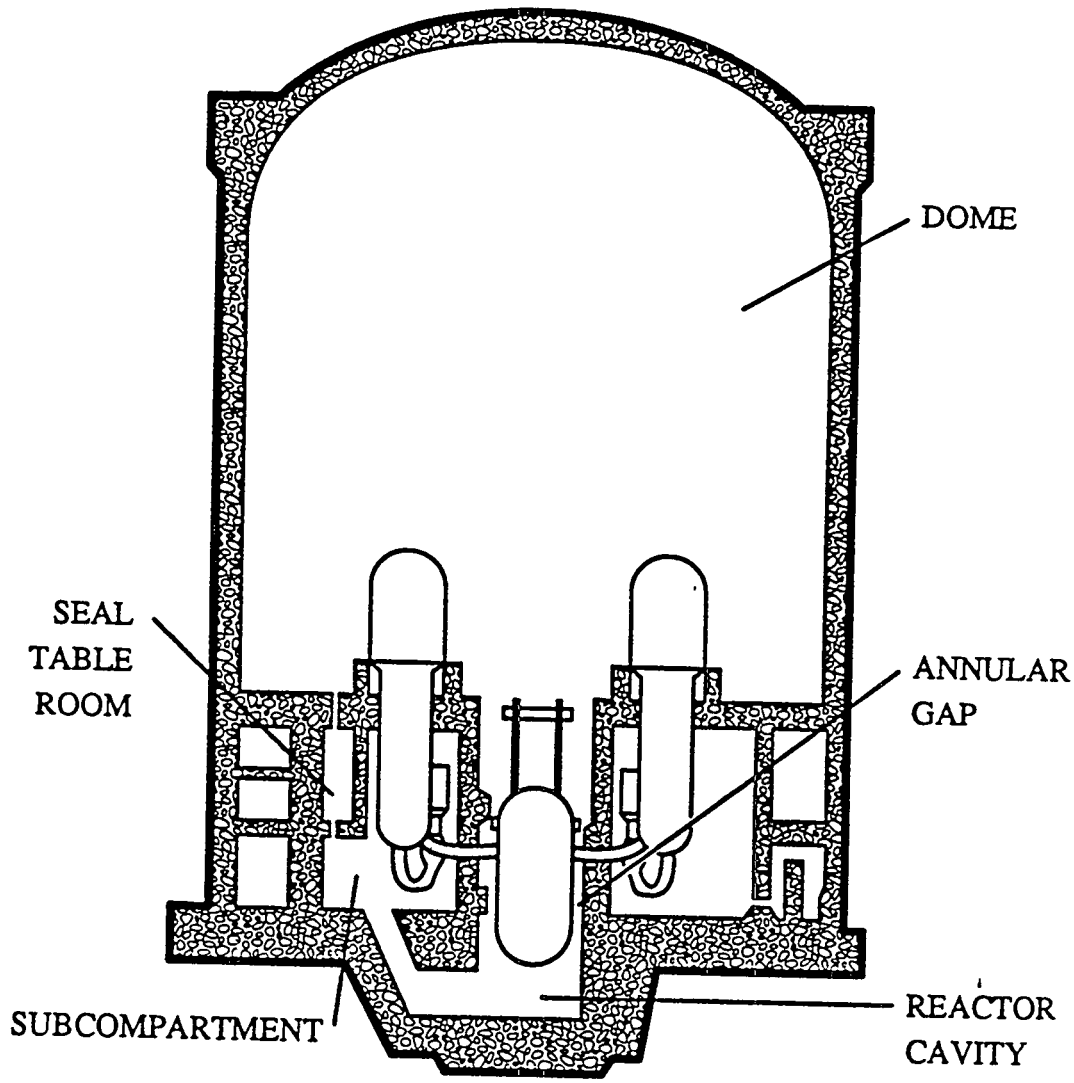

Figure 3.3. Zion nuclear power plant.

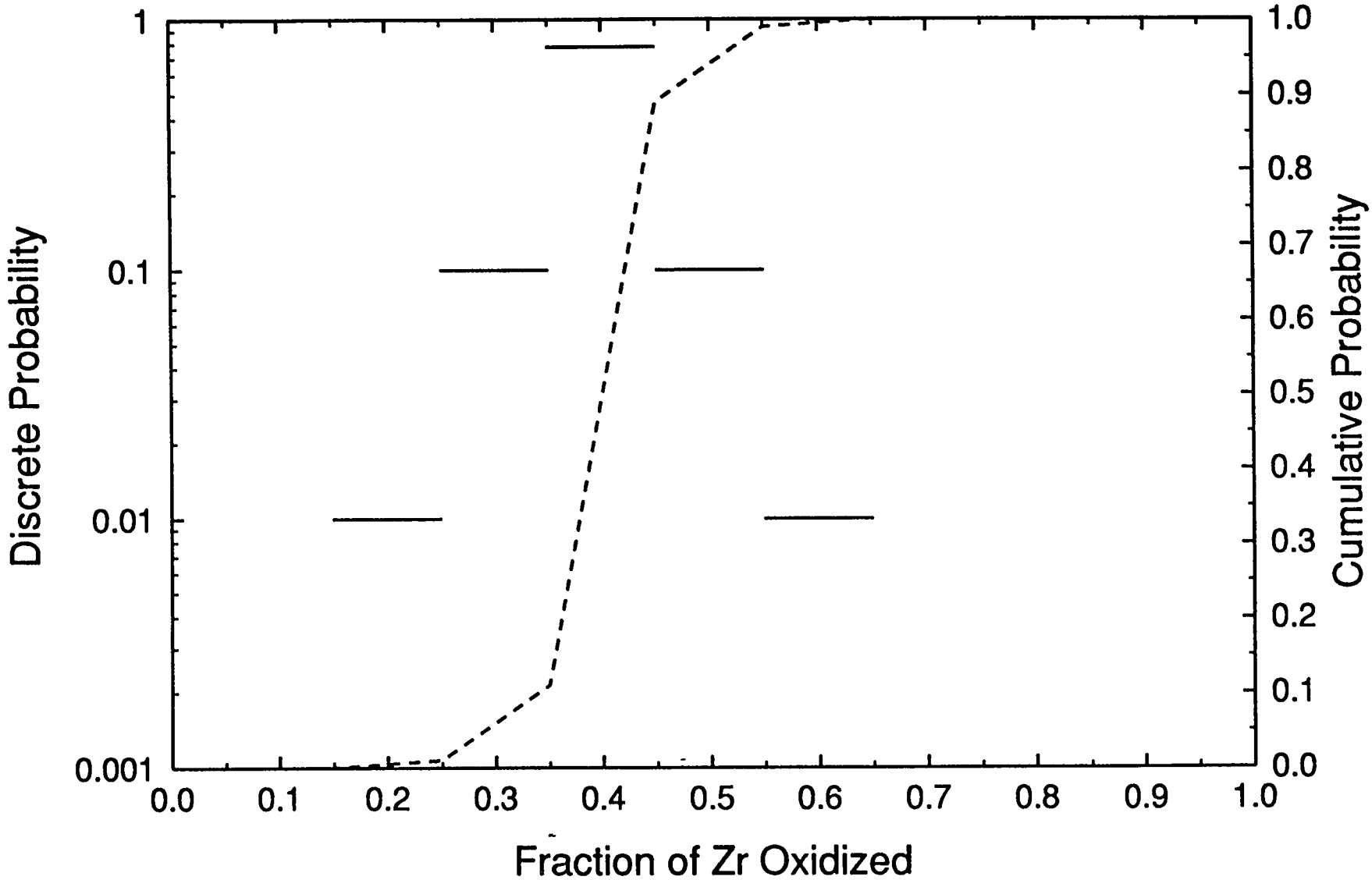

Figure 3.4. Distribution for fraction of Zr oxidized (core-wide) in Scenarios V and VI.

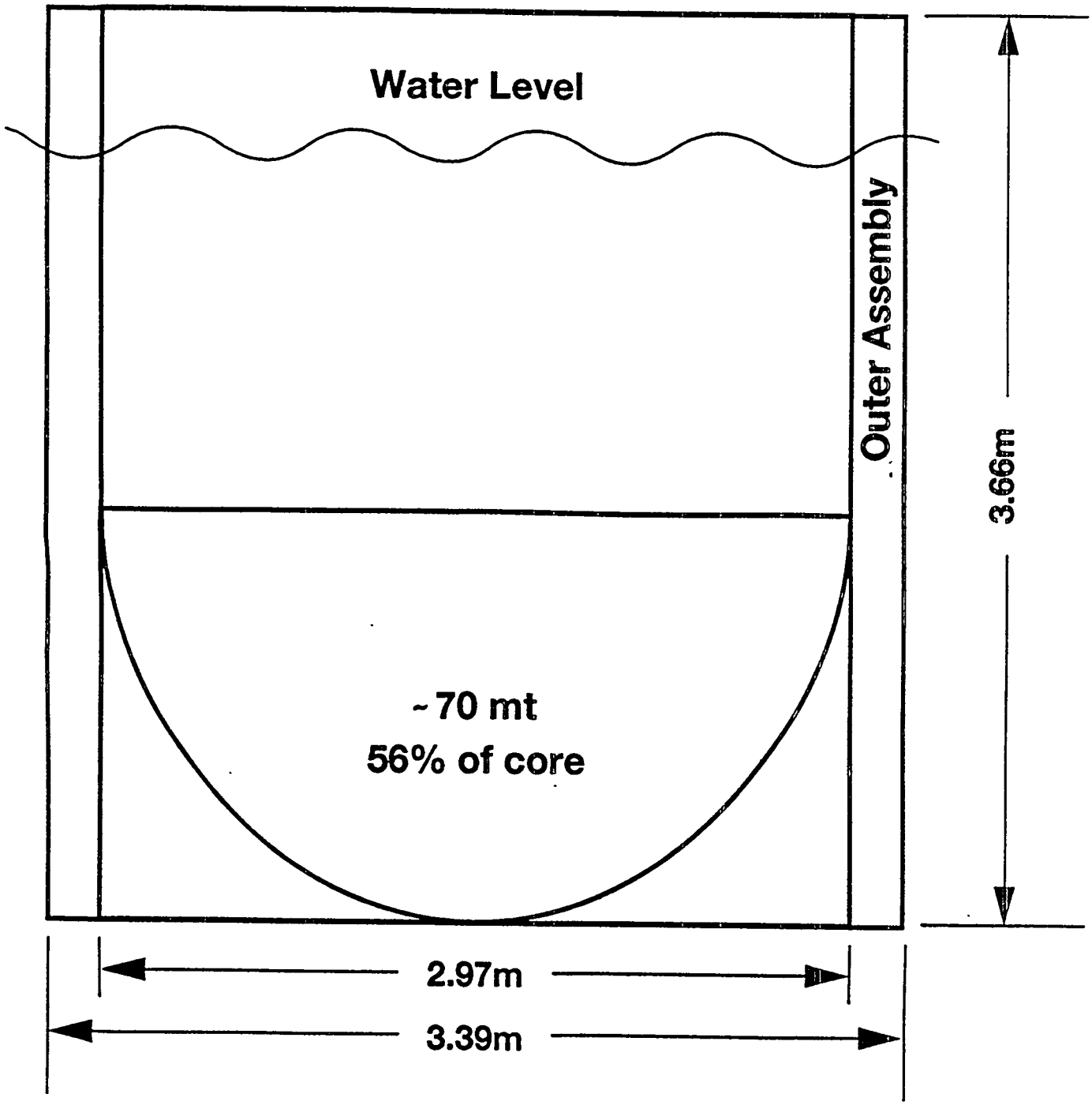

Figure 3.5. Crucible formation in a flooded RPV - Scenario V.

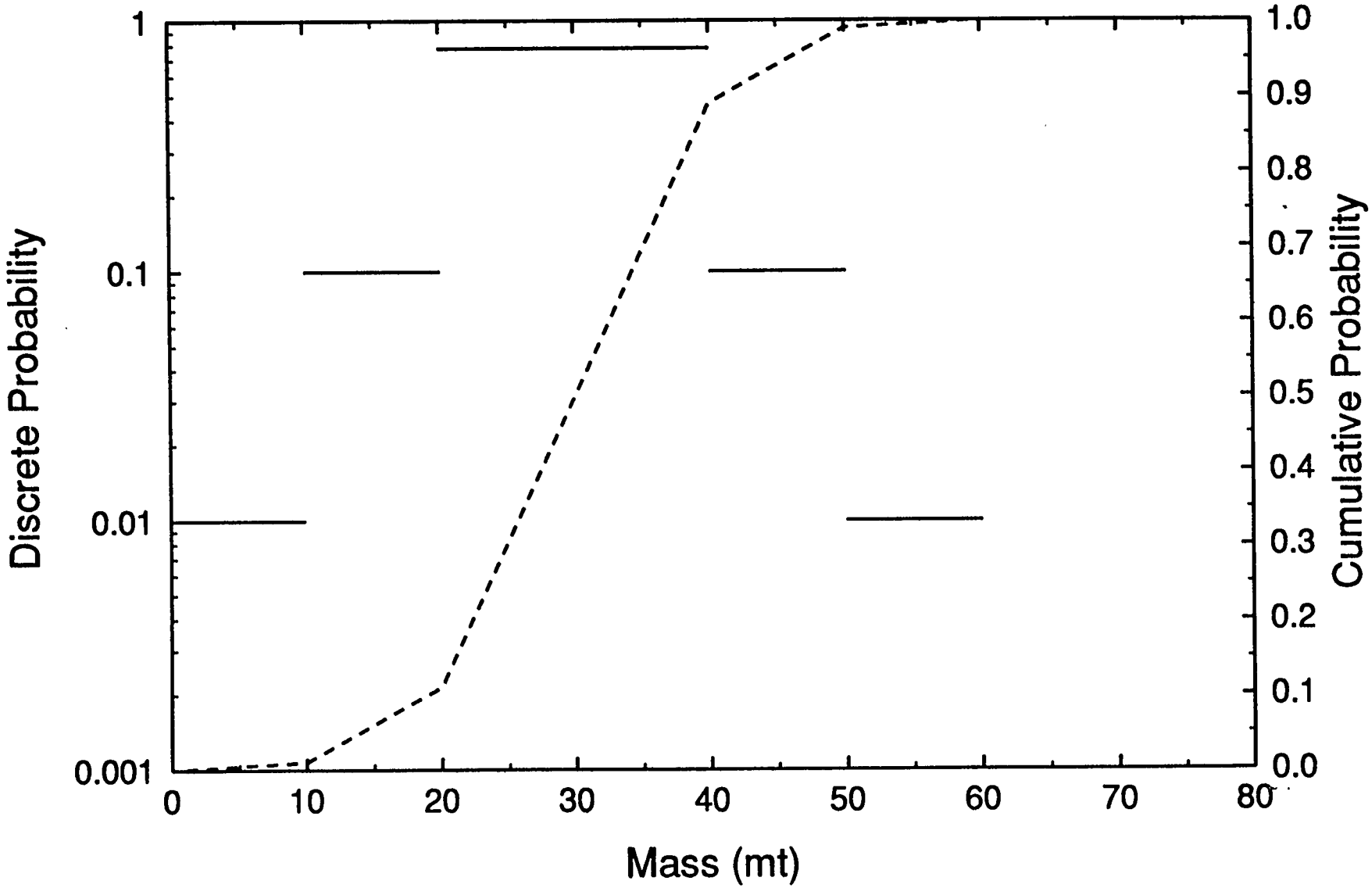

Figure 3.6. Distribution for UO_2 release from the crucible in Scenario V.

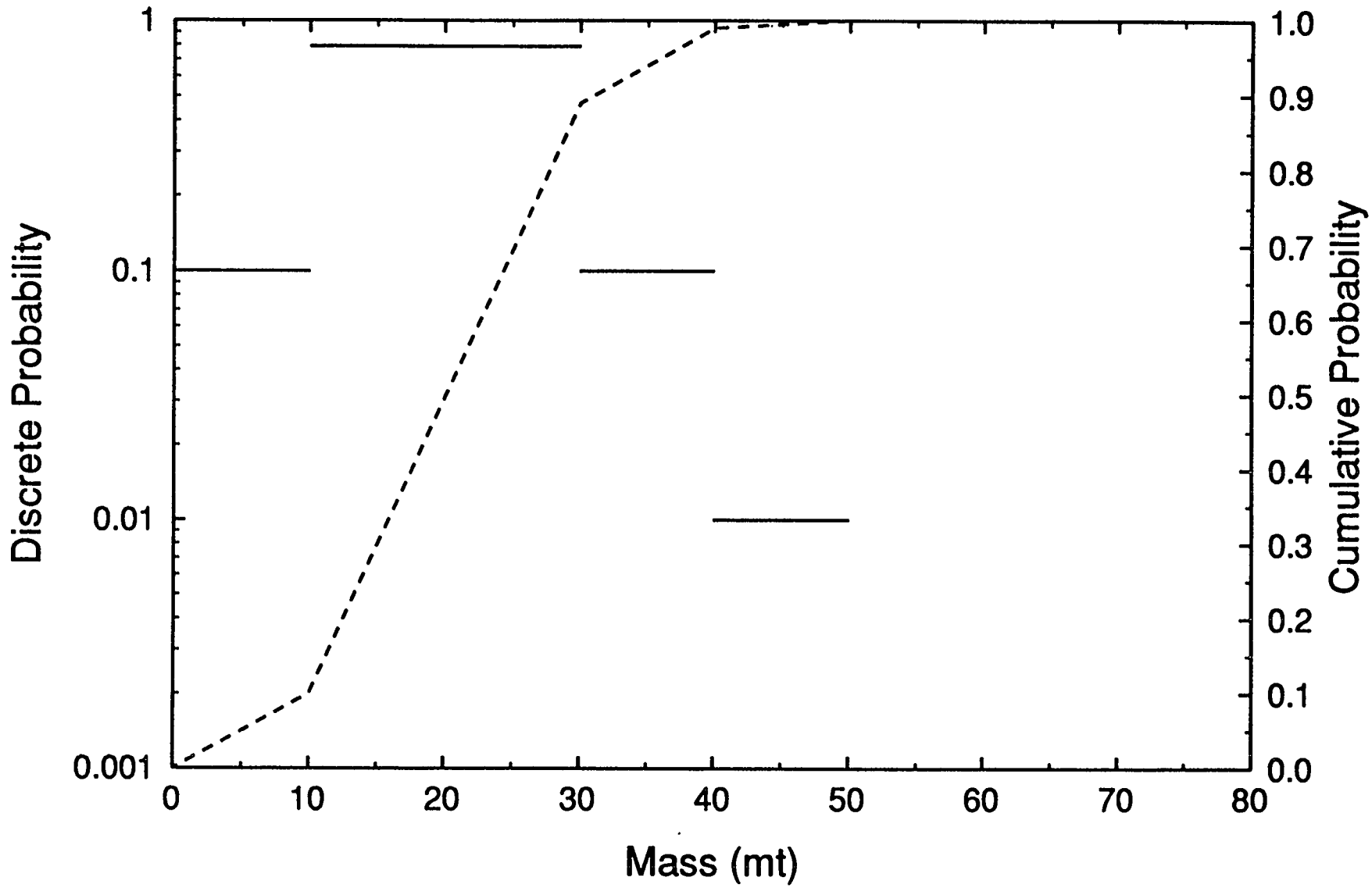

Figure 3.7. Distribution for molten UO_2 in the lower plenum at the time of vessel rupture for Scenario V.

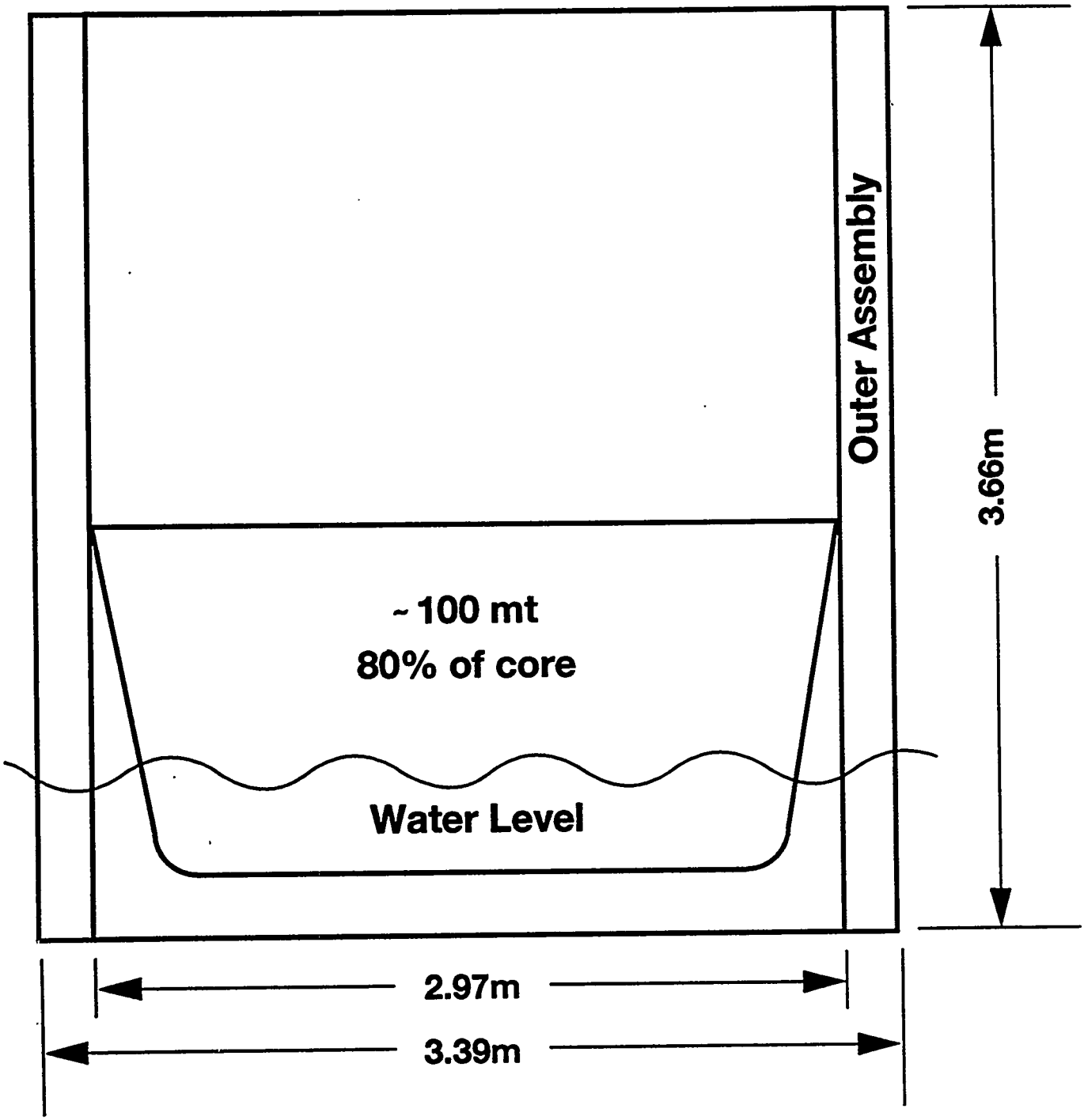

Figure 3.8. Crucible formation in wet core scenario with partial operator intervention - Scenario VI.

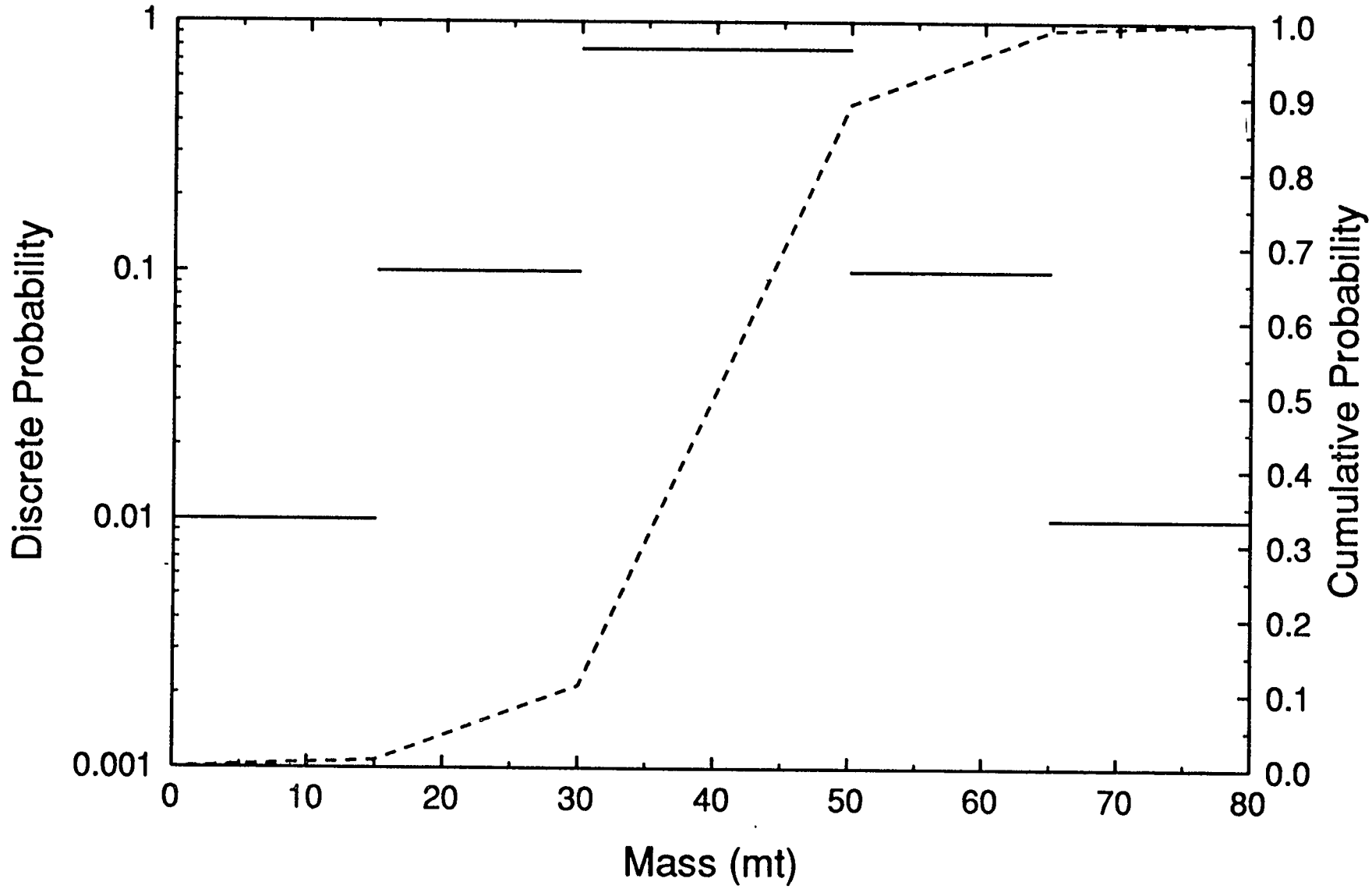

Figure 3.9. Distribution for UO_2 release from the crucible in Scenario VI.

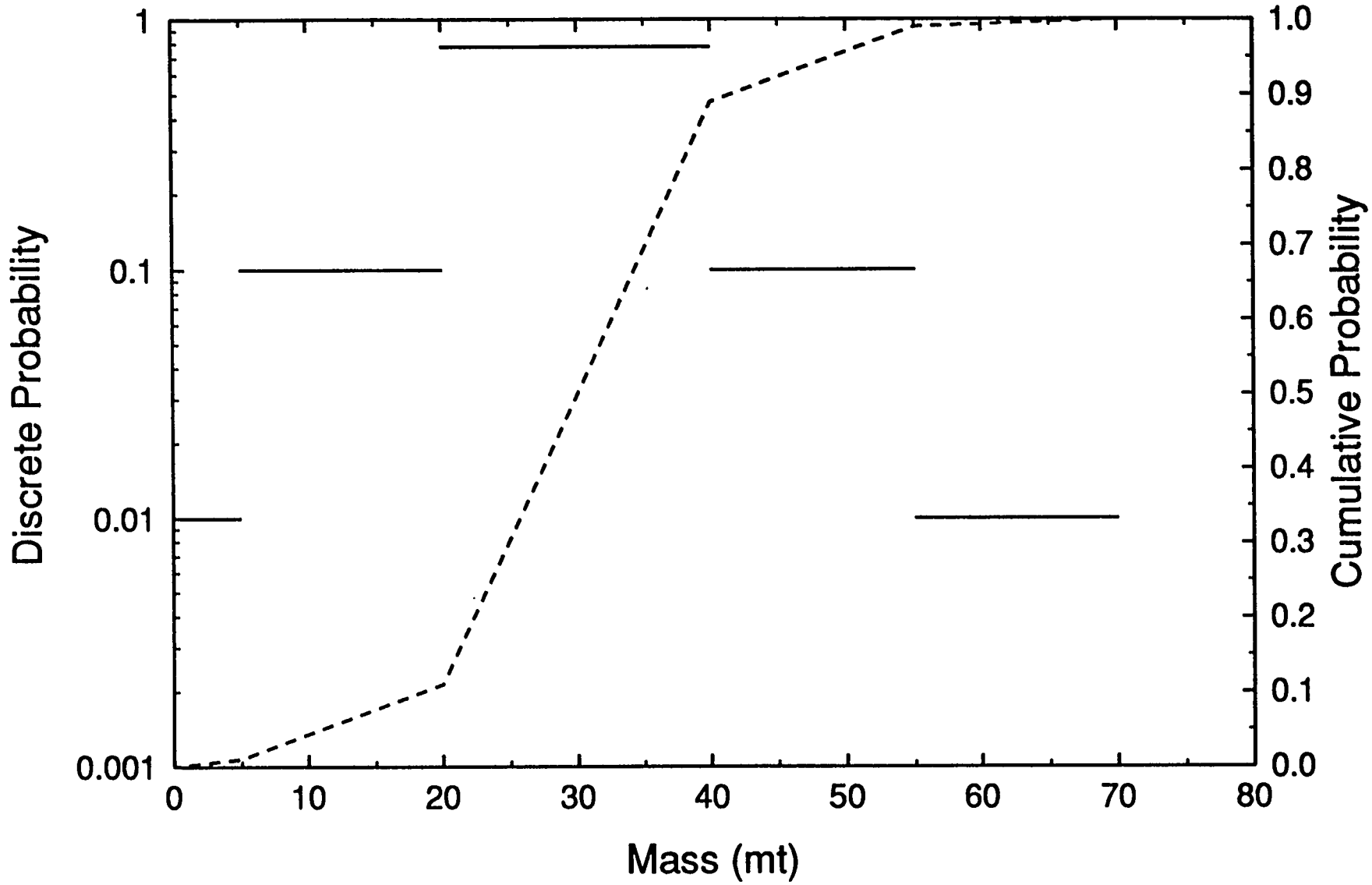

Figure 3.10. Distribution for molten UO_2 in the lower plenum at the time of vessel rupture for Scenario VI.

4.0 QUANTIFICATION OF THE DCH PHENOMENON

The quantification of the DCH phenomenon is carried out by means of a causal relation (CR1) for the containment load. CR1 is fulfilled here by the two-cell equilibrium model, which is developed in Appendix E of NUREG/CR-6075 (Pilch et al., 1994). In the TCE model, the containment pressurization can be written in terms of the various energy sources (blowdown, latent and sensible heat of debris, oxidation of metallic debris constituents, and hydrogen combustion) that can contribute to DCH,

$$\frac{\Delta P}{P^0_{RCB}} = \eta \frac{\sum \Delta E_i}{U^0(1 + \psi)} , \tag{4.1}$$

where η is an efficiency that accounts for mitigation of DCH due to the compartmentalized geometry of the containment and accounts for mitigation due to the noncoherence of debris dispersal and blowdown processes. The TCE model has been validated against the extensive database that is summarized in Table 4.1. Figure 4.1 compares model predictions with the relevant database.

Working group discussions (Appendix A) defined two new scenarios (V and VI) which involve significant quantities ($\sim$10 - 75 mt) of nearly saturated water that would be coejected with the melt into the reactor cavity. This is a situation that has not been addressed by the existing database; however, the working group (Appendix A) expressed an opinion that water in the primary system at vessel breach is expected to mitigate the impact of DCH. We note that a related experiment involving large quantities of cavity water (IET-8B; Allen et al., 1994) suggest that DCH energies went entirely into vaporizing water, pressurizing the containment to levels comparable to containment pressures observed in (essentially) dry DCH tests. RPV water (unlike cavity water) will partially flash to steam during isentropic blowdown. The contribution to containment pressure from this mechanism is less than $\sim$0.075 MPa. The calculations and results presented here are performed by ignoring any impact of coejected water. The margins to failure are high enough for Zion so that the impact of coejected water can be ignored in these analyses; however, it may become necessary to address this phenomenon explicitly in the extrapolation effort.

We note that the Zion reactor cavity will be deeply flooded in certain scenarios. A deeply flooded cavity would submerge the RPV, which may prevent its failure (although this is an area of ongoing research). The SNL/IET-8B experiment indicated that melt ejection into a half full cavity would fully quench the melt reducing the DCH event to a non-threatening steam spike. We expect that more deeply flooded situations would exhibit similar quenching behavior.

Most input parameters in the TCE model are related to initial conditions and material properties. The key modeling parameter in the TCE model is the melt-to-steam coherence ratio. Because the entrainment time is short compared with the blowdown time, molten debris is exposed to a small fraction of the primary system steam during the dispersal process. Since this steam is the medium for carrying the melt energy and the hydrogen produced by steam/metal interactions to the main containment volume, this incoherence is a crucial mitigating factor. With this understanding, it is possible to reduce most of the complexity of cavity phenomena to the coherence ratio ($R_\tau = \tau_e/\tau_b$ in the TCE model). We now focus on the coherence ratio and its quantitative representation in the calculations (i.e., *pdf4*, see Figures 2.1 and 2.2).

Appendix E in NUREG/CR-6075 (Pilch et al., 1994) develops a correlation for the coherence ratio based on experiment values obtained by a procedure best suited to the TCE model. For this application, the Zion data are best correlated by

$$R_\tau = 9.661\ f_d \left[\frac{T^0_{RCS}}{T^0_d}\right]^{\frac{1}{4}} \left[C_d\ \frac{M^0_d}{M^0_g}\ \frac{A_h V_{cav}^{\frac{1}{3}}}{V_{RCS}}\right]^{\frac{1}{2}} . \tag{4.2}$$

It is assumed that R_τ values are distributed normally about the mean given by Equation 4.2 with a relative standard deviation of 29 percent as indicated by the database. A comparison of the correlation against the Zion database is shown in Figure 4.2. The correlation has also been successfully developed for the Surry database, the differences being that the lead constant should be replaced by 12.2 and the relative standard deviation is 18 percent.

The database for the coherence ratio largely overlaps the range of individual parameters that are of interest to reactor applications (Table 4.2). However, the database does not include all possible combinations of parameters for each of the potential applications; consequently, the correlation for the coherence ratio is required to fill gaps in the database. It is significant that this process is one of interpolation rather than extrapolation.

Rapid ejection of hot melt through a breach in the RPV leads to ablation, which increases the initial hole size. Appendix J in NUREG/CR-6075 develops a model for hole ablation. The final hole size can be computed from

$$\frac{\Delta D_h}{D_h^0} = \frac{\dfrac{\tau_M}{\tau_D}}{1 + 0.6934 \left[\dfrac{\tau_M}{\tau_D}\right]^{2/3}} \tag{4.3}$$

where

$$\tau_M = \frac{M_d^0}{\dot{M}_d} = \frac{M_d^0}{\rho_d C_d \dfrac{\pi (D_h^0)^2}{4} \left[\dfrac{2}{\rho_d} (P_{RCS}^0 - P_c^0)\right]^{1/2}} \tag{4.4}$$

is the characteristic time to eject all the melt from the RPV in the absence of ablation and where

$$\tau_D = \frac{D_h^0}{\dot{D}_h} = \frac{D_h^0}{\left[\dfrac{2\, h_{d,w}\, (T_d^0 - T_{mp,w})}{\rho_w \left[C_{p,w}(T_{mp,w} - T_w) + h_{f,w}\right]}\right]} \tag{4.5}$$

is the characteristic time to double the initial hole size by ablation. Figure 4.3 validates the model against the existing database. This figure also illustrates that ablation increases the hole size only slightly for initial hole sizes characteristic of lower head rupture; consequently, ablation will not have a strong influence on the calculations performed for this report.

A second phenomenological uncertainty concerns hydrogen combustion during DCH. The working group emphasized that hydrogen combustion should be treated in a manner consistent with the expected conditions in the containment. Appendix E addresses the issue of jet combustion, entrainment into a jet, stratification, global mixing, and volumetric combustion phenomenology in more detail. Our conclusions regarding hydrogen combustion during DCH events can be summarized as follows:

1. DCH-produced hydrogen (plus some entrainment of H_2 from the preexisting atmosphere) can burn as a jet in the dome and contribute to peak containment pressures. This is consistent with NUREG/CR-6075.

2. Stratification of jet combustion products will occur in the dome, thus impeding the mixing of combustion products with the preexisting atmosphere.

3. Flame propagation is difficult to achieve in a stratified containment atmosphere and the burning process is too slow and inefficient to contribute to peak loads except possibly at the upper end of H_2 distribution. Explicit treatment of this process (not considered in NUREG/CR-6075) to better define and bound uncertainties in hydrogen combustion is included in the supplement analyses. The fraction of the preexisting hydrogen that can burn on DCH time scales and contribute to peak loads is given by

$$f_{pre} = \eta \left[1 - \frac{\dot{E}_{HT}}{\dot{E}_{H2}} \right] . \tag{4.6}$$

Even for finite combustion completeness (η), heat transfer to structures can exceed the energy release rate due to the deflagration so that the deflagration does not contribute to peak DCH loads. These enhancements had negligible impact on the predicted containment load distributions for scenarios with ~50 percent steam in the containment atmosphere. Deflagration enhanced DCH loads are predicted for a TMI-like scenario with essentially no steam in the atmosphere, but the increased pressure is offset by the lower initial pressure in the containment.

4. Slow volumetric combustion of preexisting hydrogen does not contribute to peak loads.

5. Sudden volumetric combustion (autoignition) of preexisting hydrogen is essentially impossible in a stratified atmosphere because heating of the containment atmosphere is mixing limited. However, to better bound uncertainties in hydrogen combustion phenomena, we have reduced the autoignition temperature from 1100 K (NUREG/CR-6075) to ~950 K.

6. Combustion initiated by mixing of hot gases with the preexisting atmosphere is too slow to contribute to peak pressure. This is because the mixing (and combustion) time scale is long compared to the heat transfer time scale.

These insights and recommendations are consistent with peer review comments concerning the autoignition temperature and the need to consider partial combustion of the preexisting hydrogen. These recommendations have been factored into the calculated results presented in Section 6.

The amount of material participating in DCH is typically less than the melt mass on the lower head at the time of bottom head failure. The SNL/ANL counterpart experiments exhibited melt retention in both the crucible (scaled to the bottom head of the RPV) and the reactor cavity below the RPV. On average, 93 $\pm$ 4.4 percent of the melt was ejected into the cavity in these experiments. A conservative upper bound of 100 percent is used for all the scenarios in the supplement. The SNL/ANL counterpart experiments have also shown that only 76 $\pm$ 7.2 percent of the melt in the cavity is dispersed into the containment. We assign a dispersal fraction of 85 percent to all scenarios in order to bound the experiment results. These assessments are fully consistent with NUREG/CR-6075.

The SNL/ANL counterpart experiments have shown that 8.5 percent of the debris dispersed from the cavity through the instrument tunnel (not the annular gap) will enter the upper dome, some through the seal table room (located directly over the cavity exit) and some through vents above the reactor coolant pumps (RCPs). Ishii et al. (1993) report 3 percent transport to the dome in experiments using water. Of this, 2 percent is carried to the dome through the vents above the RCPs surrounding the steam generators located on either side of the cavity exit. The remaining 1 percent, which is carried to the dome through the seal table room, is nonprototypic because of low film velocities at the cavity exit. Minimal transport to the dome is supported by additional scoping experiments using water (FAI, 1991; Ginsberg, 1988). This transport to the dome is accounted for in the TCE evaluations of containment loads. For the evaluations in this supplement to NUREG/CR-6075, we assume 5 percent transport through the seal table room and RCP vents to the upper dome. Such treatment, however, is deemed conservative because the experiments did not model the seal table that blocks access into the seal table room; because the experiments did not model the "penthouse" over the cavity exit (a steel enclosure with blowout panels intended to deny unauthorized personnel access into the cavity); and because the experiments did not model the vast array of in-core instrument guide tubes that may be dispersed from the cavity with the debris (Allen et al., 1990). These assessments are consistent with NUREG/CR-6075.

A second possible flow path to the upper dome is the annular gap around the RPV. The SNL/IET-11 experiment showed that the melt-laden gas will melt the insulation and sweep it from the gap. The SNL/HIPS-8C experiment also simulated the gap without insulation. Analysis of these two experiments indicates that the fraction of dispersed debris that goes through the gap is equivalent to the minimum flow area through the gap divided by the sum of the minimum gap and tunnel flow areas (see Appendix K in NUREG/CR-6075 for a more phenomenological development of the model and validation against a database for Zion and Surry cavity designs). For Zion, the minimum tunnel flow area is ~ 5.6 m^2 and the minimum gap flow area (at the level of the nozzles) is ~ 0.54 m^2. Consequently, ~ 9 percent of all dispersed debris will be transported through the gap to the dome. This assessment of gap transport may be conservative because the experiments did not model the neutron shields or other structures in the gap and because water is expected to be coejected from the RPV with the melt. Transport through the gap can be added to the ~ 5 percent transport through the seal table room and RCP vents, so that 14 percent of all dispersed debris will enter the dome. These assessments are consistent with NUREG/CR-6075.

4.1 References

Allen, M.D., R.T. Nichols, M. Pilch (1990). *A Demonstration Experiment of Steam-Driven, High-Pressure Melt Ejection: The HIPS-10S Test*, NUREG/CR-5373, SAND89-1135, Sandia National Laboratories, Albuquerque, NM.

Allen, M.D., M.M. Pilch, T.K. Blanchat, R.O. Griffith, and R.T. Nichols (May 1994). *Experiments to Investigate Direct Containment Heating Phenomena with Scaled Models of the Zion Nuclear Power Plant in the SURTSEY Test Facility*, NUREG/CR-6044, SAND93-1049, Sandia National Laboratories, Albuquerque, NM.

FAI (1991). *Zion IPE Position Paper on Direct Containment Heating*, FAI/91-18, Submitted to Commonwealth Edison Co.

Ginsberg, T., and N.K. Tutu (1988). *Progress in Understanding Direct Containment Heating Phenomena in Pressurized Light Water Reactors*, BNL-NUREG-41751, Brookhaven National Laboratory, Upton, NY.

Ishii, M., S.T. Revankar, G. Zhang, Q. Wu, and P. O'Brien (March 1993). *Separate Effects Experiments on Phenomena of Direct Containment Heating - Air-Water Simulation Experiments in Zion Geometry*, PU NE-93/1, Purdue University, West Lafayette, IN.

4.2 Nomenclature

A_h	=	breach area in RPV
C_d	=	discharge coefficient (0.6)
$C_{p,w}$	=	heat capacity of RPV steel
D^0_h	=	initial hole diameter
f_d	=	fraction dispersed
$h_{d,w}$	=	debris/wall heat transfer coefficient during ablation (see Appendix J, NUREG/CR-6075)
$h_{f,w}$	=	heat of fusion for RPV steel
M^0_d	=	initial melt mass
M^0_g	=	initial RCS gas mass
P^0_c	=	initial containment pressure
P^0_{RCS}	=	initial RCS pressure
R_r	=	coherence ratio
T^0_d	=	debris temperature
T^0_{RCS}	=	RCS gas temperature
$T_{mp,w}$	=	melting temperature of RPV steel
T_w	=	temperature of RPV lower head at vessel failure
U^0	=	total internal energy of containment atmosphere
V_{cav}	=	cavity volume
V_{RCS}	=	RCS volume

Greek

ΔD_h	=	change in hole diameter
ΔE_i	=	energy contribution of DCH process
ΔP	=	pressure increase in containment due to DCH
ρ_d	=	mass density of debris
ρ_w	=	mass density of RPV steel
σ_{bias}	=	relative bias
σ_{rms}	=	relative (root mean squared) standard deviation
τ_D	=	characteristic time to double the initial hole size by ablation

τ_M = characteristic time to eject melt from RPV in the absence of ablation

ψ = total heat capacity of dispersed debris divided by total heat capacity of the atmosphere

Table 4.1 Survey of DCH-relevant experiments

Experiment Series	Number of Tests	Nominal Scale	Cavity Type	Water
SNL/DCH	4	1:10	Zion	None
SNL/TDS	7	1:10	Surry	None
SNL/LFP	6	1:10	Surry	None
SNL/WC	3	1:10	Zion	None Cavity
SNL/IET-Zion	9	1:10	Zion	Cavity Cavity/basement
SNL/IET-Surry	3	1:5.75	Surry	None Cavity/basement
ANL/CWTI	2	1:30	Zion-like	Cavity/basement
ANL/IET	6	1:40	Zion	None Cavity
ANL/U	3	1:40	Zion	None
FAI/DCH	4	1:20	Zion	Basement Cavity/basement

Table 4.1 (continued)
Survey of DCH-relevant experiments

Experiment Series	Driving Gas	Driving Pressure (MPa)	Melt Mass (kg)	Melt Composition	Hole Size
SNL/DCH	N_2	2.6 - 6.7	20, 80	Fe/Al_2O_3	0.06
SNL/TDS	H_2O	3.7 - 4.0	80	$Fe/Al_2O_3/Cr$	0.065
SNL/LFP	H_2O	2.5 -3.6	50, 80	$Fe/Al_2O_3/Cr$	0.04 - 0.09
SNL/WC	H_2O	3.8 - 4.6	50	$Fe/Al_2O_3/Cr$	0.04 - 0.10
SNL/IET Zion	H_2O	5.9 - 7.1	43	$Fe/Al_2O_3/Cr$	0.04
SNL/IET Surry	H_2O	12	158	$Fe/Al_2O_3/Cr$	0.072-0.098
ANL/CWTI	N_2	4.7 - 5.0	4.1	$UO_2/ZrO_2/SS$	0.13
ANL/IET	H_2O	5.7 - 6.7	0.72, 0.82	$Fe/Al_2O_3/Cr$	0.011
ANL/U	H_2O	3.0 - 6.0	1.13	$UO_2/Zr/ZrO_2/SS$	0.011
FAI/DCH	N_2, H_2O	2.4 - 3.2	20	Fe/Al_2O_3	0.025

Table 4.1 (concluded)
Survey of DCH-relevant experiments

Experiment Series	Containment Pressure (MPa)	Annular Gap Around RPV	Atmosphere Composition	Containment Structures
SNL/DCH	0.08	No	Air, Ar	Open containment
SNL/TDS	0.09 - 0.23	No	Air, Ar	Open containment
SNL/LFP	0.16	No	Ar	Compartmentalized by slab
SNL/WC	0.16	No	Ar	Essentially open
SNL/IET Zion	0.2	No	N_2, N_2/Air, N_2/Air/H_2, CO_2/Air/H_2	Zion subcompartment structures
SNL/IET Surry	0.13-0.19	No partial insulation	Air/H_2O/H_2	Surry subcompartment structures
ANL/CWTI	0.1	No	Ar	Compartmentalized by baffle
ANL/IET	0.2	No	N_2, N_2/Air, N_2/Air/H_2, H_2O/Air/H_2	Zion subcompartment structures
ANL/U	0.2	No	N_2/Air/H_2	Zion subcompartment structures
FAI/DCH	0.1	No	N_2	Zion (Like) subcompartment structures

Table 4.2 Applicability of the database to reactors

	CAVITY	f^*_{disp}	T^*_d/T^*_{RCS}	M^*_d/M^*_g	$A_h V^{1/3}_c/V_{RCS}$
Complete database	Zion, Surry	0.6 - 1.0	3.0 - 11.0	2.8 - 21.4	0.001 - 0.014
SNL/ANL IET Zion tests P^0_{RCS} = 6 MPa	Zion	0.6 - 0.9	4.2	3.9 - 6.0	0.0027
SNL/IET Surry tests P^0_{RCS} = 13 MPa	Surry	0.9	3.2	2.9	0.0033
NPP P^0_{RCS} = 8 MPa D^0_h = 0.4 m T^0_{RCS} = 1000 K M^0_d = 50 mt	Zion	~1	3.5	6.2	0.002
NPP P^0_{RCS} = 16 MPa D^0_h = 0.4 m T^0_{RCS} = 800 K M^0_d = 50 mt	Zion	~1	2.8	3.9	0.002

*Only experiments where dispersal is complete or nearly complete ($f_{disp} \geq 0.5$) considered.

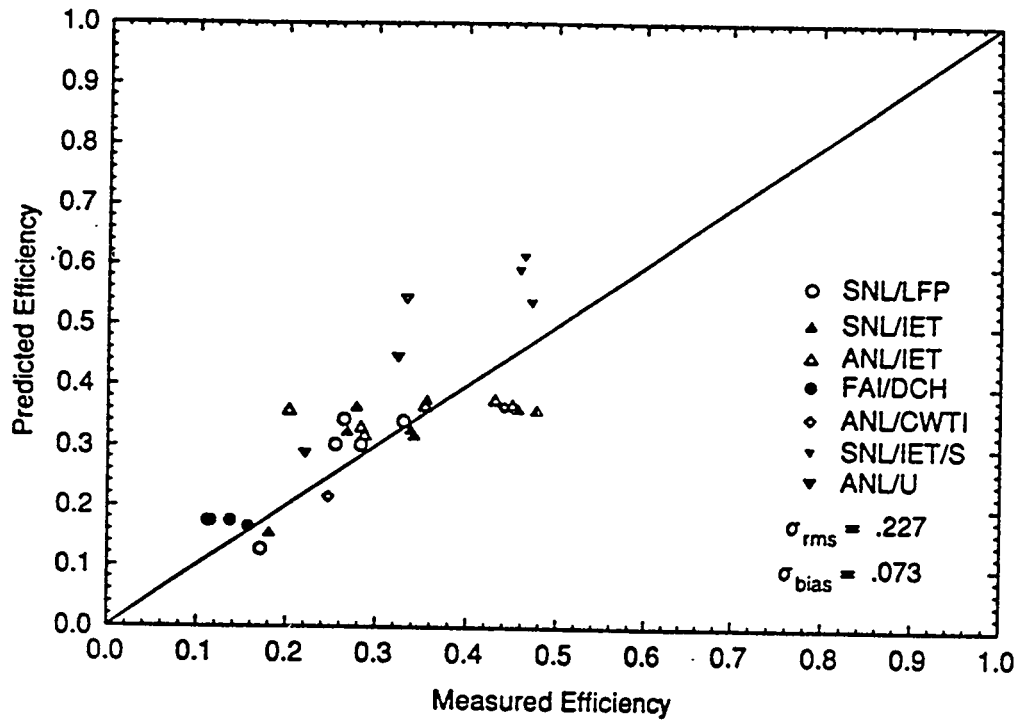

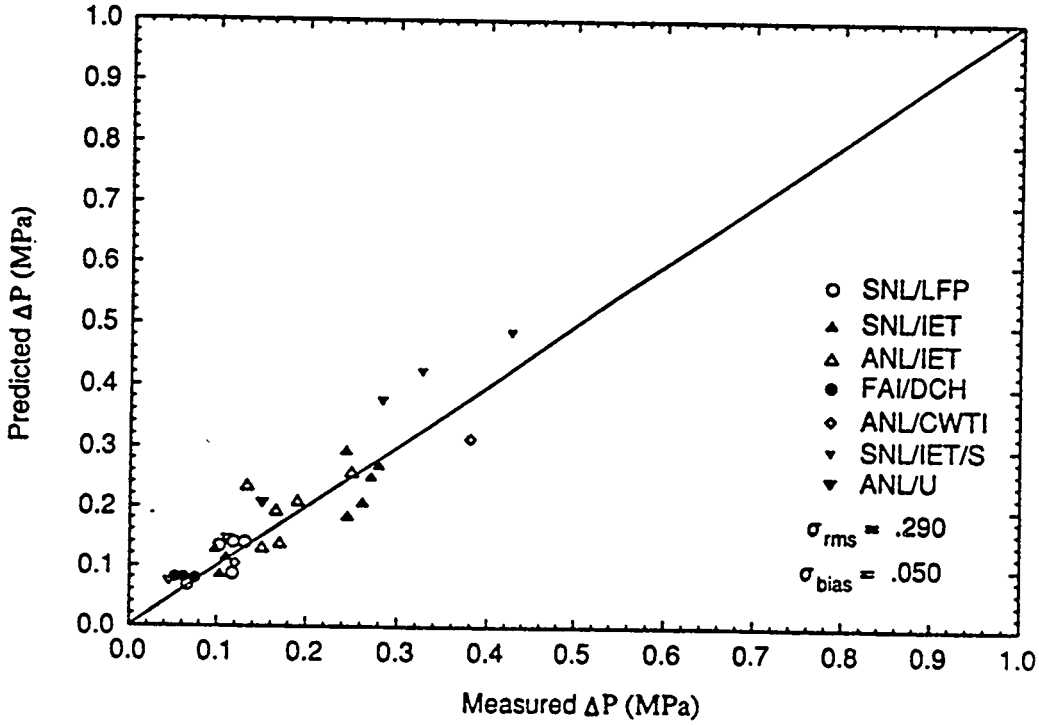

Figure 4.1. Validation of the two-cell equilibrium model against all experiments with compartmentalized geometry.

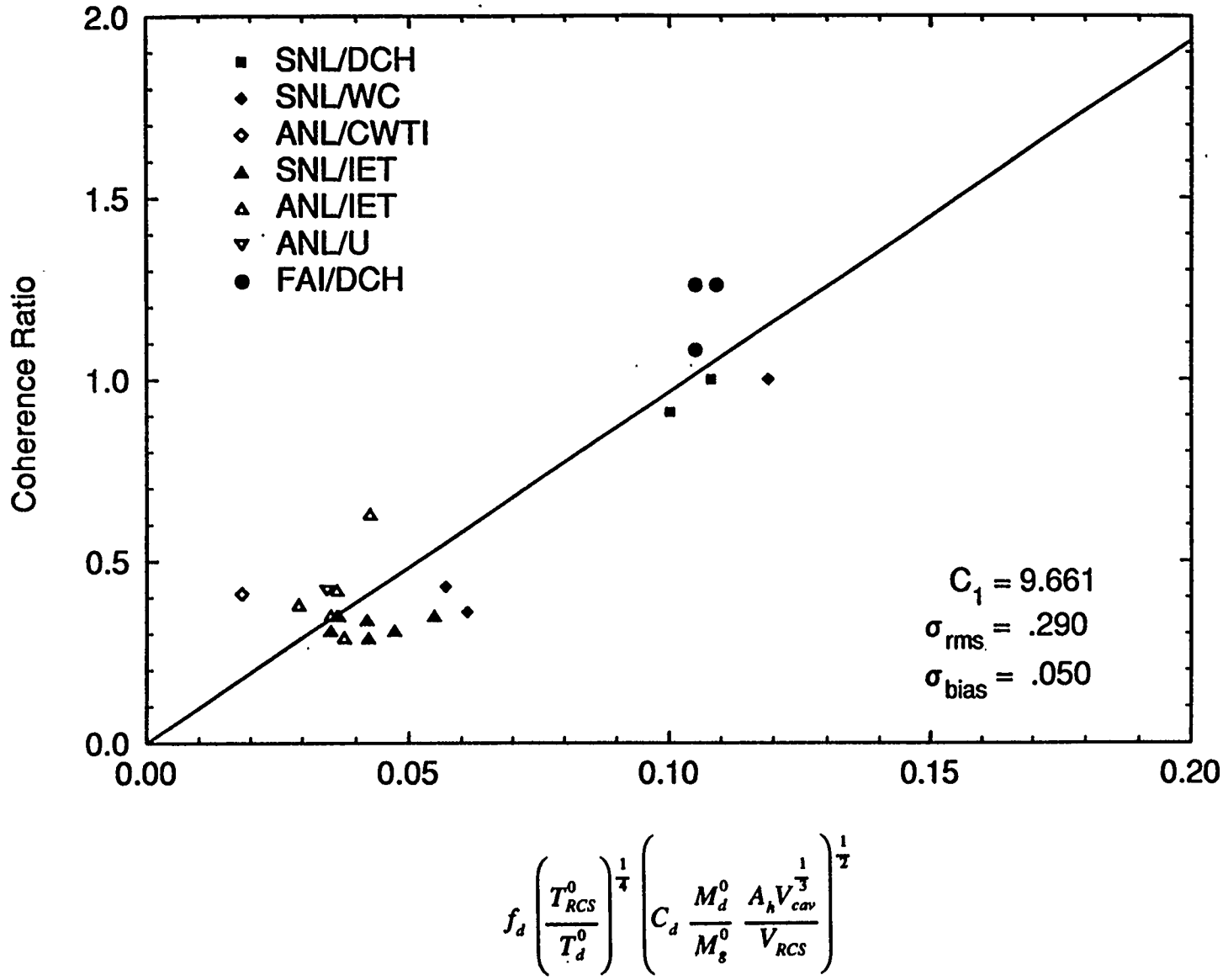

Figure 4.2. Validation of the coherence ratio for Zion-like cavity designs for scenarios without coejected water.

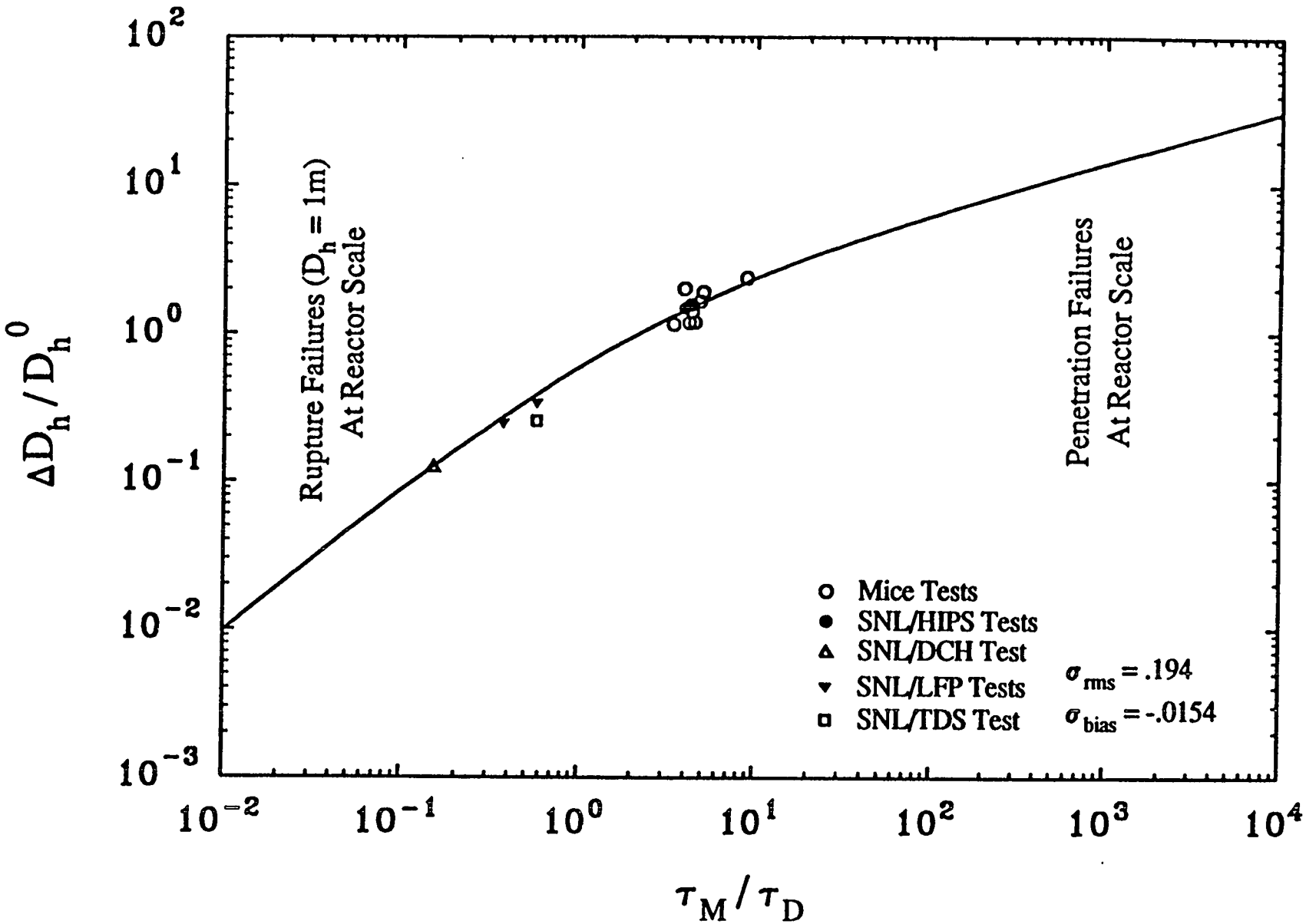

Figure 4.3. Validation of the hole ablation model.

5.0 QUANTIFICATION OF CONTAINMENT FRAGILITY

This section characterizes the strength of the Zion containment in probabilistic terms. The pressure capacity of the Zion containment is treated as a random variable because of the variability in material properties, of unknown differences between the as-built and design conditions, and modeling uncertainties. The probability that the containment failure pressure is less than a specified pressure is known as the containment overpressure fragility curve.

Fragility curves represent a probabilistic estimate of the capacity of the containment, and as such are not directly derivable from existing data or full-scale experiments. In general, they are derived from a combination of material property data, tolerances in dimensions from drawings, and judgment of the analyst. Analyst judgment is used in determining what level of analysis is required and what failure mechanisms are considered to govern the containment capacity. In addition, analyst judgment is utilized in translating the results of material property tests into a probabilistic estimate of the variability of the various material properties involved. Finally, judgment is exercised in assigning "modeling" uncertainty to the models to characterize the analyst's confidence in the ability of the selected models to represent the actual failure mechanisms involved. Modeling uncertainty could, in principle, be reduced with further analysis or testing. Funding constraints, however, usually require the analyst to exercise his judgment to reflect the uncertainty involved.

In addition, it should be noted that a containment fragility curve is, in fact, a plant-specific entity. It is to be anticipated that the fragility curves derived for a specific containment are sensitive to local design details, tolerances, and the design philosophy used for that particular containment. While it is likely that various submodels representing different local containment failure modes may be applicable to a variety of containments of a given type, it is also true that the combination of failure mechanisms existing in a given containment is unique. Thus, the reader is cautioned against reading any generic applicability into the fragility curves developed for any specific containment.

5.1 Fragility Curve Selected for DCH Evaluation

The Zion containment is a prestressed, post-tensioned concrete cylinder with a shallow-domed roof. The foundation is a reinforced concrete slab. The containment is lined with

welded 6.35-mm (0.25-inch) steel plate. The post-tensioning system is composed of 63 dome tendons, 216 vertical tendons, and 555 hoop tendons. The design pressure and temperature are 0.42 MPa-abs and 376 K (47 psig and 217°F). The free volume is about 76.9 x 10^3 m^3 (2.7 million cubic feet).

The containment fragility curve used for this study (Figure 5.1) is taken from the Zion IPE (1992). This curve reflects the most recent judgment of the licensee of the plant. As described by the licensee, the Zion IPE fragility was derived as follows.

> Analyses of the ultimate pressure capacity of the Zion containment were performed independently by Sargent & Lundy (S&L) for the IDCOR program, Brookhaven National Laboratory (BNL) for the NRC, and Los Alamos National Laboratory for the NRC. Two limiting failure locations were identified, i.e., the basemat/shell junction and the shell wall (hoop direction). The three studies show large discrepancies in the prediction of the failure pressure at the basemat/shell junction. However, only the S&L results were consistent with the Sandia 1:6 scale test. Therefore, the S&L prediction of 152 psig is adopted as the mean failure pressure for the basemat/shell junction in the containment fragility curve calculation. With regard to the failure pressure for the shell wall (hoop direction), the S&L result (134.4 psig) was in good agreement with the Los Alamos result (136 psig). The smaller failure pressure of 134.4 psig is adopted in the containment fragility curve calculation.
>
> Uncertainties in the estimated failure pressures, in terms of a coefficient of variation, are 5 and 15 percent for the hoop shell wall and the basemat/shell junction respectively. The containment fragility curve, constructed based upon the two limiting failure locations and their associated uncertainties, is shown in Figure 5.1. The mean failure pressure, where the total probability of failure becomes 50 percent, is 132 psig. Containment failure at pressures above 128 psig would most likely occur at the hoop shell wall, while failure below 128 psig would most likely occur at the basemat/shell junction. In addition, the S&L study concluded that the containment failure pressure and location would not be sensitive to the pressurization rates or temperature effects caused by any postulated failure mechanisms.

5.2 Working Group Discussion of the Zion Fragility

The Zion IPE did not tabulate values nor did any of the supporting documentation; consequently, the authors of NUREG/CR-6075 digitized the numerical data required for the calculations from the available plot.

Working group members (Appendix A) criticized this process as being potentially inaccurate and unphysical in the extreme of very low failure frequencies. Specifically, the digitizing process is subject to human error and is dependent on the quality of the curve that is digitized. In addition, low failure frequencies are obtained only as extrapolations of a theoretical curve which is fit to physically based analytical results defining the middle portions of the fragility curve. Although numerically feasible, excessive extrapolation to low failure frequencies could lose the physical basis on which most of the curve rests.

To address these issues, the NRC requested that Fauske and Associates Inc. (FAI, 1994) provide the actual pressure/frequency pairs making up the IPE fragility curve. Table 5.1 provides the data as supplied by FAI for this purpose. Graphic presentation of this information is shown in Figure 5.2.

Comparison of the FAI-supplied fragility curve with that used in NUREG/CR-6075 is shown in Figure 5.3. The coefficient of variation (COV) for the FAI-supplied IPE curve is slightly smaller than the COV of the NUREG/CR-6075 curve. At low failure frequencies, the FAI-supplied curve produces (for a given pressure) lower failure frequencies than the NUREG/CR-6075 approximation. In addition, FAI recommended truncation of the curve at 0.791 MPa (failure frequency ~ 0.01) because, in their judgment, extrapolation to lower pressures would be unphysical. This can be compared with a threshold (failure frequency = 0.0) of 0.689 MPa used in the NUREG/CR-6075 approximation. The FAI-supplied fragility curve was used in the supplement analyses for Zion.

5.3 References

FAI (1994). Fauske and Associates, Inc., 16W070 West 83rd Street, Burr Ridge, IL, 60521.
Zion IPE (April 1992). *Commonwealth-Edison Zion Station: Individual Plant Evaluation*, NRC Doc. No 9204290315.

Table 5.1 Fragility of the Zion containment

Containment Pressure		Total Frequency	Hoop Frequency	Basemat Frequency
psig	MPa-abs			
(99.8)*	(0.789)*	(0.0)*	(0.0)*	(0.0)*
100	0.791	0.111420E-01	0.000000	0.111420E-01
102	0.805	0.144660E-01	0.400000E-05	0.144629E-01
104	0.818	0.175300E-01	0.400000E-05	0.175260E-01
106	0.832	0.216800E-01	0.160000E-04	0.216640E-01
108	0.846	0.269820E-01	0.600000E-04	0.269220E-01
110	0.860	0.328700E-01	0.132000E-03	0.327380E-01
112	0.873	0.402680E-01	0.490000E-03	0.397780E-01
114	0.887	0.489920E-01	0.128200E-02	0.477100E-01
116	0.901	0.604140E-01	0.330200E-02	0.571120E-01
118	0.915	0.754180E-01	0.787600E-02	0.675420E-01
120	0.929	0.974400E-01	0.172740E-01	0.801660E-01
122	0.942	0.126856	0.334980E-01	0.933580E-01
124	0.956	0.169392	0.614960E-01	0.107896
126	0.970	0.227952	0.104018	0.123934
128	0.984	0.304952	0.163810	0.141142
130	0.998	0.397674	0.239964	0.157710
132	1.01	0.500082	0.328530	0.171552
134	1.03	0.607362	0.421320	0.186042
136	1.04	0.709642	0.512664	0.196978
138	1.05	0.798778	0.592898	0.205880
140	1.07	0.870436	0.657586	0.212850
142	1.08	0.922064	0.704518	0.217546
144	1.09	0.956902	0.734662	0.222240
146	1.11	0.978182	0.755642	0.222540
148	1.12	0.989540	0.766736	0.222804

Containment Pressure		Total Frequency	Hoop Frequency	Basemat Frequency
psig	MPa-abs			
150	1.14	0.995364	0.771732	0.223632
152	1.15	0.998204	0.774674	0.223530
154	1.16	0.99358	0.774358	0.225000
156	1.18	0.99818	0.776618	0.223200
158	1.19	0.999908	0.775880	0.224028
160	1.20	0.999988	0.774876	0.225112
162	1.22	0.999998	0.776016	0.223982
164	1.23	1.00000	0.775978	0.224022
166	1.25	1.00000	0.776508	0.223492
168	1.26	1.00000	0.774764	0.225236
170	1.27	1.00000	0.774880	0.225120

* These points added to effectively truncate the distribution as recommended by FAI.

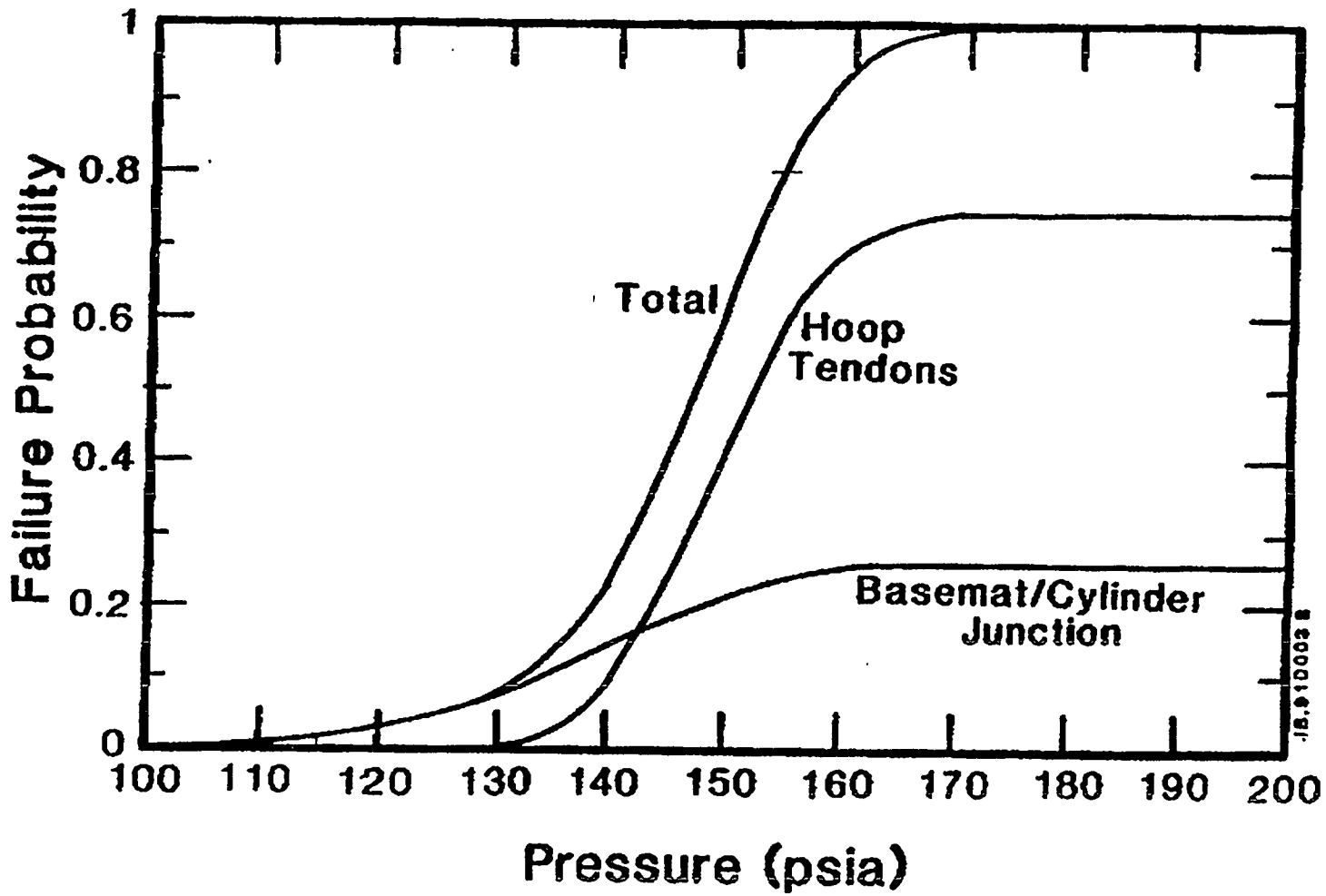

Figure 5.1. Zion fragility curve as presented in the Zion IPE.

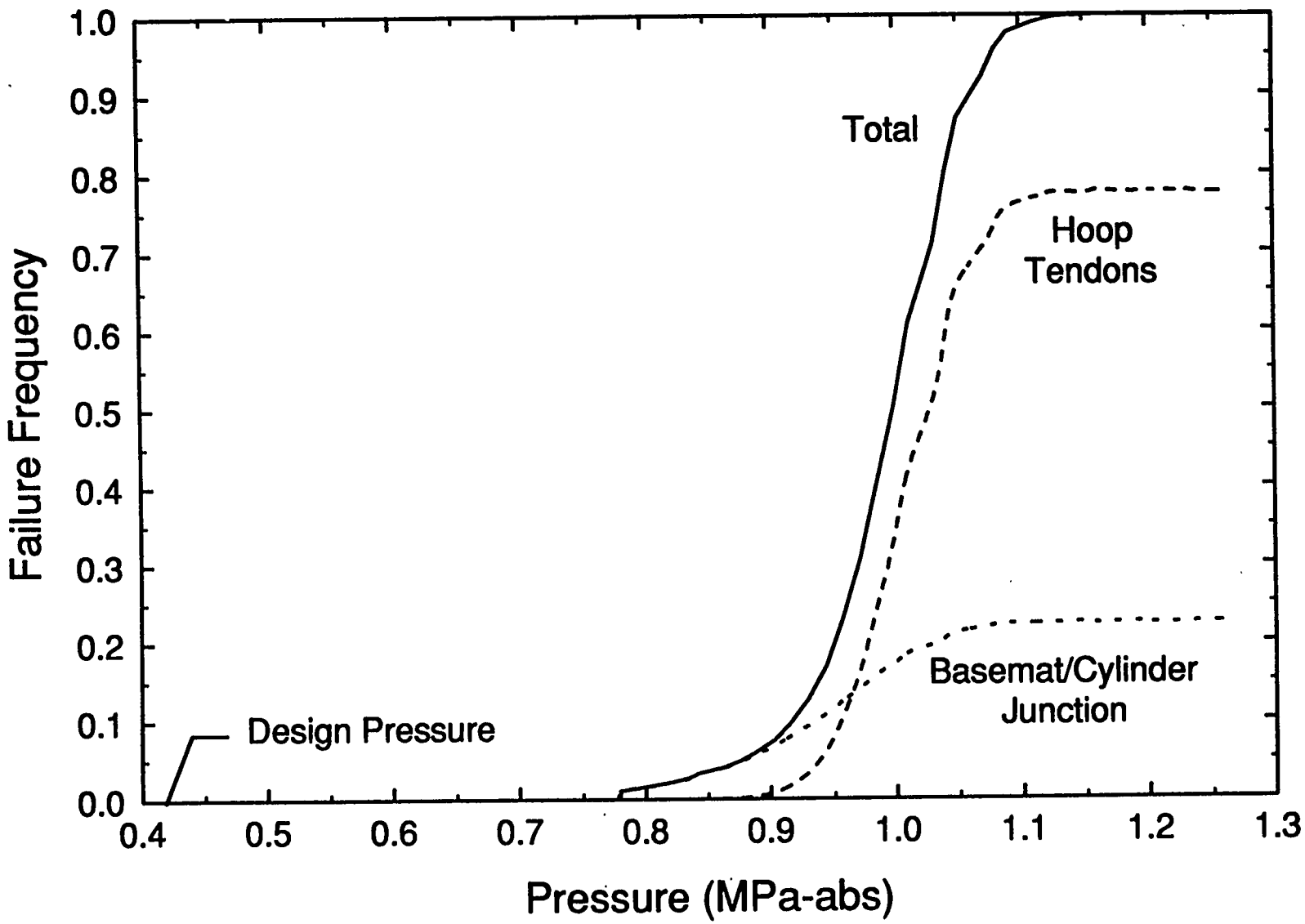

Figure 5.2. Zion fragility curve as developed by FAI for the Zion IPE.

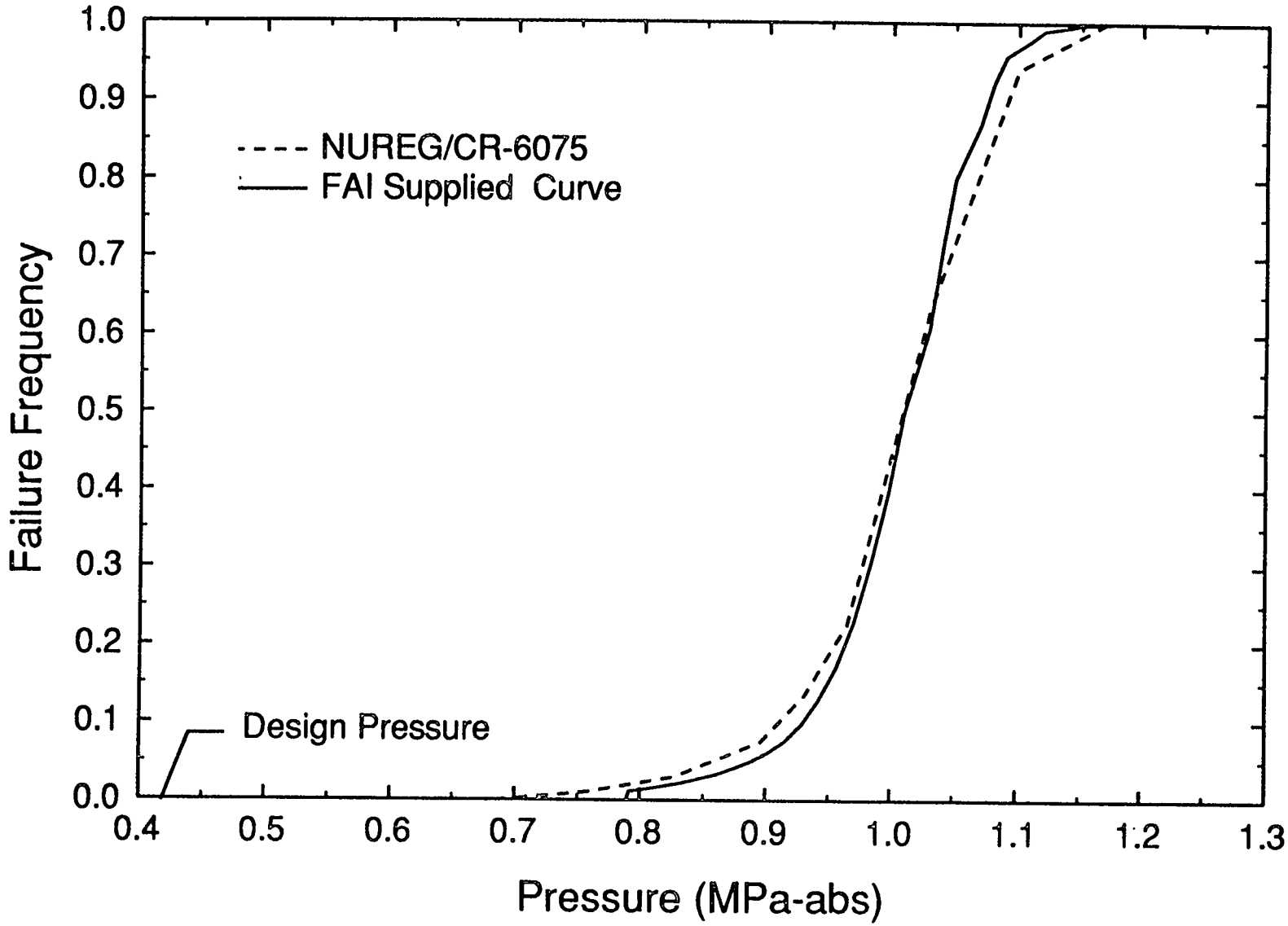

Figure 5.3. Comparison of the FAI-supplied Zion fragility curve with the approximation used in NUREG/CR-6075.

6.0 RESULTS AND SENSITIVITIES

6.1 Results

Each scenario identified in Section 3, supplemented by the respective coherence ratio distribution as discussed in Section 4 and the fragility curve of Section 5, was run through the arithmetic defined by the probabilistic framework of Section 2 to produce probability distributions for the final hole size, coherence ratio, containment temperature, and containment pressure. Finally, the containment failure probability was computed. The calculations were carried out using the computer code TCE/LHS (with 200 samples) as listed in Appendix B.

SCDAP/RELAP5 calculations have been performed (based on working group recommendations) to confirm the basic features of Scenarios VII and VIII. Three cases were run with SCDAP/RELAP5 representing the full spectrum of expected SBLOCAs: no leaks, 250 gpm/pump, and 480 gpm/pump. Appendix C presents these calculations in detail, and the results are summarized in Section 3.3. The key conclusion, however, is that hot leg failure is predicted to occur before core relocation for all SBLOCAs that proceed without operator intervention. Consequently, Scenarios VII and VIII are not further analyzed in this report.

Table 6.1 provides a concise summary of where to find each of the calculated distributions and the range of the calculated parameter organized as lower bound (LB), best estimate (BE), and upper bound (UB). The distributions for hole size, coherence ratio, and containment temperature are provided so the reader can see firsthand the range over which these key intermediate parameters vary. No intersection of the load distribution with containment fragility is predicted; therefore, we conclude that probability of containment failure by DCH in the Zion plant is zero for the scenarios analyzed.

Examination of the results led to the following observations:

1. Scenario V and VI produce comparable loads.

2. Calculated atmosphere temperatures do not exceed 675 K; thus, DCH events are far from conditions that could lead to combustion of all preexisting H_2 in the containment.

3. The calculated final breach diameters are well within the scaled range used in the experiments.

4. The debris interacts with only a fraction of the blowdown gas, as indicated by the coherence ratio.

Scenario V is an operator intervention accident with features roughly similar to the TMI-II accident. The TMI-II accident differs from Scenario V in that fan coolers were operational so that there was essentially no steam in the reactor building (compared with ~48 percent steam in Scenario V). To examine this scenario, we ran a TMI-like case with containment pressure (0.11 MPa), temperature (326 K), and atmosphere composition (X_{STM} ~ 0.039) consistent with TMI. All other parameters were the same as in Scenario V.

A hydrogen burn occurred at TMI-II when the hydrogen concentration in the dome was ~7.9 percent, which was above the local flammability limit of ~4.0 percent. Consequently, we cannot guarantee an ignition source, which would burn off the hydrogen in the containment prior to the DCH event. Deflagrations, which contribute to peak containment pressure, are expected in this scenario becuase of the high hydrogen concentration and the low steam concentration in the atmosphere. The deflagration model developed in Appendix E adequately handles this situation.

Figure 6.5 shows the results of Scenario V with TMI-like containment conditions. The upper bound pressure is 0.474 MPa-abs, which is well below the threshold (~0.79 MPa-abs) for Zion's containment fragility. The predicted pressure for TMI-like conditions is only slightly higher than for Scenario V, which had much more steam in the building. This is because the increased pressures resulting from the deflagration in the TMI-like case are offset by the lower initial containment pressure.

SCDAP/RELAP5 predicts hot leg or surge line failure for all credible SBLOCAs. Such failures lead to rapid and complete depressurization of the RCS well before predicted melt relocation to the lower head. During melt relocation, SCDAP/RELAP5 predicts a temporary repressurization of the RCS as a result of melt/water interactions in the lower plenum. We have performed a sensitivity study by arbitrarily assuming that vessel rupture occurs without delay upon melt relocation and repressurization.

Table 6.2 synthesizes the input conditions for a point calculation sensitivity study. The SCDAP/RELAP5-predicted melt composition at the time of relocation is noteworthy in that it contains a small amount of molten steel from the upper plenum (melting of the upper plenum steel is strongly correlated with the predicted hot leg failure). The metallic blockage is largely cooled by steaming in the lower plenum, but SCDAP/RELAP5 does predict relocation of a significant fraction of the control rod material (CRM) and small quantities of zirconium. The melt masses predicted by SCDAP/RELAP5 are based on the assumption of complete relocation of all melt contained within the core crucible. The containment conditions at the time of melt relocation were estimated from CONTAIN calculations with input sources taken from SCDAP/RELAP5.

The mean containment pressure due to DCH is 0.461 MPa-abs with a predicted temperature of 723 K. These loads are well below Zion's threshold for fragility (0.79 MPa-abs).

Table 6.1 Summary of results

Distribution/Result	Scenario V		Scenario VI	
	Figure Location	Range *	Figure Location	Range *
Hole size (m)	Fig. 6.1	0.403 LB 0.429 BE 0.459 UB	Fig. 6.1	0.405 LB 0.444 BE 0.483 UB
Coherence ratio	Fig. 6.2	0.021 LB 0.214 BE 0.544 UB	Fig. 6.2	0.057 LB 0.479 BE 1.15 UB
Containment temperature (K)	Fig. 6.3	424 LB 500 BE 572 UB	Fig. 6.3	438 LB 574 BE 675 UB
Containment pressure (MPa-abs)	Fig. 6.4	0.324 LB 0.382 BE 0.437 UB	Fig. 6.4	0.295 LB 0.387 BE 0.455 UB
Containment failure probability		0		0

* LB, lower bound; BE, best estimate; UB, upper bound.

Table 6.2 Sensitivity study using SCDAP/RELAP5 conditions at the time of melt relocation

Molten Mass	Case 2	Case 3	Sensitivity
UO_2 (mt)	54.3	54.9	55
ZrO_2 (mt)	13.6	15.2	15
Zr (mt)	0.5	0	0.5
Steel (mt)	8.2	5.0	8
CRM (mt)	3.3	2.2	3
TOTALS	79.9	77.3	82.5
RCS Press (MPa)	0.7	1.7	2.0
T^0 RCS (K)			800
D^0_h (m)			1
P^0_{RCB} (MPa-abs)	0.28	0.25	0.25
T^0_{RCB} (K)	400	400	400
H_2 Prod. (kg)	519	425	500
		PREDICTIONS	P_{max} = 0.461 MPa-abs T_{max} = 723 K

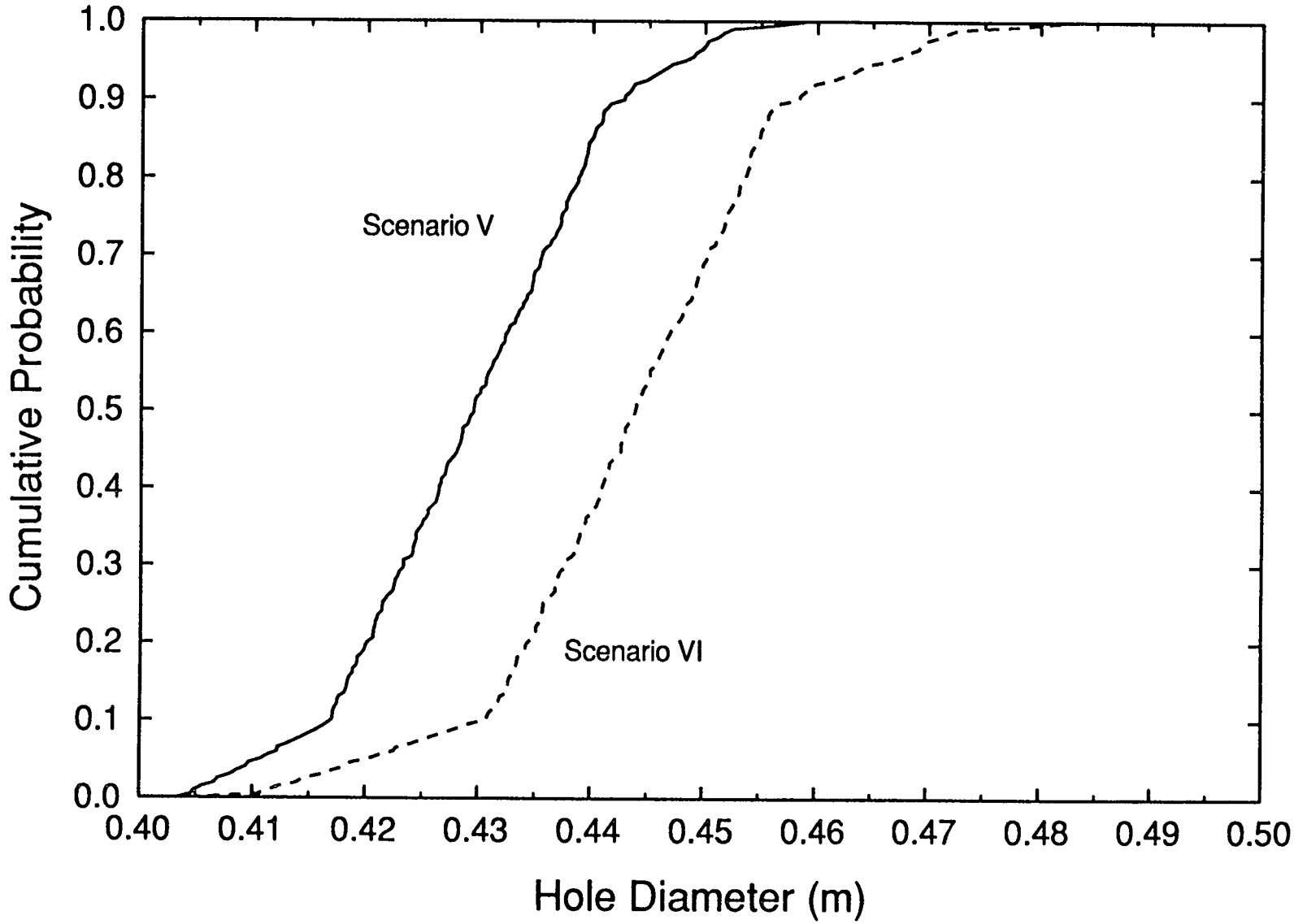

Figure 6.1. Calculated distribution for the hole size.

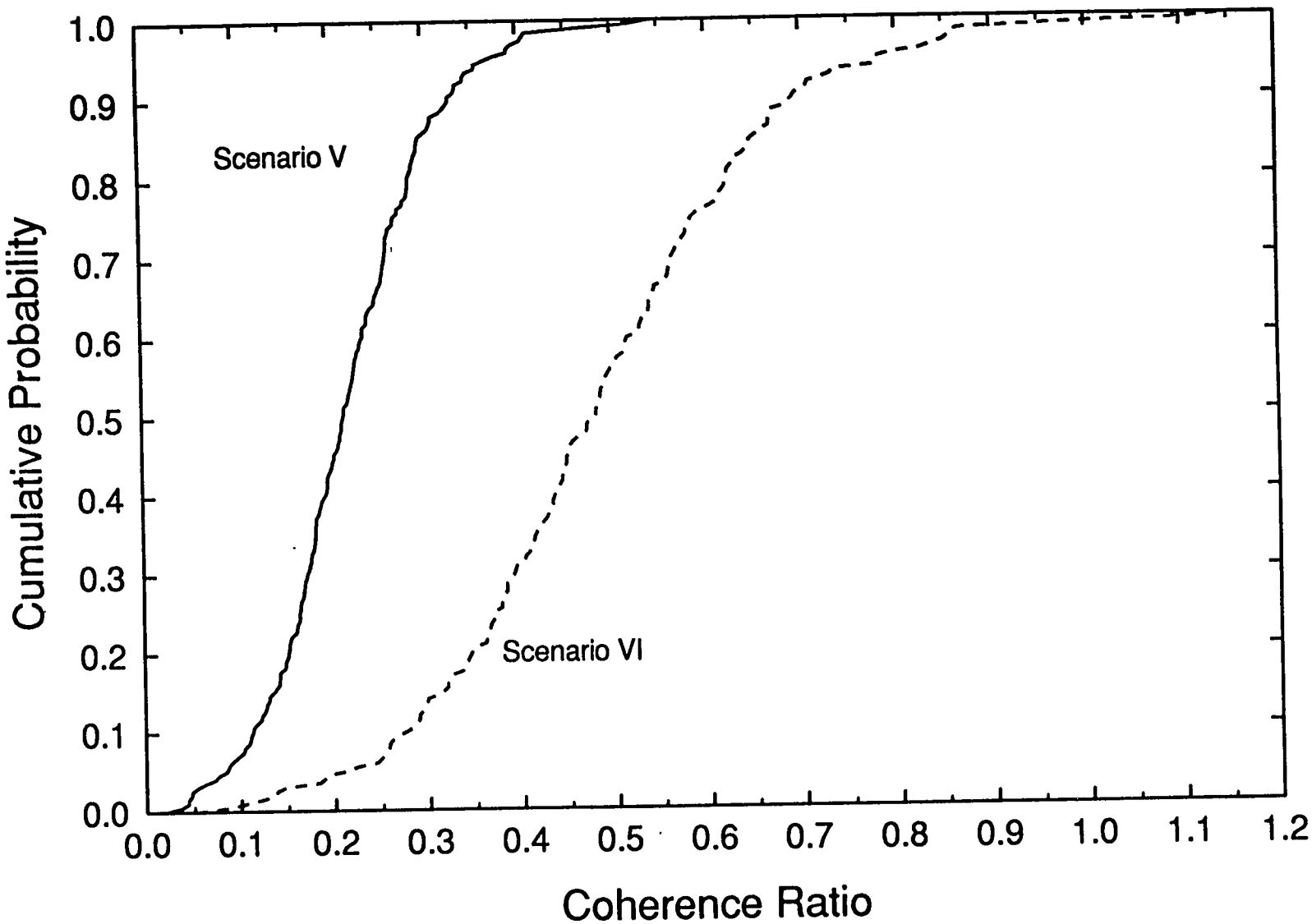

Figure 6.2. Calculated distribution for the coherence ratio.

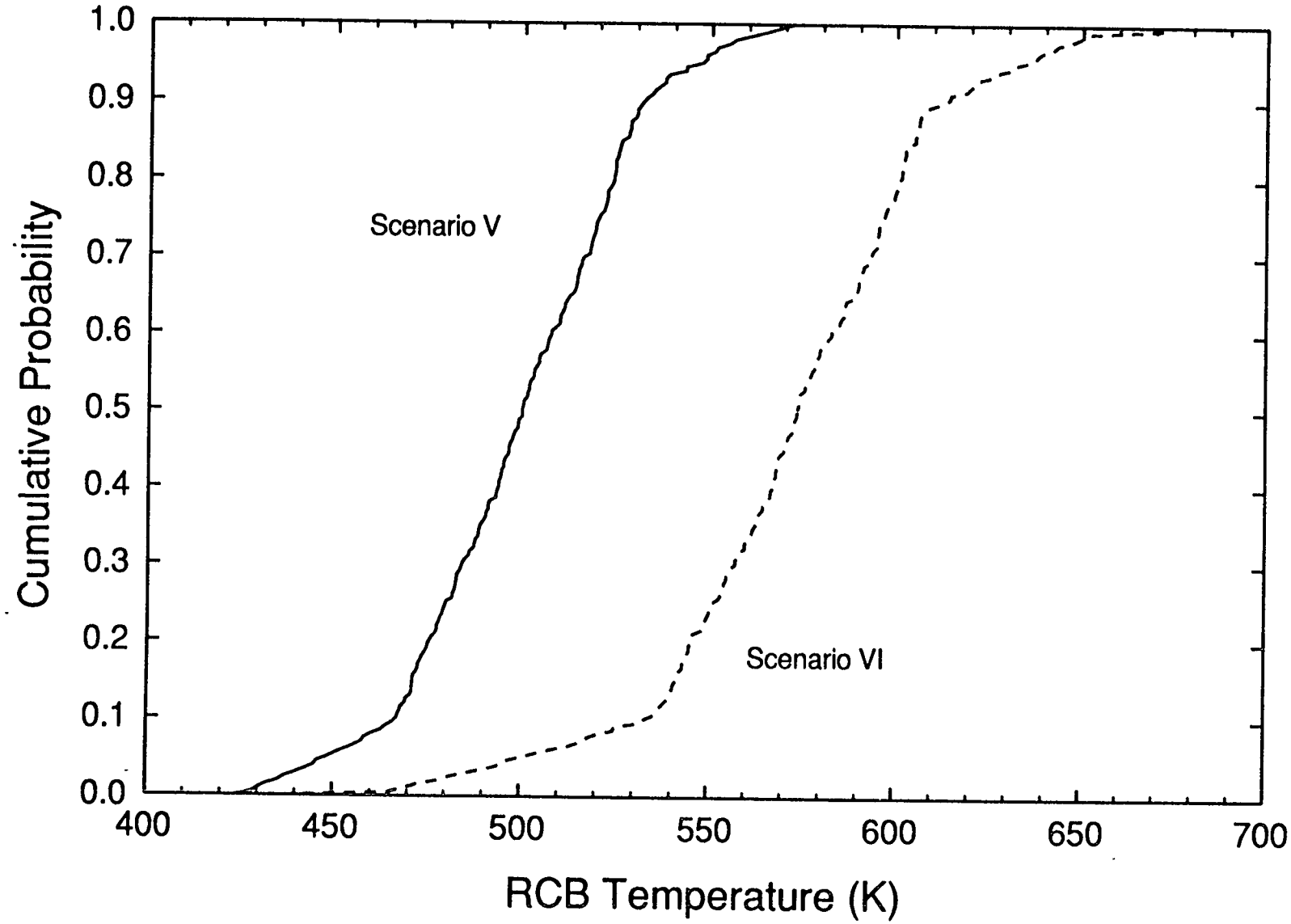

Figure 6.3. Calculated distribution for the containment temperature.

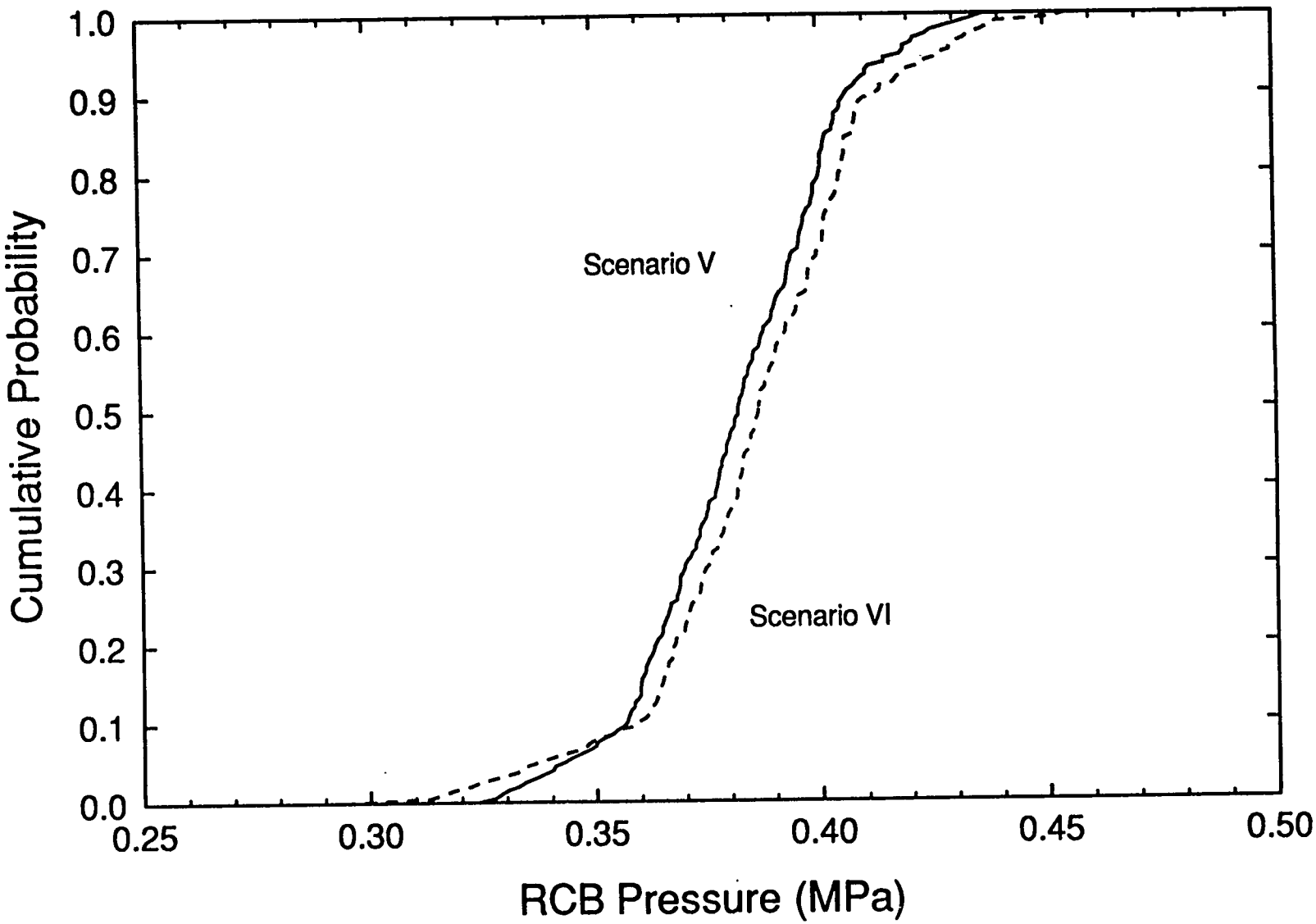

Figure 6.4. Calculated distribution for the containment pressure.

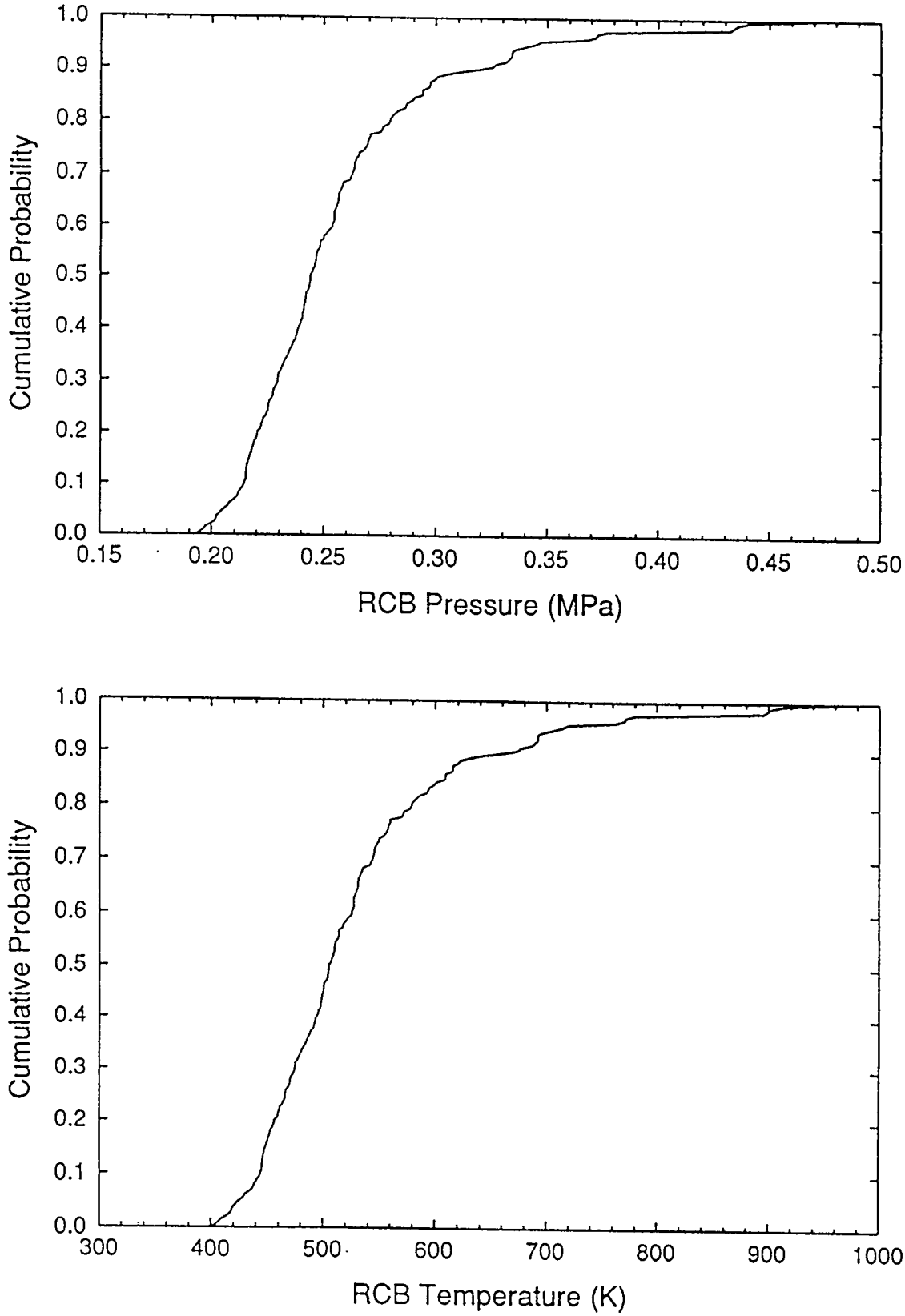

Figure 6.5. Scenario V with TMI-like containment conditions.

7.0 CONCLUSIONS AND RECOMMENDATIONS

The conclusions listed below are the result of insights from SCDAP/RELAP5 and CONTAIN analyses of three short-term station blackout cases with different leak rates and of analyses of new splinter scenarios defined in working group meetings using the methodology developed in NUREG/CR-6075.

1. SCDAP/RELAP5 was used to analyze a short-term station blackout scenario with three different leak rates: (1) no leaks, (2) 250 gpm per pump, and (3) 480 gpm per pump. In all cases analyzed, the RCS depressurized to roughly containment pressure well before lower head failure. Therefore, the RCS pressure selected in NUREG/CR-6075 (8 MPa) is conservative.

2. SCDAP/RELAP5 analyses indicate that only a very small amount of metallic debris relocates to the lower plenum. In-core metallic blockages tend to stay in place, i.e., they do not relocate to the lower plenum. The amount of metallics in the lower plenum at vessel breach predicted by SCDAP/RELAP5 were $\approx$0.5 mt Zr, $\approx$5 mt lower plenum steel, and no upper plenum steel. These amounts of metallics are less than the distributions initially considered in NUREG/CR-6075.

3. The SCDAP/RELAP5 analyses predict *molten* UO_2 masses at lower head failure that are similar to the original UO_2 melt mass distributions in NUREG/CR-6075.

4. CONTAIN calculations using input from the three cases run with SCDAP/RELAP5 resulted in containment conditions similar to those initially analyzed in NUREG/CR-6075.

5. The new splinter scenarios defined in the working group meetings were analyzed using the methodology developed in NUREG/CR-6075. There were no load-to-strength intersections and thus the containment failure probabilities were negligible for the scenarios analyzed. Therefore, the primary conclusion of this supplement to NUREG/CR-6075 is that DCH is not a problem for Zion.

APPENDIX A
PEER REVIEW OF NUREG/CR-6075

Martin M. Pilch
Sandia National Laboratories

A.1 INTRODUCTION

The NUREG/CR-6075 report describes a probabilistic framework (The Probability of Containment Failure by Direct Containment Heating in Zion) to assess the DCH issue for the Zion Nuclear Power Plant (NPP). The probabilistic approach uses several initial conditions in the form of Discrete Probability Distributions (DPDs) and a number of "Causal Relations" (CRs) for physical processes. These probability distributions and functional dependencies (in the form of CRs) are propagated through the model to arrive at the final conditional containment failure probability. NUREG/CR-6075 was prepared in January 1993 for internal Nuclear Regulatory Commission (NRC) review, and it was in final draft form by June 1993. In response to a NRC request, Energy Research, Inc. (ERI) assembled a committee of thirteen technical experts as listed in Table A.1. The NRC requested peer reviews to focus their evaluation on the following:

(a) The technical merits of the conclusions and the analysis described along with the quantification of inputs (i.e., estimate of initial and boundary conditions, containment loads, and structural response),

(b) Identification of the sources of uncertainties in the analysis and their impact on the conclusions,

(c) The necessity for further experiments or confirmatory research as suggested in NUREG/CR-6075, and

(d) Potential for application and extrapolation of the methods and conclusions to other reactor and containment designs.

Draft NUREG/CR-6075 was reviewed by the panel of thirteen experts. Comments from the reviewers were received by the NRC and forwarded, along with a summary from ERI, to the authors in October 1993. In addition, comments from four additional reviewers, as listed in Table A.1, were addressed as part of the review process. The peer reviewers' names were removed from the comments, and a letter was randomly assigned to each reviewer. Although the authors received the complete and unaltered comments, they remained blind as to which reviewer wrote the specific set of comments.

A point-by-point response to reviewer comments was prepared and submitted to the NRC in March 1994 for distribution to the reviewers. Rebuttals from the reviewers were received in April 1994. Typographical errors were corrected and minor points of clarification were incorporated into NUREG/CR-6075 to reflect the peer reviewer's comments and suggestions. NUREG/CR-6075 was then published independently to this supplement report.

Following the comment, response, and rebuttal process, two working group meetings (consisting of a subset of the original peer reviewers), were held in May 1994 to resolve two key residual concerns-initial conditions and model validity. Participation in the working group meetings is noted in Table A.1. Lastly, working group participants were given an opportunity to comment on the completed NUREG/CR-6075, Supplement 1. Their comments have been addressed in this report to the maximum extent possible.

Because of the length of this Appendix, the following index is useful in locating the desired material.

1. Comments, responses, and rebuttals

A.	Reviewer A, pp. A-4	J.	Reviewer J, pp. A-137
B.	Reviewer B, pp. A-14	K.	Reviewer K, pp. A-141
C.	Reviewer C, pp. A-39	L.	Reviewer L, pp. A-162
D.	Reviewer D, pp. A-54	M.	Reviewer M, pp. A-171
E.	Reviewer E, pp. A-65	N.	Reviewer N, pp. A-185
F.	Reviewer F, pp. A-71	O.	Reviewer O, pp. A-189
G.	Reviewer G, pp. A-95	P.	Reviewer P, pp. A-221
H.	Reviewer H, pp. A-104	Q.	Reviewer Q, pp. A-223
I.	Reviewer I, pp. A-136		

2. Minutes of Working Group, pp. A-224.

3. Working group comments on NUREG/CR-6075, Supplement 1, pp. A-238.

Table A.1. Names and affiliation of the peer reviewers

Members of the Peer Review Group		
Names	**Affiliation**	**Working Group Participation**
T. Ginsburg	Brookhaven National Laboratory	
P. Griffith	Massachusetts Institute of Technology	
R.E. Henry	Fauske & Associates, Inc.	IC, MV
M. Ishii	Purdue University	MV
M.S. Kazimi	Massachusetts Institute of Technology	
S. Levy	S. Levy, Inc.	IC, MV
J.E. Meyer	Massachusetts Institute of Technology	
M. Modarres	University of Maryland	IC, MV
F.J. Moody	General Electric Company	MV
B.R. Sehgal	Royal Institute of Technology, Stockholm	
J. Shepherd	California Institute of Technology	MV
D.A. Wesley	EQE International, Inc.	
R.J. Witt	University of Wisconsin	
Other Reviewers		
F. Eltawila	U.S. Nuclear Regulatory Commission	
H. Esmaili	Energy Research, Inc.	
W. Minners	U.S. Nuclear Regulatory Commission	
B.W. Sheron	U.S. Nuclear Regulatory Commission	

IC = Initial Condition Working Group
MV = Model Validity Working Group

Comments by Reviewer A

Review Comments on NUREG/CR-6075

I. DCH Initial Conditions

Sections Related to Comment 1:

- Executive Summary (b)
- Section 3.0 Quantification of Initial Conditions
- Section 3.3 Qualification of Primary Pressure and Temperature

The authors try to quantify the risk of the DCH problem in the Zion plant by using the probability analyses combined with a simple phenomenological model for key physical processes. Since the model is not mechanistic, it is important to use relatively conservative initial and boundary conditions. This will allow the analysis to cover all spectrum of accident conditions which may not be easily identified by mechanistic approaches. However, in their analysis, higher initial pressures for the primary system (up to 15 MPa) or larger break sizes (up to 1 m) have not been considered in the base spectrum of accident conditions. In a probability based analysis this type of exclusions should be avoided, otherwise the results can depend strongly on who performs the analysis. The purpose of this type of analysis is to put a number on the risk of a low probability accident having great uncertainty. Too restrictive ranges on the initial and boundary conditions may lead to a number representing a partial risk which can be considerably lower than the true total risk.

RESPONSE A1: *The reviewer argues that more conservative initial conditions are necessary because the models are not mechanistic even though they model the "key physical processes". This implies that capturing the key phenomenology with a simple model is somehow inferior to a detailed model that tries to model most everything that appears to be occurring. We disagree with this implication in general (for example, some CHF mechanisms are still open to investigation, but this does not stop us from using correlations).*

As a matter of philosophy, we try to avoid unnecessary conservatisms when available information suggests otherwise. NUREG-1150 assigned a 0.02 probability of bottom head failure at full

RCS pressure. More recently, SCDAP/RELAP calculations at full system pressure consistently predict RCS failure well before melt relocation into the lower plenum. A 1 m hot spot was observed at TMI-II, and the reviewer seems to suggest that a rupture this large would have occurred. We disagree, our reasoning for limited hole sizes is as follows. The TMI-II hot spot covered several lower head penetrations; consequently, we believe that rupture (had it occurred) would have been local for the reasons cited in the text. Furthermore, large strain is a predicted precursor to rupture. This ballooning will likely stress the welds on a penetration; consequently, a tube ejection is a likely precursor to rupture.

II. Model Limitations

Sections Related to Comment II:

- Section 2.0 Probabilistic Framework
- Section 4.0 Quantification of the DCH Phenomenon
- Appendix D Prediction of DCH
- Appendix E Two-cell Equilibrium Model for Predicting DCH
- Section 6.0 Results and Sensitivity

The basic assumptions of the CLCH model are as follows:

1. The molten debris is extensively dispersed in the cavity in a short time.

2. The total surface area of debris upon entrainment is very large such that the energy transfer and chemical reactions are limited by the availability of steam during the entrainment process.

3. The subcompartment traps instantaneously a major part of the dispersed debris, thus it turns off most of the debris-steam interactions.

4. A small fraction of debris can go to the dome section and react with steam further.

The TCE model uses very similar assumptions. The major difference is that TCE treats the cavity and subcompartment together.

The CLCH model is an oversimplification of the true mechanisms of the debris dispersal. The separate effect tests as well as simple mechanistic models on the entrainment and de-entrainment indicate that the following processes actually occur.

1. Some of the molten debris can be transported out of the cavity by its own momentum before the steam discharge.

2. Once the steam discharge occurs the ejection of the debris from the cavity is very rapid. During this time about half of the remaining molten debris is entrained as small droplets.

3. The remainder of the debris is ejected as liquid film without being dispersed.

4. As soon as the molten debris hits the bottom of the seal table room, it is de-entrained.

5. Some of the de-entrained debris can be re-entrained by steam in the subcompartment because of the relatively high gas velocity caused by the stagnation flow near the bottom of the real table room.

6. Most of this re-entrained debris cannot be carried over to the dome section due to the reduced steam velocity in the vertical vent sections, thus it gradually settles in the subcompartment. During this time, the steam-debris interaction can continue.

This summary indicates that the steam-debris interaction can occur both in the cavity and the subcompartment. The relative magnitude of the interactions in these two components depends on the initial pressure and the break size.

The CLCH or TCE model cannot describe these true mechanisms due to the oversimplification. Both of them use a single coherence ratio as a scale of the steam-debris interaction time. However, it can be said that the over-estimating of the cavity interaction and under-estimating of the subcompartment interaction have a compensating effect. Therefore, for cases with relatively mild interactions in the subcompartment, these models can correlate the integral test results well.

RESPONSE A2: *The TCE and CLCH are simple, but we disagree that they are overly simple because they capture the first order effects. Cavity phenomena are complex: entrainment, deentrainment, reentrainment, agglomeration, fragmentation, stratified gas velocities, etc. Mechanistic modeling of these processes may be impractical. Nonetheless, we have a reasonable expectation that thermal and chemical interactions in the cavity can achieve equilibrium (see Response M3), and comparisons of predictions with data seem to confirm this expectation. In any case, the assumption of thermal and chemical equilibrium in the cavity are clearly conservative. We do not believe that significant interactions in the subcompartment are possible in Zion geometry. Coherent blowdown gases largely displace the subcompartment atmosphere to the dome. The potential for continued interactions between coherent steam and dispersed debris in the subcompartment are irrelevant since we expect thermal and chemical processes to reach equilibrium in the cavity. Some small interactions with noncoherent blowdown gases may be possible in the subcompartment; but by this time, the debris stream (inertia dominated) and the gas stream will largely be separated (even in the subcompartment). Most debris, however, will be trapped, and any interactions of noncoherent blowdown with trapped debris will also be minimal because the surface area for interactions is largely lost (i.e., no longer highly fragmented) and the gas velocities are substantially lower.*

The applicability of the models is limited essentially to the cases when the subcompartment entrainment is not significant. This condition can be met when the initial primary system pressure is moderate ($\leq$ 8 MPa) and the break size is small ($\leq$ 40 cm). These are the conditions similar to most of the integral tests. Therefore, the models are applicable within their database.

RESPONSE A3: *We agree with the reviewer that the models are applicable within the range of their database. However, we do not interpret this statement the same as the reviewer. In the reviewer's opinion, this means only the subset of initial conditions where the RCS pressure is*

less than 8 MPa and the hole size is less than 0.5 m. This is good enough for our purposes because we have set forth a basis for these conditions as part of our base quantifications. Not surprisingly, these conditions also represent the main range for the Integral Effects Tests, which represent the main database used in this resolution. These experiment conditions where not arrived at arbitrarily, but under the guidance of the DCH Technical Review Group (TRG) which was a follow-on to the earlier SASM work. More importantly, our models are interpolating on a database that extends to 13 MPa pressures and 0.6 m hole sizes. We see nothing in these tests suggesting that somewhat more intense conditions will lead to a new behavior that is not reflected in the existing database and the TCE and CLCH models. We are confident that the models are appropriate even for the sensitivity studies at slightly larger pressures (16 MPa) and hole sizes (.7 m). We note, however, that we have carried out sensitivity studies (of an arbitrary nature) with 20% carry over to the dome (which is in the direction of the reviewers concerns about model applicability under more intense conditions); and the results show no cause for concern.

It should be pointed out, however, that the validity of the models becomes increasingly questionable as the initial and boundary conditions are changed to a higher pressure and a larger break size. Two particularly important transitions can occur at these extreme conditions. One is the occurrence of the critical flow at the cavity exit and the other is the onset of entrainment in the vertical vent sections of the subcompartment. The supersonic jet is highly dispersal. In either case, the subcompartment may not act as a effective debris trapping structure. For these cases, the debris is highly dispersed in the subcompartment and the dispersed corium can be transported by the steam flow into the dome section in a large quantity. This implies that the steam-debris interaction can be very extensive. Because of these two bifurcation phenomena, it cannot be expected that the models can be extrapolated to the extreme conditions of the higher steam velocity.

In the sensitivity analysis, the CLCH and TCE models are used to study these extreme conditions. The results show some self-limiting pressurization even at these conditions. However, these results are the consequence of the oversimplifications in the models and may not represent realistic conditions.

The above discussion indicates that the DCH models have significant limitations. However, in their analysis the uncertainty or the applicability of these models has not been addressed. This is a serious shortcoming of the report.

RESPONSE A4: *Flow from the cavity is already choked in most of the experiments conducted to date. We have not seen any evidence for an entrainment transition from the subcompartment to the dome in experiments conducted at three different scales, with real materials, with hole sizes up to ~0.6 m (full scale equivalent) and with driving pressures up to ~13 MPa. In any case, we performed a scoping calculation using a Kutadeladze criterion for the onset of entrainment from the subcompartment,*

$$Ku_c = \frac{(\rho_g V_g^2)_{SUB}}{(\rho_d g\sigma)^{1/2}} = \frac{\dfrac{\dot{m}_{RPV}^2}{\rho_{g,SUB}\, A_{SUB}^2}}{(\rho_g g\sigma)^{1/2}} \approx 10.$$

The dynamic pressure in the subcompartment can be related to the flow rate from the breach in the RPV. Using standard choked flow expressions (isentropic blowdown), the critical RCS pressure can be calculated for the onset of significant entrainment from the subcompartment, through the vents, and into the upper dome:

$$P_{RCS} \sim \left[\frac{Ku_c \rho_g\, (\rho_d g\sigma)^{1/2}}{C_d^2} \left[\frac{A_{SUB}}{A_h}\right]^2 \left[\frac{RT}{f_\gamma}\right]_{RCS} \right]^{1/2}.$$

We use the following representative values for Zion: critical Kutadeladze number, Ku_c^{-10}; discharge coefficient for RPV breach, $c_d \sim .6$; melt density, $\rho_d \sim 8000$; cross-sectional area for vertical flow in subcompartment, $A_{SUB} \sim 600\ m^2$; gravity, $g = 9.8\ m/s^2$; gas constant for steam, $R = 462$ J/Kg/K; RCS gas temperature, $T \sim 800K$; function of isentropic exponent for steam, $f_\gamma \sim .445$; surface tension, $\sigma \sim 1$ N/m; gas density flowing through subcompartment, $\rho_g \sim .3$ kg/m^3. For a 0.7m hole diameter in the RPV, we conclude that pressures in excess of four times the system set point (i.e., 4 x 16 = 64 MPa) would be required to initiate any significant entrainment to the dome. Any such calculation is inherently conservative since debris does not easily follow streamlines; consequently, debris is expected to impact structures and deentrain.

III. Reliability of Risk Oriented Accident Analysis Methodology

The reliability of the ROAAM depends on:

1. sufficiently accurate estimate of the initial and boundary conditions, and conservative estimate of the probability distributions of these.

2. reliable phenomenological models which can be applied over whole ranges of the boundary and initial conditions, and

3. in depth uncertainty analyses of the models.

As pointed out in the specific comments, the analyses on all these three areas seem to have some deficiency. The study in NUREG/CR-6075 gives an impression that the analyses are carried out rather hastily.

RESPONSE A5: *Of those parameters affecting DCH loads, some are fixed (when well known), some vary over prescribed ranges when the uncertainty is not too large, and others are treated in bounding fashion or through the use of splinters when the uncertainties are large. We believe that the models are applicable, even for the sensitivity studies of full pressure and large ruptures. Furthermore, the models have been validated over a range of conditions approaching those suggested by the reviewer. DCH processes can be quite complex, so we treat most processes with a bounding or conservative bias. Thus, modeling uncertainty and uncertainties in initial and boundary conditions are treated.*

REBUTTAL FROM REVIEWER A

1. DCH Initial Conditions

Comment on Response A1

The reviewer's initial comments implied that the simple DCH models (CLCH and TCE models) were phenomenological models based on the global observation of simulated DCH phenomena in several integral facilities. The actual key phenomena for corium dispersion and de-entrainment have not been observed directly nor measured in these integral tests. However, the results of the global observation have been used in the model as a database for the coherency factor. It appears that from the global observation the authors simply postulated the phenomenological models which may or may not represent the true physical mechanisms.

The separate effects experiments give a great insight to the basic mechanisms of the corium dispersion as indicated in the reviewer's first comments, the separate effect test results show that two fundamental assumptions of the models are only marginally good under the nominal integral test conditions. These two basic assumptions of the models are: 1) the complete dispersion of molten materials in the cavity, and 2) the instantaneous de-entrainment of molten materials in the subcompartment. At the nominal Sandia integral test conditions, less than half of the molten materials should have been dispersed in the cavity. The remaining mass go out as liquid film. Hence the reactions in the cavity can be considerably over estimated in the model. In the subcompartment, the de-entrainment process is not instantaneous, therefore there is a considerable amount of coherent steam available there. The proposed models seem to use two compensating assumptions to get a right answer.

It should be noted that the reviewer also prefers a simpler model capturing the key phenomena over a very detailed model having everything in it, simply because the analyst does not know what is important. On this point we are in full agreement. The reviewer is not against the basic approach of the authors. However, in the absence of detailed observations and measurements, the phenomenological modeling for key phenomena may miss important mechanisms outside of the database.

With the above mentioned model uncertainty, limited database and scaling uncertainty, the reviewer thinks that conservative boundary and initial conditions should be used in DCH evaluations. The accident scenario leading to the DCH phenomena itself is a highly unlikely and low probability phenomena. Under these conditions, many parameters including the primary system pressure, break size and molten mass discharge amount are difficult to estimate accurately.

II. Model Limitations

Comments on Response A2

The reviewer has no problem with the approach of the authors, if they are focusing on the prediction of the integral test results. However, one should remember that there is a big gap between the prototypic DCH and integral tests. The proposed model strongly depends on the two assumptions mentioned above and the value of the coherency factor. The thermal and chemical equilibrium in the cavity is limited by the available amount of steam through the coherency factor. Therefore, this model may not be called absolutely conservative. The subcompartment is not necessarily irrelevant even under this equilibrium condition for the cavity. If a part of the molten materials is dispersed in the subcompartment, it will continuously react with the new steam. Similar reactions occur when the de-entrainment process is not instantaneous. This steam should be considered coherent.

Comments on Response A3

The authors stated that their models were interpolating on a database that extended to 13 MPa pressures and 0.6m hole sizes. However, the reviewer thinks that this statement is misleading unless there are integral tests run simultaneously at 13 MPa and 0.6m break. If these conditions occurred in two different tests, then applying the model to conditions at 13 MPa with 0.6m hole size should be considered as a significant extrapolation, because these two parameters tend to amplify the DCH load independently.

Comments on Response A4

It was surprising to find that the authors used the Kutadeladze criterion for the onset of entrainment which was developed more than 30 years ago. There are much better correlations that have been developed since that time. The second point is that the critical flow area for the entrainment in the subcompartment is the region above the cavity exit and below the seal table room. A simple potential flow analysis can show that the gas velocity here is much larger than that based on the total vertical flow area. If the authors use these considerations, it is easy to show that with 0.7 m hole size and 13 MPa pressure, the molten materials is almost completely dispersed in the horizontal flow direction in the subcompartment. The velocity in the vertical vent section is close to onset of entrainment velocity of 60 m/s. Thus, there is a good possibility for the significant thermal and chemical interactions between the debris and steam in the subcompartment and potential for considerable debris dispersal into the upper containment.

Comments on Response A5

As the authors stated in the response, they used different approaches to different parameters. There should be a more uniform approach using probability distributions. If the parameter is well known and does not change much then the PD should have narrow spectrum whereas for a parameter with large uncertainty, a broader and flat PD should be used.

The authors really did not respond to the last comments related to the need of the in-depth uncertainty analysis of the models.

Comments by Reviewer B

As per your request, I have reviewed NUREG/CR-6075 (SAND93-1535) and the comments dated July 30, 1993 submitted by N.R. Ortiz from Sandia, those of July 20, 1993 written by J.L. Rempe of INEL, and those of July 28, 1993 prepared by D.L. Knudson of INEL. My findings can be summarized as follows:

GENERAL COMMENTS

1. NUREG/CR-6075 helps improve the perspective and reduce the concern about Pressurized Water Reactor (PWR) large dry containment failure from Direct Containment Heating (DCH).

RESPONSE B1: *We agree.*

It is unfortunate that at the same time it appears to have launched an emotional debate among engineers involved in the DCH issue. There may be several reasons for the strong emotions being voiced: they could be due to a desire by some to close the DCH issue prematurely, while others want to indefinitely pursue its resolution, or again, it may be caused by some wanting to use realistic estimates while others prefer to employ much more conservative conditions. I believe the fundamental reason for the debate may be a failure to recognize that we lack information and understanding of the processes and phenomena involved in DCH and that a much better consensus could have been reached by discussing our lack of knowledge frankly and accurately. If such an approach had been implemented it would have helped identify the current shortcomings in information and how to go about resolving the most significant remaining areas. Since all the material being reviewed was generated by contractors working for the NRC, NRC management had the responsibility of looking for and achieving a less emotional resolution.

RESPONSE B2: *We now know a great deal about DCH in an integral sense. Well scaled experiments have been performed to resolve first order issues concerning the effect of physical scale, the impact of using simulant materials instead of corium, the effect of different containment geometries, the role of cavity and containment water, and the impact of hydrogen*

combustion. Nearly universal acclaim for the testing program has resulted from the collaboration of the DCH Technical Review Group (representing universities and industry), the National Laboratories (SNL and ANL), and the sponsor (NRC). It is clear that the database does not, nor was it intended to, provide quantitative validation of all the separate effects processes that contribute to DCH. We are well along a clear path to final resolution of DCH. Specifically, we have an outstanding database, well validated models, and a focused framework for resolution in NUREG-6075. It is part of the ROAAM process, however, to address further comments and accept input from peer reviewers.

For example, NRC could have formed three groups to deal with and reach a consensus (allowing for a minority position if necessary) about

- *Core melt progression up to and including pressure vessel failure which established the initial conditions for DCH.* Lead for this group should have been vested at INEL with participation from Sandia, ORNL, and the MAAP developers (FAI).

- *DCH data modeling and correlation.* Lead for this group should have been given to Sandia with participation from UCSB, ORNL, ANL, and EPRI.

- *Containment Structural Fragility.* Lead for this group should rest with Sandia with participation from ORNL, INEL, and EPRI.

These three assessments could be integrated by the NRC on an independent subcontractor selected by the NRC and the final report so generated could then be submitted to a Peer Review. I have provided details about his more constructive approach to DCH resolution because it may be still timely and desirable for the NRC to implement it (G-1).

RESPONSE B3: *We recognize that the final step in ultimate resolution involves obtaining broad consensus on focused aspects of the problem. We believe that additional sensitivity studies, performed in coniunction with the peer reviewers, will suffice to address all concerns regarding Zion.*

2. The drop in DCH concern developed in NUREG/CR-6075 comes about from three principal sources which have been arranged in order of importance in this writer's judgement:

- Much more benign DCH initial conditions. The amount of molten materials being released, its metallic content, the reactor pressure at the time of ejection and their probability of occurrence are considerably less severe than used previously. The authors of NUREG/CR-6075 are convinced that they have selected bounding or conservative conditions. I believe that they tend to be "optimistic" as discussed later.

- Recently completed DCH tests show that only a small fraction of the ejected material will reach the containment. This finding is not subject to debate, and my comments primarily deal with lack of physical modeling, uncertainties in the results, and their extrapolation to other containment configurations.

- Development of integral models which allow correlations to be formulated for so-called coherence ratios during the DCH tests. This approach makes sense physically and my comments again deal with the need for improved physical modeling, uncertainties in the models and their extrapolation to other containment configurations.

I believe that the use of less optimistic initial conditions and a more critical discussion of the limitations of the DCH data, their modeling and uncertainties would have produced a more credible (and defensible) report.

RESPONSE B4: *We disagree with this summary statement, and our reasons will be made clear in our responses that follow.*

The containment conditional failure probability (CCFP) may increase to between 10^{-1} and 10^{-2} for the Zion plant. This would still meet the NRC safety goal of defense-in-depth (CCFP $< 10^{-1}$). <u>I recommend that the NRC modify NUREG/CR-6075 to produce a more defendable version by reducing its optimism and providing uncertainty evaluations</u> (G-2).

RESPONSE B5: *We disagree. NUREG-6075 is the first integrated assessment of DCH, including uncertainties. We cannot comment on the safety goal, but it makes no sense to be purposefully pessimistic solely because we will meet the safety goal anyway (which we do believe). This could have some undesirable ramifications when considering extrapolation to other plants.*

3. The Risk Oriented Accident Analysis Methodology (ROAAM) developed by the University of California at Santa Barbara is and has been useful in resolving selective outstanding severe accident issues. However, as pointed out by the authors of NUREG/CR-6075, "in order to apply the ROAAM methodology, one must understand the physics of an NPP accident well enough to identify a small set of the key physical processes that control the outcome." In the case of DCH, the outcome is highly dependent upon the employed initial conditions, i.e., melt release conditions after failure of the reactor pressure vessel. The key physical processes determining those initial conditions are far from being fully understood today. The authors of NUREG/CR-6075 have the responsibility to show that they have compensated for the lack of physics and understanding in the initial conditions and in the two causal relations they utilized to predict the pressure of the containment and its failure (G-3).

RESPONSE B6: *We compensate for lack of physics and understanding by considering four splinter scenarios, by attempting to envelope the expected initial conditions, by using bounding models for containment loads, and by using the utilities best assessment of Zion's fragility. Our reviewer responses on specific issues clarify our views on these issues.*

INITIAL CONDITIONS COMMENTS

1. The authors have decided to formulate their own set of initial conditions rather than to rely upon such severe accident system codes as SCDAP-RELAP5 or MAAP-4. In fact, SCDAP-RELAP5 calculations were carried out specifically for the authors of NUREG/CR-6025 to quantify the initial conditions at vessel breach. The SCDAP-RELAP5 results should have been coupled to a reactor vessel failure model to develop a set of initial conditions for DCH. INEL should have been asked to perform additional sensitivity studies to deal with potential areas of uncertainty, e.g., location of crust

failure, heat transfer from released corium to water, formation and size of hot spots in the lower head, etc. (IC-1). This approach was used in the Code Scaling, Applicability, and Uncertainty (CSAU) Evaluation Methodology (NUREG/CR-5249) and it worked satisfactorily. Also, the writer is aware that EPRI and DOE have carried out similar severe accident calculations for the Zion plant with MAAP-4 and comparison of MAAP-4 and SCDAP-RELAP5 results could provide considerable perspective about the initial conditions and their uncertainties (IC-2).

RESPONSE B7: *It is not appropriate to apply the CSAU methodology to define DCH initial conditions. As a prerequisite, CSAU requires a frozen code with well validated separate effects models and well validated integral results. This maturity clearly does not exist in the area of late phase core melt progression. A number of SCDAP/RELAP calculations were made available for this effort. If we use them in a self-consistent fashion, then our DCH quantifications are conservative and the predicted loads are very low. For example, with no pump seal leaks, surge line and hot leg failures were predicted long before melt relocation into the lower head, so complete depressurization of the RCS is expected. For pump seal LOCA scenarios, the predicted pressure at vessel breach was always below ~4 MPa if heat transfer to the water was turned off. Repressurization to 9 MPa was predicted when heat transfer to the water was calculated, but this repressurization came at the expense of quenching all the melt, so there was no molten material to participate in DCH. However, such blind use of codes should only be used to answer "what if" type questions. Qualitatively, we find that SCDAP/RELAP calculations support two of our key assessments: spontaneous failure will occur at full pressure prior to bottom head failure, and the metallic content for Scenarios I and II is quite low. We welcome any additional insight offered by MAAP-4 calculations for Zion. We were not aware that EPRI and DOE have carried out such calculations. We believe that a continued examination of code results in a critical and consistent fashion will confirm the bounding nature of our initial condition quantifications.*

2. The authors have applied considerable judgement in developing their set of initial conditions. They may be correct but, at this stage, the proposed initial conditions represent only their personal views. As pointed out by K.D. Bergeron, this may give them an unfair advantage because the individual peer reviewers are being asked to provide comments starting from the authors' position. This can lead to considerable debate and a protracted process and I shall dwell here only upon my principal concerns:

RESPONSE B8: *No comment.*

- It is not clear how the authors assign to the initial conditions of Figures 3.3 to 3.9 their probability level and the definitions in Table A.1. If it involves only their expert judgement, it should be so stated. However, since the designed probability values in Figures 3.3 to 3.9 eventually enter the containment failure probability, some supporting explanation should be given, for example, for the decision to use declining probability values by a factor of 1/10 (IC-3).

RESPONSE B9: *One should not confuse our use of "judgmental degrees of belief" with "statistical expectation". Table A.1 in NUREG-6075 provides some descriptors for various levels of judgmental degrees of belief. The numerical values assigned to these descriptors are completely arbitrary (any scale will do). We note, however, that our assigned number scale roughly corresponds to confidence levels at 1, 2, or 3 standard deviations. The numerical values are only necessary to propagate information through the arithmetic. Different scales will produce distributions of different shape. The important thing is to reinterpret the final quantitative result in terms of the same descriptors for judgmental degree of belief. See Response C9 for more details on how we make our judgements based on the physics of the process.*

For example, in the case of Scenario I, what is the basis in Figure 3.3 for the amount of UO_2 ejected to only grow by 10 metric tons as the probability decreases by a factor of 1/10. Why is a factor of 1/3 or 1/5 not more appropriate? Furthermore, the association of the "physically unreasonable" characteristic with a probability value of 10^{-3} may not be compatible with consideration of seismic events and some initiating events (large pipe break) in nuclear risk assessments which fall below 10^{-3}. For that reason, it may be desirable in Figures 3.3 to 3.9 to show values corresponding to probabilities of 10^{-3} rather than assume that they are zero.

- The initial conditions were formulated by a selective process using results from many sources possibly not compatible with each other. For example, great reliance is placed upon the TMI-2 accident, but the TMI-2 accident was a

reflooded accident and its application to a dry severe accident scenario (e.g., going from Scenario I to III) is questionable. More specifically:

RESPONSE B10: *A predictive and fully consistent approach for addressing late phase core melt progression does not exist. This was our motivation to envelope credible initial conditions. We use as much information as a basis for our quantifications. Some phenomena observed at TMI-II (i.e., crucible formation and failure) is representative of a broader class of accidents, so we can look at TMI-II for insight. Other phenomena (e.g., repressurization accompanied by vessel flooding) lead to conditions unique to TMI-II-like scenarios; and as such, must be considered in this more limited context.*

Dry core crucible scenarios are enveloped by Scenarios I and II. The amount of fuel relocated to the lower plenum is less than considered in Scenarios I and II for two reasons. First, a dry core crucible may not be as strong as one formed under wet core conditions, so an earlier failure of the crucible may be expected. Secondly, dry core scenarios favor a flatter (less hemispherical) crucible, so spill-over at the edges is expected with less melt bottled up in the crucible. There is a potential for some of the metallic blockage to melt and drip into the lower plenum where the metals will oxidize and freeze. In such a state, this relocated metal is no longer of interest to DCH. Partial relocation of the metal blockage does not alter the stability of the oxide crucible.

To answer "what if" type questions concerning large quantities of metals, we have performed a point calculation using the SASM melt composition and Zr oxidation fraction as recommended for rupture failure of the RCS with all other conditions specified in a manner consistent with Scenario II. The predicted containment pressures (using the TCE model) for Scenario II type conditions is 0.62 MPa. This containment pressure produces no intersection with the Zion fragility curve, but this illustrates the importance of metals in the melt.

a) The TMI-2 accident occurred at full pressure and it makes sense to have the base case of Scenario I be at full pressure (IC-4).

RESPONSE B11: *TMI-like scenarios with a reflooded RPV do not lead to significant DCH loads. First, it is worth noting that the RCS had depressurized to ~5 MPa at the time that melt relocation occurred. Repressurization occurred at TMI when the block valve was closed. The*

operators also started the pumps and initiated high pressure injection, reflooding the RPV with saturated water. The lower head at TMI did not fail; but if it had, only ~20 mt of oxidic melt would have been coejected from the RPV with sufficient quantities of saturated water (~100 mt) to quench the melt about 20 times during the cavity interactions.

The decision to use 8 MPa in all scenarios of Table 3.1 is questionable and results from SCDAP-RELAP5 should be used to vary that range.

b) In all accident scenarios, it is presumed that the outer row of fuel assemblies is excluded which automatically limits the material to be ejected to 70 mt. There are severe accident scenarios where the outer fuel assemblies will join the molten pool depending upon the reactor pressure, the natural circulation behavior and presence or lack of water in the bottom head. I believe a variation in that number from 0.7 to 0.9 may be more appropriate (IC-5).

RESPONSE B12: *Current system level codes do not support the notion that 90% of the core can participate. Even prior assessments of initial conditions, such as SASM, did not start from this premise. Code calculations indicate that cooling of the outer assembly, primarily to the core barrel, is sufficient to prevent their melting. Excluding only the outer assembly means that ~70% of the core can be in a degraded state.*

c) The amount of metallics in the ejected materials of NUREG/CR-6075 is quite small. It may have been based upon the TMI-2 accident, which again was a reflooded accident. One can visualize significant metallics reaching the bottom head especially during dry accidents (IC-6). Also there may be inconsistencies in having upper structure temperatures above the melting temperature of steel and no molten steel.

RESPONSE B13: *We expect that scenarios leading to significant melting of upper plenum steel will also lead to surge line or hot leg failure. This was certainly the case in the MELPROG (NUREG/CR-4742) calculations that played such a role in defining the SASM melt composition. Of the SCDAP/RELAP calculations supplied to us for Zion, only the case of a 250 gpm/pump leak lead to melting of upper plenum steel, and in this case the RCS pressure at vessel failure*

was only 3.2 MPa. The full system pressure case, 480 gpm/pump leak case, and the case of a stuck open PORV did not lead to melting of upper plenum steel, so it is not clear to us why the 250 gpm/pump leak case should. We also note that the SCDAP/RELAP calculations do not predict any Zr in the relocating melt.

d) In the TMLB' scenarios, the authors have relied upon gradual relocation. However, there could be TMLB' dry scenarios with massive relocation (IC-7). According to the authors, they were excluded because they are considered under Scenario II but Scenario II involves wet rather than dry cores (IC-8).

RESPONSE B14: *See Response B13.*

e) For a side failure of the crust, the amount of molten materials leaving the molten pool is taken at 50 percent to relatively agree with the TMI-2 results. A crust failure near the bottom assumes 75 percent is released. A slightly lower side crust failure location could raise the 50 percent to 60-70 percent and, in the case of a bottom failure, it is interesting to note from Tables D.3 and D.5 that 85% to 95% of the molten material was released from the melt generator for the SNL/IET series of tests (IC-10).

RESPONSE B15: *A range of failure locations are considered in our melt mass quantification. We do not expect a crucible to fail massively in a downward direction because the accumulation of blockage is greatest there and natural circulation patterns favor side failure. This is why we chose 75% relocation as a reasonable upper bound. There is no relationship between the 85-95% release values from the experiment melt generators and the expected release fraction from a in-core crucible. Melt generator retention is controlled by freezing on the walls with some possible effect from blowthrough during melt ejection. The experiments do not attempt to simulate the in-core crucible and its failure, and interpretation of the melt generator as representing in-core behavior is incorrect.*

f) The work of Dosanjh and Pilch (1991) is used to justify that "as steel becomes molten, it will relocate to the bottom of the debris bed and refreeze on the lower head." It is not clear why the molten steel does not

arrive with molten UO_2 and the molten steel due to its lower density does not float above the molten UO_2 (IC-11).

RESPONSE B16: *The work of Dosanjh and Pilch starts with debris bed already on the lower head that is heating up from a fully quenched state. Their analyses have nothing to do with relocation dynamics to the lower head. Gradual relocation into the lower head leads to the debris bed that is the starting point of their analyses.*

- The authors have selected four scenarios to estimate the initial conditions for DCH: two SBLOCA scenarios with crucible formation, both wet, one with early vessel penetration failure and the other with early vessel rupture; and two TMLB' scenarios with gradual relocation, both dry, one with delayed penetration failure and the other with late vessel rupture. I believe that <u>it would be preferable for SBLOCA to consider both a wet scenario at design pressure and a dry scenario at reduced pressure each with a penetration and a vessel failure. Crucible formation should be assumed for all four cases and both a side and a bottom crust failure should be included</u>. This provides a total of 8 cases for SBLOCA. In the case of <u>TMLB' dry scenarios, it might be preferable to consider both gradual and massive relocations at reduced pressure (incorporating the pressure rise associated with relocation). The massive relocation results from crucible formation similar to that formed during SBLOCA. Here again both a side and bottom crust failure should be considered</u>. This provides a total of 6 cases for TMLB'. As previously noted, it is important that the results for dry cases not be extrapolated from wet ones (IC-12).

RESPONSE B17: *All cases proposed by the reviewer are already enveloped by the four scenarios discussed in NUREG-6075. The reviewer suggests a bifurcation on vessel failure mode (penetration vs. rupture). This is already considered in our base quantification. The reviewer suggests a bifurcation on crucible failure location. We already use crucible failure location to define the uncertainty in the amount of material that relocated to the lower head. The reviewer suggests a bifurcation between crucible formation under dry core and wet core conditions. We expect dry core conditions to be similar or bounded by wet core conditions (see Response B10). Lastly, the reviewer suggests considering high pressure and intermediate pressure cases for SBLOCA scenarios. We have not identified any full pressure scenarios that do not first lead to*

spontaneous depressurization of the RCS; except perhaps, TMI-II like scenarios with a reflooded RPV, and they do not lead to significant DCH loads (see Response B11). However, full pressure cases have already been treated as part of the sensitivity studies.

- On page 87, it is stated "that uncertainties in these processes (core-melt progression, melt relocation to the lower plenum, and lower head failure) are treated by considering splinter scenarios that envelope the expected phenomenologies." While the splinter scenarios can recognize alternate courses for core melt progress, they do not provide for uncertainties within a selected scenario. <u>There would be considerable merit to estimating the principal uncertainties prevailing during each scenario</u> (IC-13). For example, estimates of the uncertainty in reactor and initial containment pressure, reactor coolant system, pressure vessel and containment temperatures, initial hole size, melt temperature...etc., may be helpful to establish the overall uncertainty with each scenario.

RESPONSE B18: *The principal uncertainties are already covered in NUREG-6075. This led us identify four splinter scenarios to envelope the expected range of behavior. The distributions themselves reflect uncertainties within each splinter scenario. Other uncertain conditions (eg., as hole size, RCS pressure, melt temperature) are treated in a bounding fashion. Containment loads are relatively insensitive to some parameters such as containment temperature and pressure. Here again, we treat these parameters in a bounding fashion. The TCE and CLCH models are also developed from a bounding perspective. Taken as a whole, our assessments and models are already biased towards higher containment loads. Any additional refinement, however, will come with a disproportionate burden of justification that would be even more difficult to defend.*

- The comments made in the INEL memoranda tend to reflect similar positions to those offered above. I found these comments to be appropriate and valuable even though, at the time of this write-up, I did not have a chance to review several of the INEL references they utilized.

RESPONSE B19: *Our responses here reflect how we would respond to similar INEL comments. Reviewer comments on specific INEL input are addressed in our responses.*

DCH TESTS AND MODELING

1. The DCH test program was extensive and well done and those involved deserve to be told that it was a job well done.

RESPONSE B20: *We agree! Here is an example where consensus has been achieved between parties with very diverse perspectives on DCH. The very successful DCH test program is an example of successful teaming between a five member Technical Review Group representing (universities and industry), the National Laboratories (SNL and ANL) who performed and documented the tests, and the NRC who sponsored the activity.*

There is one remaining concern and it is whether the range of tests parameters was changed enough to validate the scaling of all significant phenomena. Let us consider, for instance, the amount of material dispersed outside the compartment. First, it is important to note that a prescribed value of 5 percent is used in the Zion power plant calculations, but three of the 11 tests in Tables D.5 and D.6 exceeded that value. Second, the increased values of material dispersal in the three highest tests tend to be associated with an increased pressure or a large reactor vessel hole size. Arguments are offered on page 50 which rely upon inadequate modeling of the cavity and seal table room to justify the 5 percent dispersal. But they do not deal with the issues of increased reactor pressure and hole size. Also, note that during one of the tests, the loadings were high enough to produce a hole in the crane wall. Consideration should be given to tests to determine the impact of reactor pressure and hole size upon the amount of material dispersed beyond the subcompartments and to the need to evaluate the integrity of the cavity and seal table room due to DCH loads (DCH-1).

RESPONSE B21: *Tests exhibiting significantly increased transport to the dome are always associated with nonprototypic structural damage to the floor, ceiling, or side walls of the seal table room mockup. Specifically, we blew a hole in the bottom of the seal table room (and the cranewall in one test) leading to enhanced line-of-sight carryover of dispersed debris to the dome region. These structures were not and could not be scaled for their structural strength in the experiments. Furthermore, they underwent repeated testing causing dehydration of the concrete, so accumulated damage and failure resulting from impingement of the melt is not surprising. Measured pressure differences are small across the seal table room. We note that the*

experiment data were obtained under prototypic ranges of RCS pressure and (scaled) hole size. We believe that transport to the dome is largely a geometric effect involving flow areas and line of sight arguments. The Zion cavity is set directly in the ground (not freestanding), so structural damage to the cavity is not expected.

2. Since the test data are used to calculate the coherence ratios in the proposed models, estimates of the uncertainties associated with the test data and to what degree they impact the calculated coherence ratios are needed (DCH-2). For example, in the TCE model, it is noted on Page E-42 that "measured values of the melt ejection fraction, melt dispersal fraction, and melt transport fractions are used in the model predictions. Measured values of the coherence time are also used in the comparisons." Experimental uncertainties in all those parameter should be estimated as well as in the measured pressures. In particular, the uncertainty in the coherence time may be quite large because, as pointed out on page E-58, "the interpretation of the entrainment interval is still inherently subjective." The Sandia comments tend to strongly reinforce that view and the emphasis should be on a realistic estimate of the uncertainties in measured pressure and in the parameters calculated from test data.

RESPONSE B22: *The main uncertainty is in extracting R_τ from the experiment data. This uncertainty is shown explicitly in Figs D.8 and D.9, which compare CLCH predictions with experiment data. For the TCE coherence correlation, the uncertainty in the correlation itself bounds the measurement uncertainties. We remind the reviewer that uncertainties in R_τ are propagated through the plant calculations. Redundant pressure measurements in the tests are taken at multiple locations in the vessel. The measurement uncertainty in peak containment pressure for any given test is negligible. However, the stochastic uncertainty in peak pressure in any given test is estimated to be ~ +/-20% (at 95% confidence). By stochastic uncertainty, we refer to the range of peak pressures that would be observed if you could repeat the same test many times. The estimated stochastic uncertainty is obtained from four pairs of replicate tests that could be identified in the database.*

3. Both the CLCH and TCE models are integral models. They both rely upon coherence ratios and percent of dispersed material beyond the subcompartments to predict plant DCH performance. They both appear to agree with the test data; yet, their formulation for coherence ratios on pages 48 and 49 show very different dependence upon the

parameters appearing in Eqs. (4.1) and (4.3), e.g., the reactor hole diameter. It is important to resolve the discrepancy in the scaling formulation for the CLCH and TCE coherence ratio and to identify the preferred equation (DCH-3). As pointed out in the Sandia comments, the discrepancy may be indicative of not enough variation in the parameters of the integral tests to discriminate among the CLCH and TCE coherence ratio formulation. I tend to favor the TCE model because a comparison of measured and predicted pressures is presented in Figure E-6. A similar comparison of predicted to measured pressures is recommended for the CLCH model (DCH-4).

RESPONSE B23: *As stated in the text, it is not necessary to adjudicate between the TCE and CLCH formulation of the coherence ratio because both formulations are being applied in an interpolation mode (i.e., both are tied to a prototypic database for the conditions arising from our base quantifications), so both are adequate for the application.*

4. Both the CLCH and TCE models rely upon overall energy balances and equilibrium conditions to predict the test and reactor pressures. Physical representations are not provided for such DCH phenomena as material entrainment from the cavity, de-entrainment in the subcompartment, temperature and hydrogen distributions, and size of particles. Phenomena important to DCH predictions need to be identified and their physical modeling considered (DCH-5). For example, modeling of the dispersion of materials beyond the subcompartments could be useful to answering comment (DCH-1). As pointed out by Sandia, the models appear to neglect the heat and hydrogen generated by the materials left in the cavity and subcompartment. The authors need to show that they play a minor role (DCH-6).

RESPONSE B24: *Trapping of debris in the subcompartment is the chief mitigating feature of DCH, as confirmed by over 30 prototypic experiments conducted in realistic plant geometries with driving pressure up to ~13 MPa and with hole sizes up to ~.6 m. The prototypicality of the results themselves is sufficient justification to rely on this basic phenomena. Coherence of debris dispersal and RCS blowdown is also of added importance, and suitable models are developed. Trapping and coherence are the foundations of the TCE and CLCH models. This allows us to treat all other cavity/subcompartment interactions in a bounding fashion.*

For RCS pressures of most interest to DCH (~8 MPa), we expect nearly complete dispersal from the cavity with only a small amount of material retained as a thin frozen film on cavity surfaces. We do not see how this small amount material can contribute in any significant way under conditions where DCH is the greatest threat to the containment. CONTAIN calculations (NUREG/CR-6109) confirm that interactions with nondispersed debris are negligible (~3% effect); and even here, we believe that CONTAIN overpredicts the effect. The dominant retention mechanism observed in the experiments with driving pressures greater than ~6 MPa is the freezing of this film on all cavity surfaces. Here, the energy of this small amount of material goes into the walls and the resulting quenching effect reduces the potential for continued oxidation and heat transfer.

5. On page E-70, it is stated that "the TCE model is developed with a conservative bias: however, comparison with experiment data shows that nature favors the extreme and the conservative bias is very close to best estimate." <u>This view of TCE best estimate instead of the repeated use of "conservative" and "bounding" adjectives should be reflected in the main body of the report</u> (DCH-7).

RESPONSE B25: *This statement will be stricken from text.*

6. The bypass of material through the annular gap around the RPV is based upon only three tests (Table 1.1). Two of the tests were performed with a Surry geometry and the third test was carried out with a "Zion-like" geometry. The proposed model to predict the bypass relies upon a simplified flow area ratio. <u>A more rigorous model of the annular bypass should be developed</u> (equal pressure drop through the annulus and through the cavity subcompartment to containment might be considered) <u>and its uncertainty estimated</u> (DCH-8).

RESPONSE B26: *A more detailed model of dispersal through the annulus was developed based upon equal pressure drops through the cavity and the annulus.*

$$f_g = \frac{\dfrac{A_g}{\sqrt{K_g}}}{\dfrac{A_g}{\sqrt{K_g}} + \dfrac{A_T}{\sqrt{K_T}}} \approx \frac{A_g}{A_g + A_T}$$

This model reduces to the area ratio recommended in Appendix I when the total loss coefficient (K) is the same in the gap and the tunnel. Since contraction and expansion losses at the restrictions play such a important role in the two directions, the loss coefficients are indeed similar, and the simplified model is justified, as also confirmed by the data. An expanded development of the model and its uncertainty will be presented in the text.

7. The conclusion that plant geometry has a minimal impact upon DCH may not be supportable. Only two integral facilities (Zion and Surry) have been tested. Also, Figures E.9 and E.10 show that the constant in the correlation for coherence ratio increases from 4.045 for the Zion plant to 5.90 for the Surry plant, or a 50 percent increase. Again, a model explaining the difference in the coherence ratio correlations for the Zion and Surry plants is needed to generalize the Zion report to other plants (DCH-9).

RESPONSE B27: *We disagree. Prototypic tests in three geometries have already supported the conclusion that the details of subcompartment geometry are not important. The potential geometry dependence of the coherence ratio is weak and of little concern since Zion and Surry like cavities are representative of most PWRs, except CE plants and ice condenser plants (which already have been excluded from the extrapolation). The essential feature of plant geometry is that most of the dispersed debris be trapped in the subcompartment before it can mix with the upper dome. This is supported by prototypic integral experiments, which have been conducted with detailed representations of the Zion and Surry subcompartment structures. It should be noted that the subcompartments in these two plants are really quite different. Lastly, the LFP tests crudely simulated containment compartmentalization with a simple concrete slab placed above the cavity exit. All these tests, with very diverse representations of the subcompartment, can be predicted with the TCE model, which knows nothing about any of these subcompartment details. Thus, we see no strong effect of geometry on DCH loads. These validations use measured values of the coherence ratio, which Appendix E suggests might be cavity specific*

(Appendix D sees no significant dependence on geometry). IDCOR characterized plants according to their cavity design. Most existing PWRs, excluding ice condenser plants and CE plants, have cavities similar to Zion or Surry, so the appropriate data base already exists. In reality, however, Appendix E shows there is a great deal of overlap in the Zion and Surry data primarily because of the uncertainties in estimating the coherence ratio from measurements. In fact, a correlation with combined Zion and Surry data does about as well as the Zion data alone, so the apparent difference due to geometry may not be real. This is illustrated in Figure E.1 in NUREG-6075.

Due to the short amount of time available to review NUREG/CR-6075, I may have additional comments after my examination of the other reports and some of the references. Please note that I have made no statement on the autoignition temperature because my knowledge of that topic is limited and I have deferred my comments about containment fragility until I complete my review of the report on that topic.

I hope that these comments are helpful. They were numbered from G-1 to G-3, IC-1 to IC-13, and DCH-1 to DCH-9 to help focus the concerns and to help the authors prepare a reply.

RESPONSE B28: *No comment.*

REBUTTAL FROM REVIEWER B

General Comments

1. Many, if not most, of my concerns were not responded to. In most instances, insufficient specifics were provided to justify the authors' positions as the subsequent detailed comments illustrate.

2. The peer review process being followed is not very satisfying. It has led primarily to the authors restating their views rather than developing a consensus between the authors and the reviewers.

3. The authors have decided not to respond to the summary of the peer review comments prepared by Energy Research, Inc. (ERI). That summary reveals many concerns and issues where the reviewers are close to agreement and that perspective should have influenced the authors to modify their positions.

Specific Comments

Comments on Response B2

The response does not deal with the comment that "we lack information and understanding of the processes and phenomena involved in DCH" and that "we should discuss our lack of knowledge frankly and accurately." Instead of covering the remaining lack of information and understanding about DCH, the authors, in their response, primarily describe the experimental program performed to date. There is no debate about the merits of the experimental program (see my comment and response B20).

Comments on Response B3

My comment suggested another and possibly preferable approach to reach a consensus about DCH. The response proposes that "additional sensitivity studies will suffice to address all concerns regarding Zion." Additional sensitivity studies cannot deal with all concerns as long

as they continue to use the same basic assumptions, models, and interpretations of the data. I continue to urge the approach suggested by my comment.

Comments on Response B4

The authors disagree with my summary statements but choose not to explain why. In fact, my first conclusion is that the authors have used much more benign DCH initial conditions in terms of amount of molten materials being released, its metallic content and the reactor pressure at the time of ejection, and a comparison of the SASM initial values to those in NUREG/CR-6075 supports that view. My second summary statement is the "DCH tests show that only a small fraction of the ejected material will reach the containment" which again confirms the authors' view that "trapping of debris in the subcompartment is the chief mitigating feature of DCH" (see B24). It is possible that the authors do not agree with my subsequent qualifications that there is a "lack of physical modeling, uncertainty in the results and their extrapolation to other containment configurations." Such qualifications are appropriate and tend to be supported by similar comments by other peer reviewers. My third summary statement deals with the integral modeling selected and its shortcomings and again those views are supported by several other peer reviewers.

Comments on Response B5

Here again there is no response to the statement "that the use of less optimistic initial conditions and a more critical discussion of the limitations of the DCH data, their modeling and uncertainties would have produced a more credible (and defensible) report." Instead, the authors state that "it makes no sense to be purposefully pessimistic." The intent was to be more realistic and not purposefully pessimistic.

Comments on Response B6

I cannot agree with the response because the four splinter scenarios account for differences in scenario behavior and not for lack of physics and understanding. Similarly, it is not obvious that the authors have enveloped the expected initial conditions and that their models for containment loads are bounding.

Comments on Response B7

There may be a genuine difference of opinion about the use of system codes. However, the use of SCDAP/RELAP is necessary because it makes it impossible to deal with many other scenarios and to recognize differences in reactor designs. The authors claim that they have used SCDAP/RELAP results in a self-consistent fashion but it is not clear what is meant by that statement. Their responses show that the authors have tended to utilize SCDAP/RELAP results when they support their views, i.e. no metallics (and no Zr), percent of core molten (see B7, B12, and B13). However, they have chosen to disregard SCDAP/RELAP findings that might be contrary to their views., i.e., increased pressure at time of vessel failure due to molten material heat transfer to water, melting of upper plenum in the 250 gpm/pump leak case. An alternate consistent approach would utilize SCDAP/RELAP analyses as carried out until changes to that severe accident system code have been agreed to and implemented by INEL. It is recognized that SCDAP/RELAP needs several improvements but one should be careful to include both favorable and unfavorable improvements (see ERI/NRC 93-214).

This area covering Figures 3.3 to 3.9 in NUREG/CR-6075 remains one of disagreement.

Comments on Response B9 and C9

The authors claim that they first try to identify the best estimate value based on the physics of the process and assign to it an order of unity. However, the authors do not explain how they reached their best estimate values, e.g. 20 mt in scenario 1, and why an increased value is not more appropriate. Also, the authors have not explained why that best estimate value grows by only 10 mt as their probability decreases by a factor of 1/10 and why they consider a probability of 10^{-3} to be physically unreasonable. In C9, the authors state that "they identify reasonable bounds based on the physics of the process" and that a probability of 10^{-2} was assigned to the bound. Because DCH involves a multitude of processes, one could argue that the probability of the bound could be much lower or that the amount of molten material involved is much larger. In other words, Figures 3.3 to 3.9 are primarily subjective and that subjectivity needs to be reviewed and, if necessary, modified by an independent panel of experts (see comment which produced response B4).

Comments on Response B10

I agree with the authors statement that "a predictive and fully consistent approach for addressing late phase core melt progression does not exist." In view of that statement, it is not clear how the authors can claim that "dry core crucibles are enveloped by Scenarios I and II and that the amount of fuel relocated to the lower plenum is less than considered in Scenarios I and II." Similarly, their bases for a dry core crucible being flatter (less hemispherical) and less strong than a wet crucible are not provided. Furthermore, metals can reach the bottom head prior to vessel failure not only through melting of the metallic blockage but also from being present in the core molten pool and being relocated to the bottom head through the crucible break. The calculation of predicted containment pressures for Scenario II with the SASM composition "illustrates the importance of metals in the melt" and this concern needs to be dealt with before resolving the DCH issue.

Comments on Response B11

I agree that wet scenarios do not lead to significant DCH if they involve 20 mt of molten material, reduced pressure, and considerable water in the reactor vessel as occurred at TMI-2. The issue is whether there are wet scenarios involving more that 20 mt of molten material, increased pressure, and less water in the reactor vessel which may be produced by such errors as closing block valves or reseating of power operated relief valves...etc., recognizing that their probability of occurrence may be smaller.

Comments on Response B13

Here again, the issue of SCDAP/RELAP not predicting metallics in the melt needs to be revisited. As pointed out in ERI/NRC 93-124 more eutectics and other chemical interactions as well as more complicated phase diagrams may provide different answers and have to be incorporated in SCDAP/RELAP particularly in case of dry scenarios.

Comments on Response B14

It does not provide an answer to why dry scenarios with massive relocation were excluded.

Comments on Response B15

The response puts emphasis on natural circulation patterns and a side failure of the crucible to justify the selection of a 75% relocation as upper bound. It is important to recognize the limitations of the natural circulation analyses, including the use of a homogeneously mixed core and uniformly distributed heat generation. There could be stratification of materials and heat generation as well as solids being present in the pool which might impact the natural circulation results. Also, with reduced circulation of the pool, more heat will be directed to the bottom of the crucible because the pool is the deepest at that location and failure could occur at the bottom of the crucible. The uncertainties of natural circulation patterns have to be considered in selecting the upper bound of material relocation from the pool to the bottom head and the possibility of a bottom release must be included (possibly at a lower probability level).

Comments on Response B16

The authors confirm that "the work of Dosanjh and Pilch starts with debris bed already on the lower head that is heating up from a fully quenched state" and that "their analyses have nothing to do with relocation dynamics to the lower head." My concern was related to relocation dynamics and the possibility not of a gradual release, but of a single large relocation from the bottom of a dry crucible. The work of Dosanjh and Pilch may not be compatible with such conditions.

Comments on Response B17

I cannot agree with the authors' statement that all cases proposed by the reviewer are already enveloped by the four scenarios discussed in NUREG-6075. For example, the authors state that "we expect dry core conditions to be similar or bounded by wet core conditions (see response B10)". As noted under B10, it is not clear how the authors reach that conclusion while at the same time stating that "a predictive and fully consistent approach for addressing late phase core melt progression does not exist."

Comments on Response B18

The authors claim that they have considered the principal uncertainties and have tended to treat the models and their parameters in a bounding fashion. Their view is that their assessments and models are already biased towards higher containment loads. This is debatable. For example, their models do not bound the DCH tests (see comments on response B25). Similarly, the possibility of a penetration failure as assumed by the authors is now more remote (see reference after D16) so their range of hole size needs to be re-examined, particularly when the authors admit in response C31 that there is a "lack of experimental data" relevant to vessel rupture under DCH conditions.

Comments on Response B21

The authors report that "tests exhibiting increased transport to the dome are associated with structural damage to the floor, ceiling, or side walls of the table room mockup." This is an important comment which suggests the need for a methodology to predict containment loads within the cavity and an assessment that structural damage will not occur under plant configurations and actual concrete conditions. Also, this comment supports, to some extent, that the containment loads are dependent upon cavity and subcompartment configurations.

Comments on Response B22

It is important to recognize uncertainty in the experimental data separately from uncertainties in the model. For example, the experimental uncertainty in peak pressure at the one sigma level needs to be considered in the plant predictions of DCH loadings unless it can be shown that the model results always exceed the DCH test values by that amount.

Comments on Response B23

There is considerable merit to adjudicating between the TCE and CLCH formulations of the coherence ratios. If this is not done, it will require calculating plant loads with both models and utilizing the highest values. This is particularly true in the case where the hole size is varied. Also, the authors were not responsive to providing a comparison of measured to predicted pressures for the CLCH model.

Comments on Response B24

The important roles of trapping of debris in the subcompartment and of the coherence of debris dispersal and RCS blowdown are recognized. However, it is important to evaluate that there are no other important processes or parameters that could influence the results, e.g., hydrogen formed or transported early into the cavity.

Comments on Response B25

The removal of the statement on page E-70 that "the TCE model is developed with a conservative bias; however, comparison with the experimental data shows that nature favors the extreme and the conservative bias is very close to best estimate" (a similar statement is included on page E-7) is very disturbing because it is a concluding remark in Appendix E and because it reflects behavior of the TCE model versus the DCH test results. Figure E.2 shows that the TCE model correlates well the experiments when the atmosphere was inert and that it does not bound the data. Similarly, Figure E.6 shows that the predicted ΔP's from the TCE model for all experiments do not always bound all the DCH test data. As stated on page E-45, they are in good agreement with the test results and their one sigma rms is 0.290 MPa with a bias of 0.050 MPa.

Comments on Response B27

In NUREG/CR-6075, the authors reported different correlations for the coherence ratio for the Zion and Surry plants, which tends to support the conclusion that geometry has an impact (Figure E.9 and E.10).

The authors now point out that "a correlation with combined Zion and Surry data does as well as the Zion data alone, so the apparent difference due to geometry may not be real" (Figure E.11). It should be noted, however, that the constant in the correlation for coherence ratio in Figure E.11 is 4.863 compared to 4.045 for the Zion data in Figure E.9 or about 20% greater with about the same sigma rms. The predictions of containment loadings for Zion with the TCE model will need to be modified to reflect this increase. Also, the authors will have to explain why the correlation in Figure E.11 is applicable to other cavity configurations and to what

degree the one sigma rms in Figure E.11 needs to be enlarged to cover other cavity configurations.

CONCLUDING REMARKS

1. The ROAAM process as applied by the authors in this case is quite frustrating because the input accepted from peer reviewers was very limited. This approach has forced this peer reviewer to reinforce the differences between his views and those of the authors, and by doing so, quite possibly decrease the chances of reaching a consensus.

2. The principal difference between the peer reviewer and the authors is the need to establish and assess the uncertainties in the initial conditions for DCH, the DCH test data, and the proposed integral models to predict containment loading. Without addressing this issue in a complete and tractable way, the DCH resolution will be reopened until it is dealt with. We should be willing to identify what we do not know, e.g., the lack of physics and understanding, and to provide uncertainties or margins to cover them. We should be especially interested in dealing with what we do not know that we do not know.

3. The many disagreements highlighted in this communication does not in any way detract from my initial statement that "NUREG/CR-6075 helps improve the perspective and reduce the concern about Pressurized Water Reactor (PWR) large dry containment failure from Direct Containment Heating." The opportunity to close the DCH issue is good if we are all willing to accept increased containment loadings to satisfy the common points raised by all the reviewers.

COMMENTS BY REVIEWER C

Before delving into specifics of the report, its appendices and comments from INEL and SNL, I would make the following general remarks in line with the instructions provided by the NRC:

1. The authors have concluded that, for some nominal set of parameters, the containment failure probability is very low (order 10^{-3}). Although the authors have conducted sensitivity studies based on pushing certain parameters in directions to purposely enhance DCH, I would like to see the parameters pushed a little further, if for no other reason than to see just what kind of conditions would lead to an intersection with fragility curve that would make people squirm. There is a physical basis as well for pushing these parameters our further, and this is discussed in more detail below. I'm not quite yet prepared to concede that DCH is a non-issue.

2. The tome submitted by SNL points out in great detail the simplifications and uncertainties in the two models that form the basis for predicting Δp's in containment. The concern is expressed that the agreement between prediction and experiment is the result of compensating conservative and non-conservative assumptions and may not reflect an actual NPP scenario. While this argument has some merit, it isn't at all clear to me that there exists a superior approach to tackling this problem.

RESPONSE C1: *We disagree with the suggestion of pushing the sensitivity studies further and with the reviewers concern about compensating assumptions. Our detailed responses will be addressed in the following comments.*

3. I have no objection to the approach used by the authors, but there are a number of inaccurate statements in the text and appendices that need to be corrected.

RESPONSE C2: *We will consider these on a case by case basis.*

4. The authors have done a reasonable job in Section 7.0, Extrapolations, describing the conditions under which this analysis could be applied to PWRs other than Zion. I have nothing further to add in this regard.

RESPONSE C3: *No comment.*

There are instances in which TMI-2 related data are incorrectly cited. On page 22, it is stated that the TMI-2 vessel repressurized to 2 MPa, whereas the Δp during the relocation event appeared to be about 2 MPa, raising the pressure from about 9 to 11 MPa. On page 32, the estimated melt temperature on the TMI-2 lower head is cited as 2000 K, when in fact companion sample examinations indicate temperatures exceeded 2600 K.

RESPONSE C4: *Typos will be corrected.*

The documents received from INEL indicates there are also a number of instances where SCDAP output is either cited incorrectly or it is implied that SCDAP output is incorrect. The authors are encouraged to contact INEL and work with them to make sure results/predictive capabilities are reported accurately.

RESPONSE C5: *We will consider these on a case by case basis.*

There are a couple of instances where results are reported that require some qualification. At the top of page 31, the work of Boucheron is cited indirectly to indicate that "at least 15 mt of oxide must solidify in order to heat the lower head to a point where it loses its strength and ruptures." Parametric studies performed in support of the TMI-2 VIP program indicates that vessel failure depends on a large number of parameters. The assumptions made in Boucheron's analysis should be listed so that this prediction can be evaluated by the reader and compared to other analyses.

RESPONSE C6: *Boucheron's assumptions are listed in the cited reference. The text has been modified to qualify the approximate nature of this number.*

On page 34, my work is cited as resulting in a 25% reduction in failure time to creep rupture due to the presence of a hot spot. In fairness to the authors, this is an accurate reproduction of what I submitted. However, since that time, many additional analyses have been performed. It would be better to indicate that the presence of a hot spot can reduce rupture times by tens of percent, depending on the background heat flux and the failure criterion used in the analysis. If the authors wish to continue to use 25% as a representative number, that's fine, but it should be understood that the response will vary with specific conditions.

RESPONSE C7: *We understand that 25% is not an exact number and that the actual value is on the order of 10s of percent depending on the conditions. The text will be modified to reflect this. This does not alter the quantifications.*

The authors seem to have an aversion to considering the combination of full system pressure with an oxidic melt. I understand the arguments given in defense of choosing 8 MPa, but the "peculiar" operator actions at TMI-2 indicate that full system pressure (or close to it, 14.5 MPa) is quite possible under conditions where an oxidic melt is interacting with the lower head. Given that the CFP is so low, why not consider the combination of pressure and oxidic melt? Along the same lines, the discussion in Appendix F indicated autoignition temperatures near 800 K are possible. Why not consider this limit as long as you're pushing the parameter? Finally, there is reason to believe that the hole size may exceed the bounding value of 0.7 m given on page 58. Although the contention that the initial opening will be local is plausible, the arguments given in Appendix J to defend the arrest of the opening, and the subsequent control by ablation, are not convincing. I am not saying that the failure will be global, only that this issue needs to be approached differently before it can be confidently put to rest. But aside from that, why not consider a case with autoignition temperature of 800 K, system pressure of 16 MPa (with oxidic melt) and a hole size of 2.0 m, just to see where that pushes the CFP? As of now, all you know is that if you push the parameters around the ranges you've described, you can at most get the CFP to move from 10^{-3} to 4×10^{-3}. What would it take to make it equal unity?

RESPONSE C8: *TMI-like scenarios with a reflooded RPV do not lead to significant DCH loads. When the block valve was closed, the RCS pressure started to increase from its minimum of ~5 MPa. The operators also started the pumps and initiated HPI so that the RPV was filled with subcooled water. The potential for DCH at TMI must be examined in a consistent fashion. Specifically, the vessel did not fail; but assuming that it did, we would have to consider 20 mt of oxidic melt <u>coejected</u> from the RPV with a vessel filled with subcooled water, which has the potential ~20 times over to fully quench the melt in the cavity.*

We disagree with the recommendation to perform sensitivity studies to determine what is containment threatening. Such arbitrary and excessive sensitivity studies only confuse the picture by lending credibility to clearly unrealistic conditions. We already know that containment threatening conditions can be postulated (i.e, D.C. Williams, NUREG/CR-4896; Reviewers H and O). We already know what areas can be arbitrarily contrived to maximize pressure:

hydrogen production and combustion. With regard to hydrogen production, the metallic content of the melt and RCS pressure play key roles.
We know that DCH loads are not sensitive to oxide mass. The real challenge is to focus on what's credible so that you can shed unnecessary and arbitrary conservatisms.

See Response C31 with regard to arrest of hole size.

Specific Comments: Appendices

A. The Risk-Oriented Accident Analysis Methodology (ROAAM): My background is not in PRA, and I am unable to provide much input on this appendix. I defer to other reviewers to decide if the charge made by SNL is accurate, namely that, "Appendix A contains biased arguments that are misrepresentative. Furthermore, Appendix A contains considerable criticism of well-accepted and thoroughly reviewed methods and results." As a reader, I would suggest that additional discussion is in order regarding how one assigns an order of magnitude likelihood to a particular process. Perhaps specific examples contrasting processes with clearly different levels of likelihood would help non-experts appreciate Table A.1.

RESPONSE C9: *Each quantification in this report is a specific example. Additional examples can be found in the Mark-I Liner Report. The process we follow is quite simple and uses the subjective levels of belief listed in Table A.1. First, we try to identify the best estimate value based on the physics of the process; and as such, we assign a probability of order unity. We then try to identify reasonable bounds based on the physics of the process. Usually, we judge that physical conditions leading to the bound are highly unlikely, so we assign a probability of* $\sim 10^{-2}$. *We then try to fill in the distribution. We note that the numerical values for the subjective probabilities are arbitrary and only necessary to carry out the arithmetic. The important thing is to reinterpret the numerical results with the same subjective scale.*

B. Gradual Relocation Versus Crucible Phenomenologies: This appendix makes the case that a different relocation process than observed at TMI-2 is plausible and must be included as a splinter in ROAAM. I have no objections or comments on this appendix.

RESPONSE C10: *No comment.*

C. The Main Lower Head Failure Bifurcation: There are a number of places where text needs to be revised to reflect INEL concerns and results of more recent TMI-2 simulations. In the first paragraph on page C-2, SCDAP/RELAP5 is quoted as predicting lower head rupture at 1700 s. INEL indicate vessel failure times ranged from 400 to 4500 s, and that these analyses represent lower bound, rather than upper bound, times. The authors need to consult with INEL to assure the statements made here regarding SCDAP/RELAP5 are accurate.

RESPONSE C11: *The statement in the text is correct, but first we note that the vessel failure times are not used in any quantitative fashion for this Scenario. They are merely quoted to give the reader some perspective on the sequence. The SCDAP/RELAP calculations that were supplied to us, and as referenced in the report, show a vessel failure time of ~ 1700 s for the case where the melt was fully quenched. Without quenching, the reported failure times by SCDAP/RELAP are ~ 400 s. The important point is that these calculations were intentionally biased to accelerate lower head failure; and as such, they cannot be used to assess realistic failure times. The text will be modified to indicate the range of failure times predicted by SCDAP/RELAP and to qualify the use of such numbers. None of the SCDAP/RELAP calculations supplied to us indicate a failure time of 4500 s. The statement that available analyses represent an upper bound to the rupture does not refer to the SCDAP/RELAP calculations as clarified above.*

The authors quote a paper I've submitted regarding the acceleration of creep rupture failure due to the presence of a hot spot on the lower head. In fairness to the authors, the number they report is an accurate assessment of what I submitted. However, the TMI-2 Vessel Investigation Project has been an on-going process, and many additional cases of hot spots on different levels of background heat flux have been undertaken. The actual percent reduction in time to failure is sensitive to level of background heat flux and failure criterion. I am currently revising the paper to reflect these new results, and the text here should be changed to be consistent with those revisions. I would suggest the statement, "Witt (1993) has shown that hot spots on the lower head could accelerate rupture, by 25% in the TMI-2 application that was analyzed" be revised to "Witt (1993) has shown that hot spots on the lower head could decrease rupture times by tens of percent, depending on the background heat flux outside the hot spot and the failure criterion used in the evaluation." If the authors wish to use a 25% reduction as a representative value and a basis for their arguments, that's fine, but there should be more

indication that the actual number varies from case to case. The use of this number with a longer rupture time from INEL will change the lower bound value of 1000 s quoted at the end of this paragraph.

RESPONSE C12: *Our response, C7, applies here as well. The lower bound of ~ 1000 s comes about by adjusting the 1550 s bound of Pilch and Dosanjh to account for hot spot accelerated rupture.*

The authors will also need to change the statement just before this to, "Such hot spots can form as a result of partially quenched material accumulating in a nonuniform manner on the lower head." The reference to jet impingement should be eliminated for the following reason. The hot spot in this context refers not only to a temperature range, but a time interval; that is, the hot spot is not defined as such unless it is sustained for a period of time required to induce metallurgical changes and present a potential structural threat. Jet impingement does in fact produce very high temperatures on the vessel surface, but this lasts only for tens of seconds as the high thermal conductivity of the steel flattens the temperature gradient.

RESPONSE C13: *We disagree. The actual shape and form of failure will be associated with some nonuniformity of damage to the lower head. Although the temperatures eventually flatten out, the nonuniformity of damage is not wiped out.*

At the bottom of page C-4 and top of page C-5, some additional modifications are necessary. At the bottom of C-4, the authors argue that "the hot spot not only accelerates rupture, but the rupture is likely to occur around such penetrations because of local stress concentrations that are double the free field stress." In the revised paper, Witt (1993),there is some discussion of the failure mode, and a local failure of the type described here is indeed plausible, but I would suggest it's plausible for other reasons. Stress concentrations, while existing around discontinuities such as instrument penetrations, are usually associated with elastic stress fields, and the stress states in the vessel under these conditions are not going to be elastic. When we examine the deformation of the lower head in the presence of hot spots and a significant background heat flux, we observe substantial rotations of the vessel midplane from its original geometry, especially when the failure criterion is based on mechanical instability. An

instrumentation tube penetrating the vessel will be severely twisted as it attempts to resist this rotation through its support outside the vessel. Although I can't describe this process quantitatively, it seems intuitive that the deformations and stresses in the vicinity of the tube under these conditions would be extreme (perhaps far worse that those associated with an elastic stress concentration) and that a local rupture around the tube is indeed plausible.

RESPONSE C14: *We believe that the existence of a penetration will initiate a local failure. Stress concentrations near the penetration will lead to a nonuniformity of damage in that region that will not be wiped out even if plastic deformation or creep occurs. The reviewer is correct that the penetrations will be severely twisted as the vessel deforms, and that this is an additional source of local stress in the vessel. Lastly, large vessel deformations are expected prior to rupture. This deformation, or ballooning, will stress the welds holding the penetrations in place. Thus, we envision that tube ejection can occur as a precursor to rupture. The text will be modified to reflect this expanded discussion.*

A more difficult issue is deciding whether the rupture opening remains small, and is subsequently determined by ablation, or enlarges as it depressurizes. Additional comments regarding this issue are reserved for a discussion of Appendix J. The statement, "Witt's (1993) TMI-2 calculations stop short of defining the rupture size because of numerical difficulties", should be removed. My algorithm, like most approaches, treats the structure as a continuum. Explicitly simulating the presence of a tear and subsequently tracking its propagation would represent an extremely aggressive simulation and is probably beyond the current state-of-the-art. (I don't believe that well-regarded finite element codes like ABAQUS have this capability either.) Deciding how large an opening results will not be possible through numerical simulation and requires the input of individuals knowledgeable of how these structures actually fail. More comments follow in Appendix J.

RESPONSE C15: *No criticism was intended. We recognize that the definition of hole size is beyond the current state of the art for numerical simulations. This is exactly what we meant by our statement. The text will clarify this point.*

Finally, there seems to be a mislabelling of Figure C.4. From comments in the text, it would seem the dashed line is intended to reflect the metallic. This would otherwise imply high liquid fractions of oxide at short times.

RESPONSE C16: *Figure C-4 is labeled correctly. The figure presents results for a debris bed containing quenched fuel and steel. As the bed heats-up, you would expect the metallic components to melt first. This is what Figure C-4 says.*

D. The Prediction of Direct Containment Heating: I would recommend a paragraph at the bottom of page D-4 be included to provide more details of the relationship between the CLCH and TCE models. Are there instances where one would clearly be superior to the other? A complementary paragraph needs to be inserted in Appendix E.

RESPONSE C17: *The physics of the TCE and CLCH models is basically the same: debris/gas interactions are largely confined to the coherent portion of the blowdown. This physics is implemented in a different, but complementary, fashion in the two models; TCE is best thought of as a batch process while CLCH is best thought of as a flow process. The combustion of hydrogen plumes is also implemented differently in the two models. However, as the results of this report indicate, the two models give similar results and neither approach is preferable to the other (except as a matter of taste).*

I strongly disagree with the assertion at the bottom of page 13 that a system pressure of 14 MPa is "not possible...at the time of lower head failure." The TMI-2 pressure history contains pressures of just such a magnitude during a time following relocation which corresponds to peak local temperatures. The author may intend to suggest that, following lessons learned at TMI-2, operators would not behave in such a way as to cause system pressure to reach these levels. The way the passage is written, however, suggests that such pressures are physically impossible. This wording needs to be revised, at the very least, to make clear exactly what the authors mean.

RESPONSE C18: *See Response C8.*

In Figure D.10, and similarly in Figure E.7 (Appendix E), different pressure traces are presented. It is not clear from either of these figures just how τ_m is defined. There are two time intervals marked on Figure D.10, for instance. The pyrometer trace in Figure E.7 is potentially another basis for defining τ_m. both appendices need to include statements detailing the procedure used to determine this quantity and show it on the graphs.

RESPONSE C19: *The entrainment interval and its uncertainty is clearly marked on Figure D.10. Figure E.8 will be modified to show uncertainty ranges also. Note, however, that the required information is different in the CLCH and TCE models. The CLCH model uses the entrainment interval as input while the TCE model uses the end of the entrainment interval as input.*

At the bottom of page D-16, in the section on "Prediction of the DCH-scale, the authors describe the criteria used to exclude certain test results. The discussion here is too brief. It is stated that tests were ignored in which the determination of τ_m and/or τ_s from the available data was ambiguous. Under what conditions are τ_m and/or τ_s ambiguous? Could the authors provide two traces for comparison, one showing a case where these quantities are clearly defined and a second illustrating ambiguity? How often does rejection occur? Similarly, in what percentage of the cases was observed dispersal greater than 70%? If the cases with dispersal less than 70% are included (just as an exercise), does the agreement between experiment and prediction get substantially worse? How often was the discharge coefficient found to be too low and by what means could an internal restriction develop?

RESPONSE C20: *The attached figure is an example of where it is difficult to define the entrainment interval. Situations such as this were excluded. We expect essentially complete dispersal in the reactor applications, so we sought the most prototypic data for comparison. The cut-off point on dispersal is somewhat arbitrary, the intent was to exclude those tests where the dispersal was very poor.*

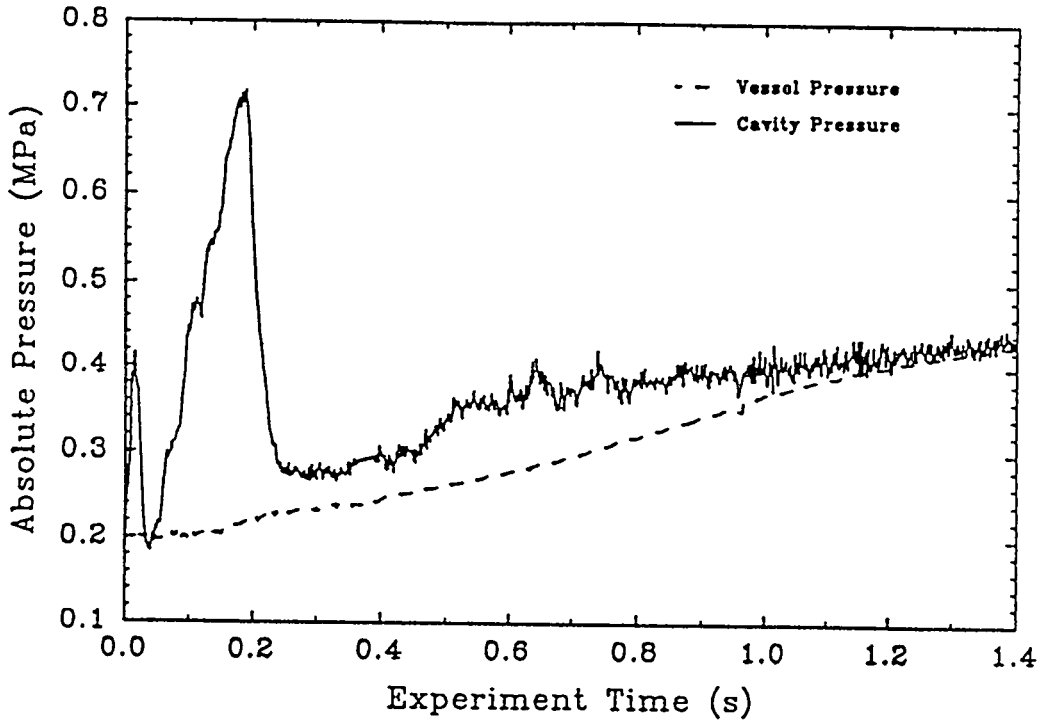

Figure 17. Cavity pressure and Surtsey vessel pressure versus time in the IET-7 experiment.

Similarly, additional explanation is needed in discussing the results on page D-19. The sentence, "Test #3 is the only one where even the L limit overpredicts the data-such a low measurement is not seen in any of the other tests and it must therefore be considered suspect," deserves more explanation. Was there no indication of the source of the problem that would lead to such a low measurement?

RESPONSE C21: *We can only speculate why SNL/IET-3 is different: the plug at the top of the seal table room remained in place and the melt/water interactions were particularly benign. These two factors have the potential to limit hydrogen production.*

E. A Two-Cell Equilibrium Model for Predicting DCH: Some of my comments on this appendix complement remarks made on the previous appendix. There needs to be more discussion of the relationship between the two models, most appropriate appended to the introduction on page E-8, and a consistent method of defining τ_m (or τ_e in this case) from the pressure or pyrometer traces needs to be described.

As in Appendix D, the authors restrict their attention to cases "where the dispersal is nearly complete (i.e., $f_{disp} \geq 0.5$) and [where] peculiar blowdown histories [are excluded]." More information, as outlined above in remarks for Appendix D, is again needed. In addition, why are dispersal fractions exceeding 50% acceptable in this case, when they needed to exceed 70% in the previous method?

RESPONSE C22: *The text describes why the 50% cutoff was chosen. Specifically model assumptions are clearly violated: cavity flow is not choked, dispersed flow assumption is violated, and gravity effects become important. Six points (out of 44 possible) fall into this category and they can be clearly identified in Table E.8 as having dispersals less than 50%. Three additional tests (ANL/IET-1R, ANL/CWTI-5, and FAI/DCH-4) are excluded because of peculiar blowdown histories. ANL/IET-1R was excluded because it had an unknown quantity of water in the melt generator. ANL/CWTI-5 was excluded because of a discontinuous blowdown history caused by valve actions. FAI/DCH-4 was also excluded because it had a discontinuous blowdown history for unknown reasons. The text will be modified to identify these tests explicitly.*

This represents my major concerns. In addition:

1. The statement at the bottom of page E-7, "This does not invalidate the conservative bias of the model. It merely means that nature favors the extreme; consequently, the distinction between conservative bias and best estimate becomes blurred," is vague. Can the authors reword these sentences to make their meaning clearer?

RESPONSE C23: *A provocative statement for sure and we will delete it from the text. Clearly, the models are developed with a bounding and conservative bias for the first order processes. When compared to experiment data, it is seen that the models also have the flavor of being best estimate. The bounding aspect simplifies the defense of the model and simplifies the extrapolation rationale to other plants. The best estimate flavor means that we do not carry excessive conservatisms. The statement in the text accurately conveys these thoughts.*

2. On page E-42, measured values of coherence time are referenced to Figure E.3, which plots measured versus predicted hydrogen generation.

RESPONSE C24: *This is a typo. The text will be modified to correctly cite Table E.8.*

3. On page E-54, the sentence on the third line from the bottom trails off.

RESPONSE C25: *This is a bad page break; text will be corrected.*

4. If M°_{g} is represented by the ideal gas law, there is a $(T^{\circ}_{RCS})^{3/2}$ power in the second brackets that offsets the $(T^{\circ}_{RCS})^{-1/4}$ in the first brackets to give a dependence on $(T^{\circ}_{RCS})^{+1/4}$, not the inverse $(T^{\circ}_{RCS})^{-1/4}$.

RESPONSE C26: *We agree; the typo will be corrected.*

F. Autoignition Temperature in DCH Events: Although this topic is outside my area of expertise, the discussion in this appendix is off in that there seems to be considerable evidence for low ($\simeq$ 800K) autoignition temperatures, while the authors conclude, on page F-7, "The threshold for more energetic events, that might be of interest to DCH, might be in the 1000-1100 K range." Objections raised by SNL regarding this selection seem warranted.

RESPONSE C27: *This comment will be addressed in Response F33.*

G. The Sandia Integral Effects Test Series: did not review.

RESPONSE C28: *No comment.*

H. Results of Direct Containment Heating Integral Experiments at 1/40 Scale at ANL: did not review.

RESPONSE C29: *No comment.*

I. The Role of the Annular Gap Around the RPV: Does this merit a separate appendix?

RESPONSE C30: *Absolutely! Debris dispersal through the gap is important because this debris bypasses the mitigation that occurs in the subcompartment. This appendix defines the method by which gap transport can be assessed for other plants.*

J. Continued Enlargement of the Initial Failure Site in the Reactor Pressure Vessel: I have no objection to those sections of the appendix which concern ablation, but section J.7, Hole Expansion Following Rupture, will have to be entirely rewritten. The problem here is that once a finite tear opens in the structure, methods used to decide if the tear grows or is arrested bear little resemblance to methods used for continuous structures. The use of a Larson Miller Parameter (LMP) under these conditions is completely inappropriate. What is needed here is input from an individual with a lot of experience in dynamic, ductile fracture. Such a person could probably devise a criterion for deciding if the tear grows or stops. The other complication is that discharge from a local region would create asymmetric loads on what might have initially been a symmetric problem. Unlike the creep problem, which evolves slowly enough to be quasi-static, the sudden discharge would have to be treated dynamically, essentially as an impact problem. The complication here is that, even if the initial tear is arrested, the asymmetric impact loads from discharge may precipitate a failure in some other region of the lower head. The problem is far more complicated than described here.

RESPONSE C31: *We disagree because the DCH situation is quite unique. Rupture is immediately accompanied by melt discharge and ablation, which has the effect of blunting any tear. In addition, rupture of the lower head will be accompanied by large strains. We expect that the rupture will be confined to regions of large strain. We've also examined this problem from the perspective of fracture mechanics and concluded that unstable crack growth is unlikely under DCH conditions. None of these perspectives is wholly suitable to the problem, especially given the lack of relevant experiment data.*

K. Comparison of Melt Mass Composition Quantifications with Prior Work: My only comment is to emphasize that INEL claims different results are predicted by SCDAP/RELAP5 than are presented here. Sections related to SCDAP/RELAP5 should be rewritten to reflect the input from INEL.

RESPONSE C32: *Reviewer comments on specific INEL input are addressed in our responses.*

Specific Comments: Evaluation of INEL, SNL Concerns

RESPONSE C33: *Reviewer comments on supplemental SNL and INEL comments have not been addressed as part of our responses.*

REBUTTAL FROM REVIEWER C

This letter is in response to author's responses to comments on NUREG/CR-6075, "The Probability of Containment Failure by Direct Containment Heating in Zion." I am generally satisfied with the response of the authors to my comments, but I would like to make one additional comment with respect to Appendix J, Continued Enlargement of Initial Failure Site in the Reactor Pressure Vessel. The authors' state in their responses, C31, that they have "also examined the problem from the perspective of fracture mechanics and concluded that unstable crack growth is unlikely under DCH conditions." I would recommend that these fracture-based analyses also be included in Appendix J so that readers are aware that more than one approach was used to evaluate the issue. I have no other comments at this time.

Comments by Reviewer D

This letter constitutes my review of NUREG/CR-6075, "The Probability of Containment Failure by Direct Containment Heating in Zion", and the attachment includes my comments on the additional material supplied by national laboratory personnel. Before presenting my review, let me say I have considered this report from the viewpoint of whether it is sufficient justification for the NRC to make a substantive conclusion with respect to this severe accident phenomenon. Hence, this consideration is separate from whether I agree completely with detailed physical mechanisms, assumptions in the analyses, application to the experiments and application to the reactor system. Moreover, this higher level evaluation needs to be made in light of the various types of reactor designs, the spectrum of accident scenarios and recovery conditions that must be considered by the NRC. In this regard, this is similar to the evaluation requested on the assessment for Mark I liner melt-through, i.e., is the approach and documentation sufficient for the NRC to make a substantive decision on severe accident phenomena?

To begin my review, I will divide the discussion into six categories:

1. Could a high pressure melt ejection (HPME) and direct containment heating (DCH) happen as a result of a spectrum of accident sequences that should be considered?

2. If HPME were to happen, what would matter in the process and are these addressed in the report?

3. What do that available DCH experiments tell us and is this addressed by the report?

4. What do the available analyses tell us and are these clearly discussed in the report?

5. What is claimed by the report and is this adequately demonstrated in the report?

6. Is the composite of the information sufficient for the NRC to make a substantive conclusion with respect to this severe accident phenomenon?

1. <u>Could a high pressure melt ejection (HPME) and direct containment heating (DCH) happen as a result of a spectrum of accident sequences that should be considered?</u>

For considerations of HPME/DCH, the accident must result in core debris relocating to the lower plenum and overheating of the reactor pressure vessel (RPV) wall, with the primary system at a sufficiently high pressure to cause high pressure melt ejection. The report is, of course, clear in this definition and considers two types of RPV failure, i.e., penetration failure or a rupture of the RPV wall. Typically, such sequences would evolve from station blackout like or small break LOCA type of conditions. In the latter case, the water injection to the RCS is insufficient to maintain the core covered, and the RCS pressure remained at least at a few MPa.

In these scenarios, the single-phase gas natural circulation from the core to the upper plenum, and possible into the steam generators (for those designs like Zion with inverted U-tube type steam generators), could experience sufficient energy transfer that the hot legs could reach temperatures that are too high for the internal pressure, i.e., they could experience a creep rupture behavior. If this were the case, the RCS would likely be depressurized to a level insufficient to support HPME. This part of the accident scenarios is discussed in the report and characterized as having a maximum pressure of about 8 MPa. I agree with this, with one exception, and that is when the damaged core is recovered as it was in the TMI-2 accident. Under these circumstances, the natural circulation could be negated and the pressure could be higher, yet the vessel could be essentially full of water. The report does not address these conditions. I believe these conditions are much less threatening to the containment but more likely to occur due to the recovery actions likely to be taken.

RESPONSE D1: *See Response C8.*

In any case, the report should address these conditions. Also, those designs with once-through steam generators (OTSGs) may not have the same magnitude of natural circulation. This should be considered with respect to hot leg creep rupture when extrapolating from Zion to other designs.

RESPONSE D2: *We agree, as stated explicitly in Recommendation B in our summary and conclusions. However, recent experimental work suggests that hot leg or surge line failures in plants with OTSGs occur on a time scale comparable to plants with U-tube steam generators. M. di Marzo's experiments (1993 NHTC) suggest that hot leg failure occurs in ~4500 - 5500 s and that surge line failure occurs in 4000 - 5000 s. These times can be compared to SCDAP/RELAP calculations for Zion (Knudson, April 1993) and Surry (Knudson, NUREG/CR-5949) under similar core heatup rates and RCS pressures. The SCDAP/RELAP calculations give ~6000 - 6500 s for hot leg failure and ~4600 - 5300 s for surge line failure. Comparing failure times, we conclude that there is no significant difference in natural circulation phenomena for OTSGs and U-tube steam generators. This comparison will be cited in the text. We note, however, that the focus of NUREG-6075 is Zion, and that extrapolation issues are intended to be addressed more completely in NUREG-6109.*

2. <u>If HPME were to happen, what would matter in the process and are these addressed in the report?</u>

   Of course, the major parameters are the mass of material accumulated in the lower plenum, the pressure in the reactor coolant system (RCS), the unreacted metals in the melt and the containment conditions. These are adequately represented in the report. However, the influence of water in the RCS, as discussed above, should be discussed since this could have a substantial influence on the heat transfer and oxidation processes. In particular, with water in the RCS, failure of the RPV would result in a release of core debris, <u>then the water</u> (some of which could flash) <u>would be discharged</u>, followed by the blowdown of the high pressure gases in the RCS. This is a substantially different set of processes than those addressed in the report and the influence of high pressure, high temperature water should be addressed.

RESPONSE D3: *See Response C8. We note that substantial mitigation was observed in SNL/IET-12, and that inadvertent coejection of saturated water has been identified as one of two likely explanations.*

Two failure sizes are considered: in an-core penetration failure and a rupture of the RPV wall. Experiments of high temperature melt submerging a full size PWR type penetration (Hammersley, et al., 1993) show a penetration would not be expected to fail.

It is appropriate for the report to consider penetration failures, but the likelihood of such failures should be stated in a manner consistent with the available experiments.

RESPONSE D4: *We treat penetration failures as splinter scenarios because we are not convinced that you can rule out failures of this type. Although we may have some opinion as to likelihood, we stop short of assigning probabilities to various splinter scenarios.*

3. <u>What do the available DCH experiments tell us and is this addressed in the report</u>?

The principal behavior demonstrated by the available DCH experiments at different scales is that internal compartmentalization of the containment building does have a substantial mitigating influence on the pressurization if an HPME were to occur. This is the main focus of the report and is adequately addressed in the report.

RESPONSE D5: *No comment.*

Another focal point of the integral experimental program is the influence of scale. Specifically, the data has shown linear scaling is appropriate and there is no significant influence of scale. Both models discussed in the report also conclude linear scaling is appropriate and this is adequately addressed in the report.

RESPONSE D6: *No comment.*

Two related aspects of the HPME/DCH process are the extent of unreacted metals in the melt discharged and the potential for combustion in the containment atmosphere. The authors have considered a spectrum of possible conditions with respect to unreacted metals. One difference between the available experiments and the reactor system is the oxidation rate of the metals. Specifically, the thermite used to simulate the molten core debris has some excess aluminum. At the melt temperature, aluminum has a significant vapor pressure and can possibly experience vapor phase burning. Conversely, the chromium used to simulate the remainder of the unreacted metals has a much lower vapor pressure and is a much better simulant for the Zircalloy in the reactor system. This difference with respect to oxidation rates should be addressed in the report.

RESPONSE D7: *The potential non-prototypicality of Al in the melt simulant is not significant, and we see no evidence to suggest that kinetic limitations to oxidation are more limiting with reactor materials. Thermite melts do include trace quantities of Al in solution with the iron phase. The potential oxidation of this Al accounts for only ~10% of the total* H_2 *reported as being produced during the test. This corresponds to about ~20% of the hydrogen produced and burned on DCH time scales. Furthermore, the vapor pressure of Al in solution with Fe is not very high. Thus, the potential for a significant vapor phase reaction does not really exist.*

We see no evidence to support the reviewers suggestion that kinetic limitations to oxidation are potentially more limiting with reactor materials. We see no kinetic limitations to oxidizing the Cr in our thermitic melts, and ANL tests using a real corium simulant do not reveal any significant kinetic limitations to oxidation. Note, however, that if the reviewers concern where true, then our model predictions would be conservative, and already we do not predict containment threatening pressures. The text will address this issue.

Of equal importance is the influence of the containment atmosphere in terms of inerting against a hydrogen burn. The experimental program has included conditions in which the containment atmosphere has been classically inerted and the results have shown burning did not occur. In fact, the experiments have shown the burning of preexisting hydrogen in the atmosphere is also very limited, if at all. Both are explicitly considered in the report, including the possibility of autoignition of the containment atmosphere.

RESPONSE D8: *No comment.*

Containment compartmentalization has a first order effect on the distribution of high temperature core debris and the oxygen in the atmosphere. Linear scaled experiments at different scales are a major step forward in understanding the accident behavior with respect to hydrogen combustion. The report addresses this effect through the use of the two interpretive models and through discussion of the potential for stratification of high temperature hydrogen in the upper containment regions. In addition, the report gives a perspective of what could be measured in future experiments to resolve any questions associated with the hydrogen behavior in the dome.

RESPONSE D9: *No comment.*

In summary, the report addresses the major issues related to the available DCH experiments. However, the specifics related to aluminum oxidation rates in the experiments should be addressed more completely.

RESPONSE D10: *See Response D7.*

4. <u>What do the available analyses tell us and are these clearly discussed in the report</u>?

The available analyses include those discussed in the report as well as integral code calculations for the spectrum of accident sequences to be considered. One of the specific evaluations from integral code calculations is the potential for creep rupture of one or more hot legs for core damage sequences at elevated RCS pressures. As mentioned previously, this is dependent on the natural circulation between the RPV upper plenum and the steam generators, which in turn is dependent on the steam generator design. Consequently, one would anticipate this circulation, for the same RCS pressure, would be different for designs with inverted U-tube designs and the OTSG designs used in B&W designs. These RCS differences are not addressed in the report and should be considered when extrapolating the results to other reactor systems.

RESPONSE D11: *See Response D2.*

Integral analyses also evaluate the core melt progression including the quantity and rate at which the melt progresses into the lower plenum. As discussed in the report, these are currently best described as parametric models. However, with some parameters, these models can calculate more melt draining to the lower plenum than is considered to have significant probability in this report. It is not clear what are realistic values for some of these parameters controlling the freezing of molten materials, the hydraulic resistance of coolant channels with frozen debris, the strength of a crust, etc. Consequently, it is difficult to determine the extent to which current integral code calculations support the probability distributions given for the material masses considered for Scenarios I, II, III, and IV. It is recommended the authors expand the justification for these probability distributions since these are central to the conclusions. One possible approach to consider, in line with the current reasoning, is that since the TMI-2 core was submerged for about half an hour before the 20 mt drained to the lower plenum, the crust

is as strong as it could be for any accident sequence. To challenge this crust requires a melt magnitude and temperature that are greater than or equal to that expected for any other sequence. If this can be justified, it would add substantially to the foundation for the melt distribution.

RESPONSE D12: *We agree. This will be noted in the text.*

5. <u>What is claimed by the report and is this adequately demonstrated in the report</u>?

The principal conclusion is that a DCH event in the Zion plant would not result in a challenge to containment integrity. This is due to the compartmentalization of the containment, the lack of a line-of-sight path for significant debris to be transported to the dome region, and the strength of the Zion containment building. Mechanistic considerations of these features through the ROAAM do not produce any significant intersections of creating large containment loads and the containment fragility curve. Hence, a challenge to containment integrity is considered to be physically incredible.

Is this adequately demonstrated? Appropriate causal relationships are defined and are applied to four generalized accident sequences likely sufficient to consider the spectrum of conditions that could be expected during an accident. However, failure of the RPV with water in the RPV should be included in the report. Analytical models have been formulated for the dominant physical processes, compared to the scaled experimental results and to the reactor systems for the spectrum of conditions assigned to the generalized accident sequences. These have then been used to develop probability density functions to characterize the likelihood of challenging the containment. Thus, the methodology has exercised the advertised approach and made specific conclusions with respect to Zion-like reactor/containment systems. With the exception of needing more foundation for the probability distributions used to characterize the molten mass participating in the HPME, and including a scenario with water in the RPV, I find that what is claimed in the report for Zion-like systems is adequately demonstrated.

RESPONSE D13: *See Response C8 for a discussion of the RPV water issue.*

In addition, there are extrapolations made to other reactor systems given certain containment compartmentalization and the lack of significant water in the reactor cavity. Here I believe the report considerations are too general. For example, the TMI-2-like B&W designs have support skirts for the RPV with holes in the skirts and reactor cavities closed off by concrete block or other structural material. Does this represent a path for significant melt transport to the upper region? Probably not, but this cannot be decided based on the information in Section 7. Furthermore, both the design and the sequence determine how much water would be in the reactor cavity. Even Zion has SBLOCA sequences where the reactor cavity is completely full and there is four feet of water on the containment floor. In this case, the lower half of the RPV is submerged and the vessel likely could not be failed by high temperature debris. These conditions should be addressed before extrapolations are made.

RESPONSE D14: *We recognize that geometry and accident sequences vary from plant to plant and a more careful review of these considerations is required as part of the extrapolation process. The amount of water in the Zion cavity can vary from condensate levels to a fully flooded cavity with an additional four feet of water on the basement floor. Experiments have shown that condensate levels of water have no discernable impact on DCH. Experiments with a half filled cavity essentially quenched the melt (SNL/IET-8B) reducing the loads to a nonthreatening steam spike. A flooded cavity would immerse the RPV, which may prevent its failure (Hammersley, PSA93).*

6. Is the composite of the information sufficient for the NRC to make a substantive conclusion with respect to this severe accident phenomenon?

This report provides a good first step to the issue resolution process. It specifically addressed Zion-like plants which represents a minimum of 15 plants, and perhaps more, which is obviously an appropriate starting point. ROAAM considers a spectrum of accident sequences with a range of melt quantity and composition. It is in this area that the current approach should be expanded to either include a larger range or provide additional justification for the present values.

The report addresses the available experiments in impressive thoroughness using both the CLCH and TCE models. The authors are to be specifically complemented for their considerations of the DCH experimental database.

In short, this report needs to be expanded to provide the basis for NRC to resolve the issue for Zion-like designs. With resolution of concerns related to the melt mass, melt composition and sequence definition, I am confident this approach will provide the necessary basis for issue resolution for Zion-like plants. As discussed above, the extrapolation to other designs needs to be expanded before resolution is complete for other designs.

RESPONSE D15: *It is within the ROAAM process to address further comments and accept input from the peer reviewers.*

My comments related to the national laboratory comments are in the Attachment to this letter. If you should have any questions related to my comments, please feel free to call at any time.

RESPONSE D16: *Reviewer comments on supplemental SNL and INEL comments have not been addressed as part of our responses.*

Reference

Hammersley, R. J. , et al., 1993, "Experiment to Address Lower Plenum Response Under Severe Accident Conditions," Probabilistic Safety Assessments, International Topical Meeting, Clearwater Beach, Florida, pp. 193-198.

REBUTTAL FROM REVIEWER D

Via a letter dated March 11, 1994, Brian Sheron asked that I review the authors' responses to my peer review comments on NUREG/CR-6075 to assure that my concerns have been adequately addressed. I have reviewed the responses to my comments and there are two places where I believe additional considerations should be asked of the authors.

The first is with respect to the consideration of water within the reactor coolant system and the general conclusions associated with accidents like the TMI-2 event where the system could remain at elevated pressure. In response D3, the authors refer to response C8 and in addition note that substantial mitigation was observed in SNL/IET-12, as a result of flow ejection of saturated water. In reviewing response C8 it is stated "TMI-like scenarios with a reflooded RPV do not lead to significant DCH loads." This is a substantial conclusion by the authors that should be added to the report since this is perhaps the most interesting situation to utilities when evaluating potential accident management strategies. If the authors believe they have the justification for this important statement, the addition of this statement and the associated justification to the report are sufficient to address my concern.

Secondly, in response D7 to my concern with respect to which metals have reacted in the thermite reaction, the authors have provided their interpretation of what is realistic to assume for the reaction and the observation that the model predictions in the report are conservative. I agree that calculations presented by the authors are conservative. However, my comment is related to the interpretation of the experiments. Specifically, does experimental data exist regarding the relative extent of reaction for aluminum and chromium such that the molten mass ejected from the simulated RPV can be well characterized. Specifically, can one justify complete oxidation of the aluminum with the chromium remaining in unreacted form or should this be treated as an assumption with a reasonable uncertainty? I think a clear statement of what is known and what is not known with respect to the melt discharged from the simulated RPV would be helpful in the report. Of course, this does not change the conservative nature of the calculations but adds to the strength of the arguments presented by the authors in NUREG/CR-6075.

If these two comments are addressed, along with the changes noted in the other responses included in the March 11th document, then my major concerns will be addressed. Should you have any questions regarding these additional comments, please feel free to call at any time.

Comments by Reviewer E

REVIEW OF CONTAINMENT PRESSURE CAPACITY USED IN NUREG/CR-6075

1. INTRODUCTION

As part of the resolution of the Direct Containment Heating (DCH) issue for Pressurized Water Reactors, a significant research effort has been completed and documented in NUREG/CR-6075, "The Probability of Containment Failure by Direct Containment Heating in Zion" (Ref. 1). In Reference 1, the containment failure probability from DCH is determined from the convolution of the demand (containment internal pressure and temperature) with the fragility (containment pressure capacity), both described in probabilistic terms for Zion. This review concentrates on the fragility description of the Zion containment pressure capacity as described in Reference 1.

The Zion fragility description was developed by Sargent & Lundy (S&L) as part of the Zion IPE (Ref. 2). Two failure modes were found to dominate: shell wall (hoop) failure with a mean pressure capacity of 134.4 psig and Coefficient of Variation (COV) of 0.05 and failure at the shell wall/basemat junction with a mean pressure capacity of 152 psig and COV of 0.15. Some additional deterministic calculations have been completed by Sandia (Ref. 3) but no results were available for review.

RESPONSE E1: *No comment.*

2. FRAGILITY DESCRIPTION

The fragility description used in Reference 1 consists of a combination of the S&L hoop failure and shell wall/basemat junction failure modes. The mean hoop value of 134.4 psig represents a mean factor of safety of about 2.86 when compared to the 47 psig design pressure with a mean factor of safety of about 3.23 for the wall/baseslab failure. These are consistent with results of other fragility evaluations of similar post-tensioned large dry PWR containments. Short of a detailed review of the S&L calculations, these values are judged to represent realistic mean values for the above two failure modes.

RESPONSE E2: No comment.

A number of additional possible failure modes exist for the Zion containment which were not addressed in Reference 1. Among these are:

a. Membrane (axial) failure of the cylinder
b. Membrane failure of the dome
c. Local liner tearing at locations of liner strain concentration
d. Ovaling at the equipment hatch penetration or failure of the sleeve
e. Failure of the equipment hatch
f. Failure of the personnel airlock bulkheads or doors
g. Shear or flexural failure of the baseslab
h. Purge valve failure
i. Interference effects due to large deformation of the concrete shell on pipe penetrations or the fuel transfer tube.

Presumably these and possible other failure modes have been evaluated by S&L and found to be noncontrolling. However, experience with the evaluation of similar containment structures indicates that membrane failures of the cylinder and dome typically have only somewhat higher capacities than the cylinder hoop failure mode. Normally, their capacities are similar and have the same COV since the strengths of the tendons, reinforcing steel, and liner can be expected to be similar for all those modes in addition to similar failure criteria and modeling assumptions. Whether local liner tearing is likely to occur prior to failure of the tendons is dependent on the elongation properties of the tendons and liner (including biaxial strains), and the degree of strain concentration which in turn depends on thickness variations in the liner and the liner anchorage details. Whether the local liner tear results in a small controlled leak is dependent on the ability of the tendons and reinforcing steel to carry the additional load from the failed liner. This is dependent on a number of parameters including the size of the liner tear and the stress and elongation in the adjacent tendons and reinforcing steel. This mode of failure is highly plant specific and may have relatively high variability, particularly that associated with leak area.

Ovaling of the equipment hatch has been investigated by Sandia (Ref. 3), but no pressure capacity is included in Reference 1. Failure capacities of equipment hatches and personnel

airlocks have typically been shown to be above major concrete structural failure capacities except at extreme temperatures or long times at high temperatures when deterioration of the elastomeric seals may occur. Similarly, failure of the electric penetration assemblies requires very high temperatures. These conditions are not encountered in DCH scenarios.

Baseslab failure can occur from either shear or flexure and has controlled the pressure capacity of several U.S. large dry containments. The strength of the baseslab is controlled by the reinforcing steel and concrete rather than by the tendon strength as in the case of membrane failures in the shell. Purge valve failure is normally very unlikely, but leakage due to interference effects has been predicted for several plants at pipe penetrations or at the fuel transfer tube. Again, these failure modes are highly site specific.

Although the above failure modes are typically expected to have higher mean capacities than the two failure modes included in the Reference 1 containment fragility, their inclusion could possible influence the overall containment fragility.

RESPONSE E3: *We recognize the importance of evaluating fragility on a plant specific basis. For Zion, we rely on the plant specific assessment as reported in their IPE. Examination of the S&L analyses (IDCOR T10.1) indicates that only purge value failure (mode h) was not considered explicitly, and the reviewers own assessment suggests that purge value failure is not likely. Of those additional failure mechanisms considered by S&L (failure modes a-i, excluding h), none was considered limiting for pressures less than ~10 MPa (~134 psig). With regard to extrapolations, we specifically state the need for plant specific evaluations, possibly through the IPEs. The issue of extrapolation is treated more completely in NUREG-6109.*

A COV of 0.05 was used in Reference 1 to account for the uncertainty expected in the hoop failure mode. This valve must include variability in the tendon strand ultimate strengths, tendon strength based on individual strand strength properties, tendon stain at failure, variability in the reinforcing bar strength at tendon failure strain, variability in the liner strength (including biaxial strain conditions) at tendon failure strain, possible liner strain concentrations, dimensional tolerances, and analytical modeling uncertainty. For Zion, plant specific material properties were presumably used to the extent possible. Typical strand COV for strength are normally in the range of 0.04 or slightly less. Therefore, an overall COV of only 0.05 may be somewhat

too low when considering the above possible sources of variability. A COV in the range of 0.08 to 0.10 for hoop failure is considered more realistic.

RESPONSE E4: *The IPE curve represents the utilities best assessment of Zion's fragility for hoop failure. Although we do not have all the details, we expect that the plant specific information, including material properties, has been employed in the evaluation. We do not know how the variabilities were combined, but we agree with the reviewer that the COV may be low, especially at the low end of the curve.*

The COV of 0.15 is higher for the shell/basemat junction failure mode due to the more complex mode of failure. In addition to the uncertainty associated with concrete strength, many of the variables listed above also contribute to the overall uncertainty for this failure mode. Results of other analyses by Brookhaven National Laboratory and Los Alamos National Laboratory for the NRC for this failure mode were dismissed as unrealistic by S&L. None of the analysis details were available for review. However, clearly an increased variability for analytical modeling is warranted for this mode of failure. The overall COV of 0.15 for this mode of failure is probably realistic, but could also be somewhat low.

RESPONSE E5: *Basemat failure at Zion may well be unrealistic. If this is shown to be true, then our predictions should be viewed as being only more conservative because of our current use of the IPE fragility curve.*

Many of the potential failure modes discussed above are highly correlated while others are essentially independent. The membrane failure modes are highly correlated since they are largely controlled by the tendon strength and elongation properties. Local liner tearing and interference-induced failure modes are also highly correlated with the membrane failure modes. The shell/basemat failure is expected to be partially correlated with the membrane failure mode as well as the baseslab shear and flexure modes. The hatch failure modes are expected to be essentially uncorrelated for the DCH conditions.

RESPONSE E6: *No comment.*

3. SUMMARY

Details of the calculations leading to the fragility descriptions for the Zion containment pressure capacity were not available for review. However, based on previous experience, the mean values used for the two dominant failure modes appear realistic. A coefficient of variation (COV) of 0.05 for the hoop failure mode is judged to be low. A number of potential failure modes were not discussed. Their potential contribution to the pressure fragility is unknown. However, unless one or more of these modes has an unexpectedly low capacity, the change in overall risk from DCH is not expected to be significantly changed unless the expected DCH pressures/temperatures are increased above those described in Reference 1.

RESPONSE E7: *No comment.*

4. REFERENCES

1. Pilch, M.M., H. Yan, and T.G. Theofanous, "The Probability of Containment Failure by Direct Containment Heating in Zion," NUREG/CR-6075, SAND93-1535, June 1993.

2. Zion IPE (April 1992), "Commonwealth - Edison Zion Station, Individual Plant Evaluation," NRC Doc. No. 9204290315.

3. Bohn, M.P., et al (June 1993), "A Mechanistic-Specific Analysis of the Zion Containment Overpressure Fragility," Draft Report, SAND93-1346, Sandia National Laboratories, Albuquerque, NM.

REBUTTAL FROM REVIEWER E

In general, I found the author's response to review comments to be satisfactory. Of primary concern, the author noted that most other potential modes of failure were investigated by Sargent and Lundy and found to be non-controlling. The author agreed that a COV for the controlling failure mode may be low. No evaluation using a larger COV was proposed or sensitivity study was prepared. However, in view of the pressures and temperatures predicted for the Zion DCH condition, an increased COV would not be expected to alter the overall risk significantly. Finally, the author states that basemat failure at Zion may well be unrealistic. No basis is given for this statement, and basemat failure has been shown to be an important and sometimes controlling mode of failure for some other large, dry PWR containments.

In summary, the responses of the author are considered satisfactory and no further resolution is considered necessary.

Comments by Reviewer F

Review of NUREG/CR-6075, "The Probability of Containment Failure by Direct Containment Heating in Zion," by Pilch, Yan, and Theofanous.

General Remarks

This report attempts to synthesize a wide range of material on accident progression, DCH experiments, models, containment failure and risk analysis. This is a challenging task but necessary if the NRC is ever to resolve these safety issues. The authors have clearly made an enormous effort to put all this together and should be commended for their work.

RESPONSE F1: *No comment.*

Despite the exertions of the authors, this document is still very preliminary. What this report needs more than anything else is a professional editor. I found the report difficult to read and also full of omissions and typographical errors. The language is often verbose and obscure, full of references to jargon and tediously repetitious. Entire sections, particularly those dealing with ROAAM, could be drastically reduced in size without any loss of information. The sections written by different authors have not been integrated. Material is repeated and conflicting interpretations are given in some cases. Little effort has been made to compare the results of the modeling efforts by the two groups.

RESPONSE F2: *We agree. The report will be reviewed by a Technical Editor.*

Fully two-thirds of the report is Appendices, much of which are central to the authors' conclusions. Either these appendices should be directly incorporated into the main body or else the document should be split into parts. Some of these appendices report, apparently for the first time, the results of modeling studies. This material really needs to be judged separately from main conclusions of the report. I would prefer to see a separate write-up of the modeling with more in-depth comparison to the experiments and justification of the approximations.

RESPONSE F3: *We disagree. Our intent in the main body of the report was to provide a clear and concise accounting of how the various elements integrate to yield the probability of containment failure. We intentionally left many details to appendices so that the reader could judge their merits separately from the integration logic and results.*

Beyond these mechanical deficiencies, there are some technical issues that must be addressed in the revision. Some of these issues are simply matters of clarifying nomenclature. Others are much more serious and challenge the technical credibility of this work. In my review, I have chosen to emphasize those technical issues with which I am most familiar and I feel are most significant. I have made no effort to be comprehensive and I chose not to examine the other reviewers remarks before writing this review in order to maintain some semblance of impartiality.

Finally, I found a disturbing tendency for the authors to make assertions without justification. Rather than present an quantitative analysis, they pass on their own qualitative judgements about approximations and the agreement between data and models. I believe that it is important to critically evaluate models and ideas and justify your work fully. This report suffers from a lack of this critical spirit and as a consequence, the basis for deciding this issue is substantially weakened. It will be very difficult to defend the technical basis of the conclusions in front of a knowledgeable audience of scientists and engineers.

RESPONSE F4: *These will be addressed on a case by case basis.*

Detailed Remarks

Appendices D, E, and F and the related experimental data in Appendices G and H form the main basis for the technical evaluation of DCH. I have focused my review on evaluating this material.

Appendix D

The model presented in this section is extremely simplified given the complexity of the physical processes involved in DCH. The model is based on the energy balance principle of elementary thermodynamics and completely neglects heat transfer or any details of the flow. This sort of

model is often very useful as a first effort in understanding the issues and placing upper bounds on the peak pressure for a process such as DCH. However, it is quite surprising to find that this model is being used to make regulatory decisions. After at least a decade of studying this problem, I would expect that much more progress toward a realistic model would have been made. Although it might be argued that the very complexity of the problem prevents realistic modeling, this also suggests that simplified models may be particularly unreliable at estimating the effects of scale.

RESPONSE F5: *Although our models are developed with a bounding perspective of the first order effects, they are also very close to best estimate (see, for instance, Fig. E.6). This greatly simplifies the problem of scaling or extrapolation and greatly simplifies the problem of bounding scale effects.*

The discussion in Section 4.0 indicates that the key parameter derived from the models is the "coherence ratio." This is discussed at some length in the appendices. The coherence ratio is obviously a key parameter of the CLCH **model** but this is merely a consequence of the model equations and the preconceptions of the authors. It is in no way demonstrated on a physical basis that this is the key scaling parameter. This parameter is simply a way of partitioning the energy of the melt into a portion that goes into the gas and a portion that is transferred into the containment and associated interior structures. Heat transfer and fluid mechanics have not been considered (beyond very elementary order-of-magnitude estimates) in these models and the appropriate experiments show little effect of scale.

It is important for the NRC to recognize that the idea of the coherence ratio is a preconceived notion that is not a result of the modeling but rather an assumption. It may, in fact, be a very useful assumption but that has not been demonstrated in a convincing fashion. The scaling of the coherence ratio is based on separate arguments (given in Sections D.5 and E.4.1) that are also quite simplistic and involve a large number of approximations. Again, this derivation is rather crude and more in the way of a back of the envelope computation rather than a derivation. Furthermore, the discussions in Section D-5 and E.4.1 are inconsistent and based on completely different mechanisms for the characteristic entrainment time scales.

RESPONSE F6: *The coherence ratio is not an arbitrary modeling parameter. Pyrometers at the cavity exit clearly demonstrate that debris dispersal is noncoherent with much of the*

blowdown process. Furthermore, gas temperatures, as they vent from the subcompartment to the dome, also peak on a time interval consistent with debris dispersal. We try to capture only the main scaling dependencies in our development of correlations for the coherence ratio. Since we can't adjudicate between the models, modeling uncertainty is accounted for by using both models in the load assessments. The important thing to recognize is that these correlations are used in reactor applications that also interpolate on the database.

p. D-6 and D-7

As admitted on p. D-6 "detailed interactions of the melt-steam interactions in the cavity/chute region have not been examined in any direct way so far: however..." and the authors go on to construct an entire scenario with apparently very little or no direct experimental evidence! For this reason, the CLCH model should be used very cautiously.

p. D-8

The model should be physically derived from a set of assumptions rather than just stating the equations in Table D.1. A careful discussion of the level of approximation and the implications for scaling must be given if this model is to be used to resolve this issue. Whenever possible, each separate portion of the model or submodel should be validated against the experiments. Examples: the perfect-gas model for the steam blowdown out of the primary system should be compared to Surtsey data; the melt energy retained in the subcompartment can be estimated with the experimental measurements of temperature and flow rate and compared to the model predictions.

RESPONSE F7: *The notion that debris dispersal is noncoherent with much of the blowdown process is based on direct physical evidence as noted in response F6. Our approach to blowdown modeling follows the discussion by Wulff (BNL) in the SASM report (NUREG/CR-5809). Comparison of measured and predicted blowdown histories exists in some of the ANL experiment reports. Excluding an initial period of two-phase discharge, the models predict the blowdown reasonably well. Other examples of separate validation are: the coherence ratio (e.g., Fig. E.9 - E.11), DCH loads in inert atmospheres (Fig. E.2), hydrogen production (Fig. E.3), and DCH loads with hydrogen combustion (Fig. E.5).*

This model and the related TCE model both completely neglect heat transfer from both the gas and melt to the containment and other interior structures. This aspect of the modeling must be discussed and justified.

RESPONSE F8: *We do not believe that heat transfer to structures affects peak containment pressure in any significant way, so we wish to bound these processes. Simple scoping calculations indicate that structure heat transfer in the dome region is way too slow to affect peak pressure. Measured pressure and temperature (gas) histories in the dome region of experiments indicates that cooldown takes ~20 - 40 times longer than heatup during the DCH event. The cavity surface area is too small for any significant heat transfer; and in any case, the surfaces are coated with a thin layer of hot melt that reduces the potential for heat transfer from the gas. Lastly, control volume type calculations for the subcompartments suggest that structure heat transfer might have a noticeable, but not dominant effect on containment pressure in some experiments where no hydrogen combustion occurs. Such assessments, are particularly difficult to do correctly because experiment observations indicate that the gas is not well mixed in the subcompartment and that there is some tendency for the gas to "tunnel" through the subcompartment to the available vents. Structure heat transfer only affects the thermal energy contribution of debris to peak pressure. Hydrogen combustion, a significant energy source in DCH, occurs in the dome and is not affected by subcompartment heat transfer. Furthermore, structure heat transfer is a surface-to-volume effect, so its impact is expected to be reduced at reactor scale. For these reasons, we do not believe that heat transfer to structures affects peak containment pressure in any significant way, so we simply chose to bound these processes in our models. These points will be clarified in the text.*

Apparently, these models do not conserve energy since a substantial fraction of the melt energy is "lost." Since the model does not start with a control volume analysis and proceed logically, it is not clear that the equations presented in the Table are consistent either. For these reasons, I want to see a detailed accounting of the energy balance in this problem-an energy budget so to speak. Numerical values of the energy change associated with each process and substance should be given.

RESPONSE F9: *We disagree. The models need only focus on the energy transferred to the atmosphere. The remaining energy remains in the debris as latent or sensible heat that could*

not be transferred to gas, or as metals that were not oxidized, or as preexisting hydrogen that was not burned.

p. D-10 Equation D-11

The results of the sensitivity study with this model (Fig. D.3c) indicate that the percentage of "preexisting" hydrogen in the containment one of the key parameters. However, only a very limited percentage is considered in both cases. The consequences of increasing the hydrogen concentration above 4% must be discussed. Both models have arbitrarily limited the amount of hydrogen in the containment to less than this amount. The amount of "preexisting" hydrogen and the zirconium fraction in the melt are related and this relationship must be considered when determining the possible combinations of parameters.

There is some discussion of this issue on p. D-13 but hydrogen concentrations of greater than 3.5% are dismissed simply because that would require oxidizing greater than 50% of the core. Since the peak pressure and flammability limits are very sensitive to the hydrogen faction, this issue should be considered much more carefully. Examining the tradeoff between the Zr fraction remaining in the melt and preexisting hydrogen, a more useful upper bound on peak pressures could be developed.

RESPONSE F10: *Hydrogen concentrations greater than 3.5% are <u>not</u> dismissed as the reviewer contends. The equivalency between 3.5% preexisting hydrogen in the atmosphere and 50% Zr oxidation is cited to provide the reader with some perspective of what is likely. In reactor applications, the tradeoff between preexisting hydrogen and in-vessel Zr oxidation is handled in a fully consistent and dependent fashion (see Eqs. 3.2 and 3.3). For additional perspective, we note that in the extreme of 75% Zr oxidation (in-vessel) that ~5.5% preexisting hydrogen exists in the containment. Response F33 suggests that hydrogen combustion phenomena does not differ significantly over the range of 3.5% to 5.5% hydrogen during DCH events.*

p. D-9

The asymptotic limit of the CLCH model is not really surprising. After all, isn't this just equivalent to the one-cell equilibrium model? As discussed in Appendix E (p. E-7), the one cell equilibrium model produces an upper bound which "often far exceeds experiment observations

by a margin to large to be useful in reactor analyses." This is contrary to the statement on p. D-10 "the asymptotic loads produced here are rather modest and possible to live with, even though they may be somewhat conservative."

Which is correct and what is the relationship between the two models? Some direct comparisons between the two models should be performed and the two authors should agree on interpretation.

RESPONSE F11: *The relationship between the one-cell equilibrium (OCE) model and the asymptotic limit exhibited with R_τ is subtle. The OCE model assumes that debris/gas interactions come to equilibrium with the entire containment atmosphere. This unrealistic situation leads to very severe loads. A more realistic treatment allows debris/gas interactions to come to equilibrium with coherent blowdown gas. The asymptotic limit occurs when the entire blowdown is allowed to interact with debris. Blowdown gas is still much less than the entire containment atmosphere, so debris/gas thermal interactions are much more limited leading to much reduced loads.*

Section D.4

I do not consider Figs. D.11 and D.12 as being "remarkable agreement with the data" or that the "these parameters have been varied over significantly wide ranges". This sort of hyperbolic and self-serving language diminishes the value of the comparison. There are systematic variations of the experimental data which are not explained by this model. These are apparently being ignored.

RESPONSE F12: *No comment.*

There are no error bars or efforts at an uncertainty analysis. No other possible correlations have been considered. The actual range of parameters is less than an order of magnitude. The effect of scale is mixed in with the effects of geometry since several different configurations are being compared. Can the LFP-1 and LFP-2 experiments really be "deemed an adequate approximation of the main subcompartment feature" (p. D-20)? This is a key point since without the extended data range and with some realistic uncertainties, a constant value for τ_m would be just as reasonable as a linear correlation to Eq. D.16. Further, the constant 0.2 in D.16 has apparently been chosen to give the best fit. Is this the case and if so, isn't the agreement rather artificial?

RESPONSE F13: *A relative standard deviation of 12.5% is applied to the CLCH coherence ratio. The coherence ratio is applicable so long as it is not applied outside the data range on which it is based. These ranges are cited in the text, and the reactor applications fall within the database. The LFP tests are adequate because we observe that the structure is effective at confining the debris to the subcompartment and not allowing it to mix with the dome; this is the test of adequacy. The scaling arguments are only intended to identify the key parameter dependencies. It may be hopeless to predict the constant of proportionality from first principles; consequently, it is determined by fitting the correlation to the data.*

Section D.5

The DCH-Scale derivation is ad hoc and totally inconsistent with the discussion of E.4.1 The discussion refers to Eq. D-2 and in-pedestal recirculation time in the derivation of Eq. D-13. However, Eq. D-13 is just the mass flow rate for the choked flow of a perfect gas from a reservoir. Apparently, the flow time L/U is being used to estimate τ_m, the melt sweep out time. This has nothing to do with recirculation or the droplet entrainment mechanism discussed in E.4.1.

RESPONSE F14: *We cannot adjudicate between the two coherence ratio correlations. This kind of model uncertainty is accommodated in ROAAM by performing reactor calculations with both correlations. As the results indicate, both models with their respective coherence correlation lead to similar containment loads. This is because both coherence correlations are being applied to reactor cases that interpolate on the existing database, so they give similar values to the coherence ratio.*

Section D.6

The "L" and "U" methods of estimating hydrogen are not clearly explained in the text. The material presented on p. D-10 to D-12 is rather confusing and I was unable to reproduce the results given in Tables D-7 and D-8. Debris chemical compositions and the assumed oxidation states for the various metals are needed to complete this discussion. Because of these omissions, this section was not intelligible to me.

RESPONSE F15: *Text will be modified for clarity.*

Appendix E

This section describes two slightly different models for the DCH process. In common with the previous section, the models are based on energy balances and elementary thermodynamics. These models have the same general deficiency that heat transfer processes are completely neglected and further, this issue is not discussed at all.

RESPONSE F16: *See response F8.*

Section E.1

The introduction is a good overview of the history of testing and modeling for this problem. This material should be moved up into the main portion of the text.

RESPONSE F17: *We disagree that this material should be moved to the main body of the report. We want the main body to remain as a concise accounting of how the various elements integrate.*

Section E.2

This model is developed in a much clearer fashion than the CLCH model. There are a number of niggling inconsistencies in notation and problems with the references that careful proofreading could eliminate.

As with the previous model, an energy budget with typical numerical values is needed. The statements about the role of ψ on the top of p. E-15 are rather peculiar. I do not understand at all the remark "This is a second order effect on a containment-wide basis". Second order compared to what?

RESPONSE F18: *Appendix E will be proofread. The models need only focus on the energy transferred to the atmosphere. With this in mind, the energy balance is quite simple in the SCE and TCE models. The total energy that is available to heat the containment atmosphere is given by $\Sigma\Delta E_i$ in the SCE model. At equilibrium, the fraction, $1/(1 + \psi)$, could actually be delivered to the atmosphere with the rest remaining in the debris. In the IET experiments, $\psi \sim .15$ on*

a containment wide basis and has even smaller values in typical reactor applications. These containment wide values represent second order effects because ψ is compared to unity. The efficiency in the TCE model further reduces the energy that is delivered to the atmosphere. This additional reduction comes about because additional thermal energy remains with the melt (higher equilibrium temperatures in the subcompartment), less hydrogen is produced (steam limitations or incomplete oxidation), and because most preexisting hydrogen is not burned. Table E.6 shows that typical efficiencies for the IET tests is ~35%. Of the energy actually delivered to the containment atmosphere in a typical IET experiment, ~50% comes from hydrogen combustion, ~30% comes from latent and sensible heat, ~15% comes from exothermic oxidation reactions, and ~5% from the blowdown.

Section E.2.1

This section indicates that the ideal gas model used in the previous section is in error for high-pressure steam near saturation. The compressibility factor is really a function of the thermodynamic state within the vessel and the blowdown should be analyzed using the real-gas isentrope if compressibility is significant rather than just trying to fix up Eqn. E-15.

I am surprised that neither group has presented comparisons of the blowdown expressions with experimental data. If the state in the vessel is near saturation, then the ideal gas expression will be grossly wrong and cannot be fixed up by just including Z. The correct treatment for real gases and saturated mixtures is well understood and there is no reason for these ad hoc models. See the discussion of vessel blowdown by Moody in **Unsteady Thermofluid Mechanics.**

RESPONSE F19: *The blowdown modeling adopted here was presented in Appendix K (prepared by W. Wulff, BNL) of NUREG/CR-5809 as part of the SASM investigation of DCH. The important thing is to correctly characterize the amount of steam initially in the RCS. This can be done with either a compressibility factor derived from virial coefficients for steam (Keenan and Keys) or taken directly from steam tables.*

Sections E.2.x

The concepts of energy and enthalpy are frequently mixed together when discussing the energy balance equations. While both concepts are useful in this context, the present treatment is

inconsistent and invites criticism. These problems could be avoided if a more careful control volume analysis was carried out.

RESPONSE F20: *Text will be modified to reflect a consistent treatment.*

Clarify the entries in Table E.2 What reactions do the Δh_r refer to, steam or oxygen? What is the sign convention and the reference temperature? What does the symbol Δu_d refer to? Is this some portion of Eqn. E.6? What are the reference temperatures and what temperature is C_d evaluated at?

RESPONSE F21: *As the text indicates, Δh_r refers to oxidation metal in steam. The nomenclature will be modified to further clarify this point. The reference temperature is 298K and all reactions are exothermic. The text and nomenclature define ΔU_d as the specific molar internal energy of debris, and it is used specifically in Eq. E.19 to calculate the total thermal energy in the melt. It is referenced to 298K. The text states that the debris heat capacity, C_d, is averaged over the temperature range 300 - 2500K.*

Reporting the actual correlation between the one-cell model and the experiments would be useful. It appears that the actual pressures could be approximated as simply some fixed fraction of the predicted pressures. That might be just as useful a model as the artificial "coherence ratio" method proposed in Appendix D.

RESPONSE F22: *We disagree. The SCE model overpredicts data by a margin too large to be useful in reactor applications. An empirical correlation would still have excessive scatter without addressing the issue of extrapolation. It becomes essential to identify the dominant mitigating mechanisms, i.e., trapping in the subcompartment and the noncoherence of dispersal and blowdown processes. This is the motivation for the TCE and CLCH models.*

Section E.3.0

The wording used to describe flow paths (p. E-32) is confusing. Is the sum $\eta_1 + \eta_2$ equal to the η given in Table E.6?

RESPONSE F23: *The description of the two flow paths is described in Section 3.0. However, for greater clarity, Fig. 3.2 will be modified to explicitly identify these two flow paths and a callout to this figure will be cited in Section 3.0. The total DCH efficiency will be clarified in the nomenclature and Table E.6.*

Section E.3.1

What does the first sentence mean at the top of p. E-33? Is mass flow rate proportional to the flow area?

RESPONSE F24: *The mass flow rate* <u>*is*</u> *proportional to flow area. Here, however, we are referring to quantities not rates. Thus, the amount of debris that ends up in the subcompartment equals the cavity flow area that communicates with the subcompartment divided by the total flow area from the cavity. See Appendix I.*

The term "heat sink" is poor terminology. The containment walls and other internal structures are the more obvious choice for heat sinks.

RESPONSE F25: *We favor the term, which must refer to* <u>*gaseous*</u> *heat sinks because we're dealing with an adiabatic model. This distinction will be clarified in the text.*

What is f_{al} in Eqn. 3.30 and E. 31? Is this also a volume ratio?

RESPONSE F26: *As defined in the nomenclature, f_{al} is the fraction of the total flow area from the cavity that communicates with the subcompartment. It defines how much of the blowdown and dispersed debris ends up in the subcompartment. It is not a volume ratio.*

The phrase "second order effect" is used repeatedly in connection with ψ. This phrase is meaningless. Numerical values of ψ should be given. If ψ is large it certainly cannot be second order or neglected! It is incorrect to say that "debris/gas heat transfer can be reduced drastically because of large values of ψ". The present considerations have nothing to do with heat transfer rates! The heat transfer rate is in fact considered to be infinitely fast in the present model. The equilibrated temperature is lower when ψ is larger but this is simple thermodynamics.

RESPONSE F27: *The equilibrium temperature is higher for larger values of ψ, not lower as the reviewer suggests. Large values of ψ mean not much gas and/or lots of debris. In these cases, the equilibrium temperature favors the initial debris temperature, not the initial gas temperature. The phrase "second order effect" is correct and meaningful with regard to ψ on a containment-wide basis (see Response F18 and F29). The local value, ψ, in the subcompartment can be ~3 - 4, which corresponds to significant mitigation since $1/(1 + \psi)$ is the fraction of thermal energy that can be transferred from the melt to the gas.*

Eqn. E.32 requires more explanation with regard to the factors f_{coh} and f_{vl}. This is the key part of this model and results in the pressure reductions due to the subcompartment interactions with the debris. The origin of these factors and numerical values should be given. Some sort of derivation should be presented for this equation. The relationship between the CLCH model and this model should be discussed at this point.

RESPONSE F28: *Eq. E.32 is a secondary aspect of the model. Equation E.32 defines a mixture temperature between blowdown and subcompartment gases before DCH interactions occur. This has only a weak impact on the predicted loads. A few words of clarification will be added to the text. The key features of the model are embodied in Eqs. E.29, E.36, and E.40.*

The correction to the thermal term in Eqn. E.30 cannot be both "quite insignificant" and "important" simultaneously (p. E-34).

RESPONSE F29: *ψ is generally a second order effect on a global basis (i.e., containment wide, see Response F18); but when evaluated on a local (subcompartment) basis, ψ can be quite significant because the (gaseous) heat sink is small compared to the containment atmosphere.*

The difference between gas internal energy and the total energy in a subcompartment should be more clear distinguished in the discussion of Eqn. E.32. It should be made clear that the terms involving the reference temperature are somewhat artificial and involve a degree of arbitrariness associated with the choice of reference temperature. In particular, the choice of a reference temperature should certainly not be cited as a "mitigating factor" (p. E-35).

RESPONSE F30: *The term, $N_d C_d (T_l - T_r)$, is an artifact of the reference temperature arising from the use of tabulated internal energies. The term has nothing to do with the physics of DCH. This will be clarified in the text.*

Section E.3.2

What is f_{a2} and how is it determined? What is the effect of the gas displaced from the subcompartment on the energy balance of Eqn. E.37? Eqn. E.39 needs more explanation and relating to Eqn. E.32.

RESPONSE F31: *f_{a2} is a compliment ($f_{a2} = 1 - f_{a1}$) to f_{a1}; it represents the fraction of material (blowdown and dispersed debris) that is transported to the dome. This term (f_{az}) will be added to the nomenclature. These two fractions are also complimentary, $f_{az} = 1 - f_{a1}$. Displaced gas is only a few percent of the atmosphere, and it is conservative in that the dome gains what the subcompartment loses. Thus, on a containment wide basis, there is no net gain or loss of energy. Eqs. E.39 and E.32 are analogous, one applying to the subcompartment while the other applies to the dome. This will be explicitly stated in the text.*

Section E.3.3

There is something wrong with Eqn. E.47.

RESPONSE F32: *Eq. E.47 is correct given the stoichiometry given in Eq. E.49.*

There are really three issues related to hydrogen combustion. One is the combustion of the hydrogen in the jet, possible augmented by the combustion of hydrogen in the entrained atmosphere. The second is the ignition and propagation of a flame in the dome region. The third is the so-called volumetric oxidation in the dome. These issues need to be clearly identified and treated separately.

RESPONSE F33: *Our perceptions of hydrogen combustion during DCH events can be summarized as follows: 1) that DCH produced hydrogen (plus some entrainment of H_2 from the preexisting atmosphere) can burn as a jet in the dome and contribute to peak containment pressures, 2) that flame propagation is difficult to achieve and that the process is too slow and*

inefficient to contribute to peak loads, 3) that slow volumetric combustion of preexisting hydrogen is too slow in a stratified atmosphere to contribute to peak loads, and 4) that sudden volumetric combustion (autoignition) of preexisting hydrogen is essentially impossible.

The combustion of hydrogen as jets venting from the subcompartments to the dome is treated explicitly in both the TCE and CLCH models. Such treatment is inherently conservative since all DCH produced hydrogen plus some hydrogen entrained into the jet is assumed to burn. In reality, not all DCH produced hydrogen will vent into the dome on DCH time scales. Some will remain in the oxygen starved subcompartments. This hydrogen that lags behind may eventually mix with the dome, and possibly burn, but any such mixing and burning is too slow to contribute to peak pressures.

In the extremes of the distributions (75% Zr oxidation), the preexisting hydrogen concentration could be as high as ~5.5% for our initial containment pressure of .25 MPa. Considering a range of realistic containment pressures, $P_c \sim .2 - .3$ MPa, the maximum concentrations of preexisting hydrogen could be $X_{H2} \sim 6.8\% - 4.8\%$. The corresponding range of steam concentrations is $X_{stm} \sim 36\% - 58\%$. The upward and downward flammability limits are ~6 - 10% and ~9% hydrogen respectively, provided that $X_{stm} \leq 55 - 65\%$; otherwise, propagating flames cannot exist. Thus, the potential to propagate flames is limited for most DCH situations.

Flame propagation may be possible in some extreme situations; however, the energy release rate is too slow to contribute to peak pressures. This can be seen by comparing the energy release rate due to a propagating flame with the heat transfer rate to structures,

$$\frac{\dot{E}_{H2}}{\dot{E}_{HT}} = \frac{\eta_c X_{H2} \Delta e_{H2}}{\tau_{H2}} \frac{\tau_{HT}}{C_v \Delta T} .$$

where the combustion time constant is given by

$$\tau_{H2} \sim \frac{L}{v_f}.$$

The dome of the Zion containment is L ~ 50 m high. For a DCH event that produces containment threatening pressures (P ~ .7 MPa), then ΔT ~690K; and the heat transfer time

constant to structures is ~80s. The molar heat capacity is $C_v \sim 30$, and the molar combustion energy is $\Delta e_{H2} \sim 2.4 \times 10^5$. Turbulent combustion velocities are $v_f \sim 1.4 - .2$ m/s for $X_{H2} \sim 6.8\% - 4.8\%$, and the corresponding completeness of reactions is $\eta_c \sim .3$ respectively for both cases. Thus,

$$\dot{E}_{H2}/\dot{E}_{HT} \sim .05 - .5.$$

Therefore, the maximum energy release rate, under extreme conditions, is too slow to contribute to peak pressures, and propagating flames need not be considered in the models. We note, however, the sensitivity to steam and hydrogen concentrations.

Slow volumetric combustion can occur at elevated temperatures. We envision the atmosphere to be stratified on DCH time scales. Hot combustion products (from the jets) stratify at the dome, and the cooler preexisting atmosphere is displaced downwards; thus, volumetric combustion of the preexisting hydrogen is insignificant without some mixing with hotter dome gases. To assess the potential of slow volumetric combustion to contribute to DCH, we use the reaction rate expression given by De Soete (La Rivista dei Combustibili, Vol. XXIX, 1975)

$$\frac{\dot{E}_{H2}}{\dot{E}_{HT}} \sim \frac{630\ \Delta e_{H2}\ X_{H2}^{2.7}\ X_{O2}^{0.2}\ e^{-8050/T}}{\dfrac{C_v\ \Delta T}{\tau_{HT}}}.$$

At ~800K (the limit of his database),

$$\dot{E}_{H2}/\dot{E}_{HT} \sim 5x10^{-3};$$

band extrapolating to ~1100K,

$$\dot{E}_{H2}/\dot{E}_{HT} \sim .07.$$

We therefore conclude that slow volumetric combustion of hydrogen cannot contribute to peak DCH loads.

The Froude number of the gases venting to the dome is ~3 in the SNL/IET experiments. Therefore, inertial forces exceed the buoyancy forces, and some mixing can be expected. If the mixing zone is sufficiently hot (~900K), then a mixing limited volumetric combustion may occur in the mixing layer. This process is treated in Appendix F where it is shown that these mixing

processes are too slow to contribute to peak pressures. At reactor scale, the Froude number is much lower, Fr ~ .3, so that the tendency to mix is much reduced because buoyancy forces are stronger and the tendency to stay stratified is greater. Consequently, slow volumetric combustion and mixing limited volumetric combustion cannot contribute to peak loads, and they need not be modeled.

Sudden volumetric combustion (autoignition) of the preexisting atmosphere is essentially impossible in DCH events because of the stratification and mixing limitations discussed above. But even if the atmosphere is well mixed and uniformly heated, then autoignition is still difficult or impossible. Small scale tests (Stamps NSE 109 1991 and Fig. F.1 in NUREG/CR-6075) indicate that the autoignition temperature becomes asymptotically large at the hydrogen concentrations of interest and that the addition of steam makes autoignition even more difficult.

We recognize that flammability limits, flame velocities, and reaction completeness are all temperature dependent in such a way as to increase the potential for increased loads. The temperature of the displaced preexisting atmosphere in the stratified dome is difficult to characterize, but is expected to be relatively cool. Actual DCH experiments are the best simulation of the real situation.

All these assessments are consistent with the SNL/IET-11 experiment. This is the most severe DCH experiment ever run. Peak pressures are consistent with combustion of DCH produced hydrogen as a jet plus some entrainment of preexisting hydrogen. Propagating flames and mixing limited combustion were indicated by a prolonged glow in the vessel and posttest gas analyses indicating that much of the preexisting hydrogen was burned. Using the measured heat transfer time constant and the glow interval as a lower bound to the combustion time, then

$$\dot{E}_{H2}/\dot{E}_{HT} \sim .1$$

for the combined processes of flame propagation and mixing limited combustion. Thus, flame propagation and mixing limited combustion did not contribute to peak pressure loads. Containment pressurization was continuous and it did not show any sudden discontinuity suggesting autoignition. Lastly, all these processes are independent of scale, so these experiment observations are indicative of full scale behavior under similar conditions.

Unless there is oxygen in the jet, there must always be entrainment in order for there to be combustion within the jet. In order for the combustion to actually take place, there must be both ignition and stability of the jet. Williams' ignition criteria does not appear to be based on either an analysis of the ignition process of experimental data. It is well known that in a diffusional mixing situation, the local temperatures cannot be estimated using a well-mixed approximation such as Eq. E.55. I do not consider this to be a sound approach to the ignition problem. Either experimental data need to be obtained on this aspect of the problem or else the jet should be assumed to burn.

RESPONSE F34: *The Williams criteria for jet extinction is essentially impossible to achieve in reactor applications. The extinction threshold is ~5% O_2. This is consistent with observations from the NTS tests, where Shepard (1987) noted that hydrogen diffusion flames extinguished when the background oxygen concentration dropped below ~5% - 8%. To satisfy the Williams criteria, the steam concentration in the atmosphere must be 75% which corresponds to ~.3 MPa of steam to compliment the ~.1 MPa of air initially in the containment. These conditions are essentially impossible to achieve in a DCH event. However, low oxygen concentrations existed in a few DCH experiments where hydrogen combustion was suppressed. The Williams criteria was used to explain these results. In this context, the discussion will be expanded to also cite the NTS observations.*

A jet or plume entrainment model should be used to determine the amount of hydrogen from the atmosphere that is being entrained and burned.

Section E.3.4

What are the values of all the parameters used in the model to make these predictions? Exactly how many of these are adjustable and how were they chosen?

RESPONSE F35: *Validation of the TCE model against experiment data requires <u>no</u> adjustable parameters. All input parameters are taken from the experiment reports. In addition to initial and boundary conditions, the coherence ratio is also important. These values are also obtained from the data reports for each experiment. All important input data is listed in Table E.8 and all results are listed in Table E.6. For reactor applications, the dispersal fraction is treated in*

a bounding fashion and the coherence ratio is obtained from a correlation as explained in the text.

Section E.4

"The primary heat sink for debris/gas interactions is smaller..." smaller than what?

There is something wrong with Eq. E.66.

RESPONSE F36: *Smaller values of the coherence ratio means less coherent blowdown gas (heat sink) with the dispersal process. A few words of clarification will be added to the text. Typo in Eq. E.66 will be corrected.*

Section E.4.1

The symbols for velocity in this section are inconsistent.

RESPONSE F37: *Symbols for velocity are used in a consistent manner in this section. Perhaps the reviewer is confusing volumes with velocities. All velocities and volumes are defined consistently in the nomenclature.*

What is the control volume for Eq. E.69?

RESPONSE F38: *The control volume is the cavity. This will be clarified in the text.*

What is the film referred to in the sentence before Eq. E.76?

RESPONSE F39: *The film refers to molten material spread over cavity surfaces. Text will clarify this point.*

The Kutateladze number is incorrectly defined (not dimensionless) in Eq. E.70.

RESPONSE F40: *Typo will be corrected.*

If the debris velocity is less than 10% of the gas velocity then either the flow is transient or there are significant wall-debris interactions that are being neglected in this treatment. This analysis is really more of a back of the envelope approximation than a derivation. There is also apparently no independent experimental verification. The ad hoc nature of this analysis should be more clearly stated.

RESPONSE F41: *This model is not intended to be a detailed accounting of all transient processes that occur in the cavity; rather, it is intended to identify key parameter dependencies with the further intent of correlating the experiment database. This point will be clarified in the text.*

The choked flow approximation used in this analysis is not supported by the data shown in Fig. E-7. The pressure ratio is not sufficiently high to obtain choking for most of the flow duration.

RESPONSE F42: *Consistent with Response F41, the intent is only to identify characteristic rates. For this purpose, the model assumes that the gas density is determined by upstream conditions. This is strictly true when the flow is choked and approximately true when the flow is nearly choked. More importantly, however, the critical pressure ratio can be much reduced when two phase flow effects are taken into account.*

This entire discussion appears peripheral to the TCE model because the f_{coh} parameter has not been related to the coherence parameter or entrainment time. So apparently the coherence ratio is not really relevant to the TCE model and the statements made in Section 4 about the importance of this parameter for both models is incorrect. The relationship between the TCE model and the coherence ratio really must be explicitly discussed.

RESPONSE F43: *The fraction of the blowdown gas that is coherent with debris dispersal is given by,*

$$f_{coh} = 1 - \frac{M_g^0}{M_{g,e}} = 1 - \left[\frac{P_e}{P^0}\right]^{\frac{1}{\gamma}} = 1 - \left[1 + \frac{\gamma - 1}{2} R_\tau\right]^{\frac{-2}{\gamma - 1}}.$$

For $R_\tau \leq .5$, $f_{coh} \sim R_\tau$. This relationship between f_{coh} and R_τ will be clarified in the text.

Section E.4.1

The discussion in this section makes it clear that entrainment has never actually been measured. We only know that debris is being pushed out of the cavity. Nothing more. This emphasizes further the speculative nature of the present models.

p. 68 is missing.

RESPONSE F44: *We apologize for the pagination error. This will be corrected.*

Section E.4.5

Eq. E.91 is useless for the purpose of assessing DCH scaling. Further, it has not been demonstrated that physical scale is unimportant since many key physical processes such as heat transfer (which are strongly scale dependent) have been completely neglected.

RESPONSE F45: *The scaling implications of the model is <u>very</u> useful because of its simplicity if not for its completeness. The TCE model is developed with a <u>bounding</u> perspective; thus, the scaling implications must be viewed with the same bounding perspective. This simplifies both the model and the scaling implications. As it turns out, the models also have an element of being best estimate; thus, the scaling implications are also complete. We recognize that many kinetic processes are scale dependent, but it does not appear that these processes are limiting in any significant way.*

Section E.6

The claim that "comparison with experimental data shows that nature favors the extreme and the conservative bias is very close to the best estimate" is nonsensical. What is the author really trying to say here?

RESPONSE F46: *This statement will be deleted from the text.*

Appendix F

I am completely baffled by this appendix. The available experimental data and the analyses both indicate that a temperature of about 800 to 900 K is sufficient to ignite the mixtures of interest yet the author concludes that the "autoignition temperature for NPP analyses" is 1100 K. In what way is this conservative?

RESPONSE F47: *See Response F33.*

Ignition is a local phenomena for which transport processes (mass and energy) and the spatial localization of singularities are extremely important for the correct prediction of the threshold. This is notoriously difficult problem and the techniques used in this section are inadequate.

First, it is not clear that the standard reaction mechanism developed for hydrogen-air flames far from the lean limit (this is what is usually supplied with CHEMKIN) is appropriate for this problem. At temperatures of 800 K and lower, a number of studies show that the predicted reaction times are one to two orders of magnitude lower than the measured times. See M.L. Vermeersch, A Variable Pressure Flow Reactor for Chemical Kinetics Studies, Ph.D. Thesis, Princeton University, 1991. The recent high-temperature combustion studies carried out at BNL obtained "significant" hydrogen oxidation at 650 K within a time frame of minutes.

Second, the model is being misused. The equations should really be the time and spatial dependent ignition equations with suitable loss terms in the energy and species equations. Maas and Warnatz, Combustion and Flame, Vol. 74, p. 53, 1988, give a complete discussion of the correct model.

RESPONSE F48: *We agree. We will delete from Appendix F any attempt to predict autoignition.*

Third, the amount of preexisting hydrogen in the atmosphere will have a strong influence over the outcome of this process. If sufficient hydrogen (> 4 to 5%) is present, a propagating flame could actually be initiated in the dome region. This possibility has been completely neglected in the present analysis.

RESPONSE F49: *We agree. See Response F33.*

Sections G and H

I would like to see one-to-one comparisons of the experimental results from the two facilities. These comparisons should be carried out in properly scaled variables in order to clearly display the effect of scale. So much has been made of this effort to compare the varicus scales that I would actually like to see the comparison. In addition, it would be useful to have a critical analysis of this comparison, strictly based on the experimental data alone.

RESPONSE F50: *This has been done, in part, in a letter report to the NRC (Pilch, Binder, Allen, 1992). The comparisons in Fig. E.6 include experiments conducted at 1:40th, 1:30th, 1:20th, 1:10th, and 1:6th scale.*

REBUTTAL FROM REVIEWER F

I have looked over the replies to my review of the referenced document. It appears that the authors have made a diligent effort to constructively respond to my comments. On this basis, I expect that the issues I have raised will be adequately addressed by the authors.

However, I await the final revised document before making any conclusive statement about resolution of these issues. In a number of cases, it is unclear exactly how much revision will actually occur. But on the surface, I believe that the proposed revisions are appropriate.

Comments by Reviewer G

SUMMARY COMMENTS

Here are what I perceive as the big questions involving the DCH issue, and comments:

The Three Big Questions

1. **Can the DCH issue be resolved for a given system, using the available experimental information and computer simulation models?**

   I think the framework and information is available for estimating the probability of containment failure from DCH, provided that input probability distributions are skewed far enough to satisfy recognized experts that moderate conservatism is introduced in the result.

2. **Is the problem understood well enough to obtain resolution?**

   The fact that experts disagree on various aspects of DCH problem does not mean that the problem is not understood well enough for resolution. It does mean, however, that the level of resolution achievable may not be acceptable; that is, it may be ultra-conservative, whereas more understanding of several key phenomena could bring an acceptable resolution.

3. **What level of resolution is acceptable, and is further study needed to make it acceptable?**

   I think that the DCH issue is close to an acceptable resolution whereby recognized experts will have participated in the ROAAM process and come to a unified position on the expected range of inputs employed. This achievement may require additional study by working groups whose mission is to propose and carry out what is necessary to satisfy valid concerns.

RESPONSE G1: *We agree.*

A Proposed Resolution Process

The philosophy of a resolution process described in NUREG/CR-6075 is as follows:

1. Employ a basic thermodynamic model for a region, which gives pressure as a function of energy, mass, and volume. The CLCH and TCE models start here.

2. Obtain a formulation which shows the limits of containment integrity in terms of pressure and thermal loads which could be imposed by adjacent thermodynamic states.

3. Recognize that the time-dependent energy and mass contained in any region depend on the rates of transport across boundaries which separate regions in the containment.

4. Further recognize that the energy and mass transport rates are determined by pressurized discharge phenomena, geometry of flow paths, entrainment mechanisms of corium, and chemical reaction of hydrogen formation, ignition, and burning.

5. Allow for the fact that transport uncertainties exist because the transport rates depend on a range of possible initial conditions, geometry, and local states which depend on accident sequences, and can change rapidly.

6. Process the known information in a way that compares the predicted thermodynamic states with containment integrity limits, using the range of possible input combinations.

7. Interpret the results in terms of the likelihood of containment failure.

8. The ROAAM process provides a framework for combining current knowledge, experimental data, and uncertainties into a probabilistic framework which yields a failure probability.

9. The technical concerns expressed by national laboratory staff mostly criticize NUREG/CR-6075 for either neglecting, misinterpreting, or misapplying their experimental results in obtaining inputs for important parameters.

10. I think that two additional steps would be useful in resolving the DCH issue:

    (a) Let the authors of NUREG/CR-6075 respond to the criticisms, first in writing, then at a round table, as was done in the Mark I Liner issue. This provides a forum for both supporters and critics to converge on how best to handle remaining differences of opinion.

    (b) Form working groups for the purpose of strengthening the weakest inputs by either additional computer studies, or other studies in order to achieve reasonable agreement among participants, as in the Mark I process.

RESPONSE G2: *It is within the ROAAM process to address comments and accept input from peer reviewers and any follow-up potential activities.*

ADDITIONAL REMARKS

The rest of my remarks are organized according to the format requested in the July 2, 1993 letter from Brian Sheron, confirming my participation in reviewing reports addressing the resolution of the DCH issue.

(a) The technical merits of the conclusions and the analyses described along with the quantification of inputs (i.e., estimate of initial and boundary conditions, containment loads, and structural response).

The report makes use of the ROAAM procedure for obtaining the probability of violating containment limits. The framework for employing ROAAM involves causal relations for containment peak pressure, and containment failure probability as a function of pressure. Two independent models are employed for prediction of the containment peak pressure: The Convection Limited Containment Heating, CLCH, and the Two Cell Equilibrium, TCE, models.

Comments in reviews by national las challenge the statements made about independent models, because the authors have worked together on the DCH issue. I was present on different occasions when each of the models was introduced. In my opinion, the CLCH and TCE models represent two different means of distributing energy and mass throughout the containment. These models were conceived at different time by two authors, and I think that whether one influenced the other or not is immaterial. Whether energy is confined to a region of the containment, or its release to heat the containment atmosphere is otherwise retarded, the end result is containment pressure, and both models reasonably agree.

Both the CLCH and TCE models include the amount of corium dispersal and consequent containment gas heating, hydrogen generation, and combustion, all of which are intimately associated with the melt dispersal (or entrainment) and blowdown characteristic times. These times appear as the ratio of (dispersal or entrainment time)/(blowdown time), called the coherence ratio, CR. Entrainment models and experimental studies show that the dispersal time is difficult to predict. Therefore, the containment pressure in the CLCH model is obtained for a range of CR between zero and 2.0. Surprisingly, containment pressure is relatively insensitive to CR greater than 0.5. This is one of the advantages of simple models, relative to multinode systems, in that they show behavior trends, and display the importance of different parameters, assumptions, and initial conditions.

The CLCH and TCE models are based on spatially uniform systems (top down approach) with energy and mass accounting to obtain the thermodynamic state. Uncertainties arise in the amounts of mass and energy that are transferred to a system (bottom up approach), which may depend on the initial conditions as well. The CLCH and TCE models are independent formulations which yield the containment pressure as fundamental functions of gas mass,energy, and volume. The gas mass, including hydrogen, and thermal energy of the gas, have possible ranges that require quantification.

Extensive discussions are given in NUREG/CR-6075 for obtaining expected values and standard deviations of the parameters which affect mass and energy quantities. Phenomena, computer code predictions, and experiments are cited and employed to obtain inputs for the ROAAM computations. The study draws heavily, as would be expected, on work reported throughout the industry, and does a nice job of citing, discussing, and interpreting the references.

Comments by national labs state that some information has been misinterpreted, misapplied, or neglected altogether. These comments require response from the authors and probably subsequent dialogue to be resolved.

The authors have given a strong case for their conclusion that containment failure by DCH in Zion type plants is physically unreasonable. Remarks made by national labs are not in agreement, citing their concern that such a position is vulnerable at this stage. They also object to such a conclusion coming from a small number of experts. While the authors may be correct in their conclusion, it is important to use the present work as a springboard for achieving a unified conclusion among both the authors and the labs. Such a conclusion, based on current knowledge, may not be tolerable for some plants, but the groundwork for further refinement would be a joint effort.

I've seen the ROAAM process work on the Mark I liner issue. An initial in-depth prediction of a failure probability is made, every recognized expert is invited to challenge results, rebuttal and modifications are allowed, and where input issues are unresolved, expert committees are enlisted to determine what is required to resolve them. The process stops when participant's concerns have been addressed and they are satisfied with the probability ranges and causal relations employed in ROAAM.

RESPONSE G3: *No comment.*

(b) Identification of the sources of uncertainties in the analysis and their impact on the conclusions.

The important uncertainty described in NUREG/CR-6075 is the ratio of melt dispersal time to the blowdown time, or coherence ratio, CR. Although the blowdown time can be easily bounded for a given discharge hole size and initial conditions in the vessel, corium dispersal is a complex phenomenon, not easily predicted with certainty. Geometry of the cavity and subcompartment play a role in the corium dispersal time, as well as entrainment and trapping, which are difficult to predict accurately from deterministic models.

The CLCH model displays a relative insensitivity to the CR above 0.5, which implies that at higher CRs, the not-easily-predicted processes embraced by the CR have lesser influence on the

end pressure. This observation is significant, because it helps in ranking the importance of phenomena with large uncertainties.

A potential weak spot in the analysis of uncertainties involves hydrogen formation and combustion. National lab comments are both supportive, and cautious about how to properly include hydrogen effects. Resolution and a unified judgement is needed here.

RESPONSE G4: *See Response F33.*

(c) The necessity for further experiments or confirmatory research as suggested in the report.

There are three items noted in NUREG/CR-6075 that require further attention of a confirmatory nature. These involve (a) deeply flooded cavities, (b) system pressure level, and (c) containment strength. These appear to be plant specific concerns, which may be of secondary importance when contrasted with concerns raised by the national labs.

I think that time and effort would be well spent in providing a forum where all qualified experts can state their concerns, and then join forces to discuss what it would take to eliminate their concerns. In some cases, it might be increasing the standard deviation or moving the expected value of a parameter with uncertainties. In other cases, it might require a computer substudy of the sensitivity to a particular parameter in order to gain confidence about its representation in ROAAM. Still other cases may require additional experiments or confirmatory research to obtain agreement among experts.

RESPONSE G5: *We agree.*

(d) Potential for application and extrapolation of the methods and conclusions to other reactor and containment designs.

The basic CLCH and TCE models will not change from one plant to another, although the mass and energy transport rates will vary. The generalizations given for extrapolation in NUREG/CR-6075 are logical, but not verified. For example, even though there may not be a direct pathway for debris into the main containment volume, the wrong combination of other

geometric and thermodynamic parameters could make the Zion system analyzed nonrepresentative of a similar system. Detailed computer models can help by providing fine structure calculations for expected or bounding parameters, which could then be compared with pressures and temperatures obtained for the Zion system.

RESPONSE G6: *We disagree. The present models capture the key physics and involve no arbitrary parameter selection. Attempts at more detailed models would be plagued by numerous parameters in an attempt to characterize poorly understood phenomena in complex geometries.*

Small scale-model systems could be built for plant specific applications to predict debris dispersal and time available for FCI and hydrogen generation. Such systems already have been built and have provided data on dispersal. More might be needed, depending on how representative available data is of a given system being considered. This could provide expected values and standard deviations to use in ROAAM.

RESPONSE G7: *Experimentally, we know that Zion and Surry are dispersive and that these cavities are representative of most PWRs (excluding CE and ICE condenser plants). We assume that 85% of the melt is dispersed in the 8 MPa cases and assume complete dispersal in the 16 MPa sensitivity studies. We also assume (see Response M3) that heat/mass transfer processes go to equilibrium during the dispersal process and that heat transfer to structures is minimal. These are conservative assumptions. Thus, a detailed representation of these processes is not needed.*

Extrapolation does not seem to be a valid issue until the technical community is unified in the determination of a containment failure probability for the Zion plant.

RESPONSE G8: *We agree. The Zion document is intended to identify issues important to DCH resolution. However, we are also forward looking and view our discussion of extrapolation as providing insight into how DCH could be resolved for most PWRs.*

REBUTTAL FROM REVIEWER G

I have no rebuttal to the authors' responses to my earlier discussion of the subject report. They have adequately explained their disagreement with one of my comments expressing reservation about extrapolating NUREG/CR-6075 to other plants (see Response G6).

Let me comment on several concerns expressed of other peer reviewers.

The authors' CLCH and TCE models are still viewed as either "too simple to be correct," or lacking in essential physics by some of the reviewers. I fully support these models, which are based on first principles of mass and energy conservation.

Some reviewers have expressed concern that the energy is not properly taken into account. The authors have responded by noting that only energy which is added to the atmospheric contents creates pressure increase. This is a key point. If energy remains locked up as internal energy in hot debris, or as chemical energy in unburned hydrogen, it does not raise the containment pressure. The questions asked by several reviewers is, "Where is the rest of the energy?" The authors correctly point out that it is there, but not all of it has transferred to the containment air by the time maximum pressure occurs.

The CLCH and TCE models yield containment pressure in terms of mass and energy in the air space. The formulations make use of the coherence ratio, (melt dispersal time/system depressurization time). The exact value of coherence ratio is now known because it depends on the fine-structure, or bottoms up phenomena, (droplet entrainment, trajectories, transient heat transfer from droplets, metal/water interactions. etc.) which are not yet fully understood. However, the results show that even for a broad range of the coherence ratio, maximum pressures become relatively flat. In my opinion, this was a breakthrough for the DCH issue resolution. It employs a macroscopic model, based on fundamental physics, to show (somewhat surprisingly) that you don't need to know all of the fine structure details to reasonably bound the containment maximum pressure.

In a way, this is like classical turbulent flow problems. The fine structure of turbulence is not fully understood, but we can closely predict the conditions for which it occurs, and then design for it.

I think that there is enough technology tied together in NUREG/CR-6075 to resolve DCH for Zion now.

Additional peer-reviewing, dialogue, round tables, and substudies will:

1. Make it possible to extrapolate Zion results to other plants;

2. Refine distributions used in the ROAAM;

3. Help diminish some remaining reservations held by various experts;

4. Increase confidence in the initial conditions.

Comments by Reviewer H

1. Page 5, first paragraph: The authors claim that "...the initial melt parameters are to be quantified as probability density functions, representing modeling uncertainty in the parameters (variations from stochastic processes are assessed to be insignificant relative to modeling uncertainty)." The authors should not claim that modeling uncertainty is totally captured by their pdfs and CRs. Typically, the following uncertainties are not addressed in a ROAAM type analysis:

a) Uncertainty associated with the highest level model used (i.e., the ROAAM decomposition model itself). One may argue that although a ROAAM decomposition model may ultimately reflect the consensus of experts, its accuracy and completeness still carries some uncertainty. This modeling uncertainty is not reflected in the ROAAM process and is very difficult to model.

b) While the parameter uncertainty due to stochastic variations is believed to be much smaller than modeling uncertainty, this cannot be proved.

c) Although the DPDs assigned to the initial parameters can theoretically capture the modeling uncertainty, the process of building the DPDs by experts is informal and highly subjective. These DPDs reflect the uncertainty that the authors subjectively place on the available literature. Other analysts may suggest different DPDs. If their views are not adequately reflected, an uncertainty about the accuracy of the DPDs may still exist.

Based on the discussions above, it appears that although modeling uncertainty is better addressed by ROAAM than other methods such as NUREG-1150, all uncertainties are not reflected in the final ROAAM calculations.

RESPONSE H1: *We agree that modeling uncertainty is better addressed in ROAAM than other methodologies. Uncertainties associated with the decomposition itself are intangible in nature and cannot be quantified. We expect that any difficulties, if they exist, will surface as part of the review process. We cannot prove that modeling uncertainty dominates stochastic uncertainty. Although the DPDs represent <u>our</u> judgement, we do seek consensus amongst knowledgeable experts as part of the ROAAM process. However, the sensitivity studies performed by Reviewers H and O suggest that the results are not sensitive to our judgements of the DPDs.*

2. Paragraph 1, page 6: Scenario I UO_2 mass is based on the TMI-II experience. How does the DPD representation capture modeling uncertainty here?

RESPONSE H2: *Modeling uncertainty is captured by examining the controlling phenomenology and noting any similarities to TMI-II. In Scenario I, and in TMI-II, crucible formation and failure is the controlling phenomenology. Thus, we use TMI-II observations to guide our selection of the best estimate UO_2 mass. Modeling uncertainty associated with the formation of a crucible is treated by considering Scenarios III and IV where crucible formation is not assumed. Modeling uncertainty on crucible failure is recognized by considering the range of the credible failure locations. This is reflected in the spread of the UO_2 distribution about its mean. Thus, modeling uncertainty is captured by splinters as well as by DPDs.*

3. Paragraph 2, page 6 and footnote 4: DPD is not a pdf format. The authors should differentiate between these two probabilistic representation methods. DPDs can be converted into a pdf, but the two should not be used interchangeably. In the Mark I Liner Issue, it was highly recommended by several reviewers that for displaying uncertainty range, pdf representation be used.

RESPONSE H3: *The point is a matter of semantics. DPDs and PDFs convey the same information and can be used interchangeably. This is a matter of taste.*

4. Equation 2.3: This equation assumes that m_{UO2}, $X_{Zr,j}$, and $m_{ss,k}$ are independent. The general form of this equation should assume dependence, thus

$$P_{ijk}(m_{Uo2},X_{Zrj},m_{ss,k}) = P_i(m_{Uo2}).P_j(X_{Zrj}|m_{Uo2}).P_k(m_{ss,k}|m_{Uo2},X_{Zrj})$$

Of course, if elements m_{UO2}, X_{Zrj}, and $m_{ss,k}$ are independent, then this equation reduces to equation (2.3) of the report. It is difficult to argue that these processes are absolutely independent. In fact, comment 12 discusses certain factors that make m_{UO2}, X_{Zrj}, and $m_{ss,k}$ dependent.

Similarly, $R_{r,l}$ in its general form, is dependent on the values of m_{UO2}, X_{Zrj}, $m_{ss,k}$), accordingly

$$P_{ijk}(m_{Uo2},X_{Zrj},m_{ss,k},R_{r,l}) = P_{ijk}(m_{Uo2},X_{Zrj},m_{ss,k}).P_l(R_{r,l}|m_{Uo2},X_{Zrj},m_{ss,k}).$$

RESPONSE H4: *The equations in Section 2 are intended to be general. In some scenarios, one or more of the distribution parameters is strongly correlated with another as discussed in Sections 3 and 4. Equations 2.3 and 2.4 are still applicable provided the probability of a dependent parameter is appropriately interpreted as conditional on the required input. Table 3.1 summarizes the key dependencies for each scenario (indicated by an equation evaluation for the strongly correlated parameters). Section 2 will be clarified to reflect these points.*

5. Equations 2.1-2.3, 3.1, and 4.3: Terminology is inconsistent in these equations. For example, UO2 mass is represented by m_{UO2} in equations 2.1-2.3, by M_{UO2} in equation 3.1, and by M_d in equation 4.3.

RESPONSE H5: *Capital letters will be used for mass quantities in the body of the report.*

6. Section 2: Uncertainties are not always expressed in form of DPDs as claimed in this section and as Appendix-A suggests. While pdf1, pdf2, and pdf3 are presented in DPD forms (not for all scenarios, for example, steel mass for scenario II and IV are represented by equations), the coherence ratios based on TCE and CLCH models are assumed to follow normal distributions with assumed relative standard deviation values of 12.5 percent and 28 percent, respectively.

   Additionally, if normal distributions with assumed relative standard distributions are used, in what ways the modeling uncertainty about the scaling up model for coherence ratio is accounted for?

RESPONSE H6: *Normal distributions are used, but we intend that they convey judgmental degrees of belief, not any statistical significance. Modeling uncertainty is further accounted for by using two different correlations in the plant evaluations. The coherence correlations are based on experiments ranging from 1:40th to 1:6th scale. No significant effect of scale is observed in the data and no scale effect is reflected in the correlations. They can be applied to reactor scale provided they are not applied outside their database. Fortunately, both models are evaluated in reactor applications that interpolate on the database.*

7. Page 21, paragraph 2: SCDAP/RELAP5 calculations in NUREG/CR-5949 is based on Surry reactor only, not Surry and Zion reactors.

Since SCDAP/RELAP5 calculations are based on TMLB' sequence, in what ways these calculation are applicable to SBLOCA-like sequences of Scenarios 1 and 2?

RESPONSE H7: *We do not use SCDAP/RELAP results in any direct way. We have examined SCDAP/RELAP results for both Zion and Surry, along with other information, when formulating our quantifications. NUREG/CR-5949 is Surry specific while similar calculations were supplied to us for Zion (Knudson, 1993). These calculations considered a range of pump seal leaks characteristic of SBLOCAs.*

8. Page 22, paragraph 1: The 8 MPa enveloping pressure, while somewhat consistent Knudson and Dobbe calculations, is inconsistent with TMI-II accident of 10 MPa. The authors have considered this as a "peculiar" case since it is extremely unlikely. In a probabilistic treatment of rare events such as DCH, the whole spectrum of events occurred regardless of their likelihood should be considered as viable evidence. From a probabilistic view point, the TMI sequence is the strongest and most confident evidence that we currently have. This underlines the importance of presenting our state of uncertainty about the RCS pressure at the time of vessel breach in form of a DPD instead of an enveloping value. Such a DPD represents the RCS pressure variability in the available literature and the degree of belief that can be placed on them. Similar to the use of TMI melt mass of 21 tones as a best estimate for M_{UO2} DPD, the TMI's RCS pressure should be factored into estimating the RCS pressure DPD.

RESPONSE H8: *TMI-like scenarios with a reflooded RPV do not lead to significant DCH loads. The RCS pressure at TMI continued to drop to a low value of ~5 MPa at the time that the block valve was closed. Repressurization was accompanied by pump startup and HPI. Thus, operator actions leading to high pressure also caused the vessel to fill with subcooled water. Had the vessel failed, which did not occur (presumably because of water in the lower plenum), then >100 mt of subcooled water would have been coejected with the ~20 mt of oxidic melt from the RPV. This water has the capacity to fully quench ~20 times the melt present at TMI-II. We recognize that the crucible phenomenology at TMI-II is more generally expected but that*

operator actions lead to a situation (flooded RPV) where DCH loads would be reduced to a steam spike because of coejected water (even if the vessel was fully pressurized).

9. Page 22, paragraph 2: The argument provided for bounding of the RCS pressure to 8 MPa is inadequate. I suggest to treat RCS pressure as a random variable represented by a DPD in the ROAAM decomposition hierarchy. Especially since sensitivity studies show that full 16 MPa pressure does not alter the final quantification, the spread of this distribution should not affect the final result. From SCDAP/RELAP5 calculations (Knudson and Dobbe--NUREG/CR-5949), it appears that an overwhelming majority of the RCS pressures at the time of vessel breach are at low pressures (-1.38 - 6.89 MPa). See Table 10 of Knudson and Dobbe for different RCS pressure probabilities.

RESPONSE H9: *We resist suggestions to include full pressure scenarios in our base quantification based on the argument that it makes no difference in the results. We view the RCS pressure as bounded by ~8 MPa; we cannot defend any distribution of RCS pressure. For perspective, we note that the probability of being at full pressure at vessel failure was only ~.02 in NUREG-1150 and that recent SCDAP/RELAP calculations all indicate surge line or hot leg failure at full system pressure. However, we recognize the concerns expressed by some reviewers and some members of the NRC with regard to RCS pressure. If at the end of the peer review process, this issue is not satisfactorily resolved, we will change the report accordingly.*

10. Page 27, paragraph 2: If the TMI accident was not arrested, it appears that the amount of relocated UO2 may have been higher at the time of vessel failure. Thus the use of TMI-II melt mass of -21 mt as a "best estimate" for Scenario I UO2 mass distribution may be somewhat low.

RESPONSE H10: *It is important to understand the relationship between TMI-II and Scenarios I and II. Scenario I represents a penetration failure occurring during or shortly after relocation. Consistent with the TMI-II experience (which is the strongest and most confident evidence we have), ~20 mt of relocated material makes sense for Scenario I. The reviewer then speculates that additional material may have relocated if failure had occurred at some later time (neither occurred at TMI-II). This is analogous to our Scenario II.*

11. Page 27, last paragraph: The discussions provided in this paragraph clearly describe the subjectivity of the DPDs used. The DPDs are simply judgements of the authors and are not obtained through a formal expert elicitation process. Based on the arguments presented in this paragraph, I can equally claim that with 90% probability the reasonable bounds of UO2 in the melt ranges from 10 to 30 mt lower and upper extreme ranges can each have a 5% probability. Thus, the following distribution can be used (maximum entropy representation). Why not use this distribution?

Similar arguments can be made for other DPDs described in this report. For example, for Zr oxidized which ranges from 20-60 percent, a probability of 0.90 can be used. Accordingly, for 0-20 percent and 60-100 percent Zr oxide, a probability of 0.05 can be used.

RESPONSE H11: *Construction of our DPDs represents our judgment. Formal elicitation is also very judgmental. We seek consensus in this judgement process, while avoiding maximum entropy arguments. However, it makes no difference for the case cited since Reviewer O could not achieve containment threatening pressure with ~100 mt of UO_2 in his sensitivity studies.*

12. Section 3: The issue of dependency among the initial parameters is not adequately discussed. I believe that there is a varied degree of dependency between m_{UO2}, X_{Zrj}, and $m_{ss,k}$. These are some sources of dependencies:

a) Amount of stainless steel in the melt depends on the total amount of melt. Core steel, upper plenum steel (due to natural circulation melting of upper plenum that occurs at high pressures) and lower plenum steel (due to direct contact with melt) varies depending on the RCS pressure, amount of melt and timing of vessel failure.

b) Fraction of Zr oxidized depends on the amount of UO_2 mass.

c) Zr oxidized depends on RCS pressure.

To account for these dependencies, parametric treatments such as the use of a linear correlation coefficient may be used. The degree of correlation can be estimated by authors. For example, one can use low, medium, or high dependence.

RESPONSE H12: *We cannot justify additional correlation between the parameters beyond what is already done. In some cases we chose to bound any such correlation to maintain clarity of the processes. As the reviewer suggests, steel mass is already explicitly correlated in Scenarios I and II with the total amount of relocated material. This will be clarified in the text. In Scenarios III and IV, we bound the correlation of steel with additional Zr oxidation by considering that all upper plenum steel has relocated to the lower plenum. We see no correlation between the fraction Zr oxidized and UO_2 mass; and for that matter, we see no correlation between UO_2 mass and the fraction Zr oxidized. The latter is covered by bounding the amount of UO_2 in crucible and gradual relocation scenarios. We arrive at our quantification of Zr oxidation by examining code calculations appropriate to the Scenarios and RCS pressures of interest. We believe that they are conservative.*

13. Section 3: Instead of a DPD, for scenario II and scenario IV steel mass is obtained from equations 3.5 and 3.8 respectively. In effect, these equations are assumed to have a probability of 1 for yielding the correct answer. Considering the uncertain nature of these equations and their underlying assumptions, what is the justification for using point estimates as opposed to DPDs?

RESPONSE H13: *Our explicit treatment of correlating steel mass with relocated material (Eq. 3.5) is intended to <u>bound</u> the process. For example, we note that not all submerged steel was melted at TMI-II. In fact, only a few nozzles melted while many remained fully intact even though they were covered with melt. Equation 3.5 applies only to lower plenum steel. If upper plenum steel is also molten (and we argue that it is not), then both upper and lower plenum steel must be considered. In Eq. 3.8, we intend to bound the steel mass with contributions from both the upper and lower plenums.*

14. Page 30, last paragraph: Justify the assumption that up to 75 percent of degraded core will relocate.

RESPONSE H14: *We do not expect a crucible to fail on the bottom. The core blockage and crucible are most dense on the bottom while convective patterns in the molten pool strongly favor failure high on the sides of the crucible.*

15. Equation 3.6: $M_{S,LP}$ appears both in the right-hand side and in the left-hand side of this equation.

RESPONSE H15: *Typo will be corrected.*

16. Section 3: The discussions justifying the shape and form of DPDs should be extended to help the independent reviewers reach a consensus. If convincing arguments cannot be made, then maximum entropy distribution would be a better alternative.

RESPONSE H16: *Maximum entropy should not be used "as the easy way out" to avoid reaching a consensus on tough issues. In our quantifications, we bound the process. Usually, physical arguments suggest that the processes leading to the bound are judged highly unlikely; consequently, we assign low probabilities to the bound. We will clarify our reasoning in each case in the text. Maximum entropy distributions have their greatest value in examining the range of behavior, but often this does not give a clear answer for all cases. If the uncertainties are sufficiently large, then additional decomposition may be warranted as an alternative to maximum entropy.*

17. Page 48: The probabilistic treatment of the CLCH model is questionable. The authors have used the scaling equation 4.1 to estimate the coherence ratio for the full scale reactor. However, based on the variability that they observed in the coherence ratios of the IET experiments (which have a relative standard deviation of 12.5%) they extended the same variability to the full scale estimation of the coherence ratio. Accordingly:

    a) Only the variability in the experimental results that are mostly attributed to experimental measurements in the SNL/IETs is counted.
    b) The treatment violates the ROAAM process of accounting for uncertainties associated with the model as well as the variability in the available data in form of a DPD.
    c) Choice of a tight normal distribution (12.5% relative standard deviation) based on only a handful of experimental data points is not supported nor seems reasonable.

RESPONSE H17: *We disagree. Modeling uncertainty is accommodated by using two different correlations as well as by providing a distribution. The important thing is that each correlation is being applied to reactor scenarios that interpolate on the database; consequently, the two coherence ratios give similar results. The relative standard deviations differ substantially in the two correlations, reflecting two complementary philosophies: one that is selective by considering only the most consistent data, and one that tries to be all-inclusive. However, as the load distributions indicate, the results are not sensitive to these differences in relative standard deviations. The reviewers own sensitivity study (comment 7 on the ALPHA code) confirms this conclusion.*

18. Page 49: Similar concerns discussed for the uncertainty treatments in the CLCH model also applies to the TCE model. In the TCE model a relative standard deviation of 28 percent is used. Why do we need two different models for measuring the same value? If we are uncertain about the accuracy of each model, why the authors do not incorporate this uncertainty in their probabilistic treatments as the ROAAM process dictates?

RESPONSE H18: *See Response H17.*

19. Page 51: The authors have not clearly shown the CR1 family of curves for converting a set of initial parameters into a containment pressure. This is an important element of this report and should be adequately discussed in the main body of the report. A simple graphical representation of CRs in the main body of the report is necessary.

RESPONSE H19: *CR1 cannot be fully represented because there are two many parameters to present on two dimensional plots. Some attempt to convey this information using the CLCH model is shown in Table D.2 and Figures D.2-D.5. The attached figures show selected results using the TCE model.*

FIGURES CITED IN RESPONSE H19

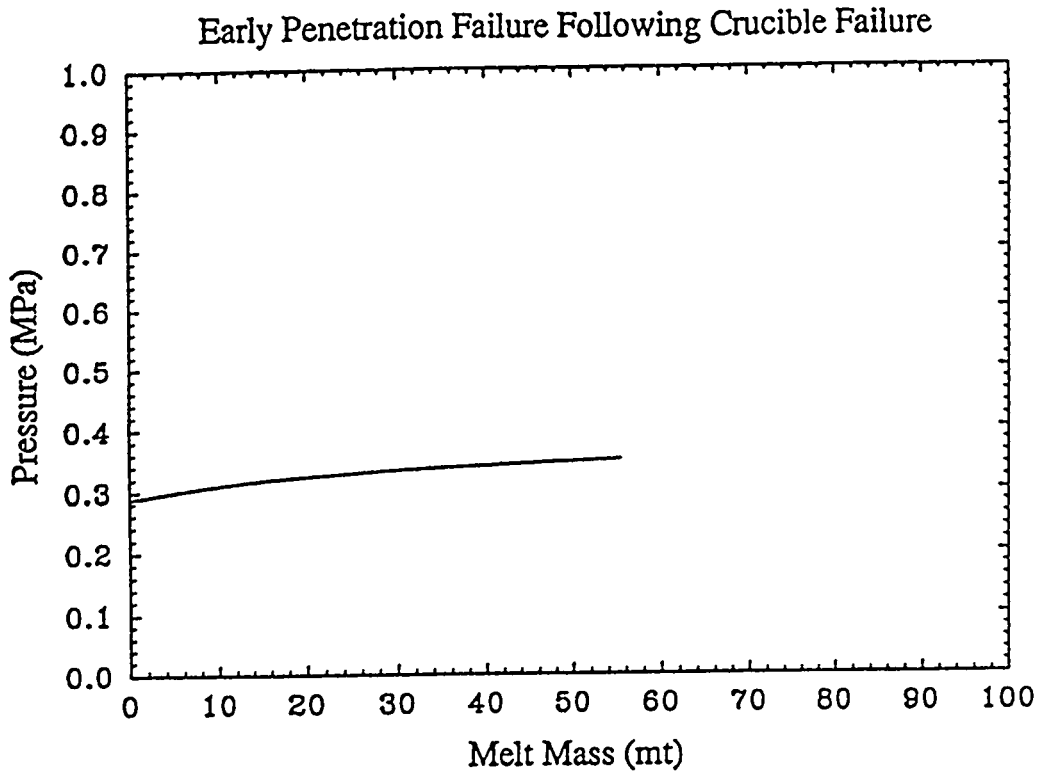

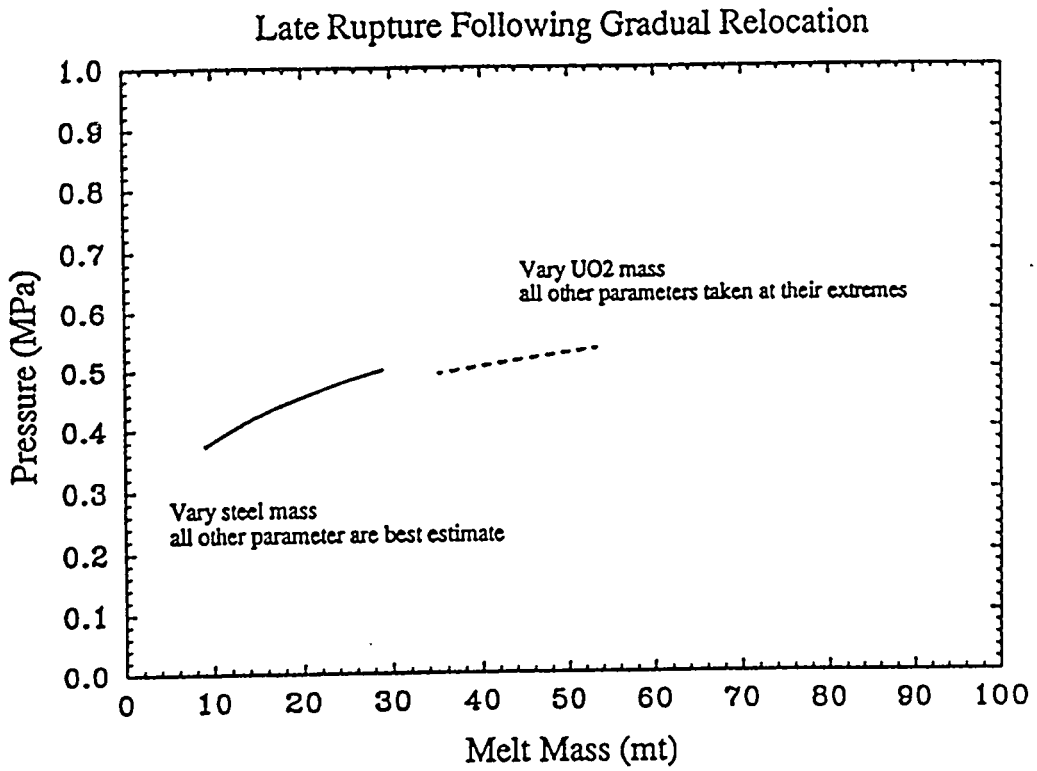

20. Page 54, figure 5.1: This figure is out of scale for the containment pressures of our interest. Since the pressures that we are interested are in the 20-60 psig range, a fragility curve for this range of pressure should be used to calculate the likelihood of failure. The use of containment failures of less than 10^{-3} in the report based on this curve cannot be supported by using Figure 5.1. Probabilities higher than 10^{-3} cannot be ruled out. Also, it would be desirable to develop families of fragility curves to represent the uncertainty associated with CR2. The IPE fragility curve uses some coefficient of variations to account for this uncertainty, but this falls short of a full uncertainty consideration through families of fragility curves.

RESPONSE H20: *Fully reviewed families of fragility curves that more systematically account for uncertainty do not currently exist. The IPE curve represents the best assessment of the utility. The Zion IPE curve has a threshold at 0.68 MPa.*

21. Page 57, paragraph 2: The reason for no intersection between the containment loads and the fragility curve CR2 is due to the scaling problem with the CR2 curve used as discussed in comment 20.

RESPONSE H21: *See Response H20.*

22. Page 60: Multiple changes in some key assumptions shows some sensitivity, with respect to Scenario IV. Furthermore, only the mean probability of containment failure is shown. It would be beneficial to show the whole distribution.

RESPONSE H22: *The reported probabilities are a high confidence bound. It is not possible to show a plot of probability versus failure frequency. Such a plot can only be generated when families of fragility curves exist.*

23. Section 7.0: Extrapolation to other plants seems premature before reaching a consensus on the Zion results.

RESPONSE H23: *We agree that Zion resolution must be resolved first. We envision that extrapolation will be based on insights gained in the Zion resolution process; however, some additional confirmatory (plant specific) information must first be obtained.*

24. Page A-4, paragraph 2: The use of weighted averaging of experts is described as inappropriate for cases where "issues" are involved. If ROAAM is supposed to converge the experts and some experts remain skeptical of the probability distributions used, the uses of some form of averaging technique or further decomposition of the ROAAM hierarchy is the most reasonable alternative.

RESPONSE H24: *Additional decomposition (splinters) may be necessary if consensus cannot be achieved. It is within the ROAAM process to address comments and accept input from peer reviewers.*

25. Appendix D: Appendix D reports seven Surtsey IET experiments, and explains that the facility is being converted to a Surry geometry. Appendix E uses eleven Surtsey experiments including some based on Surry geometry. Appendix G describes nine IETs including some to verify ANL experiments. The inconsistencies should be corrected.

RESPONSE H25: *Inconsistencies will be corrected. Inconsistencies arise because the report was being completed simultaneously with the completion of the experiment programs. Appendices G and H are incomplete accountings of the recent experiment programs. However, all experiments are fully documented elsewhere and they are appropriately cited in the text.*

26. Appendix D Nomenclature: Subscripts a and c are the same. Correct the error.

RESPONSE H26: *Typo will be corrected.*

Comments on the ALPHA Code

1. The code is difficult to follow. Detailed comments in the subroutines are necessary. Most of the variables are not defined in the code. One can only infer what they are.

RESPONSE H27: *The ALPHA code was not intended for production calculations by casual users. The ALPHA codes is not well commented and it is difficult to follow. SNL is currently reviewing the ALPHA code to ensure that the FORTRAN accurately reflects the text.*

2. The normalization procedure of the DPDs appears to have a bug. See for example Figure 1. Normalized DPD of the UO2 mass shown in this figure must give equal probabilities over various ranges of UO2 mass (similar to the DPD for Fraction of Zr oxidized). I observed that this error occurs for cases where the DPD is represented by an odd number of points in each range.

RESPONSE H28: *We have examined the FORTRAN and can find no error. However, we note that we always use even numbers of points.*

3. To see the sensitivity of the results to the probabilities assigned to various DPD ranges, a uniform distribution was used over the same ranges. For example, the normalized input DPDs for UO2 mass and Fraction of Zr Oxidized are shown in Figure.

4. The results for some key outputs such as containment pressure is also shown. The effect of this change was negligible. For all other scenarios a change to uniform DPDs over the whole range (by keeping the mean of the uniform DPDs approximately the same as the DPDs assigned by the authors in NUREG/CR-6075) didn't result in any appreciable change in the mean containment pressure. Thus it appears that the choice of DPD <u>probabilities</u> for various ranges is insensitive to the mean containment pressure. Although the shape of the output distributions is somewhat changed, the mean values remained largely unaffected. See comment 10 for a possible explanation.

5. To test the effect of the range of the input parameters, the input DPDs were shifted to the right and to the left by 33% (accordingly the mean is shifted by 33% too). Again, no appreciable effect in the mean containment pressure for any of the four scenarios was observed. Comment 10 may offer a reason for this insensitivity.

6. I have also made input distributions mildly dependent on each other, again no major change in the mean containment pressure is observed. Finally, input DPDs are made strongly dependent (i.e., for high UO2 mass, SS mass is made biased toward high values) and still no effect on the containment pressure is observed.

   One conclusion here is that the results (e.g., containment pressure) is not strongly related to any of the input DPDs. This, however, appears difficult to understand and justify.

Especially, if this is true, then why should we bother modeling them in the hierarchy? What other factors then control the mean values of the output DPDs (for example, containment pressure?)

7. A change in the relative standard deviation in normal distribution representing the coherence ratio (from 12.5% to 50%) calculated through the CLCH model did not affect the final results.

RESPONSE H29: *It is not clear to us why this is true without running the cases ourselves. We would expect slightly broader distributions for containment loads with no change in the mean.*

8. The output DPD of the diameter of ablated hole for some values of input would yield DPDs with almost random probability values. For example, see Figure 3 showing some output DPDs for Scenario-II based on the input values of NUREG/CR-6075. The DPD representing the ablated hole diameter does not have a defined shape. Since the hole diameter is governed by some physical parameters which have defined DPD shapes, this distribution should also have a defined shape. For example, it should show that certain ranges of hole diameter are more likely to occur than others. For some other input values it has a defined shape (for example, see Figure 4 which shows scenario III output DPDs). Is it possible that this is due to a programming error?

RESPONSE H30: *We have examined the model and the coding, and we can find no problem. Such apparently random behavior is common in DPD when the nodalization is coarse.*

9. Since I did not review the coding of the ALPHA program and I concentrated on calculating the effects of changes in the inputs to ALPHA, I believe that it is important that the code be independently and rigorously reviewed. The code should also be independently verified by using standard Monte Carlo codes.

RESPONSE H31: *The results have been independently verified using Monte Carlo techniques at Sandia. In addition, this Reviewer (H) and Reviewer O have also provided independent verification.*

10. By examining the energy balance equation in the code, contribution from the ultimate containment temperature (and thus containment pressure) is coming from three major terms: 1) heat contribution of molten mass, 2) heat contribution of O_2, N_2, Steam, and H_2, and 3) heat contribution of hydrogen combustion. Scenario-I calculations of the ALPHA code estimates the temperature rise contribution from O_2, N_2, Steam, and H_2, term to be the dominant factor (90% - 95%). With the other two terms having equal contribution to the temperature rise (about 5% - 10% contribution). Therefore, the input DPDs which influence these two terms would not be expected to play a major role in the final containment pressure. Other scenarios with somewhat higher melt mass do, however, result in slightly higher containment pressures. Accordingly, the ROAAM decomposition model has a small effect on the containment pressure since its input DPDs influence insensitive terms of the energy balance. Rather, non-DPD inputs such as amount of steam, accident scenario, containment and vessel physical characteristics determine the final pressure.

RESPONSE H32: *We recognize the insensitivity to oxide mass (see Response H19). Reviewer O found only a weak dependence of loads on oxide mass all the way up to full core. This is expected on physical grounds. The addition of more oxide mass increases the debris/gas equilibrium temperature. For relative small amounts of oxide, the equilibrium temperature approaches the initial melt temperature. The addition of more oxide cannot increase the equilibrium temperature beyond the initial melt temperature; consequently, the sensible and latent heat of this additional material cannot contribute to heating of gas or containment loads. The small sensitivity associated with oxide mass is attributed to increased amounts of transported material to the dome. Parameters not represented as DPDs are still part of the ROAAM decomposition and quantifications. Such parameters are treated in a bounding manner to remove sensitivity to hard to quantify details.*

11. The code indicates that 10% of the melt enters the upper plenum, whereas Table 3.1 of NUREG/CR-6075 assigns 9% to this value. While the difference is insignificant the discrepancy underlines the uncertainty about accuracy of the code as a whole.

RESPONSE H33: *Table 3.1 states that transport to the dome consists of 2 contributions, 9% through the gap and 5% through the seal table room, for a total of 14%. Transport to the dome*

is correctly implemented in the TCE model. We believe that the final working version of the ALPHA code also had dome transport correctly implemented in the CLCH model.

12. The ALPHA code is not a generic code. It should be adapted to each problem separately. For example, each of the four scenarios has a separate version of the code. Many of the scenario specific parameters are hard coded in the ALPHA code. It would be nice that simple editing facilities be made available so that decomposition model, DPDs and CRs can be easily entered for any physical phenomena. If needed the code can always call an external subroutine for any phenomena specific calculation.

RESPONSE H34: *See Response H27.*

FIGURE 1

Scenario I -- Initial Distribution

(Original)

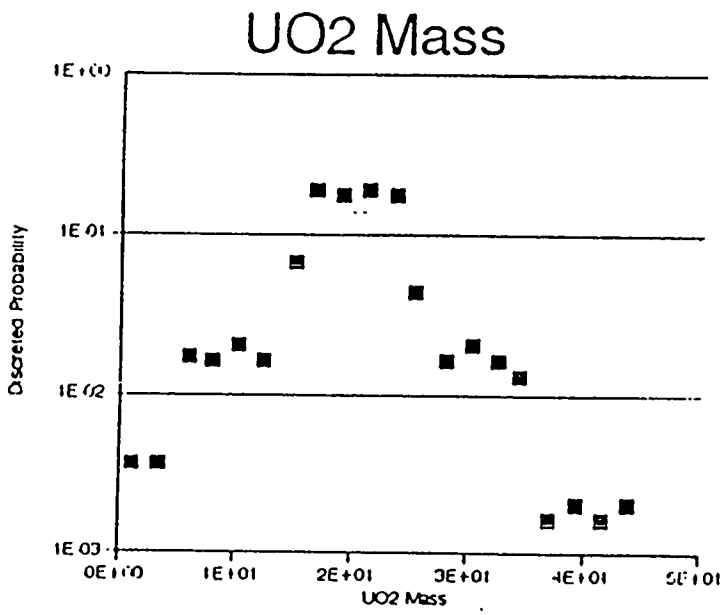

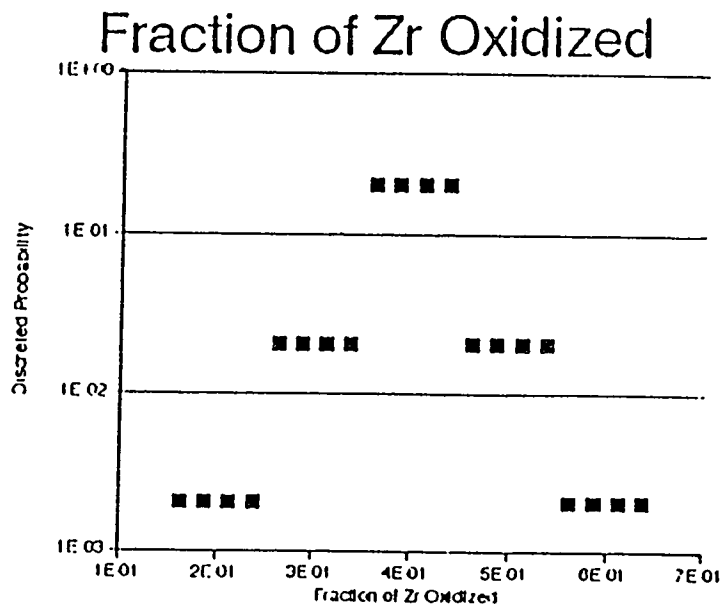

FIGURE 2

Scenario I -- Initial Distribution

(Uniform)

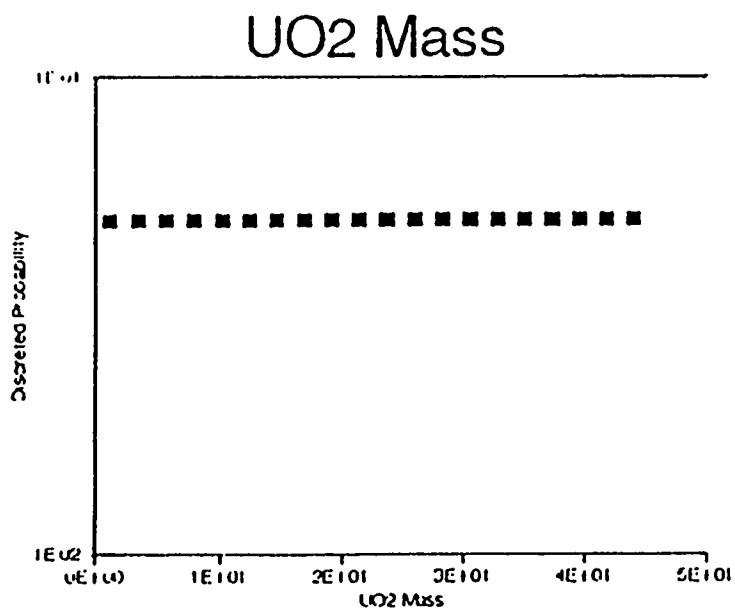

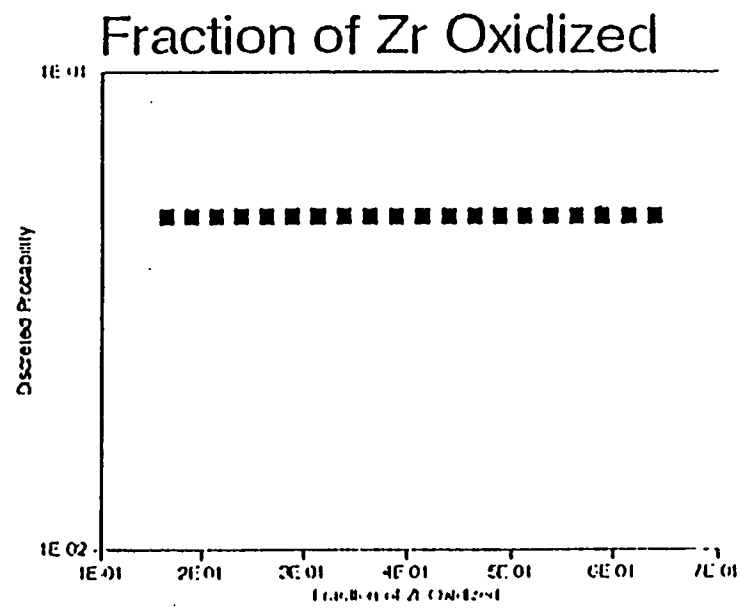

FIGURE 2 (Cont.)

Scenario I -- Output Distribution
(Uniform)

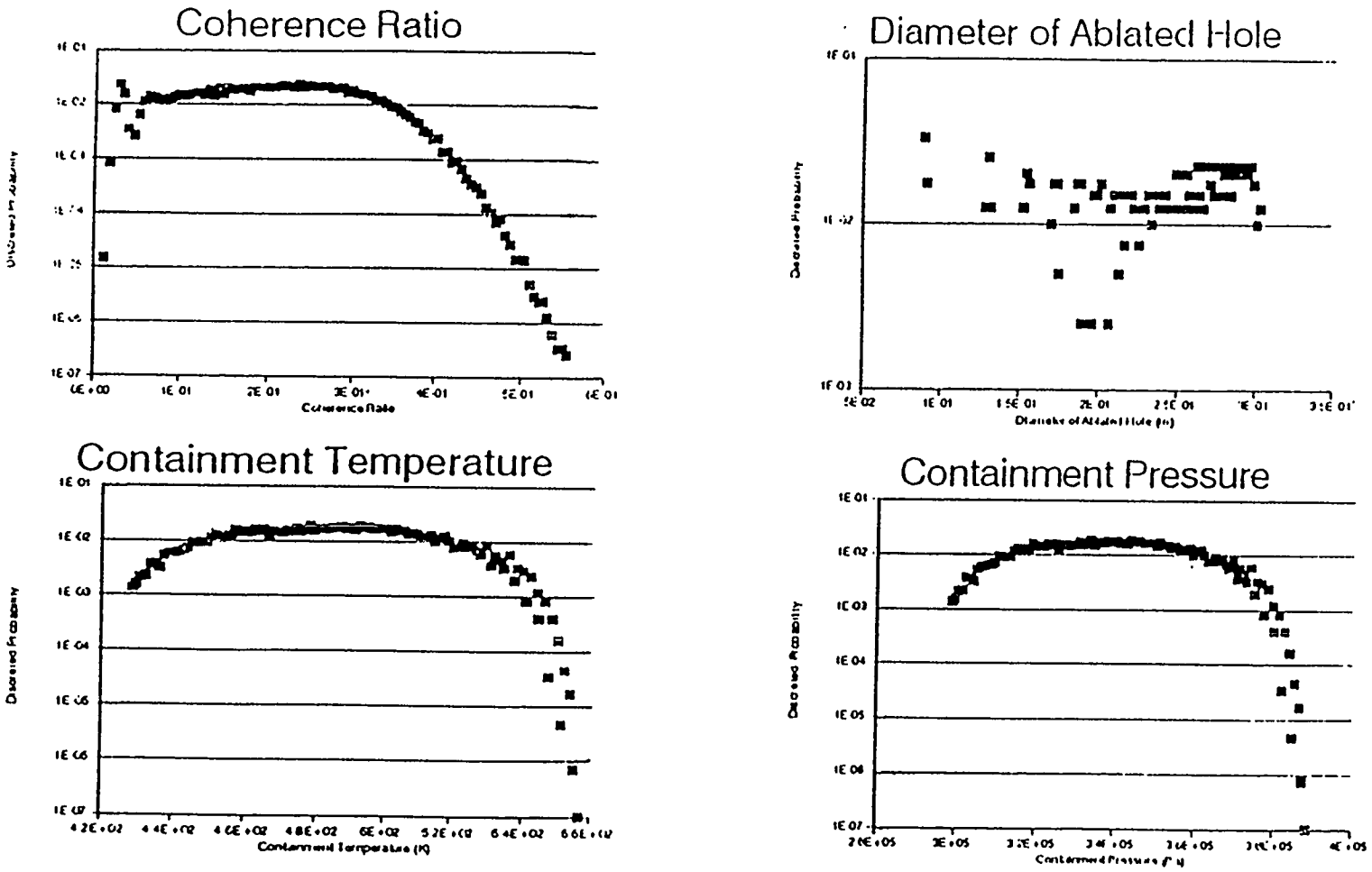

FIGURE 3

Scenario II -- Initial Distribution

(Original)

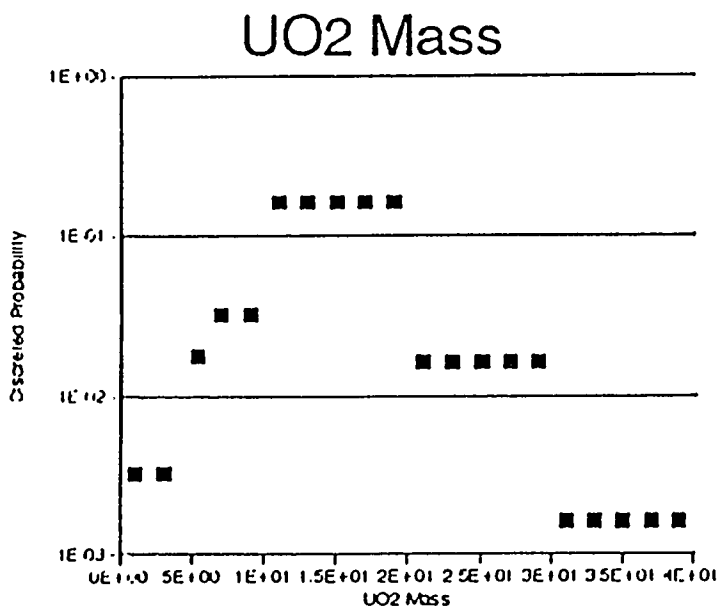

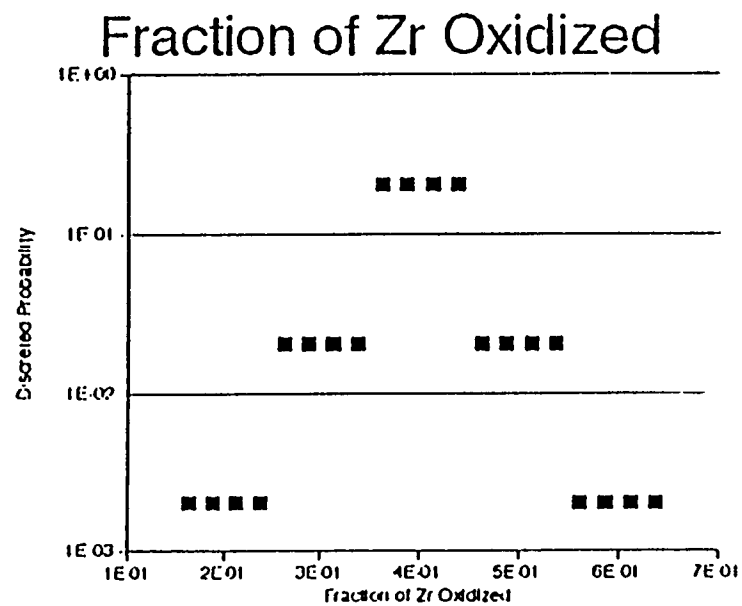

FIGURE 3 (Cont.)

Scenario II -- Output Distribution
(Original)

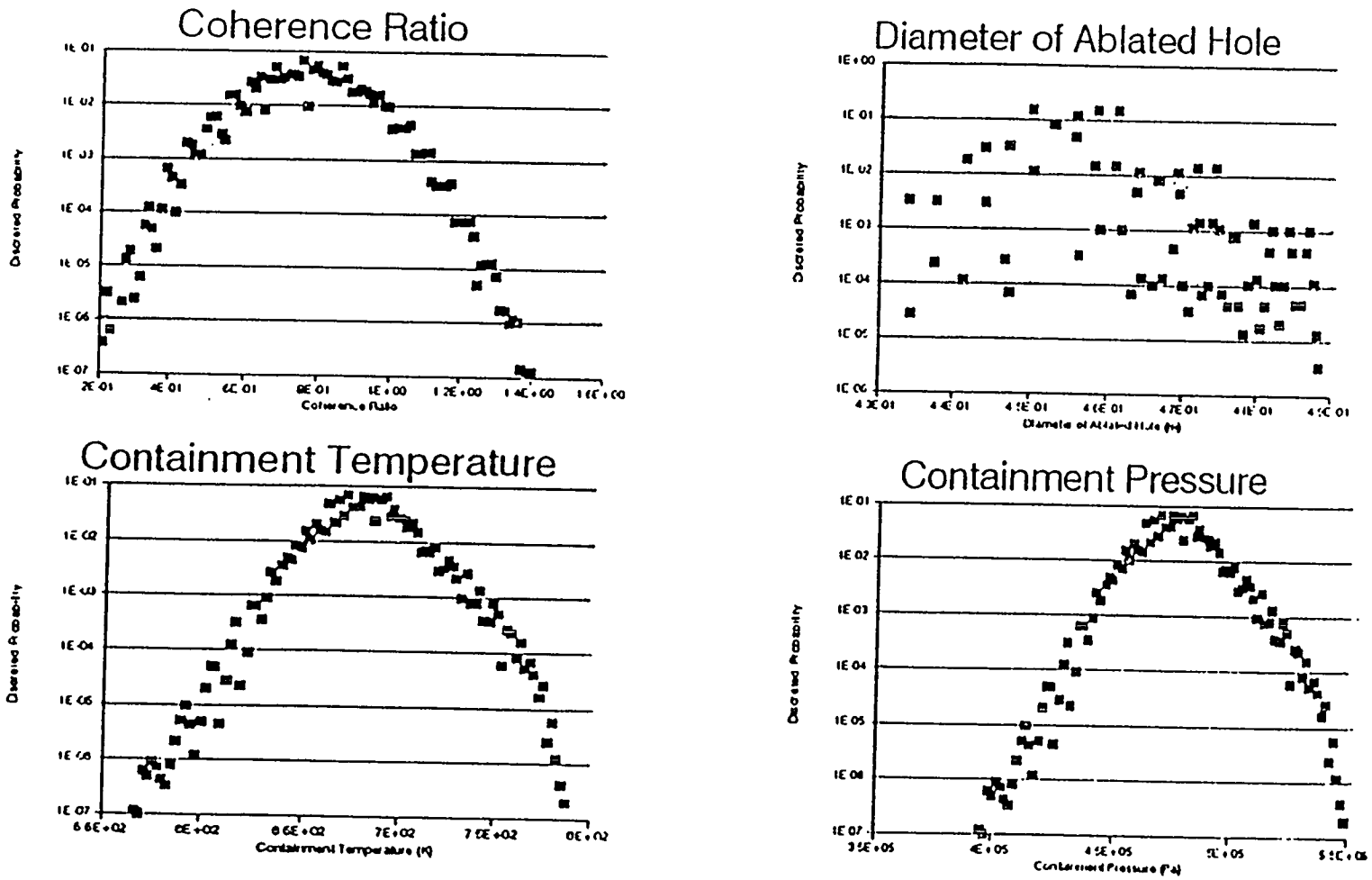

FIGURE 4

Scenario III -- Initial Distribution

(Original)

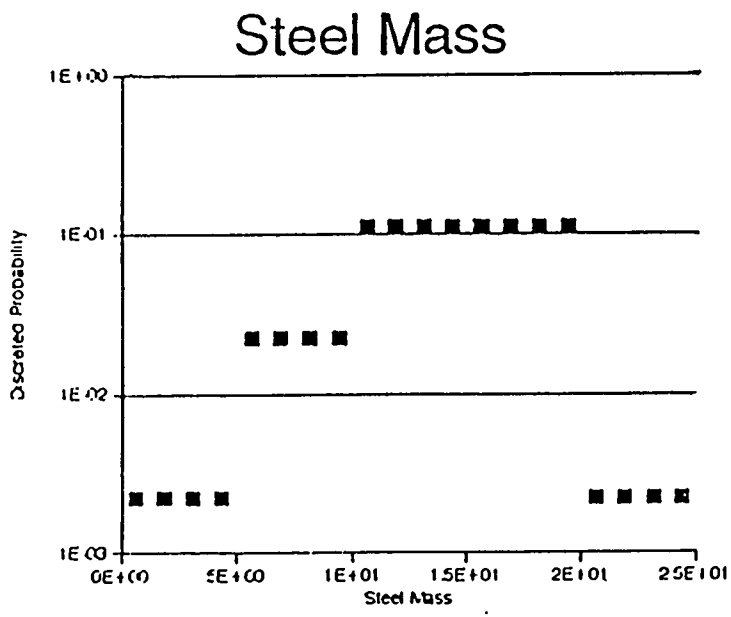

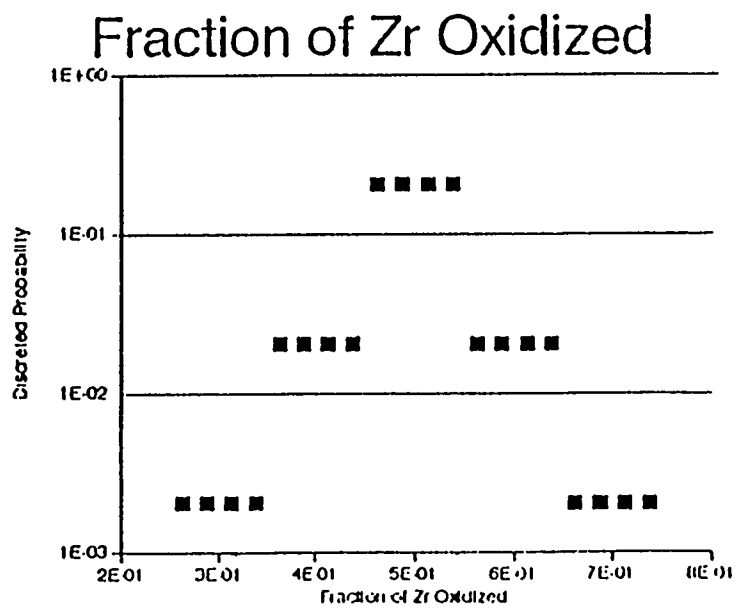

FIGURE 4 (Cont.)

Scenario III -- Output Distribution
(Original)

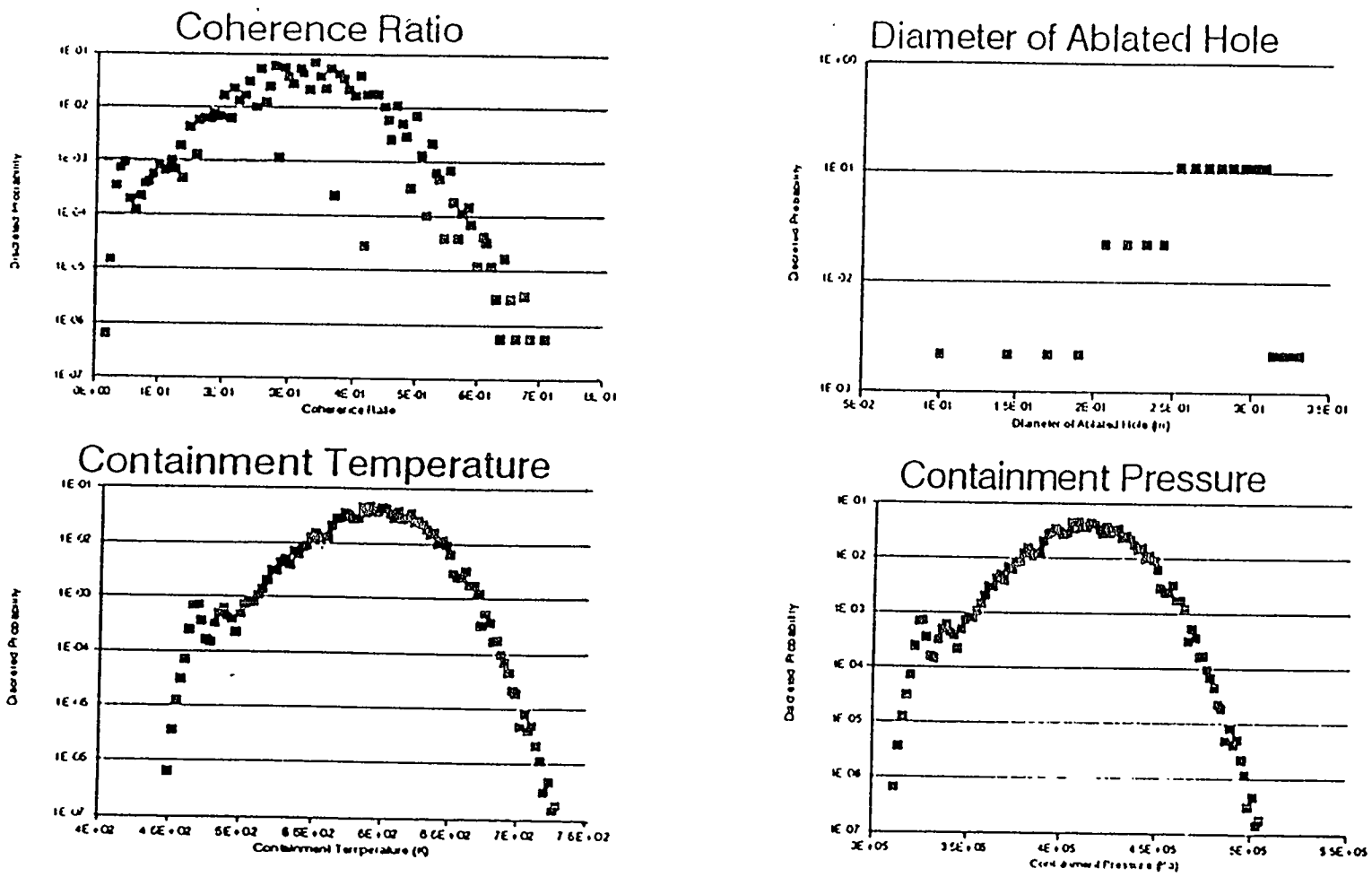

REBUTTAL FROM REVIEWER H

Comments on Response H1

The main point about comment H1 is that ROAAM can better capture modeling uncertainty than other methods used. However, it does not guarantee that the uncertainty (including modeling uncertainty) is totally captured and quantified in a ROAAM process. The authors should clarify this point in the final report.

Comments on Response H2

Response to comment H2 is adequate.

Comments on Response H3

The difference between DPDs and PDFs are not a matter of semantics. DPDs and PDFs are fundamentally different. There were several comments exchanged on this issue during the BWR Mark-I Liner Melt issue. I believe that we were agreeing that DPDs and PDFs are quite different. Furthermore, we agreed that a PDF is a better way of displaying probability distributions than a DPD. A PDF can visually show the relative frequency of a random variable about a specific range. A DPD doesn't show this. The final report of the Mark-I Liner issue used both PDF and DPD representations. Do we still have disagreement on this issue?

Comments on Response H4

This comment is meant to show the most general form of the equation. Equations 2.3 and 2.4 are only the special form of the suggested general equations:

$$P_{ijk}(m_{Uo2,i}, X_{Zr,j}, m_{ss,k}) = P_i(m_{Uo2,i}) \cdot P_j(X_{Zr,j} | m_{Uo2,i}) \cdot P_k(m_{ss,k} | m_{Uo2,i}, X_{Zr,j})$$

and

$$P_{ijk}(m_{Uo2,i},X_{Zr,j},m_{ss,k},R_{\tau,l}) = P_{ijk}(m_{Uo2,i},X_{Zr,j},m_{ss,k}) \cdot P_l(R_{\tau,l} | m_{Uo2,i},X_{Zr,j},m_{ss,k}).$$

In fact the correlated equation for m_{ss} used in sections 3 and 4 show $P_k(m_{ss,k} | m_{Uo2,i})$ and not $P_k(m_{ss})$.

The comment is to emphasize that $m_{Uo2,i}$, $X_{Zr,j}$, and $m_{ss,k}$ should be assumed dependent. If, however, the authors believe that this dependence is not strong, and if there are convicting evidence to that effect, then one can assume that $P_j(X_{Zr,j} | m_{Uo2,i}) = P_j(X_{Zr,j})$.

It is incorrect to assume that the readers should "appropriately interpret" $P_k(m_{ss})$ as a conditional probability. There is no reason to be informal and implicit in treating dependencies.

Comments on Response H5

Response to comment H5 is adequate.

Comments on Response H6

Comment H6 stresses two points. The first point relates to the probabilistic treatment used in which a mixture of PDFs and DPDs is used. As suggested in comment H3, the PDF representation is a better choice. The second point is emphasizing that while the statistical variation in the experimental results suggest small relative standard deviations (12.5 percent for TCE and 28 percent for CLCH), scaling up may not necessarily result in the same uncertainties and distributions? A point is made in the response that no major variation in the shape and relative standard deviation observed in the experiments at either 1:40th and 1:6th scales. From the viewpoint of modeling uncertainty, this is not enough to assume the normal distribution and its parameters equally applies the full scale case. I have not seen any convincing argument to satisfactorily address this issue.

Comments on Response H7

I am confused about the role of INEL calculations using SCDAP/RELAP, NUREG/CR-6075 implies that INEL calculations form the basis for developing DPDs and formulating a consistent probabilistic treatment of the phenomena. The response to this comment indicates that INEL

calculations are only indirectly used. I believe the role of INEL results should be clearly defined, and the way SCDAP/RELAP calculations are used in NUREG/CR-6075 should be clarified.

Furthermore, the ranges of seal LOCA used in the INEL calculations are concerning a TMLB' sequence. That is, they represent a transient induced LOCA and not an SBLOCA. This appears to be a scenario different from the four scenarios used.

Comments on Response H8

The response, while satisfactory, is inconsistent with the argument that the authors make in the report about the 10 MPa pressure based on the TMI experience. They considered this pressure as a "peculiar" case while they now indicate that the RCS pressure would have dropped to about 5 MPa, had the accident continued. Then what would be the role of 10 MPa in the report?

Comments on Response H9

The argument provided in support of using 8 MPa bounded RCS pressure is based on two points that a DPD representing RCS pressure cannot be defended, and the pressure plays an unimportant role. First, the bounding pressure of 8 MPa is not adequately defended, and as such the use of a distribution is much more appropriate and defendable here. The response already gives a probability for being at full pressure which violates the choice of the bounded pressure. Second, the unimportance of RCS pressure on the final result is not a good argument for treating it lightly. I am more convinced than ever that at this point the best way to treat RCS pressure is to represent it probabilistically and as part of the decomposed model.

Comments on Response H10

Response to comment H10 is adequate.

Comments on Response H11

Whatever the outcome, the probabilistic arguments used should be consistent and accurate. The ROAAM process is a "means" to reach the "end" (likelihood of a DCH failure). The end,

however, should not play any role in the formulation of the "means." The point of this comment was to ask the authors to offer reasons for rejecting my interpretation of data shown by the PDFs that I suggested. My interpretation is still consistent with the data and arguments provided by the authors. The response has no discussion about inaccuracy of my interpretation. I am stressing the accuracy and consistency only because they ultimately translate to credibility of the results, no matter if they influence the end results.

Comments on Response H12

It is counterproductive to a satisfactory resolution of raised issues by such responses as "...we see no correlation between Zr oxidized and Uo2 mass" without offering a convincing reason. The idea is to more specifically say why such a correlation does not exist and support it with the studies by others, or by their own experimental observations. The response to this comment also indicates that sometimes the authors use "bounding" to model correlations so as to maintain clarity to the process. I believe that accuracy is more important than clarity. The clarity issue can be remedied by better explanation, but inaccuracy cannot. Correlations should be clearly defined, a priori, and should be treated explicitly where possible. Only those elements of an ROAAM that cannot be adequately quantified should be conservatively bounded. A consistent adherence to the ROAAM process rules, and an accurate estimation of all input parameters and correlations is necessary.

Comments on Response H13

Since the equations 3.5 and 3.8 are bounding equations, this must be clearly stated in the report. Furthermore, an argument about the appropriateness of the bounding should also be presented.

Comments on Response H14

It is still unclear why 75 percent of the degraded core will relocate. Why not 95 percent?

Comments on Response H15

Response to comment H15 is adequate.

Comments on Response H16

I agree that a consensus reached with the reviewers would result in better and tighter distributions. Certainly, this consensus is a necessary element of the ROAAM decomposition model. However, when the shape and form of the DPDs are in dispute, the only other alternative is to use a maximum entropy distribution (the inexpensive path) or a formal expert elicitation (the expensive path). Unfortunately, I believe that the response to this and other relevant comments are not helpful for reaching a consensus on the shape and form of the DPDs. For example, in comment H11 I suggested other forms of the input distributions which were also consistent with the literature and data available, but the response was simply rejecting them since they were based on maximum entropy. I was interested to know whether the tails of the suggested distributions represented physically impossible values. For example, is there any hard evidence to show that some subsets of the range 20-60 percent Zr oxidized are more probable than other subsets as assumed by the authors? Where are such evidences? In the absence of concrete evidences, the best argument is the use of maximum entropy distribution.

Comments on Response H17

Response to comment H17 is adequate. However, again I want to emphasize that insensitivity to the final result should not be an excuse to lightly address an issue.

Comment on Response H18

Response to comment H18 is adequate.

Comments on Response H19

It would be important to graphically show the CRs. Perhaps the authors should include an appendix to the report for this purpose.

Comments on Response H20

The only parameter that controls the final conclusion of small probability of DCH caused failures for Zion is this fragility curve. I believe that the authors should avoid using this curve in the

range 20-60 psig. If such a curve does not presently exist (like now) then we should either perform a careful structural analysis to build the curve for this range, or use expert judgement for this purpose. Accordingly, the probability of 10^{-3} used in the report is incorrect. At this point we are unable to prove that a containment pressure of, say, 60 psi is less than 10^{-2}. Only carefully developed families of fragility curves between 20-60 psig can reveal an acceptable probability of containment failure. I want to emphasize again that this fragility curve is the ONLY explicit factor in the DCH ROAAM approach that dominates the final conclusion at this point. As such, it deserves a much better attention and reevaluation.

Comments on Response H21

See rebuttal H20.

Comments on Response H22

To propagate the effect of all uncertainties, it is beneficial to develop and use the families of fragility curves.

Comments on Response H23

Response to comment H23 is adequate.

Comments on Response H24

I am looking forward to seeing how the differences between the DPDs that I suggested in comment H11 and those used by the authors are resolved. The response to comment H24 is, however, adequate.

Comments on Response H25

Response to comment H25 is adequate.

Comments on Response H26

Response to comment H26 is adequate.

Comments on ALPHA Code

Comments on Response H27

In the SNL review of the ALPHA code, it would be important to insert an adequate number of comments so that the code can be easily followed by other users.

Comments on Response H28

Although I have presented a clear evidence that the code has a problem in handling DPD normalization when an odd number of nodal points are used, the authors are discounting any error. I fail to see the rationale for rejecting this error. Did the authors actually run a case with odd number of nodal points which did not result in the error that I identified? If they did, they failed to report it. If they didn't there is no justification for rejecting the comment.

Comments on Response H29

The response to the sensitivity study that I have reported in this comment doesn't seem satisfying to the authors. Apparently, they plan to independently verify them (which is quite reasonable). However, the authors keep referring to my sensitivity results in their responses to other reviewers' comments to justify their arguments. What I am most interested at this point, however, is to know what actually controls the final containment load? My sensitivity study did not identify any of the input DPDs, or other distributions and assumptions as important. If the authors are performing a sensitivity study, it would be important to identify the sensitivity of all factors involved, including parameters and assumptions which are implicit in this study. As I have indicated in comment H32, my belief is that non-DPD parameters such as the amount of steam, choice of the accident scenario, and fragility of the containment appear to be the controlling factors.

Comments on Response H30

The authors should use finer nodalization here.

Comments on Response H31

Due to the errors identified by this reviewer and observed by reviewer O, my point in raising this comment was to emphasize the need for an independent party to carefully examine the ALPHA code. For example, an independent review by SNL or other organizations.

Comments on Response H32

This was a key comment. The reason that DPDs and other assumptions in the report are so insensitive to the end results is because of other parameters treated by some bounds, and are represented in the models used in the ALPHA code. The comment is raising the issue that these sensitive factors are not clearly identified in the report, and their bounding values need to be appropriately justified.

Comments on Response H33

Response to comment H33 is adequate. However, I am not sure about the version of ALPHA code that we reviewed.

Comments on Response H34

The response is irrelevant to comment H34. Since ROAAM is a process for assessing probabilities of physical phenomena, it appears important that a generically based code should also be available to carry out the mechanics of the process. Such a code should get the decomposition hierarchy, the DPDs, and CRs as input and should produce the final probabilities. For generating the DPDs and CRs for a specific problem, tailor-made codes may be written to produce the CRs. For example, a separate code routine may be developed to solve the CLCH model. The result of such a run provides a CR which would be an input to the generic ROAAM code.

Some Other Comments:

1. Regarding Response J3, the response is contrary to my comment H32 where I found from the ALPHA code calculations that the heat contribution from hydrogen combustion is less than 10 percent of the total heat. Thus, hydrogen combustion during DCH is an unimportant contributor to containment loads.

2. References made by the authors in their responses to my comments are not provided.

Comments by Reviewer I

Comments not provided.

Comments by Reviewer J

I write to provide comments on the draft report NUREG/CR-6075 "The Probability of Containment Failure by Direct Containment Heating in Zion." The comments I have at this time are of generic nature, not of a detailed nature, mostly because it was not possible to devote as much time as needed for this effort over the past few weeks. Additionally, because of the many phenomena involved here and the contentious arguments around certain issues between the authors and the national lab reviewers, resolving the issues requires the review of several other documents. Given the limitation of time, I will confine my comments to basic principles and evidence from the simulation experiments discussed in this report.

(1) The objective of this report is the development of a framework that incorporates the important factors in assessing the consequences of DCH in PWRs. However, it is hampered by several exclusions. Because of the modeling assumptions, the authors exclude CE reactors and ice condenser reactors. They also acknowledge that a factor that does not get addressed is the impact of preexisting water on the steam availability for reactions with dispersed corium. The probability of having water in the cavity in accidents with potential for DCH is not discussed to allow the reader a clear understanding of the impact of this assumption. There is some evidence that the water present in the cavity would lead to a higher pressure rise than predicted by the report (e.g., SNL/IET-8B results). The degree to which this may occur in the reactor case should be addressed to make the case more complete, given that the probability of not having water in the cavity is low.

RESPONSE J1: *See Response D14.*

(2) Another issue that I do not find answered completely is the hydrogen issue. The threshold temperature is assumed to be in the 1000 - 1100°K range for the more energetic events "that might be of interest to DCH" (page F-7). This follows a discussion that concludes by a statement that for Zion specific conditions, the SENKIN based predicted autoignition temperature is 790°K. SENKIN appears to do well in predicting dependence on the volume scale in experimental findings of the autoignition temperature (Table F-4). It is not clear why the scale arguments do not also apply to the

energetic events, thus leading to a lower temperature for the reactor than the 1000 - 1100°K for the simulation scale. The report (page F-10) argues that for DCH relevant time-scale, preexisting hydrogen would not fully participate and hence the energetic temperature threshold is conservatively selected to be 1100°K. A preferred approach might be to choose a hydrogen burn efficiency dependence on temperature that represents the expected fraction, but less than full potential, of additional energy from the hydrogen during DCH. Such dependence can allow for some additional energy, increasing with temperature between the 790°K and the 1100°K. That is clearly more conservative than the approach used here and perhaps a better representation of the observed behavior in the SNL/IET tests (Table F-5).

RESPONSE J2: *See Response F33.*

Additionally, given the uncertainty in this phenomena, I expected a more explicit discussion of its implication in the main text. A sensitivity analysis of lowering the temperature to 950°K was used, but no probability was given to that or any other value.

RESPONSE J3: *Hydrogen combustion during DCH is an important contributor to loads. See Response F33 for a significant clarification of these issues. It is inappropriate to assign probabilities to sensitivity studies.*

(3) While the above two points are about factors that may lead to higher containment loads than what is predicted in the report, there are also some mitigating factors which are not addressed. In particular, the non-equilibrium effects and the non-adiabatic conditions in the real world would tend to limit the loads. It might be useful to attempt to show that load reduction possible due to these factors. This is particularly so given that previous treatments of these subjects by the CONTAIN code exist and can be the basis for estimating the margin of conservatism.

RESPONSE J4: *We are comfortable with bounding the loads; however, we believe that the margins are not excessive. We do not believe that heat transfer to structures limits loads in any significant way (see Response F8). Furthermore, scoping calculations indicate that thermal and chemical equilibrium are reasonably achieved in the cavity (see Response M3). Nonetheless, it is expected of the ROAAM process for those who have tools to use them.*

(4) I will need more time to review the adequacy of the treatment of the two major parameters in the analysis presented, namely the vessel breach size and the coherence ratio. In both cases, the focus of my concern is the range of their values in the sensitivity analysis. In addition, I would like to further consider the viability of having two analyses for the coherence ratio, with differing dependencies. Of particular concern is the implication of their extrapolation to containment geometries from experimental findings in much smaller scales.

RESPONSE J5: *Both correlations are used in reactor applications that interpolate on the existing database; therefore, they give similar results. For example, the applicability of the TCE coherence correlation to reactor applications is addressed in Table E.9. In Table E.9, the various dimensionless groups in the TCE coherence correlation are listed. Evaluations of these groups for the database span the range of evaluations for expected reactor applications. Thus, a scaling analysis within the context of the correlation itself suggests that the correlation can be applied to reactor applications. We recognize that controlling phenomena might change with increases in physical scale and that these unrecognized phenomena would not be represented in the current scaling analysis. However, the database includes experiments ranging from 1:40th to 1:6th scale, and no significant effect of scale is observed, so we feel confident in applying our correlations to reactor applications.*

REBUTTAL FROM REVIEWER J

I have reviewed the responses of the authors of NUREG/CR-6075 to my comments. I believe they have answered most comments in a reasonable way as far as the Zion plant is concerned.

As I stated earlier relative to the hydrogen issue, the sensitivity of the results to the participation of the preexisting hydrogen and to flame propagation assumptions necessitates a more suitable approach. For example, allowing for a finite probability for ignition temperatures below the 1100°K, with lower hydrogen burn efficiency might be more convincing than the approach used here. The report assumes zero probability for the lower ignition temperatures.

Comments by Reviewer K

Introduction - The problem of direct containment heating (DCH) has so many facets that, until this work was completed, it is possible to say we had no solution to the problem. Bounding calculations showed DCH was possible but the assumptions behind the calculations were so conservative, no one was sure that DCH was even real. This report quantifies some of the major uncertainties and arrives at the conclusion that DCH even when fuel damage occurs is very unlikely, less than 10^{-3}/reactor year. This low probability is to be multiplied by a comparable low probability of a reactor even getting to the state where a DCH accident is possible so the probability of a DCH accident in an LWR is vanishingly small.

In order to arrive to this conclusion, a number of experiments were performed on two scaled models of one plant geometry, that of Zion, and interpreted in such a way that the extrapolation to full scale conditions indicated there was no problem. The purpose of this review is to see whether this is a convincing conclusion and to suggest what needs to be done if it isn't

In particular the reviewers are asked to comment on the following:

a) The technical merits of the conclusions and the analyses described along with the quantification of the inputs (i.e., estimate of the initial and boundary conditions, containment loads and structural response). (By this I presume they mean the appropriateness of the initial conditions selected and the correctness of the answers.)

b) Identification of the sources of the uncertainties in the analysis and their impact on the conclusions.

c) The necessity for further experiments or confirmatory research as suggested in the report.

d) The potential for application and extrapolation of the methods and conclusions to other reactor and containment designs.

In order to meet these goals, the body of this report will examine those items listed above under the general headings of possible Analytical Improvements and possible Additional Experiments. In the conclusions we will return to the issues raised above and make recommendations.

Before getting into a discussion of the specifics, however, I would like to say this piece of work represents a substantial advance in the resolution of the DCH issue. It can be published just as it is.

RESPONSE K1: *No comment.*

Whether additional work is needed on the items touched on in this review depends on what the competing reactor safety problems are. The combination of an unlikely approach to state where DCH is even possible and the small probability of a DCH event failing the containment I think makes the value of further work on DCH small.

RESPONSE K2: *No comment.*

The application of the analyses to other plants should be done, however as it isn't clear how plant-specific the procedure advanced in this report is.

In doing this review my first priority has been to find surprises, that is important factors that have been left out, rather than to suggest improvements in the details of the scenarios and models that the authors have put forward. No real surprises were found. There are, however, some enhancements and suggestions which will, I think, improve the report.

RESPONSE K3: *No comment.*

Many of the technical issues raised in this review are touched on in NUREG/CR-5809, EGG-2659.[4] The utility of this report would be considerably enhanced if the assumptions, which are often based on data included in the above report, were justified by citing this report and

---

[4] "An Integrated Structure and Scaling Methodology for Severe Accident Technical Issue Resolution," NUREG/CR-5809, November 1991.

appendix in which the assumption is justified. The body of this report has no references. In addition an appendix which translates the acronyms is needed.

RESPONSE K4: *NUREG/CR-5809 will be cited as appropriate. The main report is referenced appropriately at the end of each section. A table of acronyms will be provided.*

ANALYTICAL IMPROVEMENTS

Enlarging the Data Base. There are a number of ways in which a small amount of additional analytical work could increase our confidence in the results presented here. Chief among these is to tie these experimental results to the larger field of two phase flow.

The whole justification for limiting the melt heat transfer to the gas in the containment relies on data taken in two scaled facilities using a simulant for the melt. While the number of runs is convincingly large only a single geometry has been tested, and that at only two scales.

RESPONSE K5: *Multiple geometries have been tested: Zion and Zion-like geometries, Surry, and simple compartmentalization. The database includes experiments at 5 different scales; 1:40^h, 1:30^h, 1:20^h, 1:10^h, and 1:6^h scale.*

A good range of initial conditions has been tested.

RESPONSE K6: *We agree.*

This is an acceptable database if the phenomena we rely on to limit the pressure rise in a DCH transient turn out to be what we'd expect from what we already know about two phase flows and heat transfer. An empirical correlation of data without tying the results to well understood phenomena is not enough.

RESPONSE K7: *The dominant mitigating mechanisms are trapping in the subcompartment and noncoherence of debris dispersal and RCS blowdown. Consistent with experiments, the predicted particle sizes (Ishii, PU NE-93/1) are ~1mm at reactor scale. Particles of this size are sufficiently large that they cannot easily follow streamlines; consequently, we expect particles to intercept structures and deentrain. On the other hand, ~1mm particles are sufficiently small*

that we can expect efficient debris/gas interactions in the cavity (see Response M3). Consistent with our knowledge of two-phase flows, the TCE coherence correlation is developed from the assumption that debris/gas slip is large in the cavity.

The two essential quantities extracted from these experiments are:

1. **The particle size** - If the particle size is really small the particles will be widely dispersed and the heat transfer will be excellent. DCH would than be a problem. Are the particles found in these experiments what we would have expected to find from existing correlations? I would suggest using the Ishii drop size distributions and the data which has been taken in this program (but which is not included in this report) and see how well the measured and calculated sizes compare. If they are not too far out of line, good, then I'm not very concerned about this issue.

RESPONSE K8: *Ishii's predicted drop sizes (NUREG/CR-5809, PU NE-9311) are consistent with measured drop sizes in DCH experiments. Mass mean drop sizes ~1 mm have been reported by SNL in some experiments. Ishii predicts similar drop sizes for reactor applications and his models are qualitatively validated by recent experiments. These drop sizes are sufficient to ensure rapid heat transfer but are much too large to follow gas streamlines.*

2. **The slip between phases** - In essence the reason that so much melt is left behind in the cavity when blowdown is complete is due to the existence of slip between the phases and the short duration of the blowdown. Lots of data on slip exist. Very little has been taken during transients. None-the-less, I think properly used steady state data can be used to predict what has been found. (The data giving amount of melt left behind in the cavity can be converted into a void or liquid fraction and existing slip correlations compared to it.) I think this comparison will turn out to be pretty good. The same calculation can be repeated for the reactor. I believe the Ishii flow regime based drift flux model constants should be used for this calculation.

RESPONSE K9: *Freezing on cavity surfaces, not slip, seems to be the dominant retention mechanism in the experiments using prototypic melts with RCS pressures of interest to DCH.*

3. **Nodalization** - Closely related to this suggestion is the issue of suitable nodalization for calculations on other containment geometries. It's obvious that a single node gives an unacceptably conservative answer. Two nodes seem to do a good job. Does going to three, or four or more give any real improvement? The nodalization issue needs further study.

Discussion on Nodalization. If two nodes give an asymptotic solution which is close to what three or more nodes would give, one of my concerns about nodalization will have been addressed. I'm uncomfortable if the answer depends in an important way on the nodalization scheme selected. This is particularly true if there are no nodalization guidelines included in the instructions.

The other concern about nodalization is it is not clear what physics are we trying to capture. I think I know but it certainly isn't clear from this report. I believe we are relying on a large slip ratio plus a short blowdown time to confine most of the melt to the tunnel. One node for the tunnel and another for the containment volume seems to give a solution which reflects this. Will more tunnel nodes give a similar result? Several containment nodes won't hurt either though I believe one is enough in-so-far as the spacial pressure variations throughout the containment volume are quite small. If we look at a whole variety of containments (many of which we will probably not have any data for), where should the control volume boundaries be drawn?

I think I'd nodalize as follows. Each passage to the containment volume would be represented by at least one control volume. For the Zion containment I'd have one or more tunnel nodes plus a node connecting the volume below the vessel through the gap around the vessel. The tunnel might better be nodalized into two pieces as one piece is horizontal and one is inclined. The equations governing the slip in these two segments are not necessarily the same so different nodes are probably called for. If there were different rooms or chambers separated by barriers that impose substantial flow resistances, these barriers should define the volumes and nodes. Looking ahead, this report will be used to frame the models used to see if other containment geometries are subject to DCH. To do this properly, nodalization guidelines are needed to insure that the models proposed in this report are used properly.

RESPONSE K10: *Consistent with SASM (NUREG/CR-5809), our approach treats processes in 4 regions of the containment: RCS, cavity, subcompartment, and dome. We believe this nodalization is sufficient for the task. This is supported by experiment data which shows that containment loads are insensitive to details of the subcompartment geometry.*

4. **Hydrogen Explosion** - At some point in this report the question as to why TMI-2 had a hydrogen explosion and you don't must be addressed. While it's considered incredible here, the question will come up. In this report, a hydrogen explosion is categorically excluded by showing that, for a reasonable amount of hydrogen, the mixture never becomes explosive. The mixture is outside the flammability limits. There must be a significant difference between the Zion plant and the TMI-2 plant for this conclusion to be valid. What is that difference? How prevalent is this difference? Are most plants like Zion with little potential for an explosion, or are they like TMI-2 with explosion potential?

   Discussion of Hydrogen Explosion. The margin between when an explosion can occur and the amount of hydrogen that has been calculated to be present at Zion is small enough so that I'd worry about the margin. Over the years, the various experiments in the heat transfer laboratory have experienced a variety of breaks, some of them releasing steam. Both because of the steam temperature and the fact that it's of a lesser molecular weight than air, the steam from the break stratifies in the room. This occurs whatever the orientation or the elevation of the break. A cloud of steam collects in the two feet below the ceiling as a white, stable cloud. This tendency for low density gases to stratify will tend to make even a small amount of H_2 prone to explosions as it will concentrate locally. I see no reason to assume anything different will happen for the breaks that discharge hydrogen and not steam. I think you'll get an H_2 rich mixture on the ceiling and it will only dissipate very slowly. The average H_2 concentration for the entire volume is almost irrelevant if stratification occurs. Why should the breaks that I'm familiar with always stratify while the Sandia experiments apparently did not? I don't know. I think stratification must be treated parametrically before I'll be comfortable with the answer based on a well mixed model.

RESPONSE K11: *TMI-II exhibited a hydrogen burn not an explosion (Henrie, RHO-RE-EV-95P, 1987). The composition of the containment atmosphere at the time of the burn*

was estimated to be ~ 7.9% hydrogen and only ~ 3.5% steam. The atmosphere was well mixed. These conditions are quite different from what is expected during DCH scenarios, i.e., ~ 3% hydrogen and ~ 50% steam.

5. **Steam Explosion** - The steam explosion shown on Figure G-6 is dismissed without much discussion. Though the spike is of short duration, the peak pressure is quite high. Will a similar steam explosion occur in the prototype? I'd like to see a more thorough look at the steam explosion problem.

RESPONSE K12: *Prediction of steam explosion phenomena is outside the scope of this work. FCI phenomena cannot be ruled out in DCH scenarios with cavity water. In the case of Zion, such phenomena cannot damage the cavity because it is set in bedrock. High cavity pressures themselves are of no concern because experiments have shown that such pressures are fully dissipated in the dome.*

6. **Melt-Superheat** - One misfit between the early Sandia experiments and the reactor system was the melt superheat. In the reactor system the melt is really more like a slurry of the low melting temperature components and the still-unmelted high-melting point components. In order to match the energy inputs, using thermite as a simulant, the melt was greatly superheated. This meant a lot of heat had to be extracted in order to cause melt solidification. This also meant more than prototypical carry over into the containment because the very hot melt tended to melt the concrete walls rather than freeze on the walls removing it from the containment. It isn't possible to tell from this report whether the superheat in the thermite used to simulate the corium was prototypical or not. Some simple calculation and a few words would settle this issue.

RESPONSE K13: *The measured superheat in thermite is ~ 200K. This may indeed mean that thermite exhibits a more fluid behavior compared to corium. If true, our models would give even more conservative predictions of DCH loads. This issue of thermite versus corium was put to the test at ANL who performed 3 tests with a prototypic uranium based melt. Measured DCH loads were comparable or slightly less than what would be expected with thermite; therefore, real materials do not exhibit significantly different behavior.*

ADDITIONAL EXPERIMENTS

The models advanced in this report are well enough established and understood so that they can usefully be presented without any further experimentation. However, there are several directions in which experiments may well increase the margin which has already been identified or which will explore items in the scenarios which are omitted from the current program. These items will be covered in this section.

6. **Flashing of the Melt** - The choked mass velocity for a flashing two phase flow is often much lower than it is for a solid liquid flow of the same composition experiencing the same pressure difference. The real melt is a complex mix of compounds which might flash a dissolved gas or low boiling point material when the pressure drops. This could substantially reduce the ejected mass velocity and cause a change from a coherent liquid jet in the thermite simulation to a dispersed jet with a much wider divergence angle and a lower impact velocity on the walls and floor of the tunnel. An experiment, if possible, might well show the time to empty the melt is considerably greater than we are assuming. Flashing in the melt will attenuate the blowdown and reduce the severity of DCH as a result.

   A large amount of gas is not needed. The sonic velocity in a bubbly mixture can be as little as (1/30) of the sonic velocity in pure liquid. The "throat" pressure at the break would then be higher than the exit pressure and the resulting mass flow out the break reduced. While some calculations might show that outgassing is possible, the final answer, for a problem of this kind can only come from an experiment.

RESPONSE K14: *We disagree. The DCH processes are driven primarily by steam blowdown following the melt ejection phase. Furthermore, a breach in the RPV acts more like an orifice during melt discharge where the primary expansion occurs outside the vessel. Such outgassing is evident in the JETA tests (reported in Frid NUREG/CR-4508) where thermite was ejected by pure hydrogen, which is highly soluble in the iron phase under RCS pressures and melt temperatures. Although outgassing is quite evident in the JETA tests, it did not have any significant impact on the blowdown process (unpublished data).*

7. **Side Rupture** - The details of the annular gap and, hot and cold leg piping are such that it isn't clear whether a bottom rupture is always worse than a side rupture or not. One reason a side rupture could be worse is the melt and steam could hit the outer walls of the annular gap and a substantial fraction of the melt be deflected directly up and out into the main containment volume. If that is never possible because of the system geometry, no experiment is needed. If it is possible, a scaled experiment might be desirable to see if the amount of melt that is released into the main containment is small enough to insure that the containment is not challenged.

   Before any such experiment is run, however, it is desirable that a close look at the geometry of the gap, piping, and insulation in the gap be made to see if there is any problem at all.

RESPONSE K15: *We do not believe that side failures are limiting. In an extreme of ~60 mt, the lower head is filled to a depth of only ~40% of its radius; thus, a side failure still has a significant downward component. More importantly, a side failure is likely to leave significant melt behind in the vessel.*

8. **Steam Explosions** - Perhaps the most significant omission in this report is the treatment of steam explosions. Whether these are a problem and how serious a problem it is depends on both the plant geometry and the scenario. The amount of water that can be found on the floor and the depth of the resulting pool depend on both of these factors. Figure G-6 shows steam explosions are possible.

   Discussion of Steam Explosions. For a shallow pool, the amount of water that can even be contacted by melt is quite limited. If water is vaporized gradually, heat transfer to the walls will temper any pressure rise so that isn't a problem. A severe steam explosion might be a problem, however.

   The fact that a single experiment does not show a steam explosion is not significant in itself because they are notoriously unpredictable. What is needed is a way to calculate the magnitude and duration of the pressure surge resulting from a steam explosion and some experiments to show the validity of the model.

On the face of it, it doesn't look as though damage to either the concrete or the heavy steel structure within the containment is likely or even matters. The peak cavity pressure that can exist is obtained when a given amount of melt contacts water in the cavity can be calculated. The amount of water in the cavity can be treated as a parameter and the resulting pressure rise in the containment volume also calculated. A series of experiments to establish how good these calculations are would do a lot to settle the issue of whether steam explosions are a serious safety issue or not.

Though Figure G-6 shows the cavity pressure for the wet runs of 8A and 8B, the comparable pressure traces for the containment volume are not shown. If these containment volume traces do not show a major effect due to the steam explosions than further experimental work on them is probably not justified.

RESPONSE K16: *See Response K12.*

Conclusion - The letter charging us with reviewing this report listed four issues which the sponsors wished to have this review address. These items are as follows:

1) "The technical merits of the conclusions and the analyses described along with the quantification of inputs (i.e., estimates of initial and boundary conditions, containment loads and structural response)."

By focusing on the one stage of a scenario common to all DCH scenarios, High Pressure Melt Ejection (HPME), the authors of this report have managed to reduce the overall probability of DCH to a tolerable level, that is less than 10^{-6} per reactor year. This probability consists of two factors, the first a probability of 10^{-3} pre-DCH events per reactor year. This figure is from LWR experience.[5] The other, a probability of 10^{-3} per reactor-year, the likelihood that a given event leading to a HPME is severe enough to challenge the containment. The approach chosen and the answer the authors have obtained means there is little incentive to pursue further experiments directed toward understanding the many phenomena entering in the wide range of scenarios leading to

[5] TMI-2 is the only LWR which had a molten core in approximately 3000 reactor-years of LWR operation.

DCH. The one process common to all DCH transients HPME is unlikely and serious consequences from an HPME are equally unlikely.

For the reasons given above, initial and boundary conditions need not be ranged. Ranging may still be required on other reactor systems as a great variety of LWR containments are currently used in this country. On the face of it though, they all appear safe. Only calculations using the models put forward in this report are required. Given the containment loads, I find the conclusion that the containments won't fail convincing.

RESPONSE K17: *We agree.*

2) "Identification of the sources of uncertainties in the analysis and their impact on the conclusions."

The principal uncertainty is the effect of different cavity and containment geometries on the carry over of melt. A satisfactory range of conditions has been tested and the scale of the experiments sufficiently wide. How one should nodalize new geometries is not clear nor has a nodalization study, showing whether going to more than two nodes makes any difference, been performed. Until such a study has been completed the conclusion that the DCH issue has been laid to rest must be regarded as tentative.

RESPONSE K18: *See Response K10.*

Also needed is a clarification of the physics we are trying to capture in the untested geometries. I think the essential physics is a combination of a large slip ratio and a brief transient so much liquid is left behind. If that is the essence of the model, tying the liquid left in the cavity to existing slip and drop size correlations would tremendously increase my confidence that further calculations on different geometries are valid.

RESPONSE K19: *Measured drop sizes are ~0.5 mm. Particles of this size are too large to follow streamlines, so we expect them to de-entrain in the subcompartment. Subcompartment velocities are too low to re-entrain material and carry it to the dome. For conditions of most interest to DCH (~8 MPa) experiments indicate that most material is dispersed from the cavity and that the dominant retention mechanism is freezing on cavity surfaces.*

3) "The necessity for further experiments or confirmatory research as suggested in the report."

At this time no new experiments appear essential. Uncertainties can probably be reduced and larger margins uncovered if they are run but whether such experiments should actually be run should be determined after looking at alternative safety issues.

RESPONSE K20: *We agree.*

4) "Potential for application and extrapolation and conclusions to other reactor and containment designs."

This can be done now if the essential physics that needs to be captured is articulated and nodalization guidelines for different containments are provided. Depending on how close to containment failure these calculations come, there may or may not emerge a need for further work. At this time, however, the results appear to be general and the conclusions robust. The containments are a long way from failure.

Even if one or a few containments appear much more prone to fail than Zion, it does not mean a major program to reduce the uncertainty or improve the strength of the containments is called for. The probability of a DCH transient in a given containment is so small that it is unlikely it is worthwhile to spend a lot of money on a program directed at improving the safety only of one or a few containments. Training and operational changes make far more sense. There are many opportunities to terminate an accident before high pressure melt ejection occurs. These opportunities should be explored.

RESPONSE K21: *We agree. It makes far more sense to prevent accidents, regardless of what loads are predicted. This, however, is outside the scope of our work.*

REBUTTAL FROM REVIEWER K

Comments on Response K1

No further comment.

Comments on Response K2

No further comment.

Comments on Response K3

No further comment.

Comments on Response K4

Rather than list a number of general references at the end of each chapter, the assumption should cite the source and page in which the justification for the assumption was made. The most important role played by this report is to establish (to the extent that it is true) that DCH is not a problem. The data and assumptions needed to accomplish this should be arranged into a case which is built logically to the conclusion. I think all the raw materials needed to do this for the Surry and Zion type plants are at hand, only the case needs to be constructed more carefully.

Comments on Response K5

There are two essential phenomena which Pilch identified as responsible for limiting the temperature rise of the atmosphere in the containment.

1) The freeze out of melt on the walls of the structure between the vessel and the main volume that constitutes the containment.

2) The particle size, .5 to 1mm which is the same for both the experiments and the prototype. This size is such that the particles have different velocities and trajectories

than the gas and thus are redeposited while they are still hot. The complicated shapes of the various cavities and chambers trap much of the melt and limit the amount of gas that the melt is exposed to.

These ideas are not developed as well as I'd like to see in the report. Let me be more specific.

The melt freezeout fraction can be estimated from a transient conduction calculation. There must be some evidence, from the many experiments that have been run, which can show how good such a calculation is and, indicate how much would be frozen out in the prototype. I think this is needed to make this explanation convincing. This is a good idea, it needs only to be developed better.

The drop sizes which are mentioned in several places in the reports and the responses are not developed very completely. The meaning of the drop (or particle) size that he mentions varies from 1 mm or .5 mm is not clear. Is this the size that half the melt mass is above and half is below? Is it the size where 95% of the mass is below? Is it the largest size that could exist in turbulent flow field that occurred in the tunnel? What is it?

Once we know what the drop or particle size actually means, it will be possible to compare the sizes observed in the experiments and predict what we might see in a prototype.

Personally, I don't think that the scale of the experiment has any effect on particle size in the ranges we're interested in. The melt is ejected at high velocity on the floor of the tunnel and splashes and flows up the walls and down the tunnel. When most of the melt that is going to be ejected has been ejected, a rush of hot steam and hydrogen follows. Some, that is not frozen out, is re-entrained and carried downstream and perhaps re-deposited. In any case, the relevant dimension of the problem is not, in my opinion, the tunnel diameter but the film thickness remaining on the walls of the tunnel. Just as the relevant dimension for flooding goes from tube diameter to film thickness in air-water flows at a pipe size of 2.5 inches this one switches too. In flooding we go from a Froude number to a Kutateladze number type flooding correlation. I think the slip goes from a Froude number to a Kutateladze too. Most, if not all, the experiments and all the prototypes are probably at the Kutateladze number limit.

Comments on Response K6

While the initial conditions chosen seemed adequate to me, many of the other reviewers seem to be unhappy with them. Under the circumstances, I suggest the rationale for selecting the ones chosen needs a more thorough explanation.

Comments on Response K7

My response number K5 clarifies what I would like to see here.

Comments on Response K8

At the time I wrote the original review I didn't grasp the essence of the underlying assumptions in the correlation used behind the report. I'm not sure, at this time, how to proceed in establishing that most of the melt, even that which is entrained, is left behind in the cavity. At this point, the wide range of the experiments and the lack of a size effect is the best evidence. I would still like to see a comparison of particle size spectra and mass mean sizes with the Ishii curves of NUREG/CR-5809.

Turbulent deposition results in about half the drops entrained being deposited in 5 L/D's. A well established curve by Liu and Agarwal[6], among others, shows this. If these drops are immediately re-entrained and subsequently re-deposited, they would be skipping down the tunnel. The time it would take them to get to the end could then be compared to the time it would take to blow the vessel and system down and would indicate how much melt might be left behind after the system was blown down. It is also true that the vapor which was not in the vessel is probably much colder than the melt and would cause freezing as well as entrainment. In any case, I'd like to see a quantitative comparison of melt retention in the experiments and the prototype based on a model that is clearly explainable.

---

[6] Liu, BYH, Agarwal, JK (1974), "Experimental Observation of Aerosol Deposition in Turbulent Flow," Aerosol Science, vol. 5, pp. 148-155.

Comments on Response K9

If freeze retention accounts for most of what we observe, this is a sufficient mechanism for me.

Comments on Response K10

I still think nodalization guidelines are called for. The four nodes you mention in your response are satisfactory for me, I just wonder if, with the variety of containments out there, whether a user would know how to nodalize all of them.

Comments on Response K11

I mis-spoke using the word explosion, and withdraw it. There still seems to be some question of flammability limits for steam-air-hydrogen mixtures, so I suggest leaving the question of what they really are on the table to be considered if further experiments are contemplated. Other uncertainties might well be more worthwhile to investigate if other experiments are performed.

Comments on Response K12

The issue of the effect of cavity water, in general, is still open in my opinion. A shallow pool will have a minimal effect. Whether deep pools are likely enough or the resulting pressure spikes would do much to the containment is still unknown. This along with other uncertainties should be considered if further experiments are performed.

Comments on Response K13

The experiments you cite are sufficient to satisfy me on this question.

Comments on Response K14

The distinction between melt ejection and steam blowdown was one I missed and withdraw the comment.

Comments on Response K15

This response is sufficient to settle my concerns.

Comments on Response K16

No further comment.

Comments on Response K17

No further comment.

Comments on Response K18

No further comment.

Comments on Response K19

No further comment.

Comments on Response K20

No comment.

Comments on Response K21

No further comment.

DCH Closure Report Outline

I. Introduction

A. Why this report is needed.

1. Procedures used in the Surry and Zion reports not the same.
2. The target for what constitutes safe is not given nor is the rationale for selecting it clear.
3. Documentation in Surry and Zion reports is not complete. The physics they are trying to capture isn't clear, the evidence that they need to make a case is missing and the required nodalization is not clear.
4. Operator actions are completely omitted. (For slow transients operators are bound to do something.) Something has to be said about this.
5. Clear instructions on nodalization, the scenario and the figure of merit are needed if other plants and containments are to be examined.
6. Too much homework needs to be done by readers in putting the DCH closeout case together to convince many people that the problem is solved. Skipping from report to report, then to comments, and then to responses is too much to ask of most readers. The whole case needs to be consolidated and cleaned up.

B. This report

1. Probabilities of a substantial radioactive release
2. DCH scenario
3. Processes mitigating heatup during DCH
4. Predicting DCH pressure rises
5. Containment failure prediction
6. Conclusions

II. Assessing the probability of containment failure by looking at the components.

P = (P1)(P2)(P3)(..)...etc. The probability of containment failure is the product of the following probabilities (and perhaps others).

P1 - The probability of core uncovery (use experience for this, in about 3000 reactor-years of LWR use, 1 core (TMI-2) has been uncovered. P1 $\leq$ or 10^{-3}.

P2 - The probability of vessel failure. This number will have to be obtained from analytical work completed up to this time. It might be simpler to assume this is one if the other probabilities are much less than one.

P3 - Probability of HPME (High Pressure Melt Ejection). This too will have to be obtained from analytical work completed in this program and elsewhere, to get a number.

P4 - Probability of containment failure. The results of this work given in the containment failure report should provide the answer to this. Other probabilities might be inserted into th "P" equation above if they can be identified. This is a good place to identify the essential steps leading to DCH in which more work could make a difference.

III. Scenario for DCH Leading to Containment Failure

A. LOCA leading to core uncovery
B. Core relocation
C. Vessel overheat
D. Failure
E. HPME
F. Pressurization of the containment
G. Containment failure

Comments. This scenario needs to be fleshed out justifying the choices made and discussing the omissions. I would like to see operator intervention discussed here.

IV. Processes Mitigating the Heat Up Which is Due to HPME

A. Freeze out of corium in tunnel

B. Redeposition of hot corium, in the tunnel, so that the gas in the containment doesn't get heated.

Comments. The extensive experiments performed at SNL, ANL, BNL and any other places should be cited. Drop sizes and their likelihood of being redeposited should be mentioned. A calculation of the amount of melt frozen on the walls of the tunnel is needed. Times for the processes to occur in the reactor are needed. Many reviewers of the Zion report expressed concern about the initial conditions for HPME. These concerns should be addressed in this section. This section should end with a statement of the essential physics that must be captured when evaluating an untested cavity or tunnel geometry. This section is where the substance of what has been learned in the experiments is displayed.

V. Predicting DCH Peak Pressure

A. Nodalization recommendations

B. Why one control volume is not enough but more than four are not needed

C. How complex geometries should be viewed

D. Perhaps some examples and a discussion of why the nodalization selected was chosen

Comments. This section must be specific enough so that a person reading only this report would use the recommendations for calculating the DCH pressure rise correctly.

VI. Containment Failure

A. Modes

B. Probabilities

C. Recommendations

Comments. The containment failure results should be summarized with simple calculations for failure laid out for estimating purposes. Some discussion of the ranges of containment types is

probably needed with recommendations for both steel and reinforced concrete containments of various shapes made. I believe too, that the definition of failure, particularly for reinforced concrete, is very conservative, and mention that even a "failed" containment provides a lot protection should be included.

VII. Conclusions

A. A method of calculating the pressure rise due to DCH is described.

B. Containment failure criteria and probabilities are descried for typical plants, Surry and Zion. Failure probabilities less than 0.1 are calculated if DCH occurs.

C. Combined with the probability of core uncovery and other essential processes leading to DCH, the probability of a substantial radioactive release due to DCH is found to less than 10^{-6}/reactor-year, an acceptable level.

Comments. These will have to be revised and enlarged as the report is written.

Comments by Reviewer L

Thanks for inviting me to review the subject report, entitled "The Probability of Containment Failure by Direct Containment Heating in Zion," by M.M. Pilch, H. Yan, and T.G. Theofanous, and the associated comments on this report made by the staff of the Idaho National Engineering Laboratory (INEL) and the staff of the Sandia National Laboratory (SNL). I have reviewed the subject report and the associated comments but have not yet reviewed the set of reports from INEL and SNL that you transmitted to me through your letter of September 1, 1993. In the following paragraphs, I am providing you my comments only on the NUREG/CR-6075 and the associated comments made on it by the INEL and the SNL staff.

The direct containment heating (DCH) issue has been around for a long time. Perhaps, history should be recalled, even though the perspective is mint. DCH was identified as a threat for early containment failure during the time the containment loads working group deliberated. Sandia performed the initial experiments and developed the single cell conservative model, which predicted containment failure with approximately 20% of core melt. The first realistic experiments on DCH were sponsored by EPRI on the 1/30 scale CWTI facility at ANL, and the data obtained showed consistently that the DCH efficiencies were 20 to 40%; and that was ascribed by EPRI to the presence of water, structures and the restricted flow path between the upper compartment and the dome. Sandia ascribed that to the small trajectory lengths of the dispersed particles in the small scale CWTI facility.

Next, USNRC sponsored the construction of the 1/10 scale Surtsey facility at SNL and Sandia performed the DCH-1 to DCH-4 tests, which again showed relatively low efficiency (appr. 33%) for DCH. Reasons were found for the observed low efficiency and the models still predicted containment failure with DCH.

Next, the models were improved, in particular, a two region model showed very substantial reduction of calculated pressure loads due to DCH. However, the combustion of hydrogen, produced due to oxidation of all the Zirconium contained in the melt, became a very large pressure loading, since it was postulated to burn in the form of a deflagration in the dome region. The DCH loading had to be combined with the simultaneous hydrogen burn loading, in order to fail Zion or Surry containments.

The Surtsey experiments and their data were heavily criticized by the industry for lack of proper scaling and lack of representation of the water and structures present in the containments. USNRC recognizing scaling as a fundamental issue for the conduct of all severe accident experiments asked Dr. Zuber to lead the development of the severe accident scaling methodology (SASM), and its application to the DCH scenario. The SASM was developed, however, its application to DCH was not wholly successful. The SASM activity, nevertheless, crystalized the physics and the inter-related phenomenology of the DCH event; and pointed the way towards a realistic and extrapolatable experimental program. The resulting program employed the same 1/10 scale Surtsey facility at Sandia and a 1/40 scale CWTI facility at ANL and performed counterpart (i.e., same initial conditions, materials and containment representations) tests. These were complemented by a few tests in the 1/6 scale concrete containment facility and a few tests with the uranium-based thermite in the CWTI facility. The data from these tests forms the first consistent data base on DCH.

What have the data demonstrated? From my perspective, we have found that (1) the DCH process is not very efficient, (b) the DCH physical phenomena are almost equally active at scales ranging from 1/40 to 1/5.75, (c) the hydrogen, initially resident in the containment, generally does not burn, (d) the variations of parameters employed have not resulted in any discontinuous increases in the pressure-rise due to DCH, and (e) the hydrogen formed during the DCH process burns as diffusion flames as it is formed. All of these observations were expected in one form or another, except for the absence of scale effect in the pressure-increase due to DCH.

Now, I do not believe that safety issues are resolved on the basis of models developed by one person or another. They are resolved only if a sufficient amount of realistic data, favoring resolution (one way or another), are obtained. By realistic, I imply reasonably large-scale representations of the prototypic accident situations. A case in point is the LOCA-ECCS issue, whose resolution occurred only after the series of LOFT experiments, in which the clad temperature never approached the limit of 2200°F.

Scaling will always be an important issue as long as the experiments can not be performed at full scale. Computer code solutions can not be trusted as valid scaling vehicles, since physical phenomena change or affect differently with scale. Data obtained at different scales, as accomplished in the recent DCH test program, certainly provide a much more robust vehicle for developing a scaling rationale.

RESPONSE L1: *No comment.*

I believe that the observed results from the DCH test program were the inspiration for the TCE model developed by Dr. Pilch and the CLCH model developed by Prof. Theofanous. These models are attempting to describe the observed character of the DCH process, i.e., relatively low efficiency, relatively low production of hydrogen (which burns as diffusion flames) and relatively small scaling effect. The essential idea in both models is that the heat sink is limited to the amount of steam that is coherent with the melt dispersal process. The amount of hydrogen produced is also limited by the coherent steam. I consider that this limitation model is valid <u>only</u> for the time frame in which the peak value of the pressure is reached, through the rapid heat transfer from particles to the containment atmosphere.

RESPONSE L2: *The TCE and CLCH models found their inspiration elsewhere. The models only need to predict the peak pressure, there is no need to be valid for longer times.*

Both the TCE and the CLCH models are very simple and, I believe, that the authors probably do not claim them to be valid for the whole DCH event, in which heat transfer to the gas may occur from the films deposited on the surfaces, or more hydrogen may be produced by the steam arriving subsequent to that which participated in the initial dispersal process.

RESPONSE L3: *We claim to model only what contributes to peak pressure in any significant way, and we do not believe that the processes cited contribute in any significant way.*

The modeling of hydrogen production and hydrogen burn in the TCE and the CLCH model has been questioned. Certainly, a deflagration burn in the dome region would be of concern, thus, the autoignition temperature for the DCH conditions is a concern. I am not convinced by the arguments made in NUREG/CR-6075 for raising the autoignition temperature to 1100 K to compensate for the mixing limitations. Perhaps this physical phenomena should be investigated further. There may be some cogent explanation even for the observation in the most recent IET-10 test, performed in the 1/6 scale facility, in which a substantial amount of initially-resident hydrogen burned, but did not affect the peak pressure obtained. I believe, the hydrogen modeling in the TCE and CLCH models should embody the mixing process explicitly.

RESPONSE L4: *We have outlined our position more completely in Response F33. We recognize that a weak deflagration may occur under some conditions. We conclude that any deflagration, even if it can occur, will propagate too slowly and inefficiently to contribute to peak pressure. Explicit representation of mixing processes that do not contribute to peak pressure is not necessary.*

Further, regarding the hydrogen produced during the coherent dispersal process, the SNL comments point out that perhaps larger amounts of hydrogen were produced than modeled in the TCE and CLCH models. This additional (than calculated) hydrogen will also burn as a diffusion flame, raising the temperature in the dome region, however, the timing may be later than that associated with the attainment of the peak pressure. I believe this aspect of the hydrogen combustion during the DCH event also needs additional investigation.

RESPONSE L5: *We disagree. The models predict the amount of hydrogen produced (and burned if possible) on DCH time scales. These predictions are well validated for tests with nonreactive atmospheres and no containment water (e.g., Fig. E.3). Hydrogen measurements in tests with reactive atmospheres and water in the containment are distorted for the reasons cited in Section E.3.4. Recent scoping calculations using MELCOR (SAND93-1475) qualitatively support the cited reasons. More importantly, the measured load in the experiments are not consistent with the production and combustion of significantly greater quantities of hydrogen as the reviewer suggests.*

The TCE and the CLCH models do not incorporate adequate description for the initial melt - water interaction in the cavity or the melt - particle - water-droplet interactions in the upper compartments. This is perhaps due to the experimental observations of very small effect of water presence on the peak pressures measured. There are obviously compensating effects of pressure-rise due to steam production versus that due to atmosphere heating. Perhaps, this aspect of DCH needs further investigation.

RESPONSE L6: *See Responses C8 and D14.*

The SNL comments on the CLCH and the TCE models point out that besides the neglect of the melt-water interactions, these models did not consider (a) the role of the non-airborne debris, (b) possible greater transport into the dome region, (c) non-adiabatic and non-equilibrium effects,

and (d) 'Bottom-up' modeling. All of these deficiencies have been cited to claim that the TCE and the CLCH models are physically unrealistic. I believe what is being stated is that the TCE and CLCH models are not fully mechanistic. It is a good statement; however, the authors of the TCE and the CLCH models probably, do not, or can not claim them to be fully mechanistic. From my point of view, they are heuristic models, which derive a scaling rationale and then use the measured data to extrapolate to the prototypic situation. They do not start with conservation equations and then track streams of particles, films, structures, etc., of the DCH event in a particular containment. Such work was started earlier at Sandia but did not lead to a satisfactory methodology, which could be used productively to explain the DCH measurements.

RESPONSE L7: *No comment.*

The alternative model presented in the SNL comments, illustrating the possibility of obtaining agreement with the measured data on three different scales does not comply with the observation that in each test the melt dispersed as particles, which provided the surface area for the heat transfer to the containment atmosphere. In addition, that model had three constants to fit the data.

RESPONSE L8: *No comment.*

Perhaps, the pertinent question to ask is whether the TCE and the CLCH models describe those aspects of the DCH event sufficiently well, which are required for the regulatory purpose of the DCH issue resolution. These models may not have as much bottom-up experimental support as is perhaps desirable.

RESPONSE L9: *The reviewer understands the problem when he noted previously that bottoms-up modeling did not lead to a satisfactory methodology. Additional bottoms up support is given in Response M3 (cavity interactions) and Response F8 (heat transfer to structures). The problem is that it is very difficult to quantify many DCH processes in a defensible manner. The bounding nature of our models sidesteps the need for detailed bottoms-up modeling and data. Additional support for hydrogen combustion phenomena is given in Response F33.*

I must comment on the choice of the inputs in the ROAAM formalism. The probability distribution functions selected for the melt mass and the Zirconium oxidized in scenarios 1 to

4, appear to me to be optimistic, rather than conservative. Probably, the same comment can be made about the choice of values for the vessel pressures and the steam temperatures prior to vessel failure. The hole size choice limited to 0.4 meters may also be optimistic. It may also be necessary to treat the hole size with a PDF. The appendix J model is based on data from experiments with thermite on steel plates, which cover only a small segment of the regime of interest.

The description of the core melt scenarios in section 3 have some inaccuracies. I recommend that the specification of the PDF 1, 2, 3 may need further support. I am not aware of any great new knowledge in the phenomenology of late phase melt progression.

RESPONSE L10: *Sensitivity studies indicated that no single process or parameter has a controlling influence.*

Lastly, I will attempt to respond to the questions raised in your letter of July 20, 1993.

1) I believe that the TCE and the CLCH models are the heart of this issue-resolution report. I think they are technically sound and since they are tied to a good database, the conclusions based on their application should be sound. I do, however, have reservations about the choice of initial conditions.

RESPONSE L11: *It is within the ROAAM process to address comments and accept input from peer reviewers.*

2) The uncertainties in the analysis are largely in the choice of initial conditions and the sensitivity studies have tried to cover those. I am not wholly convinced that the sensitivity analysis performed covers all uncertainties. The sensitivity analysis perhaps should be strengthened.

RESPONSE L12: *The sensitivity studies preformed by Reviewers H and O compliment those in the report. In addition, we have performed point calculations with the SASM melt composition (see Response B10).*

3) I do not envision any new confirmatory experiments. The confirmatory work recommended in NUREG/CR-6075 applies primarily to the extrapolations to other containment geometries. I believe that would be helpful.

RESPONSE L13: *No comment.*

4) I am quite convinced that the methods of NUREG/CR-6075 can be applied to other containment designs. However, some of the containment geometries may not have the dispersive character, and the same cavity upper compartment arrangement, as found in the Zion and Surry plants. Thus, the extrapolations should be performed carefully and the conclusions stated after due consideration.

RESPONSE L14: *We agree that extrapolations should be done carefully. Note, however, that we focus on the retentive character of the subcompartment, not the details of geometry. Our current assessments only become more conservative if cavities are identified that are more retentive than Zion or Surry. Our focus in NUREG-6075 is Zion. NUREG-6109 is intended to provide a more complete look at the extrapolation issue.*

I am a bit late sending this review of NUREG/CR-6075 and the associated comments received from INEL and SNL. There has been a considerable hurry in sending this letter out. I may have missed making some comments, therefore, I may want to provide more comments later on. I hope you will not preclude my right to do so.

REBUTTAL FROM REVIEWER L

I have reviewed the transmittal on the subject, along with the earlier transmittal by the Energy Research Inc. of the peer review comments that were made on the report NUREG/CR-6075. I have reviewed the authors' responses to not only my comments, but also to the comments made by other peer reviewers, to obtain a perspective as to your statement that the responses are focused on the resolution of the DCH issue for the Zion containment.

One of my main concerns, and of other reviewers, i.e., the contribution to the DCH loads from hydrogen combustion was responded to in F33. The authors have provided a good response, however, it is not completely convincing, since the scenario (time) dependence has not been considered. I believe they should consider the station black out scenario and determine the spatial distribution of hydrogen in the containment at the time of HPME. The hydrogen release from the vessel occurs only about half an hour before vessel failure and the release location may not be directly communicating with the dome.

My other main concern is about the initial conditions, i.e., the melt mass, composition (metal content) and the probabilities assigned. Almost all of the reviewers have questioned the chosen values. The authors responses are not adequate. Basically, the chosen values are their expert choices and they have not provided adequate rationale for those values. If the metal content is increased the loads increase substantially. I still do not understand why the metal content chosen is so low.

The authors have not adequately responded to the comment made by Reviewer D that the operator actions may change the classic TMLB' scenario (as they did in TMI-2) and it is important to consider a situation like that of TMI-2 experiencing HPME.

In general, the authors have provided good, honest and thoughtful responses to my and other reviewers' comments. I believe that the concern of the reviewers about the initial conditions, and their probabilities assignment, will need further study. The hydrogen combustion scenario also will need further study. A face to face meeting between the authors, the reviewers and the NRC staff may clarify the remaining differences and help formulate the questions to be

answered, through further study, by ad-hoc expert groups; as it was done prior to the resolution of the MARK-I liner melt-through issue.

Comments by Reviewer M

1. INTRODUCTION

I have performed a limited-scope review of NUREG/CR-6075. This document presents, under one roof, a presentation of the DCH models, actually two sets of models, used to provide the authors assessment of DCH loads, a comparison of the models with the available database, a description of the probabilistic framework used to derive the pressure load distributions, and a presentation of the input distributions which largely control the magnitude of the computed pressure loads. The sections which present the models contain discussions of many diverse areas of phenomenology which the authors have had to come to grips with and make judgements about. My basic feeling about this review is that I have had barely the time to scratch the surface of much of the material presented, even after having been involved with selected aspects of the problem for several years. Because of the limitations of this review, I have asked myself the following questions:

(i) Do the authors provide interpretations of the available database which can plausible be applied to predictions of DCH loads in full-scale plants?

(ii) Do the input distributions adequately reflect the uncertainties in the phenomenology?

(iii) Are the conclusions plausible?

I will address these questions in this review. Questions which I cannot answer are: (i) is there an alternative interpretation of the data which would scale to plant conditions in a quantitatively different manner?, (ii) are the calculational results accurate? These questions can only be answered, I believe, by independent analysis, which was not possible during a limited review.

Section 2 below provides my comments on the models and their assessment and Section 3 discussed input distributions. My summary assessment is presented in Section 4.

RESPONSE M1: *No comment.*

2. MODELS AND ASSESSMENT WITH AVAILABLE DATABASE

Comments on Models:

The question of DCH models is dealt with first because it is the most important. The authors developed their models based upon their understanding of the available DCH database. These models are the tools which provide the "scale-up" from the experiments to full-scale conditions. The issues of model adequacy, therefore, is certainly not academic. If there are any "distortions" in the models developed from scaled experiments, these distortions will be carried through to full-scale plant calculations.

The authors have provided a good review of all points of view which have been presented over the years and which have been used to provide estimates of the magnitude of the DCH pressure loading. They have carefully examined the large number of separate effects experiments related to DCH phenomena, have analyzed the integral experimental database and have examined a number of DCH modeling studies which helped to shed light on the controlling phenomenology. They recognize the complexity of the microphenomena involved and they acknowledge the limitations of the ability to predict the details of the flow processes. The authors have developed their two conceptually-similar, but not identical, approaches based upon examination of all these factors.

Both authors focus on the impact of compartmentalization on the DCH pressure loading. This feature of DCH and the potential limits it imposes on DCH loading has been understood for several years: Melt trapping in the subcompartment above the reactor cavity has been recognized as a mitigating feature, and the effect of the heat capacity of melt and lower subcompartment to lead to equilibration of melt and gas phases has also been recognized as important mitigating factors. Two concepts were involved: (i) the melt trapping feature was viewed as one which placed a limit on the "flight path" of millimeter debris particles and (ii) the equilibration feature limited the energy which could be transferred to the containment atmosphere due to temperature "saturation."

A DCH model which incorporated the "flight path" approach would have to provide detailed mechanistic models of droplet size, heat and mass transfer rates and would limit the extent of heat and mass transfer by limiting the time, or distance, available to the droplets to complete the

transfer processes. Neither author adopts this approach. Yet, this is a possible alternative explanation for the relatively small experimental pressure rises observed in the scaled experiments. Now, it is possible that the authors have rejected this approach after attempting to analyze the results using such a model. Pilch says (p. E-4): "Some researchers felt that the observed containment pressurizations were substantially lower than would be expected at full scale because the time scale for heat and mass transfer is compressed in small scale experiments." However, he also observes that (p. E-5): "This testing program in Zion geometry is now complete. No strong effect of physical scale on containment loads or hydrogen production was found." It is not clear whether the authors have dismissed this modeling approach because they tried it and it didn't "work" to correlate the data, or because they simply didn't try it. This approach is different than the approach used by the authors, and would likely provide different scale-up to plant conditions. **If the authors have done some work which shows that "flight-path" limited heat and mass transfer is not the operative limiting mechanism, they should present this work and dismiss the approach as not capable of explaining the data. Otherwise, this alternative will loom as another possible alternative approach which should be compared with the data and used to scale to plant conditions.**

RESPONSE M2: *Time-of-flight limitations to heat and mass transfer have been tried in the past with no clear conclusion because the rate processes are so difficult to characterize and validate for realistic plant geometries. These rate processes depend on a lot of details: particle size distributions, slip, breakup, entrainment, deentrainment, reentrainment, flow patterns, etc. Some progress has been made in an overall sense, but we know of nothing that can scale these processes. How far do you go with verification? We chose to bound all these processes, since we have a* <u>*reasonable*</u> *expectation that thermal and chemical equilibrium is achieved in the cavity. Detailed treatment of kinetic processes typically show a scale dependence; however, kinetic processes do not appear to be limiting. In any case, our scaling is still bounding based on the nature of the models.*

The authors adopt two models with the intent of demonstrating "...a certain bounding feature of resulting pressurization with the DCH scale, which may be very convenient when such a bounding quality in predictions is desirable" (Theofanous, p. D-4) and with "...the intent of enveloping each of the processes that contribute to containment pressurization" (Pilch, p. E-7). The models are based upon a similar concept, one which I believe at least partially should account for the observation that measured pressure rises are significantly below ideal

thermodynamic limits. The models are based on the idea that the melt interacts only with a limited volume of gas within the large containment building, resulting in limits on both heat transfer and chemical reaction. **This idea is basically sound and has been cited in the past to explain calculational results based on the CONTAIN code.** The question in my mind, however, is **whether this factor alone** is sufficient to explain the experimental results. CLCH (Theofanous) assumes that the melt sees only steam blowdown gas in a flowing, time-dependent equilibration process, while TCE (Pilch) assumes that the melt can interact with either all the gas in the lower subcompartment, or with the blowdown gas, in a sort of static equilibration process. In neither model do heat or mass transfer **rates** play a role. While the authors have not explicitly stated it, they are, in effect, assuming that the debris-gas heat and mass transfer rates are sufficiently high that equilibration can take place in the reactor cavity, in the case of CLCH, and in the cavity and subcompartment in TCE. While the authors do not use the debris particle size data anywhere in their analyses, it appears to be a presumption that the bulk of the debris are sufficiently small so that equilibration can occur. Is this consistent with the results coming out of Purdue's separate effects experiments?

RESPONSE M3: *We have a* <u>*reasonable*</u> *expectation that thermal and chemical equilibrium is achieved in the cavity, so that flight path limitations are not controlling. To make this assessment, we follow SASM (NUREG/CR-5809) and compare the interaction time between dispersed debris and coherent blowdown with the heat transfer and oxidation time constants. The interaction time (entrainment interval) is inferred directly from the SNL/IET experiments to be* $\tau_e \sim 0.3s$. *The heat transfer time constant,* $\tau_{HT} \sim \Delta E_{i,EQ}/R_{HT}$, *can be evaluated in a manner similar to Pilch et al. 1992. Experimentally determined particle sizes* ($D_d \sim .5mm$) *and dispersal fractions* ($f_{disp} \sim 0.7$) *are used in evaluating the heat transfer time constant. The heat transfer time constant is* $\tau_{HT} \sim 0.015$ *so that* $\tau_{HT}/\tau_e \sim 0.05$. *Thus, we reasonably expect thermal equilibrium in the SNL/IET experiments. A similar process for oxidation yields* $\tau_{ox}/\tau_e \sim .01$, *so we can also reasonably assume chemical equilibrium in the cavity. These experiment based estimates are quite crude and any departure from equilibrium at other scales or in other geometries becomes a difficult scaling problem. Therefore, we are motivated to assume thermal and chemical equilibrium in all our assessments, and successful comparisons with the DCH database further support this bounding modeling approach. Ishii's correlations (PU NE-93/1) predict similar particle sizes at reactor scale. This discussion will be added to the text.*

The models are presented as bounding in nature. It appears to me that, given the effect of melt removal resulting form compartmentalization as being real, it does indeed seem that the two models should provide bounding results, in the sense that the only limitations to heat and mass transfer are the gas phase heat capacity and availability of oxidant in the gas phase. Both the CLCH and TCE models are simplified models of the phenomena and the conservation equations are not very complicated-looking. However, their derivations, including assumptions and basic form of the conservation equations, are not presented in sufficient detail and clarity. Both models purport to handle the small quantities of melt that are transported to the dome, but I don't see the terms explicitly in the model equations. While I don't doubt the abilities of the authors, **I cannot vouch for the "correctness" of the model equations.** As a reviewer, I don't want to have to rederive equations, I would like to see them explicitly derived from fundamentals, or as close to it as possible. Table D.1 is confusing to follow, and the inherent assumptions, meaning and derivation of Eqs. E.37-E.39 are not clear. If there are separate papers or reports which deal with the development of model equations, they should be made available.

RESPONSE M4: *The TCE model explicitly shows DCH contributions in the subcompartment and dome regions (see for instance Equations E.29, E.36, and E.41). The derivation and meaning of Eqs. E.37 and E.38 follow that given for the single cell equilibrium model (Section E.2). Only here the variables are specific to the subcompartment. The text will clarify this point. Eq. E.39 is a mixture temperature for 2 volumes of gas, and the text will clarify this point. The CLCH model discusses dome interactions. The CLCH equations for dome interactions are not shown explicitly because the author of Appendix D wishes to maintain clarity and conciseness in the presentation.*

The TCE model is an unusual approach for modeling a dynamic process. It relies on bounding approximations for estimates of individual energy exchange magnitudes. I have to admit that the approach makes me a little uncomfortable, since I am used to looking for transient solutions to the DCH problem. But, I'm open to a new approach, and if the approach is reasonable and it agrees with the data, then I'm willing to be convinced.

RESPONSE M5: *No comment.*

The authors' treatment of preexisting hydrogen in the dome recognizes the uncertainties in autoignition phenomena. I'll just add that in recent BNL experiments in a 10-cm diameter cylindrical stainless steel vessel, we observed significant hydrogen-air reaction rates at 650K, for mixtures as lean as 15% and as rich a 50% hydrogen by volume. The rich reaction rate was consistent with those measured by DeSoete and with DeSoete's reaction rate equation. I think that 1100K is very likely too low an estimate, although experiments have not been done in the range of several percent hydrogen. Considering the potential importance of the autoignition temperature, some thought should be given to turning it into an additional uncertain parameter with a distribution.

RESPONSE M6: *We agree that 1100K is too low an autoignition temperature for DCH events (see Response F33 for additional justification). This will be further addressed as part of an expanded treatment of hydrogen combustion issues during DCH. The reaction rates at 650K are on the order of minutes. This energy release rate is too slow to cause pressurization in DCH events, and we understand that no pressurization was observed in the BNL experiments.*

The authors correctly interpret the available database to conclude that the cavities under consideration would retain little melt under the driving pressure conditions considered. Their treatment of the melt dispersal time scale as an uncertain parameter is also reasonable, although I have not evaluated their approach to modeling their "coherence ratio" or "DCH-Scale." I should point out, however, that the potential for mitigating hydrogen generation as a result of limited steam resulting from melt dispersal time scale which is smaller than the vessel blowdown time was discussed by Tutu and myself back in 1987.[7]

RESPONSE M7: *Your contribution will be appropriately cited in the text.*

One comment about both models: **In neither model is a variable defined, dimensionless or otherwise, which reflects the initial thermal and chemical energy density of the melt.** The CLCH Equation D.12 does not have such a variable and, in addition, it also does not have a variable which defines the initial temperature of the melt, as far as I can detect. Neither does it have heats of reaction. Without these variables how does one go from thermite to corium?

---

[7] Ginsberg, T. and N.K. Tutu, "Safety Research Programs Sponsored by Office of Nuclear Regulatory Commission, Quarterly Progress Report, April 1 - June 30, 1987, NUREG/CR-2331, Vol. 7, No. 2 (1987).

RESPONSE M8: *Thermal and chemical energy densities are shown explicitly in Eqs. E.19 and E.20 for the TCE model, and Eq. D.20 for the CLCH model.*

Neither author presents a clear argument as to the basis for using their models to extrapolate from the largest experimental scale to full-scale plant conditions. The CLCH discussion presents a set of dimensionless parameters. Are these complete? How does one use these variables to extrapolate to full scale conditions? For TCE, are there dimensionless variables which characterize the process? How are these used in scale-up arguments?

RESPONSE M9: *The discussion of this issue will be expanded in Allen et al., NUREG/CR-6074, 1993. The SNL/IET experiments and the ANL/IET experiments were scaled by matching the various terms in Eq. E.13 to expected values in a reactor evaluation. This amounts to energy/volume scaling. This dictates the melt mass in the experiments, and it also dictates that prototypic RCS and containment conditions be achieved. Lastly, geometric scaling was employed. Taken together, all terms in the TCE model are reasonably matched also.*

Comments on Model Assessment Against Experimental Database

I have been able to give only the most superficial look at the large database that is now available for testing of DCH models, so that I cannot be a good judge at this point of the trends of the data compared with the models. From this viewpoint, the authors comparisons of their models with the experimental database is pretty good, especially considering the simplicity of the models. Both models, each in their own way, appear able to provide reasonable estimates of the pressure rise and hydrogen production data. It is easier to judge the comparisons with the graphical presentation presented by Pilch for TCE and I would recommend that the CLCH results be treated similarly. The data for the coherence ratios are also reasonably well predicted by the two sets of models.

RESPONSE M10: *The author of Appendix D disagrees with the need for new figures. The presentation of information in the CLCH model and the TCE model complement each other.*

It would be helpful, in the case of the CLCH model, which is able to predict the transient pressure response, to show the detailed time-dependent predictions of the model with the actual

transient data, in order to get a better feeling for the ability of the model to predict the experimental results.

RESPONSE M11: *The CLCH model predicts the right pressure by using the experimentally observed entrainment interval; consequently, the pressurization rate must also agree with the data.*

3. INPUT DISTRIBUTIONS AND OTHER DATA

The benign DCH pressurizations which are predicted by both models are, I believe, due to two factors: (i) the mitigative feature of melt removal and limited melt-gas contact resulting from the subcompartmentalization, discussed above, and (ii) the limited melt masses which were assumed in the calculations. Arguments are presented in Section 3.4 of the report which lead to the distributions of Figs. 3.3-3.9. The authors have waded through quite a bit of information to arrive at their input distributions. I have not had the luxury. Nonetheless, considering the major uncertainties in the process of relocation of material from the core to the lower plenum and the subsequent sequence of events, I believe that too low a probability is given to the high end of the melt mass distributions. In the case of Scenario I, for example, I consider reasonable the estimate that the outer 30% of assemblies will stay in place. I believe that adopting the TMI-II estimate of about 20 mt may be placing too much reliance on this piece of data, even if it is a very expensive piece of data. But, even if I accept 20 mt as best estimate, I believe that taking 45 mt at a process likelihood of 0.01 is biasing the distribution to melt masses which ar too low considering what I believe are tremendous uncertainties. I don't see very good reason for two orders of magnitude of likelihood in going from 20 mt to 45 mt. I would go for a factor of ten at best. As a result, I would suspect that the likelihood of containment failure by DCH may be somewhat understated in this report. By how much, I don't know. I believe that there is a high degree of subjectivity here. **I'd like to see a calculation done with this modification to the input distribution.** This would also serve as a test of the sensitivity of the computed probability distribution to the input melt mass distribution. We would see if there are any surprises.

RESPONSE M12: *Numerical input and results (DPDs) must both be interpreted against the same subjective (although arbitrary) scale. The numerical numbers do not convey frequensic or statistical meaning, only subjective levels of belief. See Responses B9 and C9 for additional*

detail. However, this reviewers concerns may be at least partially alleviated by sensitivity studies performed by Reviewers H and O. Maximum entropy distributions were used in some cases; and in another case, the mass varied up to 100% of core. No strong sensitivity was evident.

As I've mentioned above,I believe that there are significant uncertainties in characterization of the autoignition temperature for hydrogen-air-steam mixtures. The SNL observation is that they do not see autoignition of preexisting hydrogen in the containment. Their explanation relates to stratified gas conditions in the containment atmosphere. A temperature of 1100K is likely too high as a best estimate of the autoignition temperature. We observe chemical reactions at temperatures as low as 650K, with measurable changes in hydrogen concentration occurring on a time frame of 30 seconds to a minute. **I would recommend a sensitivity calculation at 800K, despite SNL's observations, just to look at sensitivity over a broader temperature range.** It may also be appropriate to parameterize the autoignition temperature as a distribution parameter if the sensitivity calculation indicates that it is warranted. If so, I'd be happy to offer a distribution.

RESPONSE M13: *The type of slow volumetric combustion described here does not contribute to DCH loads. We disagree with the need to treat autoignition with a distribution since we believe that autoignition (sudden volumetric combustion) is essentially impossible during DCH events. See Response F33.*

The estimate of 14% melt transport to the containment dome is, I believe, a reasonable choice. However, I have not seen any data from the large scale SNL experiments for the extent of transport to the dome. ANL reports, on p. H-8, fractions of melt transported out of the cavity of about 10%, in their 1/40-th scale experiments. I have not seen any scaling arguments to help extrapolate to full scale from the largest scale experiment that we have. It is not clear, therefore, what we should take as an upper bound. The 20% estimate used in sensitivity calculations may or may not be conservative. Pilch concludes, on p. 1-2, that 9% of the melt can be transported to the dome through the annular gap, in the case of Zion. What about the total fraction to the dome, including through the subcompartment? While this may not be very important if the melt mass discharged to the cavity is around 20 mt, it becomes more important if the likelihood of larger melt masses is greater than as proposed by the authors.

RESPONSE M14: *The total fraction of dispersed melt that goes to the dome is discussed in Section 4 of the report. Total transport consists of contributions through the gap and subcompartment. The experiments were conducted with scaled geometries and prototypic RCS pressures, so the experiment observations are directly applicable to our reactor cases. Transport to the dome is largely dependent on geometry (flow area ratios and line-of-sight arguments); consequently, we do not expect much sensitivity to RCS pressure (except possibly at very low pressures where the dispersed melt has insufficient momentum).*

4. SUMMARY ASSESSMENT

I started with three questions in Section 1, and it is with responses to them that I will summarize:

(i) The authors have presented two models which are intended to predict DCH containment loadings under full-scale accident conditions in plant geometry. The models are highly simplified descriptions of the phenomena, and are based upon the assumption that the dispersed melt comes to thermal and chemical equilibrium with either the steam discharged from the reactor vessel, or with the subcompartment gas. The melt is trapped, except for a relatively small fraction, within the subcompartment. The implication is that the heat and mass transfer processes are very fast during the time period of contact between gas and melt. Hydrogen discharged into the upper subcompartment generally burns as a diffusion flames, while preexisting hydrogen generally does not burn on the time scale of the DCH pressure rise. The two models are significantly different in their treatments of the phenomena. The derivations of the models are not explained to my satisfaction, and I cannot vouch for their physical correctness from a modeling point of view. If I am given more detailed description, then I will then make a judgement. However, I believe that the models are indeed bounding, as stated by the authors. With these caveats, I believe that the authors have demonstrated, by comparison with the available experimental data, that their models provide a reasonable explanation of the observations. Agreement of model predictions with DCH pressure rise, hydrogen generation and coherence ratio are demonstrated to be reasonable. On this basis, I believe that the models can plausibly be applied to DCH plant calculations. However, I do have some reservations. These are related to the

scale-up from the largest experiments which are available to full-scale conditions, a factor of 5.75 in linear scale, which is accomplished using the model.

RESPONSE M15: *Experiments ranging from 1:40th to 1:6th scale indicate that there is no strong effect of physical scale on DCH loads. This experiment observation, coupled with our ability to predict the data with our models gives us confidence that we can predict DCH loads at full scale without excessive conservatism. Some clarification of the TCE model development will be added to the text.*

It is not clear to me, as discussed above, whether the "limited flight path" argument might also explain the experimental data and, therefore, be used to model the full-scale plant with, perhaps, different results.

RESPONSE M16: *See Response M3.*

(ii) I believe that the input distributions for the masses of molten material discharged from the vessel do not adequately represent the major uncertainties in prediction of the in-vessel phenomena. I believe that the distributions are biased towards low melt mass. I have provided some guidance as to how to modify and perform a sensitivity calculation. The phenomena involving reactions of preexisting hydrogen are uncertain, and these uncertainties can have a significant bearing on containment loads. I suggest a wider range of sensitivity calculations, involving burn of this hydrogen. Taken on face value, however, it is difficult to argue with the experimental observations. I think that reasonable choices have been made with respect to other input parameters.

RESPONSE M17: *The sensitivity studies already performed by Reviewers H and O already satisfy this reviewers request.*

(iii) Given (1) the basic mitigation mechanism hypothesized resulting from containment compartmentalization, (2) the distribution of melt masses used in the calculations, (3) the "no-burn" of preexisting hydrogen assumption which is generally implemented, and (4) the containment fragility curve employed, the result of the NUREG/CR-6075 study is that containment failure by DCH is "physically unreasonable." However, when I

compare th results of the present study with those of NUREG/CR-5282[8], a Zion DCH loading study using the CONTAIN code with which I am familiar, I am not surprised by the judgement that containment failure is highly unlikely. As discussed above, I believe some of the assumptions in the present study may be overly optimistic and should be looked at more carefully.

RESPONSE M18: *As part of the ROAAM process, we recognize that some confirmatory activity may be necessary to achieve consensus on some initial conditions.*

---

[8] Tutu, N.K., et al., "Estimation of Containment Pressure Loading Due to Direct Containment Heating for the Zion Plant," NUREG/CR-5282 (March 1991).

REBUTTAL FROM REVIEWER M

Comments on Response M1

No further comment.

Comments on Response M2

I agree that treatment of rate processes is difficult. I also accept the physical notion that if the melt is largely trapped in the lower subcompartment, then this will significantly limit the extent of heat and mass transfer. I am still somewhat uncomfortable with the remaining scaleup required. For example, we don't know how to scale the fraction of melt transported to the upper dome. If this should turn out to be larger than expected, then rate processes could be more important than assumed in the TCE and CLCH models. This would, of course, require more detailed understanding of the processes. So, while the authors' thermal and chemical equilibrium assumption appears to satisfactorily explain the experimental data, I am still somewhat uncomfortable with the extrapolation of the models. My comfort level might improve if the TCE and CLCH predictions were supplemented by more detailed CONTAIN-type calculations, using the best information we have to date about the rate processes. Of course, we would still have to either make some assumption about the fraction of melt transported to the dome region, or embark on an effort to better be able to predict the transport of droplets in complex geometries.

Comments on Response M3

No further comment.

Comments on Response M4

When I see the final text, then I'll judge the adequacy of the response.

Comments on Response M5

No further comment.

Comments on Response M6

Mistake in my original response, as the authors picked up. I should have said "...that 1100K is too high an estimate.." instead of "...too low...." I agree that at 650K, reaction rates are low. We need to know how the reaction rate varies with temperature above this. Perhaps the autoignition temperature should not be chosen as the uncertain parameter. Maybe the time scale for chemical reaction should be selected instead. It is clear to me, however, that there is uncertainty in the extent of hydrogen reaction during the DCH time period and on the DCH pressure rise which should be represented as a probabilistic variable.

Comments on Response M7

No further comment.

Comments on Response M8

TCE author is correct. CLCH: I don't see an Eq. D.20 in the text, last equation is D.16.

Comments on Response M9

Question of scale-up not settled, as far as I observe.

Comments by Reviewer N

SECTION 2.0

1. DPD METHODOLOGY

The probabilistic framework outlined in this section is based on the use of DPD (discrete probability distribution) methodology, but the methodology is not defined nor are any references given.

RESPONSE N1: *The use of discrete probability distributions is a technique (not a methodology) that is not new. It has been used and extensively reviewed as part of the Mark I report (NUREG/CR-5960). Historically, it has been used in seismic studies also.*

In particular, there is no discussion of the crucial choices of bins and the condensation procedure. Since the probability of containment failure may be a sensitive function of the tails of the pressure distribution and the fragility curve, it is essential that the effect of these tails not be distorted by the DPD methodology. There would need to be a full discussion of this issue before any judgements can be made as to its adequacy.

RESPONSE N2: *Condensation is a two step process that is carried out in such a way as to preserve the tails of the distributions. First, the minimum probability of interest is 10^{-3}, so any point with probability significantly less than this is discarded. Typically, the cut is 10^{-3} or 10^{-4}, and the remaining points are renormalized so that the total probability remains unity. The cut point is chosen so that the total probability of all discarded points is insignificant. In the second step, the number of points remaining is reduced by binning. In this process, a number of points is replaced by a single "equivalent" point in such a way that the total probability of the bin is preserved. The equivalent point takes on the expected value of the assembly. Bin sizes are chosen so that the expected value and the variance are the same before and after the binning procedure. Our results have been independently verified using Monte Carlo techniques at SNL and by Reviewer O, who used a stratified Monte Carlo technique.*

2. ASSUMPTION OF INDEPENDENCE

Equations (2.3) and (2.4) assume that the four parameters of m_{UO2} (UO_2 mass released from vessel), m_{ss} (stainless steel mass released from vessel), X_{Zr} (fraction of zirconium oxidized) and R_r (coherence ratio) are mutually statistically independent. However, since the first three are strong functions of the pressure and temperature in the reactor vessel, their distributions should be strongly positively correlated. The effect of the independence assumption could be to significantly underestimate the DCH pressure load and the failure frequency. If equations (2.3) and (2.4) are used, then it must be shown that the independence assumption on which they are based does not significantly bias the results.

Also, the blowdown time of R_r is a function of the first three parameters directly (Zr oxidation being an exothermic reaction) or indirectly (mass released from the hole in the vessel ablating the hole). Evidence that R_r is independent or that the dependence does not bias the results is necessary.

RESPONSE N3: *See Response H4, this will be clarified in text.*

3. EQUATION (2.9)

It is unclear why the subscript "r" appears. If r is omitted, this equation yields the failure frequency as a function of the pressure distribution and the fragility curve. The use of the subscript should be explained.

RESPONSE N4: *Typo will be corrected.*

4. SECTION 5.1

The containment fragility curve used for this study is taken from the Zion IPE. As shown in the attached figure, the Zion NUREG-1150 fragility curve will produce a larger containment failure frequency at low pressures. Use of the IPE curve instead of the 1150 curve needs to be justified. Sensitivity studies should be performed to show the impact.

RESPONSE N5: *The IPE fragility curve is used because it represents the best assessment of the utility. We expect that the IPE curve is more plant specific. Furthermore, the utility had the advantage of NUREG-1150 results before making their IPE assessment. We note that the NRC sponsored Containment Performance Under Severe Accident Conditions Program is tasked with identifying deterministic failure criteria and integrating them in a probabilistic framework. Here, we expect that modeling uncertainty will be represented as families of fragility curves. The fragility issue should be revisited if this program significantly alters the current estimates of containment fragility.*

SECTION 6.0

Pg. 57, 1st Paragraph

There should be a complete description of the computer code ALPHA and the independent Monte Carlo calculations made to verify the ALPHA code results. This description is needed to provide a basis for judging the extent to which the Monte Carlo calculations verify the ALPHA code results.

RESPONSE N6: *Reviewer can examine the additional verifications provided by Reviewer O using a stratified Monte Carlo technique. At this time, we do not intend to provide a more complete description of the ALPHA code. The code is not well commented and it is difficult to follow. SNL is currently reviewing the ALPHA code to ensure that the FORTRAN accurately reflects the text.*

Pg. 58 - 60

The sensitivity study should encompass the effects of high correlations among the input parameters in Equation (2.4).

RESPONSE N7: *See Responses H4 and H12.*

Since the parameter distributions and other expert judgements on which the report's results are based were apparently due only to the authors, the use of the ROAAM or an equivalent process is essential for the credibility of the conclusions. From the last paragraph on pg. A-8, it seems that the ROAAM process is now being carried out or is planned. If so, then it should be stated who the experts are and to what extent the current report will be used.

RESPONSE N8: The reviewer has already participated in the review phase of ROAAM. All reviewer comments and the responses will be published in full along with the report. Any follow-up activities, if necessary, have not yet been defined; but if such activities become necessary, they will be carefully documented with due credit to those who participated in the process.

According to the first paragraph in Section A-3, a "physically-based probability scale" is used to convert qualitative expert judgements into probabilities for calculational purposes. Since the same qualitative judgement can correspond to different probability levels for different people, it is unclear how this method can be consistently applied to a panel of experts. This issue should be discussed.

RESPONSE N9: See Response B9.

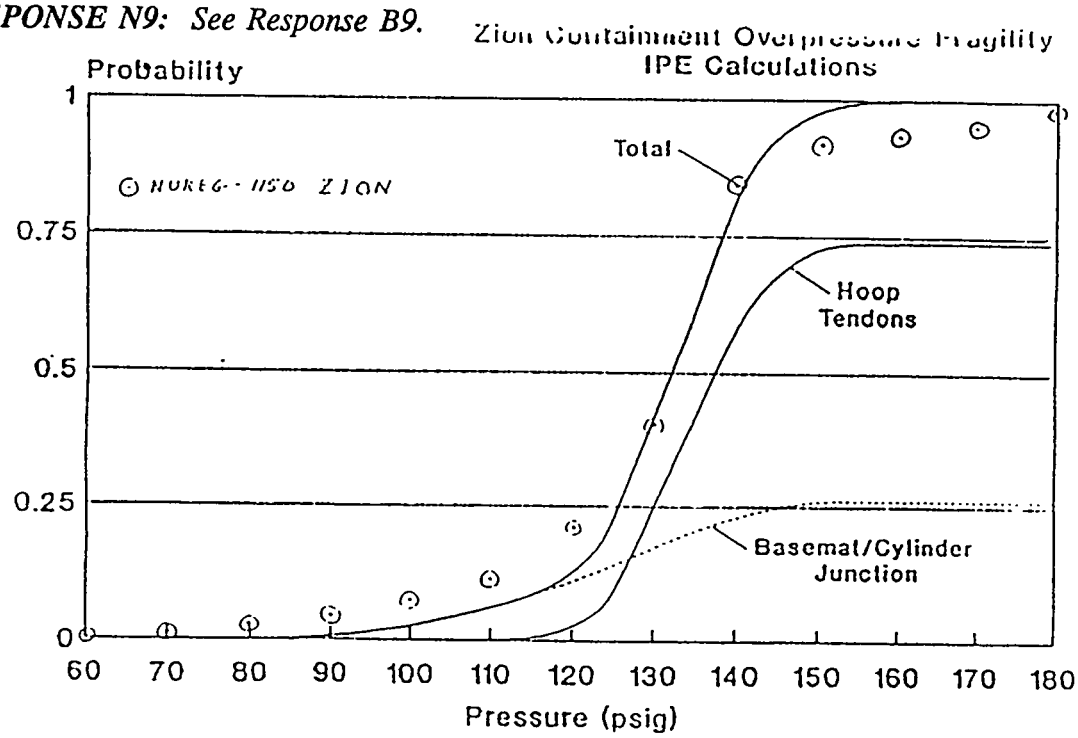

Values obtained from a figure in another document. Hence there is some plotting inaccuracy.

Comments by Reviewer O

1. REVIEW COMMENTS ON NUREG/CR-6075

1.1 Comments on the Probabilistic Framework

The approach in the NUREG/CR-6075 is based on ROAAM. The probabilistic approach uses several initial conditions in the form of Discrete Probability Distributions (DPDs) and a number of "Causal Relations" (CRs) for physical processes. These probability distributions and functional dependencies (in the form of CRs) are propagated through the model to arrive at the final conditional containment failure probability [1]. In practice, this approach also suffers from the same shortcomings as other probabilistic techniques, such as the traditional fault tree/event tree approach used in the majority of level 2 PRA studies worldwide (e.g., NUREG-1150); namely, the use of expert opinion, and the assignment of subjective probabilities. In fact, the formal approach to elicitation of expert opinion, as embodied in NUREG-1150 type studies is often more transparent and defensible since it could potentially reduce the impact of any biases introduced by one or more expert. Appendix A of Reference [1] gives the impression that issue resolution could not be achieved within the PRA framework, and ROAAM is the answer to resolution of outstanding severe accident issues.

RESPONSE O1: *The intent of NUREG-1150 type studies is to survey the range of expert opinion in order to identify what is important to risk. Having identified DCH as an issue, the next step is to resolve the problem. Here, a more focused treatment following improved phenomenological understanding is a stated philosophy of ROAAM aimed at reaching consensus on individual elements of the problem. We recognize that other techniques (such as expanded NUREG-1150 type event trees) could be used for this purpose.*

The main probabilistic framework for the assessment of containment pressurization due to DCH loads is rather simple. Uncertainties are associated with the amount of molten UO_2 in the reactor pressure vessel lower head at vessel failure, the fraction of Zr oxidized, and the mass of steel in the melt. These are the three basic input uncertainty distributions. Another input distribution is the coherence between the steam and the melt. This uncertainty is only applicable to the CLCH (Convection Limited Containment Heating) or the TCE (Two Cell Equilibrium)

model that predicts the containment pressurization. There are other uncertainties that are not discussed in Section 2 of NUREG/CR-6075 [1]. These include the amount of preexisting hydrogen (as a result of Zr oxidation prior to vessel breach) in the containment atmosphere that can be entrained into the flame (in the NUREG/CR-6075 [1] analysis, 10% of the preexisting hydrogen is entrained into the flame) and the uncertainty in the containment temperature at which spontaneous ignition occurs. There are also uncertainties regarding the RCS initial conditions (e.g., pressure and temperature). The justification for choosing a single RCS pressure and temperature is acceptable since sensitivity analyses at full system pressure have also been performed. It appears, however, that much larger uncertainties are associated with the autoignition temperature and entrainment of the preexisting hydrogen into the hydrogen flame.

RESPONSE O2: *We believe that sudden volumetric combustion (autoignition) of preexisting hydrogen is essentially impossible during DCH events. See Response F33. The entrainment of preexisting hydrogen is treated differently in the CLCH and TCE models. The 10% entrainment assumed in CLCH is based on modeling of entrainment into the plume. The TCE model bounds the process by assuming that entrainment is sufficient to burn all hydrogen in the plumes and any preexisting hydrogen carried into the plume with the oxygen necessary to achieve complete combustion. These approaches compliment each other.*

The probability distribution for the initial melt mass and composition is given by Equation (2.3) in NUREG/CR-6075 [1]. This equation assumed that these events are mutually exclusive (i.e., the final probability distribution is simply the product of the individual input probability distributions). However, as discussed in Section 3 of the report, the amount of steel, Zr, and ZrO_2 in most cases is weighted by the amount of UO_2. Therefore, Equation (2.3) needs to be modified (see, for example, Equations (3.4) through (3.8) in section 3 of NUREG/CR-6075 [1].

RESPONSE O3: *See Response H4.*

On page 7, line 4 in NUREG/CR-6075 [1], the expression ($m_{m,i}$, $_{Zr,j}$, $\omega_{ss,k}$, $R_{r,l}$) should be replaced by ($m_{UO2,i}$, $x_{Zr,j}$, $m_{ss,k}$, $R_{r,l}$) to be consistent with the definitions given in Equations (2.1) through (2.4).

RESPONSE O4: *Typo will be corrected.*

In Figure 2.2 on page 10 [1], the cumulative probability distribution for the containment fragility (CR2) is given by two curves (at 5% and 95%), however, it is not discussed how the uncertainties in the containment fragility curve will be integrated into the final containment failure frequency.

RESPONSE O5: *As noted in footnote 2 in Section 2, only a single fragility curve is available; but the discussion has been generalized to accommodate desired improvements in information.*

1.2 Comments on the Quantification of Initial Conditions

The basic idea in quantifying the initial mass and composition of molten material in the lower plenum at vessel breach is based on two accident sequences that are believed by the authors to envelope the scenarios that may challenge the containment integrity due to DCH loads. These accident sequences are the Small Break Loss of Cooling Accident (SBLOCA), and station blackout sequences (TMLB'). The SBLOCA-like accidents are associated with wet core scenarios, and the TMLB'-like scenarios occur under dry core conditions. In addition, these two accident sequences are further "splintered" into two additional scenarios that are associated with early failure of a single penetration and early rupture for the case of SBLOCA-like accidents, and delayed failure of a single penetration and late rupture for the case of TMLB'-like accidents.

The initial conditions for each scenario are quantified as probability distributions as shown in Figures (3.3) through (3.9) [1]. The upper bounds for Scenarios I, II, and IV are compared to previous estimates of the SASM report [2] and NUREG-1150 which in some cases are different. For example, in Scenario I no CRM or steel is present in the melt, whereas Reference [2] reports upper bounds of 2.34 mt and 4 mt for the CRM and steel. It should also be mentioned that Reference [2] does not assign probability distributions to the initial conditions and the assignment of upper bound to the values in Reference [2] is purely based on the judgement of the authors of NUREG/CR-6075 [1].

RESPONSE O6: *The rationale for not including CRM and steel in the melt for Scenario I is discussed in Section 3.4.1; in summary, however, they are not molten at vessel failure. We will not interpret SASM melt compositions as upper bounds. This point will be clarified in the text.*

The assignment of the probability levels to the UO_2 mass appears rather optimistic. For example, in scenario I, the best estimate UO_2 mass (20 mt) is obtained from a single observation (i.e., TMI-II accident) with a high probability assigned to it. The upper bound value of 45 mt is assigned a likelihood of 0.01, and no probability is assigned to values greater than 45 mt. Therefore, the probability distribution constructed in Figure 3.3 of Reference [1] indicates a very narrow range of values for the UO_2 mass, and the probabilities assigned to 35 mt and 45 mt UO_2 mass are 1 to 2 orders of magnitude smaller than the best estimate. In addition, it is not clear why there is no zirconium or steel in the melt, even at the upper bound values as has been assumed in the SASM report [2] (see Table K.1 [1]). Scenario II is a continuation of Scenario I according to NUREG/CR-6075 and the same comments regarding the distribution of UO_2 mass also apply here.

RESPONSE O7: *The UO_2 mass is bounded based on the maximum volume of a credible crucible. The probabilities assigned to the various mass ranges are subjective as discussed in Responses B9 and C9; the important thing is to interpret results against the same subjective probability scale. Zr metal is retained as a metal blockage in the core. We anticipate that scenarios leading to significant melting of upper plenum steel will also lead to surge line or hot leg failure (see Response B13), and there is no time to melt lower plenum steel in Scenario I (penetration failure at time of relocation).*

Scenarios III and IV correspond to TMLB' scenarios with delayed penetration failure and rupture of the lower head under dry core conditions. In these scenarios, a gradual relocation of core material to the lower plenum is assumed. In scenario III, there is no UO_2, ZrO_2, or Zr in the melt and no probability distribution is assigned to these values. It is stated on page 12 of NUREG/CR-6075 that "The SCDAP/RELAP5 calculations are reviewed to provide insights for estimating the pressure at vessel breach. However, due to the parametric nature of the lower plenum modeling and the lack of complete modeling of lower head failure mechanisms, the calculations cannot be used directly to estimate the melt mass at vessel breach." It is not clear why the authors have not relied more on the results of the code calculations, even though the parametric nature of the code calculations can be used as a basis for constructing uncertainty distributions for the initial melt mass and composition. The same comments also apply to scenario IV.

RESPONSE O8: *We relied on existing calculations to the extent that we felt comfortable given their parametric nature. The available SCDAP/RELAP calculations were intentionally biased to accelerate lower head failure. We did not have the time, resources, or mandate from the NRC to perform parameter studies with SCDAP/RELAP in the manner suggested by the reviewer. The available SCDAP/RELAP calculations all predict crucible formation and failure; and as such, they provide insight into Scenarios I and II, but not Scenarios III and IV.*

1.3 Comments on the Quantification of DCH Phenomenon

The quantification of the DCH loads is based on the CLCH and TCE models which are discussed in Appendices D and F in Reference [1]. The key input parameter in quantifying the final containment pressure is the coherence ratio. The coherence ratio is defined as the ratio of the melt dispersal time scale to the primary system blowdown time scale. Two empirical correlations for the coherence ratio are given for the CLCH and TCE models, respectively (Equations 4.1 and 4.3 of Reference [1]).

RESPONSE O9: *No comment.*

On page 51, paragraph 2 in Reference [1], it is stated that "A second phenomenological uncertainty concerns the temperature at which sudden volumetric (autoignition) of all preexisting hydrogen occurs." Considering this uncertainty in the autoignition temperature, it is not clear why a probability distribution is not assigned to this uncertain phenomenon. In the models, the autoignition temperature has a constant value of 1100 K. The same constant autoignition temperature is applied to all four scenarios even though the mole fraction of the preexisting hydrogen in the containment is dependent on the scenario (e.g., in scenario 1, the mole fraction of preexisting hydrogen is expected to be lower than in other scenarios where additional hydrogen is produced due to Zr and steel oxidation). It is further stated that in the SNL/IET-11 experiment significant combustion of the preexisting hydrogen occurred. As far as the CLCH model is concerned, a complete combustion of the preexisting hydrogen is equivalent to a volumetric combustion (i.e., in both cases the entire energy release due to hydrogen combustion is transferred to the containment volume). In addition, a higher fraction of the entrained preexisting hydrogen into the flame (in the CLCH analysis, it is assumed that 10% of the preexisting hydrogen burns in the flame) may make the conditions just right for autoignition.

RESPONSE O10: *The TCE and CLCH models treat only those hydrogen combustion mechanisms that can contribute to peak pressures. See Response F33.*

1.4 Comments on the Results and Sensitivities

The final containment failure probability for all four scenarios is exactly zero. This means that the containment pressure load probability distribution never intersect the containment fragility curve, and the DCH-induced containment failure is absolutely impossible rather than "physically unreasonable" as stated in paragraph 2 on page 57 in Reference [1]. In addition to these base case calculations, a number of sensitivity analyses are also performed. These include a lower autoignition temperature of 950 K, a higher initial hole size of 0.7 m for scenarios II and IV, a higher percentage of debris transport to the dome (20%), and a calculation at full system pressure.

RESPONSE O11: *No comment.*

As far as the sensitivity to the autoignition is concerned, there is no discussion to the physical significance of this sensitivity calculation, i.e., how was this autoignition temperature determined? In addition, an examination of the base case DPDs for the containment temperature indicates that maximum temperature of <950 K is obtained in the worst case scenario (IV). It is clear that lowering the autoignition temperature to 950 K does not change the results. Therefore, a sensitivity calculation with an autoignition temperature of 950 K is absolutely irrelevant.

RESPONSE O12: *As the text states, sensitivity studies are arbitrary. If we could ascribe any credibility or physical meaning to the sensitivity values, then they would be part of the base quantifications. Multiple simultaneous sensitivities were performed where the dome temperature occasionally exceeded 950 K. More importantly, we believe that autoignition is essentially impossible in DCH events. See Response F33.*

The sensitivity study with the full system pressure (16 MPa) seems relevant only if it can be proven that at full system pressure, the initial distributions of melt mass and composition are the same as the intermediate pressure of 8 MPa. The choice for a sensitivity study of higher hole

size of 0.7 m is not made clear in the report. The same is true for the higher total debris transport to the dome.

On page 58, paragraph 1 in NUREG/CR-6075 [1], it is stated that "systematic sensitivity studies were also performed by *arbitrarily* varying the key inputs...as to produce higher loads." There is no objection to an arbitrary variation of these inputs, however, the level of importance of these sensitivities and the way they influence the containment pressurization and other derived key parameters in the model (e.g., the coherence ratio) must be made clear. This is more important than simply performing several sensitivity calculations without providing a physical basis.

RESPONSE O13: *Table 6.5 indicates that large hole sizes in conjunction with low autoignition temperatures has the most impact on containment loads.*

Figures 6.4, 6.8, 6.12, and 6.16 in NUREG/CR-6075 [1] indicates that both the CLCH and TCE model give similar probability distributions for the containment pressure (the maximum containment pressure is slightly higher in the CLCH model). The Containment Failure Probability (CFP) for all individual sensitivity calculation are also similar as shown in Tables 6.2 through 6.5 in NUREG/CR-6075 [1]. However, a simultaneous combination of these four sensitivities at 16 MPa indicates a significant difference between the CFPs predicted by the TCE and CLCH models (the CFP for the TCE model is $< 10^{-3}$ whereas the CFP for the CLCH model is $\sim 2 \times 10^{-2}$ which is at least an order of magnitude higher). It would be interesting for the reader if an explanation to the cause of this large difference is made in NUREG/CR-6075. On page 60 in NUREG/CR-6075 [1], the authors maintain that the containment failure probability by DCH for Zion is less than 10^{-3} which indicates a "physically unreasonable" phenomenon. They also suggest that the results of the sensitivity calculations do not alter this basic conclusion, even though a sensitivity calculation at full system pressure (with the simultaneous variation of all sensitivity variables) has indicated a containment failure probability of $\sim 2 \times 10^{-2}$ for the CLCH model.

RESPONSE O14: *The results of this report stand <u>solely</u> on the merits of the base quantifications. The reviewer should not confuse sensitivity results with <u>credible</u> containment failure probabilities. The difference in results (TCE vs. CLCH) for the 4-way sensitivity cited come primarily from the different hole size dependence in the coherence ratio correlations.*

1.3 Comments on the Extrapolations

The authors of NUREG/CR-6075 [1] state that encouraged by the very low CFPs for the Zion containment ("physically unreasonable" event), the Zion DCH loads can be extrapolated to other plants with large, dry containments. There are some concerns regarding the extrapolation:

(a) The idea of extrapolation to other plants seems reasonable only if the approach to issue resolution is found acceptable for Zion. This is not yet the case.

RESPONSE O15: *We agree. We understand that Zion must be resolved first. When this is accomplished, we believe that resolution for most other PWRs will follow quite easily, pending certain confirmatory information as listed in the report. Extrapolation issues are addressed more completely in NUREG-6109.*

(b) The DCH pressure loads that were obtained from the CLCH and TCE models are strongly dependent on the coherence ratio. These coherence ratios were empirically obtained from a limited number of experimental observations from the IET experiments for the Zion and Surry specific geometries. The same correlations may not be directly applicable to other geometries (see also section 3.7 of this report).

RESPONSE O16: *The IDCOR categorization of cavity designs indicates that Zion-like and Surry-like cavities are representative of most other PWRs, excluding CE and ICE condenser plants. This should be verified on a plant by plant basis, possibly through the IPEs. We note, however, that Zion and Surry are quite different designs. The CLCH model for coherence shows no apparent dependence on cavity design and the TCE model for coherence shows some dependence on cavity design, but the uncertainties are large (~28%). The correlation based on combined Zion/Surry data does almost as well as correlations based on Zion and Surry data individually. Any less dispersive geometries, if they exist, will lead to lower DCH loads.*

(c) The similarity of the containment fragility curves for other plants with large, dry containments to that of Zion is not yet established.

RESPONSE O17: *We agree. We have established the similarity of containment loads. We identified similarity of containment fragility as a confirmatory activity.*

The process of extrapolation to other plants based on the assumptions that the melt quantities, the containment volume, and the RCS volume for different plants are proportional to the reactor power is reasonable.

RESPONSE O18: *No comment.*

1.6 Comments on the Conclusions and Recommendations

It is stated on page 89 of NUREG/CR-6075 that "Even though we show that melt expulsion with maximum primary system pressures do not lead to any significant concerns for Zion, we cannot categorically exclude system pressures above 8 MPa at this time for all plants." This is not discussed in section 7 of NUREG/CR-6075.

RESPONSE O19: *We will first raise this issue in Section 7.*

If Zion DCH loads at full system pressure do not lead to containment failure (CFP = 0), why would the extrapolation to other plants be sensitive? If the extrapolation process is deemed justified, then the CFP for other plants at full system pressures can be carried out and the results can be compared to the fragility curves for the individual plants. The concern is therefore not the fact that system pressures above 8 MPa can be excluded for other plants, but if the DCH loads at full system pressure predict loads that are high enough to challenge containment integrity.

RESPONSE O20: *Our quantifications are not (and should not be) driven by anticipated margins of safety. We think it is important not to carry excessive conservatism through the assessments; after all, some plant with an uncharacteristically weak containment might be identified in the future.*

1.7 Comments on the Prediction of Direct Containment Heating

A summary of the CLCH model is given in Appendix D of NUREG/CR-6075 [1]. The derivation of the melt dispersal time scale is given on pages D-16 and D-17. The time scale for the blowdown is known from Equation (D.4). The empirical correlation for the coherence ratio is obtained from the melt dispersal time scale based on seven IET experiments (ANL/IET-7,

ANL/IET-8, SNL/IET-1, SNL/IET-6, SNL/IET-9, SNL/IET-10, SNL/IET-11). It should be mentioned that the first four experiments correspond to Zion geometry while the last three experiments correspond to Surry geometry. It is stated that in arriving at the correlation for the melt dispersal time, other experiments that produced "ambiguous" data were discarded. It is not mentioned in what way these data were ambiguous for the determination of melt dispersal time.

RESPONSE O21: *See Responses C20 and C22.*

The comments concerning the empirical correlation given by Equation (D.16) and comparison to the experimental data shown in Figure D.11 are the following:

(a) The empirical correlation is based on only a limited number of experiments.

(b) The left hand side term in Equation (D.16) is a dimensional quantity. It is not clear why an empirical correlation for the melt dispersal time scale is obtained rather than for the DCH-scale (or coherence ratio).

(c) It appears that the melt dispersal time sale correlation shows better agreement with the experiments for the Zion tests (see Figure D.11 in NUREG/CR-6075 [1]). For the Surry tests, the predicted melt dispersal time scale does not significantly change as the experimental values become higher, especially for the extended data range. The range of application of the correlation given by Equation (D.16) is not quantified.

RESPONSE O22: *The database covers a broad range of conditions including 3 different scales ranging from 1:40th to 1:6th scale, 2 different cavity geometries, hole sizes ~.35 - .6m (full scale equivalent), and driving pressures ~4 - 13 MPa. Equation D.16 is dimensionally correct. The dispersal time (Fig. D.11) and coherence ration (Fig. D.12) are <u>both</u> correlated. The coherence ratio correlation, like any other correlation, should only be applied in the range of its data. The applicable ranges will be cited in the text.*

The CLCH model equations are given in Table D.1 [1]. The ratio T/τ_s in Equation (D.1) should be replaced by t/τ_s. In Equation (D.7), the term dT_c/dt should be replaced by dT_s/dt.

RESPONSE O23: *Typos will be corrected.*

Appendix D [1] should also tabulate the CLCH predicted containment pressures and the experimental data.

RESPONSE O24: *We disagree. The information is adequately represented in the figures.*

2. POINT ESTIMATE SENSITIVITY CALCULATIONS

A number of point estimate sensitivity calculations were performed to estimate the containment pressurization and failure frequency with the CLCH model using the ALPHA code.

RESPONSE O25: *These sensitivity studies will be of interest to some reviewers. We would like to emphasize the arbitrary and conservative nature of these studies, which were performed to determine where containment failure might be expected.*

2.1 Sensitivity to Melt Mass and Composition

The mass and composition of the melt at the time of vessel breach affect the DCH loads. A comparison of the containment pressure and failure frequency are made for two cases that include variation of the UO_2 and steel melt mass and fraction of Zr oxidation keeping other parameters constant (the amount of Zr, ZrO_2 and steel in the melt is calculated according to Equations (3.1) and (3.4) through (3.8) in NUREG/CR-6075 [1]):

Case (a): Best estimate UO_2 melt mass and Zr oxidation for each scenario from NUREG/CR-6075 [1].

Case (b): 98.2 mt of UO_2 melt mass (entire core) and 100% Zr oxidation for each scenario.

The results of the calculations for the two cases are shown in Table 1. The uncertainties in the coherence ratio are not considered in these calculations (12.5% standard deviation in the coherence ratio is assumed in the report). For the best estimate case in Scenario I, this variation of the coherence ratio results in less than 1% change in the final containment pressure.

The values in Table 1 indicate that using the CLCH model, the maximum pressure variation occurs for Scenario II (42%) if the entire UO_2 core inventory is discharged and the entire Zr is

oxidized. For the first three scenarios, the containment failure probability is zero, i.e., it is not needed to consider probability distributions for the mass of UO_2 and fraction of Zr oxidation (keeping other parameters constant). For Scenario IV, the containment failure probability is still very low (10^{-3}). The containment failure probability in these cases were calculated by comparing the DCH loads with the Zion fragility curve. The final containment pressures indicate that using probability distributions for the fragility curve is not expected to considerably change these results. The conclusion from these sensitivity calculations is that according to the CLCH model, the melt mass and composition are not expected to greatly affect the final results of the distributions (i.e., containment failure probability).

RESPONSE O26: *The insensitivity to melt mass (oxidic melts) is well known. What limits DCH in these extremes is the amount of blowdown gas available to absorb energy from the melt. See Response H32.*

Table A.2. Comparison of the containment pressure and failure frequency as a function of melt mass and composition for different scenarios

	Scenario I		Scenario II		Scenario III		Scenario IV	
Case	(a)	(b)	(a)	(b)	(a)	(b)	(a)	(b)
UO_2 (mt)	19.0	98.2	15.0	98.2	0.0	98.2	0.0	98.2
% Zr oxidation	40	100	40	100	50	100	60	100
ZrO_2 (mt)	2.1	27.0	1.7	27.0	0.0	27.0	0.0	27.0
Zr (mt)	0.0	0.0	1.2	0.0	0.0	0.0	0.0	0.0
Steel (mt)	0.0	0.0	2.2	7.6	15.0	25.0[a]	15.0	25.0[a]
p_c[b] (bars)	3.4	4.7	4.3	6.1	4.3	5.7	5.2	7.0
$[(p_c)_b-(p_c)_a]/(p_c)_a$	+38%		+42%		+33%		+35%	
F_f[b]	0	0	0	0	0	0	0	10^{-3}

(a) The mass of steel in scenarios III and IV correspond to the upper bound values.
(b) P_c, T_c, and F_f are the containment pressure, temperature, and failure frequency, respectively.

2.2 Sensitivity to Hydrogen Combustion

The results of the previous section indicated that the variation of the melt mass and composition (using 100% Zr oxidation and entire UO_2 inventory in the melt) do not significantly challenge the Zion containment integrity. The energy release from the combustion of hydrogen, on the other hand, is expected to greatly influence the final containment pressure. As mentioned in NUREG/CR-6075 (see page 51, paragraph 2), in the SNL/IET-11 experiment a significant combustion of preexisting hydrogen occurred. The results of the calculations in NUREG/CR-6075 are presumed to include combustion of 10% of the preexisting hydrogen (for the CLCH model).

A number of sensitivity calculations are performed assuming combustion of 10%, 30%, 60%, and 99% of the preexisting hydrogen. Entrainment of 100% of the preexisting hydrogen into the combustion flame is theoretically equivalent to a spontaneous ignition of the preexisting hydrogen in the containment as far as the energy release is concerned. In addition, a higher percentage of hydrogen entrainment and combustion may lead to a condition (containment temperature) where the spontaneous ignition of the remaining preexisting hydrogen could possibly occur.

For these sensitivity calculations, two cases are considered:

Case (a): Best estimate UO_2 melt mass and Zr oxidation for each scenario from NUREG/CR-6075.

Case (b): Upper bound of UO_2 melt mass and Zr oxidation for each scenario from NUREG/CR-6075.

Table 2 shows the mass and composition of the melt at the time of vessel breach. The results of the sensitivity calculations for these cases are shown in Tables 3 and 4.

Table A.3. Comparison of the best estimate and upper bound melt mass and composition for different scenarios

	Scenario I		Scenario II		Scenario III		Scenario IV	
Case	(a)	(b)	(a)	(b)	(a)	(b)	(a)	(b)
UO_2 (mt)	19.0	45.0	15.0	40.0	0.0	0.0	0.0	20.0
% Zr oxidation	40	65	40	65	50	75	60	80
ZrO_2 (mt)	2.1	8.1	1.7	7.2	0.0	0.0	0.0	4.4
Zr (mt)	0.0	0.0	1.2	0.7	0.0	0.0	0.0	0.8
Steel (mt)	0.0	0.0	2.2	3.9	15.0	25.0	15.0	25.0

The results in Table 3 indicate that even a 99% hydrogen burn in the containment does not lead to containment failure for scenarios I through III, however, a 1% containment failure frequency is predicted for scenario IV.

Table A.4. Sensitivity to fraction of preexisting hydrogen burnt for the best estimate melt composition (case a)

	Fraction of Preexisting Hydrogen Burnt					
	10%			30%		
	P_c(bars)	T_c(K)	F_f	P_c(bars)	T_c(K)	F_f
Scenario I	3.4	479	0	3.7	531	0
Scenario II	4.3	621	0	4.7	673	0
Scenario III	4.3	624	0	4.7	689	0
Scenario IV	5.2	744	0	5.7	823	0

Table A.4. (continued)

	Fraction of Preexisting Hydrogen Burnt					
	60%			99%		
	P_c(bars)	T_c(K)	F_f	P_c(bars)	T_c(K)	F_f
Scenario I	4.2	609	0	5.0	710	0
Scenario II	5.2	751	0	5.9	851	0
Scenario III	5.5	787	0	6.3	915	0
Scenario IV	6.5	941	0	7.6	1094	0.01

The results for the upper bound melt mass and composition show that a 60% hydrogen burn in the containment may lead to 50% cumulative failure probability for scenario IV. The results for 99% hydrogen combustion for scenario IV are similar to the 60% case, since a 60% hydrogen burn heats the containment atmosphere (1455 K) to a point where a volumetric combustion of preexisting hydrogen occurs. Therefore, a containment failure under these conditions cannot be ruled out for scenario IV. Notice that in these sensitivity calculations, no probability distributions to the melt mass and composition have been assigned.

Table A.5. Sensitivity to fraction of preexisting hydrogen burnt for the upper bound melt composition (case b)

	Fraction of Preexisting Hydrogen Burnt					
	10%			30%		
	P_c(bars)	T_c(K)	F_f	P_c(bars)	T_c(K)	F_f
Scenario I	3.8	548	0	4.4	632	0
Scenario II	4.8	690	0	5.4	775	0
Scenario III	4.7	679	0	5.4	778	0
Scenario IV	6.2	893	0	6.9	999	0

Table A.5. (Continued)

	Fraction of Preexisting Hydrogen Burnt					
	60%			99%		
	P_c(bars)	T_c(K)	F_f	P_c(bars)	T_c(K)	F_f
Scenario I	5.3	759	0	6.5	924	0
Scenario II	6.3	902	0	7.4	1066	0.008
Scenario III	6.4	926	0	8.4	1218	0.04
Scenario IV	10.1	1455	0.48	10.1	1455	0.48

RESPONSE O27: *In the extremes of melt mass and composition, containment threatening pressures can be achieved. This illustrates the importance in resolving hydrogen combustion issues.*

A comparison of the predicted pressure loads with sensitivities to the hydrogen combustion and initial melt mass and composition has indicated that the results are more sensitive to the hydrogen combustion uncertainties and the effects of the initial melt mass and composition are of secondary importance. However, it should be noted that the initial conditions (i.e., fraction of Zr oxidized and the quantity of the metallic components in the melt) also determine the amount of the preexisting hydrogen in the containment which is directly related to the energy release in the hydrogen combustion process. It is therefore suggested, that the fraction of hydrogen burned and hydrogen autoignition temperature in the containment be integrated as probability distributions in the DCH models.

RESPONSE O28: *We disagree. See Response F33 for an expanded discussion of our perceptions of hydrogen combustion in DCH events.*

3. PROBABILISTIC SENSITIVITY CALCULATIONS

The probabilistic sensitivity calculations presented in this section include:

(a) Determination of the uncertainty distributions in the containment pressure, temperature, and failure frequency with the CLCH model using a stratified Monte Carlo (i.e., the Latin Hypercube Sample (LHS) technique, and

(b) Sensitivity to H_2 combustion using uncertainty distributions for the fraction of preexisting hydrogen combustion and the autoignition temperature. The CLCH model was used in these calculations.

3.1 Results of the Monte Carlo Simulation Technique

The LHS technique in conjunction with the CLCH model was used to predict the uncertainty distributions in the containment pressure and temperature and the containment failure frequency. The initial conditions corresponding to Scenario I were used for this calculation. The melt mass and composition were derived from the initial probability distributions shown in Figures 3.3 and 3.4 [1]) using the 'user distribution' option in the LHS input file, and a normal distribution was used for the coherence ratio. The number of LHS samples was 40 in this calculation. Figures 1 and 2 show comparisons of the probability distributions for the containment pressure and temperature. Figures 3 and 4 show the comparison of the cumulative probability distributions for the coherence ratio and the final hole size. The results of the LHS technique show good agreement with the distributions calculated using the method in NUREG/CR-6075. Therefore, these results have independently confirmed the results presented in NUREG/CR-6075.

RESPONSE O29: *This is a third, but welcome, confirmation of our results. SNL Monte Carlo results and Reviewer H have also verified our results.*

3.2 Probabilistic Sensitivity to Hydrogen Combustion

The point estimate calculations presented in Section 2 of this review report indicated that the containment pressure and temperature show rather strong sensitivities to the uncertainties associated with the combustion of hydrogen. These include the combustion of preexisting hydrogen entrained into the jet and the volumetric combustion of the preexisting hydrogen when the containment reaches the autoignition temperature. The sensitivities to the fraction of the preexisting hydrogen combustion and the autoignition temperature were taken into account by constructing probabilities to ranges for the fraction of preexisting hydrogen combustion (between 0.0 and 0.50 with a mean at 0.25), and the autoignition temperature (between 600 K and 1100 K with a mean of 850 K). These probabilities are used only to demonstrate the sensitivity to these variables. In these calculations, the probabilistic approach of NUREG/CR-6075 has been adopted, however, Equation (2.4) in NUREG/CR-6075 was modified to reflect

the inclusion of these probabilities. The modified version of Equation (2.4) for these calculations becomes:

$$P_{ijklpq}(m_{UO2,i}, x_{Zrj}, m_{ss,k}, R_{r,l}, f_{H2,p}, T_{H2,q}) = P_{ijk}(m_{UO2,i}, x_{Zrj}, m_{ss,k})\ P_l(R_{r,l})\ P_p(f_{H2,p})\ P_q(T_{H2,q})$$

where the additional terms f_{H2} and T_{H2} are the fraction of preexisting hydrogen that burns and the autoignition temperature. Figures 5 and 6 show the probability distribution for each of these variables.

These sensitivity calculations have been performed for Scenario I. Figures 7 and 8 show the results of these sensitivity calculations. In these calculations, the probabilistic approach in NUREG/CR-6075 with Equation (1) has been employed. The results indicate that for Scenario I, the containment failure probability is zero even though the containment pressure and temperature are higher than those obtained in NUREG/CR-6075 (i.e., the containment pressure cumulative probability does not intersect the Zion fragility curve). This observation for Scenario I is not surprising since the point estimate calculations in Section 2 of this report also did not predict a containment failure for Scenario I even if all the preexisting hydrogen is assumed to burn. The coherence ratio and the hole size distributions ar obviously not sensitive to these two additional input parameters (f_{H2} and T_{H2}) as shown in Figures 9 and 10. The most severe case occurred for Scenario IV (see Section 2 of this review report), therefore, it appears that sensitivity calculations for this scenario should also be performed in NUREG/CR-6075.

RESPONSE O30: *We already know from your earlier sensitivity studies that hydrogen combustion phenomena for Scenario IV are important, so additional sensitivity studies shed no new light on the issue.*

4. REFERENCES

1. M.M. Pilch, H. Yan, and T.G. Theofanous, "The Probability of Containment Failure by Direct Containment Heating in Zion," NUREG/CR-6075, June 1993.

2. Technical Program Group, "An Integrated Structure and Scaling Methodology for Severe Accident Technical Issue Resolution," Draft Report for Comment, NUREG/CR-5809, 1991.

Figure 1 Comparison of the calculated containment pressure cumulative probability. ——— : NUREG/CR-6075, ◇: LHS, - - - -: Zion Fragility.

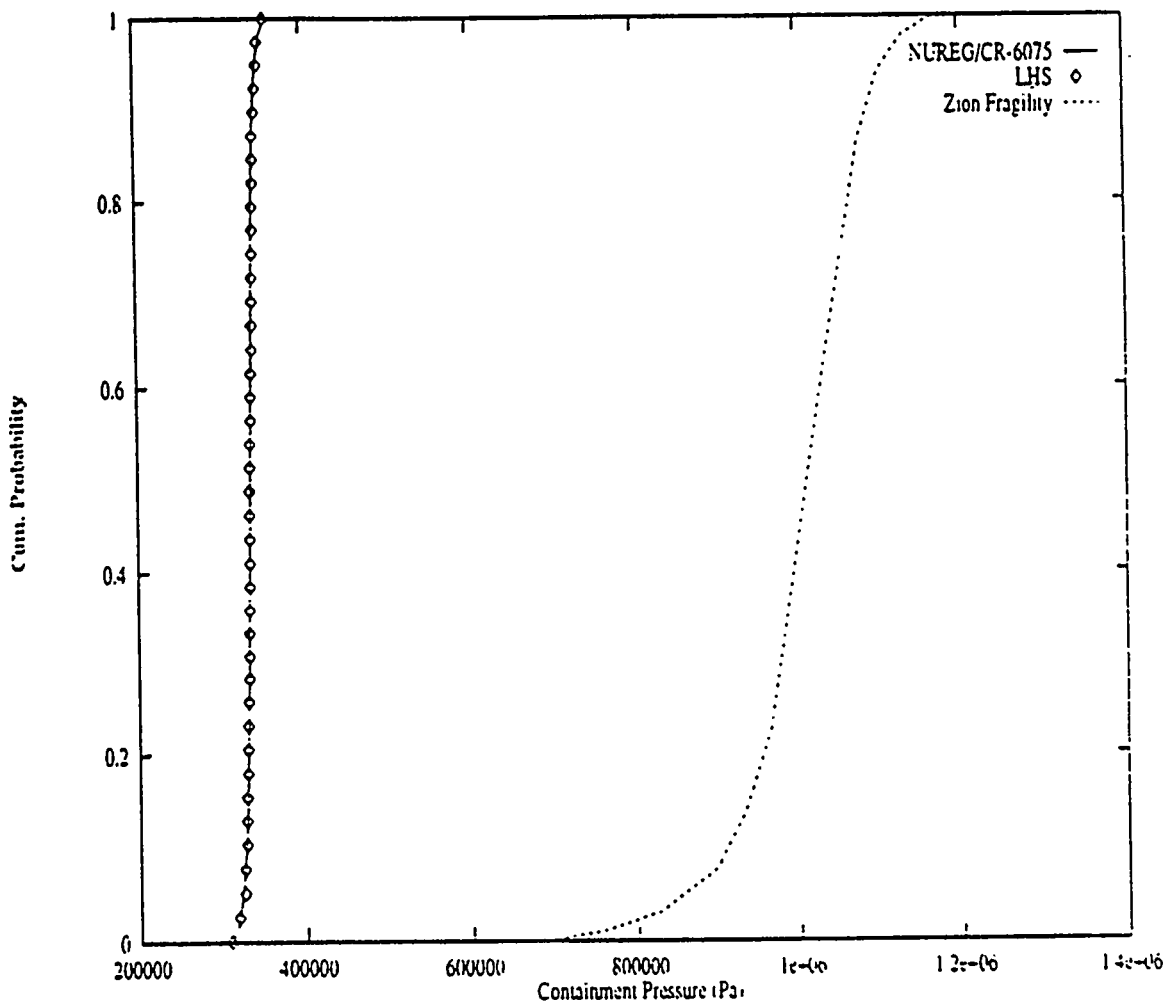

Figure 2 Comparison of the calculated containment temperature cumulative probability. ——— : NUREG/CR-6075. ◇: LHS.

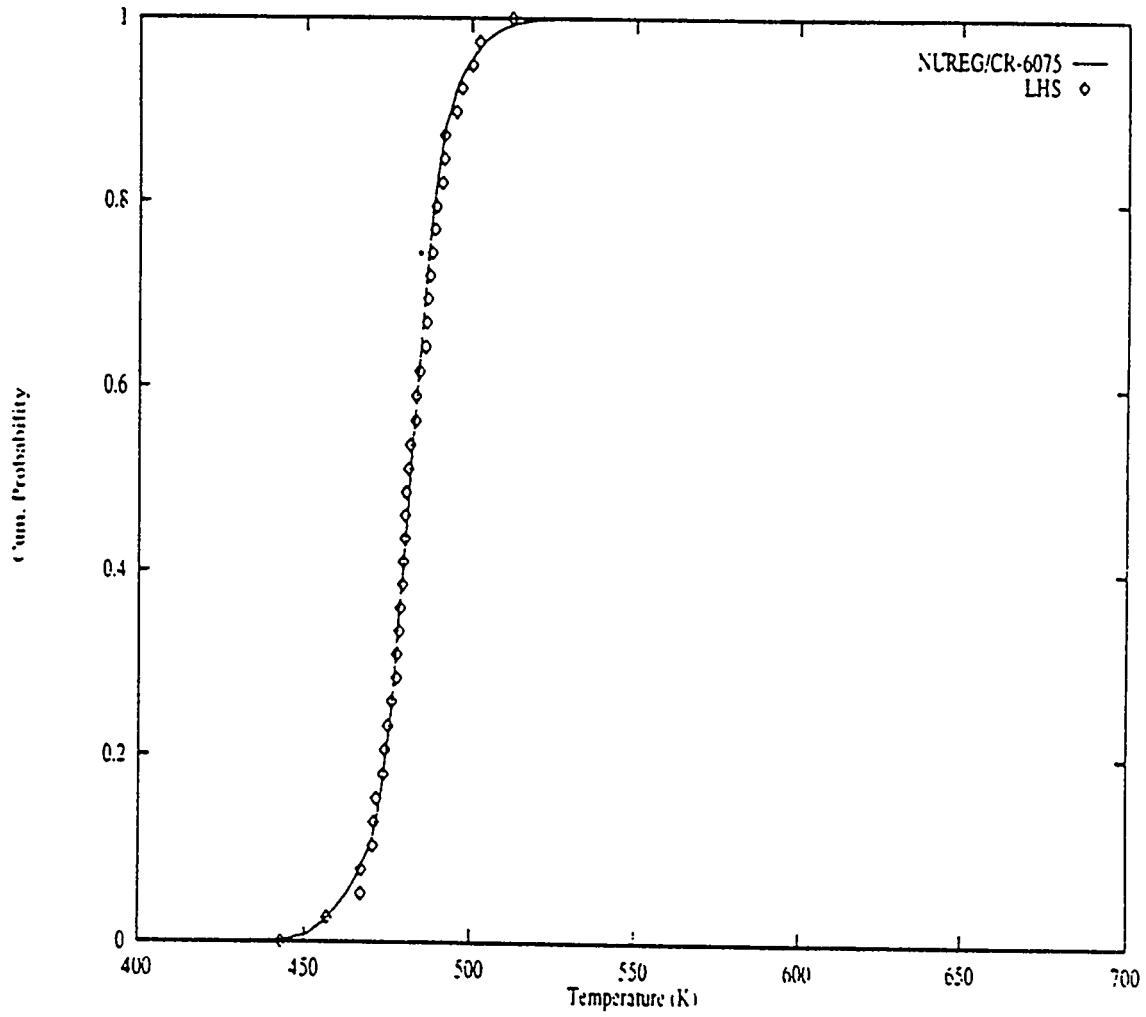

Figure 3 Comparison of the calculated coherence ratio cumulative probability, ——— : NUREG/CR-6075, ◇ : LHS.

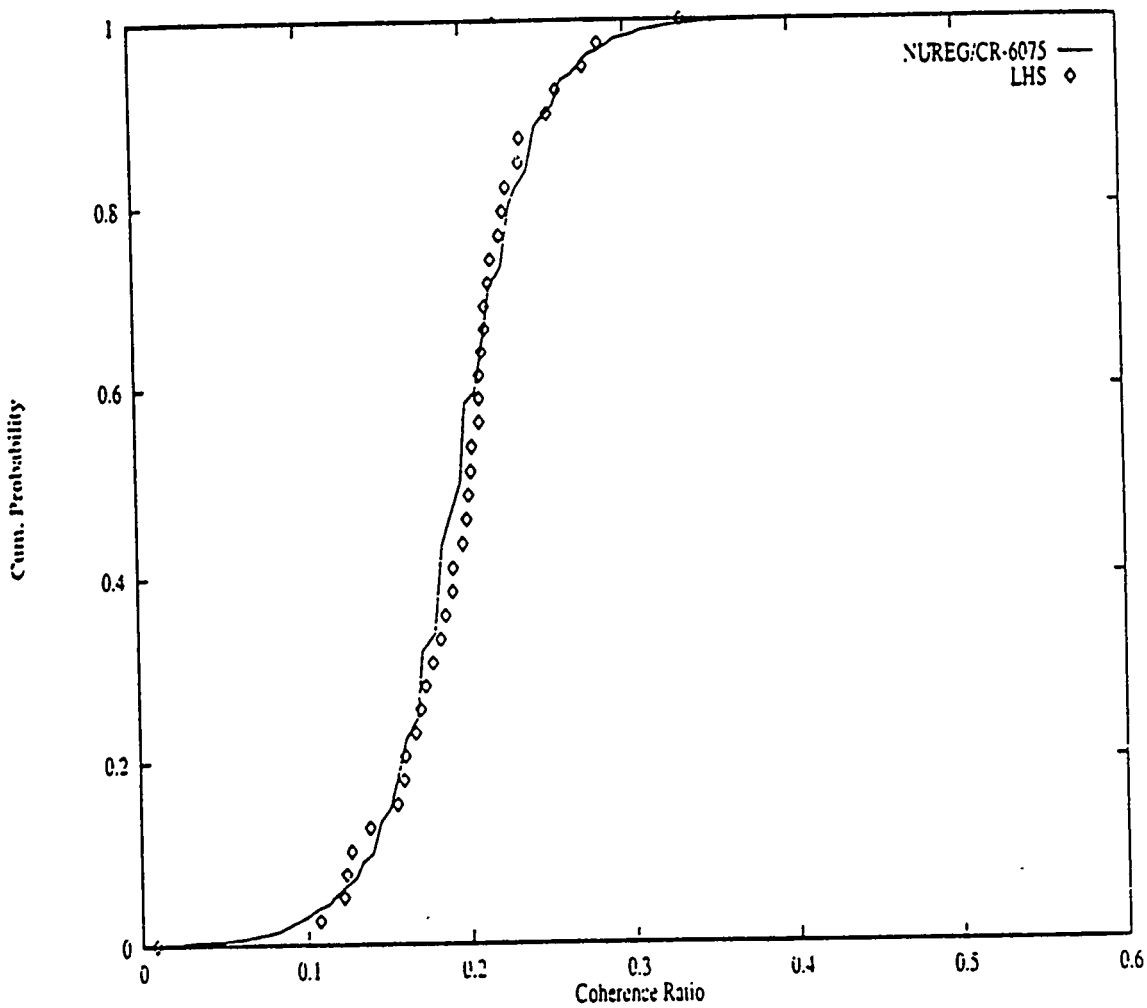

Figure 4 Comparison of the calculated final hole size cumulative probability, ——— : NUREG/CR-6075, ◇: LHS.

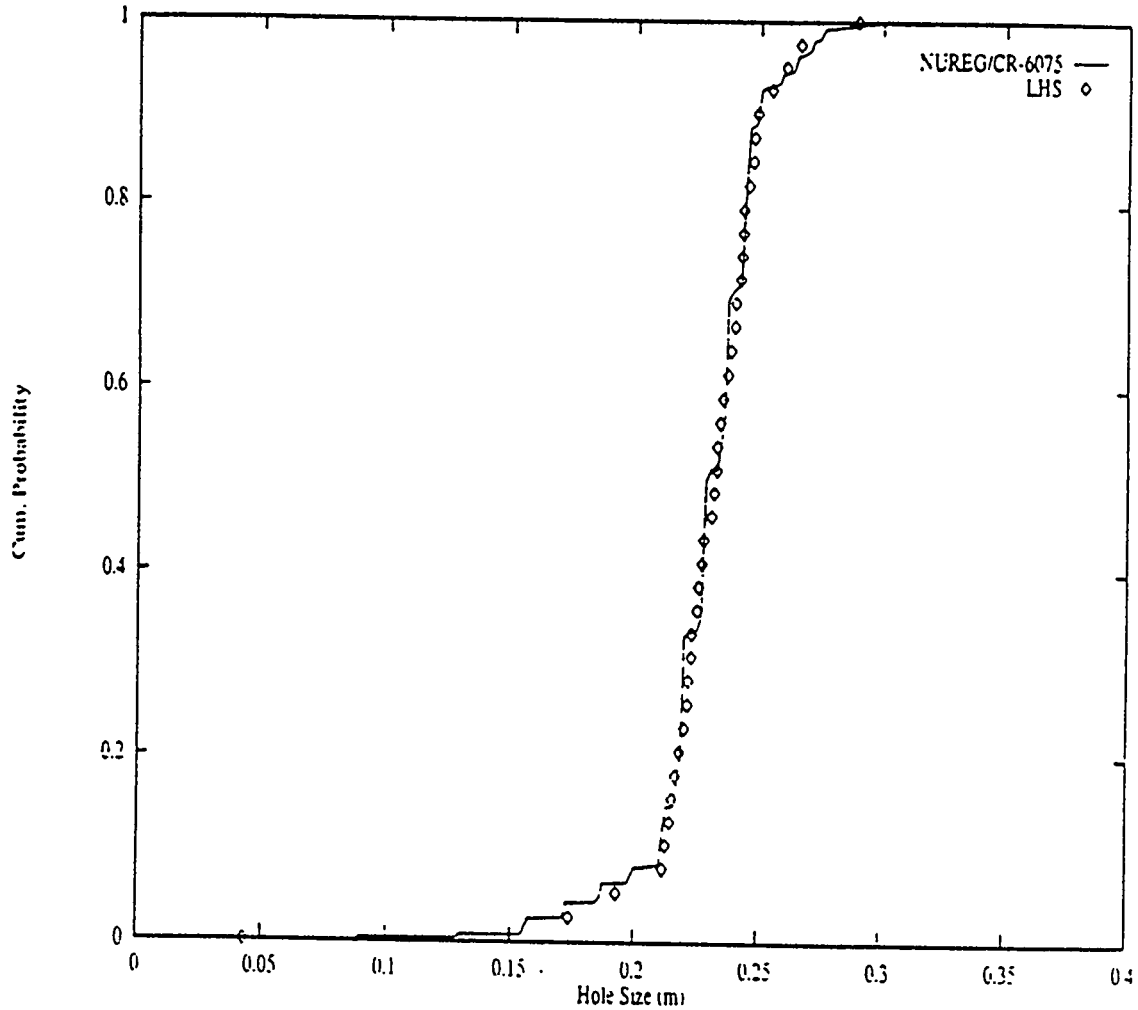

Figure 5 Distribution of the fraction of preexisting hydrogen combustion (f_{H2}).

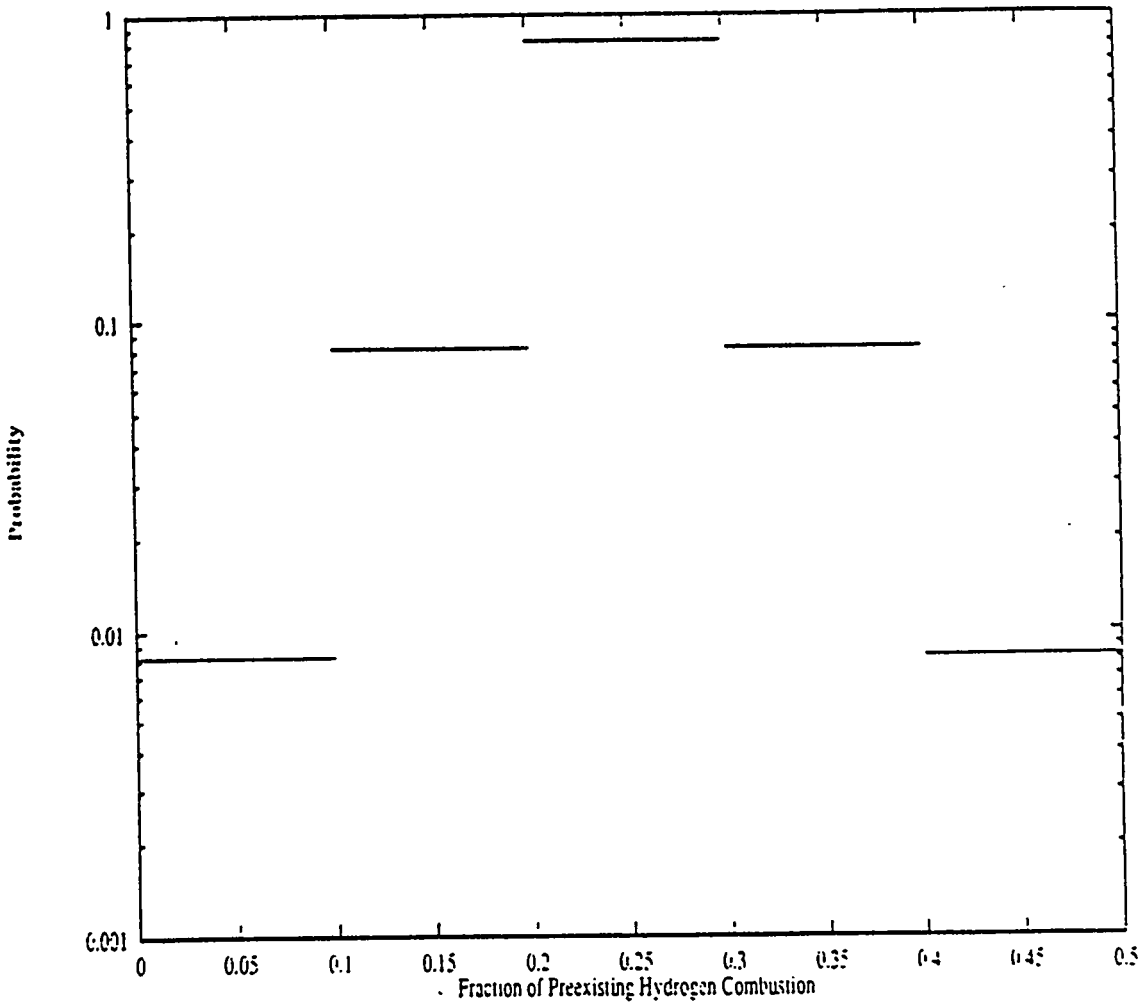

Figure 6 Distribution of the autoignition temperature (T_{H2}).

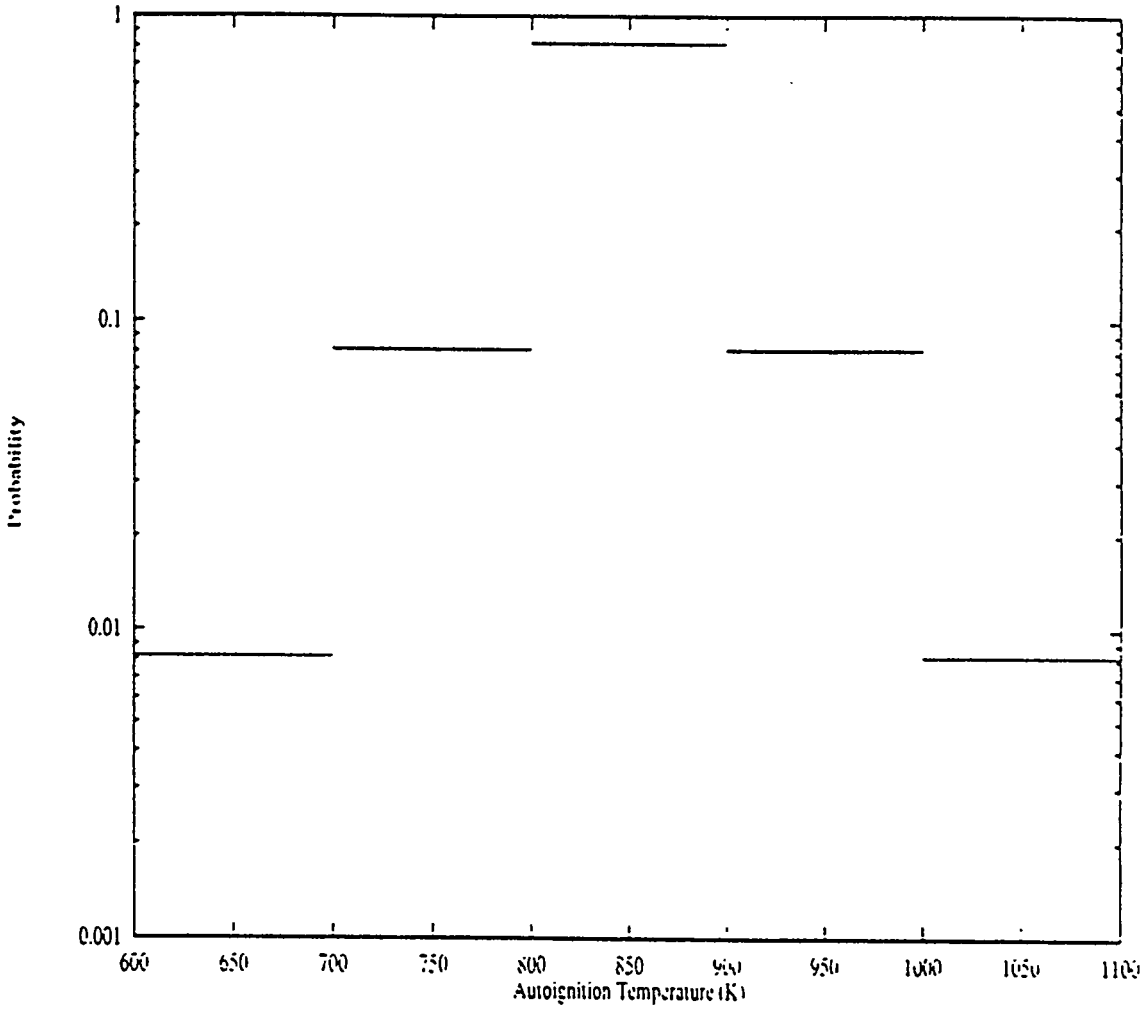

Figure 7 Comparison of the calculated containment pressure cumulative probability (SC-1), ——— : NUREG/CR-6075, — — — —: Sensitivity to f_{H2} and T_{H2}, - - - -: Zion Fragility.

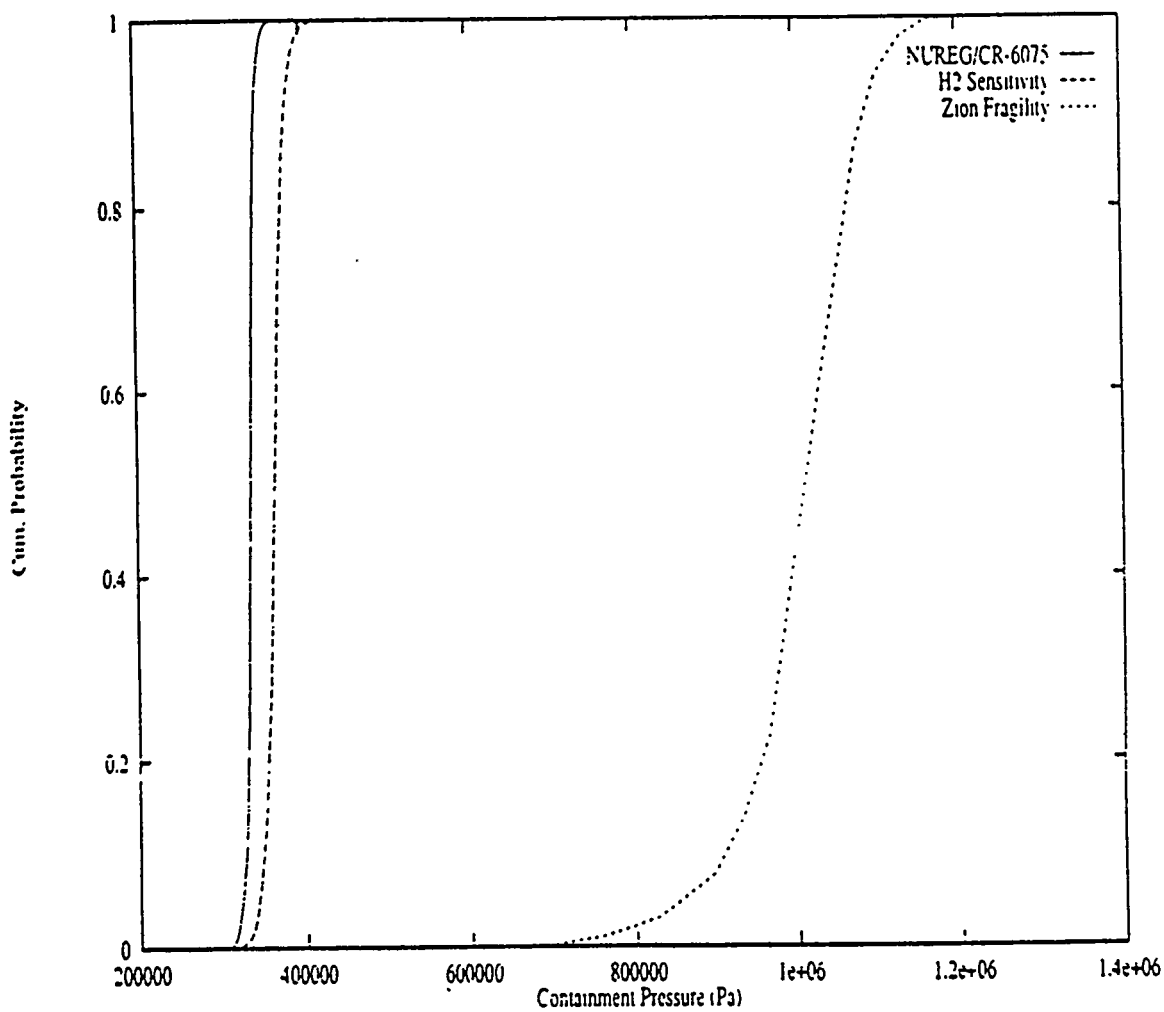

Figure 8 Comparison of the calculated containment temperature cumulative probability (SC-I). ——— : NUREG/CR-6075, — — — —: Sensitivity to f_{H2} and T_{H2}.

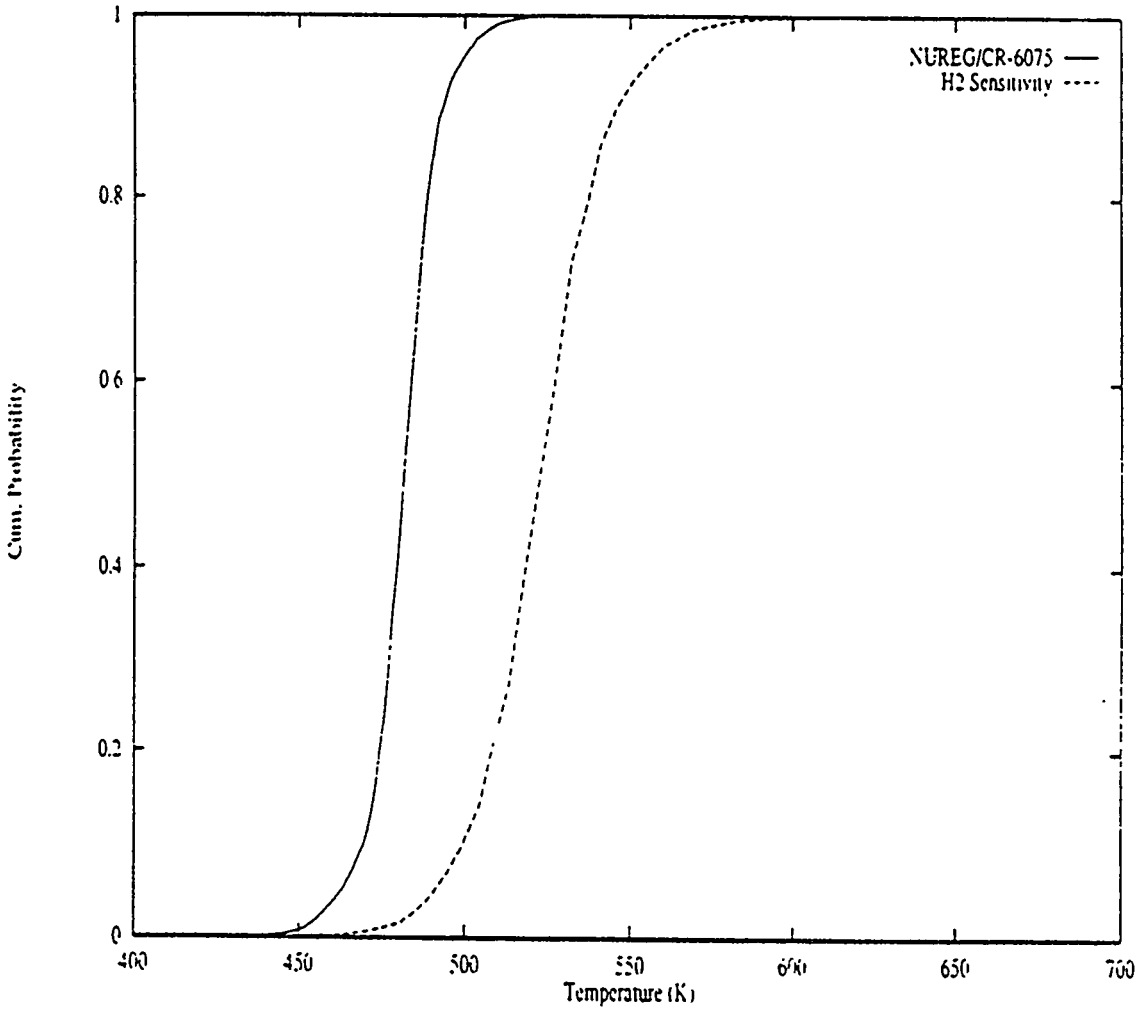

Figure 9 Comparison of the calculated coherence ratio cumulative probability (SC-I), ——— : NUREG/CR-6075; — — — —: Sensitivity to f_{H2} and T_{H2}.

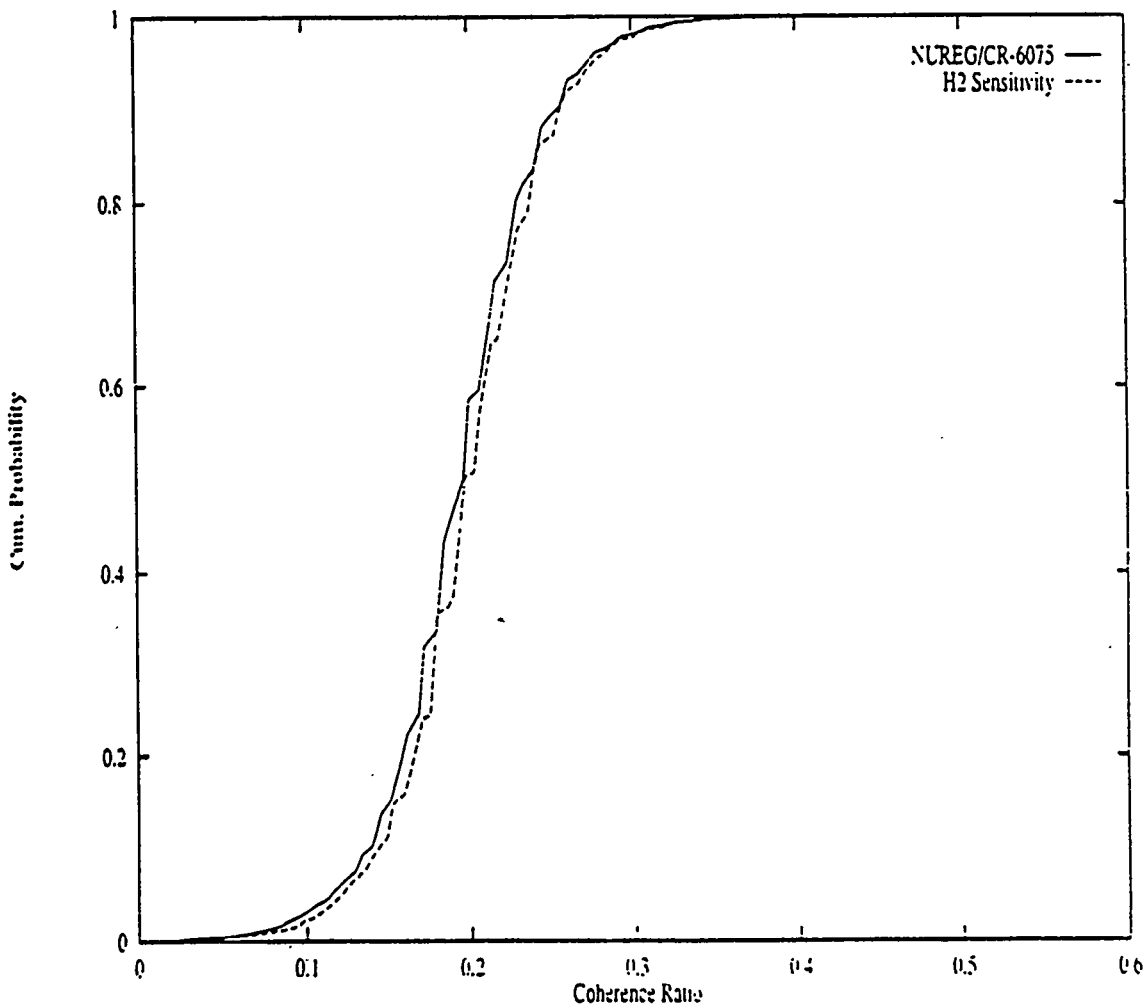

Figure 10 Comparison of the calculated final hole size cumulative probability (SC-I). ——— : NUREG/CR-6075. — — — —: Sensitivity to f_{H2} and T_{H2}.

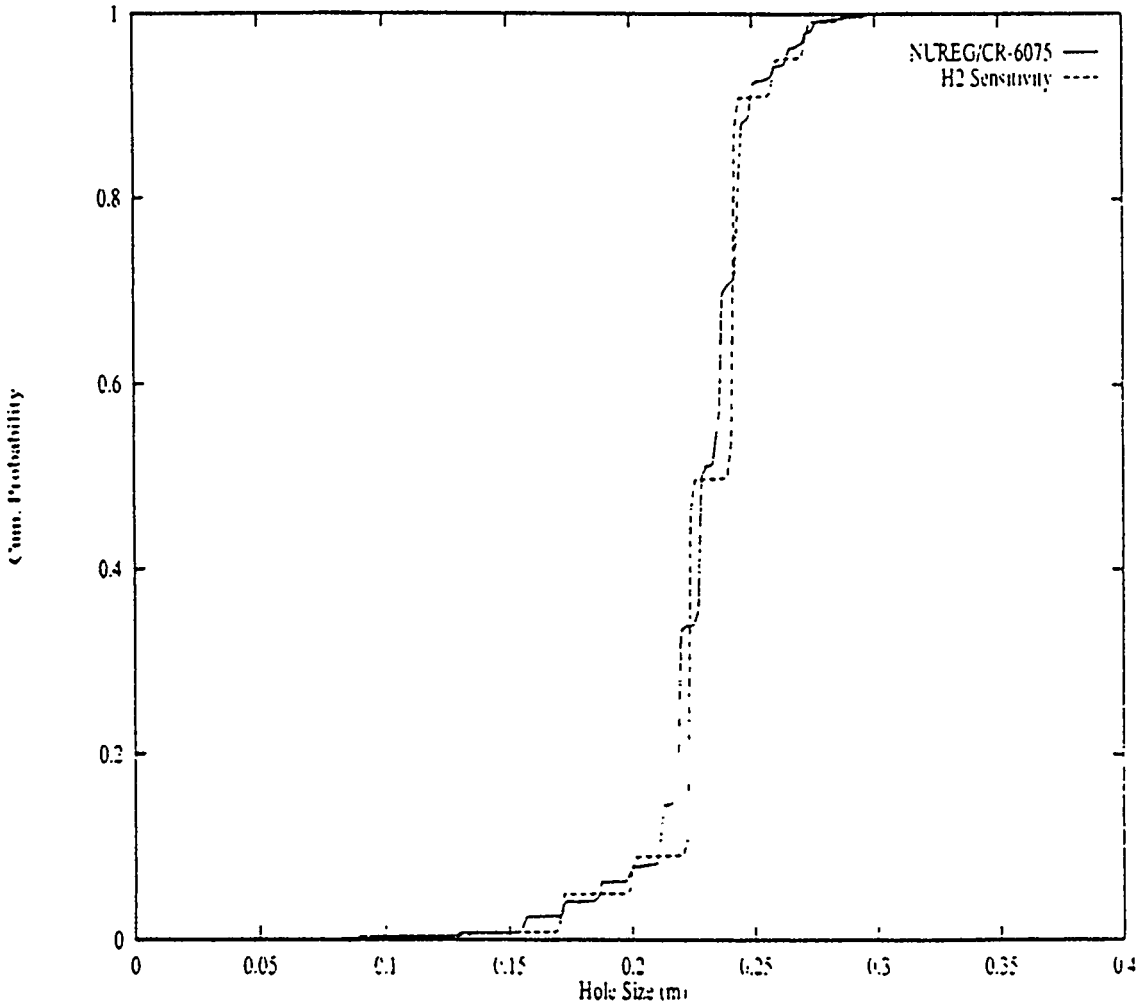

REBUTTAL FROM REVIEWER O

Comments on Response O1

This should be stated in the final report.

Comments on Response O2

The two models use different approaches for the treatment of the preexisting hydrogen combustion and I do not understand what the authors mean by the statement that these approaches "compliment" each other. The authors should explain that in the CLCH model, the 10% criteria is used for all predictions (if this is indeed the case) including Zion and the IETs, since this is an important model parameter in the CLCH model.

The information provided in response F.33 should be expanded to provide the basis for the numerical values (e.g., turbulent combustion velocities as a function of hydrogen concentration, the combustion efficiency, and the Froude number) in the final report. I suggest that the authors also include a discussion of what the conditions in the IET-11 test (Surry geometry) were that prevented autoignition, even though very high temperatures were observed in the dome (e.g., provide a similar argument regarding the steam and hydrogen mole fractions). This was the only test that demonstrated the severity of the DCH and hydrogen combustion (the initial hydrogen concentration were 2.4% and 2% in the IET-9 and IET-10 tests and these values are below the flammability limits). There should be more discussion in the report to close the gap between the analysis in Appendix F (pages F-1 through F-7) that arrives at the autoignition temperature of 790 K for Zion (albeit this is called the benign threshold in NUREG/CR-6075) and the conclusion that the autoignition temperature <u>might</u> be in the 1000-1100 K range.

Considering that the SENKIN results indicated that at the containment temperatures of 850-900 K, the reaction times are much lower than the DCH time scale (15 s) and the uncertainties associated with the autoignition temperature and the experimental evidence from only a single test (IET-11) where the average dome temperature was above 900 K, an uncertainty distribution regarding combustion of the preexisting hydrogen should be included in the analysis. Note also

that the mitigating effect of stratification was not observed in some of Zion SNL/IET experiments (e.g., IET-6 as noted by the SNL peer review of NUREG/CR-6075).

Comments on Response O5

I know that the authors have used a single fragility curve, however, they do not discuss the nature of the distribution between the 5% and 95% limit lines.

Comments on Response O7

I already know from my sample sensitivity calculations (Table 1), that even if the entire core would be assumed molten at the time of vessel breach, the maximum containment pressure is still below the containment capacity for scenarios I and II. Therefore, I am satisfied with the results for scenarios I and II and would not recommend any additional base case calculations with more conservative initial distributions of the melt mass and composition.

In fact, the authors of the NUREG/CR-6075 could have avoided a lot of controversy regarding their quantification of initial melt mass and composition by simply indicating that the final pressure would not be high enough to challenge the containment integrity even if the entire core were assumed to participate in DCH. Since the authors had decided to present an elaborate discussion of their quantifications, I wanted to make the point that the initial conditions may be considered rather optimistic (even though I do not think that the final results would be significantly altered according to my point estimate sensitivity calculations).

Comments on Response O10

See my comments on response O2.

Comments on Response O12

I know that the authors' sensitivity studies are arbitrary, however, the point I was trying to make here was that since the temperature in all four scenarios never reached 950 K, clearly the authors must have known that this sensitivity would not change the results. In their response, they state that "Multiple simultaneous sensitivities were performed where the dome temperature

occasionally exceeded 950 K" which means that autoignition occurred. The authors should provide a discussion of the conditions under which autoignition occurred in the final report.

Comments on Response O13

I can see from Table 6.5 that the large hole size in conjunction with low autoignition temperature has a higher impact on the CFP. Incidentally, this is true only for the CLCH model, while the TCE model does not show any sensitivity. Still, there is no discussion why this is the case. The final report should include an expanded discussion of the results.

Comments on Response O14

I did not confuse the sensitivity results with the base quantification. However, my point was that the simultaneous combination of the sensitivities (at 16 MPa) for scenario IV indeed change the CFP (based on the CLCH model), i.e., 2×10^{-2} for multiple variations vs. $<< 10^{-3}$ for the base quantification.

Comments on Response O20

I think this case can be verified on a case by case basis. We can get an idea how sensitive the results are to the primary system pressure if the authors would also provide the Zion results for full system pressure in a manner shown in Table 7.2.

Comments on Response O21

I agree that it is difficult to define the entrainment interval by noting the pressure history for IET-7. If the dispersal for this case was very poor, I expect that the model would predict higher pressures for this case since the coherence ratio was based on tests that met the criteria of dispersal greater than 70%. However, an examination of Figures D.8a and D.8b in NUREG/CR-6075 indicates that the model is actually underpredicting the data even though a more "conservative" coherence ratio was employed.

Comments on Response O24

The information in Figures D.8a and D.8b is not adequately represented. It is difficult to interpret the results since the same line types are used for some of the tests. If the authors are resistant to tabulate the results, then they should present the results in these figures in a more intelligible way.

Comments on Response O27

See my comments on response O2.

Comments on Response O28

See my comments on response O2.

Comments on Response O30

See my comments on response O2.

Comments by Reviewer P
Brian W. Sheron

I attended the presentation of Marty Pilch's paper at the Water Reactor Safety Information Meeting last Monday. I think he did a good job of summarizing the DCH work on Zion as documented in NUREG/CR-6075. At the end of his paper, I had raised my hand to ask a few questions, however, the press of time prevented no more than the one or two questions from the audience. Therefore, I will give you my questions. I understand that they may be duplicative of some of the peer reviewer comments. I would appreciate if you would see that these questions get addressed as part of the ongoing peer review.

My first question has to do with the treatment of the initial pressure. It would appear that by assuming that all scenarios start at 8 MPa, this is equivalent to assigning a probability of 1 to the initial pressure. This seems inconsistent however, with the results presented in Table 3.8 of NUREG/CR-6109, which show finite probabilities for an initial primary pressure range of 6.89-16 MPa. Moreover, in other areas of the report, such as initial melt mass, the authors select a mean range and then select distribution tails of 0.1 and 0.01. The distribution tails on initial pressure would appear to be of the same magnitude as the distribution tails on other parameters. Hence, I see no justification for treating initial pressure any different from other parameters that have uncertainties. While I realize that the authors address the issue through sensitivity studies, one could argue that they could deal with all uncertainties through sensitivity studies rather than probabilistically. I think the authors need to deal with all parameters that have uncertainties in a consistent fashion.

RESPONSE P1: *The authors of NUREG/CR-6109 do show finite probabilities for RCS pressures greater than 6.89 MPa, but we do not know what is intended as the upper limit. Our intent was to bound RCS pressures at 8 MPa and not to imply that 8 MPa RCS pressures occur with probability unity. However, we recognize the concerns expressed by some reviewers and some members of the NRC with regard to RCS pressure. If, at the end of the peer review process, this issue is not satisfactorily resolved, we will change the report accordingly. It may be necessary to treat RCS pressure as a distribution if consensus on a reasonable upper bound cannot be reached. Alternatively, RCS pressure could be treated as an additional splinter. The best course of action should be decided if consensus on an upper bound cannot be reached.*

My second question deals with the uncertainty distributions chosen. While I understand the authors' basis for selecting a mean and its range, I found no basis for the assumed values of the tails of the distribution. All I can figure is that for most of the distributions, the authors arbitrarily assumed tails that had two discrete values on either side of the mean, namely 0.1 and 0.01. Similarly, the range for each of these values was arbitrarily selected to be roughly equal to the range of the mean for that particular distribution. Without any justification, these distributions would seem to be only the opinion of the authors, and I do not believe these distributions can be considered a "base case" as they currently are. In other words, these distribution functions are a considerable source of uncertainty themselves, and therefore need to be treated like any other parameter that has a large uncertainty in the ROAAM process.

While I realize the authors could argue that the peer review process will pass judgement on the acceptability of the presumed distributions, this does nothing more than reduce ROAAM to the expert elicitation process of NUREG 1150. Also, running sensitivity studies to show insensitivity to the results does not justify retaining the author's arbitrary distributions as the "base case." The objective of the ROAAM process should not be to put arbitrary distribution functions in front of peer reviewers, but to truly identify sources of uncertainty and deal with them in the process up front, such as by treating them as a splinter. Without doing this, the assumed distribution functions become nothing more than an expert elicitation of one.

RESPONSE P2: *Large sources of uncertainty are treated as splinters. Other less severe sources of uncertainty can be treated as distributions. We rely on the phenomenology to identify the mean and bounds of the distribution. With only this information we could construct a maximum entropy distribution. In most cases, however, the processes leading to the bounds are judged very unlikely based on the physics (e.g., bottom failure of a crucible); consequently, they are assigned a probability of 10^{-2}. We then attempt to fill in the distribution. The text will clarify why we think the bounds of the distribution are judged very unlikely. See Response B9 for further discussion of the number scale.*

Comments by Reviewer Q

Farouk Eltawila

I would like to bring to your attention an issue that should be addressed by SNL as part of its response to the peer reviewers comments with respect to the DCH issue resolution as described in NUREG/CR-6075, "The Probability of Containment Failure by Direct Containment Heating in Zion," The issue is that during a TMLB' accident, the reactor cavity in the Zion plant has the potential for being completely flooded with water. This is due to a unique feature of the Zion plant in which a dedicated containment spray system will be operative even in the event of a TMLB' accident. Therefore, the resolution of the DCH issue for the Zion plant in NUREG/CR-6075 needs to address this issue of a flooded reactor cavity during a high pressure melt ejection.

RESPONSE Q1: *Water in the Zion cavity can range from condensate levels to fully flooded (plus 4' in the basement). Such deeply flooded situations would submerge the RPV, which may prevent its failure (although this is an area of ongoing research). The SNL/IET-8B experiment indicated that melt ejection into a half full cavity would fully quench the melt reducing the DCH event to a nonthreatening steam spike. We expect that more deeply flooded situations would exhibit similar quenching behavior. Structural damage to the Zion cavity resulting from potential steam explosions is not a problem since the Zion cavity is set in bedrock.*

MEMORANDUM
ENERGY RESEARCH, INC.

TO: R. Henry, FAI
M. Ishii, Purdue
S. Levy, S. Levy, Inc.
M. Modarres, UMCP
F. Moody, GE
J. Shepherd, Cal Tech
F. Eltawila, NRC
R. Lee, NRC
C. Tinkler, NRC
M. Pilch, SNL
C. Allison, INEL

FROM: H. Esmaili H.E.

SUBJECT: Zion DCH Issue Resolution

DATE: June 9, 1994

This memorandum is intended to summarize the proceedings of the Zion DCH issue resolution (NUREG/CR-6075) meeting that was held in Albuquerque, NM on May 16-17, 1994. The purpose of the meeting was to resolve the outstanding peer reviewers' concerns. To this end, two working groups were formed to focus on two aspects of the issue, namely, the specification of the initial and boundary conditions (Working Group 1; May 16, 1994), and the modelling of the DCH phenomena (Working Group 2; May 17, 1994).

The working group 1 peer review members included S. Levy, R. Henry, and M. Modarres, while the working group 2 members included S. Levy, R. Henry, F. Moody, J. Shepherd, and M. Ishii. NRC was represented by F. Eltawila, C. Tinkler, and R. Lee. The other participants included M. Pilch, M. Allen, J. Kelly, and N. Ortiz of SNL; and D. Knudson and C. Allison from INEL. In addition, during the two day meeting, other experts from SNL also provided supplementary information towards the resolution of the issues.

Initial and Boundary Conditions (Working Group 1)

The discussion of the first day meeting was focused on the specification of the initial and boundary conditions for the Zion DCH study (Draft NUREG/CR-6075). The members of the peer review group expressed their concerns regarding the consistency in the initial conditions for Zion. The insights from the SCDAP/RELAP5 calculations for Zion are to be used to arrive at a more defensible initial conditions. The members of the peer review group, INEL, NRC,

and SNL finally reached an agreement on how the scenarios and the initial and boundary conditions should be specified. The conclusions are listed below:

(1) The consistency in the initial conditions requires that at high primary system pressures, the amount of melt mass in the lower plenum must be relatively low (and the vessel breach size is expected to be small). On the other hand, for low system pressures, the melt mass in the lower plenum is expected to be higher and the breach size should be larger.

(2) For high pressure scenarios[1] (i.e., full system pressure), the primary system must contain a large amount of water as a result of operator intervention. The modeling of this case requires ejection of water from the primary system (together with debris and steam). The effect of water in the primary system at vessel breach is expected to mitigate the impact of DCH. Even though this consideration would not be required for the Zion application (the document should acknowledge this effect), it may become necessary for other applications. The effect of the pre-existing water in the cavity at the time vessel breach would be to mitigate the DCH loads (this provides a heat sink for the debris).

(3) The dry core scenarios are expected to contain a large amount of metallic debris, however, the primary system pressures associated with these scenarios are expected to be relatively low. INEL will provide the expected range of the primary system pressures and the melt mass.

(4) SCDAP/RELAP5 calculations should be performed with more realistic modelling parameters (e.g., a lower heat transfer coefficient between the melt and the lower head) to provide estimates of the lower plenum melt mass and composition at vessel breach. The specification of the initial melt conditions in the lower plenum for Zion application should take advantage of the SCDAP/RELAP5 results.

(5) For the upper bound quantification of the initial conditions (e.g., the melt mass at vessel breach), a probability scale of 0.01 seems reasonable.

Based on the conclusions reached, 6 scenarios were considered for the Zion evaluation as listed in Table 1. For the Wet Core Scenarios, the results of the rupture calculations are expected to bound the expected pressure loads during a postulated DCH event. Therefore, only scenarios II and IIA need to be considered in the evaluation process, however, scenarios I and IA should be acknowledged in the revised document. For scenarios IIB and III, INEL will perform SCDAP/RELAP5 calculations to provide the primary system pressures and melt masses at vessel breach.

---

[1] Dry high pressure sequences will most likely depressurize due to hot leg or surge line rupture.

DCH Modeling Approach (Working Group 2)

On the second day of the meeting (May 17, 1994), the discussion centered around the DCH modeling effort. Two models have been used in NUREG/CR-6075 to predict the DCH loads, namely, the Two-Cell Equilibrium (TCE) and the Convection Limited Containment Heating (CLCH) models. The most important modeling parameter for both models were the specification of the coherence ratio (i.e., coherence between steam and debris during the interaction period). In the revised version of NUREG/CR-6075, the members of the peer review group reached consensus regarding the use of the TCE model for the quantification of the containment loads. The issues that were considered included:

(1) Coherence Ratio

(2) Range of Applicability of the Model (TCE)

(3) Hydrogen Combustion

(4) Containment Fragility

(5) Extrapolation to Other PWRs

Coherence Ratio

Different cavity designs may have a bearing on the empirically determined coherence ratio correlation for the TCE model (e.g., the constant parameter in the correlation ranges from 4.045 for the Zion geometry to 5.9 for the Surry geometry). The characterization of the length scale as the cube root of the cavity volume may be a possible cause. The conclusions and the actions that would be taken to resolve the coherence ratio issue in the TCE model are outlined as follows:

(1) Different length scales (e.g., the chute length) should be explored to show the sensitivity to this parameter. This examination would be addressed as part of the extrapolation process and is not a requirement for the closure of the Zion DCH study (NUREG/CR-6075).

(2) The revised document should be expanded to include a discussion of the experimental conditions used in the determination of the coherence ratio (e.g., some of the experiments were performed with a larger initial hole size diameter of ~ 1 m, while others included over-scaled masses of debris discharged to the cavity).

(3) PWRs with Zion or Surry cavity geometries should use the corresponding empirical coherence ratios for extrapolation purposes. Cavity geometries that show similarities to either Zion or Surry should use the respective coherence ratios, however, the

uncertainties in the coherence ratio must include a broader range (within the standard deviations measured experimentally).

Range of Model Applicability

The concern involved the TCE model applicability for sequences with high primary system pressures and very large hole sizes. The analysis by Ishii indicated that under these conditions, a higher fraction of the debris will be transported to the upper compartments and there would be a large coherence even in the subcompartments. This was also observed to be the major scaling issue.

However, the initial conditions proposed during the first day of the meeting suggested that scenarios with high primary system pressure involve smaller hole diameters. The action at this point would be to use the TCE model. Ishii will perform the separate effect tests focused on the assumption of the negligible coherence between the steam and debris in the subcompartment at high primary system pressure (up to 15 MPa) and large hole sizes (up to 0.5 m). Based on these test results and simple dispersion model, the limit of the applicability of the TCE model will be established. For the Zion application, this issue was resolved.

Hydrogen Combustion

The peer reviewers were also concerned with the extent of hydrogen combustion (including the DCH produced hydrogen and pre-existing hydrogen) that can burn as a flame. There were also some uncertainties regarding the auto-ignition temperature. The discussion regarding the sudden volumetric combustion of pre-existing hydrogen satisfied the peer reviewers and they agreed that this mode of combustion may not be feasible on the DCH time scale. The conclusions reached with respect to the extent and mode of hydrogen combustion were as follows:

(1) The recommendation of the peer reviewers was to rely on the existing IET database and other available information on hydrogen combustion to determine the magnitude of pre-existing hydrogen combustion. The DCH produced hydrogen would burn as a diffusion flame. The complex flow dynamics as far as the formation and development of the flame is concerned, require further consideration. J. Shepherd will provide M. Pilch with additional information regarding the entrainment of pre-existing hydrogen that could possibly burn as the diffusion flame enters the upper compartment.

(2) The CONTAIN code would be used to strengthen the arguments and hypotheses regarding the rate of heat transfer to structures during the DCH event. These rates would be compared to the energy release rates occurring during hydrogen combustion to determine their effects on the peak pressures..

(3) The specification of the initial containment conditions such as pressure and gas composition for scenarios IIB and III would require utilization of system codes (e.g., CONTAIN and SCDAP/RELAP5) to provide consistency.

(4) CONTAIN and SCDAP/RELAP5 results would also be used to assess the possible combustion of hydrogen as it vents from the RCS at high temperatures and ignite the pre-existing hydrogen, even though this scenario would no longer be a DCH problem.

Containment Fragility

The issue involved the accuracy of the lower bound tail of the containment fragility curve that was used to calculate the conditional failure probability. The issue was resolved for the Zion application. It was recommended to use the current IPE fragility curve, however, exact values from the fragility distribution should be used to avoid any errors that may occur as a result of "eyeball" extrapolations used in the draft NUREG/CR-6075 (R. Henry would provide the necessary information to M. Pilch). In addition, for IPE's with failure pressures below design pressure, the corresponding values should be truncated. This issue would be further clarified by the NRC.

Extrapolation to Other PWRs

The issue of extrapolation to other PWRs would be approached based on geometrical considerations, differences in the core power and Zr content, and a figure-of-merit for screening purposes which is based on a quantitative value of the containment conditional failure probability currently set to 0.1. Specifically, the following recommendations will be used to resolve this issue:

(1) The insights, data, and correlations from the separate effects tests in the Purdue experiments would be used in the CONTAIN code to assess the critical discharge flow of two-phase gas/liquid from the primary system and the entrainment of debris. CONTAIN would also be used to assess the energy release as a result of debris interaction with the atmosphere and the associated heat sinks provided by the dispersed water, and the dominant mode of heat transfer to the structures.

(2) The geometrical considerations require evaluation and identification of potential paths (or those that could be formed) to the upper containment and dome region. These conditions could occur as a result of high local pressures in the cavity during debris discharge from the pressure vessel. The recommended action would be to estimate the structural loadings on the cavity boundaries through asymmetric load evaluations which will be examined by NRC.

(3) The extrapolation to other PWRs should take into account the variations in the core thermal power and Zr content. The development of natural circulation and the possibility of hot leg/surge line failure would also be considered as it provides an effective means of primary system depressurization before vessel breach.

(4) The specification of the figure-of-merit (or conditional containment failure probability) would be further examined by NRC (currently a figure-of-merit of 0.1 is used in the

evaluation of PWRs that may be susceptible to DCH loads). NRC will re-examine the sequences that may lead to core damage at high pressure. Based on the specification of the initial conditions proposed during the meeting on May 16, 1994, it may be worthwhile to take credit for scenarios that progress to low pressure (e.g., Sc-III).

cc: M. Khatib-Rahbar, ERI

Table 1 Listing of the Initial Conditions for Different Scenarios

Crucible Formation			Gradual Relocation
Penetration Failure	Rupture		Rupture
Wet Core		Dry Core	Dry Core
Sc-I Operator Action RCS Pressure (16 MPa) Flooded Vessel Oxidic Melt (TMI-II) ~ 20 mt UO_2 (best estimate) ~ 40 mt UO_2 (upper bound) Zr content 0/1/2 mt No Steel T_{debris} = 2800 K Early Failure (D = 0.025 m) f_{Zr} ~ 0.15/0.40/0.65 90% H_2 release to containment	**Sc-II** Operator Action RCS Pressure (16 MPa) Flooded Vessel Oxidic Melt (TMI-II) ~ 20 mt UO_2 (best estimate) ~ 40 mt UO_2 (upper bound) Zr content 1/1/2 mt No Steel T_{debris} = 2800 K Delayed Failure (D = 0.4 m) f_{Zr} ~ 0.15/0.40/0.65 90% H_2 release to containment	**Sc-IIB*** RCS Pressure (< 3-4 MPa) Oxidic/Metallic Melt ~ 60 mt UO_2 (upper bound) ~ 30 mt Steel (upper bound) ~ 1 mt Zr (upper bound) T_{debris} = 2800 K Failure Size (TBD) f_{Zr} ~ 0.15/0.40/0.65 100% H_2 release to containment Metal Blockage Remains in Place	**Sc-III*** RCS Pressure (< 2-3 MPa) Full Loop Circulation Oxidic/Metallic Melt ~ 60 mt UO_2 (upper bound) ~ 30 mt Steel (upper bound) ~ 10 mt Zr (upper bound) T_{debris} = 2800 K Failure Size (TBD) f_{Zr} ~ 0.3/0.6/0.8 100% H_2 release to containment Metal Blockage Relocates
Sc-IA RCS Pressure (~ 8 MPa) ~ 10 mt H_2O in vessel Oxidic Melt ~ 30 mt UO_2 (best estimate) ~ 50 mt UO_2 (upper bound) Zr content 0/1/2 mt No Steel T_{debris} = 2800 K Early Failure (D = 0.025 m) f_{Zr} ~ 0.15/0.40/0.65 90% H_2 release to containment	**Sc-IIA** RCS Pressure (~ 8 MPa) ~ 10 mt H_2O in vessel Oxidic Melt ~ 30 mt UO_2 (best estimate) ~ 50 mt UO_2 (upper bound) Zr content 1/1/2 mt Some Steel (TBD) T_{debris} = 2800 K Delayed Failure (D = 0.4 m) f_{Zr} ~ 0.15/0.40/0.65 90% H_2 release to containment		

* For scenarios IIB and III, SCDAP/RELAP5 calculations will be performed by INEL to provide the primary system pressure and the melt mass at vessel breach.

Sandia National Laboratories

P.O. Box 5800
Albuquerque, New Mexico 87185-1137

May 31, 1994

Dr. H. Esmaili
Energy Research, Inc.
P.O. Box 2034
Rockville, MD 20847

Dear Dr. Esmaili:

I have reviewed the minutes of the May 16, 17, 1994 meeting on DCH Issue Resolution. I would like to suggest two modifications.

Pp. 3, Coherence Ratio: Item 1 suggests exploration of different length scales. This should be addressed as an extrapolation issue and not as a requirement for closure of NUREG/CR-6075.

Pp. 4, Containment Fragility: It is recommended to use exact values from the fragility distribution. It needs to be clarified that I can do this only if someone (Henry) provides me with the values.

Feel free to call me at (505) 845-3047 if you have any questions.

Sincerely,

Martin M. Pilch
Severe Accident Phenomenology
Department 6422, MS1137

MMP:6422:mlg

Copy to:
MS1137 M. D. Allen (6422)
MS0742 J. E. Kelly (6414)

H. Esmaili
Energy Research, Inc.
P. O. Box 2034
Rockville, MD 20847

June 7, 1994

These are my comments on the proceedings of the Zion DCH issue resolution meeting of May 16-17, 1994, which you sent to me.

I was assigned to working group 2, which concentrated on the DCH modeling approach. Because of a schedule conflict, I could not attend the meeting. Therefore, I am sure that my comments are lacking continuity which comes from actual attendance and participation in resolution discussions. However, I appreciate being kept in the loop, and having the opportunity to comment on the conclusions proposed.

COHERENCE RATIO

The coherence ratio, namely the ratio of (melt dispersal time/system depressurization time), or (melt entrainment time/steam blowdown time), depending on whether the T. Theofanous or M. Pilch model is used, embraces a tremendous amount of bottom-up (fine structure) effects, even though it is a top-down (macroscopic) parameter. In my opinion, any two vessel -containment systems which have similar basic components will have DCH peak containment pressures which can be macroscopically correlated with the coherence ratio, and the initial containment atmosphere properties and melt composition.

It can be shown analytically that for a given quantity of thermal energy introduced to a region of gas, the resulting pressure increase does not depend on the distribution of that energy. Regarding the DCH phenomena, the released thermal energy can be confined to the cavity, or uniformly distributed between all containment regions, and the maximum pressure will be the same. However, the <u>amount</u> of thermal energy transferred does depend on flight paths, the surrounding gas state, and other heat and mass transfer effects.

The coherence ratio includes effects of the melt mass, vessel steam mass and initial pressure, hole size, and cavity geometry, especially the length. I think that the conclusions and actions outlined in the summary notes will perhaps slightly refine determination of the coherence ratio. However, the significant value of (1) studying the effect of length scales, (2) discussing experimental conditions used in

determining the coherence ratio, and (3) including a broader range of uncertainties in the coherence for extrapolation purposes, will be to reduce lingering questions and to provide a stronger case for issue resolution.

RANGE OF MODEL APPLICABILITY

In my opinion, high primary system pressures and very large hole sizes are reflected in the coherence ratio definition, unless different flow regimes are encountered, or additional flow paths to the containment are opened. Melt entrainment could become a melt plug discharge if the steam blowdown rate was high enough through a large hole. However, if a melt plug made a trajectory through other zones of the containment, heating of the containment atmosphere would not be efficient as for entrained droplets, and lower pressures could occur. Large hole sizes would be expected to create higher pressures in the cavity, but containment pressures due to steam would be the same.

Since the initial condition working group suggested that high pressure steam is consistent with smaller holes, the high pressure - large hole size may be academic. But even if it is not, I think that the DCH maximum pressure could be less for this case.

HYDROGEN COMBUSTION

The burning of pre-existing hydrogen is expected to be not feasible on the DCH time scale. The recommendations made for fully resolving this issue make use of the most recent pre-existing hydrogen combustion data (IET), and structural heat transfer and initial condition computational tools.

Without the burning of initial hydrogen, I think the peak DCH containment pressure is dominated by the coherence ratio, with effects of initial melt composition, which partly controls DCH produced hydrogen.

There was no mention of the mitigative effect of water on essentially all DCH scenarios, although it has been strongly suspected by a number of experts.

CONTAINMENT FRAGILITY

My understanding of containment fragility is limited, and I have no comments on this discussion.

EXTRAPOLATION TO OTHER PWRS

I think that the only thing that would preclude use of the TCE model extrapolations to other PWRs would be the introduction or exclusion of the basic phenomena employed. It may be repetitive, but when it comes to simple debris heating of the cavity, subcompartment, or containment atmosphere, with a given amount of thermal energy, the equilibrium pressure is not affected by how the heating is distributed. That may be one subtle reason that the coherence ratio is such an important parameter. It governs how much thermal energy can be transferred to the surrounding atmosphere during the time of its active dispersal.

Regarding the Purdue tests (1), it is my opinion that minimal new macroscopic (top down) information will come to light from the Purdue experiments, although microscopic (bottom up) understanding will be enhanced. More understanding on the debris energy transfer rate to the surroundings will likely correlate with the coherence ratio. The effect of water would be expected to be further clarified.

The geometrical considerations (2) will help to resolve questions about high cavity pressures and the effect on the dome region. If it is true that containment equilibrium pressure depends on the <u>amount</u> of energy transferred from the debris and not its <u>distribution</u>, high pressure in the cavity would not automatically yield higher dome pressure.

The core thermal power and Zr content (3) are expected to influence the amount of energy transferred from debris in a given time interval. Its effect should be included in extrapolations to other PWRs, as recommended.

I have no comment on (4) regarding the figure-of-merit.

Yours truly,

Frederick J. Moody

Frederick J. Moody
GE Nuclear Energy, MC-747
175 Curtner Avenue
San Jose, CA 95125
(408) 925-6434

June 7, 1994
Aeronautics, 105-50
Caltech
Pasadena, CA 91125

H. Esmaili
Energy Research, Inc.
PO Box 2034
Rockville, MD 20847-2034

FAX 301 881 0867

RE: Zion DCH Resolution

Dear Dr. Esmaili:

I have reviewed your memorandum of May 23 regarding the DCH resolution meeting in Albuquerque on May 16 and 17. In regard to hydrogen combustion, some clarifications about my position are in order.

Item 1

I do not recommend that we rely exclusively on the existing IET database to determine the extent of hydrogen combustion. These experiments are very complex and difficult to interpret, particularly the hydrogen combustion aspect. A very limited range of preexisting hydrogen has been examined and I am still concerned that the boundaries of the test conditions are too limited to draw very general conclusions. For these reasons, all available information on hydrogen combustion should be utilized in making the safety assessment. Unfortunately, a great deal of extrapolation is required in many cases and there is conflicting evidence (for example, concerning the autoignition temperature of lean mixtures) about many phenomena. I think that this means that there are still substantial uncertainties regarding hydrogen combustion phenomena in DCH. However, this does not necessarily translate into an appreciable uncertainty in risk.

A selection of references on transient plumes and jets is attached to this letter. The key result for the present problem is that the fluid within a "turbulent puff" is roughly equal parts ambient and source fluid. That is, the entrainment rate for transient jets or plumes is much lower than steady flows.

Sincerely,

Joseph E. Shepherd

Tel: 818 395 8663
Fax: 818 449 2677

References on Transient Jets and Plumes within Enclosures

1. The primary reference in this area is the book

J. S. Turner 1973 **Buoyancy Effects in Fluids,** Cambridge University Press.

A very brief discussion of "starting plumes" is given on pp. 186-192.

2. A recent study on mixing of a jet and the creation of a mean vortical within a confined volume is given in

R. E. Breidenthal, V. R. Bounadonna, and M. F. Weisbach 1990 "Molecular mixing via jets in confined volumes" J. Fluid Mechanics **219**, 531-544.

This study gives scaling laws for the amount of circulation created in the vessel and the mixing time for a two-dimensional situation.

3. The classical reference on plumes within an enclosed volume is

W. D. Baines and J. S. Turner 1969 "Turbulent buoyant convection from a source in a confined region" J. Fluid Mechanics **37**, 356-368.

4. I applied this model to the problem of jet and plume fires in the NTS tests and this is discussed in NUREG/CR-4534 (Analysis of Diffusion Flame Tests by J. E. Shepherd).

5. A simple model for entrainment (based on Turner's ideas) in fireballs in an unconfined region is given

J. A. Fay and D. H. Lewis, Jr. 1977 "Unsteady Burning of Unconfined Fuel Vapor Clouds," 16th Symposium (Intl.) on Combustion, 1397-1405.

PURDUE UNIVERSITY

SCHOOL OF NUCLEAR ENGINEERING

June 8, 1994

Dr. H. Esmaili
Energy Research, Inc.
P.O. Box 2034
Rockville, Maryland 20847

Dear Dr. Esmaili:

Re: Memorandum Summarizing the DCH Issue Resolution Meeting

I have one comment concerning the statement you have made in the second paragraph on page 4. The second line reads, "the action at this point would be to use the TCE model and Ishii will further confirm his analysis." I would like to change this sentence to the one given below to clarify the point which I made in the meeting.

The action at this point would be to use the TCE model. Ishii will perform the separate effect tests focused on the assumption of the negligible coherence between the steam and debris in the subcompartment at high primary system pressure (up to 15 MPa) and large hole sizes (up to 0.5m). Based on these test results and simple dispersion model, the limit of the applicability of the TCE model will be established.

Sincerely,

M. Ishii/bjm

M. Ishii
Professor of Nuclear Engineering

MI/bjm

1290 NUCLEAR ENGINEERING BUILDING • WEST LAFAYETTE, IN 47907-1290

Fauske & Associates, Inc.

October 10, 1994

Dr. Mohsen Khatib-Rahbar
Energy Research, Inc.
Post Office Box 2034
Rockville, Maryland 20847-2034

Dear Mohsen:

I have reviewed NUREG/CR-6075, entitled "The Probability of Containment Failure by Direct Containment Heating and Zion". I find that the authors have in general been responsive to my comments. I have several minor comments that are detailed in the attachment. None of these comments are of a serious nature, but I believe that by incorporating these, the authors can improve the fidelity of the final document.

Should you have any questions regarding any of the enclosed comments, please feel free to call any time.

Sincerely yours,

Bob

Robert E. Henry
Senior Vice President

REH:lab
Attachment

16W070 West 83rd Street • Burr Ridge, Illinois 60521 • (708) 323-8750
Telefax (708) 986-5181

Comments on NUREG/CR-6075

The authors have been responsive to the major points brought up by the Technical Review Group. In particular, the addition of SCDAP/RELAP5 and CONTAIN calculations provides added depth to the conclusions and a greater perspective on the influence of how hot leg creep rupture reduces (or eliminates) the sensitivities to other phenomena. The following is a list of comments that could add to the usefulness and fidelity of the document.

1. The title of this document is specific to the Zion nuclear station. While Zion was used to develop the experimental models, the intent of the analysis and the experiments are to address a class of reactors that are Zion-like. Specifically, it is my impression that the experimental scaling is not sufficiently detailed that one could tell the difference between Zion, Byron, Braidwood, etc. On the other hand, I believe that the results are as applicable to these other reactors as they are to Zion. Therefore, I would recommend that in the title, the executive summary, and the conclusions that the text be modified to address Zion-like containment configurations.

2. At the bottom of page 18, the next to the last sentence should read "is so degraded that it can no longer withstand...".

3. Top of page 21: Fourth line should read "core former plates". The core former wall is made up of numerous steel plates.

4. Last sentence of the first paragraph on page 21: This reads as if the TMI-2 vessel should have failed because molten material froze while transferring heat to the lower head. I would suggest that this sentence be altered to say: "that some material will freeze as a heat is transferred to the lower head causing the temperature to increase to levels where failure might be expected. While this was the case of the TMI-2 accident, the post-accident examination revealed that rapid cooling of the lower head region occurred after these elevated temperatures were achieved."

5. First paragraph in Section 3.7, the second sentence discusses the SCDAP/RELAP5 prediction of surge line failure before bottom head failure. Tables C.7, C.9 and C.11 list the major timing of events in the three sequences evaluated with SCDAP/RELAP5. In these tables, the failure is always the hot leg nozzle and not the surge line. It would be helpful to the reader if this inconsistency was rectified, or if there is no inconsistency, further explained for the readers benefit.

6. On page 52 there is a discussion of the influence of insulation around the reactor pressure vessel. The discussion mentions experiment SNL/IET-11, then suggests that the melt-laden gas will melt insulation as it moves through the available gap between reactor vessel and the biological shield. It should also be mentioned that the iron thermite used in the experiment likely results in the highly superheated molten iron being discharged first since the iron is heavier than the aluminum oxide. However, for the reactor system, the first material discharged would be the oxidic melt, and as

discussed further in the text, would be followed by the blowdown of saturated water. Both of these would tend to promote much less ablation than molten iron followed by superheated steam. Hence, the experiment is a conservative representation of the reactor system in that it would result in more ablation, hence a larger flow path between the reactor pressure vessel and the biological shield. This aspect of the experiment should be mentioned in the text.

7. On page 64 the following statement is made: "To address these issues, the NRC requested that Fauske & Associates, Inc. (FAI, 1994), the organization responsible for the Zion IPE, ...". The organization responsible for the Zion IPE is Commonwealth Edison Company, not FAI. FAI was one of the organizations that worked with Commonwealth Edison to perform the Zion IPE, but the plant operator is responsible for the IPE effort. This statement must be changed.

8. On page 71 there is a discussion of the upper bound pressure determined from the TCE calculations and the Zion containment fragility curve. The fragility curve given in Figure 5.3 has an abcissa which is confusing as to whether it is the containment pressure as absolute or containment pressure minus the atmospheric pressure, i.e. a gauge pressure. The discussion on page 71 does not mention whether these pressure are absolute or gauge. While this does not influence the conclusions, the text should be clear.

9. On page C-23 the following statement is made "the conclusions of this analysis are specific to the Zion PWR." While the SCDAP/RELAP5 calculations were done for a Zion input deck, it would seem that the conclusions are valid for a Westinghouse 4-loop NSSS design with a thermal power approximately 3,000 MW, zirconium clad fuel and silver-indium-cadmium control rods. Hence, these conclusions should be valid for Zion-like PWR designs. In other words, this statement indicates that the authors could differentiate between Zion and any other reactor system with essentially the same NSSS design. Is this really true? It would seem to me that the level of uncertainties in the analyses presented are greater than those that would be considered as small differences between the reactor designs and their behavior under severe accident conditions. I recommend that the conclusions can be broadened substantially.

10. On page D-1 the following statement is made: "The quench tank is located in the annulus volume (outside the crane wall) of the containment (Henry, 1994)." Why reference a personal communication with respect to the location of the quench tank when Figure D.1 shows the pressurized relief tank (also called the quench tank) located in the annular volume? It would seem more appropriate to refer directly to Figure D.1.

11. Again on page D-1 the following statement is made: "From Henry (1994) the hot leg is reinforced inside the shield and therefore, ...". The hot leg itself is not reinforced inside the biological shield, rather near the vessel wall the hot leg is thicker as part of the weldment fitting; see Figure D.1. Furthermore, the strain to failure for something as large as a hot leg could experience interference with the concrete in the biological shield, thereby altering the location of the failure site. The specifics should be cleaned

up in the final version.

12. On page D-6, the first paragraph discusses Figure D.38 and specifically the behavior of the jet autoignition temperature for low hydrogen concentrations. The abcissa in Figure D.38 is the water vapor concentration with the notations by the individual data points evidently being the hydrogen concentration. It is recommended that this figure be re-drawn for clarity and that the relationship of the numbers next to the data points be clearly identified in the figure and not left to the presumption of the reader.

PURDUE UNIVERSITY

SCHOOL OF NUCLEAR ENGINEERING

October 19, 1994

Dr. Khatib-Rahbar
Energy Research, Inc.
P.O. Box 2034
Rockville, MD 20847-2034

Dear Dr. Khatib-Rahbar:

I have completed the review of the Supplement 1 of NUREG/CR-6075. Following are my comments on the report:

1) General Comments

This report is well organized to document the peer review comments for NUREG/CR-6075 and the authors' responses to these comments. In general, these responses are technically accurate and satisfactory. Some of the remaining issues were discussed by the Technical Program Group for DCH and SNL followed up these issues with additional analyses. The summary of this effort is also reported here.

2) Specific Comments

An additional analysis for the DCH problem for Zion geometry has been carried out based on the SCDAP/RELAP5 calculations. Although there are some discussions on the uncertainties of these calculations in Appendix C, these uncertainties are not quantified. It is clear that there are numerous and large uncertainties in modeling of the melt progression and vessel failure, as indicated by the complicated multiphase flow phenomena and available options in the code. However, the code also indicated that earlier hot leg failure can occur well in advance of the vessel failure. The uncertainty of this hot leg failure may be more easily characterized, since it is a problem of vapor convection and metal heating up. The quantification of this uncertainty will strengthen the analysis and increase the confidence level of the results.

Sincerely yours,

M. Ishii
Professor of Nuclear Engineering

MI/ks
cc: Richard Lee (NRC)

1290 NUCLEAR ENGINEERING BUILDING • WEST LAFAYETTE, IN 47907-1290

LEVY & ASSOCIATES

3880 S. Bascom Ave., Suite 112
San Jose, CA 95124
408/369/6500
FAX 408/369-8720

September 27, 1994

Mr. Wayne Hodges, Director
Division of Systems Research
Office of Nuclear Regulatory Research
Nuclear Regulatory Commission
Washington, D. C. 20555

Dear Wayne:

As per your request of September 15, 1994, I have reviewed the draft copy of Supplement 1 of NUREG/CR-6075 "The Probability of Containment Failure by Direct Containment Heating in Zion" and my comments are as follows:

1. Supplement 1 strengthens the NUREG/CR-6075 argument that DCH is not a problem for Zion and I concur with that conclusion. The Supplement also illustrates how to couple the SCDAP/RELAP5 and CONTAIN computer codes to predict containment pressure and that methodology could be applied to a broader spectrum of severe accident scenarios as well as their probabilistic evaluation through Monte Carlo treatment.

2. The Supplement provides results for an increased primary pressure and an augmented release of molten materials from the vessel by comparison to those used in NUREG/CR-6075. A comparison of the containment pressures calculated in the Supplement (Table 6.1) versus those in NUREG/CR-6075 should be included to help quantify the impact of the modified parameters upon containment pressure.

3. On page 24, it is not clear why a containment pressure of 0.25 Mpa is selected at the time of vessel breach when CONTAIN calculations in 1990 and in Appendix D show increased values. A SCDAP-RELAP5/CONTAIN calculations for the high pressure scenario studied in Supplement 1 might have helped to establish the containment pressure at vessel break more reliably. While this is not considered essential for Zion due to its large margin to containment failure such a coupled calculation may become necessary for plant designs with less margin.

4. One could imply from the statement on top of page C-20 and in the middle of page C-23 that it might be possible to produce increased primary pressures during station blackout TLMB' scenarios with operator actions and core recovery with water. If INEL believes that this might occur, INEL should be challenged to find such sequences and to define their probability of occurrence.

5. The range of containment pressures in Table 6.1 is quite small going from the lower bound to the upper bound values. For example, under Scenario V they cover pressures of 0.324 Mpa to 0.437 Mpa and in Scenario VI the corresponding values go from 0.295 Mpa to 0.455 Mpa. This small range of ± 20 percent suggests that DCH containment pressures are not overly sensitive to presumed variations in parameters and scenarios. Another possibility is that insufficient variations were considered in Supplement 1. The DCH work performed to-' ' has identified three important parameters: (1) primary pressure which has been varied to its maximum extent in Supplement 1; (2) metallic content which was considered over a narrow range in Supplement 1, e.g., 0 to 1.5 mt of Zr and 0 to 2.3 mt of steel in Scenario V; and (3) hydrogen combustion or deflagration which played a limited role in Supplement 1 at the time of peak DCH pressure. It may be worthwhile to quantify the role of increased metallics and change in hydrogen combustion/deflagration timing to determine where and if they can produce a sharp rise in containment pressure. Also it may be desirable to consider other scenarios which involve different types of core recovery or operator actions to ascertain that they cannot lead to significant increases in containment pressure. (See comment 4)

6. With the current successful application of SCDAP/RELAP5 and CONTAIN computer codes, consideration should be given to sensitivity studies of the codes to not only study other scenarios but also the impact of such important input code parameters as those listed in Table C.4. Other assumptions such as variations in the countercurrent flow parameters listed in Table C.2 or such as the mode of debris-to-coolant heat transfer should also be evaluated. 'In particular, the current version of SCDAP/RELAP5 allows the debris-to-coolant heat transfer to be either on or off. In the scenarios evaluated in Supplement 1, the heat transfer was turned on in all calculations in order to increase the potential for pressurization of the primary system during quenching. However, in all Scenarios evaluated in the Supplement the reactor always remained depressurized; and, a set of calculations with the heat transfer turned off might be valuable to understand to what degree it might change the amount of metallics and molten materials that could be released from the vessel at low pressure.

7. Scenarios VII and VIII were not analyzed in Supplement 1 because they produced complete depressurization of the primary system before lower head failure and, therefore, they were judged not to be relevant to DCH. However, Scenarios VII and VIII may have other impacts upon containment integrity and particularly in terms of loads from molten material-coolant interactions, hydrogen combustion, and concrete ablation. These are outside the scope of DCH but they still need to be considered under overall containment integrity assessment.

8. On page 26, it is noted that SCDAP/RELAP5 predicts localized degradation of the outer assemblies. However, on page 17 the outer row of fuel assemblies is excluded from contributing to the core melt at vessel breach. It is suggested that these statements be reconciled or shown to have a negligible effect upon containment pressure.

In summary, a good case has been made for DCH not being a problem for the Zion plant. The worst calculated containment pressure was 0.46 Mpa (Table 6.1 and 6.2) which is well below the Zion's 0.79 Mpa threshold for fragility. For that reason, it would be best not to perform the additional evaluations suggested herein for the Zion plant and

instead to consider them in extrapolating the DCH methodology to plants with less robust designs or containments.

Before closing, let me finally command the NRC, its supporting national laboratories, and particularly SNL and its consultants for a job well done.

Sincerely yours,

Salomon Levy

Salomon Levy

cc: Dr. R. Lee, NRC

M. Wayne Hodges, Director
Division of Systems Research
Office of Nuclear Regulatory Research
Washington, D. C. 20555-0001

October 10, 1994

Dear Dr. Hodges,

These are my comments on NUREG/CR-6075 Supplement 1.

It is my opinion that Sandia National Laboratories has adequately performed the necessary calculations to render the DCH issue closed for Zion.

Even though reviewer comments and rebuttals show that concerns expressed by some reviewers did not receive completely satisfactory responses from Sandia, the conclusion of zero containment failure probability for each scenario seems to be well supported.

We are considering containment pressurization and strength responses. The initial conditions and microscopic (fine structure) thermal-hydraulic phenomena are somewhat random, and play a significant role. However, the supporting analyses, experimental data, and computer studies have provided a strong framework to arrive at containment load distributions from which defensible conclusions can be drawn.

The greatest uncertainty in DCH involves the energy released to the containment. The TCE model captures the functional dependence of containment pressure on energy released, making it possible to determine if the containment load distribution and fragility curves intersect. Present results are based on extensive studies and sub-studies, based on reviewer inputs. Sandia's arguments convincingly show that further refinements in physical understanding would not be expected to change the conclusions.

Yours truly,

Frederick J. Moody

Frederick J. Moody
GE Nuclear Energy, MC-747
175 Curtner Avenue
San Jose, CA 95125
(408) 925-6434 (phone)
2790 (fax)

cc: Dr. M. Khatib-Rahbar

UNIVERSITY OF MARYLAND AT COLLEGE PARK

DEPARTMENT OF MATERIALS AND NUCLEAR ENGINEERING
RELIABILITY ENGINEERING

Dr. Mohsen Khatib-Rahbar
Energy Research, Inc.
P.O. Box 2034
Rockville, MD 20847

October 2, 1994

Dear Dr. Khatib-Rahbar:

I have completed my review of Supplement 1 of NUREG/CR-6075. I have concluded that the authors have adequately considered and addressed my outstanding concerns about NUREG/CR-6075. Also, they have appropriately dealt with the issues raised during the working meetings, including the peer review meeting on "initial conditions" in which I participated. Accordingly, I concur with the conclusion of the report that suggests closure of the DCH issue for the Zion plant.

In reviewing the Supplement 1, I have identified a small number of specific comments and corrections for improving the quality of the report. I have listed them below:

page iii (one line from the bottom):
Instead of ". . . containment probability was zero . . . ", use ". . . containment probability was negligible . . .".

Page xvii (4th paragraph):
My last name is misspelled.

page xxi (one line from the bottom):
Similar to the first comment, change "zero" to "negligible".

page 16 (2nd paragraph):
Change "pilot operated relief valve" to "power operated relief valve".

page 18 (2nd paragraph of section 3.5):
Eliminate ". . . corresponds roughly to a 2σ confidence limit". Also, the interpretation for the probability levels provided in Table 3.2 and in the text of this section are different. I prefer the interpretation of the text instead of the one in Table 3.2.

page 40 (Figure 3.4):
In my original review of NUREG/CR-7075, I suggested using a PDF instead of a DPD.

COLLEGE PARK, MARYLAND 20742-2115 • (301) 405-5209 • FAX: (301) 314-9467 • E-MAIL: roush@eng.umd.edu

This allows a better visualization of the relative frequencies. In Figure 3.4 and all other distributions shown in Supplement 1, besides the DPD form, a cumulative probability distribution function (CPDF) is also shown. This is another way of displaying the relative frequencies (instead of PDFs). Accordingly, the distributions shown in NUREG/CR-7075 should also include CPDFs, so that they become comparable with Supplement 1 distributions.

page 64 (last paragraph):
The containment threshold of 0.689 MPa in the text is inconsistent with the 0.789 MPa in Table 5.1. It appears from the discussions elsewhere in the report that 0.789 is the correct threshold.

page 65 (Table 5.1):
The frequencies shown in this table are cumulative frequencies. The table uses the rare event approximation to calculate the "Total Frequency". This is done by summing the frequency of the hoop failure at each pressure level with the corresponding frequency of the basemat failure. This approximation is only good for events with small probabilities. As such, some errors could occur at high containment pressures. For example, the frequency of hoop failure at 170 psig is less than the hoop failure frequency at 154 psig. Also, the frequency of basemat failure at 166 psig is less than the frequency of the basemat failure at 158 psig. Clearly, these are physically unexplainable and, most likely, incorrect. I believe that this may have been caused by trying to assure that the total frequency does not exceed 1.00 (as happens when rare event approximation is used when summing high probabilities). I suggest to redo this table using: Total Cumm. Freq. = Hoop Cumm. Freq. + Basemat Cumm. Freq. - (Hoop Cumm. Freq.)(Basemat Cumm. Freq.). All cumulative frequencies should be reevaluated, and they should increase as the containment pressure increases.

page 72 (last paragraph):
Change " The predicted containment pressure. . .", to "The mean containment pressure . . .".

Page A-3 (Table A.1, second column):
Change "Massachusetts" to "Massachusetts Institute of Technology".

I would like to commend the authors of NUREG/CR-7075 and Supplement 1 for their excellent work and their cooperation with the peer reviewers. Please don't hesitate to call me at (301)405-5226, if there are any questions.

Sincerely yours,

Mohammad Modarres
Professor of Nuclear
Engineering

October 22, 1994
Aeronautics, 105-50
Caltech
Pasadena, CA 91125

Dr. Mohsen Khatib-Rahbar
Energy Research. Inc.
P. O. Box 2034
Rockville, MD 20847

FAX 301 881 0867

Re: NUREG/CR-6075 Supplement 1

Dear Dr. Kahtib-Rahbar:

I have examined the referenced document, and primarily directed my attention to Appendix E. My comments are as follows:

1. The discussion is for the most part significantly improved over the previous version.

2. The experimental evidence is that current reaction mechanisms for low temperature hydrogen combustion are fundamentally incomplete. In some cases these mechanisms *overpredict* the reaction time - not underpredict as claimed on p. E-17. There is no basis for arbitrarily multiplying the time constants by a factor of 100. Lacking reliable experimental evidence, this is all just speculation. Neither reaction time or volumetric oxidation rates can reliably predicted under these conditions. This has to be pointed out.

Sincerely,

Joseph E Shepherd

Joseph Shepherd

CC: C. Tinkler/US NRC

MEMORANDUM
ENERGY RESEARCH, INC.

TO: M. Khatib-Rahbar

FROM: H. Esmaili HE

SUBJECT: Review of NUREG/CR-6075 Supplement 1

DATE: October 24, 1994

I have reviewed supplement 1 of NUREG/CR-6075 and determined that the authors have adequately addressed all the concerns raised in the working group meeting and reflected in the summary of that meeting (Appendix A of the Supplement). I have identified a number of minor corrections and additions that would enhance the consistency of the report even though the conclusions of the report would not be altered, i.e., DCH would not challenge the Zion containment integrity. These are listed below:

1. The last statement on the bottom of page 70 is inaccurate. The tabulated values of the containment pressures and temperatures for the best estimate and the upper bound in Table 6.1 indicate that scenario VI produces higher loads than scenario V. This is also evident from Figures 6.3 and 6.4.

2. The LHS sample size (i.e., the number of observations sampled from the probability distributions) is not specified in the supplement. I do not think that this will affect the conclusions, however, the number of observations should be cited for completeness.

3. The value of the auto-ignition temperature in Table 3.3 should be changed to 950 K. This is the value referred to in the third paragraph on page E-3.

4. The first sentence in Section 3.7 states that "... predicts surge line failure ...," which should be replaced by "... predicts hot leg failure ..."

5. The RCS gas temperature for scenario VI is 1000 as listed in Table 3.3. The input file for scenario VI lists the RCS gas temperature as 800 K (page B-8).

6. Remove "to calculate the loads" from the sentence "Next, a driver program, ..." in the last paragraph on Page B-1.

cc: R. Lee, NRC
ERI/NRC-046 file

APPENDIX B
MONTE CARLO FRAMEWORK

B.1. INTRODUCTION

The discrete probability distribution (DPD) method was used to propagate distributions through the probabilistic framework in NUREG/CR-6075. The ALPHA code, developed at the University of California at Santa Barbara (UCSB), was the software based on the DPD approach that was used in NUREG/CR-6075 to calculate containment failure probabilities. An alternative to using ALPHA was developed by Sandia for the present supplement document, with an eye towards continued use in future extrapolation efforts.

Sandia has developed software to perform either traditional Monte Carlo sampling or stratified Monte Carlo sampling (Latin hypercube sampling, LHS). The software, called LHS (Iman and Shortencarier, 1984) is user-friendly and has an established quality assurance pedigree, including code assessment and verification. The LHS software was developed in the 1980s and was substantially upgraded in 1992 (Wyss, 1994). The purpose of the software is to provide a user with a versatile facility for sampling statistical distributions. The software supports both Monte Carlo and Latin hypercube sampling methods for more than 35 types of continuous and discrete statistical distributions. It also provides a mechanism by which a user can induce an arbitrary degree of rank correlation between pairs of random variables. The software has a quality assurance pedigree that has been established through an extensive verification program, and represents the standard method by which statistical sampling is performed for risk assessment activities in many areas of Sandia National Laboratories.

The software was set up to perform the analysis in three steps, as shown in Figure B.1. In the first step, the distributions used for the particular scenario are sampled using the LHS code. Thus, the input for each TCE/LHS scenario is actually expressed as an input file for the LHS code. This input file is processed by LHS to obtain a standard LHS output file that contains sample observations for each parameter. Next, TCEDRV is run to evaluate the loads for each observation in the sample using the TCE code to calculate the loads. The driver program outputs the calculated loads in either of two formats that can be used to plot the results: (1) a format accepted by a Sandia-developed plotting program that can create various statistical plots, and (2) a tab-delimited format of the cumulative distribution function (CDF) for the

calculated variables, which can be imported into most commercial graphics packages. Further details of the software used to perform each step are provided in the following paragraphs. We will refer to the overall software for calculating DCH loads as TCE/LHS for convenience.

Figure B.2 shows a schematic of the TCE driver program, TCEDRV. TCEDRV reads in the constant values (RCS volume, RCS pressure, etc.) and distributions (melt mass, composition, etc.) in the format written by LHS, and then it repeatedly performs TCE calculations in a loop over the sample observations. Within the loop, the code reads in the sampled values, then calculates RCS, containment, and melt conditions. A subroutine is called to calculate the ablated hole diameter, and using this value, the coherence ratio is calculated. Melt properties are then calculated in the subroutine MELTPRP. Next, the peak containment pressure and temperature during DCH is estimated in the subroutine TWOCELL, which is based on the TCE model. The code then outputs the peak containment pressure and temperature, coherence ratio, and ablated hole size in the format selected by the analyst.

The TCE/LHS software was benchmarked by comparing its results with those that had been calculated with the ALPHA code for Scenario I of the initial Zion DCH analysis (Pilch, et al. 1994). The DPDs calculated by ALPHA were converted to a CDF so that the results could be compared directly with the sampled values from TCE/LHS. The input for TCE/LHS was called in a manner consistent with the ALPHA code and the results were in excellent agreement, as shown in Figure B.3.

A listing of TCEDRV and its associated subroutines is attached. The source code for TCEDRV, as well as the input and output files for all of the scenarios, have been sent to NRC on a disk.

B.2. REFERENCES

Iman, R.L., and M.J. Shortencarier (March 1984). *A FORTRAN 77 Program and User's Guide for the Generation of Latin Hypercube and Random Samples for use with Computer Models*, NUREG/CR-3624, Sandia National Laboratories, Albuquerque, NM

Pilch, M.M., H. Yan, and T.G. Theofanous (July 1994). *The Probability of Containment Failure by Direct Containment Heating in Zion,* NUREG/CR-6075, SAND93-1535, Sandia National Laboratories, Albuquerque, NM.

Wyss, G.D. (June 1994). *Recent Enhancements to Probabilistic Risk Assessment Software at Sandia National Laboratories,* SAND94-1015C, presented at the DOE Energy Facilities Contractors Group Safety Analysis Working Group Fourth Annual Safety Analysis Workshop, Albuquerque, NM.

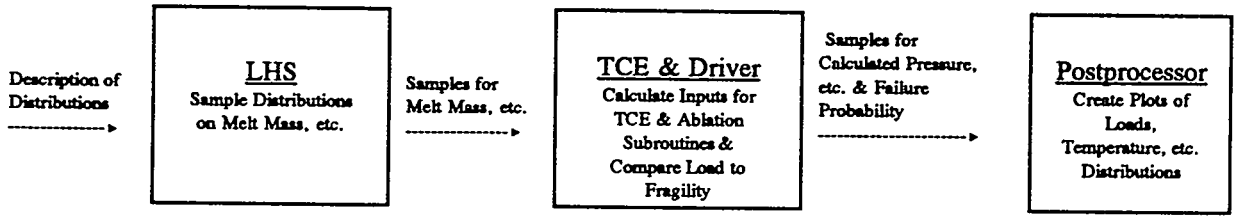

Figure B.1. DCH calculational process.

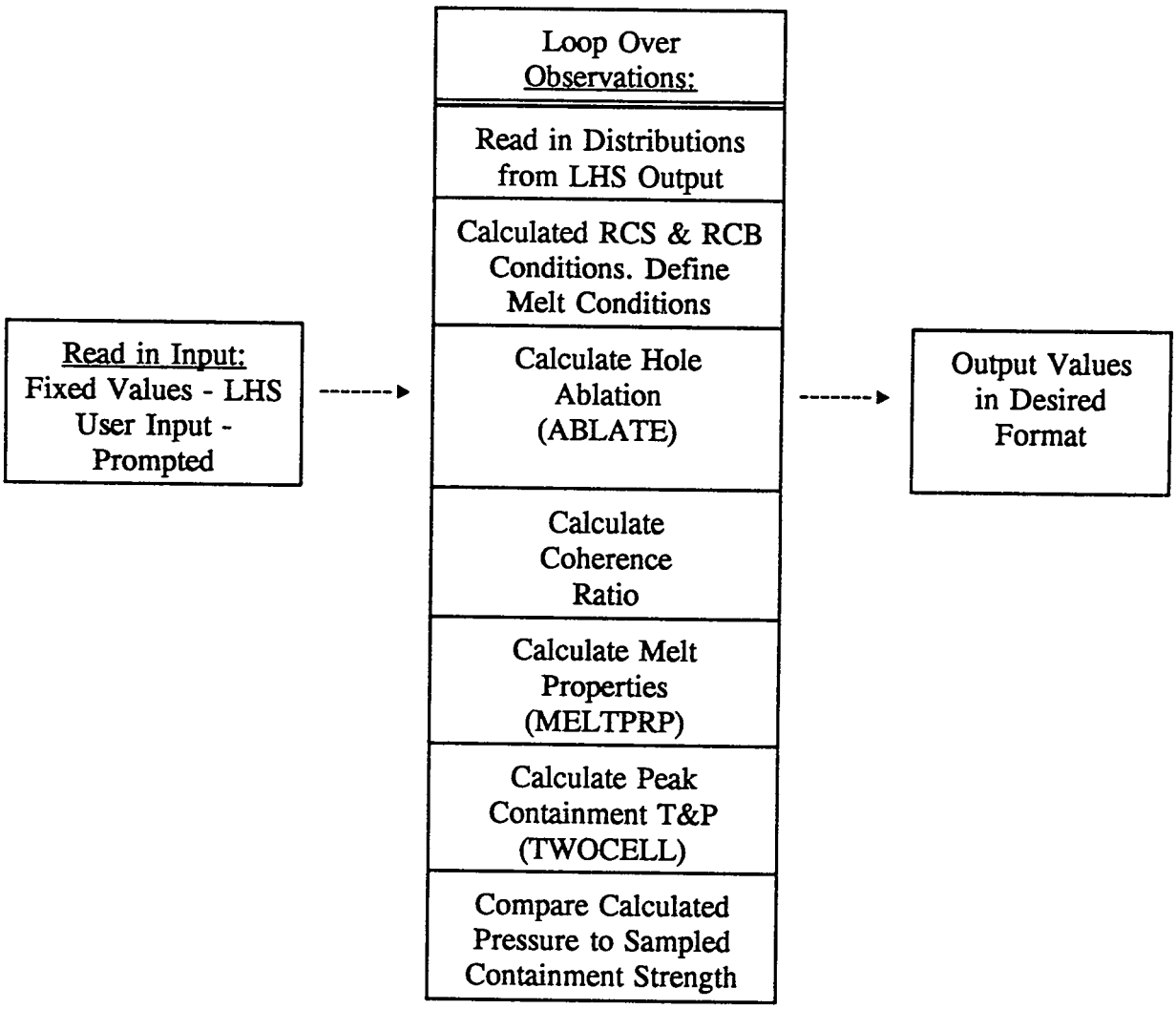

Figure B.2. Schematic of TCE driver logic.

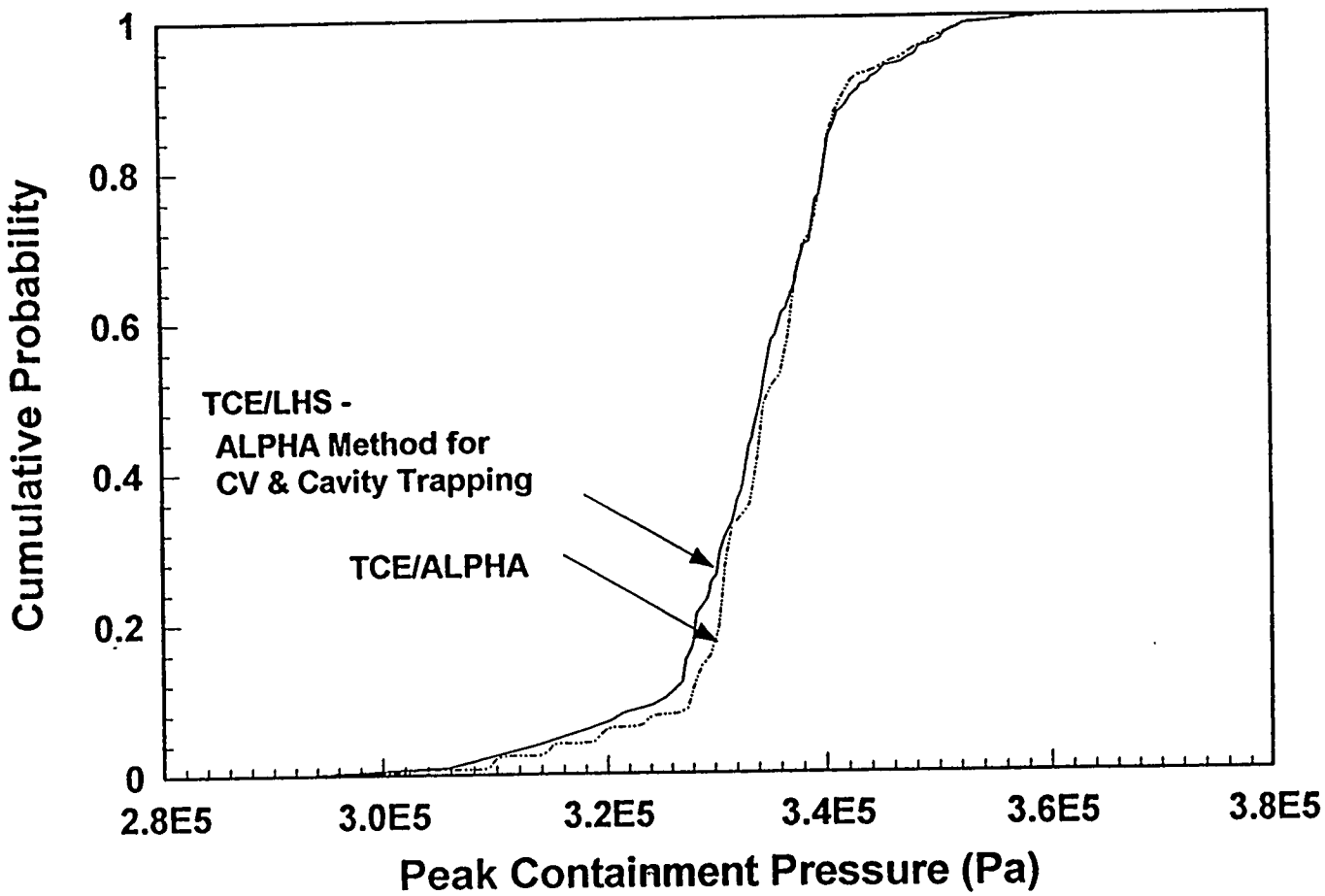

Figure B.3. Benchmarking of the Monte Carlo method using TCE/LHS against the discrete probability distribution (DPD) method for Scenario I in NUREG/CR-6075.

SCENARIO - V INPUT FILE

```
$ Scenario - V  operator intervention
Dataset:
tlhead Constant     .14   $ lower head thickness (m)
vlp    Constant     30.  $ lower plenum volume (m**3)
dh0    Constant     .4   $ initial lower head hole diameter (m)
tw0    Constant    1000.  $ lower head wall temperature at vessel breach (K)
crmm   Constant       0.  $ mass of control rod material in melt (kg)
uo2m0  Constant   98200.  $ total mass of UO2 in core (kg)
zrm0   Constant   20000. $ total mass of zr in core (kg)
stlmlp Constant   10000.  $ mass of steel in lower plenum (kg)
cohmul Constant   9.661   $ coherence ratio multiplier - plant specific
prcs   Constant   16.E6   $ RCS pressure (Pa) at vessel breach
vrcs   Constant    353.  $ RCS volume (m**3)
trcs   Constant    700.  $ RCS gas temperature (K) at vessel breach
prcboc Constant    .1e6   $ containment pressure (Pa) at operating conditions
trcboc Constant    316.  $ containment temperature at operating conditions
prcb   Constant   .25E6   $ containment pressure (Pa) at vessel breach
trcb   Constant    400.  $ containment temperature (K) at vessel breach
vrcb   Constant  76.9E3   $ containment volume (m**3)
vcav   Constant    190.  $ cavity volume (m**3)
fasub  Constant    .86   $ fraction of dispersed debris going to subcompartment
$                          (vs straight bypass to upper containment)
fvsub  Constant    .065   $ volume fraction of the subcompartment
tautoig Constant   950.  $ autoignition temperature (K)
tdeb   Constant   2800.  $ debris temperature (K)
fzrrel Constant   0.0    $ fraction Zr of Zr blockage relocated to lower head.
fh2rcs Constant     0.  $ fraction of h2 generated in rcs that stays in rcs.
fejec  Constant    1.0  $ fraction of debris ejected into cavity
fdisp  Constant    .85  $ fraction of debris dispersed from cavity
zro2ml Constant     1.  $ multiplier on ZrO2 - not used
stlmul Constant     0.  $ multiplier on steel mass eq 3.5
$
$ UO2 mass (kg)
uo2m   Continuous Linear 5  #
   0.  0.                 #
10000.    .10              #
30000.    .89              #
40000.    .99              #
50000.   1.
$ steel mass (kg)
stlmi  Continuous Linear 2  #
   0.  0.                 #
   1.0E-6   1.
```

```
$ fraction of Zr oxidized
fzrox   Continuous Linear 6  #
   .15   0.                 #
   .25    .01               #
   .35    .11               #
   .45    .89               #
   .55    .99               #
   .65   1.
$ distribution on coherence ratio
$                    mean   standard deviation
cohdis   Normal      0.        .29
$ containment failure pressure (Pa)
pfail   Continuous Linear 29 #
  .789E6   0.               #
  .791E6   .0111             #
  .805E6   .0145             #
  .818E6   .0175             #
  .832E6   .0217             #
  .846E6   .0270             #
  .860E6   .0329             #
  .873E6   .0403             #
  .887E6   .0490             #
  .901E6   .0604             #
  .915E6   .0754             #
  .929E6   .0974             #
  .942E6   .127              #
  .956E6   .169              #
  .970E6   .228              #
  .984E6   .305              #
  .998E6   .398              #
 1.01E6    .500              #
 1.03E6    .607              #
 1.04E6    .710              #
 1.05E6    .799              #
 1.07E6    .870              #
 1.08E6    .922              #
 1.09E6    .957              #
 1.11E6    .978              #
 1.12E6    .990              #
 1.14E6    .995              #
 1.15E6    .998              #
 1.23E6   1.
```

SCENARIO - VI INPUT FILE

```
$  Scenarion - VI operator intervention
Dataset:
tlhead Constant     .14   $ lower head thickness (m)
vlp    Constant     30.  $ lower plenum volume (m**3)
dh0    Constant     .4   $ initial lower head hole diameter (m)
tw0    Constant    1000.  $ lower head wall temperature at vessel breach (K)
crmm   Constant       0.  $ mass of control rod material in melt (kg)
uo2m0  Constant   98200.  $ total mass of UO2 in core (kg)
zrm0   Constant   20000. $ total mass of zr in core (kg)
stlmlp Constant   10000.  $ mass of steel in lower plenum (kg)
cohmul Constant   9.661   $ coherence ratio multiplier - plant specific
prcs   Constant   8.0E6   $ RCS pressure (Pa) at vessel breach
vrcs   Constant    353.  $ RCS volume (m**3)
trcs   Constant   1000.  $ RCS gas temperature (K) at vessel breach
prcboc Constant    .1e6   $ containment pressure (Pa) at operating conditions
trcboc Constant    316.  $ containment temperature at operating conditions
prcb   Constant   .25E6   $ containment pressure (Pa) at vessel breach
trcb   Constant    400.  $ containment temperature (K) at vessel breach
vrcb   Constant  76.9E3   $ containment volume (m**3)
vcav   Constant    190.  $ cavity volume (m**3)
fasub  Constant    .86   $ fraction of dispersed debris going to subcompartment
$                          (vs straight bypass to upper containment)
fvsub  Constant   .065   $ volume fraction of the subcompartment
tautoig Constant   950.  $ autoignition temperature (K)
tdeb   Constant   2800.  $ debris temperature (K)
fzrrel Constant    0.0   $ fraction of Zr blockage relocated to lower head.
fh2rcs Constant      0.  $ fraction of h2 generated in rcs that stays in rcs.
fejec  Constant    1.0   $ fraction of debris ejected into cavity
fdisp  Constant    .85   $ fraction of debris dispersed from cavity
zro2ml Constant      1.  $ multiplier on ZrO2 - not used
stlmul Constant      0.  $ multiplier on steel mass  - not used
$
$ UO2 mass (kg)
uo2m   Continuous Linear 6  #
   0.   0.                 #
 5000.    .01               #
20000.    .11               #
40000.    .89               #
55000.    .99               #
70000.   1.
$ steel mass (kg)
stlmi  Continuous Linear 2  #
   0.   0.                 #
   1.0E-6   1.
```

```
$ fraction of Zr oxidized
fzrox   Continuous Linear 6  #
   .15   0.                 #
   .25    .01               #
   .35    .11               #
   .45    .89               #
   .55    .99               #
   .65   1.
$ distribution on coherence ratio
$                    mean   standard deviation
cohdis   Normal      0.          .29
$ containment failure pressure (Pa)
pfail   Continuous Linear 29 #
  .789E6   0.                #
  .791E6   .0111              #
  .805E6   .0145              #
  .818E6   .0175              #
  .832E6   .0217              #
  .846E6   .0270              #
  .860E6   .0329              #
  .873E6   .0403              #
  .887E6   .0490              #
  .901E6   .0604              #
  .915E6   .0754              #
  .929E6   .0974              #
  .942E6   .127               #
  .956E6   .169               #
  .970E6   .228               #
  .984E6   .305               #
  .998E6   .398               #
 1.01E6    .500               #
 1.03E6    .607               #
 1.04E6    .710               #
 1.05E6    .799               #
 1.07E6    .870               #
 1.08E6    .922               #
 1.09E6    .957               #
 1.11E6    .978               #
 1.12E6    .990               #
 1.14E6    .995               #
 1.15E6    .998               #
 1.23E6   1.
```

LISTING OF TCEDRV AND ASSOCIATED SUBROUTINES

```
      program tcedrv
c
c deflagration model inplimented into tce
c
c This is the driver program for propagating distributions through the TCE
c code for calculating DCH containment failure probabilities. Distributions
c are generated external to this program using the LHS code. This program
c reads the LHS output to get distributions for melt mass, fragility, etc.
c Additional input describing the plant and scenario is contained in the input
c file fixed.dat. The vessel breach hole size is calculated using Marty
c Pilch's ablation model. The DCH pressure rise comes from Marty's property
c subroutine and two cell equilibrium model subroutine. The containment failure
c probability is determined by comparing the calculated load to a sampled
c failure pressure for each observation, and then calculating the fraction of
c observations with failure after completing the loop over observations. The
c calculated variables of interest are written out in the "LHS format" which
c allows the plotting program CRAVE to be used to plot distributions.
c
c CONSTANTS
c   gamma = specific heat ratio
c   awall = surface area in dome, m**2 (not used)
c   deh2  = molar combustion energy of hydrogen, J/mole
c INPUT VARIABLES FROM LHS:
c    uo2m = UO2 mass (kg). Zion: Fig 3.3 & 3.5 for Scenarios I & II. 0 for
c           Scenario III
c    stlmi = steel mass (kg). Zion: 0 for Scenarios I & II. Fig 3.7 for III
c    fzrox = fraction of zr oxidized. Zion: Fig 3.4 for Scenarios I & II.
c            Fig 3.6 for Scenario III.
c    cohdis = distribution on coherence ratio. Zion: Normal distribution
c             with standard deviation of 28%
c    pfail = containment failure pressure (Pa). Zion: Fig 5.1
c INPUT VARIABLES FROM FILE FIXED.DAT:
c    tlhead = lower head thickness (m). Zion: .14
c    vlp = lower plenum volume (m**3). Zion: 30.
c    dh0 = initial lower head hole diameter (m). Zion: .0254 for Scenarios
c          I and III. .4 for Scenario II base, .7 for Scenario II sensitivities.
c    tw0 = lower head wall temperature at vessel breach (K). Zion: 600,1000,800
c          for Scenarios I,II,III
c    crmm = mass of control rod material in melt (kg). Zion: 0 for Scenario I.
c           4000 for Scenarios II & III.
c    uo2m0 = total mass of UO2 in core (kg). Zion: 98200.
c    zrm0 = total mass of zr in core (kg). Zion: 3200.
c    stlmlp = mass of steel in lower plenum (kg). Zion: 15000.
c    cohmul = coherence ratio multiplier. Zion: 4.045
c    prcs  = RCS pressure (Pa) at vessel breach. Zion: 8E6 for base scenarios, 16E6 for
```

```
c           sensitivities
c     vrcs  = RCS volume (m**3).  Zion: 353
c     trcs  = RCS gas temperature (K) at vessel breach.  Zion: 800 for Scenarios I & II.
900
c           for Scenario III.
c     prcboc = containment pressure at operating conditions.  Zion: .0654E6
c     trcboc = containment temperature at operating conditions.  Zion: 311 K
c     prcb  = containment pressure (Pa) at vessel breach.  Zion: .25E6
c     trcb  = containment temperature (K) at vessel breach.  Zion:  383
c     vrcb  = containment volume (m**3).  Zion:  76.9E3
c     vcav  = cavity volume (m**3).  Zion: 190
c     fasub = fraction of dispersed debris going to subcompartment (vs straight
c           bypass to upper containment).  Zion: .86 for base scenarios, .8 for sensitivities
c     fvsub = volume fraction of the subcompartment.  Zion:  .065
c     tautoig = autoignition temperature (K).  Zion:  1100 for base scenarios, 950 for
c             sensitivities
c     tdeb = debris temperature (K).  Zion: Scenario I = 2800, II = 2500,
c          III = 1900.
c     fzrrel = factor in Eq 3.4 for Zr relocated to lower head.
c             Zion: 0. for Scenarios I & III, 0.1 for Scenario II
c     fh2rcs = fraction of h2 generated in rcs that stays in rcs.
c             Zion: 0. for the 8 MPa scenarios and .2 for 16 MPa sensitivities
c     fejec = fraction of debris ejected from cavity.  Zion: 1. for Scenarios
c           I and II, and .9 for Scenario III.
c     fdisp = fraction of debris dispersed from cavity.  Zion: .85 for base scenarios,
c           1. for 16 MPa sensitivities
c     zro2ml = multiplier on ZrO2 eqn (Eqn 3.1).  Zion: 1 for Scenarios I & II,
c             0 for Scenario III.
c     stlmul = multiplier on steel mass eq 3.5.  Zion:  0 for Scenarios I & III.
c             1. for Scenario II.
c OUTPUT VARIABLES:
c     dhole = ablated hole size (m)
c     tcoh = coherence ratio
c     pfrcb = peak containment pressure (Pa)
c     tfrcb = peak containment temperature (K)
c     cfp = containment failure probability (0/1 on observations plus mean)
c
c
      dimension fatm(6),values(200),ikeep(200),imatch(200)
      dimension fdmass(9),f(9)
      dimension var(300),dhle(10000),tch(10000),pfr(10000)
      dimension tfr(10000),cf(10000),cp(10000)
      real nim,indeb
      character*16 lhsinp(28),lhsnd(5),word
      character filenms*80,input*40,output*40,lhscard*80
      character result*11,result2*12,tab*1
c
```

```
c ***********************************************************************

c point value input from lhs output
c
      data lhsinp/'TLHEAD', 'VLP',   'DH0',  'TW0',   'STLMLP','PRCS',
     1          'COHMUL', 'VRCS',   'TRCS', 'PRCBOC','TRCBOC','PRCB',
     2          'TRCB',   'VRCB',   'VCAV', 'FASUB', 'FVSUB', 'TDEB',
     3          'TAUTOIG','FH2RCS', 'FEJEC','FDISP', 'FZRREL','ZRM0',
     4          'ZRO2ML', 'CRMM',   'STLMUL','UO2M0'/
c
c distributions from lhs output
c
      data lhsnd/'UO2M','STLMI','COHDIS','PFAIL','FZROX'/
c
c ***********************************************************************
c constants
      gamma = 1.33
      awall = 9500.
      deh2  = 2.42e5
c counter for calculating containment failure probability
      cfpsum = 0.
c
c ***********************************************************************
c call time and date routines for output file
c
      call time(result)
      call date(result2)
c
c ***********************************************************************
c
c get input and output file names from user
c
      call getcl(filenms)
      if(filenms.eq.' ') then
         write(*,100)
 100     format(///,' Enter input and output file names separated'/,
     *          ' by a blank'/)
         read(*,*)input,output
c
c Get filenames
c
      else
        k = 1
        do while (filenms(k:k).ne.' ')
             input(k:k)=filenms(k:k)
             k = k + 1
        enddo
```

```
        j = k+1
        is = 1
        do while(filenms(j:j).ne.' ')
           output(is:j)=filenms(j:j)
           j = j + 1
           is = is + 1
        enddo
       endif
c
c
c Query user for plot package being used
c
      write(*,*)' Which plot package do you want to use?'
      write(*,*)' Input a 1 for CRAVE or a 2 for tab-delimated table'
      read(*,*)iplot
c
c  ***********************************************************************
c
c    read in fixed data
c
      open(unit=71,file=input,status='unknown',err=31)
      open(unit=72,file=output,status='unknown',err=33)
      open(6,file='debug.fil')
c
c read heading from lhs output file
c
      read(71,*)lhscard
      do while (lhscard(1:1).eq.'$')
         read(71,*)lhscard
      enddo
      backspace 71
c
c read in input variables and keep counter
c
      iword = 1
      ie = 1
 10   read(71,*)lhscard
      if(lhscard(1:1).ne.'$') then
         backspace 71
         read(71,*)word,values(ie)
c
c --convert lower case to upper
c
         do 11 ib = 1,len(word)
              itest = ichar(word(ib:ib))
              if (itest.ge.97 .and. itest.le.122)
    *       word(ib:ib) = char(itest-32)
```

```
 11     continue
c
c check for all 28 input variables
c
          check:do j = 1,28
               if(word.eq.lhsinp(j)) then
                 ikeep(iword) = j
                 imatch(ie) = ie
                 iword = iword + 1
                 exit check
               endif
          enddo check
          ie = ie + 1
          goto 10
        endif
c
c check for all 28 of input variables
c
       iword = iword - 1
       if(iword.ne.28) then
          write(*,*)' Error in input variables.  Check input file'
          stop
       endif
c
c
c all variables are here - continue processing
c set variables to values  (It isn't pretty, but it works!!)
c
       do iq = 1,28
          if(ikeep(iq).eq.1) then
               tlhead = values(imatch(iq))
          elseif(ikeep(iq).eq.2) then
               vlp = values(imatch(iq))
          elseif(ikeep(iq).eq.3) then
               dh0 = values(imatch(iq))
          elseif(ikeep(iq).eq.4) then
               tw0 = values(imatch(iq))
          elseif(ikeep(iq).eq.5) then
               stlmlp = values(imatch(iq))
          elseif(ikeep(iq).eq.6) then
               prcs = values(imatch(iq))
          elseif(ikeep(iq).eq.7) then
               cohmul = values(imatch(iq))
          elseif(ikeep(iq).eq.8) then
               vrcs = values(imatch(iq))
          elseif(ikeep(iq).eq.9) then
               trcs = values(imatch(iq))
```

```
        elseif(ikeep(iq).eq.10) then
              prcboc = values(imatch(iq))
        elseif(ikeep(iq).eq.11) then
              trcboc = values(imatch(iq))
        elseif(ikeep(iq).eq.12) then
              prcb = values(imatch(iq))
        elseif(ikeep(iq).eq.13) then
              trcb = values(imatch(iq))
        elseif(ikeep(iq).eq.14) then
              vrcb = values(imatch(iq))
        elseif(ikeep(iq).eq.15) then
              vcav = values(imatch(iq))
        elseif(ikeep(iq).eq.16) then
              fasub = values(imatch(iq))
        elseif(ikeep(iq).eq.17) then
              fvsub = values(imatch(iq))
        elseif(ikeep(iq).eq.18) then
              tdeb = values(imatch(iq))
        elseif(ikeep(iq).eq.19) then
              tautoig = values(imatch(iq))
        elseif(ikeep(iq).eq.20) then
              fh2rcs = values(imatch(iq))
        elseif(ikeep(iq).eq.21) then
              fejec = values(imatch(iq))
        elseif(ikeep(iq).eq.22) then
              fdisp = values(imatch(iq))
        elseif(ikeep(iq).eq.23) then
              fzrrel = values(imatch(iq))
        elseif(ikeep(iq).eq.24) then
              zrm0 = values(imatch(iq))
        elseif(ikeep(iq).eq.25) then
              zro2ml = values(imatch(iq))
        elseif(ikeep(iq).eq.26) then
              crmm = values(imatch(iq))
        elseif(ikeep(iq).eq.27) then
              stlmul = values(imatch(iq))
        elseif(ikeep(iq).eq.28) then
              uo2m0 = values(imatch(iq))
        endif
      enddo
c
c ***********************************************************************
c
c get number of observations and number of variables from lhs output
c
      read(71,*)word
      read(71,*)word,nobs
```

```
      read(71,*)word,ivar
c
c get values from 2nd block in lhs output file
c
      iword = 1
      ie = 1
      do k = 1,ivar
         read(71,*)word
         ib = 1
c
c convert to upper case
c
         do while(word(ib:ib).ne.':')
            itest = ichar(word(ib:ib))
            if (itest.ge.97 .and. itest.le.122)
     *        word(ib:ib) = char(itest-32)
            ib= ib+1
         enddo
         ib = ib -1
c
c Search for next batch of variables
c
c check this value with Greg
c
         comp: do kk = 1,ivar
               if(word(1:ib).eq.lhsnd(kk)) then
                  ikeep(iword) = kk
                  imatch(ie) = ie
                  iword = iword + 1
                  exit comp
               endif
         enddo comp
         ie = ie + 1
      enddo
      iword = iword -1
      if(iword.ne.5) then
         write(*,*)' Input variables not correct - check file'
         stop
      endif
c
c Now write all the above to new lhs file
c
      if(iplot.eq.1) then
         zero = 0.0
         kvar = 5
         write(72,*)' $ LHS File Format Version 1.00'
         write(72,*)' $'
```

```
          write(72,*)' $ This run was executed on ',result2
          write(72,*)' $ at ',result
          write(72,*)' $'
          write(72,*)' $ the input file name is ',input
          write(72,*)' $ the output file name is ',output
          write(72,*)' $'
          write(72,*)' dhole          ',zero
          write(72,*)' tcoh           ',zero
          write(72,*)' pfrcb          ',zero
          write(72,*)' tfrcb          ',zero
          write(72,*)' cfp            ',zero
          write(72,*)' @UNCERTAINTY'
          write(72,*)'  @OBSERVATIONS    ',nobs
          write(72,*)'  @VARIABLES       ',kvar
          write(72,*)' dhole:'
          write(72,*)' tcoh: '
          write(72,*)' pfrcb:'
          write(72,*)' tfrcb:'
          write(72,*)' cfp:  '
          write(72,*)'  @SAMPLEDATA
        endif
c
c
c
c ***********************************************************************
c loop over observations from LHS - first read in distributions
c
c
c read @SAMPLEDATA card from file
c
        read(71,*)lhscard
        do 1000 iloop = 1,nobs
c
c read in 2 dummy variables, then uo2m,stlmi,cohdis,fzrox,pfail
c
          read(71,*)idum1,idum2,(var(ii),ii=1,ivar)
c
c need to fix for any order
c
          do iq = 1,ivar
             if(ikeep(iq).eq.1) then
                  uo2m = var(imatch(iq))
             elseif(ikeep(iq).eq.2) then
                  stlmi = var(imatch(iq))
             elseif(ikeep(iq).eq.3) then
                  cohdis = var(imatch(iq))
             elseif(ikeep(iq).eq.4) then
```

```
                pfail = var(imatch(iq))
            elseif(ikeep(iq).eq.5) then
                fzrox = var(imatch(iq))
            endif
        enddo
c*********************************************************************
c  calculate h2 mass and RCS conditions
c
c  moles of h2 generated by zr oxidation - Eq 3.2
      h2genn = 2./.091*fzrox*zrm0
c  moles of h2 remaining in rcs
      h2rcsn = h2genn * fh2rcs
c  partial pressure ratios for steam, h2, n2
      fn2rcs = 0.
      fh2rcs = h2rcsn*8.3143*trcs/vrcs / prcs
C   COMPUTE total MASS AND MOLES IN RCS and mole fractions
      CALL RCSPRP(PRCS,VRCS,TRCS,FN2RCS,FH2RCS,yh2,ystm,
     1          RCSm,RCSn)
c
c *********************************************************************
c  calculate remaining melt masses and compositions
c
c  zr mass - Eq 3.4 for scenario II, fzrrel will be read in as 0 for
c          scenarios I and III
c       zrm = fzrrel*zrm0*(1.-fzrox)
      zrm = .029*uo2m + fzrrel*((1.-fzrox)*zrm0-.029*uo2m)
c  zro2 mass - Eq 3.1
      zro2m = uo2m/uo2m0*zrm0*fzrox*123./91.
c  steel mass - combines Eq 3.5 for Scenario II & distribution for Scenario III
c      submergence as in NUREG/CR-6075
c       stlm = stlmul*stlmlp*(uo2m+zro2m+15000.+zrm+crmm)
c    1                  /(10400.*.82*vlp) + stlmi
c      submergence as commented on by INEL
      stlm = stlmlp*
     1      (uo2m/10400.+zro2m/5900.+10000./9660.
     2      +zrm/6500.+crmm/9250.)/vlp + stlmi
c  mass of steel constituents
      fem   = .7206 * stlm
      crm   = .1912 * stlm
      nim   = .0882 * stlm
c  other masses from experiment analyses
      alm = 0.
      al2o3m = 0.
c  total mass of debris ejected from vessel and mass fractions
      dmass = uo2m+zrm+zro2m+stlm+crmm
      FDMASS(1) = uo2m/dmass
      FDMASS(2) = zro2m/dmass
```

```
      FDMASS(3) = zrm/dmass
      fmstl = stlm/dmass
      FDMASS(4) = .7206*fmstl
      FDMASS(5) = .1912*fmstl
      FDMASS(6) = .0882*fmstl
      FDMASS(7) = crmm/dmass
      FDMASS(8) = 0.
      FDMASS(9) = 0.
c
c ***********************************************************************
c containment atmosphere conditions
c
c total moles in containment from ideal gas law
      rcbn  = prcb * vrcb / (8.3143 * trcb)
c moles of h2 released to containment
      h2rcbn = h2genn - h2rcsn
c fatm is mole fractions in order - o2,n2,h20,h2,ar,co2
      fatm(4)=h2rcbn/rcbn
c assume negligible steam at operating conditions. In air, moles of N2 =
c 3.76 * moles O2, so moles of O2 at operating conditions are
c (prcboc * vrcb)/(4.76*r*trcboc). Moles of o2 remain unchanged during
c transient, so o2 mole fraction at vessel breach is
      fatm(1)=(prcboc*trcb)/(4.76*trcboc*prcb)
c moles of n2 = 3.76 * moles of o2
      fatm(2)=3.76*fatm(1)
      fatm(3)=1. - fatm(4) - fatm(1) - fatm(2)
      fatm(5)=.0000
      fatm(6)=.0000
c heat capacity of containment atmosphere
      cv = fatm(1)*25.9+fatm(2)*24.1+fatm(3)*32.4+fatm(4)*21.2
c
c ***********************************************************************
c calculate ablated hole size
       CALL ABLATE(UO2m,ZRO2m,ZRm,FEm,CRm,NIm,crmm,al2m,al2o3m,
     1            DH0,TW0,TLHEAD,PRCS,Prcb,TDEB,DHOLE)
c
c ************************************************************************
c coherence ratio calculation - lower head hole area, coherence ratio
      ahole = 3.14159*dhole*dhole*.25
      tcoh = cohmul*fdisp*(trcs/tdeb)**.25*
     1       sqrt(0.6*dmass/rcsm*ahole*vcav**.33333/vrcs)*(1.+cohdis)
      tcoh = amax1(0.,tcoh)
c
c debris mass ejected from cavity
      dmass = dmass * fejec * fdisp
c
c ************************************************************************
```

```
c get melt properties
c
      call meltprp(dmw,indeb,der,det,stoic,cd,f,dmass,tdeb,fdmass)
c
c ***********************************************************************
c calculate DCH load
c
      call twocell(pfrcb,etasub,etadm,etaeff,
     $  det,der,stoic,deh2,cd,
     $  prcs,vrcs,trcs,rcsn,yh2,ystm,gamma,
     $  indeb,tdeb,tcoh,
     $  prcb,trcb,rcbn,vrcb,awall,h2rcbn,cv,
     $  fasub,fvsub,
     $  f,fatm,tautoig,tfrcb)
c
c ***********************************************************************
c calculate containment failure probability (each observation will either
c   be 0 or 1
      if (pfrcb .lt. pfail) then
        cfp = 0.
      else
        cfp = 1.
      end if
c
c sum up number of times containment failed
      cfpsum = cfpsum + cfp
c
c ***********************************************************************
c write out variables in LHS format
c
      If(iplot.eq.1) then
        write(72,*)iloop,5,dhole,tcoh,pfrcb,tfrcb,cfp
      elseif(iplot.eq.2) then
        dhle(iloop) = dhole
        tch(iloop) = tcoh
        pfr(iloop) = pfrcb
        tfr(iloop) = tfrcb
        cf(iloop) = cfp
      endif
 1000 continue
c
c Determine which plot package being used and plow ahead accordingly
c
      if(iplot.eq.2) then
        call sift(dhle,nobs)
        call sift(tch,nobs)
        call sift(pfr,nobs)
```

```
          call sift(tfr,nobs)
          call sift(cf,nobs)
          tab = char(9)
          write(72,2000)
2000      format(6x,'CP',14x,'DHOLE',14x,'TCOH',14x,'PFRCB',
   $          13x,'TFRCB',14x,'CFP')
          do 2001 io = 1,nobs
               cp(io) =(io-1.0)/(nobs-1.0)
               write(72,2002)cp(io),tab,dhle(io),tab,tch(io),
   $                tab,pfr(io),tab,tfr(io),tab,cf(io)
2002      format(1pe12.4,(5(a,1pe12.4)))
2001      continue
        endif
c
c  containment failure probability
        cfp = cfpsum / float(nobs)
c write out cfp to screen
        write(*,*)' Containment failure probability is
        write(*,*) cfp
        stop
   31 print 401
  401 format(' error opening input file')
      stop
c   32 print 402
c  402 format(' error reading from input.file')
c      stop
   33 print 403
  403 format(' error in opening output file')
        stop
        end
c#######################################################################
c#######################################################################
        subroutine twocell(pfrcb,etasub,etadm,etaeff,
     $    det,der,stoic,deh2,cd,
     $    prcs,vrcs,trcs,nrcs,yh2,ystm,gamma,
     $    indeb,tdeb,tcoh,
     $    prcb,trcb,nrcb,vrcb,awall,nh2rcb,cv,
     $    fasub,fvsub,
     $    f,fatm,tautoig,tgmax)
c
c calc  pfrcb = final containment pressure due to DCH
c
c  dictionary of pass-thru variables
c     pfrcb = final pressure in RCB following DCH, MPa
c     etasub= DCH efficiency of subcompartment
c     etadm = DCH efficiency of dome
c     etaeff= total effective DCH efficiency
```

```
c     det   = specific molar internal energy debris, J/mole
c     der   = specific molar oxidation energy of debris, J/mole
c     stoic = mole of h2 produced per mole of debris
c     deh2  = molar combustion energy of hydrogen, J/mole
c     cd    = molar specific heat of debris, J/mole/K
c     prcs  = initial pressure of RCS, MPa
c     vrcs  = volume of RCS, M**3
c     trcs  = initial temperature of RCS, K
c     nrcs  = moles of gas in RCS, moles
c     yh2   = mole fraction of H2 in the RCS
c     ystm  = mole fraction steam in the RCS
c     gamma = specific heat ration for the RCS
c             and the containment atmosphere
c     indeb = moles of debris participating in DCH, moles
c     tdeb  = initial debris temperature, K
c     tcoh  = coherence ratio
c             entrainment time / characteristic blowdown time
c             about twice UCSB tau-m/tau-s
c     prcb  = initial pressure in RCB, MPa
c     trcb  = initial RCB temperature, K
c     nrcb  = moles of gas initially in RCB, moles
c     vrcb  = volume of rcb, m**3
c     awall = surf area in dome region, m**2
c     nh2rcb= moles of hydrogen in the RCB, moles
c     cv    = molar heat capacity of containment atmosphere, J/mole/K
c     fasub = fraction of dispersed debris going to subcompartment
c     fvsub = volume fraction of the subcompartment
c     f     = mole fraction of debris species
c             uo2,zro2,zr,fe,cr,ni,al2o3,al
c     fatm  = atm species mole fract
c             o2,n2,h2o,h2,ar,co2
c     tautoig = auto ignition temperature, K
c     tgmax = final containment temperature, K
c
c
      implicit real (a-z)
      dimension f(8),fatm(6),stc(8)
c
c species stoichometry mole H2 / mole reactant
      data stc / 0., 0., 2., 1., 1.5, 0., 0., 1.5/
c
c*****************************************************************
c some defined quantities
c*****************************************************************
c
c fraction of blowdown gas coherent with debris dispersal
      fblow = 1.-(1.+(gamma-1.)/2.*tcoh)**(-2./(gamma-1.))
```

```
c
c  total debris heat capacity
      ncd = indeb * cd
c
c  heat capacity ratio - global
      psi = ncd / ( (nrcb + nrcs) * cv)
      psi1 = psi+1.0
c
c  fraction of flow area to dome and dome volume fraction
      fadm = 1.0 - fasub
      fvdm = 1.0 - fvsub
c
c  heat capacity ratio in subcompartment
      ngsink = amax1((fvsub * nrcb),(fasub * nrcs * fblow))
      tsink = (fasub*nrcs*fblow*trcs + fvsub*nrcb*trcb)/
     1        (fasub*nrcs*fblow + fvsub*nrcb)
      tsnk2 = (fadm*fblow*nrcs*trcs + fvdm*nrcb*trcb)/
     1        (fadm*fblow*nrcs + fvdm*nrcb)
      psisub = (fasub * ncd)/ ngsink/cv
      psisub1 = psisub + 1.0
c
c  dome heat capacity ratio
      psidome = (fadm * ncd) /
     $        ( amax1 ( (fvdm*nrcb) , ( fadm*nrcs*fblow) ) * cv )
      psidm1 = psidome + 1.0
c
c  internal energy of RCB
      urcb = nrcb*cv*trcb
c
c
c*************************************************************************
c energy sources
c*************************************************************************
c
c  blowdown energy
      tdeblw = (prcs * vrcs) / (gamma -1.0)
c
c  debris thermal energy
      tdet = indeb * det
c
c  debris oxidation energy
      tder = indeb * der
c
c  hydrogen production
c
c  max h2 if all dispersed debris oxidized
      nh2max = stoic*indeb + yh2*nrcs + nh2rcb
```

```
c
c  moles of stm coherent with debris dispersal
      nstmcoh=ystm*fblow*nrcs + fblow*yh2*nrcs
c
c  max h2 prod by oxidizing entrained reactive metals
      nh2rm=(stc(3)*f(3)+stc(5)*f(5)+stc(8)*f(8))*indeb
c
c  stm/rm limit determines actual h2 produced by rm
      nh2rm= amin1(nstmcoh,nh2rm)
c
c  stm/fe ratio after reactive metals have reacted
      if(f(4) .le. 0.) then
         dstmfe=1.e6
         dh2fe=1.e6
      else
         dstmfe=(ystm*fblow*nrcs-nh2rm)/(f(4)*indeb)
         dh2fe=(yh2*fblow*nrcs+nh2rm)/(f(4)*indeb)
      end if
      dstmfe=amax1(1.e-6,dstmfe)
c
c  equilibrium constant at 2300 K
      eqk=2.1
c
c  solve for fraction of fe oxidized
      da1=.5*eqk/(eqk-1.)*(1.+dstmfe+dh2fe/eqk)
      da2=4.*(eqk-1.)/eqk*dstmfe/(1.+dstmfe+dh2fe/eqk)**2
      xfeo=da1*(1.-sqrt(1.-da2))
c
c  total h2 produced by metal oxidation
      nh2ox=nh2rm+xfeo*stc(4)*f(4)*indeb
c
c********first pass ****************************************
c estimate dome temperature without auroignition or deflagration
c
c  fract of h2 in sub that can burn as a jet
c  blowoff criteria - NTS tests
      xo2crt=.05
      if(fatm(1) .lt. xo2crt) then
         fjet=0.
      else
         fjet=1.
      end if
c
c  fract of preexisting h2 in dome burned
c  entrainment only
      dtest=2*fatm(1)-fatm(4)
      if(dtest .lt. 0.) then
```

```
         fpreh2=0.
      else
         fpreh2=fjet*(nrcs*yh2*fblow+nh2ox)
     1          /nrcb/dtest
      end if
c
c  fract of all possible h2 burned
      fburn=(fjet*(nrcs*yh2*fblow+nh2ox)
     1       +fpreh2*fatm(4)*nrcb)/nh2max
c
c  o2 limit to h2 combustion
      fburn=amin1(fburn,(2.*fatm(1)*nrcb/nh2max))
c
c  total possible hydrogen combustion energy
      tdeh2 = deh2 * nh2max
c
c  total possible energy
      totde = tdeblw + tdet + tder + tdeh2
c
c  subcompartment efficiency
      etasub=fasub*psi1/psisub1*
     $      (1.-tdeh2/totde-tdet/totde*(tsink-298.)/(tdeb-298.))
c
c  dome efficiency
      etadm=psi1/psidm1
     $      *(fadm*(1.-tdeh2/totde)+fburn*tdeh2/totde
     1          -tdet/totde*(tsnk2-298.)/(tdeb-298.))
c
c  effective two-cell efficiency
      etaeff=etasub+etadm
c
c  pressure rise in the containment
      deltap = etaeff * prcb * (totde / ( urcb * (1.0 + psi)))
c
c  final equilibrium pressure
      pfrcb = prcb + deltap
c
c  max dome temp without voulumetric combustion
      tgmax=nrcb/(nrcb+nrcs)*pfrcb/prcb*trcb
c
c******** second pass ******************************************
c dch with possible autoignition and deflagration
c
c  fract of h2 in sub that can burn as a jet
c  blowoff criteria - NTS tests
      xo2crt=.05
      if(fatm(1) .lt. xo2crt) then
```

```
         fjet=0.
      else
         fjet=1.
      end if
c
c  fract of preexisting h2 in dome burned
c  entrainment only
      dtest=2*fatm(1)-fatm(4)
      if(dtest.lt. 0.) then
         fpreh2=0.
      else
         fpreh2=fjet*(nrcs*yh2*fblow+nh2ox)
     1          /nrcb/dtest
      end if
c  fraction of prexistion hydrogen in dome that can burn
c    as a deflagration on DCH time scales
c  deflagration basis ********************************************
c    well mixed atmosphere
c    post blowdown steam and hydrogen concentrations
c    combustion completeness and flame speed based bulk atm temp
c    structure ht based on bulk avg temp
      dum = nrcs/nrcb
      dumbotm = 1. + (1.-fblow)*yh2*dum + (1.-yh2)*dum
      xh2dum = (fatm(4) + (1.-fblow)*yh2*dum)/dumbotm
      xstmdum = (fatm(3) + (1.-yh2)*dum)/dumbotm
c  combustion efficiency
      xup = .037 + .02381*xstmdum - 5.e-5*(tgmax-373.)
      xdwn = .075 + .02381*xstmdum - 1.0135e-4*(tgmax-373.)
      xup = max(xup,0.)
      xdwn = max(xdwn,1.e-6)
      burneff = (xh2dum-xup)/(xdwn-xup)
      burneff = min(burneff,1.0)
      burneff = max(burneff,1.0e-6)
      xinert = .63 + 3e-4*(tgmax-373.)
      xinert = min(xinert,1.)
      if(xstmdum .ge. xinert) burneff=1.0e-6
c  heat transfer rate
      htrate = 5.67e-8*.8*3.1415*(6./3.1415*vrcb)**.666*tgmax**4
c  h2 burn energy release rate
      hdome = (6./3.1415*vrcb)**.333
      fvft = (tgmax/373.)**.333
c  flame speed in quiesent environment
      xupvf = .036 - 5.e-5*(tgmax-373.)
      xupvf = max(xupvf,0.0)
      vflame = 23.7*hdome**.333*(xh2dum/(1.-xstmdum) - xupvf)
     1        *exp(-4.877*xstmdum*(1.+.61677*xstmdum))*fvft
c  flame speed in turbulent environment
```

```
c       xupvf = .021 - 5.e-5*(tgmax-373.)
c       xupvf = max(xupvf,0.0)
c       vflame = 59.65*hdome**.333*(xh2dum/(1.-xstmdum) - xupvf)
c     1        *exp(-4.877*xstmdum*(1.+.61677*xstmdum))*fvft
c
      vflame = max(vflame,1.e-6)
      h2rate = burneff*(1.-fpreh2)*fatm(4)*nrcb*2.4e5/hdome*vflame
c total fraction of prexisting h2 that is entrained or deflagrates
      fpreh2 = fpreh2+(1.-fpreh2)*burneff*(1.-min((htrate/h2rate),1.))
      dumpre = (1.-fpreh2)*burneff*(1.-min((htrate/h2rate),1.))
      write(6,1919) nrcs,nrcb
1919  format(1x,8(1p,e8.2,1x),e7.1)
c
c deflagration basis ******************************************
c   stratified atmosphere
c   pre blowdown steam and hydrogen concentrations
c   combustion completeness and flame speed based init atm temp
c   structure ht based on bulk avg temp
c       xh2dum = fatm(4)
c       xstmdum = fatm(3)
c combustion efficiency
c       xup = .037 + .02381*xstmdum - 5.e-5*(trcb-373.)
c       xdwn = .075 + .02381*xstmdum - 1.0135e-4*(trcb-373.)
c       xup = max(xup,0.)
c       xdwn = max(xdwn,1.e-6)
c       burneff = (xh2dum-xup)/(xdwn-xup)
c       burneff = min(burneff,1.0)
c       burneff = max(burneff,1.0e-6)
c       xinert = .63 + 3e-4*(trcb-373.)
c       xinert = min(xinert,1.)
c       if(xstmdum .ge. xinert) burneff=1.0e-6
c heat transfer rate
c       htrate = 5.67e-8*.8*3.1415*(6./3.1415*vrcb)**.666*tgmax**4
c h2 burn energy release rate
c       hdome = (6./3.1415*vrcb)**.333
c       fvft = (tgmax/373.)**.333
c flame speed in quiesent environment
c       xupvf = .036 - 5.e-5*(tgmax-373.)
c       xupvf = max(xupvf,0.0)
c       vflame = 23.7*hdome**.333*(xh2dum/(1.-xstmdum) - xupvf)
c     1        *exp(-4.877*xstmdum*(1.+.61677*xstmdum))*fvft
c flame speed in turbulent environment
c       xupvf = .021 - 5.e-5*(tgmax-373.)
c       xupvf = max(xupvf,0.0)
c       vflame = 59.65*hdome**.333*(xh2dum/(1.-xstmdum) - xupvf)
c     1        *exp(-4.877*xstmdum*(1.+.61677*xstmdum))*fvft
c
```

```
c       vflame = max(vflame,1.e-6)
c       h2rate = burneff*(1.-fpreh2)*fatm(4)*nrcb*2.4e5/hdome*vflame
c  total fraction of prexisting h2 that is entrained or deflagrates
c       fpreh2 = fpreh2+(1.-fpreh2)*burneff*(1.-min((htrate/h2rate),1.))
c
c
c  jet entrainment, deflagration, plus volumetric combustion

      if (tgmax .ge. tautoig) fpreh2=1.
c
c  fract of all possible h2 burned
      fburn=(fjet*(nrcs*yh2*fblow+nh2ox)
     1       +fpreh2*fatm(4)*nrcb)/nh2max
c
c  o2 limit to h2 combustion
      fburn=amin1(fburn,(2.*fatm(1)*nrcb/nh2max))
c
c  subcompartment efficiency
      etasub=fasub*psi1/psisub1*
     $       (1.-tdeh2/totde-tdet/totde*(tsink-298.)/(tdeb-298.))
c
c  dome efficiency
      etadm=psi1/psidm1
     $       *(fadm*(1.-tdeh2/totde)+fburn*tdeh2/totde
     1         -tdet/totde*(tsnk2-298.)/(tdeb-298.))
c
c  effective two-cell efficiency
      etaeff=etasub+etadm
c
c  pressure rise in the containment
      deltap = etaeff * prcb * (totde / ( urcb * (1.0 + psi)))
c
c  final equilibrium pressure
      pfrcb = prcb + deltap
c
c  max dome temp with voulumetric combustion
      tgmax=nrcb/(nrcb+nrcs)*pfrcb/prcb*trcb
      return
      end
C#######################################################################
      SUBROUTINE
ABLATE(MUO2,MZRO2,MZR,MFE,MCR,MNI,MCRM,MAL,MAL2O3,
     1          DH0,TW0,LHEAD,PRCS,PRCB,TDEBRIS,DHF)
C
C  THIS PROGRAM CALCULATES THE FINAL HOLE AFTER ABLATION
C
C DICTIONARY OF TERMS ***
```

```
C  MUO2 = UO2 MASS
C  MZRO2 = ZrO2 MASS
C  MZR = Zr MASS
C  MFE = Fe MASS
C  MCR = Cr MASS
C  MNI = Ni MASS
C  MAL = AL MASS
C  MAL2O3 = AL2O3 MASS
C  MCRM = MASS OF CONTROL ROD MATERIAL, TREATED LIKE NICKLE
C  DH0 = INITIAL HOLE DIAMETER
C  TW0 = INITIAL TEMPERATURE OF RPV LOWER HEAD
C  LHEAD = THICKNES OF THE RPV LOWER HEAD
C  PRCS = INITIAL RCS PRESSURE
C  TRCB = INITIAL CONTAINMENT PRESSURE
C  TDEBRIS = TEMPERATURE CORE DEBRIS
C  DHF = FINAL HOLE DIAMETER
C  MASS(I) = MATRIX OF MELT MASSES BY SPECIES
C  MW(I) = MATRIX OF MELT MOLECULAR WEIGHTS BY SPECIES - KG/GMOLE
C  FV(I) = MATRIX OF VOLUME FRACTIONS
C  FM(I) = MATRIX OF MASS FRACTIONS
C  FN(I) = MATRIX OF MOLE FRACTIONS
C  K(I) = MATRIX OF MELT THERMAL CONDUCTIVITIES BY SPECIES
C  CP(I) = MATRIX OF MELT SPECIFIC HEATS BY SPECIES
C  VISC(I) = MATRIX OF MELT VISCOSITIES BY SPECIES
C  MTOT = TOTAL MELT MASS
C  VTOT = TOTAL MELT VOLUME
C  NTOT = TOTAL MELT MOLES
C  KM = EFFECTIVE MELT THERMAL CONDUCTIVIETY
C  RHOM = EFFECTIVE MELT DENSITY
C  CPM = EFFECTIVE MELT SPECIFIC HEAT
C  VISCM = EFFECTIVE MELT VISCOSITY
C  VELM = MELT DISCHARGE VELOCITY
C  RE = REYNOLDS NUMBER
C  PR = MELT PRANDTL NUMBER
C  HCOEF = HEAT TRANSFER COEFFICIENT
C  DDOT = ABLATION RATE
C  BETA = CORRECTION FACTOR DUE TO RAPID ABLATION
C  TAUM = CHARACTERISTIC DISCHARGE TIME ASSUMING NO ABLATION
C  TAUD = CHARACTERISTIC TIME FOR ABLATION TO DOUBLE THE HOLE
DIAMETER
C  TIME = ACTUAL MELT DISCHARGE TIME
C  KS = RPV STEEL THERMAL CONDUCTIVITY
C  RHOS = RPV STEEL DENSITY
C  CPS = RPV STEEL SPECIFIC HEAT
C  TMPS = RPV STEEL MELTING TEMPERATURE
C  HFS = RPS STEEL HEAT OF FUSION
C
```

```
      DIMENSION MASS(9), MW(9), FV(9),FM(9),FN(9),K(9)
      DIMENSION RHO(9), CP(9),VISC(9)
C
      REAL MUO2,MZRO2,MZR,MFE,MCR,MNI,MCRM,MAL,MAL2O3,
     1    MTOT,NTOT,MASS,MW,K,KM,LHEAD
C
C  MELT SPECIES
C          UO2    ZrO2    Zr    Fe    Cr    Ni   CRM  AL  AL2O3
C
      DATA MW
     1     /.270; .123, .091, .056, .052, .059, .059, .027, .102/
      DATA K
     1     /5.6, 3.0, 4.0, 38.5, 19.4, 60.0, 60.0, 115., 6./
      DATA RHO
     1     /9090.,4760.,5810.,6500.,6036.,7500.,7500.,1831.,2700./
      DATA CP
     1     /465.,942.,465.,852.,859.,750.,750.,1321.,1600./
      DATA VISC
     1     /1.50E-2,1.50E-2,1.50E-2,3.25E-3,2.87E-3,2.16E-3,
     2     2.16E-3,2.69E-4,2.91E-2/
C
C  RPV STEEL PROPERTIES
C
      RHOS = 7514.
      CPS = 720.
      TMPS = 1700.
      HFS = 2.68E5
C
C  HARDWIRE LIQUID PHASE DISCHARGE COEFFICIENT
C
      CDISCH = .6
C
C  FILL THE MASS MATRIX
C
      MASS(1) = MUO2
      MASS(2) = MZRO2
      MASS(3) = MZR
      MASS(4) = MFE
      MASS(5) = MCR
      MASS(6) = MNI
      MASS(7) = MCRM
      MASS(8) = MAL
      MASS(9) = MAL2O3
C
C  CALCULATE MASS, VOLUME, AND MOLES OF ALL MELT SPECIES
C
      MTOT = 0.
```

```
      VTOT = 0.
      NTOT = 0.
      DO I=1,9
         MTOT = MTOT + MASS(I)
         VTOT = VTOT + MASS(I)/RHO(I)
         NTOT = NTOT + MASS(I)/MW(I)
      ENDDO
C
C  CALCULATE MASS, VOLUME, MOLE FRACTIONS
C
      DO I=1,9
         FM(I) = MASS(I)/MTOT
         FV(I) = MASS(I)/RHO(I)/VTOT
         FN(I) = MASS(I)/MW(I)/NTOT
      ENDDO
C
C  CALCULATE THE EFFECTIVE MIXTURE PROPERTIES OF THE MELT
C
      KM = 0.
      RHOM = 0.
      CPM = 0.
      VISCM = 0.
      DO I=1,9
C        CONDUCTIVITY - SERIAL RESISTANCE
         KM = KM + K(I)*FV(I)
C        DENSITY - VOLUME WEIGHTED
         RHOM = RHOM + RHO(I)*FV(I)
C        HEAT CAPACITY - MASS WEIGHTED
         CPM = CPM + CP(I)*FM(I)
C        VISCOSITY - KENDAL MOORE, VANESA
         VISCM = VISCM + VISC(I)**.333*FN(I)
      ENDDO
      VISCM = VISCM**3
C
C  CALCULATE MELT VELOCITY
C
      VELM = CDISCH*SQRT(2.*(PRCS-PRCB)/RHOM)
C
C  CALCULATE UNMODIFIED HEAT TRANSFER COEFFICIENT
C
      RE = RHOM*VELM*LHEAD/VISCM
      PR = CPM*VISCM/KM
      HCOEF = .0292*KM/LHEAD*RE**.8*PR**.33
C
C  CALCULATE UNMODIFIED HEAT TRANSFER COEFFICIENT
C
      DDOT = 2.0*HCOEF*(TDEBRIS-TMPS)/
```

```
     1       (RHOS*(CPS*(TMPS-TW0) + HFS))
C
C  CALCULATE MODIFIED HEAT TRANSFER COEFFICIENT
C
      BETA = RHOS*CPS*DDOT/2./HCOEF
      HCOEF = HCOEF*BETA/(EXP(BETA) - 1.)
C
C  CALCULATE MODIFIED ABLATION RATE
C
      DDOT = 2.0*HCOEF*(TDEBRIS-TMPS)/
     1       (RHOS*(CPS*(TMPS-TW0) + HFS))
C
C  MELT DISCHARGE TIME WITHOUT ABLATION
C
      TAUM = MTOT/(RHOM*3.1315/4.*DH0**2*VELM)
C
C  CHARACTERISTIC TIME FOR ABLATION TO DOUBLE HOLE DIAMETER
C
      TAUD = DH0/DDOT
C
C  ACTUAL MELT DISCHARGE TIME WITH ABLATION
C
      TIME = TAUM/(1.0 + .6934*(TAUM/TAUD)**.666)
C
C  CALCULATE FINAL HOLE DIMETER
C
      DHF = DH0 + DDOT * TIME
C
C  ALL DONE
C
      RETURN
      END
C#######################################################################
C#########################################################################
      SUBROUTINE RCSPRP(PRCS,VRCS,TRCS,YN2,YH2,fgmh2,fgmSTM,MRCS,NRCS)
C
C  COMPUTE THE NUMBER OF GAS MOLES IN THE RCS
C  COMPUTE THE MASS OF RCS GAS
C
C  DICTIONARY
C    PRCS = RCS PRESSURE
C    TRCS = RCS TEMPERATURE
C    VRCS = RCS VOLUME
C    YSTM = FRACTION OF RCS PRESSURE ATTRIBUTED TO STEAM
C    YH2  = FRACTION OF RCS PRESSURE ATTRIBUTED TO HYDROGEN
C    YN2 = FRACTION OF RCS PRESSURE ATTRIBUTED TO NITROGEN
C    MRCS = TOTAL GAS MASS IN RCS
```

```
C   NRCS = TOTAL MOLES OF GAS IN THE RCS
C   NRCSSTM = MOLES OF STEAM IN THE RCS
C   NRCSH2 = MOLES OF HYDROGEN IN RCS
C   NRCSN2 = MOLES OF NITROGEN IN RCS
C   ZFACT = COMPRESSIBILITY FACTOR ACCOUNTING FOR NONIDEAL GAS
C         BEHAVIOR OF STEAM
C   VCOEF = VIRIAL COEFFICIENT
C   FGMH2 = MOLE FRACTION H2
C   FGMSTM = MOLE FRACTION STEAM
C   FGMN2 = MOLE FRACTION NITROGEN
C
    REAL MRCS,NRCS,NRCSSTM,NRCSH2,NRCSN2
C
C RCS CAN CONSIST OF THREE GASES:STEAM, H2, AND N2
C   COMPUTE N2 FRACTION
C
    YSTM = 1. - YN2 - YH2
C
C # MOLS OF STEAM IN THE GAS STATE IN THE RCS (NSTM)
C USE ZFACT TO CORRECT FOR NON IDEAL GAS LAW EFFECTS FOR SAT
STEAM
C ZFACT COMPUTED FROM VIRIAL EQ OF STATE
C     CONSTANTS REQ TO COMPUTE VIRIAL COEFF
        DUMC1=2.0624
        DUMC2=2.61204
        DUMC3=.1008
        DUMC4=.0349
        DUMT=1000./TRCS
        DUMPSI=DUMC3*DUMT**2/(1+DUMC4*DUMT**2)
C     COMPUTE THE VIRIAL COEF (cm**3/g)
        VCOEF=DUMC1-DUMC2*DUMT*10.**DUMPSI
C     CONVERT TO MORE USEFUL UNITS (m**3/mole)
        VCOEF=VCOEF*1.E-3*.018
        IF((YSTM*PRCS) .LE. 1.E5) VCOEF=9.99E10
C     NOW COMPUTE THE ZFACT
        ZFACT = .5*(1.+SQRT(1.+4.*YSTM*PRCS/8.314/TRCS*VCOEF))
C
C TOTAL MOLES OF H2 IN RCS
        NRCSH2 = (YH2*PRCS * VRCS) / (8.314 * TRCS)
C TOTAL MOLES OF STM IN RCS
        NRCSSTM = (YSTM*PRCS * VRCS) / (8.314 * TRCS) / ZFACT
C TOTAL MOLES OF N2
        NRCSN2 = (YN2*PRCS * VRCS) / (8.314 * TRCS)
C TOTAL MOLES ALL GAS IN RCS
        NRCS = NRCSH2 + NRCSSTM + NRCSN2
C
C COMPUTE MOLE FRACTIONS
```

```
C     H2
        FGMH2 = NRCSH2/NRCS
C     STM (H2O)
        FGMSTM = NRCSSTM/NRCS
C     N2
        FGMN2 = NRCSN2/NRCS
C
C  INITIAL MASS OF GAS IN THE RCS (kg)
C
      MRCS = NRCSh2*.002 + nrcsstm*.018 + nrcsn2*.028
C
C  ALL DONE
C
    RETURN
    END
C#######################################################################
C#######################################################################
      subroutine meltprp(mwd,indeb,der,det,stoic,cd,FDMOLE,
    $    massd,tdeb,FDMASS)
c
c  calculate effective material properties for the melt
c
c  dictionary of pass-thru variables
c     mwd   = effective molecular weight of the debris, kg/mol-deb
c     indep = moles of debris participating in DCH, mol-deb
c     der   = specific molar oxidation energy of debris, J/mol-deb
c     det   = specific internal energy of debris, J/mol-deb
c     stoic = mole of H2 produced per mole of debris oxidized
c     cd    = effective molar heat capacity of the debris
c     massd = mass of debris participating in DCH, kg
c     tdeb  = initial temperature of debris, K
C     FDMOLE() = MOLE FRACTION BY SPECIES
C     FDMASS() = MELT MASS FRACTIONS BY SPECIES
c
      implicit real (a-z)
     dimension FDMOLE(9),mw(9),hr(9),stc(9),cdeb(9),FDMASS(9)
C
c  melt speices order
c     uo2,  zro2,  zr,  fe,  cr,  ni,  al2o3,  al,  CRM
c  species molecuar weights kg/mole
     data mw / .270, .123, .091, .056, .052, .059, .102, .027, .052/
c  species reaction energies J/mol
     data hr / 0., 0., 5.98e5, 1.97e3, 2.07e5, 0., 0., 3.97e5, 0./
c species stoichometry mole H2 / mole reactant
     data stc / 0., 0., 2., 1., 1.5, 0., 0., 1.5, 0./
c species molar specific heats J/mol/K
     data cdeb / 126.55, 116.87, 42.315,
```

```
     $      47.712, 44.668, 44.25, 163.2, 35.667, 44.25/
c
c  compute effective molecular weight
      mwd = 0.
      do i=1,9
         mwd = mwd + FDMASS(i)/mw(i)
      enddo
      mwd = 1./mwd
c
c  compute moles of debris
      indeb = massd/mwd
c
c  compute mole fraction of each species
      do i=1,9
         FDMOLE(i) = FDMASS(i)*mwd/mw(i)
      enddo
c
c  compute specific oxidation energy
      der = 0.
      do i=1,9
         der = der + FDMOLE(i)*hr(i)
      enddo
c
c  compute effective stoichometric coefficient
      stoic = 0.
      do i=1,9
         stoic = stoic + FDMOLE(i)*stc(i)
      enddo
c
c  compute effective molar specific heat
      cd = 0.
      do i=1,9
         cd = cd + FDMOLE(i)*cdeb(i)
      enddo
c
c  compute specific molar internal energy
      det = cd*(tdeb-298.)
c
      return
      end
c#######################################################################
C***********************************************************************
C SUBROUTINE SIFT WILL SORT A VECTOR OF DATA IN INCREASING ORDER
C
      SUBROUTINE SIFT (XV,N)
      DIMENSION XV(N)
      M=N
```

```
10 M=M/2
   IF (M) 30,20,30
20 RETURN
30 K=N-M
   J=1
40 I=J
50 L=I+M
   IF (XV(I)-XV(L)) 70,70,60
60 A=XV(I)
   XV(I)=XV(L)
   XV(L)=A
   I=I-M
   IF (I) 70,70,50
70 J=J+1
   IF (J-K) 40,40,10
   END
```

APPENDIX C
A SCDAP/RELAP5 ANALYSIS SUPPORTING DCH ISSUE RESOLUTION FOR THE ZION PWR

D. L. Knudson
Idaho National Engineering Laboratory

C.1 INTRODUCTION

Molten core materials could be ejected into the containment building by a high pressure RCS (reactor coolant system) following reactor vessel failure during certain severe accidents. A rapid rise in containment temperature and pressure, or DCH (direct containment heating), could result from that HPME (high pressure melt ejection). In an extreme case, the pressurization associated with DCH could lead to containment failure. The potential for such a failure has driven a number of DCH-related studies, including this analysis to support resolution of the issue for the Zion PWR (pressurized water reactor). The support provided centers on a 'best-estimate' SCDAP/RELAP5 (Allison 1993) analysis of core damage progression and the behavior of the RCS during a station blackout without recovery and without operator actions.

A station blackout was considered because core damage and melting could occur, providing a potential for DCH that may or may not develop in many other postulated reactor accidents. Furthermore, it was assumed that the extent of core melting without recovery and without operator actions will reasonably bound conditions that could develop as a result of any other accident.

Analysis of RCS behavior was important because experimental results have indicated that natural circulation flows can develop without operator actions (Stewart 1986 and Stewart 1992). Those flows can redistribute core decay energy, which can lead to creep rupture failures in ex-vessel pressure boundaries (Bayless 1988 and Knudson 1993). [The surge line, the hot leg nozzles, the SG (steam generator) tubes, and the pressurizer PORVs (power operated relief valves) are the most vulnerable boundaries in the Zion PWR.] Depressurization through an accident-induced failure of the RCS pressure boundary prior to lower head failure could prevent or mitigate the severity of the HPME, and thereby reduce any associated threat to containment integrity.

And finally, an analysis of core damage progression was needed to determine melt mass, melt composition, melt temperature, and related data that can be used to develop initial conditions that contribute to containment loads. The analysis was performed using a realistic SCDAP/RELAP5 model to provide the best estimate of potential HPME conditions. A separate study of the results (and other appropriate information) is planned to determine if DCH is or is not expected to cause containment failure in the Zion PWR.

A detailed description of the SCDAP/RELAP5 model and the calculations performed is provided in Section C.2. SCDAP/RELAP5 results are given in Section C.3 while associated conclusions are summarized in Section C.4. Section C.5 contains a list of references.

C.2 SCDAP/RELAP5 ANALYSIS

The best-estimate SCDAP/RELAP5 analysis of a station blackout (without recovery and without operator actions) in the Zion PWR is described in this section. The Zion PWR is a Westinghouse-designed nuclear power station with a rated thermal power of 3250 MW_t. The core consists of 193 15x15 fuel assemblies with an active fuel height of approximately 3.66 m. There are four primary coolant loops. Each loop contains a U-tube SG, a RCP (reactor coolant pump), and associated piping. A single pressurizer is attached to the hot leg piping in one of the four loops. Two PORVs, with a combined capacity of 52.9 kg/s, can be used to relieve excess RCS pressure from the top of the pressurizer. One accumulator, with 24.1 m^3 of borated water at 325 K, is attached to each cold leg. The accumulators, which are initially pressurized to 4.24 MPa by a nitrogen cover gas, are the only operational part of the ECCS (emergency core cooling system) during a station blackout. A large, dry atmospheric containment building surrounds the reactor systems.

The specific station blackout sequence considered is designated TMLB'. This sequence is initiated by the loss of offsite power. Onsite AC (alternating current) power is also unavailable because the diesel generators fail to start or fail to supply power. Decay heat removal cannot be maintained in the long term because there is no AC power for the electrical pumps and the steam driven auxiliary feedwater pumps also fail to supply water. When the TMLB' sequence begins, power is lost to the control rod drives and pumps. A reactor scram follows, with coastdown of the main feedwater pumps and RCPs. Feedwater is quickly reduced to zero as the main feedwater valves close. The turbine stop valves close and the pressure in the SGs increase until the relief (or dump) valves open. SG pressures are maintained between the opening and closing pressures of

the relief valves thereafter. Water in the secondaries is completely vaporized as heat is transferred from the RCS to the SGs. Once water in the secondaries is depleted, the SGs no longer remove significant amounts of heat. Core decay energy then heats the RCS, resulting in system pressurization controlled by cycling pressurizer PORVs. The RCS pressure can also be influenced by RCP seal leaks, which could develop following the loss of seal cooling associated with the loss of AC power. After the RCS saturates, a high pressure boiloff begins, ultimately leading to core uncovery and heatup. Without recovery of power or equipment, the transient proceeds to severe core damage and melting.

SCDAP/RELAP5 is an integrated computer code designed for reactor accident analysis. It can be used to simulate a very wide variety of system transients of interest in reactor safety, but it is specifically designed to calculate RCS behavior during severe accidents. SCDAP/RELAP5 was developed by incorporating coding from SCDAP (Berna 1984), TRAP/MELT (Jordan 1985), and COUPLE (Lemmon 1980) into RELAP5 (Allison 1990). SCDAP provides coding for simulation of the reactor core, including logic for oxidation, hydrogen generation, ballooning and rupture of the fuel rod cladding, fission product release, fuel and cladding liquefaction, flow and freezing of liquefied core materials, and associated geometry changes. TRAP/MELT allows simulation of fission product transport and deposition, including aerosol agglomeration, deposition, evaporation, condensation, and the chemisorption of vapors by stainless steel. COUPLE provides coding for two-dimensional, finite-element heat conduction/convection calculations at user specified locations. Such detailed thermal simulation is typically used to represent molten regions in the core and/or lower head. And finally, RELAP5 contains coding to allow simulation of fluid behavior throughout the system, as well as the thermal behavior of structures outside the core, based on a one-dimensional, two-fluid, nonequilibrium, six-equation hydrodynamic representation. Feedbacks between all parts of the code have been developed to allow an integral analysis capability. The user can then provide model input to activate those parts of the code necessary to simulate the problem of interest.

Three different SCDAP/RELAP5 transient calculations were completed in this analysis. Each of the calculations required the use of (1) RELAP5 to simulate thermal-hydraulics and heat transfer affecting the plant structural mass; (2) SCDAP to simulate core components during degradation, melt, and relocation to the lower reactor vessel head; and (3) COUPLE to represent the lower head during thermal attack by relocated core materials. Generic input for each of those modules is described in Sections C.2.1, C.2.2, and C.2.3, respectively. Input necessary to distinguish each of the transient calculations is discussed in Section C.2.4. And finally, steady

state conditions (developed as a starting point for all transient calculations) are described in Section C.2.5.

Before those sections are given, it should be noted that Release B of MOD3.1, with updates, was used to complete all calculations in this analysis. The updates included (1) logic to allow user-defined relocation of in-vessel stainless steel into an in-core molten pool or the lower head (as appropriate), (2) logic to allow user control of core relocation to the lower head based on crust stability on the core periphery, and (3) minor error corrections that have been added to subsequent versions.

C.2.1 RELAP5 Input

RELAP5 input was used to develop a model to represent the thermal-hydraulics of the reactor vessel, all four primary coolant loops, the pressurizer, all four SGs, and selected parts of the secondary systems. The corresponding nodalization for the reactor vessel is shown in Figure C.1. As indicated, five parallel flow channels (with cross connections) extend from the lower plenum through the core to the upper reactor vessel head. If the appropriate conditions exist, this nodalization will allow development of in-vessel natural circulation. Core components, which will be discussed in detail in Section C.2.2, are represented by the shaded regions. Heat structures, which are represented by those areas filled with slanted lines, were included to simulate the structural mass of the reactor vessel walls, the core barrel and baffle, the thermal shield, the upper and lower core plates, and other structures in the upper and lower plena. The external surfaces of all structures were assumed to be adiabatic, with the exception of the lower reactor vessel head as discussed in Section C.2.3.

Modeling provisions were made to monitor the temperature of upper plenum stainless steel structures in all calculations. If a given structure temperature reached the melting point, that structure was relocated to the in-core molten pool (if one existed) or to the lower head through user-defined slumping input. (As previously indicated, user-defined slumping input was added to Release B of SCDAP/RELAP5/MOD3.1 for this analysis.) In addition, a modeling approximation was developed to account for thin (cross-section) stainless steel structures in the lower head that would be expected to melt as a result of being submerged in relocated core materials. Specifically, it was estimated that there is about 10 mt of thin stainless steel in the lower head of the Zion PWR. An assumption that the thin steel was a linear function of height (between the bottom of the lower head and the bottom of the core) and the depth of relocated debris was used to estimate the

amount of thin stainless steel that would be expected to melt. The appropriate mass was then added to the lower head debris through the user-defined slumping input.

The Zion PWR has a downcomer bypass configuration, which means that a portion of the total downcomer flow can pass through holes in the core barrel (just below the upper core plate) and flow downward toward the lower plenum through a region between the core barrel and baffle. Upon reaching the lower plenum, the downcomer bypass flow rejoins the bulk flow before turning upward through the core. The corresponding bypass flow path was modeled by Component 505 as shown in Figure C.1.

A junction connecting the top of the downcomer (Component 502) to the upper plenum (Component 582) at the hot leg elevation is shown in Figure C.1. This junction represents a small leak path associated with clearances between the hot leg nozzles (which are welded to the reactor vessel wall) and the internal hot leg piping (which is welded to the core barrel). The resulting gap in the hot leg piping, which allows some flow to bypass the core, is a design requirement to allow removal of the core internals.

Nodalizations of the primary coolant loop containing the pressurizer are shown in Figures C.2 and C.3. With the exception of the pressurizer and associated surge line piping, similar nodalizations were included in the model to separately represent the other three primary coolant loops in the Zion PWR.

As indicated in Figures C.2 and C.3, both fluid volumes and heat structures were included to represent the primary coolant loop piping, the pressurizer and associated surge line, and the SG with associated relief valves. Without AC power, accumulators are the only part of the ECCS that required simulation. The SG main feedwater system and associated piping were only needed to establish steady-state conditions prior to transient initiation. Auxiliary feedwater systems were not modeled because they are not operational in the subject transient. The external surfaces of all heat structures were assumed to be adiabatic. Relative elevations for the reactor vessel and primary coolant loop models (referenced to the bottom of the lower head) are listed in Table C.1.

Model input was included in all calculations to track the potential for creep rupture failures in the surge line, hot leg nozzles, and SG tubes. Consistent with the best-estimate approach of this analysis, a break was introduced at the appropriate location in the RCS pressure boundary if rupture was predicted. However, the break size was assumed to be constant at

0.02164 m^2 regardless of where the rupture occurred. That break size was derived from a previous Surry study where creep rupture failure was estimated to result in a break that was approximately 32.3% of the surge line flow area (Bayless 1988). The constant break area used was calculated by applying that fraction to the Zion surge line flow area of 0.06700 m^2. Obviously, this flow area would be too large to represent creep rupture failure of a SG tube. However, scoping calculations indicated that SG tube failures will not occur prior to lower head failure. Other uncertainties associated with this simplification, which will be discussed in Section C.3.4, are not expected to be significant with respect to resolution of the DCH issue for the Zion PWR.

A single valve was used to represent both pressurizer PORVs in the Zion PWR. The valve was appropriately sized to provide the combined flow capacity of the PORVs. Similarly, a single valve was used to represent all three pressurizer SRVs (safety relief valves), although the SRVs were not challenged in this analysis. It was assumed that plant air and battery power were sufficient to operate the PORVs throughout all calculations. Furthermore, the potential for other PORV failure modes was not considered.

Valves were also used to allow simulation of RCP seal leaks. As indicated in Figures C.2 and C.3, leaks were modeled at the discharge elevation of each RCP. (SCDAP/RELAP5 allows only one connection to a pump outlet. However, the inlet of the connected pipe is hydraulically equivalent to the RCP outlet in the code.) The relationship between transient time and valve flow areas used to model seal leakage in this analysis is described in Section C.2.4.

RCP seal leaks, discharges from the pressurizer, and break flows (if creep rupture occurs) were directed into a single component representing the Zion containment (see Figures C.2 and C.3). Component input included the total containment volume and estimates of the total mass of concrete and steel. However, calculated containment pressures are expected to be high (by as much as a factor of 2) since there was no attempt to model containment in detail. Detailed modeling was not justified because flows from the RCS will be choked most of the time in each calculation and because a separate (detailed) analysis is planned to provide a full evaluation of containment response.

The nodalization shown in Figure C.2 was used in conjunction with the reactor vessel nodalization from TMLB' initiation to the onset of core heatup in all calculations. (In this analysis, the onset of core heatup was assumed to correspond to a core exit superheat of at least 2.78 K coincident with a void fraction of at least 0.95.) During this portion of the transient, full

loop natural circulation of subcooled and saturated liquid can develop. As the core heats the primary coolant toward saturation, however, voids begin to form and collect in the top of the SG U-tubes. When that occurs, full loop natural circulation of liquid is interrupted.

At the onset of core heatup, Figure C.2 nodalization was replaced by Figure C.3 nodalization in all calculations. This substitution provided flow paths needed to allow simulation of hot leg countercurrent natural circulation. Hot leg countercurrent natural circulation became possible after saturated liquid in the hot legs flashed and/or drained to the vessel. At that time, temperature gradients from the core to the SG U-tubes can drive steam flow along the top half of the hot leg (Component 100), through a portion of the SG U-tubes (Component 110), and back to the vessel through a cooler portion of the SG U-tubes and the lower half of the hot leg (Components 111 and 101, respectively). (It should be noted that the nodalization shown in Figure C.3 will also support development of full loop natural circulation of steam if RCP loop seals clear.)

Development of the hot leg countercurrent flow model for the Zion PWR was based on a previously-developed Surry model (Bayless 1988) and Westinghouse experimental data (Stewart 1992) as follows. Flow areas (which are dependent on hot leg and SG tube splits) and loss coefficients controlling countercurrent flow were extracted directly from the Surry model and incorporated into a Zion input deck. That was justified because the primary coolant loops are geometrically similar in the two plants (although Zion has one additional loop) and because the Surry model was developed to match loop heat transfer based on experimental data.

Specifically, flow areas and loss coefficients were adjusted in the previous analysis so that a total of 29.4% of the energy generated in the core would be transferred to the three primary coolant loops in the Surry PWR during a fixed time period following the onset of countercurrent natural circulation. However, the energy transferred to the loops was found to drop to 20% when the current version of SCDAP/RELAP5 (i.e., MOD3.1) was used with previously-developed Surry model. In other words, changes in SCDAP/RELAP5 (from 1988 to the present) resulted in reduced countercurrent heat transfer by about 32% [= 100*(29.4-20.0)/29.4]. A detailed investigation was not conducted, however, it appeared that recent changes in the correlation used in the code to calculate heat transfer in tube bundles (i.e., the SGs) could be a factor in the observed reduction.

Because of similarities between Surry and Zion, the 32% reduction associated with the current calculation of loop heat transfer in Surry will affect the subject calculations of hot leg countercurrent natural circulation in the primary coolant loops of the Zion PWR. In other words, the use of previously-developed Surry flow areas and loss coefficients to represent Zion countercurrent circulation will result in heat transfer that is about 32% lower than Westinghouse experimental data would suggest. Appropriate accounting for that reduction was essential in order to perform a best estimate Zion analysis. The first step in accounting for the reduction required completion of a Zion scoping calculation using the flow areas and loss coefficients from the previously-developed Surry model. The results from that calculation indicated that a total of 23.4% of the energy generated in the core would be transferred to the four primary coolant loops in the Zion PWR by countercurrent flow. Because that result is estimated to be 32% low, appropriate model adjustments were required to increase loop heat transfer to about 34% [= 23.4%/(1-0.32)].

The adjustment process was completed by altering loss coefficients used in the nodalization shown in Figure C.3. [Flow areas associated with dividing the hot leg and assigning 35% of the SG tubes for hot flow were not changed (Bayless 1988)]. Loss coefficient alterations were made to establish loop heat transfer (as discussed above) and to refine flow patterns consistent with experimental data. Specifically, data indicated that hot and cold mixing fractions should be approximately 0.87 (Stewart 1992). (The hot mixing fraction is the fraction of hot leg flow entering the SG inlet plenum that is mixed with plenum steam before entering the tubes. Conversely, the cold mixing fraction is the fraction of tube flow entering the SG inlet plenum that is mixed with plenum steam before returning to the vessel through the bottom half of the hot leg.) The data also indicated that the recirculation ratio should be about 1.9 (Stewart 1992). (The recirculation ratio is the SG tube flow divided by the hot leg flow. A ratio greater than one indicates that SG tube-to-plenum-to-SG tube recirculation is larger than the flow entering the SG inlet plenum from the hot leg).

A trial-and-error method was required to complete the adjustment process. The process was considered complete when heat transfer, mixing fractions, and recirculation ratios in all four primary coolant loops were in reasonable agreement with target values. A comparison of the target values with the final model calculation is given in Table C.2 as evidence that an acceptable adjustment was made. Loss coefficients from the final iteration were then used in all calculations performed in this analysis.

The surge line in the Zion PWR is connected above the centerline of the hot leg pipe at an angle of about 45°. That orientation was modeled prior to the onset of core heatup as indicated in Figure C.2. However, the surge line connection was moved to the bottom of the pipe after splitting the hot leg at the time of core heatup (see Figure C.3). That modification, which is illustrated in more detail in Figure C.4, included a valve (Component 154) and a section of pipe (Component 156) to compensate for centerline-to-centerline elevation differences between the hot leg pipe halves. The valve was configured to open and close with the pressurizer PORV, providing a best-estimate approach for modeling the surge line and hot leg response as follows.

The valve isolates top and bottom halves of the hot leg pipe when the PORV is closed, consistent with experimental data indicating that the countercurrent flow streams do not mix (Stewart 1986 and Stewart 1992). When the PORV opens, the valve allows both hot and cold countercurrent flow streams to be drawn into the surge line, as one would expect. In addition, any undrained pressurizer liquid can only flow toward the reactor vessel through the bottom half of the hot leg. Interface drag prevents liquid draining when the PORV is open and the valve (realistically) prevents liquid from getting into the top half of the hot leg pipe when the PORV is closed.

C.2.2 SCDAP Input

Two criteria were used to establish the five flow channels shown in Figure C.1. The first (and most important) consideration was to split the core so that similarly powered fuel assemblies could be grouped together. Splitting the core into channels with similar flow areas was a secondary consideration. Cross sections of the resulting five channel model are shown in Figures C.5 and C.6. [Data needed for developing the split and the balance of the SCDAP input was largely based on the UFSAR (Updated Final Safety Assessment Report) for the Zion PWR.]

The 15x15 assemblies in each flow channel contain 204 fuel rods and a total of 21 lattice positions for control rods and instrument tubes. The fuel rods have a Zr clad and an active (UO_2) length of approximately 3.66 m. An initial fuel rod pressure of 5.29 MPa was assumed. The control rod material is Ag-In-Cd in the ratio of 80-15-5. Control rods are clad with stainless steel and are configured for insertion into Zr guide tubes. With only 53 CRAs (control rod assemblies), about 72.5% of the control rod guide tubes in the Zion PWR are empty.

A SCDAP fuel rod component was required in each channel to represent the fuel rods. Based on a previously developed approach (Knudson 1993), a SCDAP control rod component was used in each channel to represent the control rods, empty control rod guide tubes, and instrument tubes. Therefore, the core model was composed of a total of 10 SCDAP components. Ten axial nodes were assigned to each component consistent with the hydrodynamic nodalization shown in Figure C.1. Masses associated with the resulting SCDAP model are compared to the masses of the primary core components in Table C.3.

The SCDAP/RELAP5 implementation of a 1979 ANS (American Nuclear Society) Standard was used to calculate core decay heat. Specifically, ANS 79-3 with three fissile isotopes (^{235}U, ^{238}U, and ^{239}Pu) and a 2 yr average burnup was used. A chopped-cosine axial power profile was also used. A peak-to-average power ratio of 1.154 in the third axial node characterized that profile. (Data defining the radial power profile was provided in Figure C.5.)

SCDAP input is required to define certain core damage parameters. The values used in this analysis are listed in Table C.4. The following outlines the logic used to establish the values.

Debris formation during core degradation results in flow restrictions, which will affect core heatup. Until fully mechanistic models are developed, the user must specify the flow area to be applied in core regions where cohesive debris has formed. Any input from 0 to 100% of the nominal flow area can be specified. However, the current version of the code will set the debris flow area to zero for all inputs of 10% or less. It was clear that an input greater than 10% was needed since a flow area of zero corresponds to coplanar blockage, which has not been observed in tests performed to date. Unfortunately, there is no other basis for setting the input at this time. However, selecting large values will tend to delay core heating and melting, which could be non-conservative with respect to the potential for HPME and DCH. Therefore, the minimum flow area through cohesive debris was set to 11% of the nominal flow area in all calculations as indicated in Table C.4. Although that value is on the low end of the expected range, there is insufficient data to justify larger values without the risk of generating non-defensible results.

Relocation of the core to the lower head cannot occur until melt develops and/or spreads to the core periphery in the current version of the code. There are then two options for controlling relocation. In the first option, a simple model is used to estimate the thermal stability of a peripheral oxide crust. Relocation occurs when the crust is estimated to melt. In the second option, relocation occurs as soon as the melt reaches the periphery. (Those options are considered

an interim solution until a mechanistic crust failure model is completed.) The second option was used in all calculations because an early relocation could occur, which could affect the potential for HPME.

SCDAP input is required to specify the length of time for a molten pool to drain from the core to the lower head. A molten pool draining interval of 68 s was previously estimated for the Surry PWR (Knudson 1993). That estimate was based on Westinghouse PWR lower plenum geometry and the radial division of the Surry core used in the study. It was assumed that a lower value (~60 s) could be supported since the current analysis is based on a finer radial division of the core. However, there was no attempt to rigorously revise this estimate because the results are not expected to be sensitive to this input.

Debris-to-coolant heat transfer is either on or off in the current version of SCDAP/RELAP5. Debris quenching occurs with the heat transfer turned on, up to the limit imposed by the amount of water available in the lower head. The potential for pressurization associated with quenching was of interest in this analysis because of the corresponding implications on HPME and the DCH issue. On that basis, heat transfer was turned on in all calculations performed as indicated in Table C.4.

C.2.3 COUPLE Input

The COUPLE representation of the reactor vessel lower head is shown in Figure C.7. The axisymetric mesh includes a total of 320 nodes with 285 elements. The combined thickness of the carbon steel vessel wall and the stainless steel cladding was modeled as carbon steel using three elements. Remaining elements were initially filled with primary coolant, which can boil and/or be displaced as debris relocates from the core.

Heat transfer from relocated debris to the lower head will be affected by the debris roughness and any gases that become trapped between the debris and the vessel wall. A layer of zero-width elements was aligned with the inner surface of the lower head to provide a way to simulate that contact resistance. A constant coefficient of 500 W/m^2-K was used to represent the heat transfer across that gap in all calculations. Code-calculated convection heat transfer to the containment atmosphere was modeled on the external surface of the lower head.

C.2.4 Transient Calculations

Three different SCDAP/RELAP5 calculations were performed in this analysis where RCP seal leakage was the only input that was varied. (As previously discussed, best-estimate input was used to develop the rest of the model.) Case 1 was designed without RCP seal leakage in order to evaluate behavior of the Zion PWR under station blackout conditions at high RCS pressure. Cases 2 and 3 were completed to account for the effects of RCP seal leakage.

Under normal operating conditions, high pressure systems provide cooling water flow to the seals to offset a design leak rate of approximately 3 gpm per RCP. However, the loss of all AC power results in a loss of seal cooling water. Without cooling water, leak rates increase as RCP seal temperatures increase. Leak rates of 21 gpm per RCP have been calculated for intact RCP seals subjected to normal RCS temperatures and pressures (Boardman 1985).

Leak rates will be higher if one or more of the three seal stages in a Westinghouse RCP fail. The primary factors affecting seal behavior during a TMLB' sequence are high temperature survivability and the potential for hydraulic instability under two-phase flow conditions (Ruger 1989). Unfortunately, the prediction of failure of any particular seal stage (which leads to a particular leak rate) is not straightforward. For that reason, a panel of experts was assembled to make a probabilistic determination of RCP leak rates in Westinghouse PWRs for use in completing NUREG-1150 (Wheeler 1989). The panel concluded that the most probable leak rate was 250 gpm per RCP while the maximum leak rate (with a low probability) was 480 gpm per RCP.

Based on results from the experts, a leak rate of 21 gpm per RCP was introduced at TMLB' initiation in Cases 2 and 3 to represent leakage associated with the loss of seal cooling. In Case 2, leakage was increased from 21 to 250 gpm at the time water in the RCP reached saturation to account for potential two-phase instabilities. In Case 3, the maximum leak rate of 480 gpm per RCP was introduced at the time of saturation. The relationship between transient time and flow areas used to model seal leakage in this analysis is summarized in Table C.5.

C.2.5 Steady State

Steady state initialization of the SCDAP/RELAP5 model was required to provide a starting point for the transient calculations. Initialization involved bringing the model to a stable

state representing full power operation of the Zion PWR. Initialization was considered acceptable when calculated conditions and published operating conditions (from the Zion UFSAR) were in reasonable agreement. A comparison of selected parameters is provided in Table C.6 as evidence that an appropriate initialization was achieved.

C.3 RESULTS

A best-estimate SCDAP/RELAP5 analysis of the Zion PWR during TMLB' sequences without recovery and without operator actions was completed. Results for the three cases considered in the analysis are presented in this section. Uncertainties associated with the results are also discussed.

C.3.1 Case 1

This case was designed without RCP seal leakage in order to evaluate the behavior of the Zion PWR under station blackout conditions at high RCS pressure. The sequence of events for this case is listed in Table C.7 while DCH related-parameters are given in Table C.8. The tables provide quantitative information that may be helpful in conjunction with the following description.

The reactor scrammed and RCPs tripped due to the loss of AC power at TMLB' initiation (at 0 s). An initial RCS pressure reduction occurred because boiling on the SG secondary side was sufficient to remove core decay heat and cool the RCS. However, SG heat sinks were not sustainable without feedwater. As a result, the RCS pressure increased to the pressurizer PORV opening set point by 4960 s, corresponding with the approximate time of SG dryout. A gradual RCS heatup and boiloff followed where PORV cycling provided pressure control between 15.7 and 16.2 MPa as indicated in Figure C.8.

Core decay heat was transferred to the SGs by full loop natural circulation of liquid until 7660 s. By that time, vapor generated in the core had collected in the top of the SG U-tubes, preventing further liquid circulation. As indicated in Figure C.9, the first core uncovery began at 9216 s and was complete by 10 702 s as a result continued boiling (and PORV venting). By 9384 s, SG tube and hot leg voiding allowed development of hot leg countercurrent natural circulation. Heat transfer to the ex-vessel piping by the countercurrent flow produced a heatup and an associated creep rupture failure of the hot leg in the pressurizer loop at 15 916 s as

indicated in Figure C.10. Although a similar heatup of the other hot legs occurred as indicated in Figure C.11, the pressurizer loop hot leg failed first because of the heating contribution associated with PORV cycling. (It is important to note that SG tubes were not predicted to fail at any time during this calculation since they remained relatively cool as indicated in Figure C.10.)

A 0.166 m diameter break was introduced at the time of hot leg failure, resulting in an immediate RCS pressure reduction and the end of PORV cycling as indicated in Figure C.8. The RCS pressure decreased to the initial accumulator pressure of 4.24 MPa by 15 961 s. Accumulator injection followed, providing water sufficient to reflood the core by 16 121 s. The accumulators emptied and injection was terminated by 16 285 s. A second heatup and boiloff at low RCS pressure then occurred, with a second (and final) core uncovery completed at 17 940 s as indicated in Figure C.9.

Without a source of cooling water, fuel melting began near the center of the core by 19 905 s. The melt then spread both axially and radially until the reaching the core periphery at 23 313 s. At that time, the contents of the in-core molten pool (61 040 kg of UO_2 and 15 770 kg of ZrO_2) was relocated to the lower head over a 60 s time period, resulting in a final debris depth of about 1.33 m as indicated in Figure C.12. It was estimated that 4800 kg of thin cross-section lower plenum stainless steel would be submerged by the relocated core materials. Therefore, that steel was added to the lower head debris bed assuming that it would melt as a result of being submerged.

Partial quenching of the debris was calculated during the relocation. However, quenching was limited by the amount of water available in the lower head. The amount of water was limited because some of it was vaporized, some of it was displaced by relocating debris, and some of the water was pushed out of the lower head by the pressurization associated with the vapor generation. Consequently, the debris was only cooled from 2873 K to about 2550 K during relocation as indicated in Figure C.13. A gradual heatup of the lower head debris then followed as indicated in the figure. Once debris quenching was complete, the remaining coolant settled on top of the lower head debris and heatup of the lower head began. A corresponding failure of the lower head as a result of creep rupture was predicted at 26 965 s. The failure location was approximately 0.66 m above the bottom of the inside surface of the lower head.

The RCS pressure at the time of lower head failure was about 0.53 MPa with the water inventory shown in Figure C.14. A total of 464 kg of hydrogen was produced through oxidation

of core components as indicated in Figure C.15. All of the generated hydrogen, which corresponded to oxidation of about 52% of the in-core Zr, was ultimately vented into containment through the PORV and hot leg break as indicated in Figure C.16. Melting of upper plenum stainless steel was not predicted during this calculation. However, a small relocation of 200 kg of control rod absorber material (Ag-In-Cd) was predicted after lower head failure (at 28 410 s).

C.3.2 Case 2

This case was designed to evaluate the behavior of the Zion PWR under station blackout conditions with seal leaks of 250 gpm per RCP. The sequence of events for this case is listed in Table C.9 while DCH related-parameters are given in Table C.10. The tables provide quantitative information that may be helpful in conjunction with the following description.

The reactor scrammed and RCPs tripped due to the loss of AC power at TMLB' initiation (at 0 s). Seal leaks of 21 gpm per RCP were introduced at that time to simulate leakage associated with the loss of seal cooling that would accompany the loss of AC power. An initial RCS pressure reduction occurred because boiling on the SG secondary side was sufficient to remove core decay heat and cool the RCS. However, SG heat sinks were not sustainable without feedwater. As a result, the RCS pressure began to increase following SG dryout (at ~4800-5000 s). The pressure increase terminated at the pressurizer PORV opening set point, which was reached at 5680 s as indicated in Figure C.17. A gradual RCS heatup and boiloff then followed where PORV cycling provided pressure control between 15.7 and 16.2 MPa.

Saturated conditions were reached at the RCPs at 7466 s. Seal leaks were increased to 250 gpm per RCP at that time to simulate failures that could develop with two-phase flow across the seal faces. That rate is the most probable leakage for Westinghouse RCPs (Wheeler 1989).

Core decay heat was transported to the SGs by full loop natural circulation of liquid until 7526 s. By that time, vapor generated in the core had collected in the top of the SG U-tubes, preventing further liquid circulation. By 9045 s, SG tube and hot leg voiding was sufficient to allow development of hot leg countercurrent natural circulation.

As indicated in Figure C.18, the first core uncovery began at 8944 s and was complete by 11 196 s as a result of boiling and venting through RCP seals and the PORV. However, PORV cycling ended at 10 320 s because RCP seal flow and heat transfer to the ex-vessel structures

through countercurrent natural circulation were sufficient to remove core decay heat, allowing the RCS pressure to drop below the PORV set point. That pressure reduction persisted until the initial accumulator pressure of 4.24 MPa (and the associated injection) was reached at 14 414 s as indicated in Figure C.17.

Heat transfer to the ex-vessel piping by countercurrent flow produced a heatup and an associated creep rupture failure of the hot leg in one of the non-pressurizer loops at 16 925 s as indicated in Figure C.19. A similar heatup of the other hot legs occurred as shown in Figure C.20. Unlike Case 1, however, heating of the hot leg in the pressurizer loop was not greater than in the other loops because the heating contribution associated with PORV cycling was relatively small. (It is important to note that SG tubes were not predicted to fail at any time during this calculation since they remained relatively cool as indicated in Figure C.19.)

A 0.166 m diameter break was introduced at the time of hot leg failure, allowing further RCS pressure reduction as indicated in Figure C.17. Accumulator injection followed, resulting in a core reflood by 17 163 s and accumulator dryout by 17 169 s. A second heatup and boiloff at low RCS pressure followed, with a second (and final) core uncovery completed at 17 748 s as indicated in Figure C.18.

The first formation of an in-core molten pool occurred as a result of fuel dissolution by interaction with the Zr cladding at 14 057 s. However, the first heatup to ceramic melt conditions did not occur until 14 976 s. The melt then spread both axially and radially until the pool reached the core periphery at 23 938 s. At that time, the contents of the in-core molten pool (62 930 kg of UO_2 and 16 350 kg of ZrO_2) was relocated to the lower head over a 60 s time period, resulting in a final debris depth of about 1.65 m as indicated in Figure C.21. (Note that some debris had accumulated from prior relocations of control rod materials.) It was estimated that 5300 kg of thin cross-section lower plenum stainless steel would be submerged by the relocated core materials. Therefore, that steel was added to the lower head debris bed assuming that it would melt as a result of being submerged.

Partial quenching of the debris was calculated during the relocation. However, quenching was limited by the amount of water available in the lower head. The amount of water was limited because some of it was vaporized, some of it was displaced by relocating debris, and some of the water was pushed out of the lower head by the pressurization associated with the vapor generation. Consequently, the debris was only cooled from 3068 K to about 2900 K during

relocation as indicated in Figure C.22. A gradual heatup of the debris then followed as indicated in the figure. Once quenching was complete, the remaining coolant settled on top of the lower head debris and heatup of the lower head began. A corresponding failure of the lower head as a result of creep rupture was predicted at 26 915 s. The failure location was approximately 0.80 m above the bottom of the inside surface of the lower head.

The RCS pressure at the time of failure was about 0.56 MPa with the water inventory shown in Figure C.23. A total of 520.5 kg of hydrogen was produced through oxidation of about 58% of the in-core Zr as indicated in Figure C.24. Essentially all of the generated hydrogen was ultimately vented into containment, primarily through RCP seal leaks as indicated in Figure C.25. Approximately 2734 kg of upper plenum stainless steel melted and slumped in a period between 14 018 and 16 849 s. In addition, 17 210 kg of UO_2 and 4508 kg of ZrO_2 melted and relocated to the lower head between 23 938 s and the time of lower head failure.

C.3.3 Case 3

This case was designed to evaluate the behavior of the Zion PWR under station blackout conditions with seal leaks of 480 gpm per RCP. The sequence of events for this case is listed in Table C.11 while DCH related-parameters are given in Table C.12. The tables provide quantitative information that may be helpful in conjunction with the following description.

The reactor scrammed and RCPs tripped due to the loss of AC power at TMLB' initiation (at 0 s). Seal leaks of 21 gpm per RCP were introduced at that time to simulate leakage associated with the loss of seal cooling that would accompany the loss of AC power. An initial RCS pressure reduction occurred because boiling on the SG secondary side was sufficient to remove core decay heat and cool the RCS. However, the SG heat sinks were not sustainable without feedwater. As a result, the RCS pressure began to increase following SG dryout (at ~4800-5000 s). The pressure increase terminated at the pressurizer PORV opening set point, which was reached at 5680 s as indicated in Figure C.26. A gradual RCS heatup and boiloff followed where PORV cycling providing pressure control between 15.7 and 16.2 MPa.

Saturated conditions were reached at the RCPs at 7466 s. Seal leaks were increased to 480 gpm per RCP at that time to simulate failures that could develop with two-phase flow across the seal faces. That rate corresponds to the maximum leakage that would be expected if all seal stages in a Westinghouse RCP failed (Boardman 1985 and Wheeler 1989).

Core decay heat was transported to the SGs by full loop natural circulation of liquid until 7526 s. By that time, vapor generated in the core had collected in the top of the SG U-tubes, preventing further liquid circulation. Energy dissipated through RCP seal leaks exceeded core decay heat by 8456 s. As a result, the RCS pressure dropped below the PORV set point, which ended further PORV cycling as indicated in Figure C.26. The pressure reduction resulting from RCP seal leak flows persisted until the initial accumulator pressure of 4.24 MPa (and the associated injection) was reached at 12 312 s.

As indicated in Figure C.27, the first core uncovery began at 8644 s and was complete by 10 016 s as a result of boiling and venting through the RCP seals. By 8697 s, voiding in the SG tubes and hot legs allowed development of hot leg countercurrent natural circulation. Heat transfer to the ex-vessel piping by the countercurrent flow produced a heatup and an associated creep rupture failure of the hot leg in the pressurizer loop at 20 650 s as indicated in Figure C.28. (It is important to note that SG tubes were not predicted to fail at any time during this calculation since they remained relatively cool as indicated in Figure C.28).

A 0.166 m diameter break was introduced at the time of hot leg failure, allowing further RCS pressure reduction and injection of the remaining accumulator inventory. The accumulators emptied at 20 920 s, with a core collapsed liquid level ~0.82 m below the top of the fuel rods. A second heatup and boiloff at low RCS pressure followed, with a second (and final) core uncovery completed at 21 470 s as indicated in Figure C.27.

The first formation of an in-core molten pool occurred as a result of heating to ceramic melt conditions at 12 169 s. However, accumulator injections (starting at 12 312 s) delayed further melting until 26 610 s, when control rod absorber materials began to melt and relocate to the lower head. Core melting followed since accumulators (the only cooling water source) emptied by 20 920 s. The melt spread both axially and radially until the pool reached the core periphery at 29 212 s. At that time, the contents of the in-core molten pool (60 290 kg of UO_2 and 16 690 kg of ZrO_2) was relocated to the lower head over a 60 s time period, resulting in a final debris depth of about 1.40 m as indicated in Figure C.29. (Note that some debris had accumulated from prior relocations of control rod materials.) It was estimated that 5000 kg of thin cross-section lower plenum stainless steel would be submerged by the relocated core materials. Therefore, that steel was added to the lower head debris assuming that it would melt as a result of being submerged.

Partial quenching of the debris was calculated during the relocation. However, quenching was limited by the amount of water available in the lower head. The amount of water was limited because some of it was vaporized, some of it was displaced by relocating debris, and some of the water was pushed out of the lower head by the pressurization associated with the vapor generation. Consequently, the debris was only cooled from 2873 K to about 2500 K during relocation as indicated in Figure C.30. A gradual heatup of the debris then followed as indicated in the figure. Once quenching was complete, the remaining coolant settled on top of the lower head debris and heatup of the lower head began. A corresponding failure of the lower head as a result of creep rupture was predicted at 33 285 s. The failure location was approximately 0.66 m above the bottom of the inside surface of the lower head.

The RCS pressure at the time of failure was about 0.55 MPa with the water inventory shown in Figure C.31. A total of 423.8 kg of hydrogen was produced through oxidation of about 47% of the in-core Zr as indicated in Figure C.32. All of the generated hydrogen was ultimately vented into containment, primarily through RCP seal leaks as indicated in Figure C.33. Approximately 2240 kg of UO_2 and 569 kg of ZrO_2 melted and relocated to the lower head between 29 212 s and the time of lower head failure.

C.3.4 Uncertainties

Numerous uncertainties arise when any detailed analysis is performed with a complex computer code like SCDAP/RELAP5. In this case, there are uncertainties that could impact the predicted melt mass, melt composition, and other results that could be used to establish DCH initial conditions for the Zion PWR. There are also uncertainties that could impact the potential for HPME through their influence on the timing of predicted RCS pressure boundary failures. However, only uncertainties falling into the second category are discussed here because SCDAP/RELAP5 results indicate that HPME will not occur in the Zion PWR during TMLB' sequences without recovery and without operator actions. Since HPME is not predicted to occur, the melt mass and other DCH initial conditions are inconsequential. On the other hand, any uncertainties that could alter conclusions relative to the potential for HPME in the Zion PWR merit further discussion as outlined below.

It was recognized that hot leg countercurrent natural circulation would control ex-vessel heating and the timing of ex-vessel failures before this analysis began. Therefore, a significant effort was focused on development of a best-estimate model of countercurrent natural circulation

in the Zion PWR (within time and budget constraints). The resulting model closely correlates with previous SCDAP/RELAP5 analyses and available experimental data. Results using that model indicate that the hot leg will fail 7013 to 8562 s before relocation into the lower head begins and 9990 to 12 635 s before the lower head would fail in the sequences considered. Those margins will increase if heat transfer by hot leg countercurrent natural circulation was underpredicted and conversely, the margins will decrease if the heat transfer was overpredicted. Because experimental data is limited, there is also a possibility that the heat transfer was overpredicted to the point where lower head failure would actually occur before a hot leg (or other ex-vessel) failure. However, the potential for that result appears to be very unlikely based on the current understanding of hot leg countercurrent natural circulation.

The current version of SCDAP/RELAP5 does not allow relocation of the core into the lower head until melt develops and/or spreads to the core periphery. This restriction appears to be reasonable based on preliminary hand calculations indicating that stresses are much higher (and therefore, failure is more likely) in side wall crusts of an in-core crucible than in bottom crusts of the same thickness (personal communication with S. A. Chavez, Idaho National Engineering Laboratory, Idaho Falls, ID). Furthermore, natural circulation within the molten pool should result in relatively thin side wall crusts, providing an additional factor favoring side failure before bottom failure. However, there is no known experimental or analytical verification supporting this code feature. Therefore, some uncertainty in the results of this analysis must be acknowledged. Although it is expected to be unlikely, an early bottom crust failure could allow core relocation with a potential for lower head failure before ex-vessel failure.

There are two options in the current version of SCDAP/RELAP5 for controlling relocation to the lower head once melt is established on the core periphery. The option allowing relocation as soon as melt reaches the periphery was used in all calculations in this analysis. That approach neglects the potential relocation delay that could occur as a result of side wall crust stability. However, accounting for side wall crust stability did not appear necessary since hot leg failures were predicted well ahead of core relocation (and associated lower head failures) in all calculations.

A constant coefficient of 500 W/m^2-K was used to represent debris/vessel heat transfer in this analysis. However, there is a considerable amount of uncertainty in this parameter, primarily because the surface roughness at the debris/vessel interface in severe reactor accidents has not been characterized. It is important to note that this uncertainty is not critical with respect to the

potential for HPME in this analysis since hot leg failures were predicted to occur at least 7000 s before relocation. In other words, an infinite coefficient, which would have led to an almost instantaneous failure of the lower head, could have been used without changing the results relative to the potential for HPME.

The current version of SCDAP/RELAP5 provides two options for heat transfer between debris and coolant during core relocation into the lower head. In the first option, debris is relocated without heat transfer, providing the potential for a relatively early lower head failure. Relocating debris is quenched in the second option, within limits imposed by the amount of coolant available in the lower head. The second option was used in all calculations in this analysis because the potential for repressurization associated with debris quenching was thought to be more important than the potential for a relatively early lower head failure. However, the results indicate that either option could have been used without impact on the potential for HPME in the Zion PWR. Specifically, a relatively early lower head failure would not alter conclusions relative to the potential for HPME because hot leg failures were predicted well ahead of core relocation. In addition, the potential for HPME was not affected by any repressurization because there was a relatively small amount of water available for quenching (as a result of hot leg breaks) and because there was sufficient time to vent excess vapor and reduce RCS pressures before failure of the lower head.

Creep rupture failures of the hot leg were predicted in all TMLB' sequences considered in this analysis. Corresponding hot leg breaks were introduced at predicted failure times, consistent with the best-estimate nature of the calculations. However, a constant break flow area of 0.02164 m^2 was used based on a previous estimate for creep rupture of the Surry surge line. Although one would expect a larger break flow area to develop in the hot leg (since it is larger than the surge line), a more rigorous evaluation of breaks resulting from creep rupture was avoided by using that break flow area. Furthermore, it is clear that this simplification had no adverse impact on the results of this analysis since the break area was large enough to allow rapid and complete depressurization of the RCS. A slightly faster depressurization associated with the use of a larger (and perhaps, more defensible) break flow area would be insignificant, given the predicted margins of 9990 to 12 635 s between hot leg and lower head failures.

Uncertainties in the prediction of ex-vessel creep rupture are believed to be relatively small because rupture depends on natural convection heating and the corresponding creep damage response, which are experimentally based. Unfortunately, there are numerous (and potentially

large) uncertainties in the simulation of core melt progression leading to melt relocation and lower head failure, primarily because there is a lack of experimental data for thorough validation of the late phase core damage models. However, those uncertainties are not expected to be large enough to offset the predicted margins of 9990 to 12 635 s between hot leg and lower head failures. In other words, the uncertainties are not expected to change the respective ordering of the RCS pressure boundary failures.

C.4 CONCLUSIONS

A best-estimate SCDAP/RELAP5 analysis of the Zion PWR during TMLB' sequences without recovery and without operator actions was completed. The analysis was designed to evaluate the behavior of the RCS and the progression of core damage during accident conditions. Conclusions developed on the basis of this analysis are presented below.

Natural circulation of steam (and steam flow associated with pressurizer PORV cycling) will induce creep rupture failures in the hot leg piping before failure of the lower head.

Hot leg countercurrent natural circulation of steam will be established in the Zion PWR after the SG tubes and the hot legs are voided. Decay energy is transferred from the core to structures in the primary coolant loops by that flow. If the RCS is not depressurized by leaks, pressurizer PORVs will cycle to control the RCS pressure. Steam flows associated with the PORV cycling will also transfer heat to the loop structures. As a result, the hot legs will be heated to the point of creep rupture failure before failure of the lower head.

The RCS will depressurize through the hot leg failures before the lower head fails.

Hot leg breaks that develop as a result of creep rupture will allow a rapid depressurization of the RCS. As the pressure drops, all available accumulator inventories will be injected into the core. Some RCS repressurization can occur during the injection, depending on the amount of accumulator water available and the condition of the core. However, any excess steam will be vented through the hot leg break, allowing complete depressurization of the RCS to the containment pressure long before the lower head fails.

Creep rupture of the hot legs and the associated RCS depressurization will occur before the lower head fails over the complete RCP leak spectrum.

SCDAP/RELAP5 calculations without RCP seal leaks, with best-estimate leaks of 250 gpm per RCP, and with leaks of 480 gpm per RCP were performed. Those calculations cover the complete RCP leak spectrum since 480 gpm corresponds to the maximum leakage associated with failure of all seal stages in a Westinghouse RCP. The results from all calculations indicate that the hot legs will fail and depressurize the RCS before the lower head fails. The same result would be expected if any intermediate RCP leak rate developed.

HPME is unlikely in the Zion PWR during a station blackout without recovery and without operator actions.

The SCDAP/RELAP5 results for all TMLB' sequences considered indicate that margins between RCS depressurization (through hot leg breaks) and lower head failures are large. Although uncertainties in the results were identified, the uncertainties do not appear to provide support for any condition where the lower head could fail before failure of the hot leg. Since hot leg failure and complete RCS depressurization is expected, HPME in the Zion PWR during the sequences considered appears to be unlikely.

Conditions in the lower head at the time of failure during a station blackout without recovery and without operator actions will be characterized by low RCS pressures and relatively large oxidic melt masses.

The RCS pressure will be at (or very near) the containment pressure at the time of lower head failure as a result of (relatively early) hot leg failures. The total oxidic debris (UO_2 plus ZrO_2) in the lower head will be between 77 and 103 mt. However, a fraction of that debris will be solidified as heat is transferred from the melt to the lower head. Therefore, the molten mass of oxidic debris (available for ejection into the containment building) is estimated to be between 55 and 66 mt.

The conclusions of this analysis are specific to the Zion PWR but should be applicable to Zion-like PWRs.

This analysis was based on a best-estimate SCDAP/RELAP5 model to determine the Zion PWR response during TMLB' sequences without recovery and without operator actions. Therefore, the results and conclusions of this analysis are specific to the Zion PWR. However, the results and conclusions of this analysis should be applicable to other four loop Westinghouse PWRs with similar geometries and core powers (e.g., the Byron and Braidwood PWRs).

C.5 REFERENCES

- Allison, C. M., et al. (1990). *RELAP5/MOD3 Code Manual*, NUREG/CR-5535, EGG-2596 (Draft), Volumes 1-4, Idaho National Engineering Laboratory, Idaho Falls, ID.
- Allison, C. M., et al. (1993). *SCDAP/RELAP5/MOD3.1 Code Manuals, Volumes 1-5*, NUREG/CR-6150, EGG-2720, Idaho National Engineering Laboratory, Idaho Falls, ID.
- Bayless, P. D. (1988). *Analyses of Natural Circulation During a Surry Station Blackout Using SCDAP/RELAP5*, NUREG/CR-5214, EGG-2547, Idaho National Engineering Laboratory, Idaho Falls, ID.
- Berna, G. A., et al. (1984). *SCDAP/MOD1/V0: A Computer Code for the Analysis of LWR Vessel Behavior During Severe Accident Transients*, IS-SAAM-83-002, Revision 1, Idaho National Engineering Laboratory, Idaho Falls, ID.
- Boardman, T., et al. (1985). *Leak Rate Analysis of the Westinghouse Reactor Coolant Pump*, NUREG/CR-4294, 85-ETEC-DRF-1714, Rockwell International Corporation, Canoga Park, CA.
- Jordan, H., et al. (1985). *TRAP-MELT2 User's Manual*, NUREG/CR-4205, BMI-2124, Battelle Memorial Institute, Columbus, OH.
- Knudson, D. L., and C. A. Dobbe (1993). *Assessment of the Potential for High Pressure Melt Ejection Resulting from a Surry Station Blackout Transient*, NUREG/CR-5949, EGG-2689, Idaho National Engineering Laboratory, Idaho Falls, ID.
- Lemmon, E. C. (1980). *COUPLE/FLUID: A Two-Dimensional Finite Element Thermal Conduction and Advection Code*, EGG-ISD-SCD-80-1, Idaho National Engineering Laboratory, Idaho Falls, ID.
- Ruger, C. J., et al. (1989). *Technical Findings Related to Generic Issue 23: Reactor Coolant Pump Seal Failure*, NUREG/CR-4948, BNL-NUREG-521444, Brookhaven National Laboratory, Upton, NY.

- Stewart, W. A., et al. (1986). "Experiments on Natural Circulation Flows in Steam Generators During Severe Accidents", *Proceedings of the International ANS/ENS Topical Meeting on Thermal Reactor Safety*, American Nuclear Society, San Diego, CA.

- Stewart, W. A., et al. (1992). *Natural Circulation Experiments for PWR High Pressure Accidents*, EPRI Project No. RP2177-5 Final Report, Westinghouse Electric Corporation, Pittsburgh, PA.

- Wheeler, T. A., et al. (1989). *Analysis of Core Damage Frequency From Internal Events: Expert* Judgement Elicitation, NUREG/CR-4550, SAND86-2084, Volume 2, Sandia National Laboratories, Albuquerque, NM.

Table C.1.
SCDAP/RELAP5 model elevations relative to the lower reactor vessel head

Location	Relative Elevation (m)
Inside surface of the bottom of the lower head (reference)	0
Bottom of the active core	2.666
Top of the active core	6.323
Surge line (at the connection to the hot leg piping)	7.914
Hot leg nozzle	7.914
RCP seal leak	7.914
Pressurizer PORV	26.68
Pressurizer SRV	26.68

Table C.2.
Comparison of countercurrent flow parameters with values calculated by SCDAP/RELAP5

Parameter	Target Value	Calculated Value
Fraction of core energy absorbed by all primary coolant loops	0.34[a]	0.33
Hot mixing fraction (range: 0.85-0.89)	0.87[b]	0.87[c]
Cold mixing fraction (range: 0.85-0.89)	0.87[b]	0.89[c]
Recirculation ratio (range: 1.7-2.2)	1.9[b]	2.3[c]

a. Derived from a previous SCDAP/RELAP5 analysis of hot leg countercurrent natural circulation (Bayless 1988).
b. Derived from experiments conducted by Westinghouse (Stewart 1992).
c. Represents an average for the four primary coolant loops in the Zion PWR.

Table C.3.
Zion UFSAR core inventory compared to the SCDAP/RELAP5 model

	UFSAR Value	Modeled Value
Total mass of UO_2 (kg)	98 230	98 270
Total mass of Zr (kg)	20 200	20 210
Total mass of control rod material (kg)[a]	(not available)	2350
Total in-core stainless steel mass (kg)	(not available)	421.7

a. Zion control rod material is Ag-In-Cd in the ratio of 80-15-5. However, the material is treated as Ag by SCDAP/RELAP5.

Table C.4.
SCDAP core damage input

Parameter	Value
Minimum cohesive debris flow area	11% of nominal
Early relocation (relocation to lower head when melt spreads to core periphery)	yes
Molten pool relocation time interval	60 s
Debris-to-coolant heat transfer during core relocation to the lower head	yes

Table C.5.
Time/flow area relationship for simulating RCP seal leaks

Time	Flow Area	Case		
		1	2	3
From TMLB' initiation to lower head failure	Flow area = 0	★		
From TMLB' initiation to RCP saturation	Flow area[a] = 8.384e-6 m^2		★	★
From RCP saturation to lower head failure	Flow area[b] = 1.476e-4 m^2		★	
From RCP saturation to lower head failure	Flow area[c] = 2.833e-4 m^2			★

a. Providing a flow of 21 gpm per RCP at 549.9 K (cold leg temperature) and 15.51 MPa for intact seals exposed to normal operating temperatures following the loss of seal cooling (Boardman 1985).
b. Providing a saturated liquid flow of 250 gpm per RCP at 15.96 MPa (the midpoint between PORV opening and closing pressures), which corresponds to the most probable leak rate (Wheeler 1989).
c. Providing a saturated liquid flow of 480 gpm per RCP at 15.96 MPa (the midpoint between PORV opening and closing pressures), which corresponds to the maximum leak rate (Boardman 1985 and Wheeler 1989).

Table C.6.
Zion UFSAR steady state parameters compared to values calculated by SCDAP/RELAP5

Parameter	UFSAR Value	Calculated Value
Reactor power (MW_t)	3250	3250
Pressurizer pressure (MPa)	15.51	15.51
Pressurizer water/steam volume (%)	60/40	60/40
Total RCS flow (kg/s)	17 010	17 010
Cold leg temperature (K)	549.9	549.9
Hot leg temperature (K)	585.5	585.4
SG pressure (MPa)	4.964	4.964
Feedwater temperature (K)	493.5	493.5
Steam flow per generator (kg/s)	440.9	439.7
Liquid volume in each SG (m^3)	52.05	51.98
Liquid mass in each SG (kg)	(not available)	40 820

Table C.7.
Case 1 sequence of events

Event	Time (s)
TMLB' initiation	0
Onset of pressurizer PORV cycling	4960
Steam generators dryout (pressurizer/non-pressurizer loops)	4976/5006
End of full loop (liquid) natural circulation	7660
Collapsed liquid level falls below the top of the fuel rods	9216
Vapor in the core exit begins to superheat; hot leg countercurrent circulation begins	9384
Collapsed liquid level falls below the bottom of the fuel rods	10 702
Pressurizer drains	10 997
Onset of fuel rod oxidation	11 621
Pressurizer loop hot leg nozzle fails by creep rupture	15 916
Hot leg break initiated; break diameter = 0.166 m	15 916
End of pressurizer PORV cycling	15 916
Accumulator injection begins	15 961
First fuel rod fragmentation; in the third channel	16 012
Core is reflooded; collapsed liquid level rises above the top of the fuel rods	16 121
Accumulators empty; injection ends	16 285
Second core dryout; collapsed liquid level falls below the bottom of the fuel rods	17 940
First appearance of an in-core molten pool; through heatup in the first channel	19 905
First slumping into lower head; 61 044 kg UO_2, 15 770 kg ZrO_2	23 313
4800 kg of submerged 'thin' stainless steel added to lower head debris	23 400
Lower head failure; by creep rupture ~0.66 m above the inside bottom surface of the head	26 965
Relocation of 200 kg of Ag-In-Cd into the lower head from in-core crusts	28 410
End of calculation	28 995

Table C.8.
DCH parameters at selected times in Case 1

Parameter	@ 23 313 s[a]	@ 26 965 s[b]	@ 28 995 s[c]
Lower head pressure (MPa)	0.4989	0.5393	0.5455
Lower head liquid temperature (K)	424	428	428
Containment pressure (MPa)	0.4841	0.5272	0.5345
Containment vapor temperature (K)	411	415	416
Mass of in-vessel liquid (kg)	25 340	16 845	14 835
Integrated H_2 generated (kg)	464.0	464.0	464.0
Integrated H_2 flow into containment (kg)	458.6	464.0	464.0
Lower head debris: Ag-In-Cd (kg)	0	0	200[d]
Stainless steel (kg)	4800[e]	4800	4800
UO_2 (kg)	61 040	61 040	61 040
Zr (kg)	0	0	0
ZrO_2 (kg)	15 770	15 770	15 770
Maximum temperature (K)	2873	3514	4108[f]
Average temperature (K)	2873	3336	3794
Molten fraction[g]	1	0.71	0.82

a. Corresponding to the time that the first relocation into the lower head began.
b. Corresponding to the time of lower head failure.
c. Corresponding to the end of the calculation.
d. Corresponding to a small relocation at 28 410 s.
e. Added at the time of relocation to represent the estimated mass of thin cross-section steel in the lower plenum that would be expected to melt as a result of being submerged by core materials.
f. This temperature reflects the non-physical condition associated with retaining the melt in the lower head when it should have relocated to containment.
g. The fraction is 1 at 23 313 s because only molten materials are allowed to relocate. Values at 26 965 and 28 995 s represent an estimate of the fraction of the listed materials that were hotter than 2850 K.

Table C.9.
Case 2 sequence of events

Event	Time (s)
TMLB' initiation	0
Introduction of seal leaks of 21 gpm per RCP; leak diameters = 0.00327 m	0
Steam generators dryout (pressurizer/non-pressurizer loops)	4801/5003
Onset of pressurizer PORV cycling	5680
RCP saturation; seal leaks increased to 250 gpm per RCP; leak diameters = 0.0137 m	7466
End of full loop (liquid) natural circulation	7526
Collapsed liquid level falls below the top of the fuel rods	8944
Vapor in the core exit begins to superheat; hot leg countercurrent circulation begins	9045
End of pressurizer PORV cycling	10 320
Pressurizer drains	10 575
Collapsed liquid level falls below the bottom of the fuel rods	11 196
Onset of fuel rod oxidation	11 235
First slumping into lower head begins; 2115 kg Ag-In-Cd over ~360 s	13 616
27.5 kg of upper plenum stainless steel melts and slumps into lower head	14 018
First appearance of an in-core molten pool; by fuel dissolution in third channel	14 057
71.5 kg of upper plenum stainless steel melts and slumps into in-core molten pool	14 219
Slumping into lower head begins; 235 kg Ag, 112.7 kg SS, 2406 kg UO_2, 452 kg Zr over ~420 s	14 250
Accumulator injection begins	14 414
First heatup to molten fuel temperatures; in first channel	14 976
First fuel rod fragmentation; in the fifth channel	15 371
501.7 kg of upper plenum stainless steel melts and slumps into in-core molten pool	15 410
131.9 kg of upper plenum stainless steel melts and slumps into in-core molten pool	15 566
632.0 kg of upper plenum stainless steel melts and slumps into in-core molten pool	16 115
620.2 kg of upper plenum stainless steel melts and slumps into in-core molten pool	16 558
749.5 kg of upper plenum stainless steel melts and slumps into in-core molten pool	16 849
Non-pressurizer loop hot leg nozzle fails by creep rupture	16 925
Hot leg break initiated; break diameter = 0.166 m	16 925

Table C.9.
Case 2 sequence of events

Event	Time (s)
Core is reflooded; collapsed liquid level rises above the top of the fuel rods	17 163
Accumulators empty; injection ends	17 169
Second core dryout; collapsed liquid level falls below the bottom of the fuel rods	17 748
Core slumping into lower head; 62 930 kg UO_2, 16 350 kg ZrO_2	23 938
5300 kg of submerged 'thin' stainless steel added to lower head debris	24 000
Slumping into lower head; 3556 kg UO_2, 1039 kg ZrO_2	24 536
Slumping into lower head; 2240 kg UO_2, 569 kg ZrO_2	24 612
Slumping into lower head; 2240 kg UO_2, 569 kg ZrO_2	24 723
Slumping into lower head; 2240 kg UO_2, 569 kg ZrO_2	25 233
Slumping into lower head; 4697 kg UO_2, 1193 kg ZrO_2	25 302
Slumping into lower head; 2240 kg UO_2, 569 kg ZrO_2	26 205
Lower head failure; by creep rupture ~0.80 m above the inside bottom surface of the head	26 915
End of calculation	28 915

Table C.10.
DCH parameters at selected times in Case 2

Parameter	@ 23 938 s[a]	@ 26 915 s[b]	@ 28 915 s[c]
Lower head pressure (MPa)	0.5479	0.5588	0.5632
Lower head liquid temperature (K)	428	429	430
Containment pressure (MPa)	0.5412	0.5566	0.5620
Containment vapor temperature (K)	416	417	418
Mass of in-vessel liquid (kg)	10 768	2384	1025
Integrated H_2 generated (kg)	520.5	520.5	520.5
Integrated H_2 flow into containment (kg)	519.4	519.4	519.4
Lower head debris: Ag-In-Cd (kg)	2350[d]	2350	2350
Stainless steel (kg)	8147[d]	8147	8147
UO_2 (kg)	65 340[d]	82 550[e]	82 550
Zr (kg)	452[d]	452	452
ZrO_2 (kg)	16 350[d]	20 860[e]	20 860
Maximum temperature (K)	3068[d]	3430	3775[f]
Average temperature (K)	3068	3195	3415
Molten fraction[g]	0.85	0.64	0.81

a. Corresponding to the time that the first major core relocation into the lower head began.
b. Corresponding to the time of lower head failure.
c. Corresponding to the end of the calculation.
d. Includes 2350 kg Ag, 140.2 kg SS, 2406 kg UO_2, and 452 kg Zr from earlier relocations and 5300 kg SS added at the time of relocation to represent the estimated mass of thin cross-section steel in the lower plenum that would be expected to melt as a result of being submerged by core materials. However, the maximum temperature is applicable only to 62 930 kg UO_2 and 16 350 kg ZrO_2 that actually relocated at 23 938 s.
e. Includes 17 210 kg UO_2 and 4508 kg ZrO_2 that relocate before lower head failure.
f. This temperature reflects the non-physical condition associated with retaining the melt in the lower head when it should have relocated to containment.
g. The fraction is estimated to be 0.85 at 23 938 s because earlier relocations (of 2350 kg Ag, 140.2 kg SS, 2406 kg UO_2, and 452 kg Zr) were quenched and because the additional 5300 kg of lower plenum SS was assumed to be added at the lower plenum temperature. Values at 26 915 and 28 915 s represent an estimate of the fraction of the listed materials that were hotter than 2850 K.

Table C.11.
Case 3 sequence of events

Event	Time (s)
TMLB' initiation	0
Introduction of seal leaks of 21 gpm per RCP; leak diameters = 0.00327 m	0
Steam generators dryout (pressurizer/non-pressurizer loops)	4801/5003
Onset of pressurizer PORV cycling	5680
RCP saturation; seal leaks increased to 480 gpm per RCP; leak diameters = 0.0190 m	7466
End of full loop (liquid) natural circulation	7526
End of pressurizer PORV cycling	8456
Collapsed liquid level falls below the top of the fuel rods	8644
Vapor in the core exit begins to superheat; hot leg countercurrent circulation begins	8697
Collapsed liquid level falls below the bottom of the fuel rods	10 016
Pressurizer drains	10 526
Onset of fuel rod oxidation	10 797
First heatup to molten fuel temperatures; in first channel	12 169
Accumulator injection begins	12 312
First fuel rod fragmentation; in the fourth channel	12 707
27.5 kg of upper plenum stainless steel melts and slumps into lower head	12 751
Pressurizer loop hot leg nozzle fails by creep rupture	20 650
Hot leg break initiated; break diameter = 0.166 m	20 650
Accumulators empty; injection ends with collapsed liq level ~0.82 m below top of fuel rods	20 920
Second core dryout; collapsed liquid level falls below the bottom of the fuel rods	21 470
319.4 kg Ag-In-Cd melts and slumps into lower head	26 610
319.4 kg Ag-In-Cd melts and slumps into lower head	26 960
638.4 kg Ag-In-Cd melts and slumps into lower head	27 059
638.4 kg Ag-In-Cd melts and slumps into lower head	27 220
199.5 kg Ag-In-Cd melts and slumps into lower head	27 283
35.5 kg Ag-In-Cd, 13.6 kg SS, and 39.3 kg Zr melts and slumps into lower head	29 175
Core slumping into lower head; 60 290 kg UO_2, 16 690 kg ZrO_2	29 212

Table C.11.
Case 3 sequence of events

Event	Time (s)
5000 kg of submerged 'thin' stainless steel added to lower head debris	29 300
Slumping into lower head; 2240 kg UO_2, 569 kg ZrO_2	31 459
Lower head failure; by creep rupture ~0.66 m above the inside bottom surface of the head	33 285
End of calculation	35 285

Table C.12.
DCH parameters at selected times in Case 3

Parameter	@ 29 212 s[a]	@ 33 285 s[b]	@ 35 285 s[c]
Lower head pressure (MPa)	0.5360	0.5451	0.5497
Lower head liquid temperature (K)	428	428	429
Containment pressure (MPa)	0.5213	0.5374	0.5438
Containment vapor temperature (K)	414	416	416
Mass of in-vessel liquid (kg)	22 190	14 120	12 910
Integrated H_2 generated (kg)	423.8	423.8	423.8
Integrated H_2 flow into containment (kg)	423.8	423.8	423.8
Lower head debris[d]: Ag-In-Cd (kg)	2151[e]	2151	2151
Stainless steel (kg)	5041[e]	5041	5041
UO_2 (kg)	60 290	62 530[f]	62 530
Zr (kg)	39.3[e]	39.3	39.3
ZrO_2 (kg)	16 690	17 260[f]	17 260
Maximum temperature (K)	2873[e]	3432	3873[g]
Average temperature (K)	2873	3167	3449
Molten fraction[h]	0.91	0.71	0.84

a. Corresponding to the time that the first major core relocation into the lower head began.
b. Corresponding to the time of lower head failure.
c. Corresponding to the end of the calculation.
d. Can include vessel internal stainless steel structures and core components that melt and relocate to the lower head. The Zion core consists of 98 230 kg UO_2, 20 200 kg Zr, 2350 kg Ag-In-Cd, and 422 kg of stainless steel.
e. Includes 2151 kg Ag-In-Cd, 41.1 kg SS, and 39.3 kg Zr from earlier relocations and 5000 kg SS added at the time of relocation to represent the estimated mass of thin cross-section steel in the lower plenum that would be expected to melt as a result of being submerged by core materials. However, the maximum temperature is applicable only to 60 290 kg UO_2 and 16 690 kg ZrO_2 that actually relocated at 29 212 s.
f. Includes 2240 kg UO_2 and 569 kg ZrO_2 that relocated before lower head failure.
g. This temperature reflects the non-physical condition associated with retaining the melt in the lower head when it should have relocated to containment.
h. The fraction is estimated to be 0.91 at 29 212 s because earlier relocations (of 2151 kg Ag-In-Cd, 41.1 kg SS, and 39.3 kg Zr) were quenched and because the additional 5000 kg of lower plenum SS was assumed to be added at the lower plenum temperature. Values at 33 285 and 35 285 s represent an estimate of the fraction of the listed materials that were hotter than 2850 K.

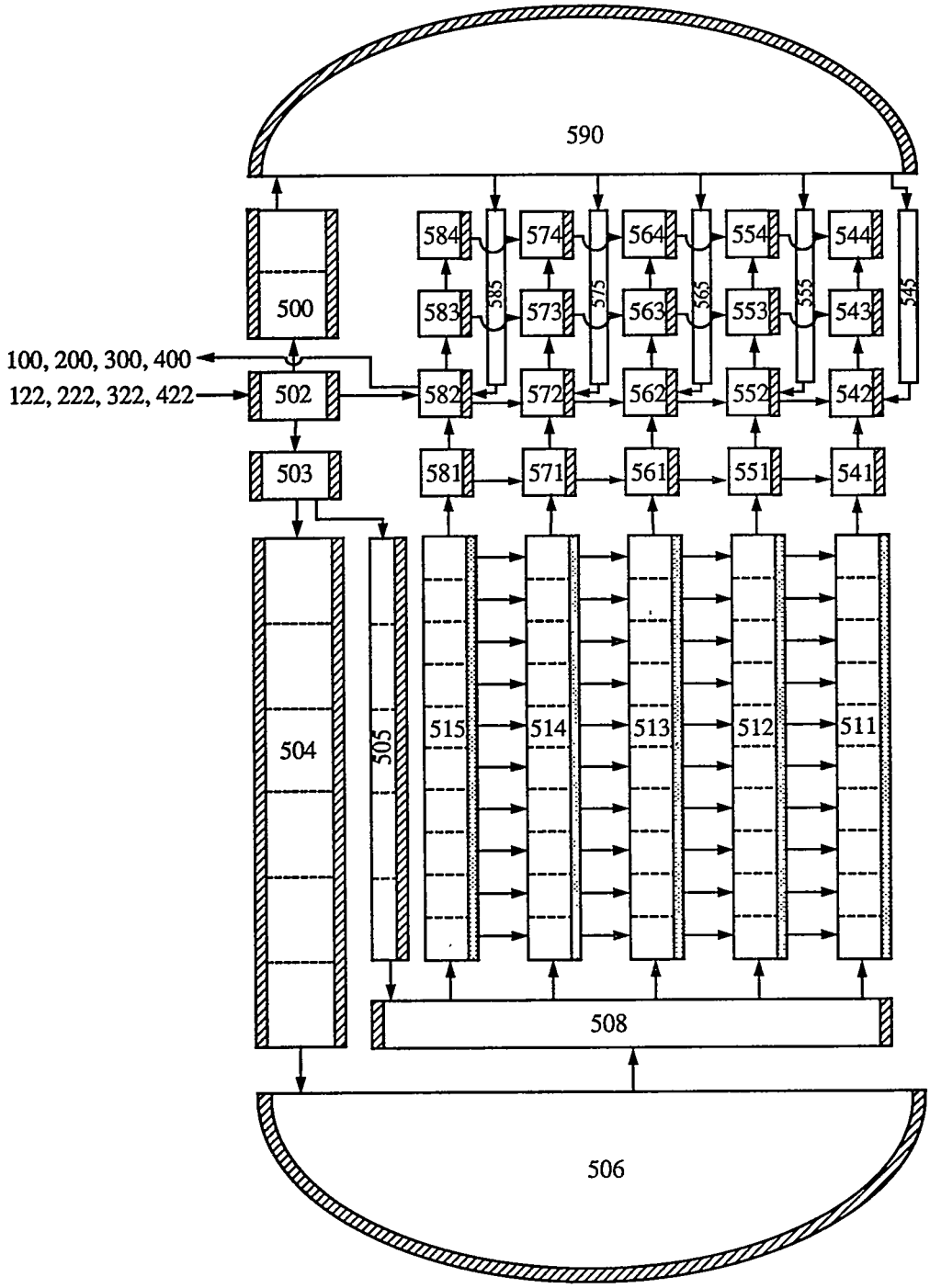

Figure C.1. Zion reactor vessel nodalization with provisions for in-vessel natural circulation.

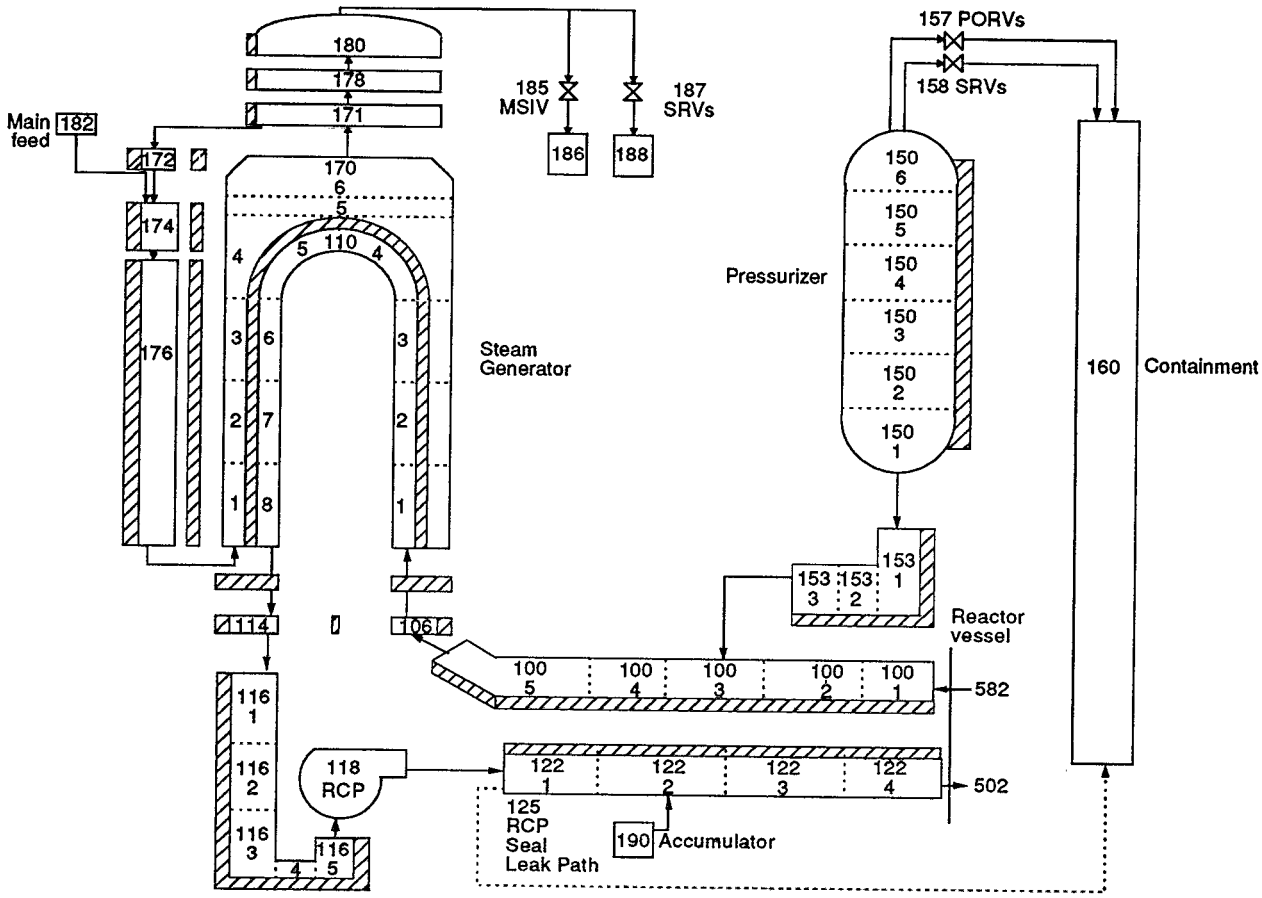

Figure C.2. Pressurizer coolant loop nodalization for the Zion PWR without provisions for hot leg countercurrent natural circulation.

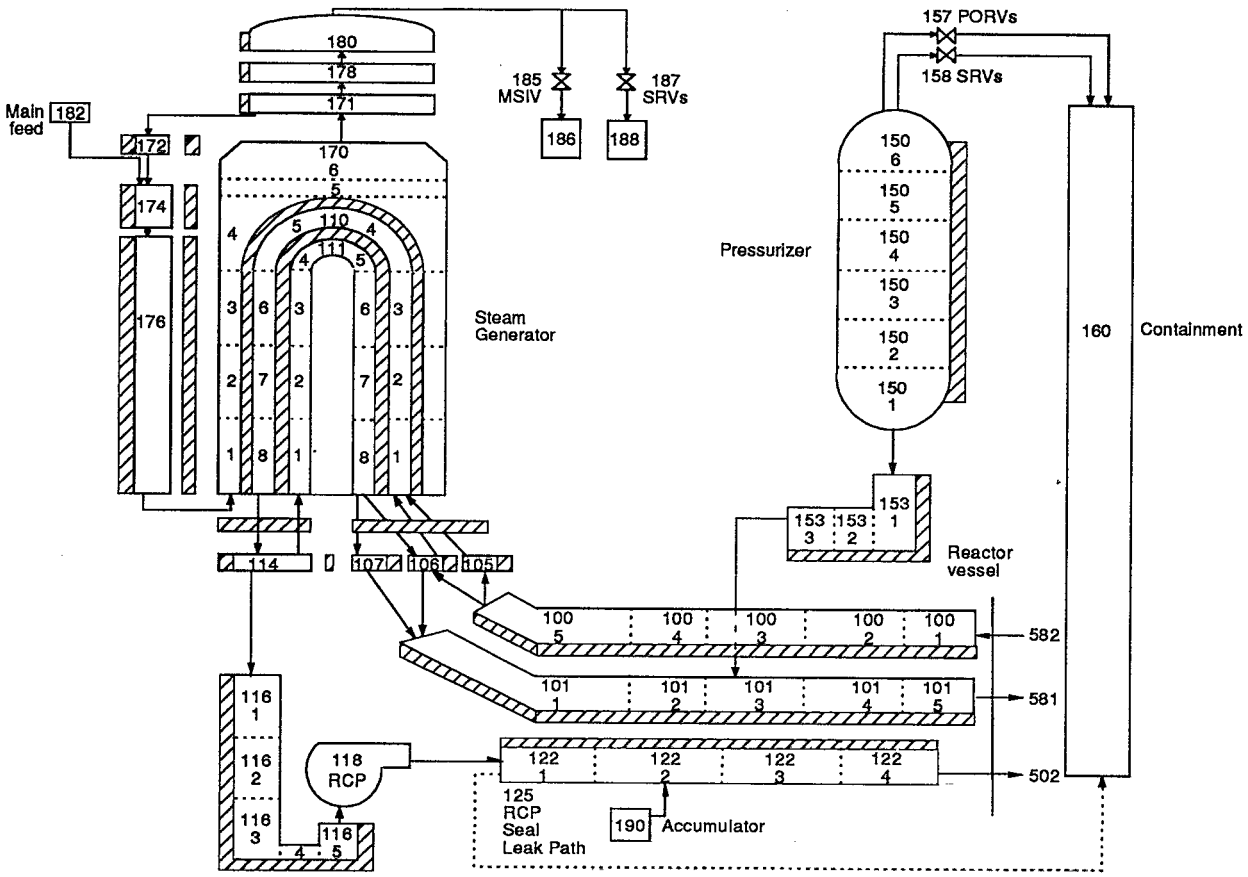

Figure C.3. Pressurizer coolant loop nodalization for the Zion PWR with provisions for hot leg countercurrent natural circulation.

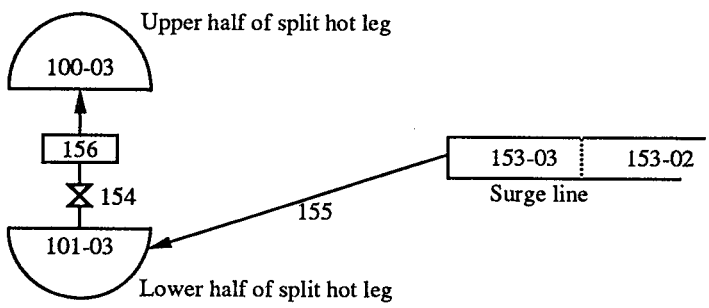

Figure C.4. Nodalization detail showing the surge line connection to the split hot legs.

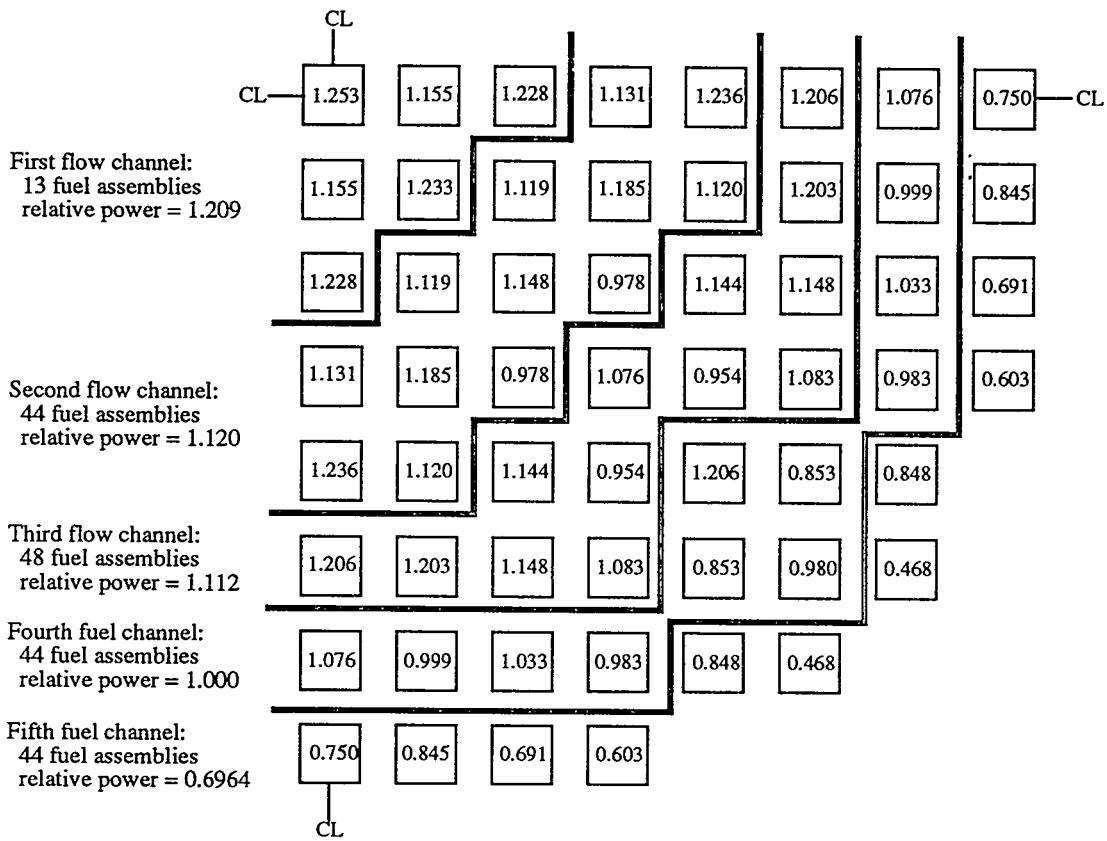

Figure C.5. Cross section of the five channel core with assembly and channel relative power levels.

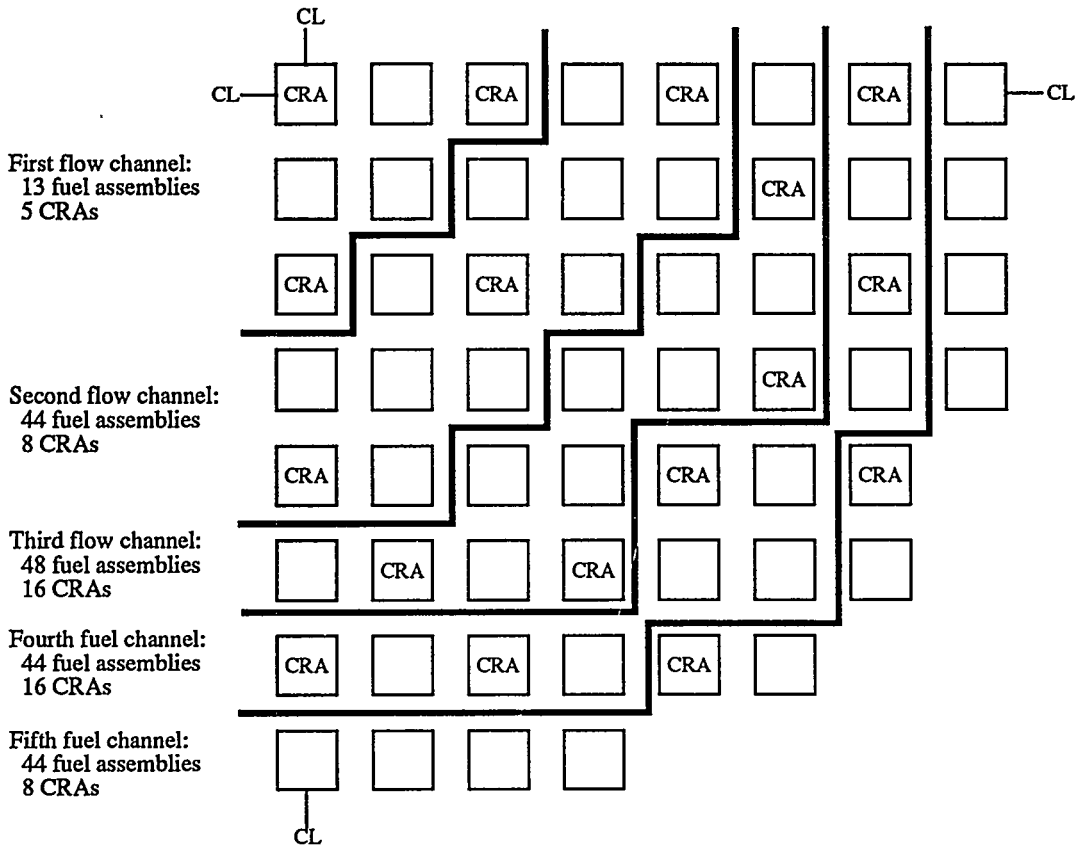

Figure C.6. Cross section of the five channel core with CRA (control rod assembly) locations.

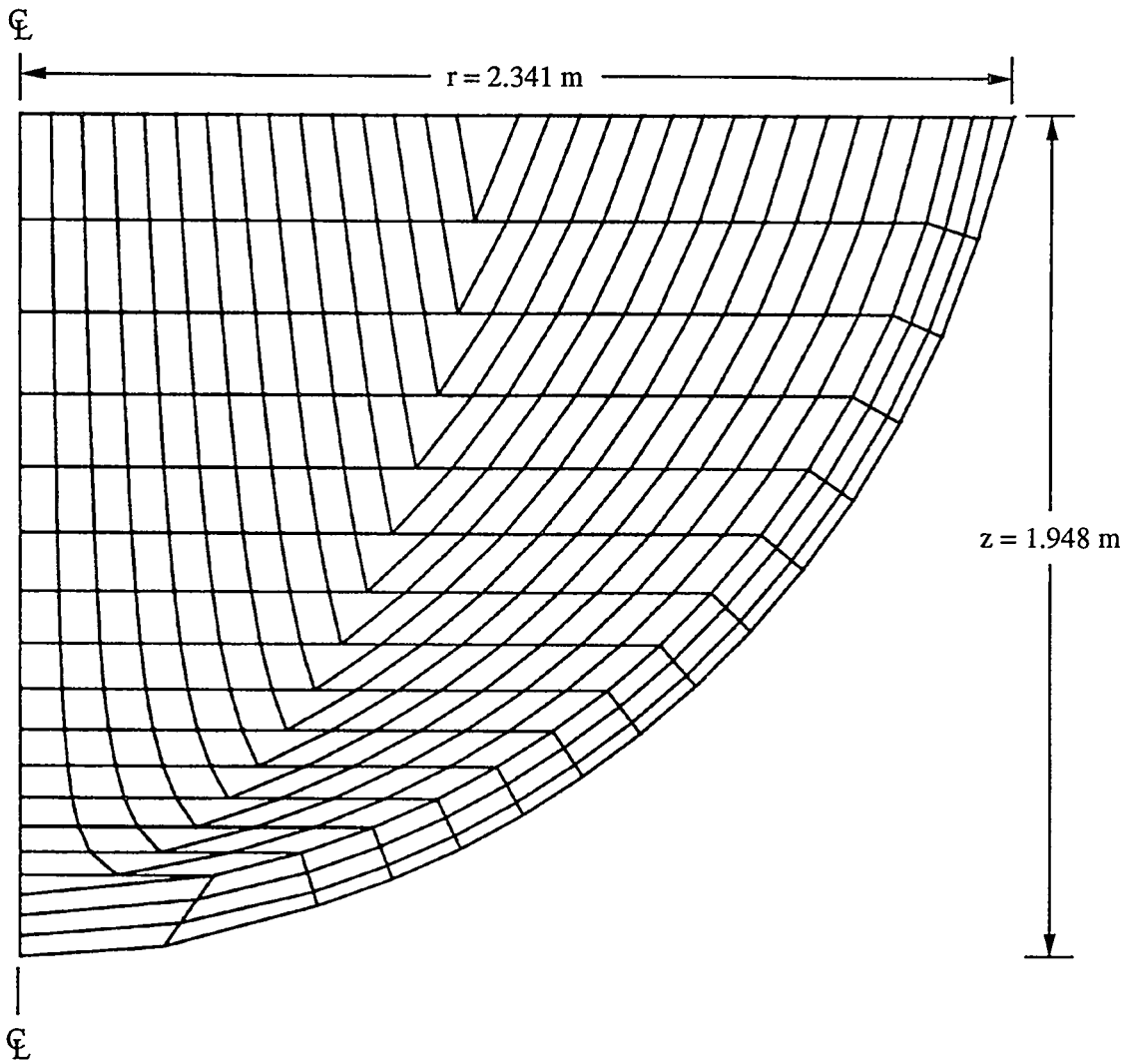

Figure C.7. COUPLE mesh representing the lower reactor vessel head of the Zion PWR.

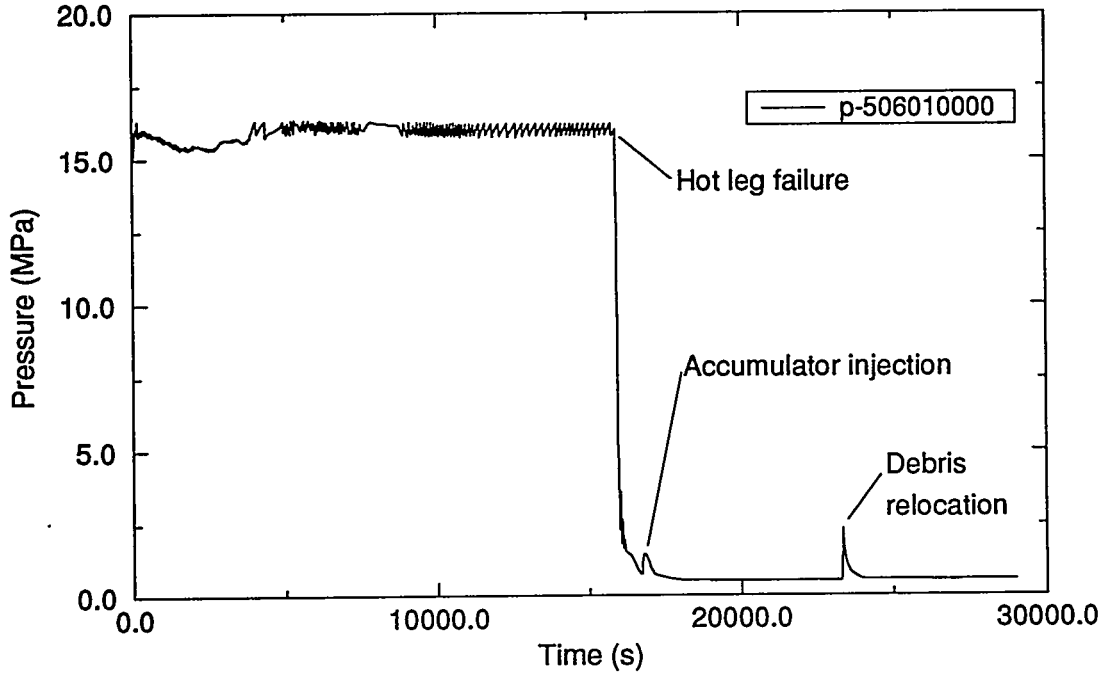

Figure C.8. Pressure in the reactor vessel lower head in Case 1.

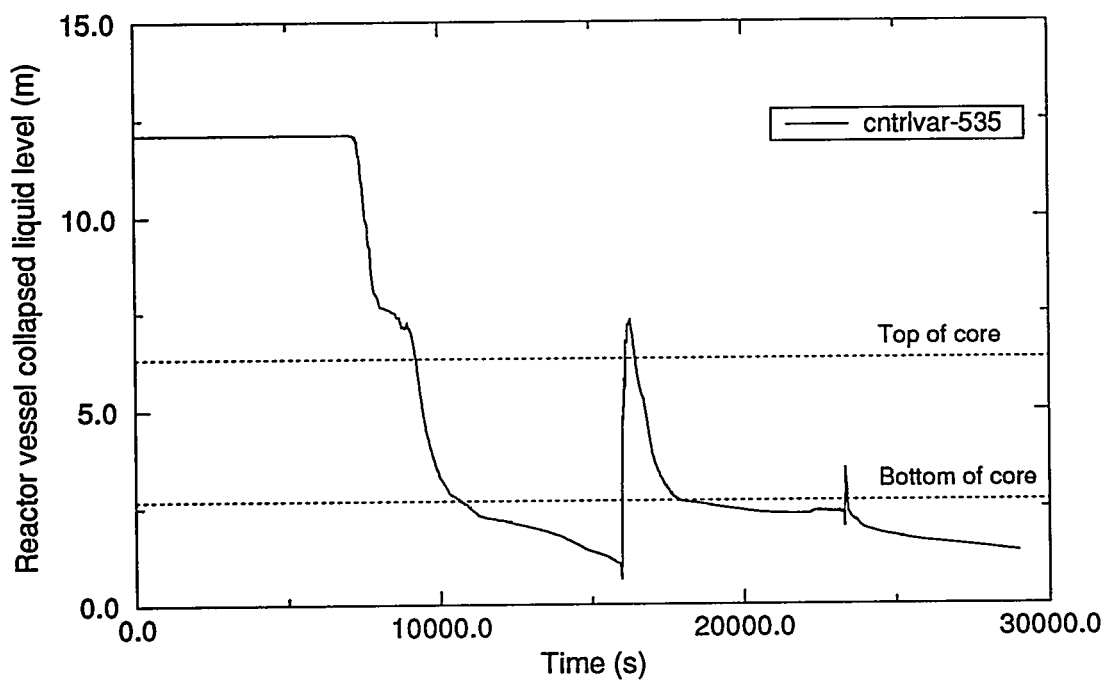

Figure C.9. Reactor vessel collapsed liquid level in Case 1.

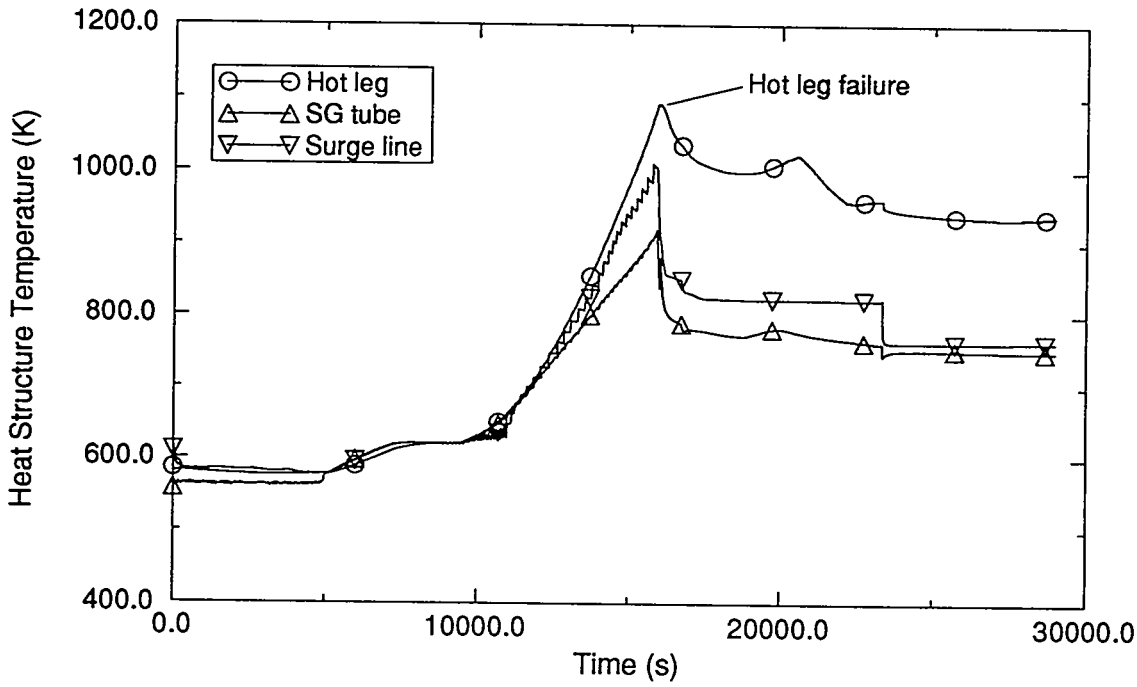

Figure C.10. Volume-averaged temperatures of selected ex-vessel structures in the pressurizer loop in Case 1.

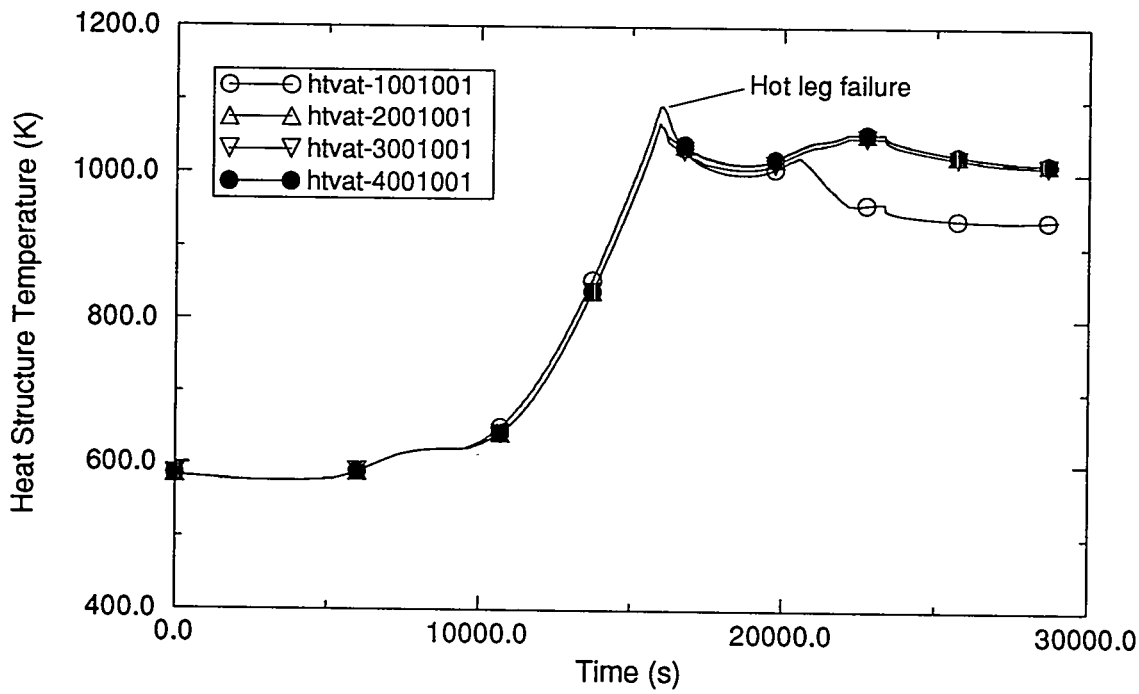

Figure C.11. Hot leg volume-averaged temperatures in Case 1.

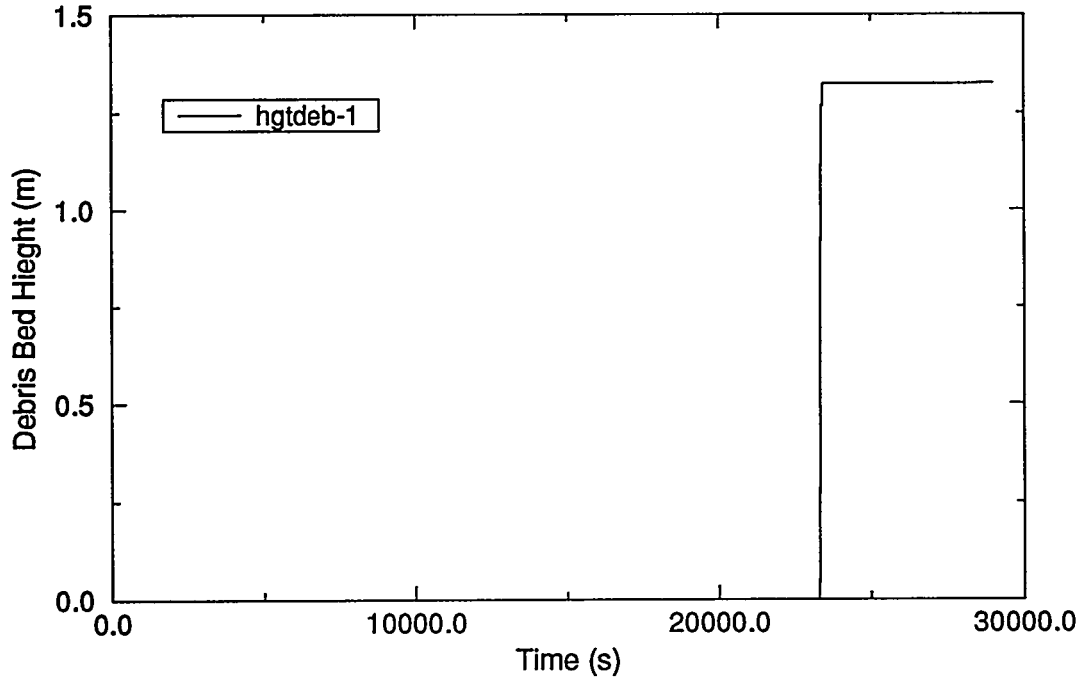

Figure C.12. Lower head debris depth (referenced to the bottom inside surface of the head) in Case 1.

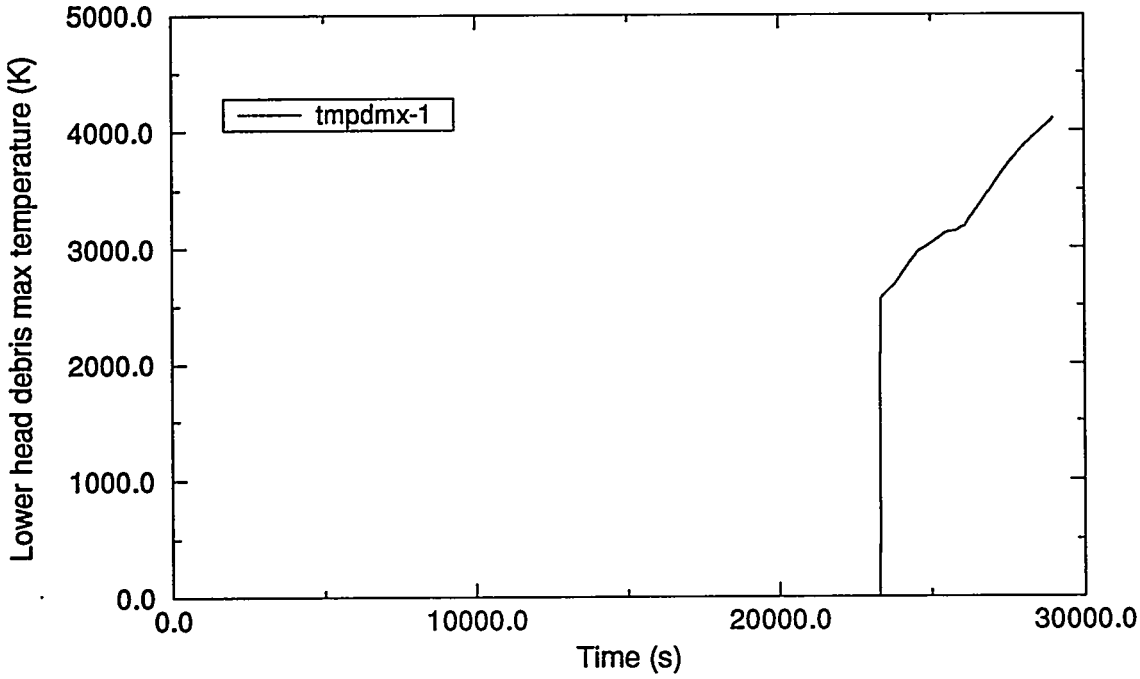

Figure C.13. Lower head maximum debris temperature in Case 1.

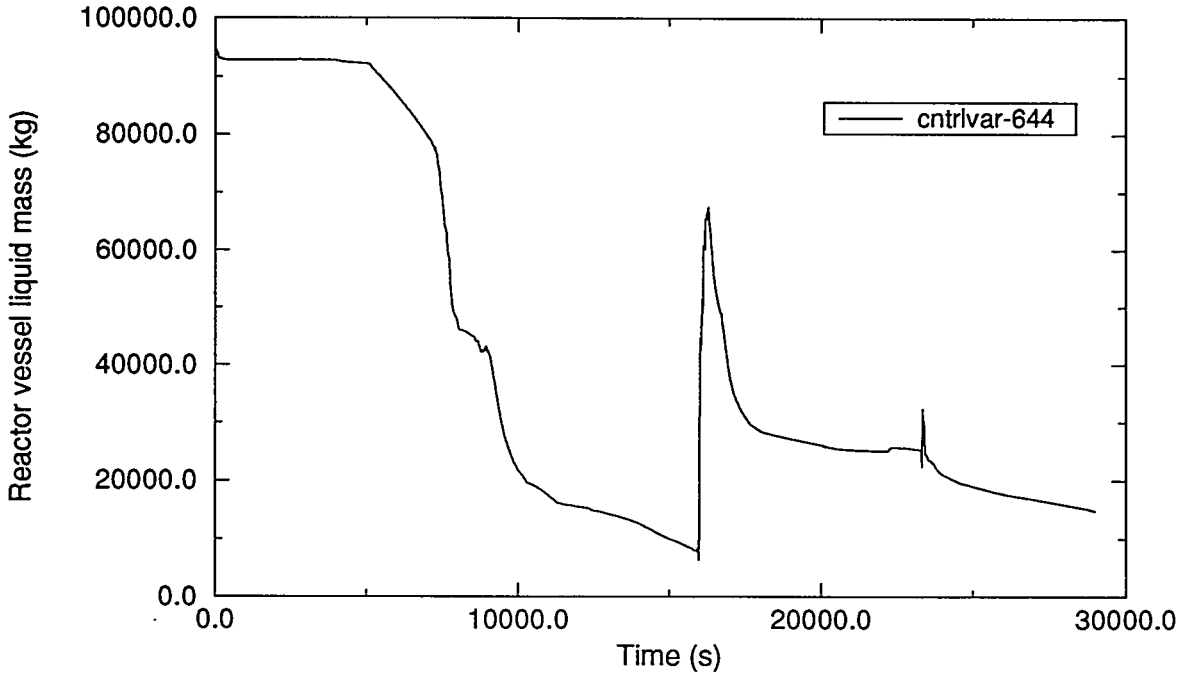

Figure C.14. Mass of liquid in the reactor vessel in Case 1.

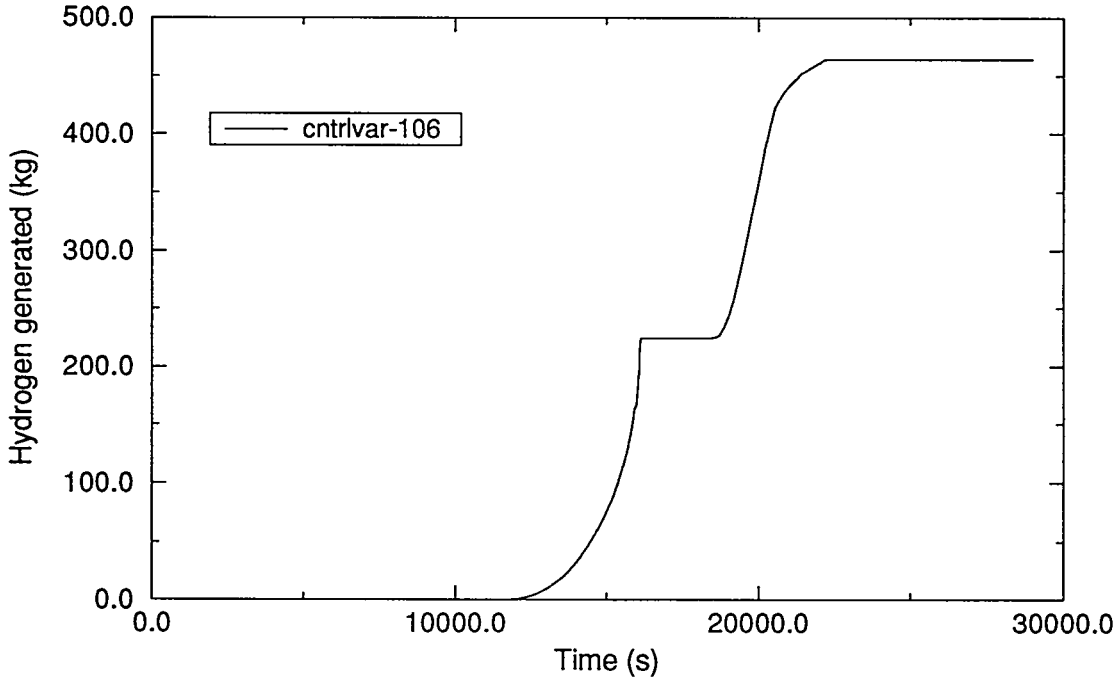

Figure C.15. Total hydrogen generated in Case 1.

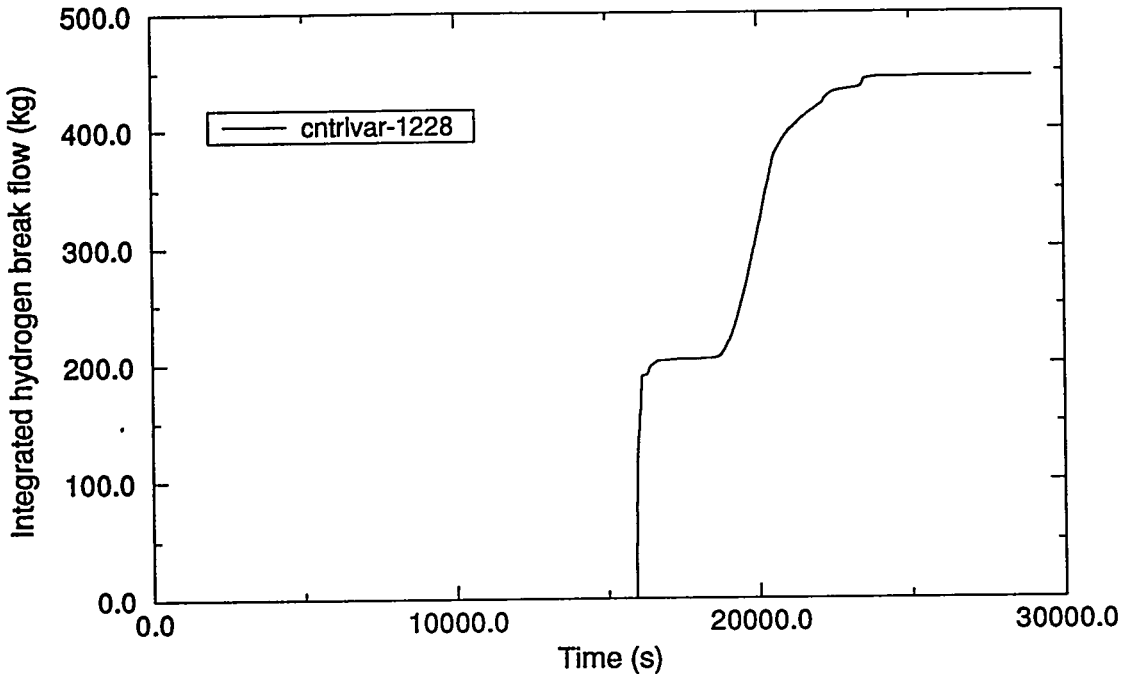

Figure C.16. Total hydrogen vented to containment through the hot leg break in Case 1.

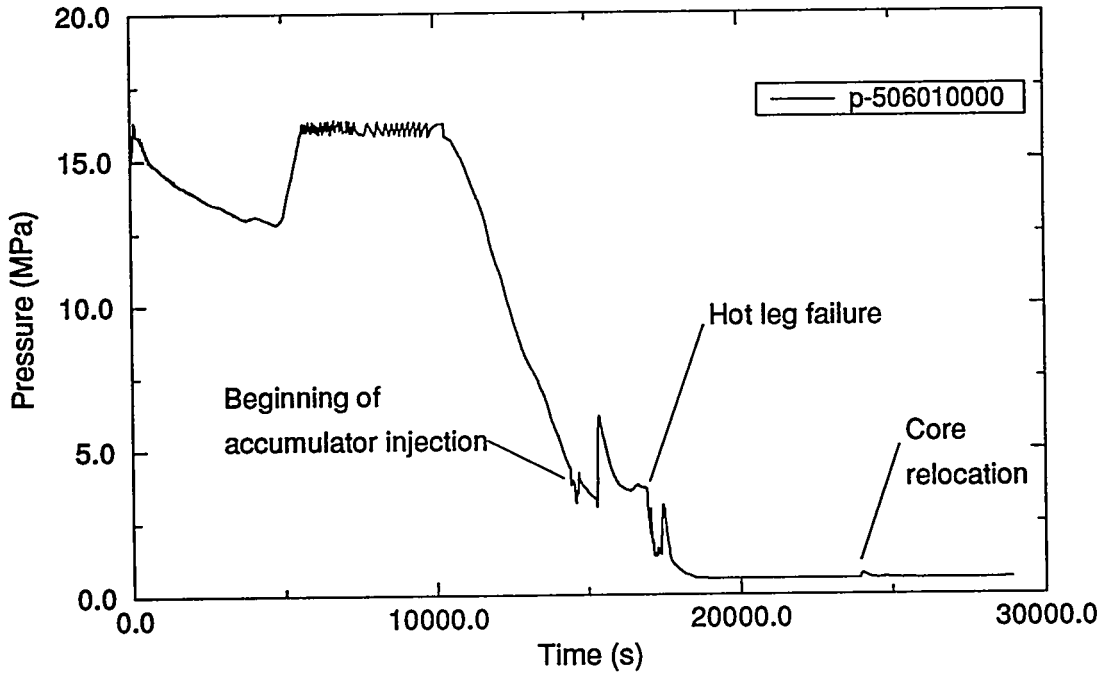

Figure C.17. Pressure in the reactor vessel lower head in Case 2.

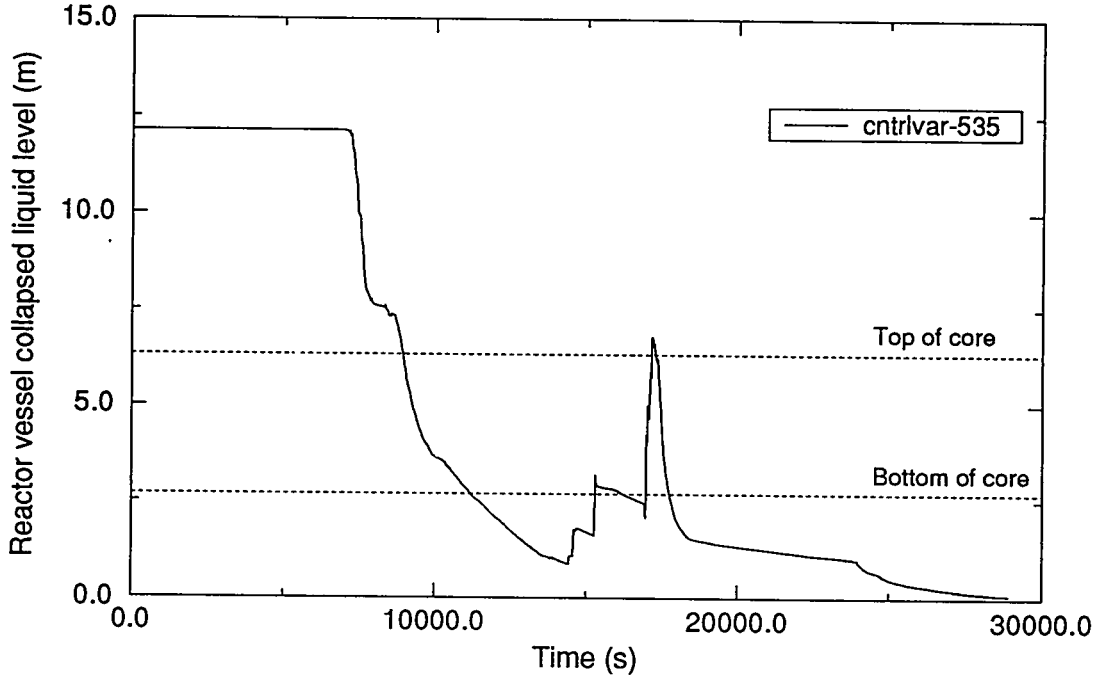

Figure C.18. Reactor vessel collapsed liquid level in Case 2.

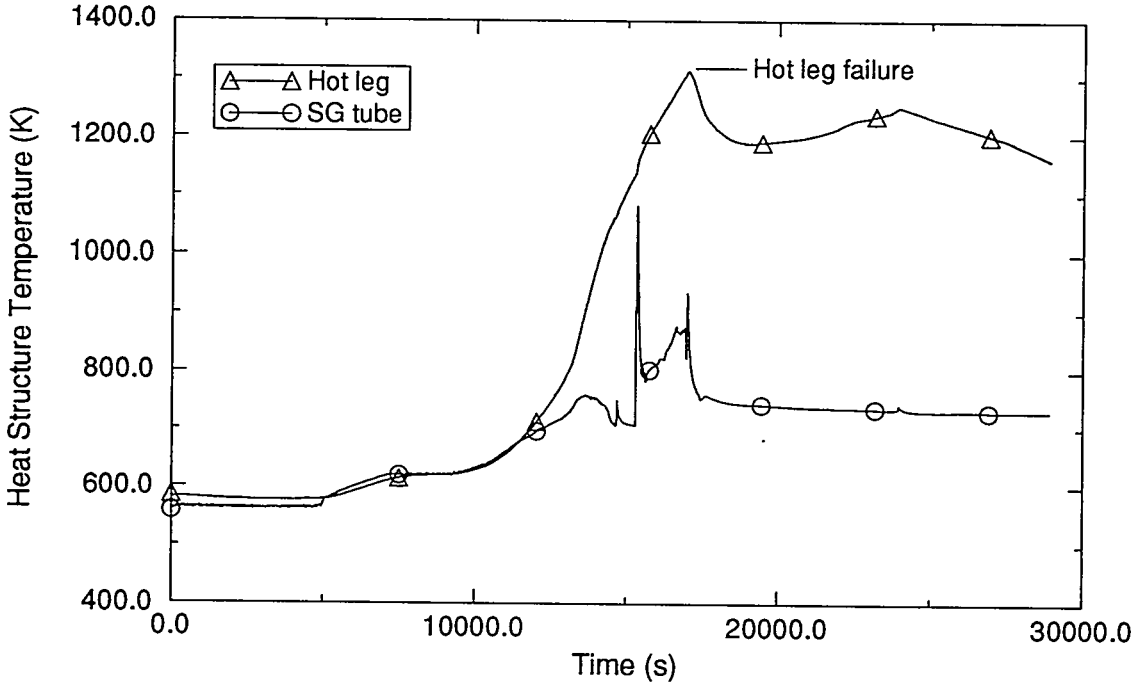

Figure C.19. Volume-averaged temperatures of selected ex-vessel structures in a non-pressurizer loop in Case 2.

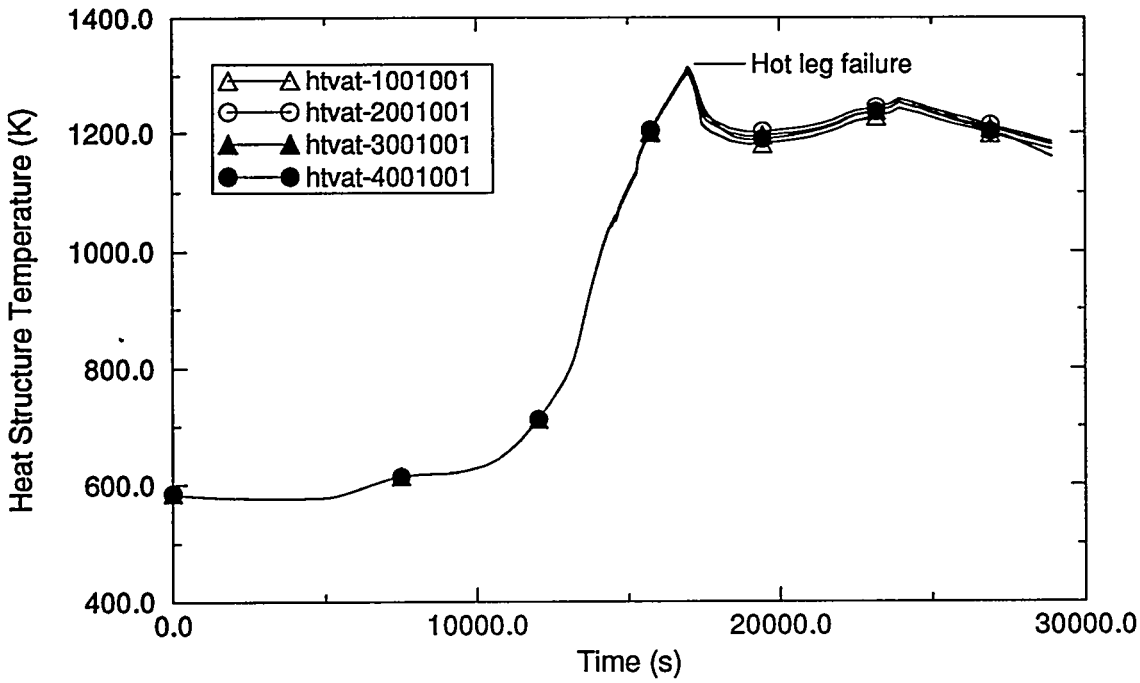

Figure C.20. Hot leg volume-averaged temperatures in Case 2.

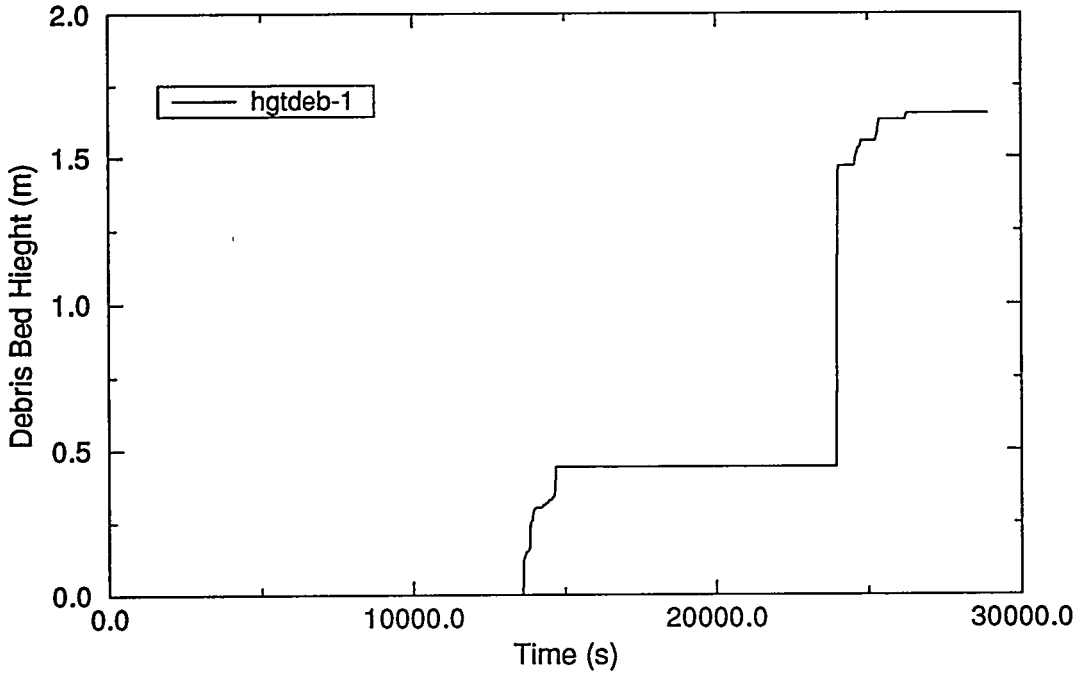

Figure C.21. Lower head debris depth (referenced to the bottom inside surface of the head) in Case 2.

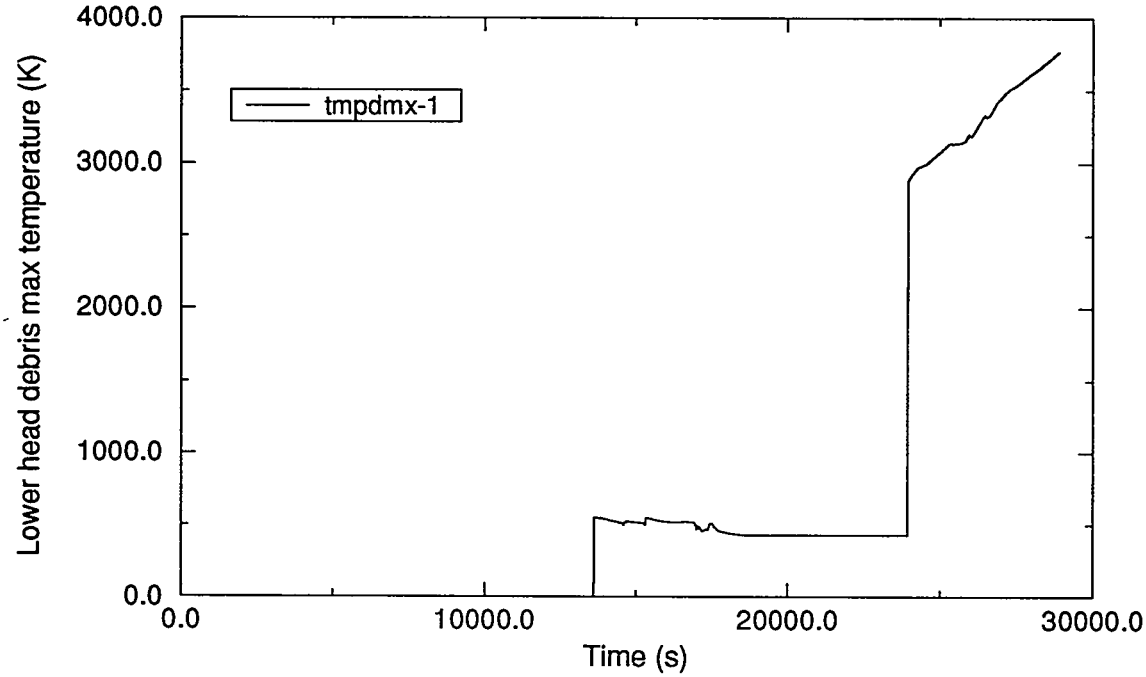

Figure C.22. Lower head maximum debris temperature in Case 2.

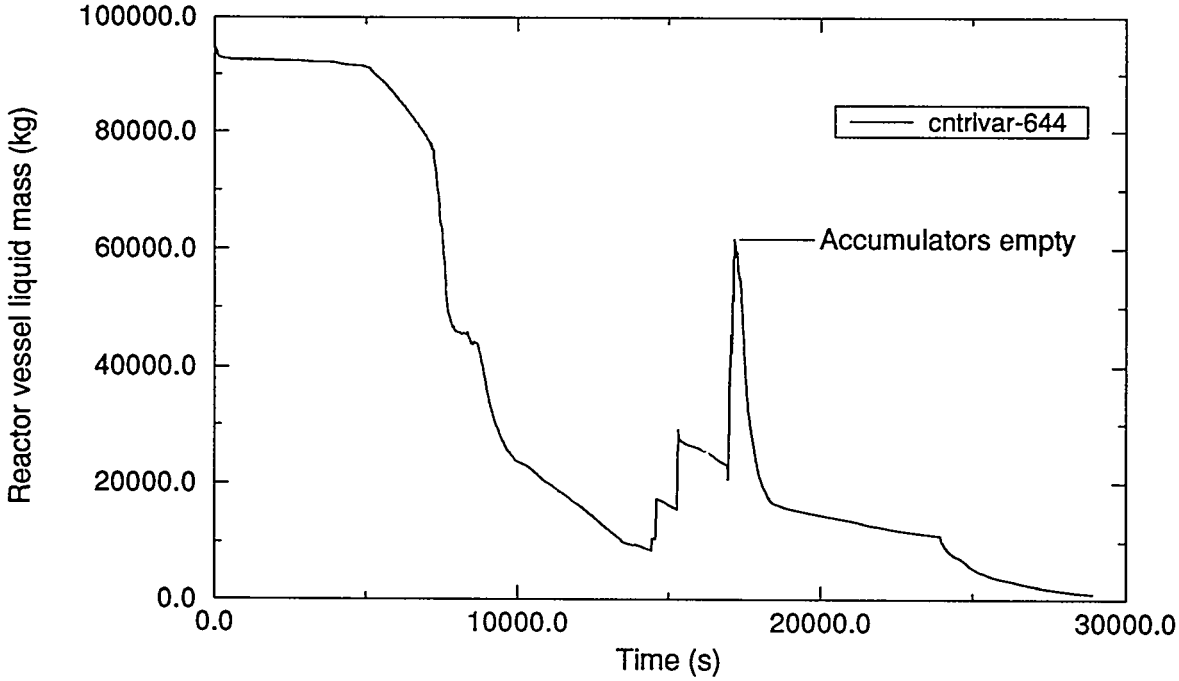

Figure C.23. Mass of liquid in the reactor vessel in Case 2.

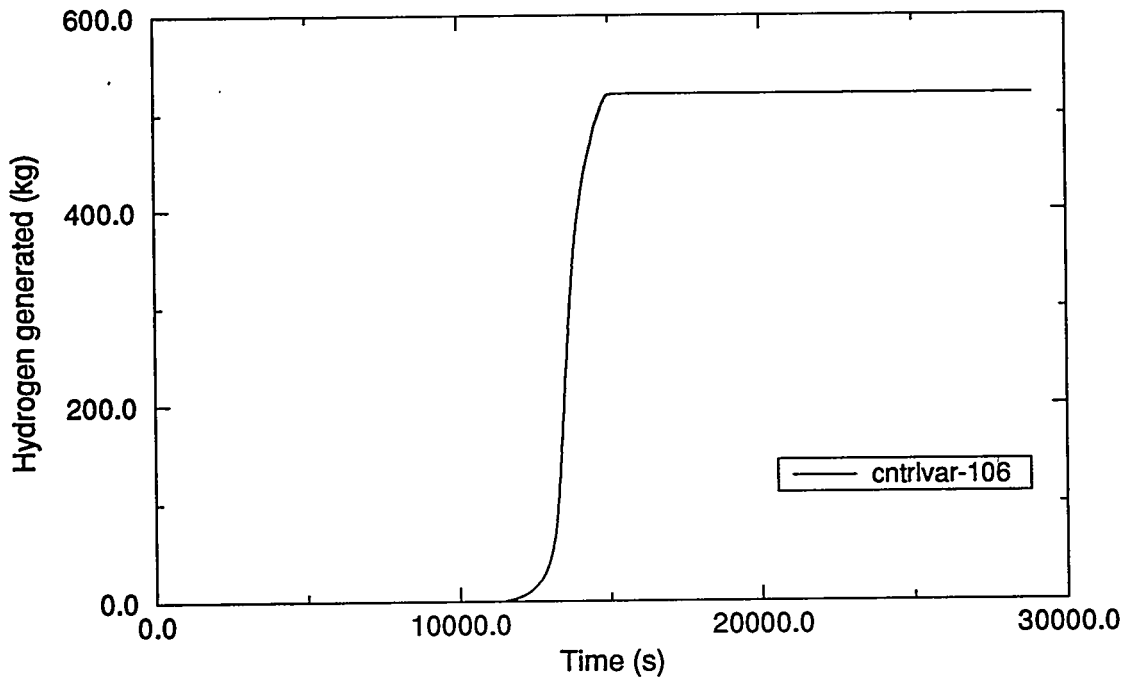

Figure C.24. Total hydrogen generated in Case 2.

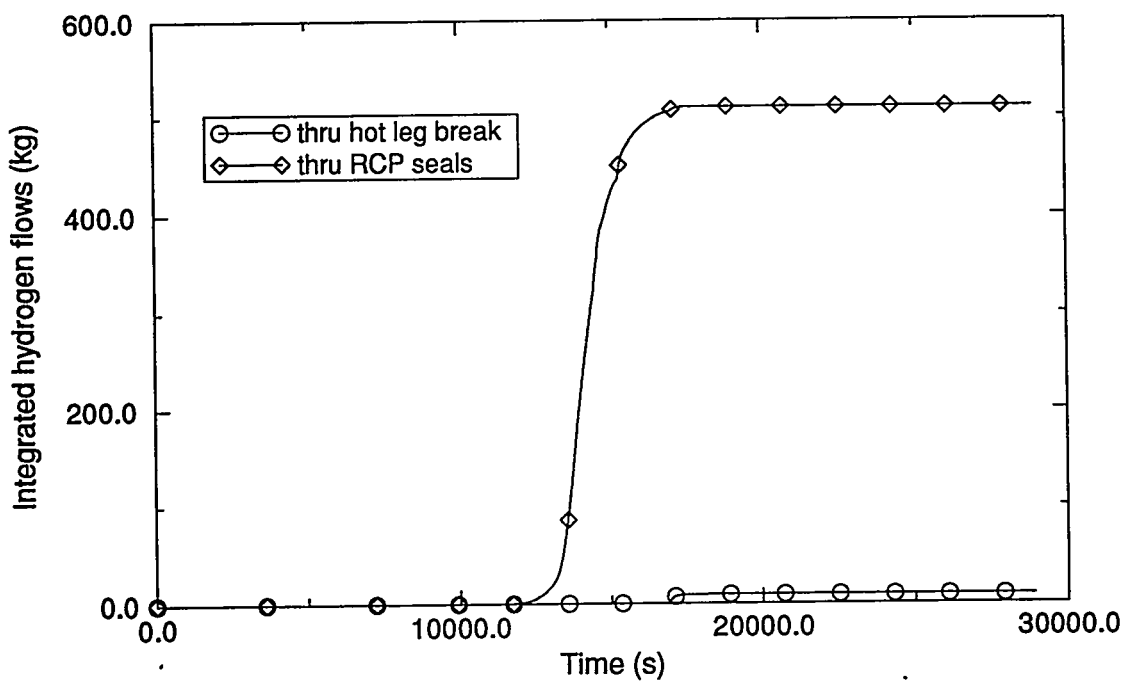

Figure C.25. Total hydrogen vented to containment through the hot leg break in Case 2.

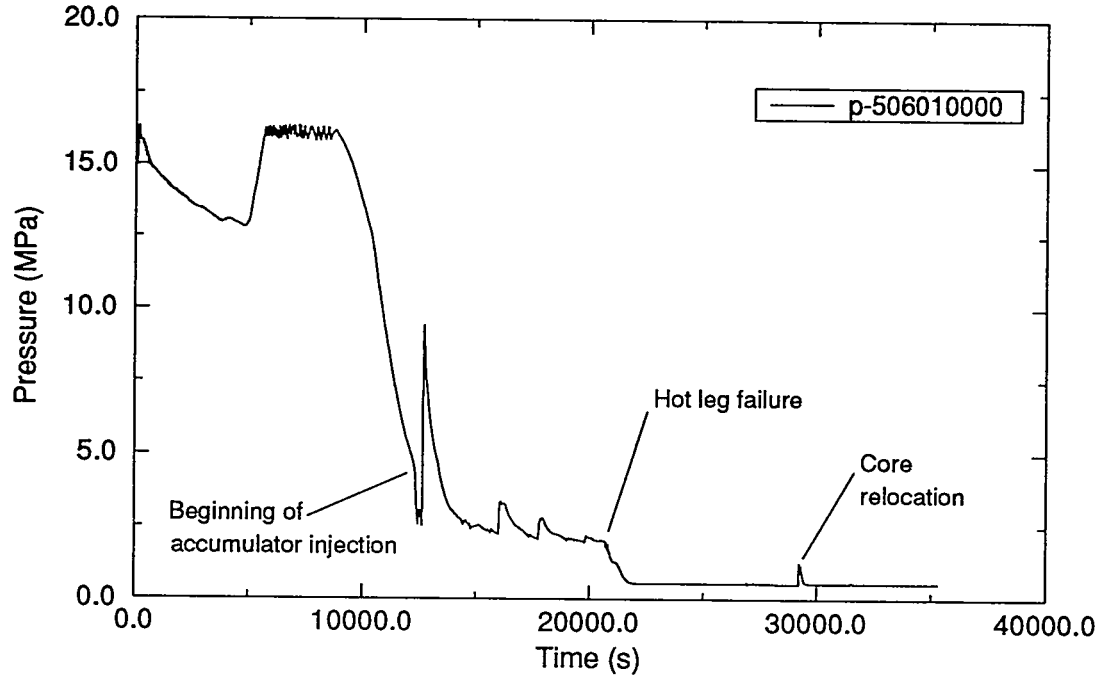

Figure C.26. Pressure in the reactor vessel lower head in Case 3.

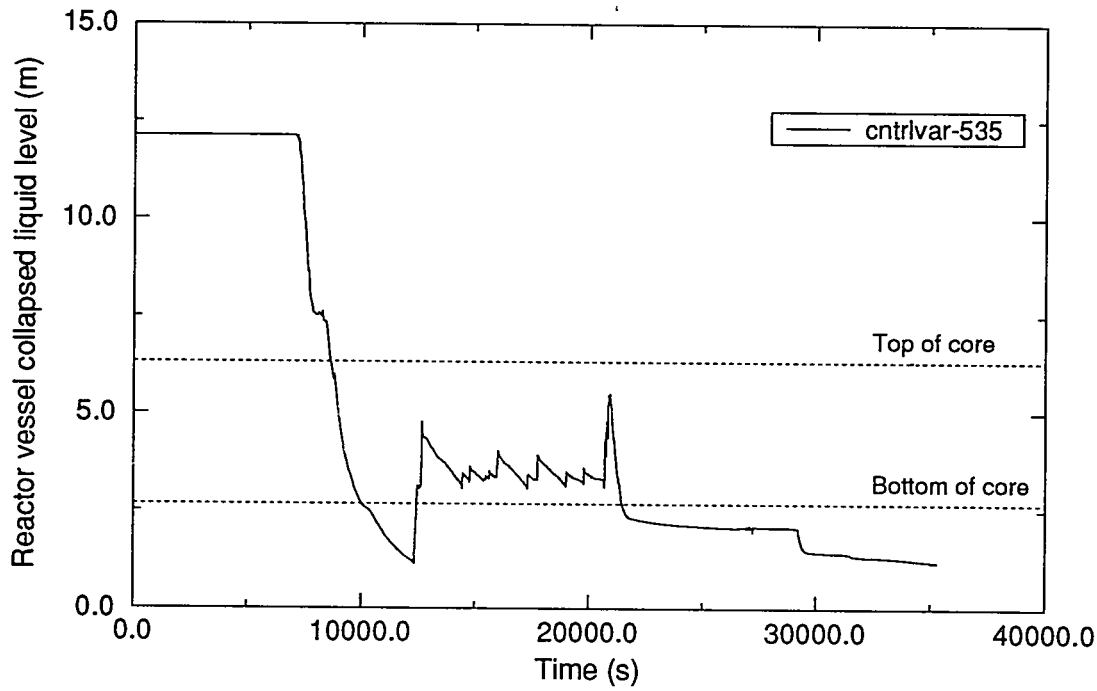

Figure C.27. Reactor vessel collapsed liquid level in Case 3.

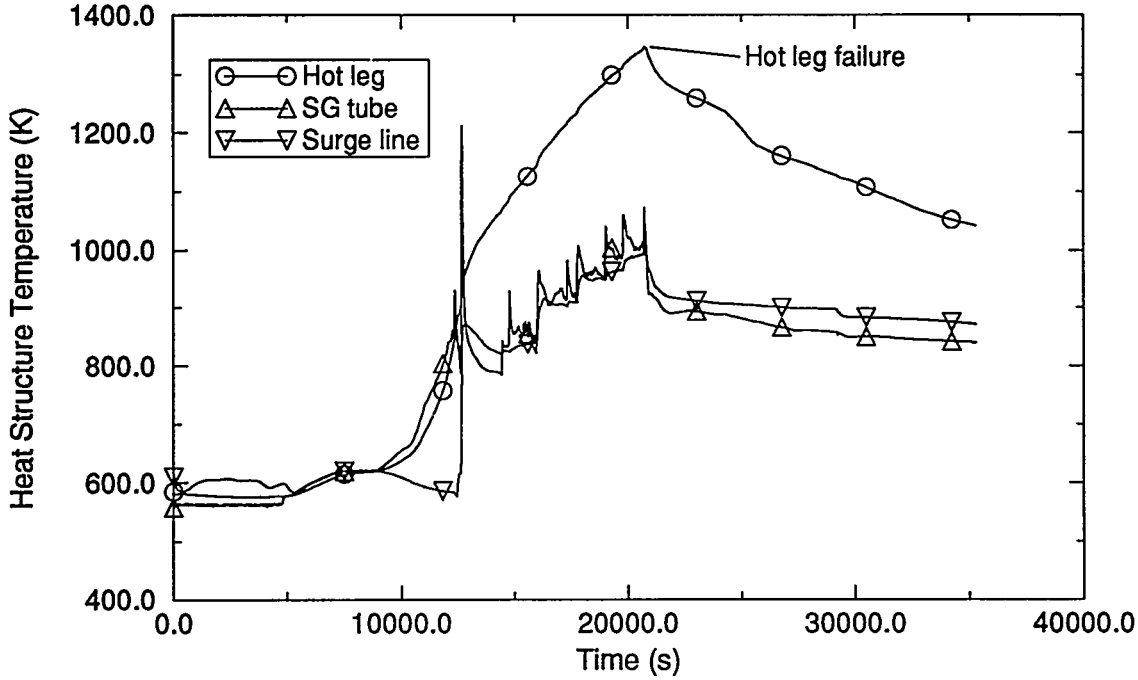

Figure C.28. Volume-averaged temperatures of selected structures in the pressurizer loop in Case 3.

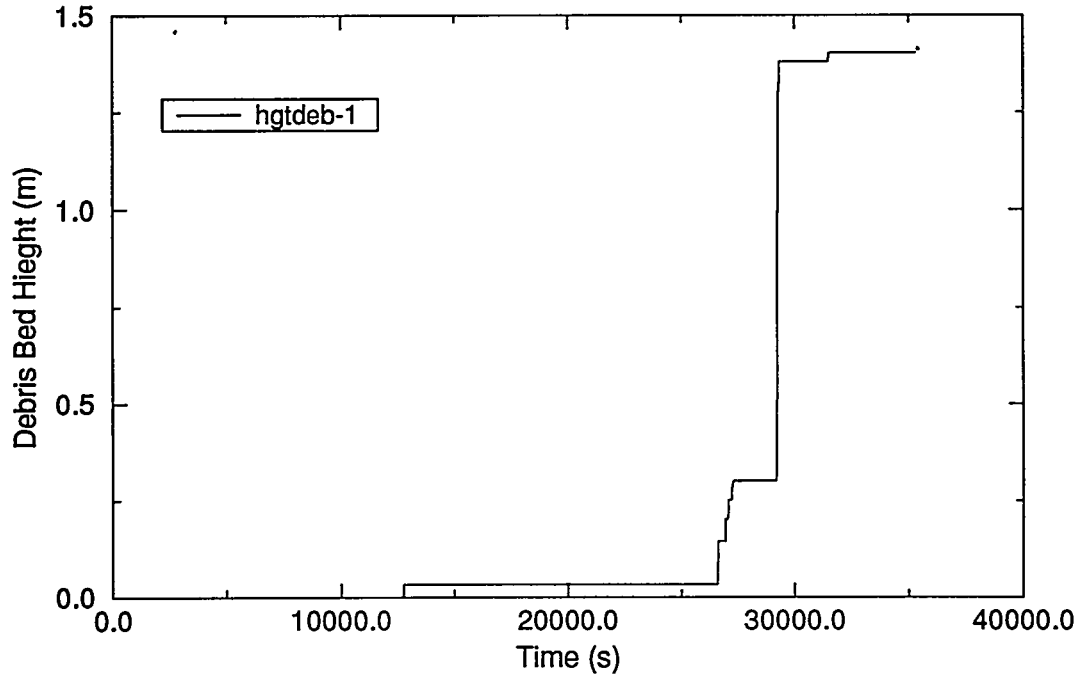

Figure C.29. Lower head debris depth (referenced to the bottom inside surface of the head) in Case 3.

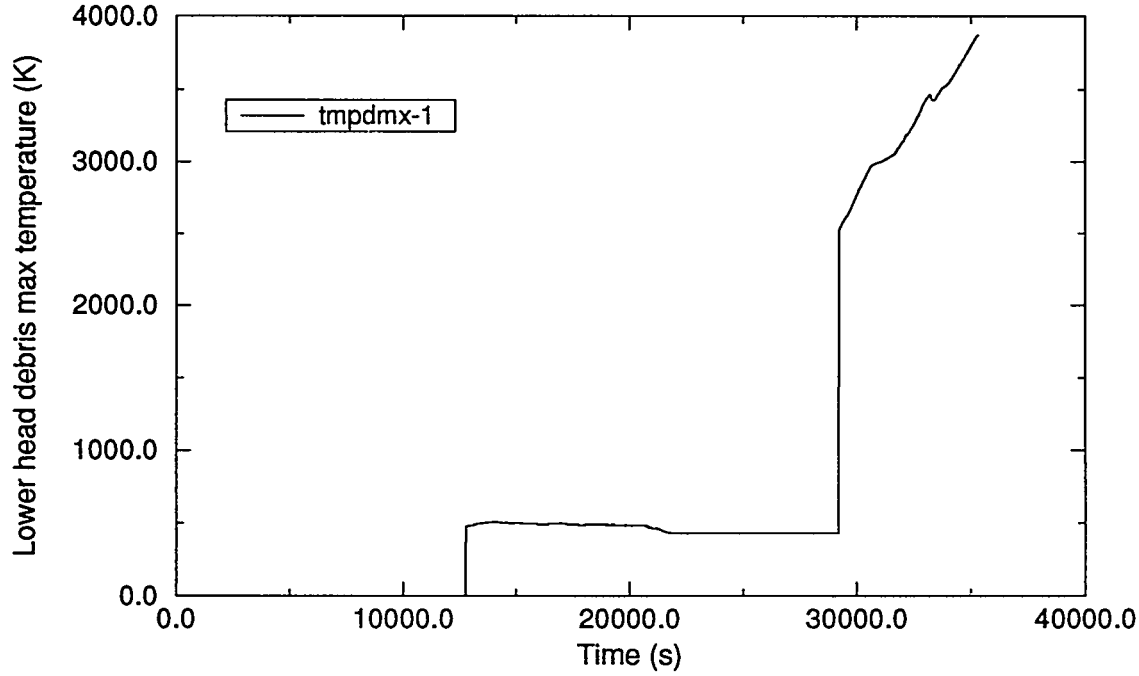

Figure C.30. Lower head maximum debris temperature in Case 3.

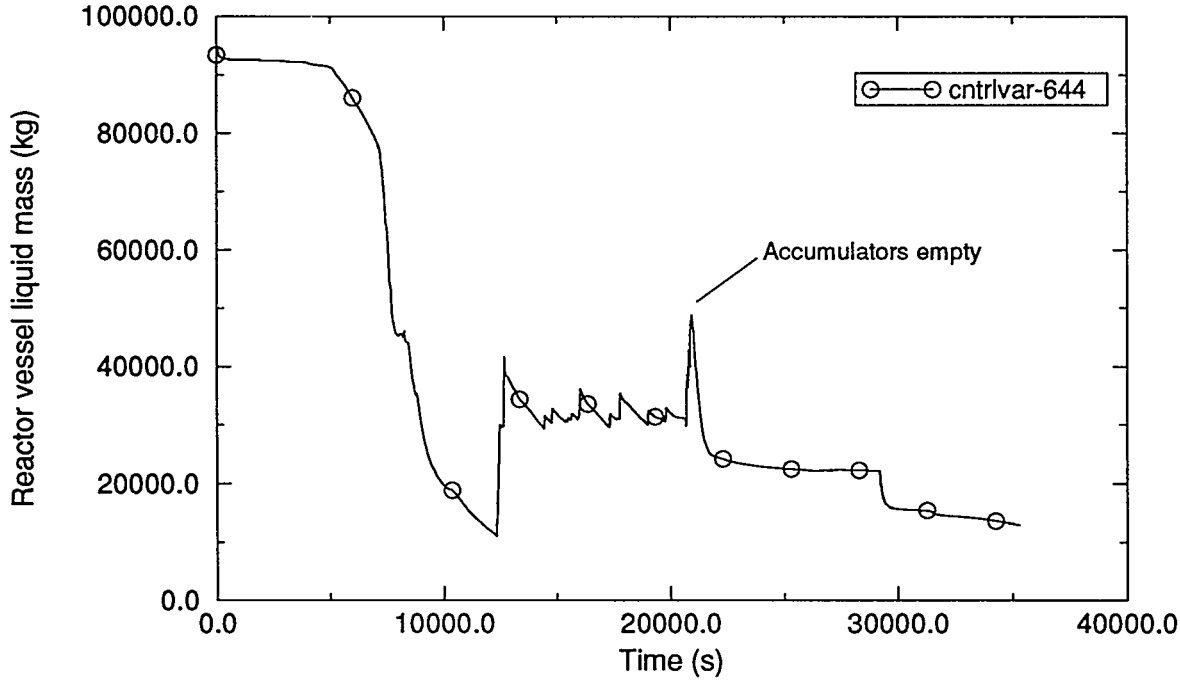

Figure C.31. Mass of liquid in the reactor vessel in Case 3.

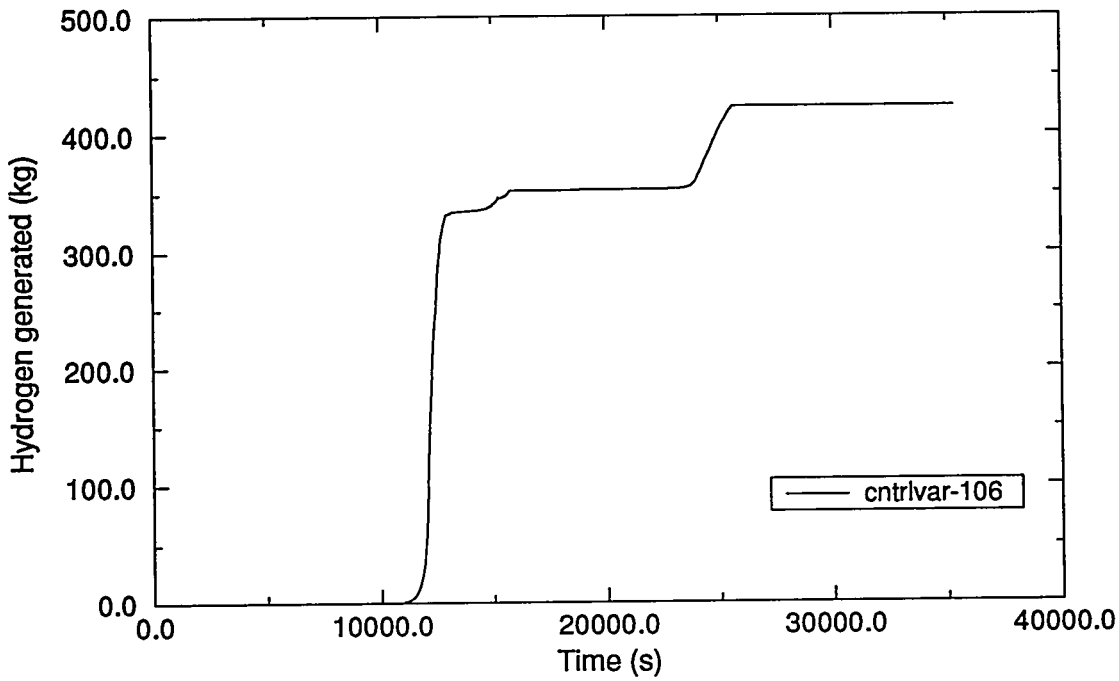

Figure C.32. Total hydrogen generated in Case 3.

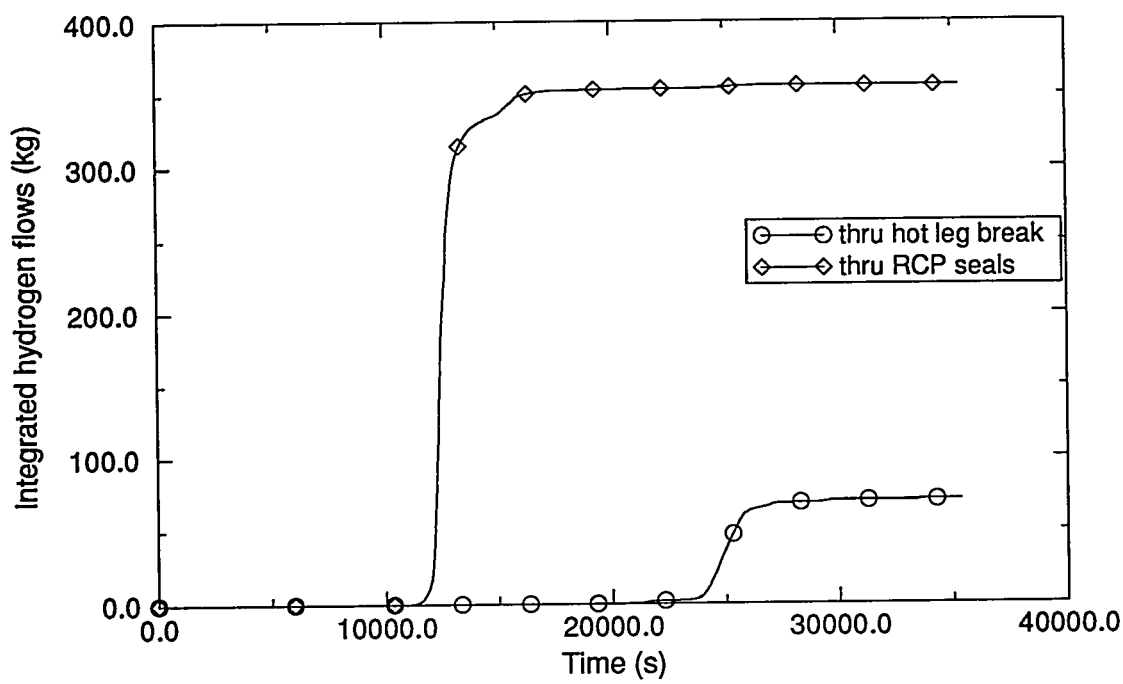

Figure C.33. Total hydrogen vented to containment through the hot leg break in Case 3.

ACRONYMS

AC	alternating current
ANS	American Nuclear Society
CRA	control rod assembly
DCH	direct containment heating
ECCS	emergency core cooling system
HPME	high pressure melt ejection
PORV	power operated relief valves
PWR	pressurized water reactor
RCP	reactor coolant pump
RCS	reactor coolant system
SG	steam generator
SRV	safety relief valve
UFSAR	Updated Final Safety Analysis Report

APPENDIX D
CONTAIN CALCULATIONS AND HYDROGEN COMBUSTION ANALYSES

Eden L. Tadios and Douglas W. Stamps
Sandia National Laboratories

D.1 INTRODUCTION

Three cases of a postulated station blackout in the Zion nuclear power plant were investigated with the CONTAIN code using liquid water, steam and noncondensible (hydrogen and nitrogen) sources obtained from Idaho National Engineering Laboratory (INEL). The SCDAP/RELAP5 code was used to predict the source rates. All three cases simulate the sequence of events after the loss of all AC power in the Zion PWR (pressurized water reactor) (Knudson, 1994a,b,c). The sequence of events for the SCDAP/RELAP5 calculations are summarized in Table D.1.

The first case, Case 1, simulates vented gases and liquid from the power operated relief valve (PORV) and from a hot leg failure. In addition to the PORV and hot leg break sources in Case 1, Case 2 simulated reactor coolant pump (RCP) seal leaks (four RCPs, 21 gpm per RCP) associated with the loss of seal cooling water flow that would accompany the loss of AC power. The initial seal leaks were introduced at the time the reactor scrammed. To simulate failures that could develop with two-phase flow across the seal faces, the seal leak rates were increased to 250 gpm when saturated conditions were reached at the RCPs. Case 3 simulates the same scenario as in Case 2, except that the seal leak rates were increased to 480 gpm when the conditions at the RCP reached saturation. Details of the three aforementioned cases are discussed in Appendix C.

Sources (liquid water, steam, hydrogen and nitrogen) from the PORV flow to the quench tank from which the PORV sources are released. The quench tank is located in the annulus volume (outside the crane wall) of the containment (Figure D.1 refers to the quench tank as the pressurizer relief tank). The hot leg is reinforced at the vessel (as part of the weldment fitting) inside the biological shield wall and therefore, the break is more likely to occur outside of the biological shield wall which is the steam generator room (SGR), and the sources are consequently discharged into the SGR. Gases and liquid released from the RCPs also flow into the SGR. From each source location, with some exceptions, the discharge consists of liquid water, steam, hydrogen and nitrogen (nitrogen originates from the accumulator). Case 1 had a

negligible amount of nitrogen discharged from the PORV and the hot leg break. In Cases 2 and 3, only steam and liquid are vented from the PORV.

D.2 NODALIZATION AND INITIAL CONDITIONS

In performing CONTAIN calculations, the user must first define the geometry of the containment and its associated structures. In CONTAIN, the containment should be nodalized into an adequate number of cells such that the desired phenomena are sufficiently captured. Defining the geometry of a nuclear power plant (NPP) containment using information from blueprints is a very cumbersome task. The recommended approach is to start with an existing input data (input deck) from a previous analysis using the same geometry. For the present analyses, an input deck from a previous Zion plant integrated containment analysis (Pasculli et al., 1988) was used as a starting point. The original input deck nodalized the containment into six cells with the external environment as the seventh cell, as shown in Figure D.1. The containment nodalization consisted of cells representing the cavity (Cell 1), reactor pressure vessel (RPV) and pressurizer (Cell 2), the steam generator room (Cell 3), the annulus (Cell 4) and the dome (Cells 5 and 6). RPV and pressurizer phenomena are not relevant to the present analyses and were not included in the CONTAIN calculations, but these volumes were included in the input data as dummy cells only for completeness.

The original containment nodalization was considered adequate for these analyses, with the exception of the containment dome. The dome was nodalized into two horizontal cells, and CONTAIN could not effectively capture the natural circulation in the dome using this modeling scheme. Additional subdivision of the dome volume might be preferred, but would require time-consuming reconfiguration of the input deck and validation efforts. Due to time constraints, an easier and a more viable option was employed in which the two horizontal dome cells (Cells 5 and 6) were combined as one cell, renamed as Cell 6. The cell combination is judged adequate for the present purposes, and it is believed to provide a better nodalization scheme than the original nodalization for this problem. The final nodalization for the present analyses is described in Table D.2.

As mentioned earlier, the Zion input deck for the present calculations was based on the input deck from Pasculli et al. (1988). The original input data was cross-checked with available Zion plant blueprints to assess the correctness of the data. Preliminary approximations of cell

volumes based on information from the blueprints demonstrated reasonable agreement with the original input data.

Initial conditions for these analyses were also obtained from Pasculli et al. (1988), which cited two sources for the initial conditions, one of which is the aforementioned SAR. Table D.3 gives the initial conditions of each cell.

D.3 DESCRIPTION OF CALCULATIONS

A set of source tables were generated for each case for the CONTAIN input using data from the SCDAP/RELAP5 calculations (Knudson, 1994a,b,c). A source table consisting of temperatures and mass flow rates as functions of time for each constituent was developed for each source location. As stated earlier, most of the sources consisted of water, steam, and noncondensibles (hydrogen and nitrogen). The nitrogen fractions in the Case 1 PORV and hot leg break sources are negligible. Case 2 and 3 PORV sources only consist of liquid and steam, no noncondensibles. For DCH (direct containment heating) purposes and the present analyses, only steam and hydrogen will be discussed. Temperature profiles and mass flow rates of the steam and hydrogen sources for all three cases are shown in Figures D.2-D.10, in which RCP1 was arbitrarily chosen to represent the RCP leaks.

Hot leg break sources and RCP leaks were located in the SGR (Cell 3), while PORV sources were located in the annulus (Cell 4). The CONTAIN calculations allowed the sources to flow into the remainder of the containment to determine the integrated containment response. Because of the complexity of the hydrogen combustion issues, CONTAIN was run with the burn model disabled. Hydrogen combustion analyses were later performed using both SCDAP/RELAP5 and CONTAIN predictions.

D.4 RESULTS

The SCDAP/RELAP5 calculations predicted a total mass of 464 kg of hydrogen generated for Case 1, 520.5 kg for Case 2 and 423.8 kg for Case 3 (Knudson, 1994a,b,c). Of the total hydrogen mass generated, 100 percent was discharged into the containment in Cases 1 & 3 and 99.8 percent in Case 2.

Using the source data from INEL, the CONTAIN calculations predicted the thermal-hydraulics response of the containment for each of the three cases described earlier. Case 1 results for the containment's cavity, SGR and dome are shown in Figures D.11-D.19. The containment pressure reached a maximum of 0.350 MPa (Figure D.11) immediately after the hot leg fails due to creep rupture at 15916 s. The cavity temperature peaked at about 485 K after the hot leg failure as shown in Figure D.13. The SGR in Case 1 experienced higher temperatures than the cavity due largely to the vented gases from the hot leg failure located in this volume. The SGR temperature reached a high of about 850 K (Figure D.15). As seen in Figure D.17, the annulus initially reached a maximum of about 640 K during the PORV cycling and after the hot leg break, the temperature reaches approximately 508 K. In the dome, the temperature profile follows a similar trend as that in the SGR, but lower in magnitude and peaked at 550 K, shown in Figure D.19.

The results from the Case 2 calculations are presented in Figures D.20-D.28. With the addition of the RCP seal leaks to the PORV and hot leg break sources, hotter gases and larger amounts of gases and liquid are vented into the containment, therefore, more severe conditions than in Case 1 can be expected. Shown in Figure D.20, the containment pressure peaked at 0.375 MPa following the hot leg failure (16925 s) and the second core dryout (17748 s). As in Case 1, no sources were vented directly into the cavity and therefore the temperatures are not expected to be as high as the other containment volumes containing the sources (steam generator room and the annulus). The temperature in the cavity only reached 405 K, shown in Figure D.22. In the SGR, the temperature had reached a temperature of about 535 K when the RCP reached saturation conditions at 7466 s. After the hot leg break in the SGR, the temperature immediately increased to about 675 K (Figure D.24). The annulus undergoes thermal cycling after the RCPs reached saturation conditions and peaks at about 570 K, gradually decreasing after the pressurizer drains, as seen in Figure D.26. Following the hot leg break, the annulus temperature rises to about 460 K. Similar to Case 1, the temperature profile in the dome follows the same trend as in the SGR. As illustrated in Figure D.28, the dome reaches a high of about 450 K after saturation is reached at the RCPs and peaks at about 460 K after the hot leg break.

Results of the Case 3 calculations are shown in Figures D.29-D.37. Although the RCP leaks (after saturation is reached at 7466 s) were larger in Case 2, the Case 3 maximum pressure is lower than that in Case 2. The maximum containment pressure reached 0.335 MPa

(Figure D.29) after the hot leg failure at 20650 s and the second core dryout at 21470 s. Sources were vented slower in Case 3 than in Case 2 and the progression of events in Case 3 were slower than in Case 2, allowing for steam condensation which reduced the maximum pressure. Case 2 and 3 temperature profiles were similar, varying only in magnitude. The cavity temperature did not progress beyond 408 K when the stainless steel melted and slumped into the lower head (Figure D.31). The cavity again reached another peak slightly above 400 K after the second core dryout. After the RCPs reached saturation, the SGR temperatures peaked at about 575 K and, after the hot leg failure, the temperature reached a maximum of about 617 K (Figure D.33). In the annulus, after saturated conditions were reached in the RCPs, the thermal cycle peaked at about 675 K shown in Figure D.35. The annulus was relatively unaffected by the hot leg break with the temperature only reaching 451 K. The maximum temperature in the dome was 20 degrees higher than in Case 2, peaking at about 480 K, as shown in Figure D.37.

D.5 DISCUSSION OF HYDROGEN COMBUSTION POTENTIAL

Cases 1-3 were analyzed using the INEL sources of gases entering the containment and CONTAIN predictions of the containment conditions to determine the amount of hydrogen, if any, that could be consumed exclusive of the DCH event. Because Cases 1-3 were station blackout scenarios, no ignition sources were considered available except for autoigniting jets. It was assumed that no hydrogen would burn until a jet autoignited. Only jet autoignition was considered since the gas temperature in each of the computational cells was below the autoignition temperature. Once a jet autoignited, a deflagration could be initiated in the source compartment and subsequent compartments if flammability limits and propagation limits were satisfied. The autoigniting jet may continue to burn as a diffusion flame even if the jet temperature drops below the autoignition temperature if diffusion flame stability criteria are met. The total amount of hydrogen consumed was estimated by including the amount of hydrogen burned during the time the jets were autoigniting and any deflagrations that could have been initiated in the containment due to the autoigniting jets. The additional hydrogen that may have been consumed if stable diffusion flames existed is beyond the scope of this analysis.

The criteria used to determine when the jets would autoignite were based on the data of Zabetakis (1956). It should be noted that the Zabetakis' data are for hydrogen-steam jets issuing into the air atmosphere while Cases 1-3 involve hydrogen-steam-nitrogen jets issuing into a

hydrogen-air-steam atmosphere. It is anticipated that background hydrogen will enhance the stability of the diffusion flame while background steam will destabilize the diffusion flame or, at sufficiently high concentrations, even extinguish it. The authors are not aware of autoignition data for jets having compositions found in Cases 1-3. The Zabetakis' data are shown in Figure D.38. His data extends to 74 percent steam (26 percent hydrogen). It can be seen from this figure that the jet autoignition temperature rises rapidly for jets with low concentrations of hydrogen. Many of the jets analyzed have conditions which extend beyond this database. Although these jets may have high temperatures the concentration of hydrogen is usually quite low. These cases will be discussed separately for the individual cases.

Jet autoignition was determined by cross-plotting the hydrogen volume concentration of the jet at each release location against the gas temperature. The mass fractions of the sources shown in Figures D.2-D.10 were converted into mole fractions. These results are shown in Figures D.39-D.52. The release locations include the PORV and hot-leg break for Case 1 and the PORV, hot-leg break, and four seal leaks from the RCPs in Cases 2 and 3. The autoignition temperature for different jet hydrogen concentrations was overlaid on the plots. For example, any jet having a temperature lower than 947 K will not autoignite regardless of jet composition. A jet with 38 percent hydrogen will autoignite when the jet temperature exceeds 1006 K. The times at which the jets would autoignite were estimated by graphical analysis of Figures D.39-D.50. The analysis of individual cases will be discussed next.

For Case 1, the jet temperature never exceeded the autoignition temperature for the PORV release as shown in Figure D.39 except at approximately 24000 s. At this time, however, there was no hydrogen in the jet. Figure D.40 shows that the gases released from the hot-leg break do autoignite between approximately 18940 s and 20540 s. During this time, the gas temperature dropped below the autoignition temperature for three short times. The amount of hydrogen released during this time is included in the estimate of total hydrogen burned during autoignition time interval. The time scale is expanded in Figure D.40 as well as in some other figures for increased clarity and includes only those times that hydrogen was released. The jet also autoignites at approximately 22170 second for about one minute. This is the last chance for ignition of a deflagration due to an autoigniting jet.

The total amount of hydrogen consumed in the autoigniting jet was estimated from the integrated hydrogen plots in Appendix C. Using graphical analysis, it was estimated that 172

kg of hydrogen was consumed during the time period between 18940 s and 20540 s. This amount of hydrogen represents approximately 37 percent of the total hydrogen that flowed into the containment.

From the CONTAIN calculations at 22170 s, the composition of the mixture in the steam generator room (source compartment) was approximately 5 percent hydrogen and 44.5 percent steam for the "no burn" calculations as shown in Figure D.14. In the case where hydrogen is consumed by the autoigniting jet, the total amount of hydrogen released into the containment is only 63 percent of the total hydrogen released in the "no-burn" case. If the hydrogen in the SGR is scaled to account for this reduction, the hydrogen concentration would be approximately 3.15 percent. Even based on data showing the widest flammability limits for hydrogen-air-steam mixtures (Kumar, 1985), this mixture is nonflammable and a deflagration is not possible.

A CONTAIN calculation was performed to determine the increase in containment pressure due to the energy released in the autoigniting jet. Developing well after the containment peak pressure, the maximum difference in the containment pressure, which occurred at about 20000 seconds, was only about 10 percent between the case with autoigniting jets and the case with no burning. The difference between the two cases was not very large in spite of the fact that 37 percent of the total hydrogen was consumed in the autoigniting jet since the energy was released over a relatively long period of time (~30 minutes).

No autoigniting jets are anticipated for the releases in Case 2. As shown in Figure D.41, the jet temperature never exceeds the autoignition temperature in the gases released from the PORV. Regardless of the temperature, however, there is no hydrogen released through the PORV. Although jet temperatures are high at various times in the RCP seal leaks shown in Figures D.42-D.45, the corresponding hydrogen concentrations in the jets are low. For example, the jet temperature is above 1100 K between approximately 15500 s and 16000 s but the hydrogen concentrations are between approximately 5 and 15 percent. Although these conditions are beyond the database, linear extrapolations indicate the jet temperature is below the autoignition temperature. The jet temperature in the hot leg break is very high (approximately 1900 K) as shown in Figure D.46, but the hydrogen concentration is very low (0.0024 percent). These conditions are so far beyond the database that it is not clear whether this mixture can autoignite given the fact that hydrogen exists in the atmosphere.

For Case 3, the jet temperature never exceeds the autoignition temperature in the gases released from the PORV as shown in Figure D.47. Regardless of the temperature, however, there is no hydrogen released through the PORV. Likewise, as shown in Figures D.48-D.51, the jet temperature never exceeds the autoignition temperature of the gas mixture for all four of the reactor coolant pump seal leaks. The jet will autoignite in the hot-leg break for a short time from approximately 24140 s to 24300 s as shown in Figure D.52. During this time, the jet temperature drops below the autoignition temperature one brief time. The jet will also autoignite briefly at approximately 24510 s, 24590 s, and possibly at 26640 s which could serve as ignition sources.

The total amount of hydrogen consumed in the igniting jet was estimated from the integrated hydrogen plots in Appendix C. Using graphical analysis, it was estimated that only 6 kg of hydrogen was consumed during the time period between 24140 s and 24300 s. This amount of hydrogen represents approximately 1.5 percent of the total hydrogen that flowed into the containment.

From the CONTAIN calculations at the latest time ignition could occur by an autoigniting jet (26640 s), the composition of the mixture in the steam generator room (source compartment) is approximately 3.7 percent hydrogen and 47.2 percent steam for the "no burn" calculations as shown in Figure D.32. Using the flammability limits data from the Whiteshell experiments (Kumar, 1985), hydrogen-air-steam mixtures would be flammable at 47.2 percent steam if the hydrogen concentration exceeded 5.6 percent. Even based on data showing the widest flammability limits for hydrogen-air-steam mixtures (Kumar, 1985), this mixture is nonflammable and a deflagration is not possible.

D.6 CONCLUSIONS

For DCH purposes, the dome conditions are most important in the analysis of containment integrity. Of the three cases investigated, CONTAIN simulations show that the Case 2 scenario has the highest load on the containment with a transient dome pressure of 0.375 MPa, most likely due to high flow rate (as much as 100 kg/s) of steam released from the RCPs. Case 3 had a higher leak rate but had a lower steam flow rate than Case 2. High temperatures occur in the subvolumes of the containment (i.e., steam generator room and annulus) but are only moderately high in the dome, the maximum being Case 1 at 550 K. Compared to Case 2, the

slower progression of events in Case 3 possibly allowed steam to condense resulting in lower peak pressures.

Hydrogen combustion analyses were performed using the results from SCDAP/RELAP5 and CONTAIN calculations. The results of the analyses indicate that the only possibility of jet autoignition occurred in the hot leg break in Cases 1 and 3. Otherwise, the temperatures of the gases released from the PORV were too low for autoignition for all cases. Likewise, gases released from the RCPs would not likely autoignite in all cases analyzed because hydrogen concentrations in the jets were very low during periods of high gas temperatures.

For Case 1, it was estimated that between 35-40 percent of the total hydrogen released into the containment could have burned as an autoigniting jet. In comparison between the case with the autoigniting jet and the no-burn case, the maximum increase in containment pressure due to the energy released from the autoigniting jet was about 10 percent at approximately 20000 seconds, well after the peak containment pressure. Although 37 percent of the total hydrogen was consumed in the autoigniting jet, the 10 percent increase was not unexpected since the energy was liberated very slowly.

Conditions for autoigniting jets were not satisfied for Case 2. For Case 3, it was estimated that approximately 1-2 percent of the total hydrogen released into the containment could have burned as an autoigniting jet. These results are for three cases that had different RCP seal leak rates (with Case 1 as having no seal leak) but were otherwise the same. The large variation in the fraction of hydrogen that could have burned for the three cases illustrates that hydrogen combustion is very scenario dependent.

Gases in the source compartments were not flammable during the time the jets were autoigniting for the three cases analyzed. The analyses accounted for the decrease in the hydrogen which was consumed in the autoigniting jets.

D.7 REFERENCES

Knudson, D.L. (July 13, 1994a). "Transmittal of Zion Case 1 Results - DLK-6-94," Letter Report to R. Lee (USNRC), EG&G, Idaho Falls, ID.

Knudson, D.L. (July 19, 1994b). "Transmittal of Zion Case 2 Results - DLK-8-94," Letter Report to R. Lee (USNRC), EG&G, Idaho Falls, ID.

Knudson, D.L. (July 29, 1994c). "Transmittal of Zion Case 3 Results - DLK-10-94," Letter Report to R. Lee (USNRC), EG&G, Idaho Falls, ID.

Kumar, R.K. (July/August 1985). "Flammability Limits of Hydrogen-Oxygen-Diluent Mixtures," Journal of Fire Sciences, V. 3, pp. 245-262.

Pasculli, A. et al. (March 21-25, 1988). "Integrated Containment Analysis of a Severe Accident in a PWR Plant Using the CONTAIN Computer Code," IAEA-SM-296/47, International Symposium on Severe Accidents in Nuclear Power Plants, Sorrento, Italy.

Zabetakis, M.G. (September 1956). *Research on the Combustion and Explosion Hazards of Hydrogen-Water Vapor-Air Mixtures*, Bureau of Mines Final Report, AECU-3327.

Table D.1. SCDAP/RELAP5 calculations sequence of events (Knudson, 1994a,b,c)

Event	Case 1 (sec)	Case 2 (sec)	Case 3 (sec)
TMLB' initiation	0	0	0
Introduction of seal leaks of 21 gpm per RCP, leak diameters = 0.00327 m		0	0
Onset of pressurizer PORV cycling, Case 1	4960		
Steam generators, dryout (pressurizer/non-pressurizer loops)	4976/5006	4801/5003	4801/5003
Onset of pressurizer PORV cycling, Cases 2 & 3 only		5680	5680
RCP saturation; seal leaks increased per RCP (Case 2 - 250 gpm, leak dia. - 0.0137; Case 3 - 480 gpm, leak dia. - 0.0190m)		7466	7466
End of full loop (liquid) natural circulation	7660	7526	7526
End of pressurizer PORV cycling, Case 3			8456
Collapsed liquid level falls below the top of fuel rods	9140	8944	8644
Vapor in the core exit begins to superheat; hot leg countercurrent circulation begins	9384	9045	8697
End of pressurizer PORV cycling, Case 2		10320	
Collapsed liquid level falls below the bottom of the fuel rods, Cases 1 & 3	10181		10016
Pressurizer drains	10997	10575	10526
Collapsed liquid level falls below the bottom of the fuel rods, Case 2		11196	
Onset of fuel rod oxidation	11621	11235	10797
First slumping into lower head begins; 2969 kg Ag over ~360 s, Case 2		13616	
27.5 kg of upper plenum stainless steel melts and slumps into lower head, Case 2		14018	
First appearance of an in-core molten pool; by fuel dissolution in third channel, Case 2		14057	

Table D.1. SCDAP/RELAP5 calculations sequence of events (Knudson, 1994a,b,c)

Event	Case 1 (sec)	Case 2 (sec)	Case 3 (sec)
71.5 kg of upper plenum stainless steel melts and slumps into in-core molten pool, Case 2		14219	
Slumping into lower head begins; 330 kg Ag, 112.7 SS, 2406 kg UO_2, 452 kg Zr over ~420s, Case 2		14250	
First heatup to molten fuel temperatures; in first channel, Case 3			12169
Accumulator injection begins, Cases 2 & 3		14414	12312
First heatup to molten fuel temperatures; in first channel, Case 2		14976	
First fuel rod fragmentation; in the fourth channel, Case 3			12707
First fuel rod fragmentation; in the fifth channel, Case 2		15371	
27.5 kg of upper plenum stainless steel melts and slumps into lower head, Case 3			12751
501.7 kg of upper plenum SS melts and slumps into in-core molten pool, Case 2		15410	
131.9 kg of upper plenum SS melts and slumps into in-core molten pool, Case 2		15566	
632.0 kg of upper plenum SS melts and slumps into in-core molten pool, Case 2		16115	
620.2 kg of upper plenum SS melts and slumps into in-core molten pool, Case 2		16558	
749.5 kg of upper plenum SS melts and slumps into in-core molten pool, Case 2		16849	
Pressurizer loop hot leg nozzle fails by creep rupture, Cases 1 & 3	15916		20650
Non-pressurizer loop hot leg nozzle fails by creep rupture, Case 2		16925	
Hot leg break initiated; break diameter = 0.166 m	15916	16925	20650

Table D.1. SCDAP/RELAP5 calculations sequence of events (Knudson, 1994a,b,c)

Event	Case 1 (sec)	Case 2 (sec)	Case 3 (sec)
Core is reflooded; collapsed liquid level rises above the top of the fuel rods, Case 2		17163	
End of pressurizer PORV cycling, Case 1	15916		
Accumulator injection begins, Case 1	15961		
Accumulator injection ends, Case 2 & 3		17169	20920
First fuel rod fragmentation; in the third channel, Case 1	16012		
Core is reflooded; collapsed liquid level rises above the top of the fuel rods, Case 1	16134		
Accumulators empty; injection ends, Case 1	16285		
Second core dryout; collapsed liquid level falls below the bottom of the fuel rods	17418	17748	21470
First appearance of an in-core molten pool; through heatup in the first channel, Case 1	19905		
319.4 kg Ag-In-Cd melts and slumps into lower head, Case 3			26610
319.4 kg Ag-In-Cd melts and slumps into lower head, Case 3			26960
638.4 kg Ag-In-Cd melts and slumps into lower head, Case 3			27059
638.4 kg Ag-In-Cd melts and slumps into lower head, Case 3			27220
199.5 kg Ag-In-Cd melts and slumps into lower head, Case 3			27283
35.5 kg Ag-In-Cd melts and slumps into lower head, Case 3			29175
Core slumping into lower head; Case 1 - 61044 kg UO_2, 15770 kg ZrO_2, Case 1, Case 2 - 62930 kg UO_2, 16350 kg ZrO_2; Case 3 - 60290 kg UO_2, 16690 kg ZrO_2, Cases 2 & 3	23313	23938	29212
Submerged 'thin' SS added to lower head debris, Case 2 - 5300 kg, Case 3 - 5000 kg	23400	24000	29300

Table D.1. SCDAP/RELAP5 calculations sequence of events (Knudson, 1994a,b,c)

Event	Case 1 (sec)	Case 2 (sec)	Case 3 (sec)
Slumping into lower head; 3556 kg UO_2, 1039 kg ZrO_2, Case 2		24536	
Slumping into lower head; 2240 kg UO_2, 569 kg ZrO_2, Cases 2 & 3		24612	31459
Slumping into lower head; 2240 kg UO_2, 569 kg ZrO_2, Case 2		24723	
Slumping into lower head; 2240 kg UO_2, 569 kg ZrO_2, Case 2		25233	
Slumping into lower head; 4697 kg UO_2, 1193 kg ZrO_2, Case 2		25302	
Slumping into lower head; 2240 kg UO_2, 569 kg ZrO_2, Case 2		26205	
Lower head failure by creep rupture, Cases 1 & 2 - ~0.80; Case 3 - ~0.66, above the inside bottom surface of the head	26965	26915	33285
Relocation of 200 kg of Ag into the lower head from in-core crusts, Case 1	28410		
End of Calculations	28995	28915	35285

Table D.2. Zion plant nodalization (Pasculli, 1988)

Cell Number	Description	Cell Volume (m^3)
Cell 1	Cavity	260.75
Cell 2	Dummy cell (RPV and pressurizer)	353
Cell 3	Steam generator room (subcompartments)	6657.3
Cell 4	Annulus	6578.4
Cell 5	Dummy cell (polar crane area)	28918
Cell 6	Dome	62309
Cell 7	External environment	

Table D.3. Initial conditions

Cell	Initial Conditions	Initial Inventory (kg)
Cell 1	T = 316.48 K P = 0.101 MPa	O_2 = 64.6 N_2 = 212.6 H_2O (steam) = 7.817
Cell 3	T = 316.48 K P = 0.101 MPa	O_2 = 1648.12 N_2 = 5427.77 H_2O (steam) = 199.58
Cell 4	T = 316.48 K P = 0.101 MPa	O_2 = 1628.6 N_2 = 5363.5 H_2O (steam) = 197.23
Cell 6	T = 316.48 K P = 0.101 MPa	O_2 = 15425.4 N_2 = 50802 H_2O (steam) = 1868

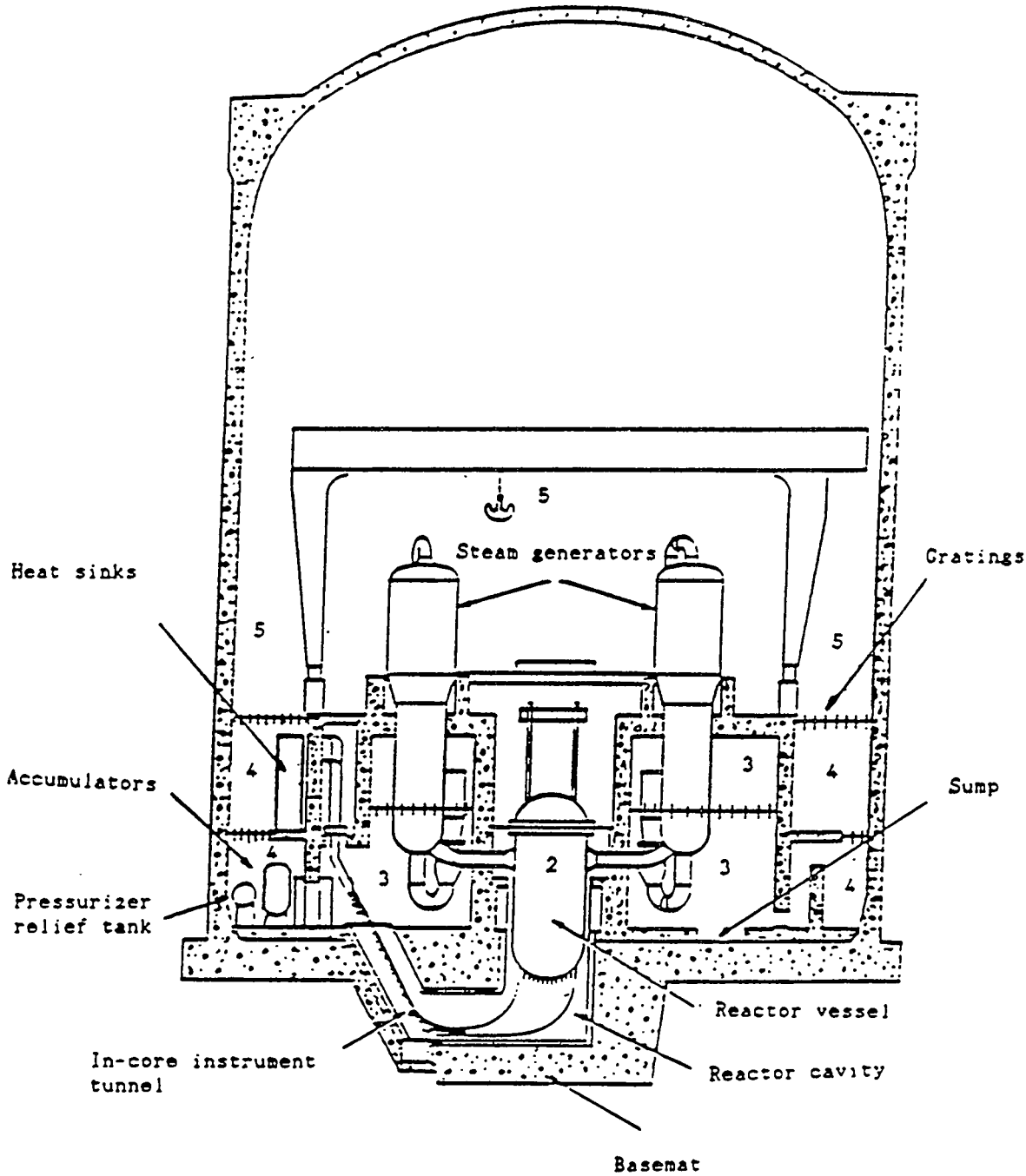

Figure D.1 Schematic of containment design and nodalization for Zion power plant (Pasculli et al., 1988).

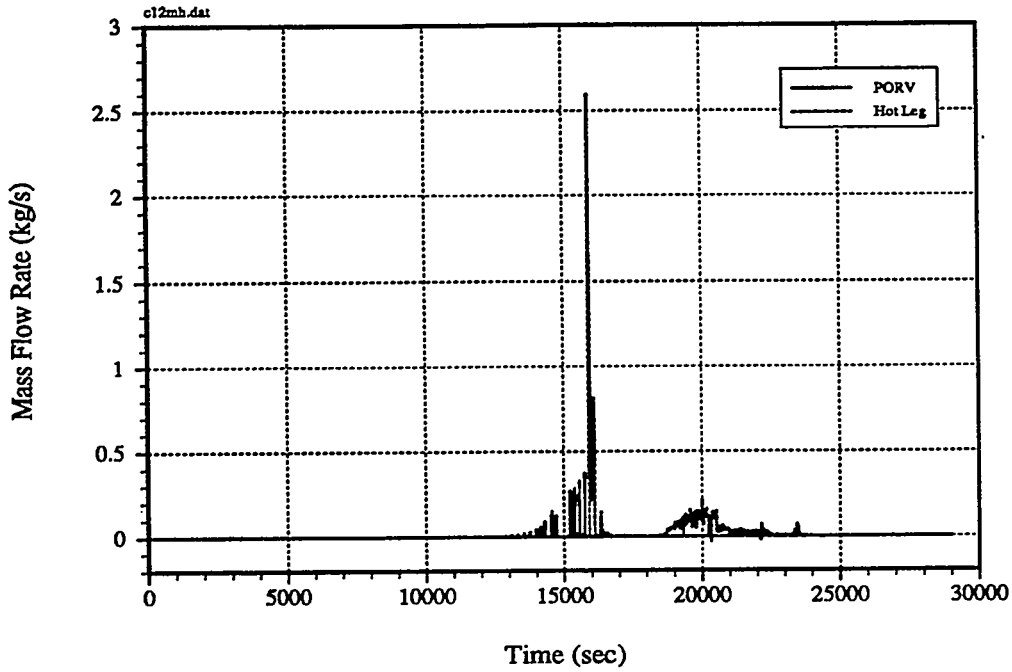

Figure D.2 Case1: Hydrogen Source Flow Rates

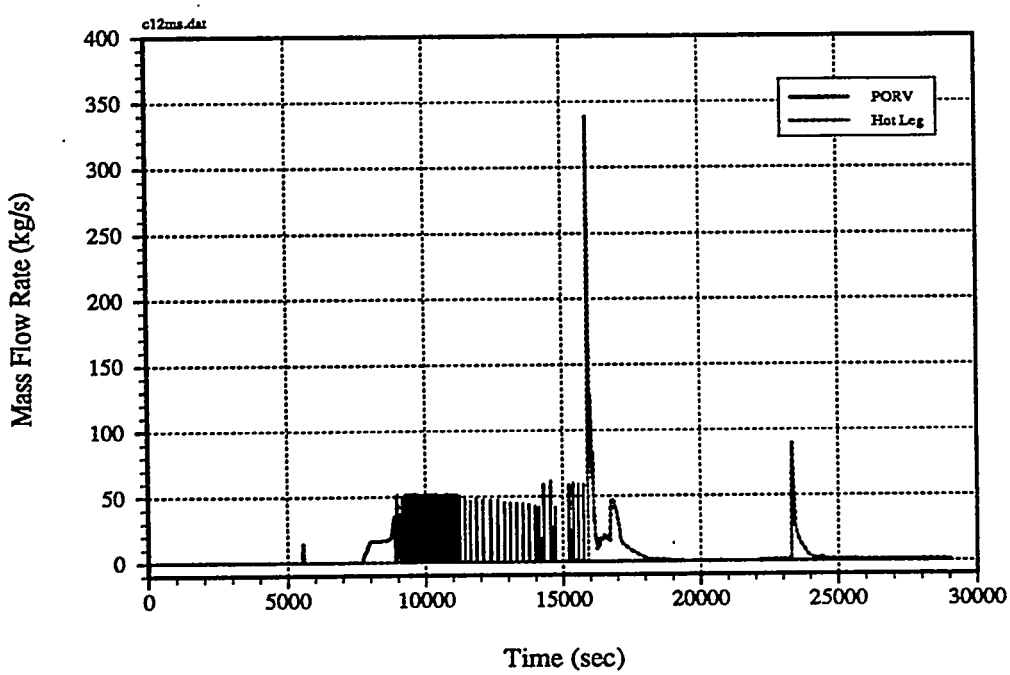

Figure D.3 Case 1: Steam Source Flow Rates

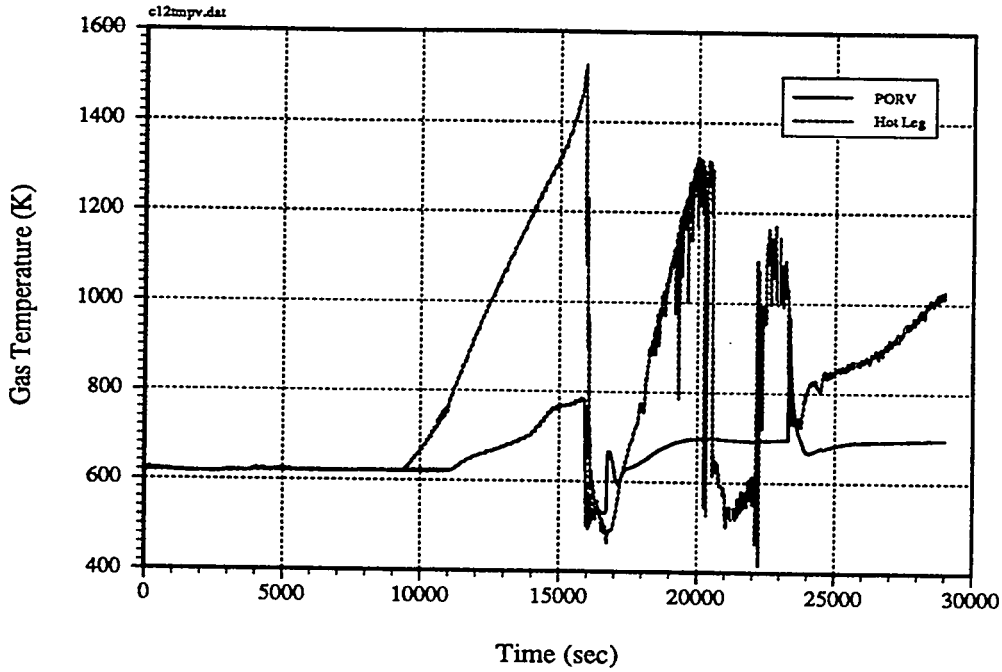

Figure D.4 Case 1: Temperatures at Source Locations

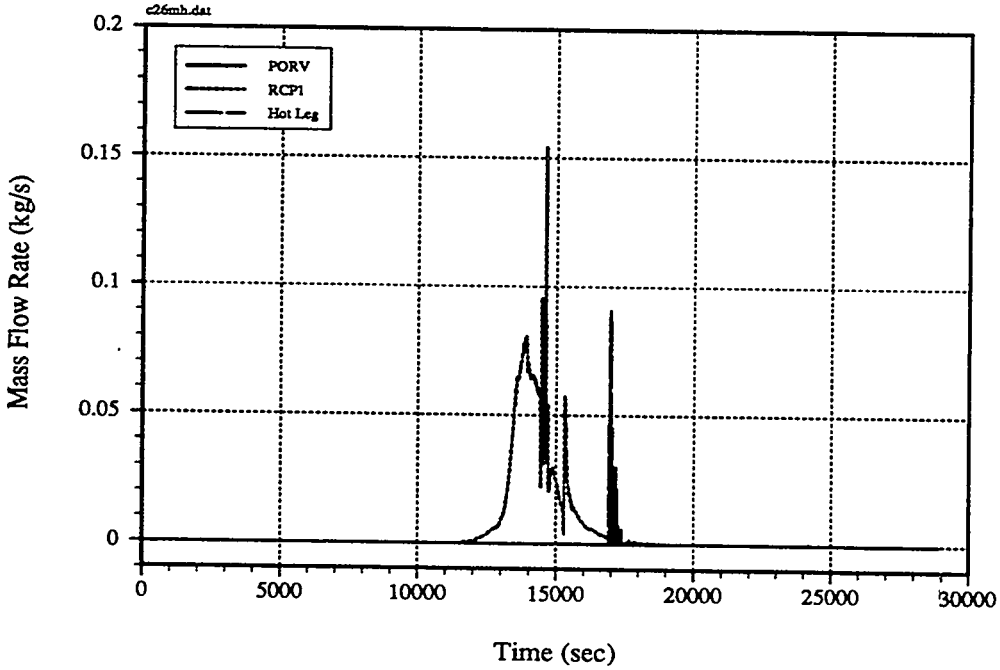

Figure D.5 Case 2: Hydrogen Source Flow Rates

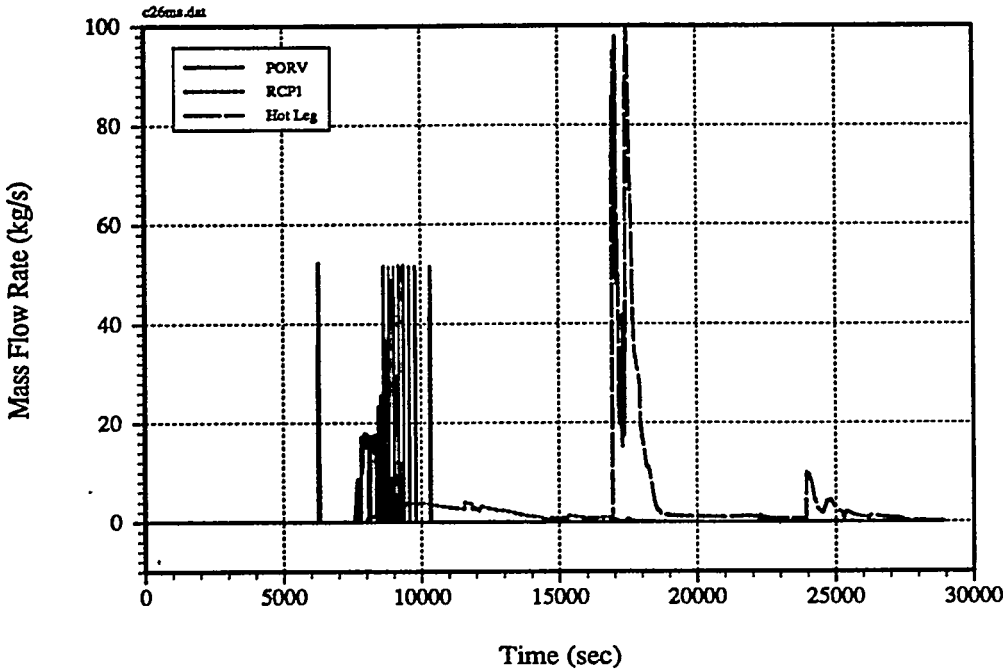

Figure D.6 Case 2: Steam Source Flow Rates

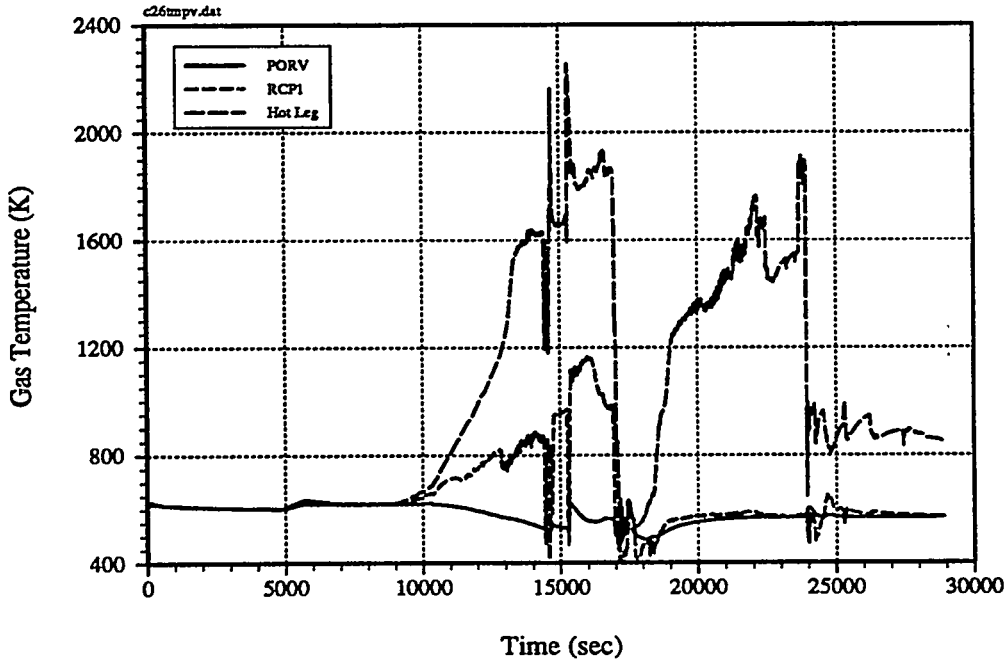

Figure D.7 Case 2: Temperatures at Source Locations

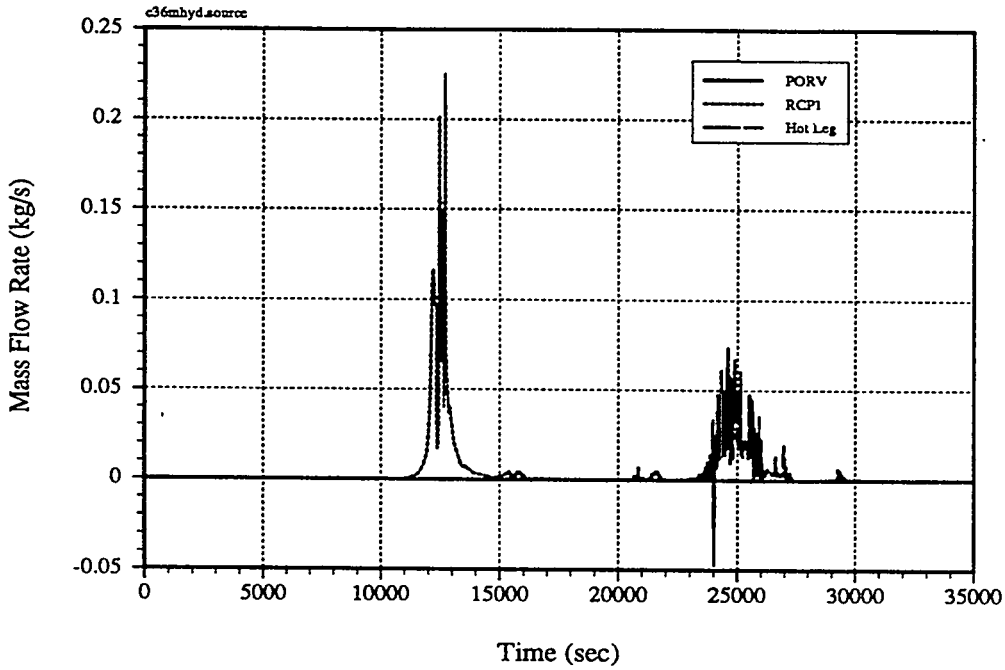

Figure D.8 Case 3: Hydrogen Source Flow Rates

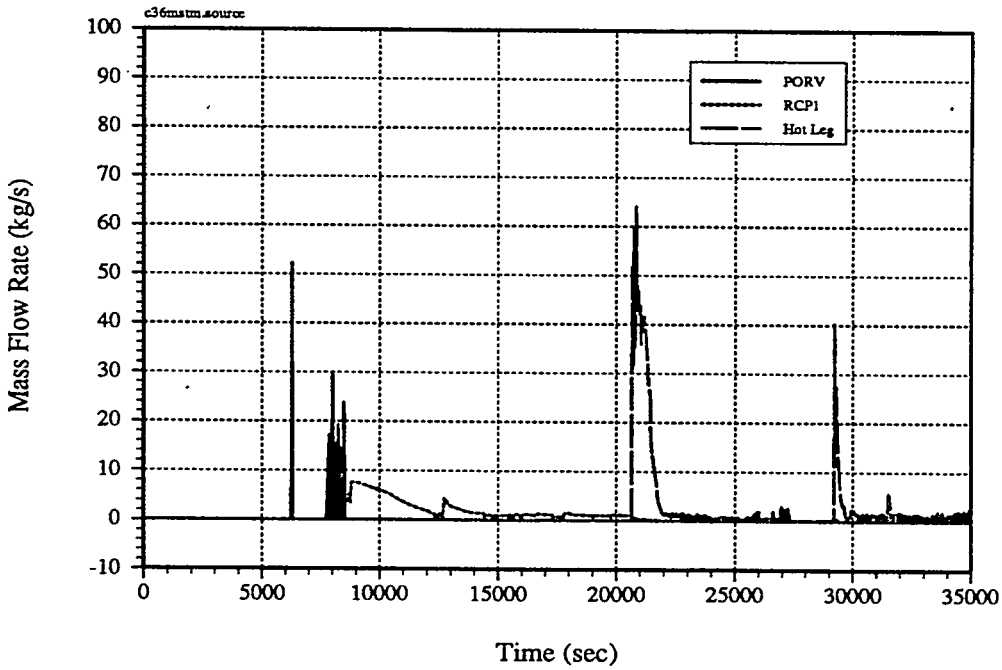

Figure D.9 Case 3: Steam Source Flow Rates

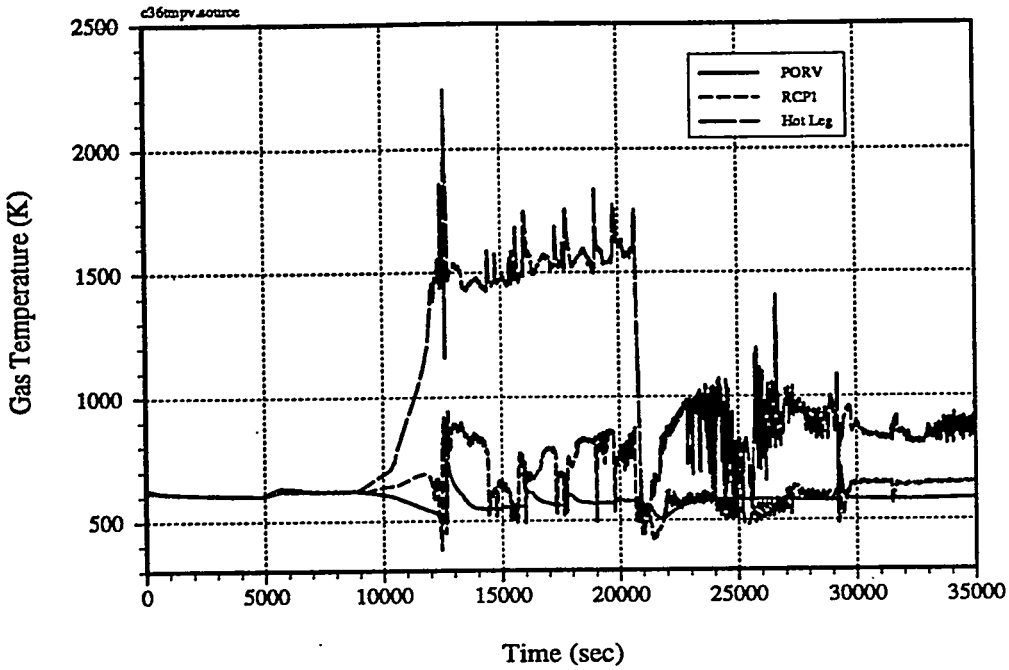

Figure D.10 Case 3: Temperatures at Source Locations

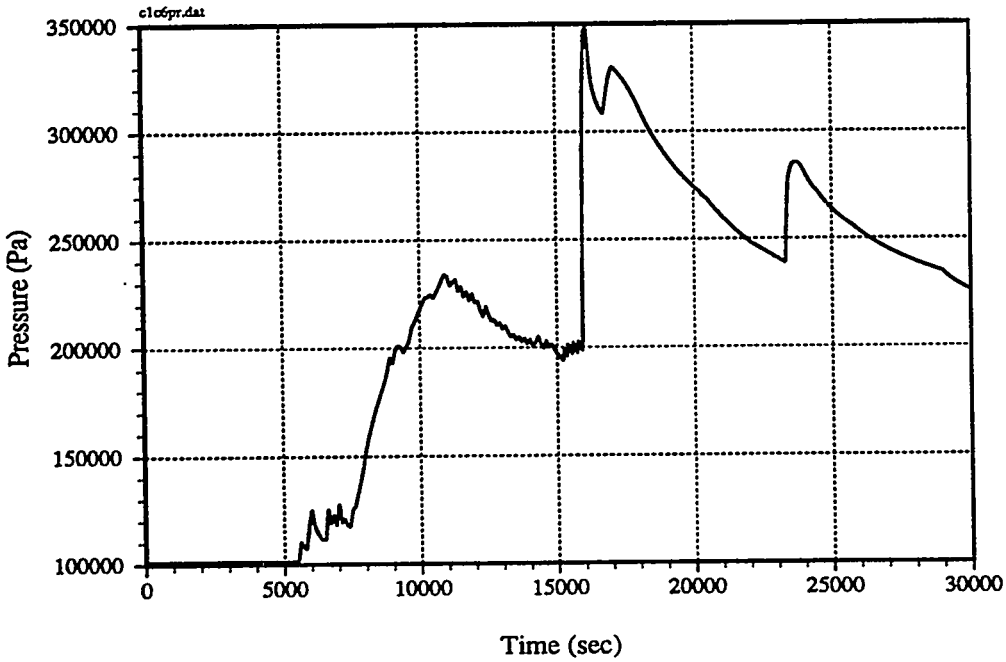

Figure D.11 Case 1: Containment Pressure

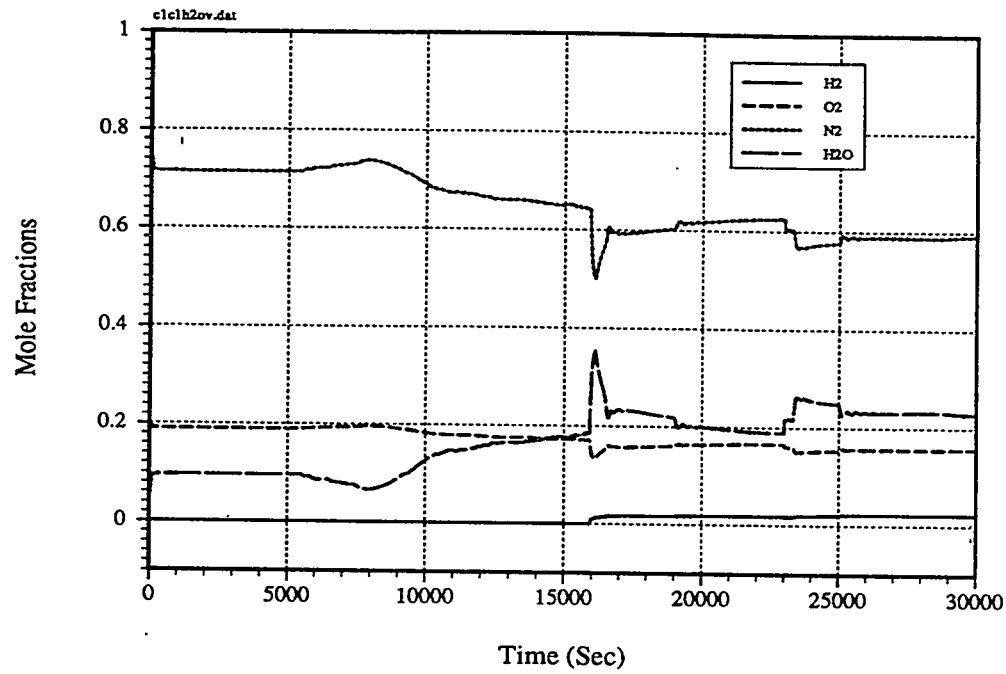

Figure D.12 Case 1: Cavity Gas Mole Fractions

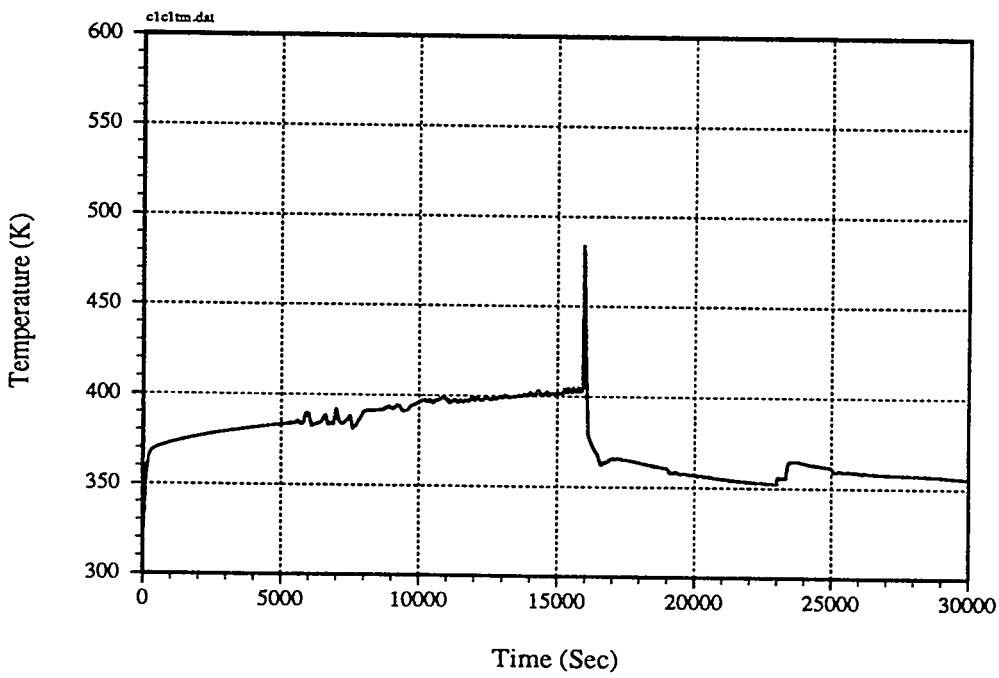

Figure D.13 Case 1: Cavity Gas Temperature

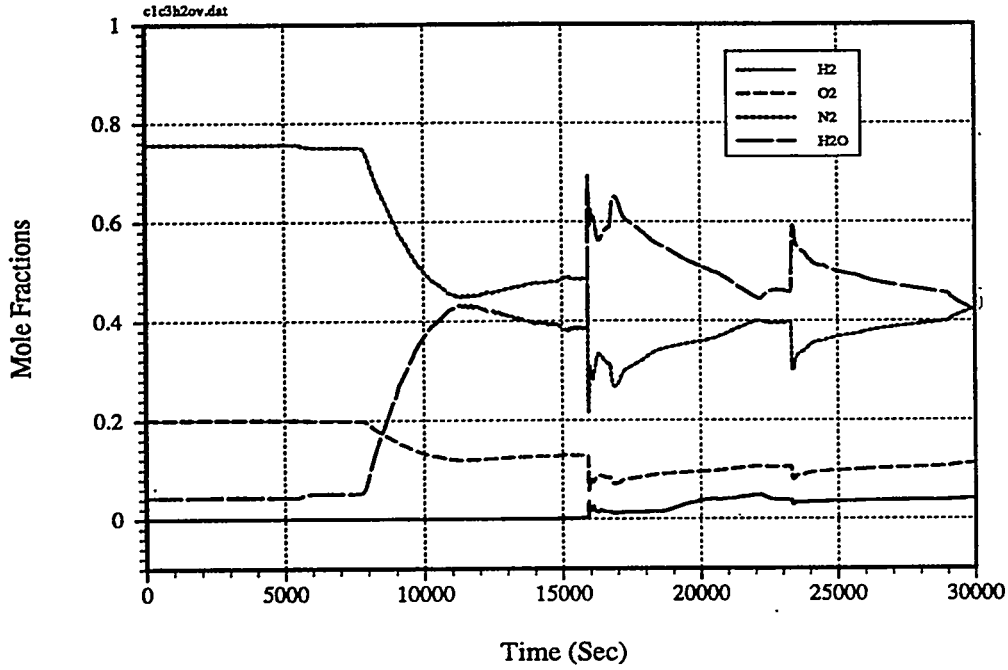

Figure D.14 Case 1: Steam Generator Room Gas Mole Fractions

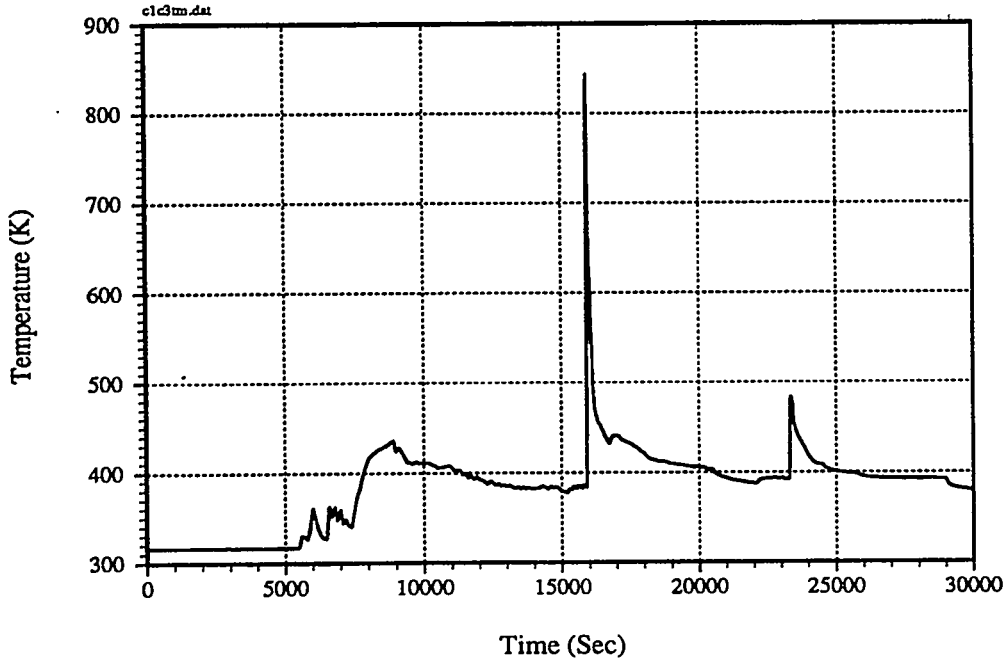

Figure D.15 Case 1: Steam Generator Room Gas Temperature

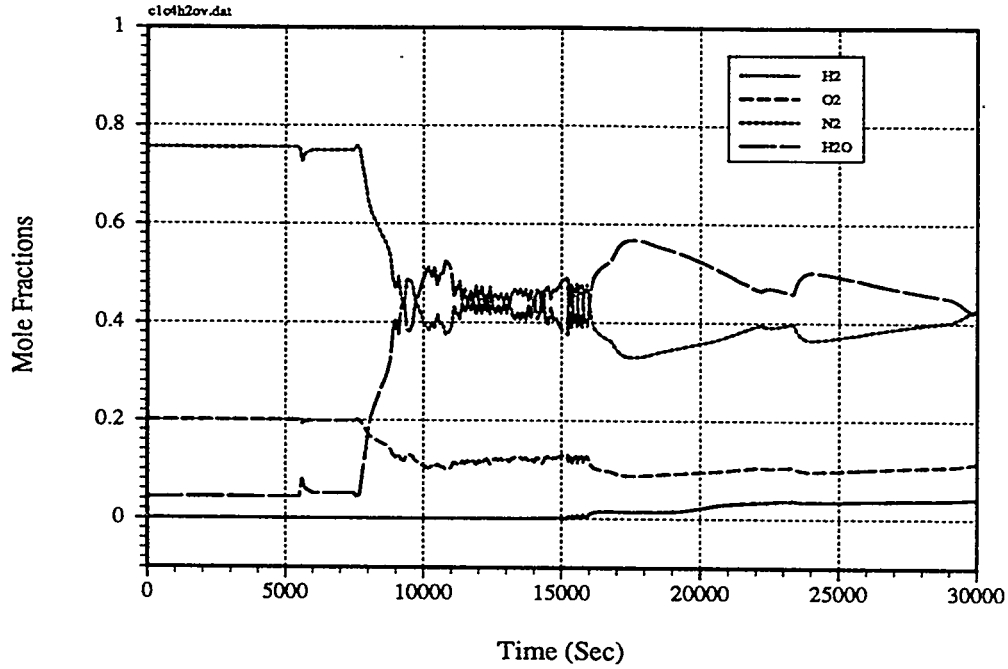

Figure D.16 Case 1: Annulus Gas Mole Fractions

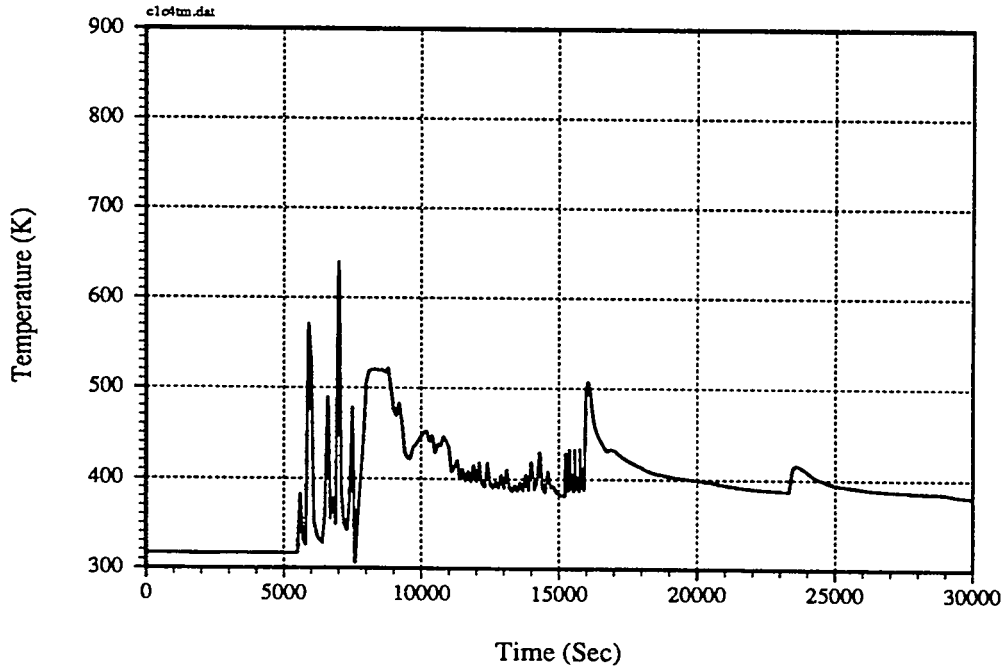

Figure D.17 Case 1: Annulus Gas Temperature

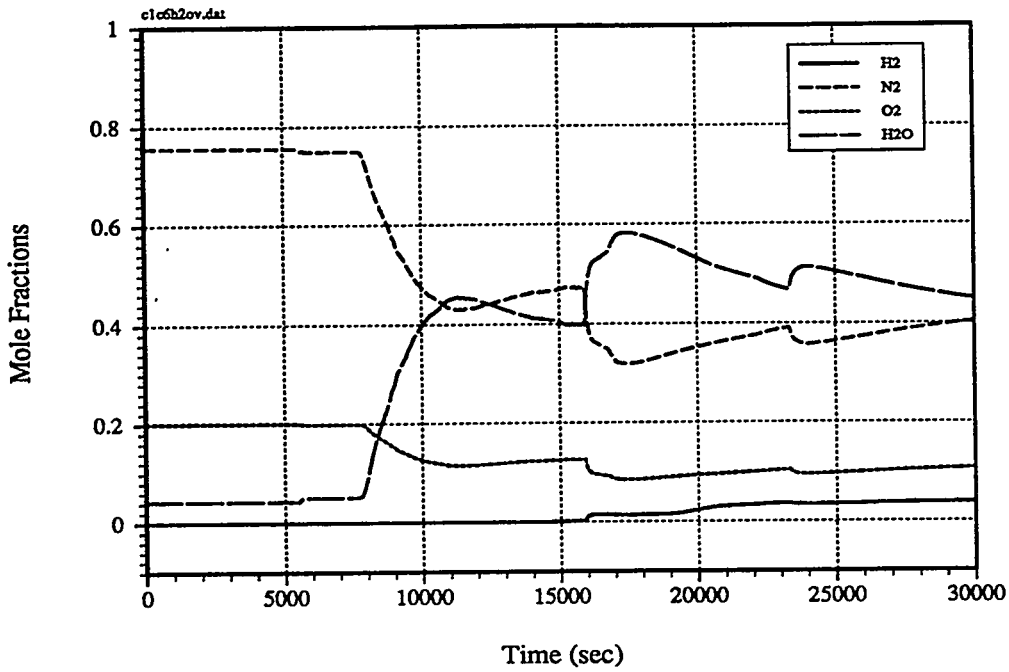

Figure D.18 Case 1: Dome Gas Mole Fractions

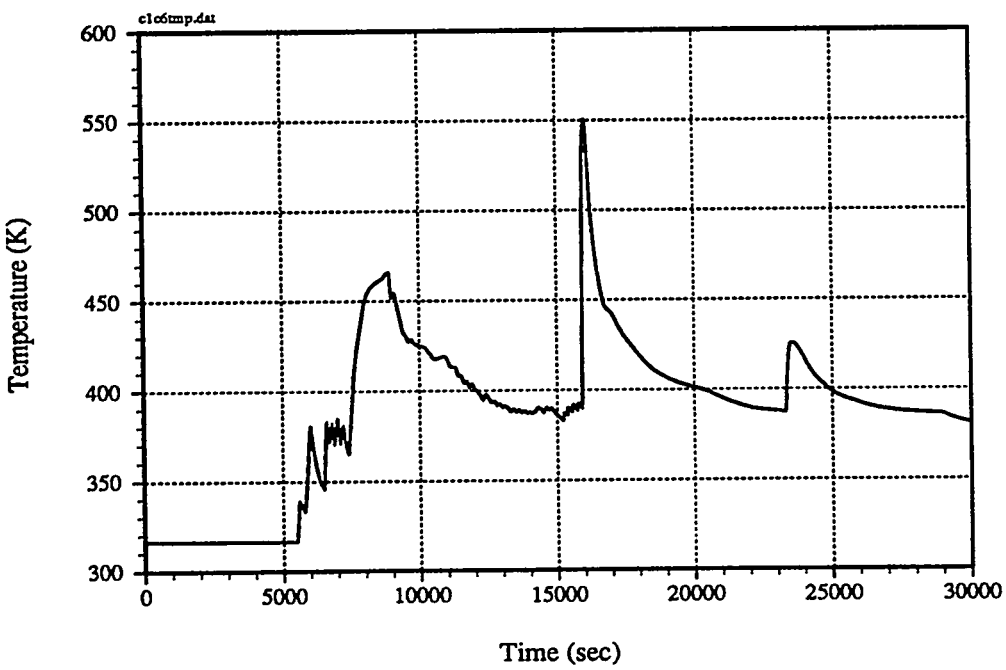

Figure D.19 Case 1: Dome Gas Temperature

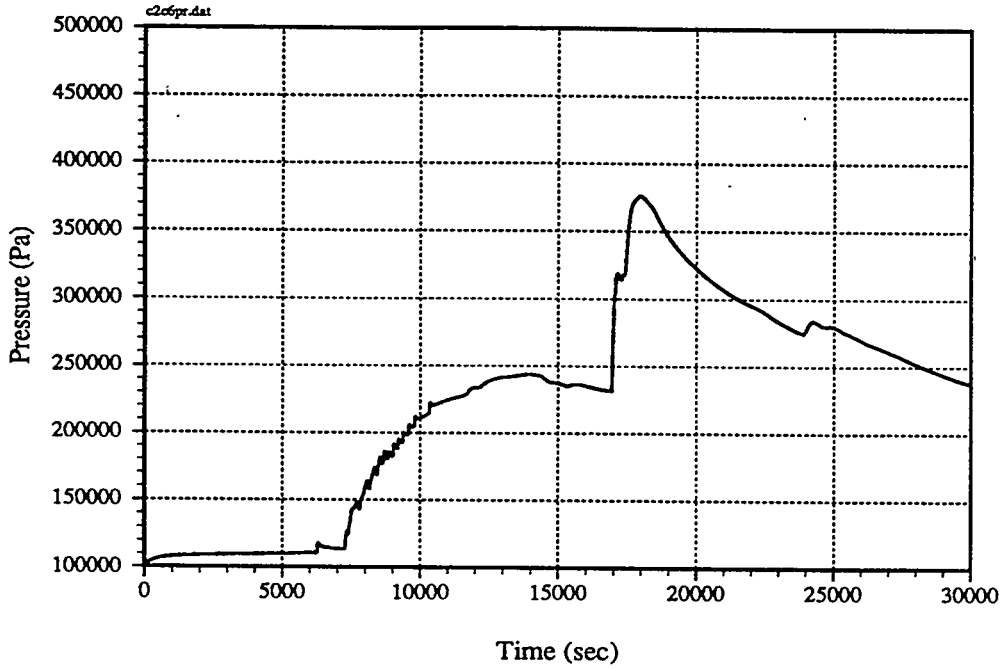

Figure D.20 Case 2: Containment Pressure

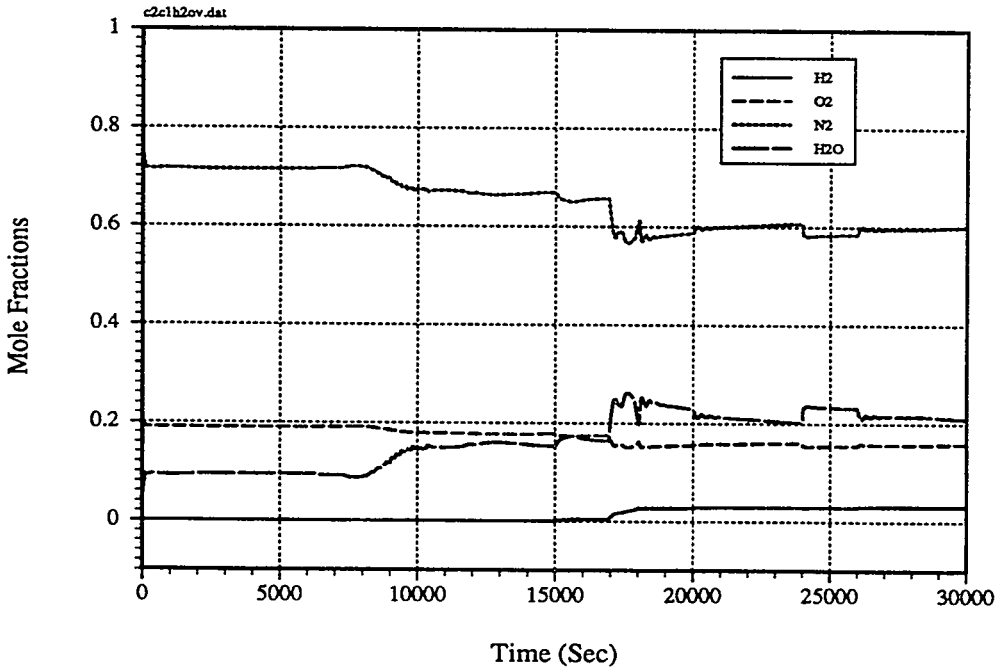

Figure D.21 Case 2: Cavity Gas Mole Fractions

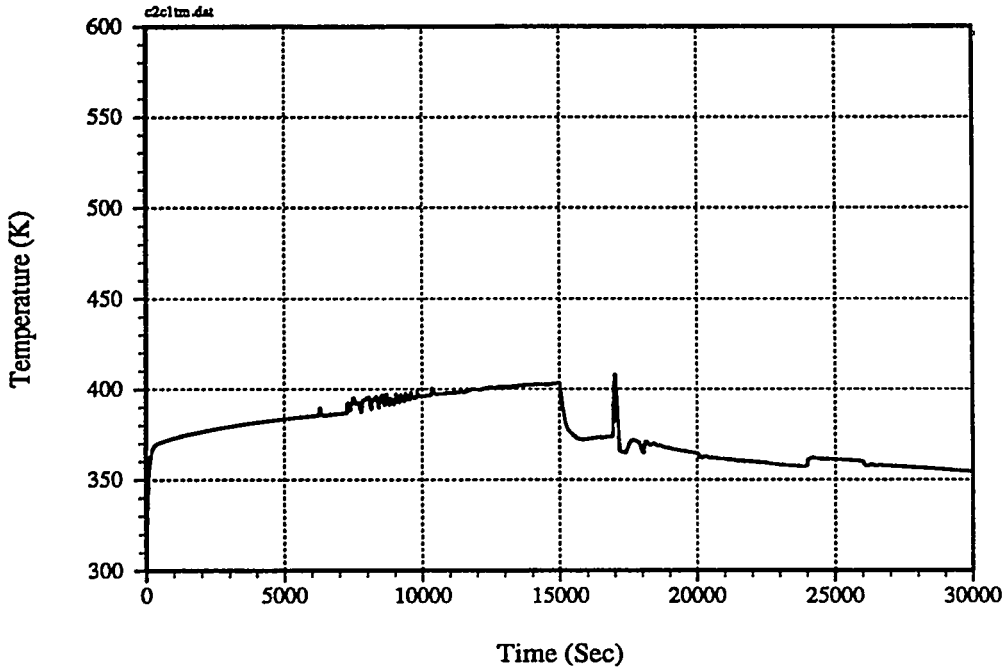

Figure D.22 Case 2: Cavity Gas Temperature

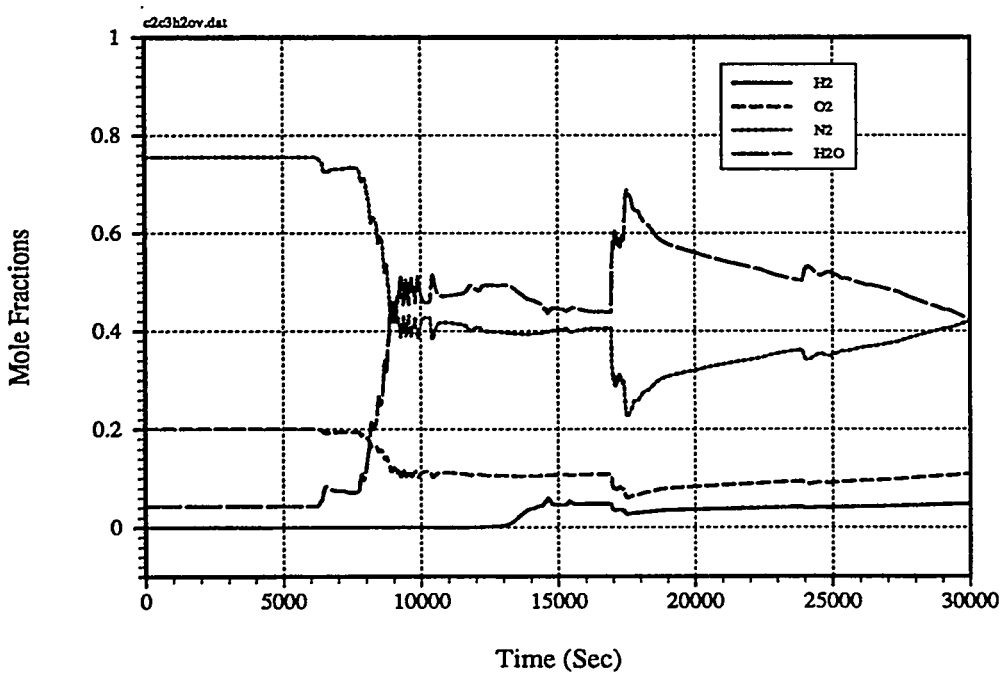

Figure D.23 Case 2: Steam Generator Room Gas Mole Fractions

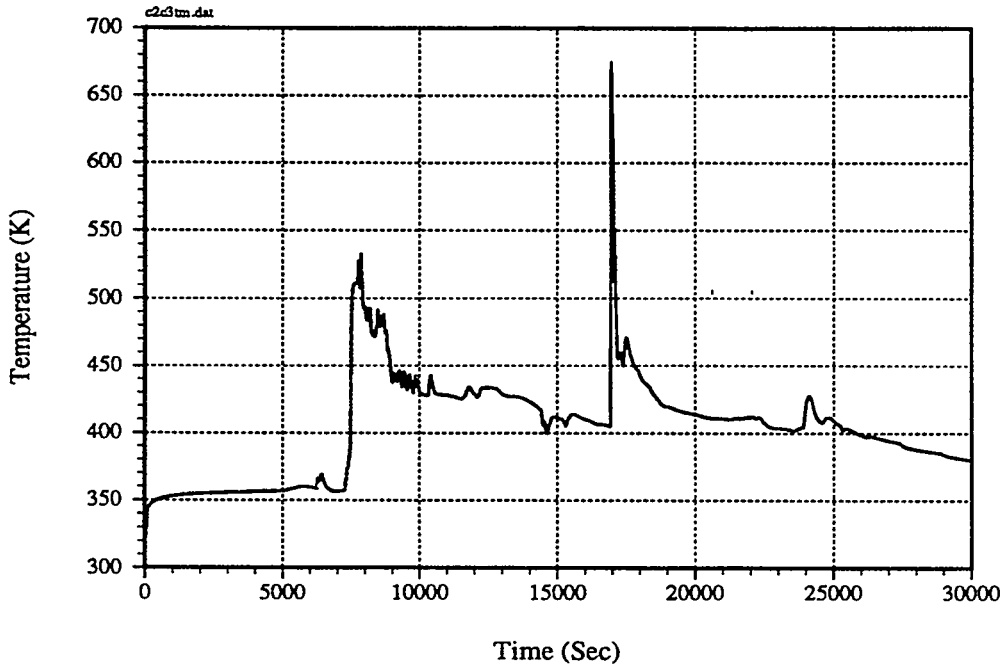

Figure D.24 Case 2: Steam Generator Room Gas Temperature

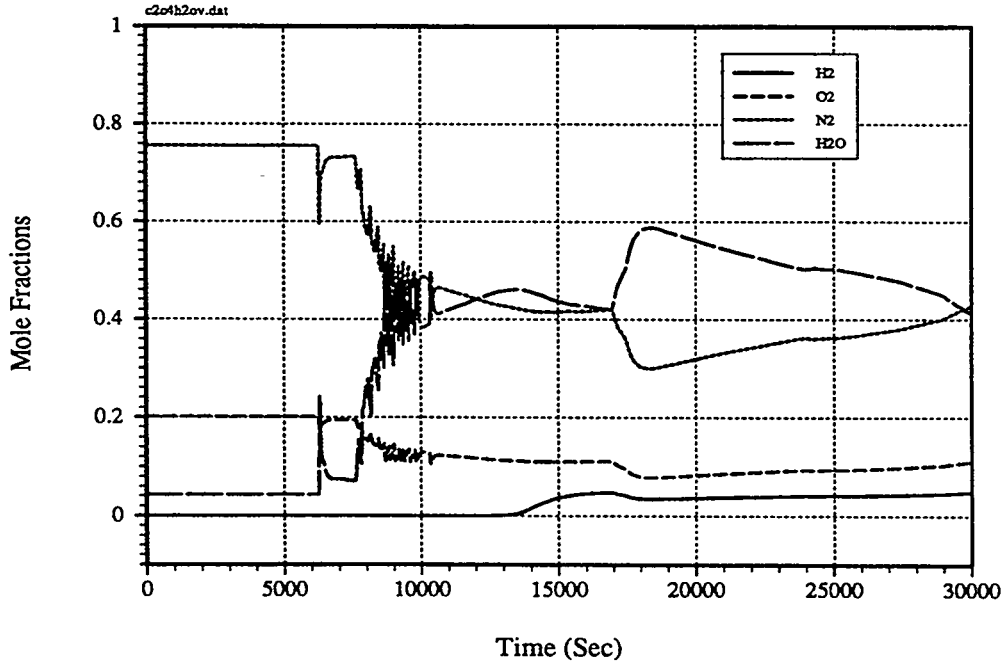

Figure D.25 Case 2: Annulus Gas Mole Fractions

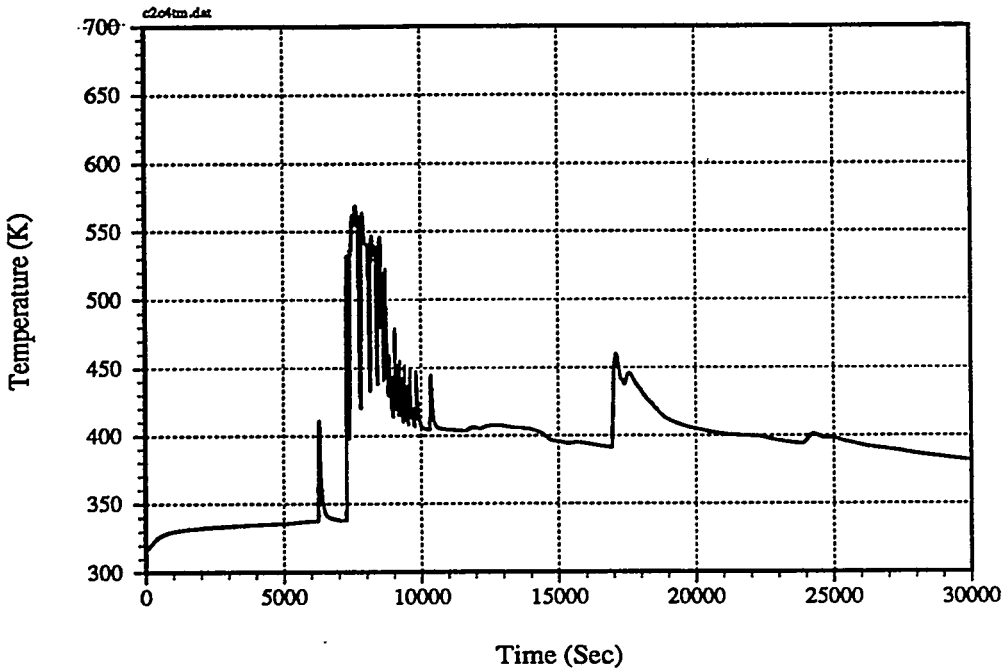

Figure D.26 Case 2: Annulus Gas Temperature

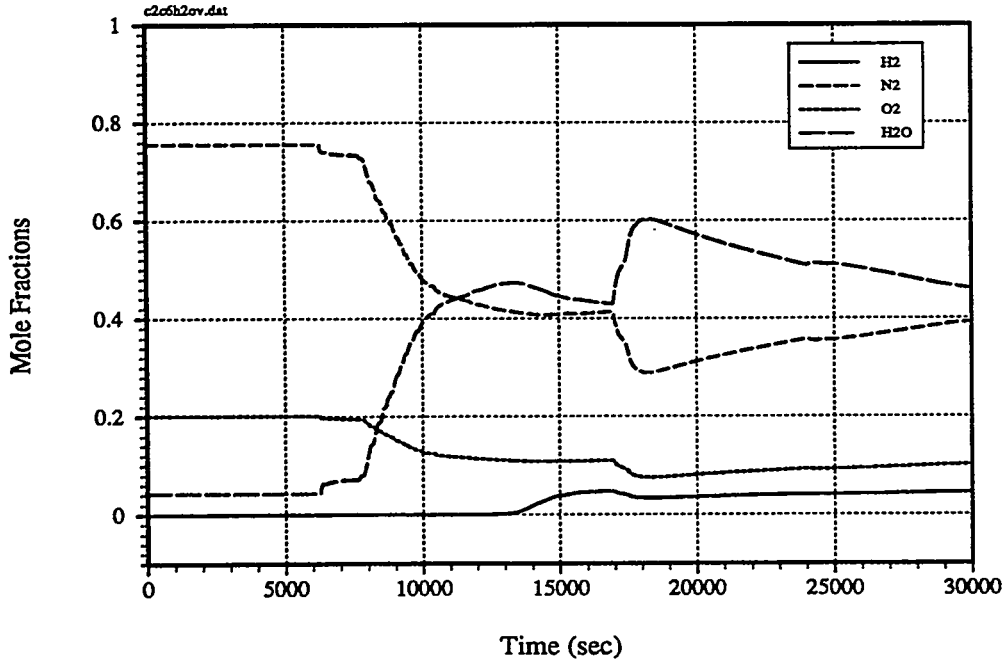

Figure D.27 Case 2: Dome Gas Mole Fractions

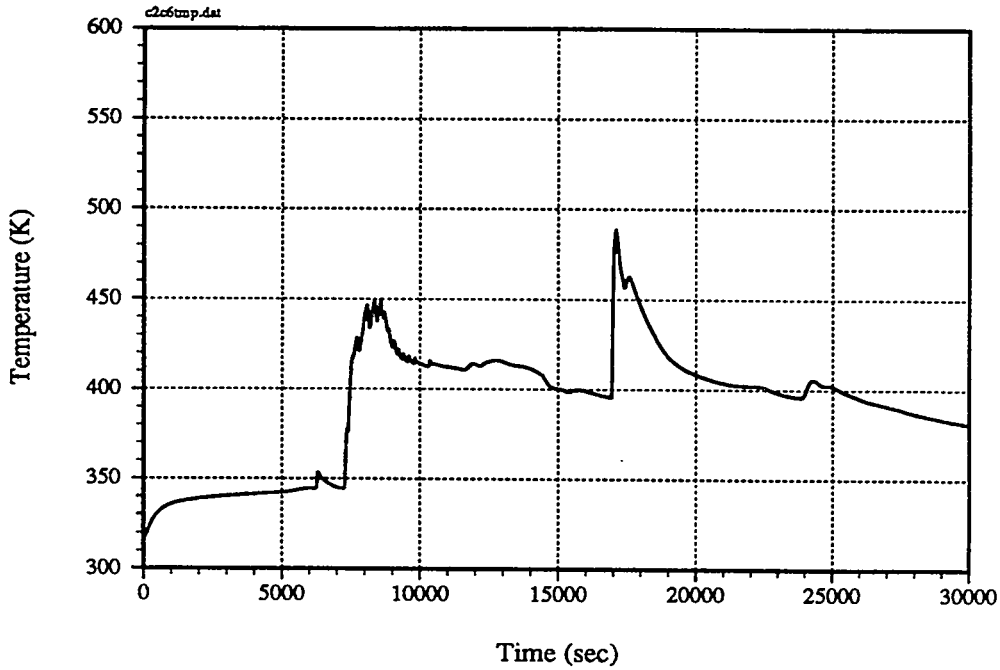

Figure D.28 Case 2: Dome Gas Temperature

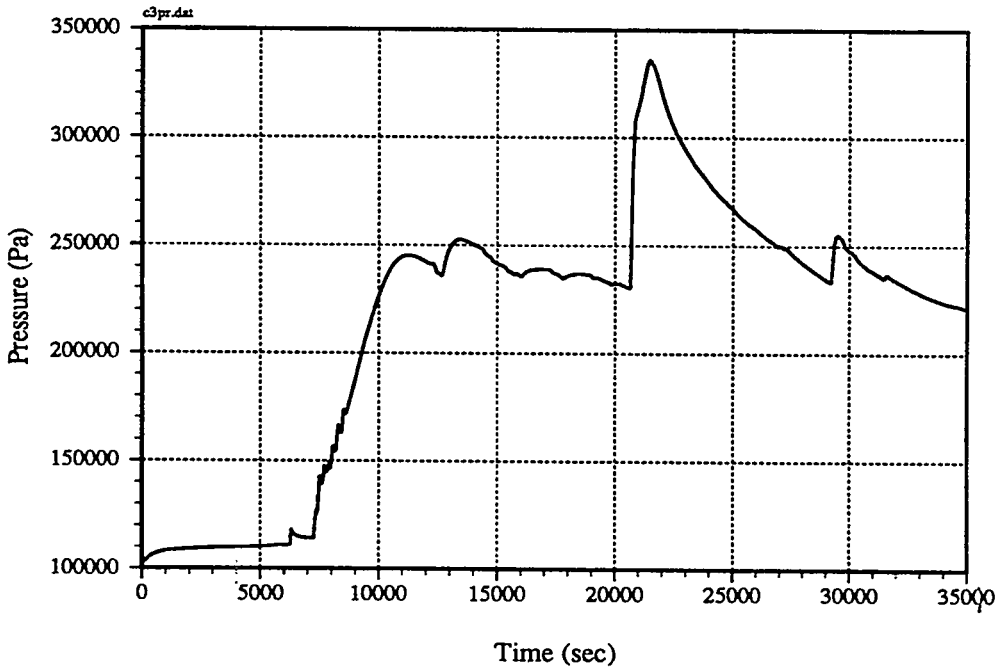

Figure D.29 Case 3: Containment Pressure

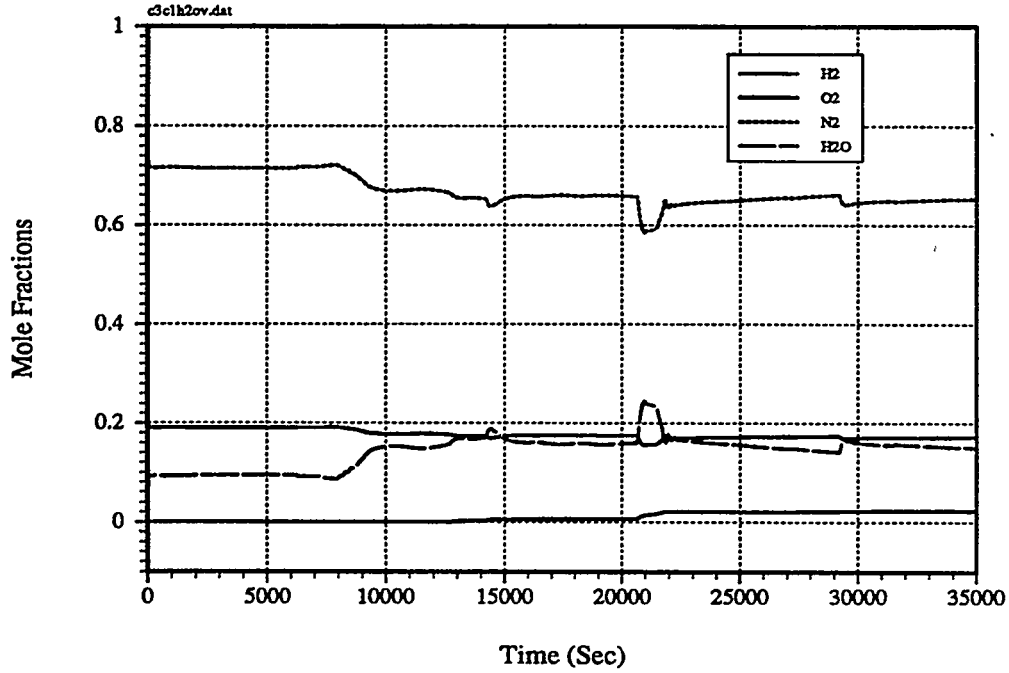

Figure D.30 Case 3: Cavity Gas Mole Fractions

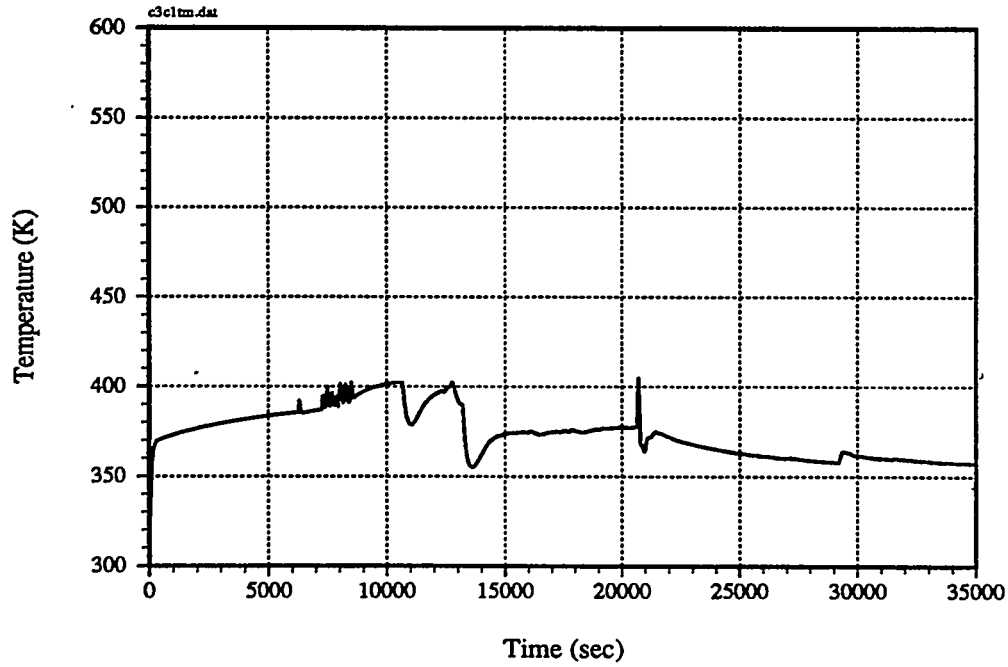

Figure D.31 Case 3: Cavity Gas Temperature

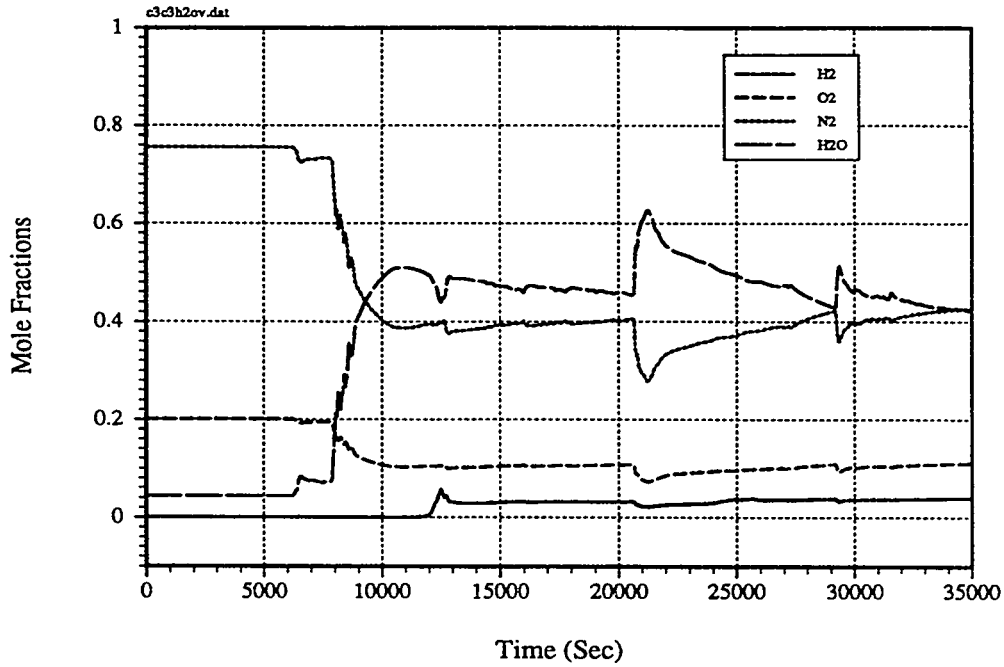

Figure D.32 Case 3: Steam Generator Room Gas Mole Fractions

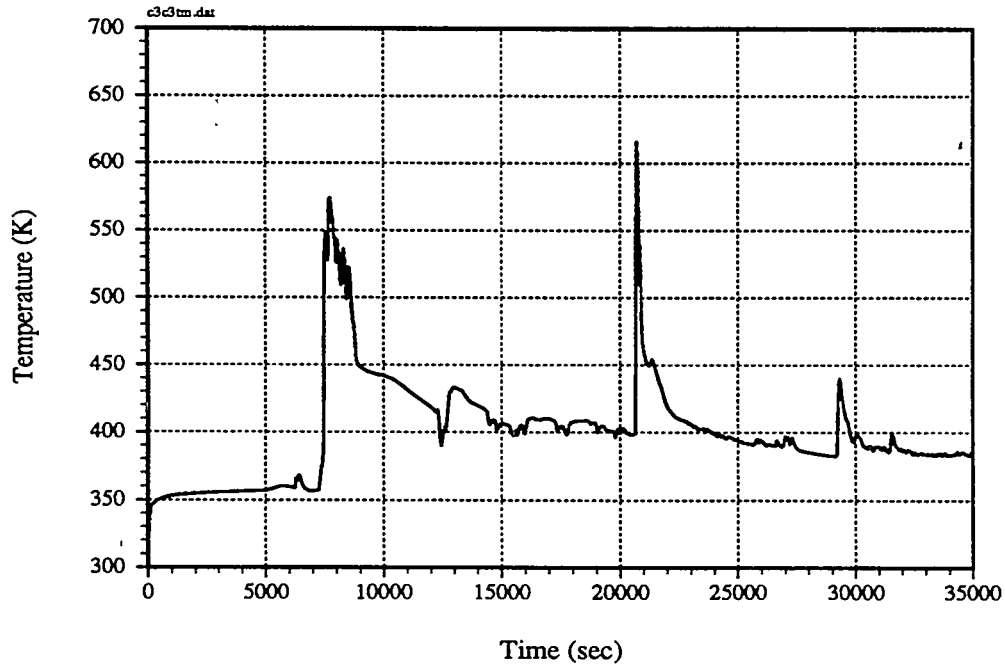

Figure D.33 Case 3: Steam Generator Room Temperature

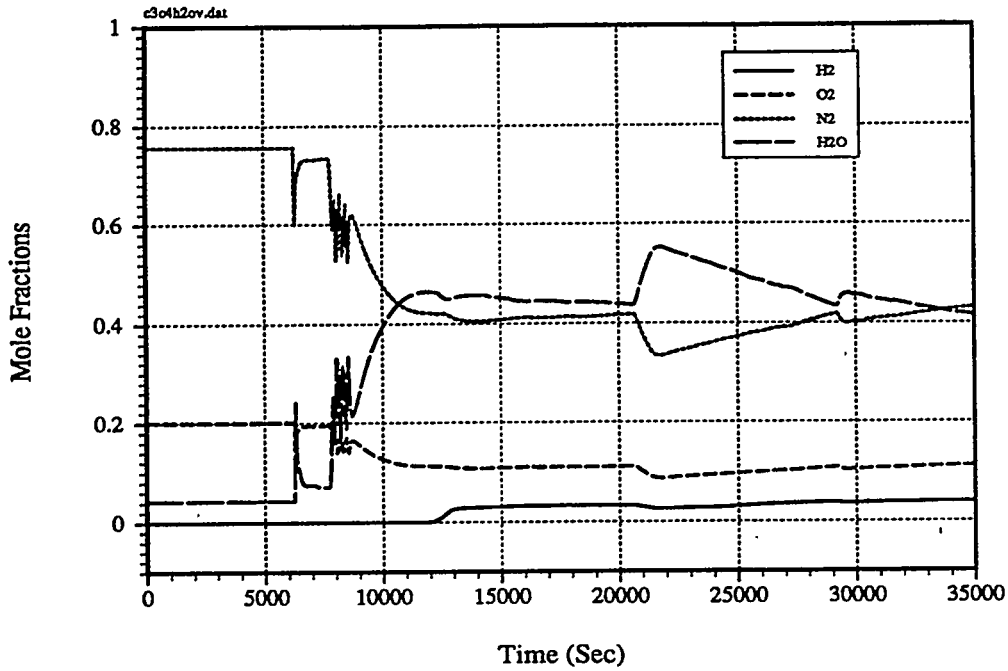

Figure D.34 Case 3: Annulus Gas Mole Fractions

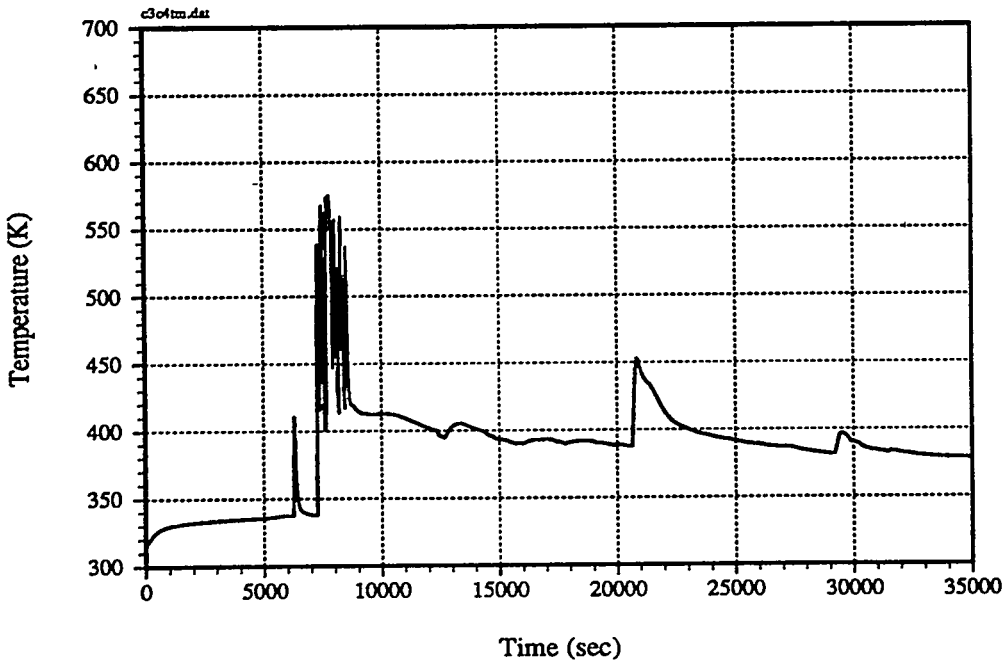

Figure D.35 Case 3: Annulus Gas Temperature

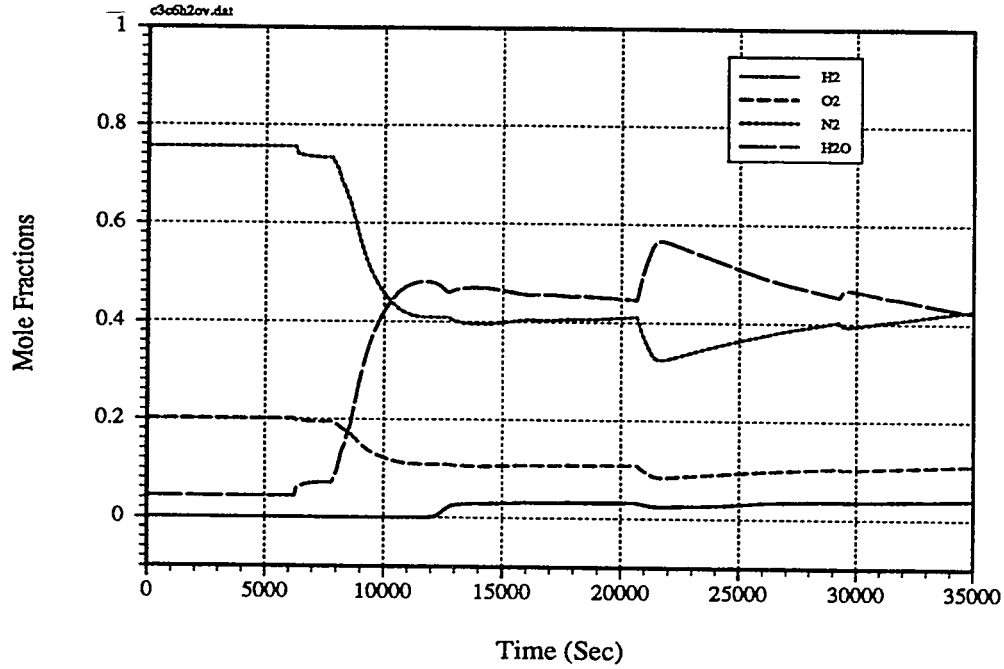

Figure D.36 Case 3: Dome Gas Mole Fractions

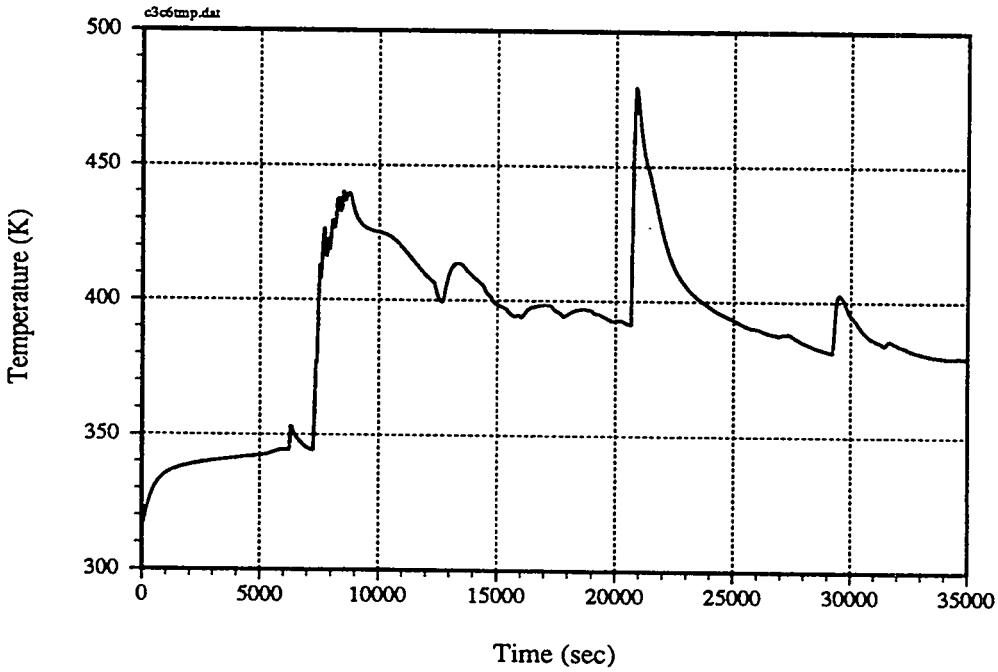

Figure D.37 Case 3: Dome Gas Temperature

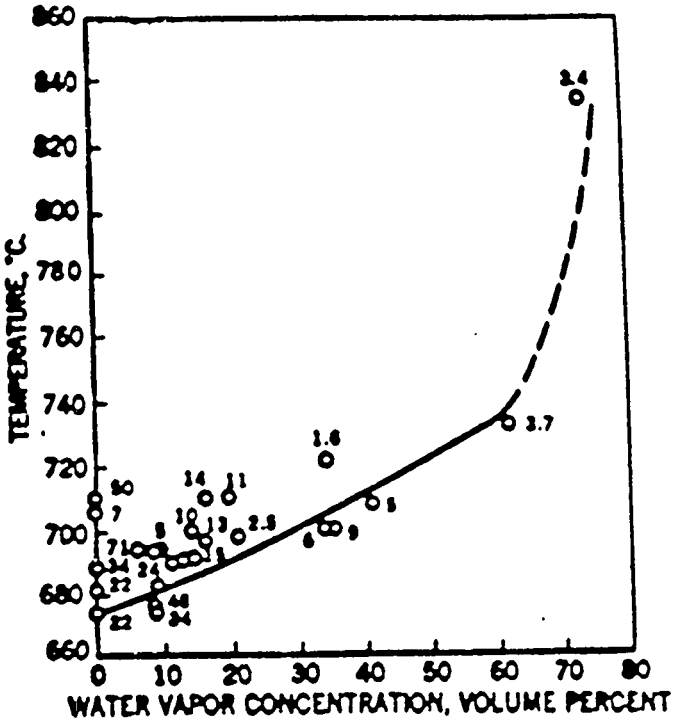

Figure D.38 Autoignition temperature data for hydrogen-steam jets (Zabetakis, 1956).

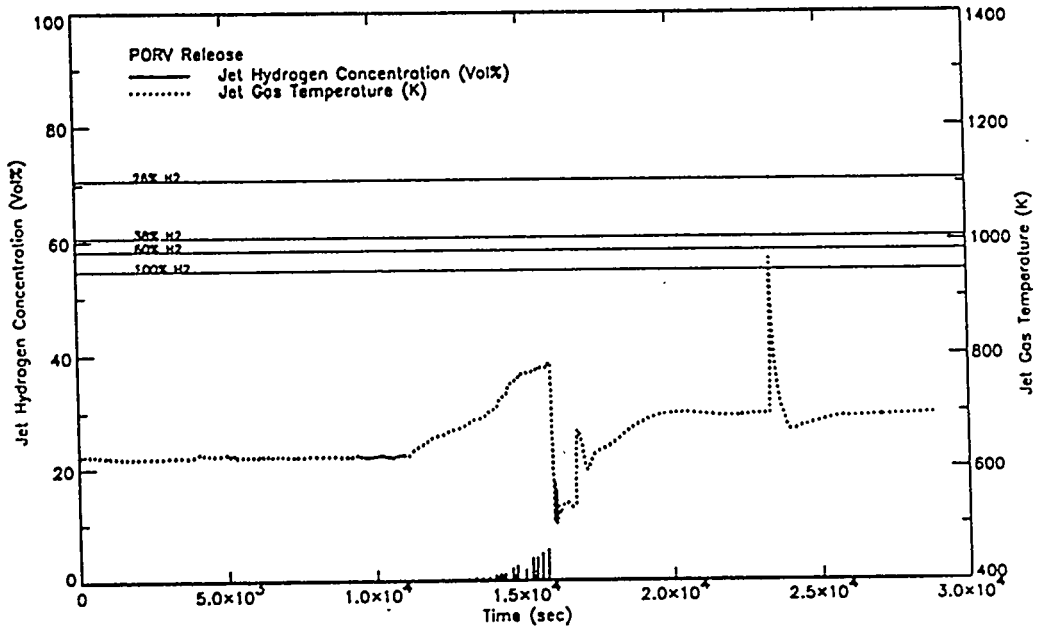

Figure D.39 Case 1: Jet hydrogen concentration and temperature of the gases released from the PORV.

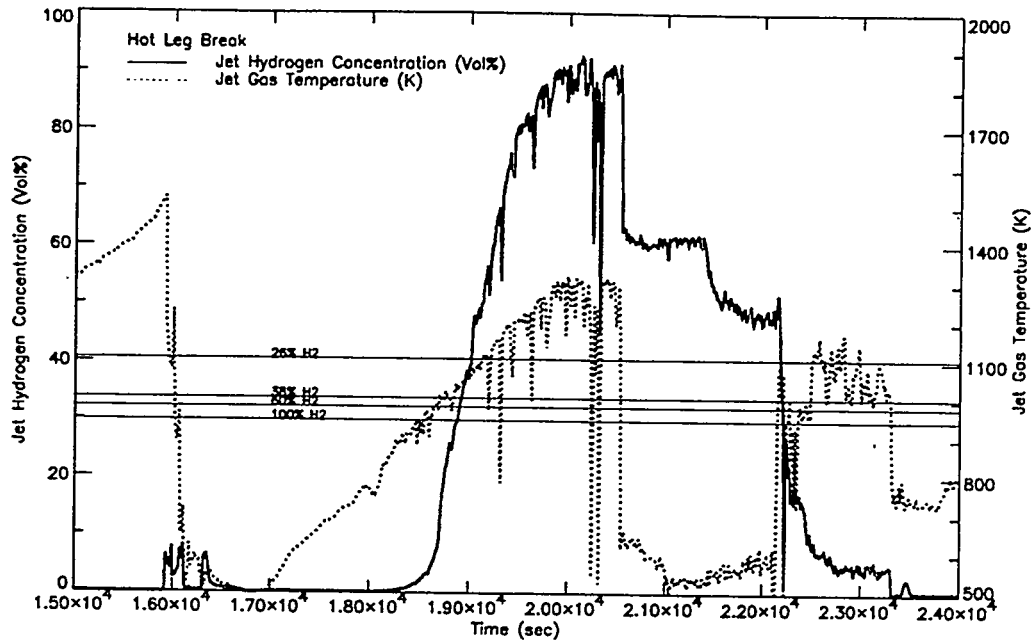

Figure D.40 Case 1: Jet hydrogen concentration and temperature of the gases released from the hot-leg break.

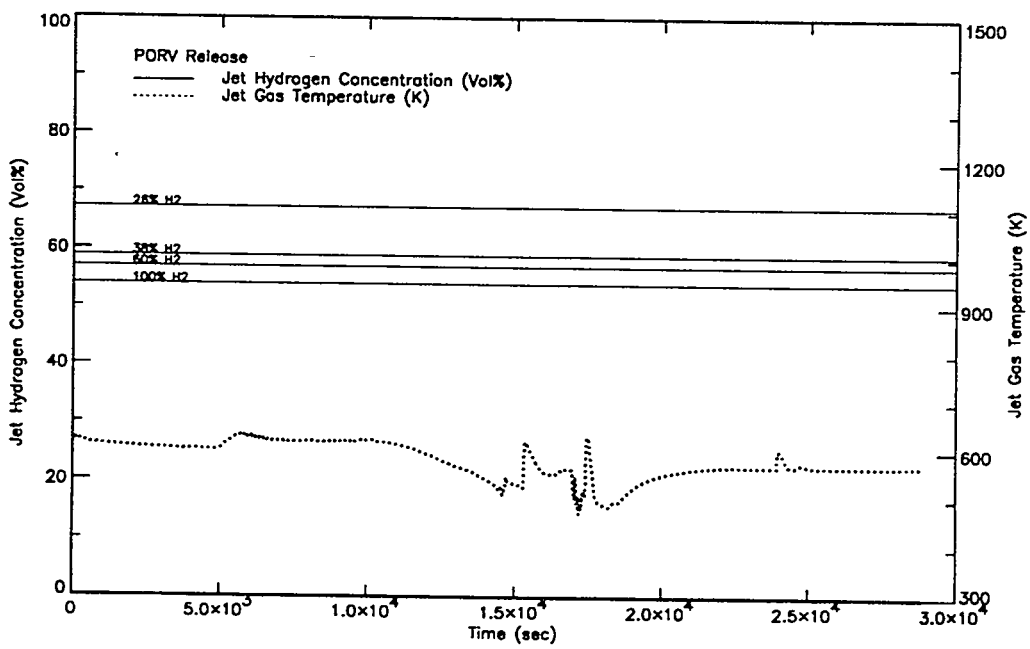

Figure D.41 Case 2: Jet hydrogen concentration and temperature of the gases released from the PORV.

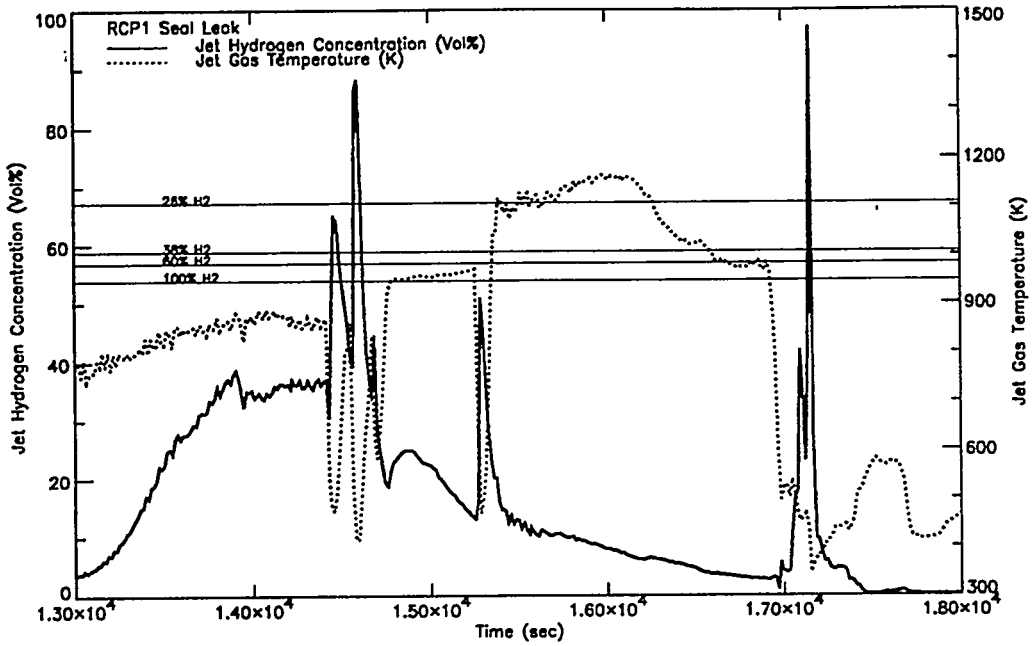

Figure D.42 Case 2: Jet hydrogen concentration and temperature of the gases released from the RCP1 seal leak.

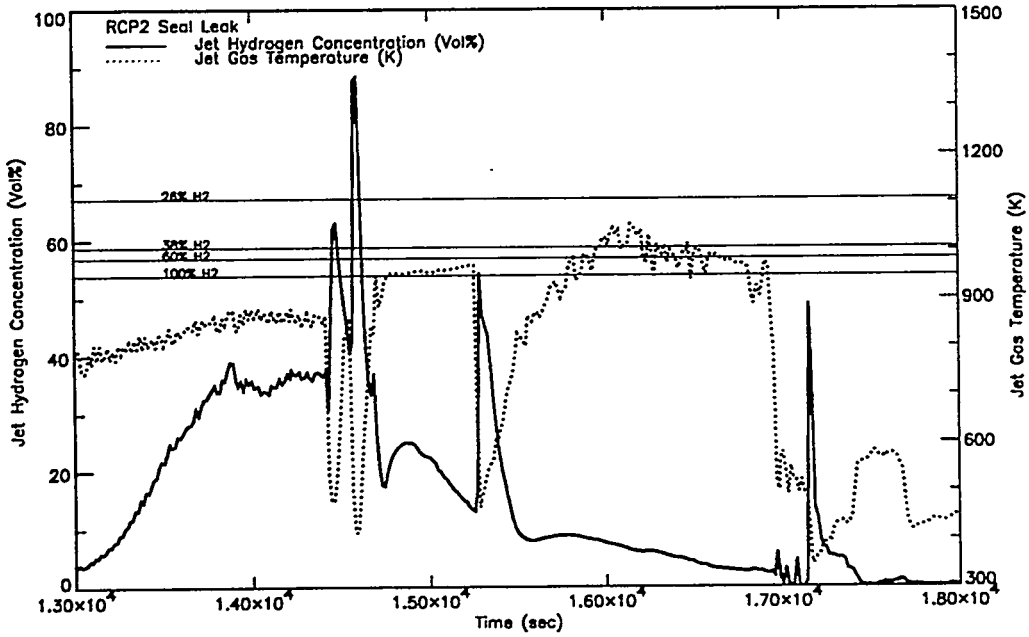

Figure D.43 Case 2: Jet hydrogen concentration and temperature of the gases released from the RCP2 seal leak.

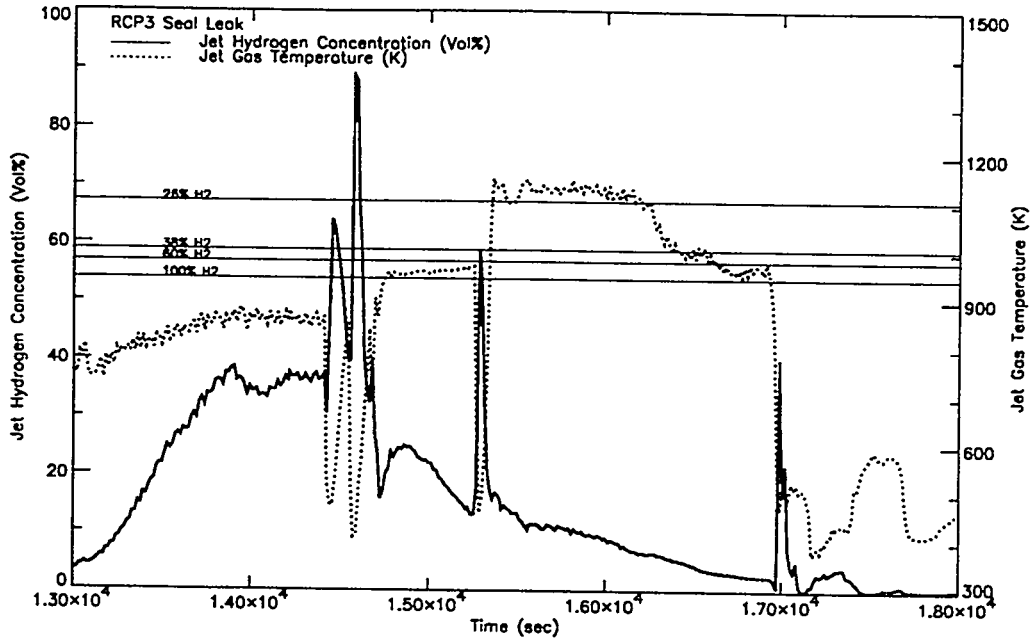

Figure D.44 Case 2: Jet hydrogen concentration and temperature of the gases released from the RCP3 seal leak.

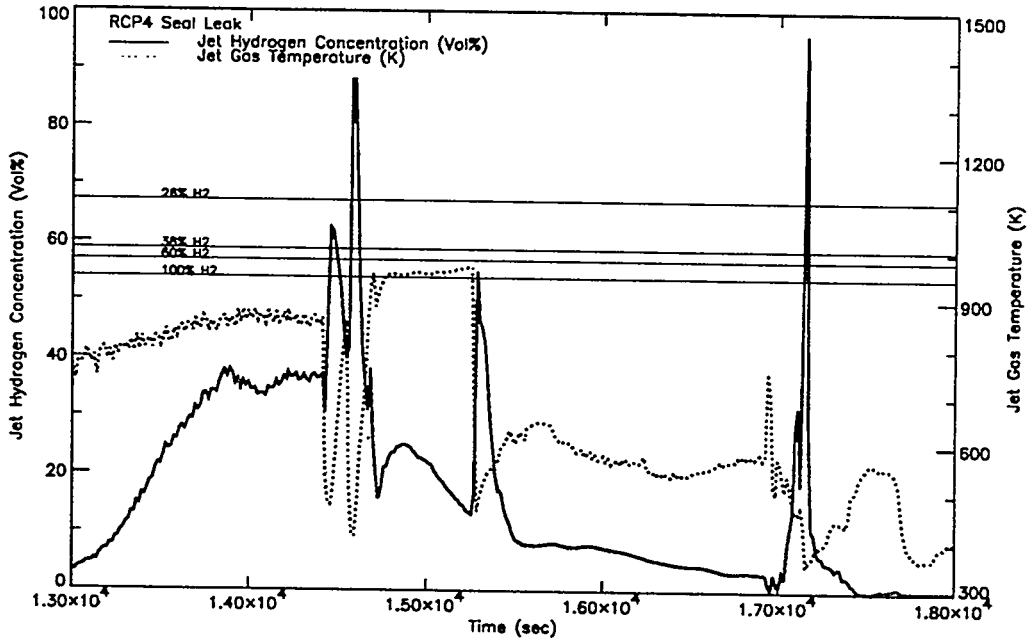

Figure D.45 Case 2: Jet hydrogen concentration and temperature of the gases released from the RCP4 seal leak.

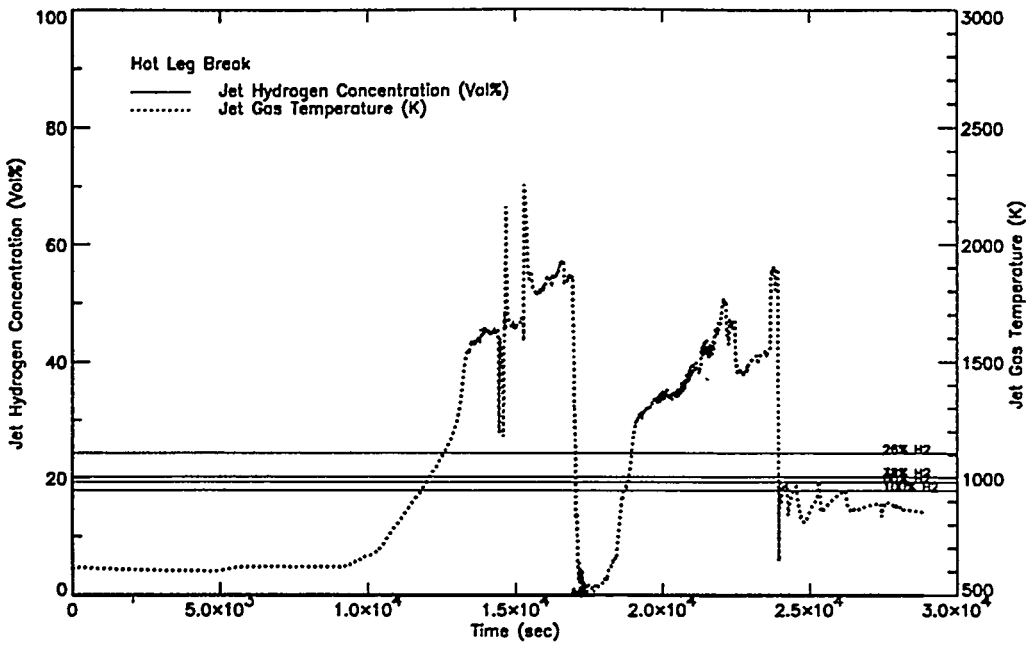

Figure D.46 Case 2: Jet hydrogen concentration and temperature of the gases released from the hot-leg break.

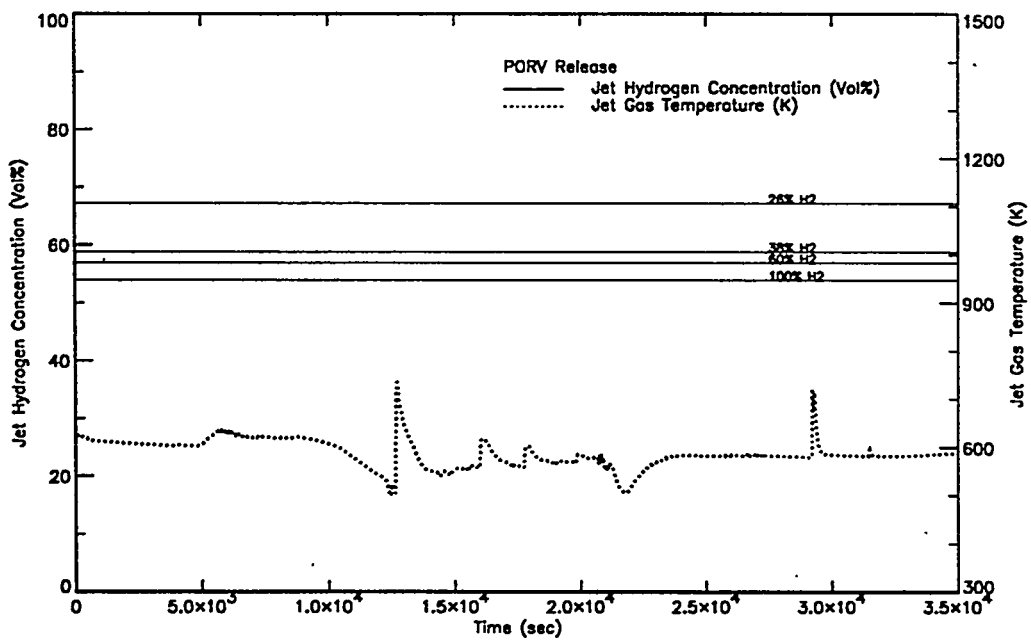

Figure D.47 Case 3: Jet hydrogen concentration and temperature of the gases released from the PORV.

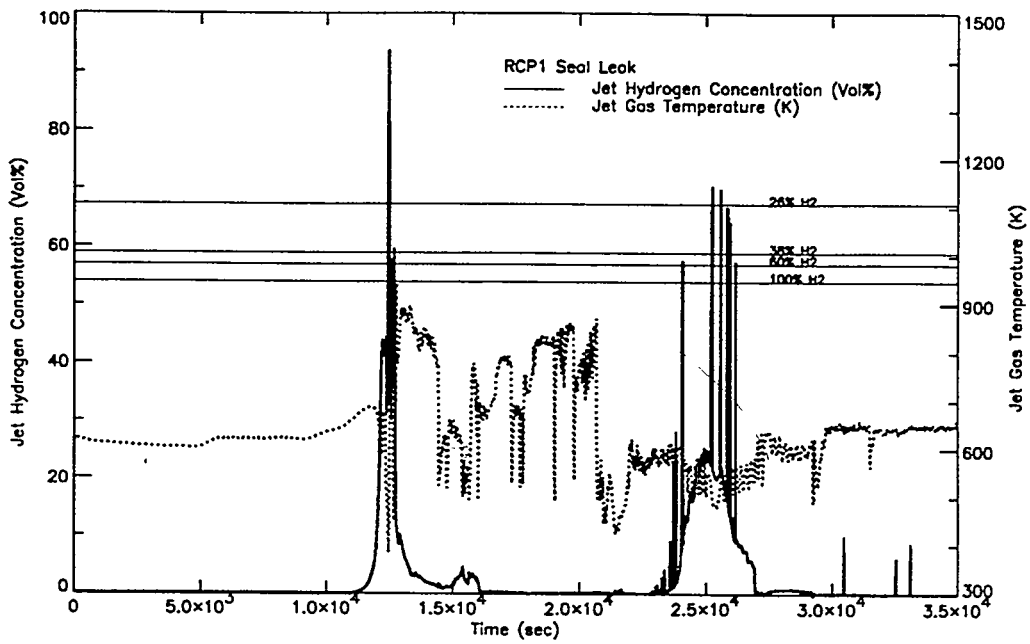

Figure D.48 Case 3: Jet hydrogen concentration and temperature of the gases released from the RCP1 seal leak.

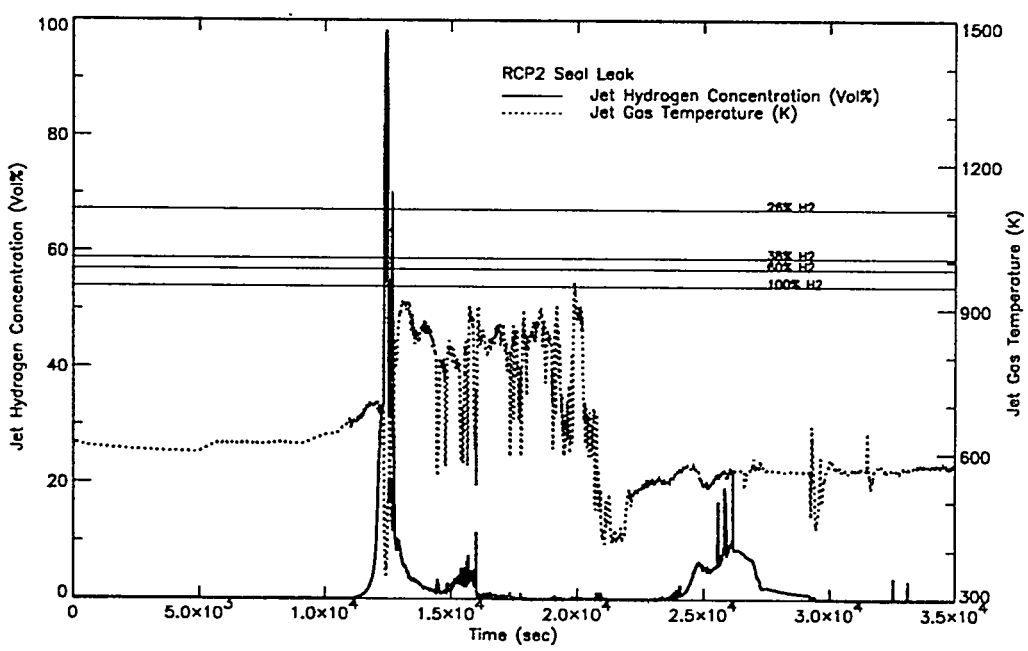

Figure D.49 Case 3: Jet hydrogen concentration and temperature of the gases released from the RCP2 seal leak.

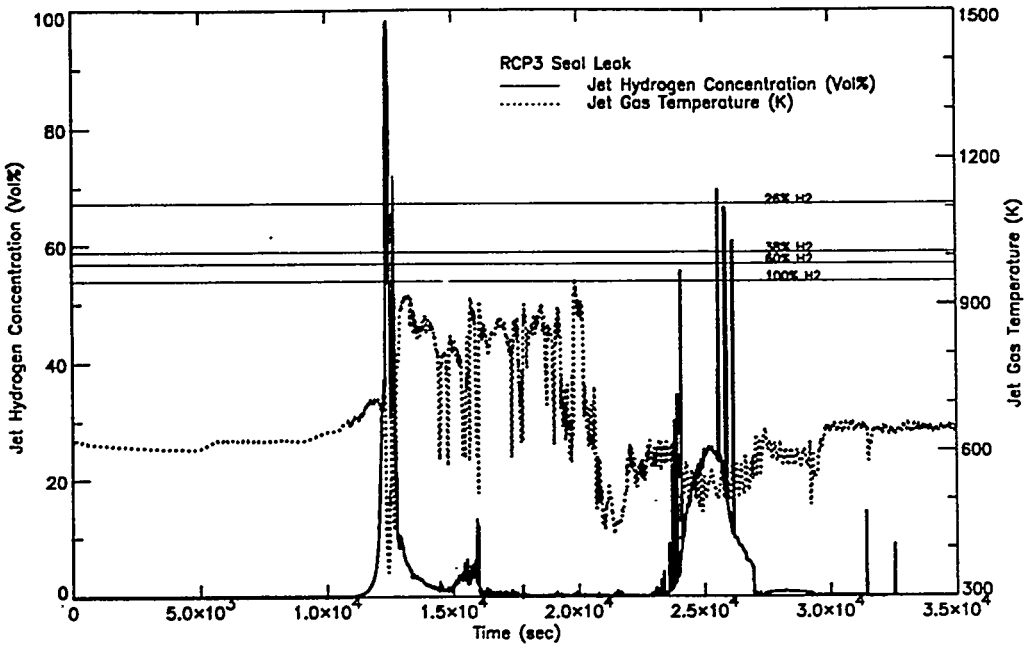

Figure D.50 Case 3: Jet hydrogen concentration and temperature of the gases released from the RCP3 seal leak.

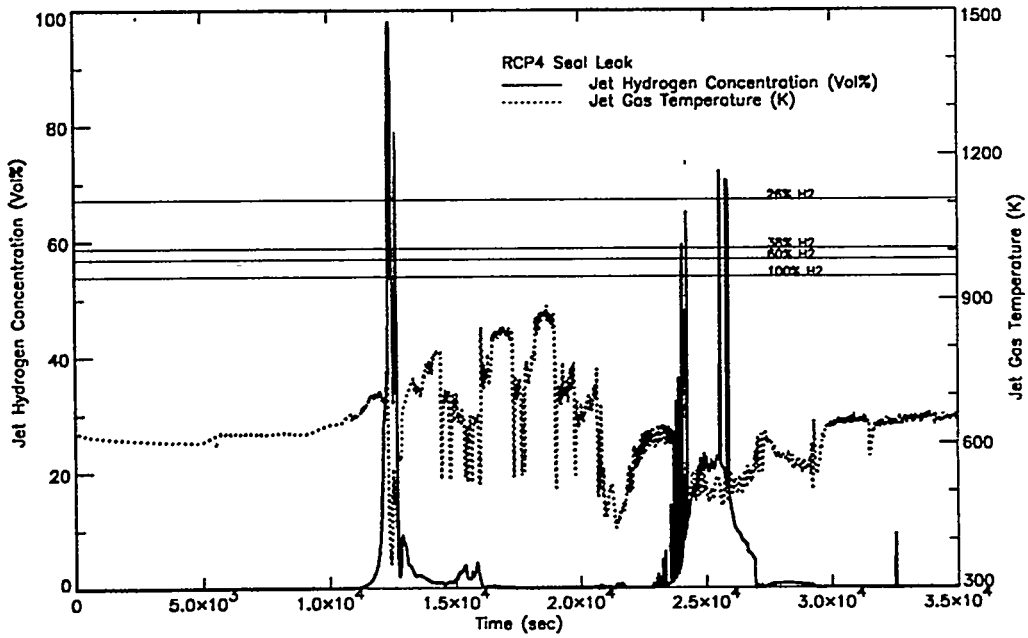

Figure D.51 Case 3: Jet hydrogen concentration and temperature of the gases released from the RCP4 seal leak.

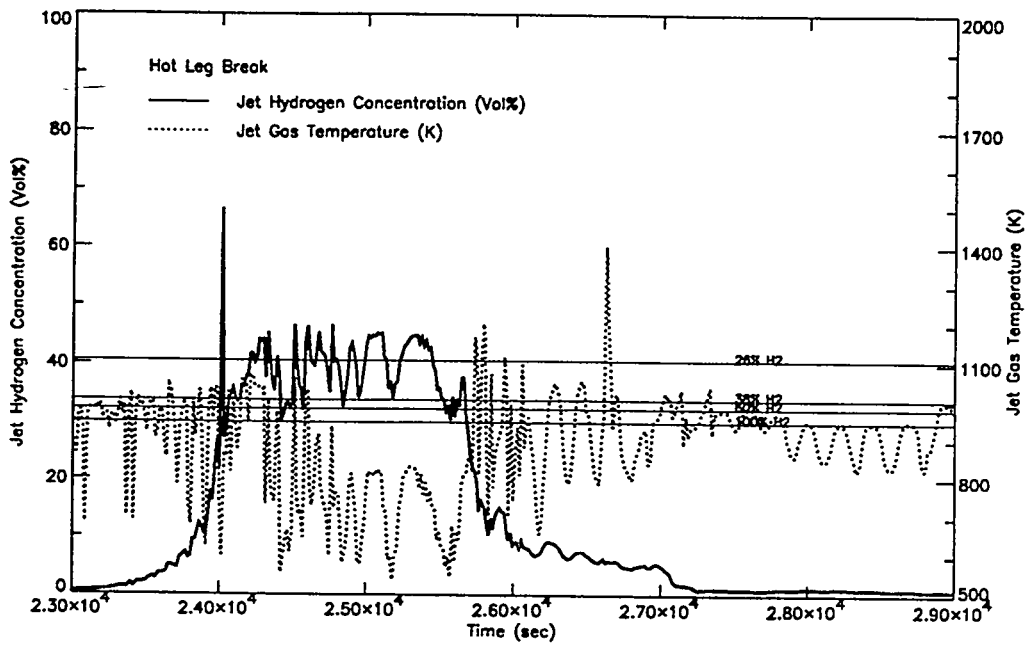

Figure D.52 Case 3: Jet hydrogen concentration and temperature of the gases released from the hot-leg break.

APPENDIX E
HYDROGEN COMBUSTION DURING DCH EVENTS

Martin M. Pilch
Sandia National Laboratories

E.1 INTRODUCTION

Figure E.1 illustrates the potential modes of hydrogen combustion during a DCH event. Hot hydrogen, produced by metal steam reactions in the reactor cavity or subcompartment, vents into the upper dome of the containment, where it can burn as a diffusion flame. The oxygen necessary to support the diffusion flame can only be supplied by entrainment of the preexisting atmosphere into the buoyant plume. This entrainment also carries H_2, present in the preexisting atmosphere, which can also burn within the plume.

The hot combustion products will impact the dome, possibly inducing mixing of the hot combustion products with the atmosphere. Again, there is the potential to burn preexisting hydrogen (and oxygen) as it mixes with the hot combustion products.

An upward propagating flame can be initiated if the preexisting atmosphere contains sufficient hydrogen and not too much steam. The preexisting atmosphere can be heated by radiation from the burning jet, by radiation from stratified combustion products in the dome, by particles of debris falling through the atmosphere, or by mixing of the containment atmosphere. With sufficient heating of the atmosphere, recombination (i.e., slow volumetric combustion) of H_2 and O_2 can occur. Because of the strong temperature dependence of the chemical reactions, a condition of sudden volumetric combustion (autoignition) can occur if heating of the atmosphere exceeds a threshold temperature.

The hot jet vents into the upper dome on a time scale of the RCS blowdown, although most occurs during the debris dispersal period. The blowdown process may void the subcompartment of any oxygen. Some hydrogen, however, could remain in the subcompartment beyond the blowdown interval, but it can burn only if it mixes with oxygen-bearing regions in the dome. Owing to buoyancy forces, this hot hydrogen will eventually mix with the containment atmosphere and possibly burn. In addition, a cool boundary layer will sink along the wall of the containment causing mixing of hot combustion products in the dome with the

cooler containment atmosphere. If the mixing region is sufficiently hot, then additional combustion of hydrogen initially in the atmosphere can occur.

Peak pressures in the containment occur on the time scale of the RCS blowdown, although experiments suggest that much of this pressurization occurs during the debris dispersal period, which typically is about half of the characteristic blowdown time. The key issue then, is not how much hydrogen burns, but how much hydrogen burns on the DCH time scale so it can contribute to peak containment pressure. Hydrogen combustion cannot contribute to peak containment pressure unless the energy release rate is greater than the heat transfer rate to structures.

Jet combustion (plus entrainment) and autoignition (~ 1100 K) were both modeled in NUREG/CR-6075. Working group discussions questioned the selected autoignition temperature and the NUREG/CR-6075 assumption that the fraction of preexisting hydrogen that is entrained and burned in the jet can be bounded by the volume of hydrogen in the atmosphere necessary to burn all the jet hydrogen. More specifically, the working group recommended that the volume of entrained atmosphere (and thus the amount of preexisting hydrogen burned) be estimated from hydrodynamic mixing models. Additionally, we have further examined whether the preexisting hydrogen could burn as a propagating deflagration at the extremes of the hydrogen distribution. Our conclusions regarding hydrogen combustion during DCH events can be summarized as follows:

1. DCH-produced hydrogen (plus some entrainment of H_2 from the preexisting atmosphere) can burn as a jet in the dome and contribute to peak containment pressures. This is consistent with NUREG/CR-6075. Estimates of hydrogen combustion of the mixture entrained into the jet based on hydrodynamic mixing considerations (Rodi, 1982) yield comparable results to that determined in NUREG/CR-6075.

2. Stratification of jet combustion products will occur on the dome, thus impeding the mixing of combustion products with the preexisting atmosphere.

3. Flame propagation is difficult to achieve in a stratified containment atmosphere and the burning process is too slow and inefficient to contribute to peak loads

except possibly at the upper end of the H_2 distribution. Explicit treatment of this process (not considered in NUREG/CR-6075) to better define and bound uncertainties in hydrogen combustion is included in the supplement analyses. These enhancements had no impact on the predicted containment load distributions for scenarios with ~50 percent steam in the containment atmosphere. Deflagration enhanced DCH loads are predicted for a TMI-like scenario with essentially no steam in the atmosphere, but the increased pressure is offset by the lower initial pressure in the containment.

4. Slow volumetric combustion of preexisting hydrogen does not contribute to peak loads.

5. Sudden volumetric combustion (autoignition) of preexisting hydrogen is essentially impossible in a stratified atmosphere because heating of the containment atmosphere is mixing limited. However, to better bound uncertainties in hydrogen combustion phenomena, we have reduced the autoignition temperature from 1100 K (NUREG/CR-6075) to 950 K.

6. Combustion initiated by mixing of hot gases with the preexisting atmosphere is too slow to contribute to peak pressure. This is because the mixing (and combustion) time scale is long compared to the heat transfer time scale.

These processes will now be discussed in more detail and their implications will be discussed in the context of the two-cell equilibrium (TCE) model. Results and observations from the SNL/IET tests confirm the general picture outlined here. In keeping with peer review comments, the limits for each combustion mode will be defined and interpreted in the context of both experiment and reactor applications.

E.2 JET COMBUSTION

The combustion of hot hydrogen as jets venting from the subcompartments to the dome is treated explicitly in the TCE model. The hydrogen in the jet comes from two sources: hydrogen produced from reactions of blowdown steam with the metallic constituents of the melt, and hydrogen carried from the RCS with the blowdown steam. The TCE model burns all jet

hydrogen plus some hydrogen entrained into the jet based on a stoichiometric criteria. Working group discussions focused on whether the stoichiometric criteria was reasonably consistent with hydrodynamic entrainment processes.

The ignition of hydrogen jets requires both an energy source and sufficient oxygen in the atmosphere into which the jet vents. The energy source in a DCH event is both hot particles and the jet (gas) temperature itself. The jet temperature at which autoignition occurs is a function of the jet velocity and composition as well as the containment atmosphere composition and temperature. Shepherd (1985) verified that pure hydrogen jets autoignited at temperatures above 903 to 1003 K. Zabetakis (1956) also observed that pure hydrogen jets autoignited above ~943 K, and the autoignition temperature increased to ~1000 K when the steam concentration increased to ~60 percent. A further increase to ~70 percent steam raised the ignition temperature to ~1110 K. Zabetakis also showed that the autoignition temperature varied with the jet velocity. The measured dependence was parabolic, with a minimum of ~943 K at ~6.1 m/s. The autoignition temperature increased to ~983 K and ~993 K when the jet velocity decreased to ~1.5 m/s and increased to ~14 m/s, respectively. Thus, the autoignition temperature of a jet is not a strong function of velocity. However, the available data on dilute (low hydrogen concentrations) suggests that autoignition may be a strong function of composition.

There must also be sufficient oxygen in the atmosphere for a hydrogen jet to ignite. Observations from the NTS tests (Shepherd, 1987) indicate that diffusion flames will not burn when the oxygen concentration drops below ~5 - 8 percent. The TCE model requires that $X_{O2} > 0.05$ in order to ignite and sustain a diffusion flame.

Table E.1 shows that jet inerting is sometimes observed in DCH experiments when the oxygen concentration in the atmosphere is below ~8 percent and jet inerting is always observed with the oxygen concentration below 5 percent. It should be noted that this oxygen limitation is a practical concern only when the containment contains ~0.18 - 0.39 MPa of steam. CONTAIN calculations (Appendix D) using input from SCDAP/RELAP5 (Appendix C) show that these conditions are achieved only early in the transient when DCH is not likely to occur because core damage is limited. However, scenarios with large quantities of cavity water or large quantities of saturated water coejected into the containment with the melt might dilute and quench the hydrogen jet to the point that a diffusion flame cannot ignite or be sustained.

Figure E.2 shows the measured temperatures in one of the vent spaces in the Zion IET experiments (Allen et al., 1994). The temperatures exceed ~1000 K; consequently, autoignition of the jet may occur for a sufficiently hydrogen rich jet. In fact, the peak temperature occurs in ~1 s, which can be compared with the reported thermocouple time constant of ~0.3 s. Thus, it seems likely that the peak temperature was higher than measured. It is interesting to note that the debris dispersal period is also ~1 s and that the blowdown period is ~3 s.

Figure E.3 shows that jet combustion was generally observed in the Zion SNL/IET tests when a reactive atmosphere (contained oxygen) was present. The SNL/IET-3 and IET-4 experiments had reactive atmospheres with no preexisting hydrogen, so jet combustion was the only mode possible. All other tests with reactive atmospheres contained ~2 - 3 percent H_2.

The TCE model bounds uncertainties associated with ignition of hydrogen jets by assuming that hydrogen jets will always burn regardless of the source diameter jet velocity, jet composition, and jet temperature. Ignition and burning of jets is subject only to the constraint that the preexisting atmosphere contain at lest 5 percent oxygen. We recognize that some situations, such as large quantities of cavity or coejected water, could create conditions where jet combustion may not actually occur.

Details of the entrainment and jet combustion processes are difficult to predict. There can be multiple vent points of irregular shape (i.e., triangles, annuli) and size, and the source, strength, and composition can vary with the sequence. For these reasons, the TCE model employs a stoichiometric argument in order to estimate the amount of hydrogen combustion in a reasonable fashion.

The hot hydrogen/steam jet can burn only because oxygen is entrained into the jet; assuming of course, that the atmosphere oxygen threshold criterion for jet combustion is met. Entrainment also carries some of the preexisting hydrogen into the hot jet, and this entrained hydrogen can also burn. The total amount of jet hydrogen and preexisting hydrogen that can burn in the diffusion flame can be written as

$$N_{H2}(flame) = N_{H2}(jet) + f_{pre}\, N^0_{H2} \qquad \textbf{(E.1)}$$

where

$$N_{H2}(jet) = f_{H2,DOME}\left(N^0_{H2,RCS} + N_{H2}(RM) + N_{H2}(Fe)\right) \tag{E.2}$$

is the total of all hydrogen that is produced in the cavity and subcompartment that has the potential to reach the dome by vents or through the annular gap around the RPV. The fraction of hydrogen produced in the subcompartment and pushed to the dome ($f_{H2,DOME}$) on DCH time scales was intentionally bounded by unity in both the TCE and CLCH models as implemented in NUREG/CR-6075.

The fraction of preexisting hydrogen that is entrained and burned in the jet can be reasonably estimated by assuming that enough atmosphere is entrained to burn all the jet hydrogen that enters the dome plus any entrained hydrogen,

$$N_{H2}(jet) + X_{H2}N_e = 2X_{O2}N_e \quad . \tag{E.3}$$

The entrained fraction is then obtained by normalizing the moles of atmosphere entrained by the initial number of moles in the atmosphere,

$$f_{pre} = \frac{N_e}{N^0} = \frac{N_{H2}(jet)}{N^0}\,\frac{1}{2X_{O2} - X_{H2}} \quad . \tag{E.4}$$

Finally, the total number of hydrogen moles burned within the flame is given by

$$N_{H2}(flame) = N_{H2}(jet)\left[1 + \frac{X_{H2}}{2X_{O2} - X_{H2}}\right] , \tag{E.5}$$

with the second term in brackets representing a correction for entrained hydrogen. This is the TCE model for jet combustion. Table E.2 evaluates the fraction of atmosphere entrained into the jet using the stoichiometric criteria.

What happens if a hot jet contains no hydrogen initially or if all the jet hydrogen has burned off and entrainment (carrying H_2 and O_2 from the atmosphere) is still occurring? Significant combustion by entrainment in this situation can be sustained only if the combustion reaction can release sufficient energy to heat the entrained gas to at least the initial jet temperature. Otherwise, the entrainment and radiative heat losses will quench the jet gas; and owing to the strong temperature dependence of the chemical reactions, the reaction itself will be quenched.

For a hydrogen-limited reaction, the criterion for sustained reactions during entrainment is

$$\delta N_e \, X_{H2} \, \Delta e_{H2} \geq \delta N_e \, C_p(T_j - T^0) \quad . \tag{E.6}$$

Representative values for both experimental and reactor applications are $\Delta e_{H2} = 2.4 \times 10^5$ J/mol, $C_p \sim 30$ J/mol/K, $T_j \sim 1500$ K, and $T^0 \sim 400$. The maximum hydrogen concentration (in the atmosphere) in Scenario V or VI is ~ 6 percent. The energy release for these values is only ~ 40 percent of what is necessary to sustain the jet temperature and significant reactions. Such an assessment is conservative because radiative heat losses from the jet were not considered. In summary, we do not expect significant additional entrainment-induced combustion once the jet hydrogen is consumed in combustion. Consequently, the stoichiometric argument provides a reasonable and a potentially conservative estimate of the amount of hydrogen burned within a jet.

We now explore the entrainment of preexisting atmosphere in the jet from a purely hydrodynamic perspective. Figure E.4 shows two extremes in the development of a jet during a DCH event. Initially, the transient jet enters the containment volume forming a mushroom cap at its leading edge. Experiments and analyses (Turner, 1962; Delichatsios, 1979) show that cap progresses at only ~ 40 percent of the source velocity. Quasi-steady entrainment is established if the cap reaches the roof before blowdown is complete.

For the conditions of the experiments, the jet is momentum driven over the blowdown period. The volumetric entrainment rate into a single jet (Rodi, 1982) of length x is given by

$$\dot{Q}_e(x) = \dot{Q}_j \left[.25 \frac{x}{A_j^{1/2}} - 1 \right] \quad , \tag{E.7}$$

which can be extended to

$$\dot{Q}_e(x) = \dot{Q}_{tot} \left[.25 \frac{x}{A_{tot}^{1/2}} \sum \left[\frac{A_i}{A_{tot}} \right]^{1/2} - 1 \right] \tag{E.8}$$

for multiple jets when each has the same source velocity. The fraction of the preexisting atmosphere that can be entrained into the jets over the blowdown period is then computed from

$$f_{pre} = \frac{Q_e}{V} = \frac{1}{V}\int_0^{t_b} \dot{Q}_e dt \tag{E.9}$$

which takes on two forms,

$$f_{pre} = \frac{\dot{Q}_{tot} t_b}{V}\left[.25\frac{1}{2}\frac{.4V_j t_b}{A_{tot}^{1/2}}\sum\left[\frac{A_i}{A_{tot}}\right]^{1/2} - 1\right] \quad for\ t_b \le \frac{H}{.4V_j} \tag{E.10}$$

$$\begin{aligned} f_{pre} = {} & \frac{\dot{Q}_{tot}\frac{H}{.4V_j}}{V}\left[.25\frac{1}{2}\frac{H}{A_{tot}^{1/2}}\sum\left[\frac{A_i}{A_{tot}}\right]^{1/2} - 1\right] \\ & + \frac{\dot{Q}_{tot}\left[t_b - \frac{H}{.4V_j}\right]}{V}\left[.25\frac{H}{A_{tot}^{1/2}}\sum\left[\frac{A_i}{A_{tot}}\right]^{1/2} - 1\right] \quad for\ t_b \ge \frac{H}{.4V_j}\ , \end{aligned} \tag{E.11}$$

depending on whether the jet reaches the dome during blowdown. This derivation ignores the accumulation of hot jet gases in a stably stratified layer on the dome; thus, the total entrainment of fresh atmosphere will be overpredicted.

Table E.2 evaluates the fraction of the atmosphere that can be entrained into the jet from a hydrodynamic perspective. These evaluations agree quite favorably with results previously obtained using the stoichiometric criteria. In particular, both criteria predict about twice as much entrainment in IET-11.

At first glance, this may seem surprising; but an explanation can be offered for the trend. The stoichiometric criteria (Equation E.6) is proportional to the amount of hydrogen in the jet N_{H2}(jet); and for a metal rich melt like thermite, the hydrogen produced is to first order proportional to the amount of steam in the jet. Likewise, the hydrodynamic criteria (Equations E.10,11) is also proportional to the amount of steam in the jet. On a scaled basis, IET-11 had ~2.4 times the amount of steam (per Kg of melt) as IET-7 because of a higher accumulator (RCS) pressure. Thus, the stoichiometric criteria correctly predicts an important trend with RCS pressure.

In summary, the stoichiometric criteria is a reasonable and potentially conservative estimate of the amount of preexisting hydrogen that is entrained and burned within the jet. The stoichiometric estimate and the hydrodynamic estimate are both independent of scale, but the latter is a function of number and size of flow paths to the dome.

E.3 STRATIFICATION

The potential for jet combustion products to stratify at the top of the dome is a function of the normalized distance to the roof (H/d_j), the vessel aspect ratio (H/D_v), and the Froude number (Fr_a) given by

$$Fr_a^{1/2} = \left[\frac{\rho_a \, V_j^2}{(\rho_a - \rho_j) \, g d_j} \right]^{1/2} . \qquad \textbf{(E.12)}$$

Figure E.5 shows a stability map for negligible aspect ratio (i.e., infinite tank diameter) taken from Peterson (1994). Table E.3 fixes the coordinates on this plot for the IET-7 and IET-11 experiments. For these representative experiments, $H/d_j > (H/d_j)_{crit}$; consequently, there is a potential for the jet combustion products to stratify on the dome and displace the cooler preexisting atmosphere downward.

The experimental evidence for stratification is straightforward. Figure E.6 shows the temperature profiles for the IET-11 experiment (Blanchat et al., 1994) as a function of elevation and time. Temperatures range from ~1500 K on the dome to ~600 K on the operating deck. Strong temperature stratification persists for ~20 - 40 s, and this represents a lower bound to material mixing. This is because heat transfer will equilibrate temperatures, regardless of composition gradients, while material mixing will also equilibrate temperatures.

Additional insight can be gained by examining the gas grab samples for SNL/IET-11, which are summarized in Table E.4. Gas grab samples are taken at two points: one at the top of the dome, and the other slightly below the midpoint of the dome. The gas grab samples are started at 15 s and 120 s, with each sample lasting 10 s. For perspective, peak pressure in the experiment occurs in ~2 - 3 s; thus, the gas samples are taken well after the main DCH event. Table E.4 confirms that significant material stratification is present at 15 - 25 s. In particular,

the top of the dome is devoid of hydrogen and is oxygen lean. By ~2 min, the dome has approached a well-mixed state.

The IET-11 experiment is close to Peterson's threshold for mixing, and the potential for mixing could increase with increasing vessel aspect ratio (H/D_v). However, ongoing work by Peterson (private communication) suggests that stable stratification is independent of aspect ratio for Fr_a characteristic of the IET experiments.

The operating conditions of the experiments were chosen so as to yield prototypic velocities and densities. The experiments were also geometrically scaled; consequently, Fr_a will be smaller at plant scale and the potential for stratification will increase.

E.4 DEFLAGRATIONS

The DCH event itself, with hot particles and autoigniting plumes, is sufficient to ignite an upward propagating flame if the atmosphere contains sufficient H_2 and not too much steam. Such conditions are typically determined by a hydrogen/air/steam flammability chart. Figure E.7 reproduces two commonly cited flammability charts by Marshall (1986) and Kumar (1985). For a fixed concentration of steam, the hydrogen concentration must exceed the lower flammability limit (LFL) for a flame to propagate through the mixture. Note also that there is a critical steam concentration of ~50 - 65 percent beyond which all concentrations of hydrogen are inerted.

Conventional flammability limits have traditionally been determined by two methods: a pressure rise criterion that is valid in enclosed volumes only and one based on the distance a flame has propagated. The data of Marshall (1986) and Kumar (1985) are representative of the two methods, respectively. At the flammability limit, however, the pressure rise approaches zero, and the limit is difficult to determine experimentally using this criterion. Generally, the limit is defined at some arbitrary pressure increment. This criterion ensures only that a specified pressure will not be exceeded. A propagating flame may exist outside of the flammability limit defined by this criterion, which may initiate fires throughout a building. The flammability limits may also be obtained by measuring the distance a flame has propagated using a series of thermocouples. The flame must propagate a sufficient distance to eliminate any effects of the ignition source and be confined in a vessel large enough that heat transfer to the walls is

negligible. The criterion based on the propagating flame yields wider limits than one based on pressure rise.

There is yet a third perspective on defining the LFL. We expect that the amount of hydrogen burned will approach zero at the LFL. Kumar (1985), Wong (1988), and Carcassi (1987), all show that (in the absence of steam) the combustion completeness is a linear function of the hydrogen concentration with the combustion completeness going to 0 and 1 at the LFL for upward and downward propagating flames, respectively. The combustion completeness is known to decrease with the addition of steam, and the LFL for upward and downward propagating flames increases slightly with steam concentration and decreases with temperature. With these in mind, we write the hydrogen combustion completeness as

$$\eta = \frac{X_{H2} - X_{H2}(UP; X_{STM}; T_{a,m})}{X_{H2}(DWN; X_{STM}; T_{a,m}) - X_{H2}(UP; X_{STM}; T_{a,m})} \tag{E.13}$$

where

$$\begin{aligned} X_{H2}(UP, X_s, T) &= 0.037 + 0.02381 X_s - 5x10^{-5}(T-373) \\ X_{H2}(DWN, X_s, T) &= 0.075 + 0.02381 X_s - 1.0135x10^{-4}(T-373) \ . \end{aligned} \tag{E.14}$$

Experiment data (Wong, 1988; Carcassi, 1987) indicates that the combustion completeness is slightly higher in very turbulent environments ($\sim$1.06 times higher than combustion completeness in a quiescent environment). Turbulent environments are characteristic of spray or fan operation in the containment. The characteristic velocity associated with spray operation is $\sim$10-15 m/s (Nelson, 1985; Marx, 1988) at plant scale, while being potentially smaller at experiment scale. The characteristic velocity associated with fan operation in the FITS tests (Marshall, 1986) is $\sim$15 m/s, and these tests are characteristic of a large part of the database with operational fans. In contrast, Section E.6 shows that the characteristic velocity for forced mixing during a DCH event is $V \sim H/\tau_{mix} \leq 0.08$ m/s (IET-11). Consequently, the DCH environment is more closely analogous to the "quiescent" database than it is to the "turbulent" database.

The lead constants (X_{H2} (UP, 0, 373 K) = 0.037 and X_{H2} (DWN, 0, 373 K) = 0.075) are fit to Kumar's (1985) data for reaction completeness for a quiescent environment. The steam correction (0.02381 X_{STM}) is also fit to Kumar's LFL chart for hydrogen/air/steam. Stamps (1991) has reviewed the temperature dependence of the LFL and found that the LFL decreases

~0.5 vol. percent/100 K for upward propagating flames and decreases ~1.0 vol. percent/100 K for downward propagating flames. The database for this temperature dependence goes up to ~800 K for dry systems and ~473 K for steam concentrations reaching ~60 percent. We note that the upward and downward flammability limits must be constrained to positive values since both go to zero at 1110 K for dry systems. This was the basis for selecting the precise value, $dX_{H2}/dT = 1.0135 \times 10^{-4}$, as the temperature derivative for downward propagating flames.

The combustion completeness correlation reproduces Kumar's (1985) data for a dry system ($X_{STM} = 0$) by design. Figure E.8 compares the combustion completion correlation to the limited database (Wong, 1988) for wet systems ($0 \leq X_{STM} \leq 0.4$). The agreement is quite good, except surprisingly for the dry data which strangely shows a lower completeness of reaction than systems with a 4 percent steam. Temperature plays a large part in explaining this apparent anomaly. The wet experiments must (of necessity) be conducted with saturated temperature (~373 K). The dry data were obtained at room temperature (~293 K). The combustion completeness correlation, evaluated at this lower temperature brings predictions and data into better (although not perfect) agreement with the dry data, as shown in Figure E.6. There is no database to validate the temperature dependence of the combustion completeness correlation.

Examination of the flammability charts (Figure E.7) show that there is a steam concentration beyond which hydrogen combustion is always inerted, regardless of hydrogen concentration. Consistent with Kumar's (1985) data, the inerting limit used here is given by

$$X_{STM}(inert) = 0.63 + 3x10^{-3}(T-373) \qquad \textbf{(E.15)}$$

where the temperature derivative, dX_{STM}/dT ~3 vol. percent/100 K was measured by Kumar over the 373-473 K temperature range.

The appropriate conditions at which to evaluate deflagrations is ambiguous for DCH applications. At the start of the event, the containment is at its initial temperature and composition. For typical initial conditions, deflagrations are only marginally possible at the upper end of the distribution of hydrogen concentration in the containment. During the DCH event, we expect the containment to favor a stratified state with blowdown and hot combustion products (jet) on the dome and the cooler preexisting atmosphere displaced downward. This preexisting atmosphere will have undergone some heating (radiation from the jet) and possibly

some mixing with the blowdown and jet combustion products. Since the completeness of reaction and deflagration rate both increase with temperature, we recommend *bounding* the treatment of deflagrations by assuming a well-mixed atmosphere. Consequently, we recommend using the bulk average atmosphere temperature in the deflagration model; and for consistency, we recommend augmenting the initial steam concentration with the blowdown steam and combustion produced steam from the jet.

Table E.5 shows that deflagrations would not be expected in the experiments or the reactor applications based on the initial conditions (augmented at blowdown) within the containment. Thus, deflagrations are difficult to initiate. Table E.5 also shows, however, that DCH temperatures have the potential to induce deflagrations where they might not be expected at dome temperatures prior to the DCH event, but only by the Kumar criteria and not the Marshall criteria. Again, we conclude that deflagrations are difficult to initiate.

Table E.5 lists the predicted reaction completeness for both experiments and reactor applications. Although the DCH event might induce deflagrations where they might not be expected, the combustion completeness normally will be limited. We note that for TMI-II conditions (X_{H2} ~0.079, X_{STM} ~0.035 T=326), the combustion completeness correlation predicts 96 percent combustion efficiency, which bounds the 86 percent value reported by Henrie and Postma (1987). Although a full scale system, TMI-II is not a stringent test of the combustion completeness correlation because the steam concentration is lower than what would be expected in most DCH events.

We now ask whether the energy release can occur on a time scale that can contribute to peak DCH loads. Heat transfer to structures is the mechanism that controls whether deflagrations can contribute to peak loads. The net energy release to the atmosphere on DCH time scales is given by

$$\Delta E_{H2} = \left(\dot{E}_{H2} - \dot{E}_{HT}\right)\tau_{DCH} \qquad \textbf{(E.16)}$$

which can be written as

$$\Delta E_{H2} = \eta \; \Delta E_{H2}(\max) \; \frac{\tau_{DCH}}{\tau_{H2}} \cdot \left[1 - \frac{\dot{E}_{HT}}{\dot{E}_{H2}} \right] \tag{E.17}$$

so that the fraction of preexisting hydrogen that can burn on DCH time scales becomes

$$f_{pre} = \frac{\Delta E_{H2}}{\Delta E_{H2}(\max)} = \eta \; \frac{\tau_{DCH}}{\tau_{H2}} \left[1 - \frac{\dot{E}_{HT}}{\dot{E}_{H2}} \right] \quad . \tag{E.18}$$

Deflagrations cannot contribute to peak DCH loads if the heat transfer rate to structures exceeds the energy release rate due to the deflagration; thus, f_{pre} must be constrained by $0 \leq f_{pre} \leq 1$. In the limit of an adiabatic containment, the DCH time scale (peak load) approaches the combustion time scale ($\tau_{DCH} \sim \tau_{H2}$) and the fraction of preexisting hydrogen that contributes to loads becomes the combustion completeness, $f_{pre} \sim \eta$.

We now develop expressions for the heat transfer and deflagration rates. Heat transfer to structures is dominated by radiation,

$$\dot{E}_{HT} = \sigma \epsilon A_s \left(T_{a,m}^4 - T_s^4 \right) \tag{E.19}$$

and the energy release rate due to deflagrations is given by

$$\dot{E}_{H2} = \frac{\eta N_{H2} \Delta e_{H2}}{\tau_{H2}} \tag{E.20}$$

where the characteristic combustion time is controlled by the dome height and a characteristic flame velocity

$$\tau_{H2} = \frac{H}{V_f} \quad . \tag{E.21}$$

Flame speeds are experimentally determined by dividing the facility scale by the pressure rise time. Wong (1988) has correlated the flame velocity in quiescent environments from a broad database,

$$V_f = 23.7\ H^{1/3} \left[\frac{X_{H2}}{1-X_{STM}} - X_{H2}(V_f, T) \right] f(V_f, T)\ \exp(-A) \tag{E.22}$$

where

$$X_{H2}(V_f, T) = 0.036 - 5x10^{-5}(T-373)$$
$$f(V_f, T) = \left[\frac{T}{373} \right]^{1/3} \tag{E.23}$$
$$A = 4.877\ X_{STM} \left(1 + 0.61677\ X_{STM}\right) \ .$$

We note that $X_{H2}(V_f, T)$ is analogous to the lower flammability limit for a dry system, and we have modified Wong's correlation to account for the temperature dependence of this term. By definition, we expect the flame velocity to be zero at the lower flammability limit, regardless of the amount of steam present. One shortcoming of Wong's correlation is that it admits finite flame velocities for hydrogen concentrations below the lower flammability limit when steam is present. Note that $X_{H2}(V_f, T)$ and V_f must be limited to positive values.

Wong's correlation for the effective flame speed depends on the cube root of the characteristic height of the combustion chamber. Such a dependence is derived by equating the buoyancy force generated by the less dense burnt gases propagating into the unburnt gases to the drag force on the rising front. The flame velocity then scales as (Wong, 1988)

$$V_f \sim \left(\left[1 - \frac{\rho_b}{\rho_u} \right] \frac{\rho_u}{\rho_b}\ gHS_u \right)^{1/3} , \tag{E.24}$$

which shows an additional temperature dependence through the density terms and the laminar flame velocity. Expressing the densities in terms of temperature (assuming negligible composition changes) and noting that $S_u \sim T^2$ (Liu and McFarlane, 1983), a temperature correction to the flame velocity can be constructed,

$$f(V_f, T) = \frac{V_f(T)}{V_f(373)} = \left[\frac{T}{373}\right]^{1/3} . \qquad \textbf{(E.25)}$$

We have modified Wong's correlation accordingly. We note, however, that there is no database to validate this temperature correction.

Table E.5 provides an assessment of whether deflagrations can contribute to peak DCH loads. For the experiments, the characteristic heat transfer rate exceeds the energy release rate; consequently, deflagrations cannot contribute to peak loads. For the reactor application and at the upper bound of the zirconium oxidation distribution, DCH-induced deflagrations can contribute partially to peak DCH loads in Scenario VI. This difference from the experiments is due in part to scale, $\dot{E}_{HT}/\dot{E}_{H2} \sim L^{-1/3}$, and in part to the higher hydrogen concentrations at the upper limit of the distribution.

E.5 VOLUMETRIC COMBUSTION

Hydrogen reacts with oxygen at all temperatures, although the reaction is strongly temperature dependent. These types of reactions occur uniformly through a constant temperature mixture; thus, we refer to this as volumetric combustion. We envision the atmosphere to be stratified on DCH time scales. The preexisting atmosphere will be displaced downward and remain cooler than the bulk average temperature. Nonetheless, the displaced atmosphere will be heated by radiation from the jets and the portion of the debris that is dispersed to the dome.

Volumetric combustion, like deflagrations, can contribute to peak DCH loads only if the energy release rate exceeds the heat loss to structures,

$$\frac{\dot{E}_{HT}}{\dot{E}_{H2}} = \frac{\sigma \epsilon A_s \left(T_{a,m}^4 - T_s^4\right)}{\dfrac{\eta N_{H2} \Delta e_{H2}}{\tau_{H2}}} \leq 1. \qquad \textbf{(E.26)}$$

Assessment is straightforward once the reaction time constant is known as a function of temperature.

Figure E.9 shows the reaction time constant as predicted by SENKIN, which is a chemical kinetics code (Lutz et al., 1991). Reviewer F (Appendix A) noted that the reaction constants in SENKIN were obtained from very high-temperature shock tube data and that extrapolation to lower temperatures is in error. Specifically, more recent lower temperature data suggest that SENKIN's rate constants can be $\sim 10^2$ too high (Vermeersch, 1991) in the temperature range of interest to DCH; consequently, SENKIN's reaction time constants should be $\sim 10^2$ larger. This is qualitatively confirmed by Hustad and Sonju (1988) and DeSoete (1975) who report τ_{H2} ~minutes for lean mixtures at ~800 - 900 K. We note, however, current reaction mechanisms for low temperature hydrogen combustion are fundamentally incomplete. We can only speculate based on the trends implied by the data of Hustad and Sonju (1988) and DeSoete (1975). For our assessments, we increase SENKIN predicted reaction times by the factor 10^2.

Table E.6 contains an assessment of volumetric combustion for the experiment and the reactor applications. Noting the strong temperature dependence of volumetric combustion, we have conservatively evaluated the reaction time constant at the bulk average temperature and have assumed complete combustion efficiency.

In all cases except IET-11, volumetric combustion is too slow to contribute to peak DCH loads. These assessments of volumetric combustion are quite conservative because they assume that the preexisting atmosphere is entirely at the bulk average temperature. This is certainly not the case in IET-11, which exhibits a strong temperature gradient (Figure E.5). Such stratification in general is to be expected (Section E.3). Moving to a region that is only ~100 K cooler (i.e., ~1000 K), the reaction rates cannot keep up with heat losses to structures. This illustrates the importance of stratification in such a severe DCH event as was observed in IET-11.

Autoignition can occur if the uniform gas temperature exceeds a critical value. Autoignition is defined as a sudden volumetric combustion of preexisting hydrogen. Autoignition, like the slow volumetric combustion discussed above, does not need a spark or pilot flame for combustion to occur. In DCH events, the strong potential for stratification precludes a uniformly-mixed high-temperature atmosphere. Such conditions can be achieved only through mixing, and Section E.6 concludes that mixing limited combustion cannot contribute to peak DCH loads.

Examination of autoignition criteria for well-mixed, uniformly heated mixtures lends more credibility to the exclusion of autoignition events. Stamps (1991) has summarized autoignition data for hydrogen/air/steam mixtures. Figure E.10, taken from Stamps, shows that the autoignition temperature becomes asymptotically large at the hydrogen concentrations (< 6 percent) of interest to DCH and that the addition of steam makes autoignition even more difficult.

Autoignition data have generally been taken near stoichiometric conditions; however, Conti and Hertzberg (1988) observed autoignition at 873 K for a dry mixture with 6 percent hydrogen. The data of Zabetakis (1956) indicate that the addition of 30 percent steam increases the autoignition temperature by ~30 K for conditions near stoichiometric. For lean mixtures (5 - 20 percent), Tamm et al. (1985) has shown that the glow plug temperature necessary to ignite a dry mixture increases ~80 K with the addition of 30 percent steam.

To ensure a conservative treatment of hydrogen combustion, we recommend evaluation of autoignition using the bulk average dome temperature and a reduction of the autoignition temperature from 1100 K in NUREG/CR-6075 to 873 + 80 ≈950 K. We note, however, that a sensitivity study in NUREG/CR-6075 showed that the containment failure probability was insensitive to a reduction of the autoignition temperature to 950 K. The dome temperatures in the supplement scenarios are lower than the NUREG/CR-6075 scenarios; consequently, we observe a similar insensitivity in the current calculations.

E.6 MIXING LIMITED COMBUSTION

Combustion of hydrogen can occur in a mixing zone if oxygen is present and the mixing zone is sufficiently hot. The hydrogen and oxygen can be brought into the mixing zone by either the hot or cold stream, or both. If the combustion is to be mixing limited, then the temperature of the mixing zone must be sufficiently hot that the reaction time scale is short compared with the mixing time scale; as a practical matter, this means that the mixture temperature must be ~900 - 1000 K. If this is not the case, then our expected conclusion (mixing limited combustion is too slow to contribute to peak DCH loads) becomes all the more true. Analogous to the discussion in Section E.3, we expect that combustion reactions will not be sufficient to maintain the temperature of the mixing zone. This quenching will greatly limit

the amount of hydrogen that can burn during mixing. Nonetheless, we further explore this combustion mode under the assumptions that the reaction is self sustaining and mixing limited.

There are three potential mixing processes that must be considered: forced mixing by the blowdown gases, buoyant mixing between the subcompartment and the dome, and mixing due to a cool wall "jet" sinking along the vessel walls. Each mechanism will now be examined and the scaling implications examined.

Section E.3 concluded that hot plumes rising from the subcompartments during blowdown would stratify at the top of the dome and thus inhibit bulk mixing of the atmosphere. The tendency to stratify is even stronger at plant scale. However, the margin of such conclusions is less well established for the aspect ratio characteristic of containment dome regions. Consequently, it is instructive to examine the implications of mixing in the total absence of buoyancy-induced stratification.

Our main goal, however, was to explore if mixing limited hydrogen combustion could contribute to peak DCH pressures. To make such an assessment, we compared the mixing limited energy release rate due to hydrogen combustion with the energy loss rate due to heat transfer from the atmosphere to containment structures,

$$\frac{\dot{E}_{H2}}{\dot{E}_{HT}} = \frac{N_{H2}\,\Delta e_{H2}}{t_{mix}}\,\frac{t_{HT}}{N_a C_v \Delta T} = \frac{X_{H2}\,\Delta e_{H2}}{t_{mix}}\,\frac{\tau_{HT}}{C_v \Delta T} \quad . \qquad \textbf{(E.27)}$$

When less than unity, this ratio implies that hydrogen combustion (although it occurs) will not contribute to peak containment pressures. For experiments, the concentration of hydrogen in the atmosphere is known, and the heat transfer time constant and temperature loss can be estimated from experiment results. Consequently, we can focus on the mixing time constant alone.

Breidenthal et al. (1990) measured the mixing time associated with jetting into a confined volume. Buoyancy forces were negligible. Breidenthal's data (Figure E.11) shows two asymptotic limits depending on the jet injection period. The asymptotic mixing times are given by,

$$\tau_{mix} = \frac{t_{mix}}{t_c} = \frac{40}{\tau_j} \qquad \tau_j^2 << 1$$
$$\tau_{mix} = 5 + \tau_j \qquad \tau_j^2 >> 1 \tag{E.28}$$

where

$$\tau_j = \frac{t_j}{t_c}$$

$$t_c = \left[\frac{\rho_a D_v^3}{T_L}\right]^{1/2} = \left[\frac{\rho_a D_v^3}{\frac{\frac{1}{2}\rho_j V_j^2 A_j}{D_v}}\right]^{1/2} \tag{E.29}$$

and where T_L is the jet thrust per unit length. The asymptotic limits are derived from simple scaling arguments and the constants 40 and 5 obtained from a fit to the data.

The mixing time, as defined by Breidenthal, corresponds to a state where local concentrations do not exceed ~2.5 percent of the mean. This is essentially an upper bound to the mixing time. Breidenthal also showed that flow circulation will loop back to the source in ~0.25 τ_{mix} and that this corresponds to the onset of significant mixing. For DCH applications, this is the more relevant mixing time scale.

Table E.7 evaluates the mixing time for the experiments. It is seen from the τ_j values that the experiments fall into the short pulse regime. Two bounds on the mixing time are listed corresponding to the onset of significant mixing and complete mixing. Forced mixing would have been a very inefficient process in the SNL/IET-7 experiment, even in the absence of buoyancy forces. The predicted mixing time for SNL/IET-11 is ~103 s. Gas grab samples suggest that the vessel is not well mixed by 15 - 25 s but that it is well mixed by 120 - 130 s; consequently, Breidenthal's correlation is consistent with experiment observation.

Table E.7 also provides an assessment of the combustion/heat transfer competition. Any combustion resulting from forced mixing cannot keep up with heat transfer to structures. Furthermore, such assessments are conservative since they neglect the propensity of the atmosphere to stratify and the propensity of the mixing zone to quench.

Following blowdown, the subcompartment will still retain some hot gases. These hot gases will then rise, under buoyant forces, through various vent spaces into the upper dome. This is accompanied by a countercurrent flow of cool dome gases back into the subcompartment.

The characteristic time to flush the subcompartment gases into the dome is approximated by

$$t_{mix} \sim \frac{V_{sub}}{v_{sd} \frac{A}{2}} \quad . \tag{E.30}$$

We use only half the available flow area to account for the counterflow. The buoyancy-induced velocities in the vent spaces arise from Taylor instabilities. For a slot or a circular vent, the rise velocity is given by

$$v_{sd} \sim .23 \left[\left(1 - \frac{\rho_s}{\rho_a} \right) gd \right]^{1/2} \quad , \tag{E.31}$$

so that the mixing time becomes

$$t_{mix} \sim 8.7 \frac{V_{sub}}{\left[\left(1 - \frac{\rho_s}{\rho_a} \right) gd \right]^{1/2} A} \quad . \tag{E.32}$$

Here d is the characteristic dimension of one of the vents and A is the total flow area for all the vents.

Table E.8 also provides an assessment of the combustion/heat transfer competition for mixing in the subcompartment. The quantity of hydrogen retained in the subcompartment and available for burning upon mixing is assumed to be ~20 percent of the hydrogen predicted to be produced during the DCH event. Table E.8 shows that any combustion resulting from buoyancy-driven mixing of the subcompartment cannot keep up with heat transfer to structures. More important, however, this process is bounded in the TCE model by assuming that all DCH-produced hydrogen (plus any from blowdown) passes to the dome, where it burns completely.

The last mixing mechanism results from cooling of the gas mixture along the walls of the dome. The cool wall layer sinks while entraining atmosphere during the process. The volume entrainment rate into the boundary layer (Peterson, 1994) is given approximately by

$$\dot{Q}_e = \pi D_v H V_e = 0.1 \pi D_v H \; Gr^{2/5} \; \frac{\nu}{H} \tag{E.33}$$

where the Grashof number is given by

$$Gr = g \; \frac{T_{a,m} - T_s}{T_{a,m}} \; \frac{H^3}{\nu^2} \quad . \tag{E.34}$$

The mixing time is then given by

$$t_{mix} \sim \frac{V}{\dot{Q}_e} \quad . \tag{E.35}$$

Table E.9 provides an assessment of mixing in the dome due to a wall jet. The mixing time in SNL/IET-11 is consistent with observations that the dome was not well mixed at ~15 - 25 s and that it was well mixed by ~120 s. The potential energy release rate due to mixing limited combustion of preexisting hydrogen cannot keep up with heat transfer to structures.

In summary, the mixing mechanisms discussed here could lead to only limited combustion of preexisting or subcompartment hydrogen, but on a time scale too long to contribute to peak containment pressures in the experiments. Extrapolation of these insights to plant scale can be examined with Table E.10. The scale dependence of the combustion/heat transfer competition is controlled by the time ratio t_{HT}/t_{mix}. Table E.10 shows that forced mixing-limited combustion is independent of scale, so the experimental evaluations and observations are directly applicable. The importance of subcompartment mixing and wall jet-induced mixing increases with physical scale; however, the experimental margin is sufficiently large that mixing limited combustion is not expected to contribute to peak pressures, even at plant scale. Mixing from the subcompartment is bounded in the TCE model by assuming that all DCH produced hydrogen is transported to the dome where it burns.

E.7 References

Allen, M.D., M.M. Pilch, T.K. Blanchat, R.O. Griffith, and R.T. Nichols (May 1994). *Experiments to Investigate Direct Containment Heating with Scaled Models of the Zion Nuclear Power Plant in the SURTSEY Test Facility*, NUREG/CR-6044, SAND93-1049, Sandia National Laboratories, Albuquerque, NM.

Blanchat, T.K., M.D. Allen, M.M. Pilch, and R.T. Nichols (June 1994). *Experiments to Investigate Direct Containment Heating Phenomena with Scaled Models of the Surry Nuclear Power Plant*, NUREG/CR-6152, SAND93-2519, Sandia National Laboratories, Albuquerque, NM.

Breidenthal, R.E., V.R. Buonadonna, and M.F. Weissbach (1990). "Molecular Mixing Via Jets in Confined Volumes," *J. Fluid Mechanics*, Vol. 219, pp. 534-544.

Conti, R.S. and M. Hertzberg (Sept/Oct 1988). "Thermal Autoignition Temperatures for Hydrogen-Air and Methane-Air Mixtures," *J. Fire Sciences*, Vol. 6, pp. 348-355.

Delichatsios, M.A. (1979). "Time Similarity Analysis of Unsteady Buoyant Plumes," *J. Fluid Mechanics*, **93**, pp. 241-250.

DeSoete, G.G. (1975). "The Flammability of Hydrogen-Oxygen-Nitrogen Mixtures at High Temperature," *La Riuista dei Combustibili*, **29**, pp. 166-172.

Henrie, J.O. and A.K. Postma (March 1987). *Lessons Learned from Hydrogen Generation and Burning During the TMI-2 Event*, RHO-RE-EV-95P, Rockwell International, Rockwell Hanford Operations, Richland, WA.

Hustad, J.E. and O.K. Sonju (1988). "Get Title", *Combust. Flame*, **71**, pp. 283.

Jain, S.C. and V. Balasubramanian (1978). "Horizontal Buoyant Jets in Quiescent Shallow Water," *J. Environ. Engng. Div. Proc. ASCE*, **104**, EE4.

Jirka, G.H. (1982). "Turbulent Buoyant Jets in Shallow Fluid Layers," in *Turbulent Buoyant Jets and Plumes (Edited by W. Rodi)*, Pergamon Press, NY.

Kumar, R.K. (July/August 1985). "Flammability Limits of Hydrogen-Oxygen-Diluent Mixtures," AECL-8890, Journal of Fire Sciences, Vol. 3, pp. 245-262.

Lee, J.H., G.H. Jirka, and D.R. F. Harleman (1974). "Stability and Mixing of a Vertical Round Buoyant Jet in Shallow Water," M.I.T. Ralph M. Parsons Laboratory for Water Resources and Hydrodynamics, Tech. Rep. No. 195.

Lutz, A.E. et al. (1991). *SENKIN: A FORTRAN Program for Predicting Homogeneous Gas Phase Chemical Kinetics with Sensitivity Analysis*, SAND87-8248, Sandia National Laboratories, Albuquerque, NM.

Marshall, B.W. (Dec. 1986). *Hydrogen: Air: Steam Flammability Limits and Combustion Characteristics in the FITS Vessel*, NUREG/CR-3468, SAND84-0383, Sandia National Laboratories, Albuquerque, NM.

Marx, K.D. (Feb. 1988). "Analysis and Computer Simulation of Confined Ring Vortices Driven by Falling Sprays," Phys. Fluids, **31** (2), pp. 263-277.

Nelson, L.S. (1983). "Behavior of Hydrogen Ignitors During Operation of Water Sprays in Containment," Twelfth Water Reactor Safety Research Information Meeting, Vol. 3, NUREG/CP-0058.

Peterson, P.F. (1994). "Scaling and Analysis of Mixing in Large Stratified Volumes," Int. J. Heat Mass Transfer, Vol. 37, Suppl. 1, pp. 97-106.

Rodi, W. (1982). *Turbulent Buoyant Jets and Plumes*, HMT, **Vol. 6**, Pergamon Press.

Shepard, J.E. (Feb. 1985). *Hydrogen-Steam Jet-Flame Facility and Experiments*, NUREG/CR-3638, SAND84-0060, Sandia National Laboratories, Albuquerque, NM.

Shepard, J.E. (Aug. 1987). *Analysis of Diffusion Flame Tests*, NUREG/CR-4534, SAND86-0419, Sandia National Laboratories, Albuquerque, NM.

Stamps, D.W. and M. Berman (1991). "High-Temperature Hydrogen Combustion in Reactor Safety Applications," Nuclear Science and Engineering, **109**, pp. 39-48.

Tamm, H., R. McFarlane, and D.D.S. Liu (March 1985). *Effectiveness of Thermal Ignition Devices in Lean Hydrogen-Air-Steam Mixtures*, AECL-7820, Atomic Energy of Canada, Ltd., Whiteshell Nuclear Research Establishment, Pinawa, Manitoba, Canada.

Turner, J.S. (1962). "The 'Starting' Plume in Neutral Surroundings," *J. Fluid Mech.*, **13**, pp. 356-368.

Vermeersch, M.L. (1991). *A Variable Pressure Flow Reactor for Chemical Kinetics Studies*, Ph.D. Thesis, Princeton University.

Wong, C.C. (Nov. 1988). *HECTR Analyses of the Nevada Test Site (NTS) Premixed Combustion Experiments*, NUREG/CR-4916, SAND87-0956, Sandia National Laboratories, Albuquerque, NM.

Zabetakis, M.G. (Sept. 1956). *Research on the Combustion and Explosion Hazards of Hydrogen-Water Vapor-Air Mixtures*, AECU-3327, U.S. Atomic Energy Commission.

E.8 Nomenclature

A_j	=	flow area of jet source
A_s	=	dome surface area
A_{tot}	=	total flow area of all jets
C_p	=	molar heat capacity at constant pressure
C_u	=	molar heat capacity at constant volume
d_j	=	jet diameter
D_v	=	vessel diameter
$\dot{E}_{HT}$	=	heat transfer rate
$\dot{E}_{H2}$	=	energy release rate due to hydrogen combustion
$f_{H2,DOME}$	=	fraction of DCH produced hydrogen and blowdown hydrogen transported to the dome
f_{pre}	=	fraction of preexisting hydrogen in the containment atmosphere that burns on DCH time scales
Fr_a	=	Froude number
g	=	acceleration due to gravity
Gr	=	Grasof number
H	=	height of dome
Ne	=	total moles of atmosphere entrained into jet
N_{H2}	=	moles of hydrogen
N_{H2} (Fe)	=	moles of hydrogen produced in the DCH event by steam reactions with iron
N_{H2} (RM)	=	moles of hydrogen produced in the DCH event by steam reactions with reactive metals
$N^0_{H2,RCS}$	=	moles of hydrogen in RCS at vessel breach
$\dot{Q}_e$	=	volumetric entrainment rate
$\dot{Q}_j$	=	jet volumetric flow rate at the source
$\dot{Q}_{tot}$	=	total volumetric flow rate of all jets
t_c	=	normalization time for jet induced mixing
t_j	=	jet time scale
t_{mix}	=	mixing time scale

$T_{a,m}$ = maximum atmosphere temperature in the absence deflagrations

T_j = temperature of gas jet venting into dome

T_L = jet thrust per unit length

T^0 = initial temperature of containment atmosphere

T_s = structure temperature

V = containment volume

Ve = entrainment velocity

V_f = flame velocity

V_j = jet velocity

v_{sd} = mixing velocity between subcompartment and dome

V_{SUB} = subcompartment volume

X_{H2} = hydrogen concentration in the atmosphere

X_{H2} (DWN; X_{STM}; $T_{a,m}$) = lower flammability limit for downward propagating flames

X_{H2} (UP; X_{STM}; $T_{a,m}$) = lower flammability limit for upward propagating flames

X_{O2} = oxygen concentration in the dome

X_{STM} = steam concentration

X_{STM} (inert) = steam concentration that inerts hydrogen combustion regardless of hydrogen concentration

Greek

δN_e = increment of molar entrainment

Δe_{H2} = molar combustion energy of hydrogen

ρ_a = mass density of containment atmosphere

ρ_j = mass density of jet gases

η = combustion completeness

ΔE_{H2} = energy release due to hydrogen combustion

τ_{DCH} = DCH time scale

τ_{H2} = hydrogen combustion time scale

σ = Boltzman constant

ϵ = emissivity

τ_{mix} = normalized mixing time scale

τ_j = normalized jet time scale

υ = kinematic viscosity

Table E.1 Inerting criteria for jet combustion

Test	Geometry	Scale	$(X_{O2})_{MEAS}$	Jet Combustion Observed
SNL/IET-1	Zion	1:10	0.000	no
SNL/IET-1R	Zion	1:10	0.002	no
SNL/IET-3	Zion	1:10	0.090	yes
SNL/IET-4	Zion	1:10	0.095	yes
SNL/IET-5	Zion	1:10	0.044	no
SNL/IET-6	Zion	1:10	0.098	yes
SNL/IET-7	Zion	1:10	0.096	yes
SNL/IET-8B	Zion	1:10	0.102	yes
SNL/IET-9	Surry	1:5.25	0.063	yes
SNL/IET-10	Surry	1:5.75	0.105	yes
SNL/IET-11	Surry	1:5.75	0.138	yes
ANL/IET-3	Zion	1:40	0.108	yes
ANL/IET-6	Zion	1:40	0.099	yes
ANL/IET-7	Zion	1:40	0.108	yes
ANL/UIB	Zion	1:40	0.057	yes
ANL/IET-8	Zion	1:40	0.077	no

Table E.2 Comparison of jet entrainment using stoichiometric and hydrodynamic estimates

Parameter	IET-7 Zion Geometry 1:10th Scale	IET-11 Surry Geometry 1:5.75th Scale
Stoichiometric Criteria		
N_{H2}(jet) (moles)	147	1100
N^0 (moles)	7129	18.8×10^3
X_{O2}	0.096	0.130
X_{H2}	0.040	0.028
f_{pre}	0.13	0.25
Hydrodynamic Criteria		
H (m)	8	8
$0.4V_j$ (m/s)	5	20
V_j (m/s)	12.5	50
t_b (s)	1.25	1.6
$t_{tran} = \frac{H}{.4V_j}$ (s)	1.6	0.4
A_1 (m^2)	0.125 vent	0.036 RPV annul.
A_2 (m^2)	0.125 vent	1.0 cont. annul.
A_3 (m^2)	0.125 vent	-
A_4 (m^2)	0.125 vent	-
A_{tot} (m^2)	0.5	1.036
$\dot{Q}_{tot}$ (m^3/s)	6.25	51.8
V (m^3)	90	282
f_{pre}	0.11	0.29

Table E.3 Potential for stratification of the atmosphere during DCH events

Parameter	SNL/IET-7 Zion Geometry 1:10th scale	SNL/IET-11 Surry Geometry 1:5.75th scale
ρ_a (kg/m^3)	2.2	1.6
ρ_j (kg/m^3)	0.16	0.18
V_j (m/s)	12.5	50
d_j (m)	0.4	1.13
H (m)	8	8
D_v (m)	3.5	7
$Fr_a^{1/2}$	6.6	15.9
$(H/d_j)_{crit}$	2	5
H/d_j	20	7.08
H/D_v	2.3	1.1

Table E.4 Composition stratification in SNL/IET-11

Species Mole Percent		
Sample Period (s)	15-25	120-130
Top Dome		
H_2	0.00	0.69
O_2	4.82	6.50
N_2	46.5	39.1
Mid Dome		
H_2	0.68	0.48
O_2	8.05	6.34
N_2	43.0	39.4

Table E.5 Assessment of deflagrations during DCH events

	IET-7 Zion Geometry 1:10th Scale	IET-11 Surry Geometry 1:5.75th Scale	Scenario V	Scenario VI
X_{H2}	0.040	0.024	0.049	0.049
X_{STM}	0.50	0.32	0.48	0.48
X'_{H2} post blowdown	0.038	0.020	0.040	0.045
X'_{STM} post blowdown	0.527	0.432	0.575	0.518
X_{H2} (UP, X'_s, 373) Marshall	0.120	0.074	0.084	0.084
X_{H2} (UP, X'_s, 373) Kumar	0.050	0.047	0.048	0.048
$T_{a,m}$ (K)	700	1100	560	680
X_{H2} (UP, X'_s, $T_{a,m}$) Marshall	0.104	0.038	0.075	0.069
X_{H2} (UP, X'_s, $T_{a,m}$) Kumar	0.032	0.011	0.039	0.033
η	0.27	1.0	0.025	0.52
N_{H2} (g • moles)	283	450	2.8×10^5	2.8×10^5
H (m)	8	8	52	52
A_s (m^2)	138	206	8.7×10^3	8.7×10^3
V_f (m/s)	0.12	0.17	0.15	0.28
ϵ	0.8	0.8	0.8	0.8
τ_{H2} (s)	66.7	47.1	342	186
$\dot{E}_{HT}$ (MJ/s)	1.5	13.4	30.3	74.3
$\dot{E}_{H2}$ (MJ/s)	0.28	2.30	5.68	187
$\dot{E}_{HT}/\dot{E}_{H2}$	5.40	5.83	5.34	0.40
f_{pre}	0	0	0.0	0.31

Table E.6 Assessment of volumetric combustion

Parameter	IET-7	IET-11	Scenario V	Scenario VI
$T_{a,m}$	700	1100	560	680
τ_{H2} (SENKIN) (s)	10^5	~1	$>>10^5$	$>>10^5$
A_s (m^2)	138	206	8.7×10^3	8.7×10^3
ϵ	0.8	0.8	0.8	0.8
N_{H2} moles	383	450	2.8×10^5	2.8×10^5
η	1	1	1	1
$\dot{E}_{HT}$ MJ/s	1.50	13.4	30.3	74.3
$\dot{E}_{H2}$ (MJ/s)	919	108	$<<0.67$	<0.67
$\dot{E}_{HT}/\dot{E}_{H2}$	613	0.12	$>>45$	>111

Table E.7 Evaluation of forced mixing

Parameter	SNL/IET-7 Zion Geometry 1:10th Scale	SNL/IET-11 Surry Geometry 1:5.75th Scale
ρ_a (kg/m^3)	2.2	1.6
ρ_j (kg/m^3)	0.16	0.18
t_j (s)	1.25	1.6
D_v (m)	3.5	7
V_j (m/s)	12.5	50
A_j (m^2)	0.5	1.036
T_L (N/m)	1.79	33.3
t_c (s)	7.26	4.06
$\tau_j = t_j/t_c$	0.138	0.394
$\tau_{mix} = t_{mix}/t_c$	290	101
t_{mix} (s)	2.1×10^3	412
$t_{mix} = 0.25\ t_{mix}$ (s)	525	103
X_{H2}	0.0397	0.0239
C_v (J/mole)	24	25
ΔT (K)	550	750
Δe_{H2} (J/mole)	2.4×10^5	2.4×10^5
τ_{HT} (s)	30	32
$\dot{E}_{H2}/\dot{E}_{HT}$	0.041	0.095

Table E.8 Evaluation of mixing between the subcompartment and the dome

	SNL/IET-7 Zion Geometry 1:10th Scale	SNL/IET-11 Surry Geometry 1:5.75th Scale
ρ_s (kg/m^3)	~1	~1
ρ_a (kg/m^3)	2.2	1.6
d (m)	0.36	0.50
A (m^2)	0.44	10
V_{sub} (m^3)	5.8	27
v_{sd} (m/s)	0.43	0.51
t_{mix} (s)	83	18
N_a	7129	18800
N_{H2}	30	220
C_v	24	25
ΔT	550	750
t_{HT}	30	32
$\dot{E}_{H2}/\dot{E}_{HT}$	0.028	0.26

Table E.9 Evaluation of mixing in the dome due to a wall jet

Parameter	SNL/IET-7 Zion Geometry 1:10th Scale	SNL/IET-11 Surry Geometry 1:5.75th Scale
T_a	800	1100
T_w	300	400
H	7	8
υ	1.7×10^{-5}	2.3×10^{-5}
Gr	7.3×10^{12}	6.0×10^{12}
v_e	0.034	0.037
$\dot{Q}_e$	2.61	6.5
V	89	282
t_{mix}	34	43
$\dot{E}_{H2}/\dot{E}_{HT}$	0.64	0.23

Table E.10 Scaling implications of the mixing mechanisms

Mixing Mechanism	t_{HT}	t_{mix}	t_{HT}/t_{mix}
Forced mixing	L	L	L^0
Subcompartment mixing	L	$L^{1/2}$	$L^{1/2}$
Wall Jet-induced mixing	L	$L^{4/5}$	$L^{1/5}$

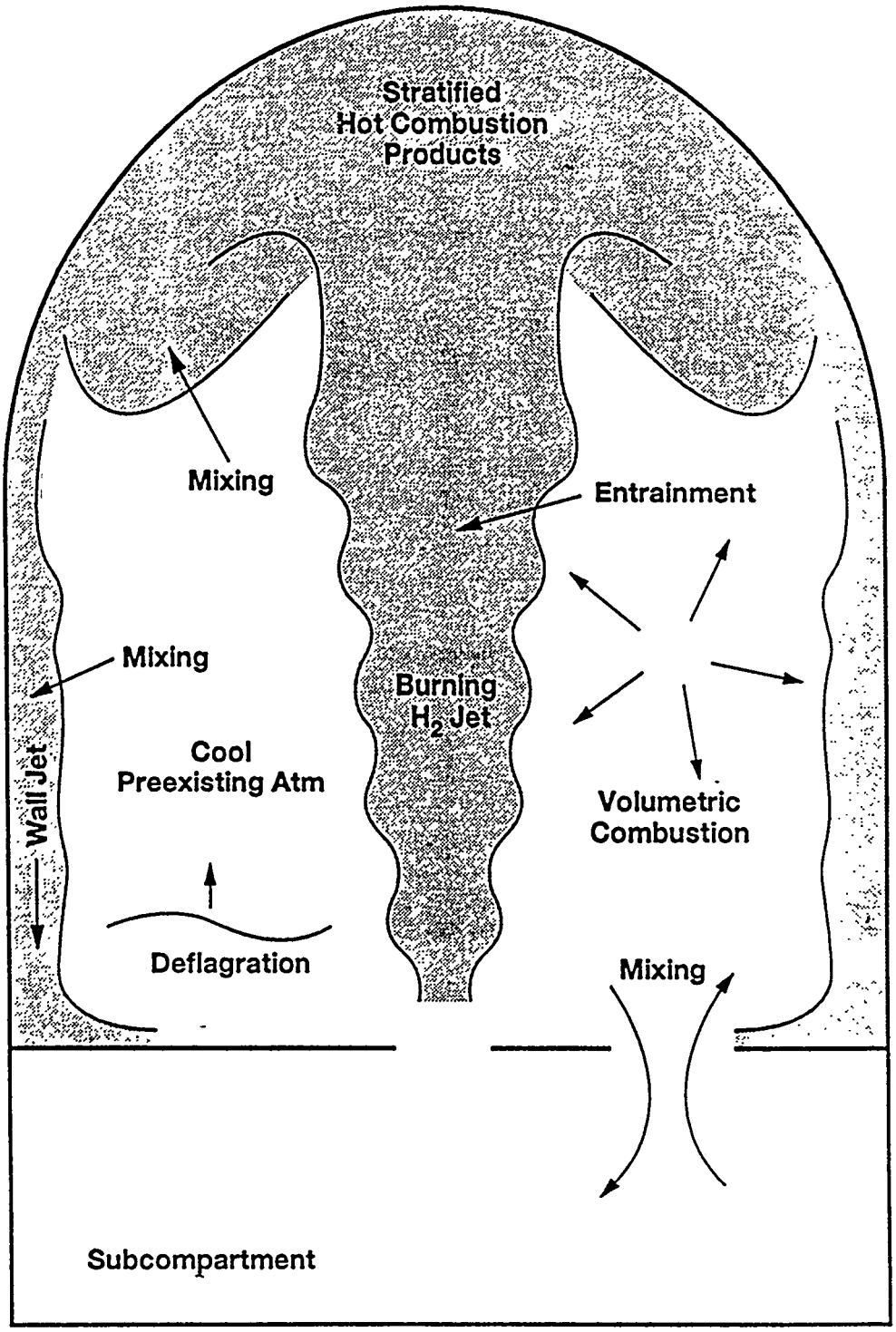

Figure E.1. Hydrogen combustion during DCH events.

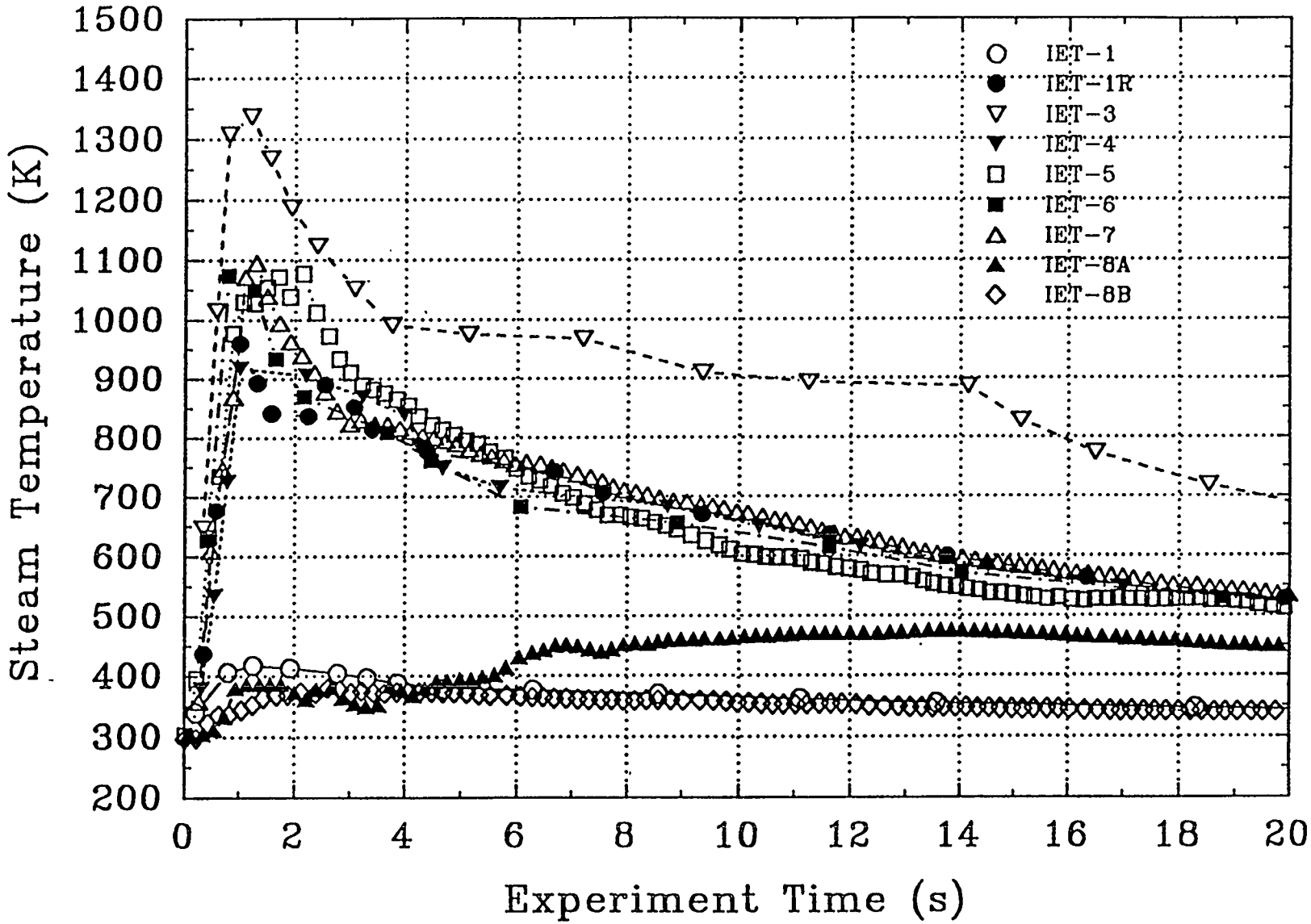

Figure E.2. Temperature history in the triangular vent space above RCP 1A in the SNL/IET experiments (from Allen et al., 1994).

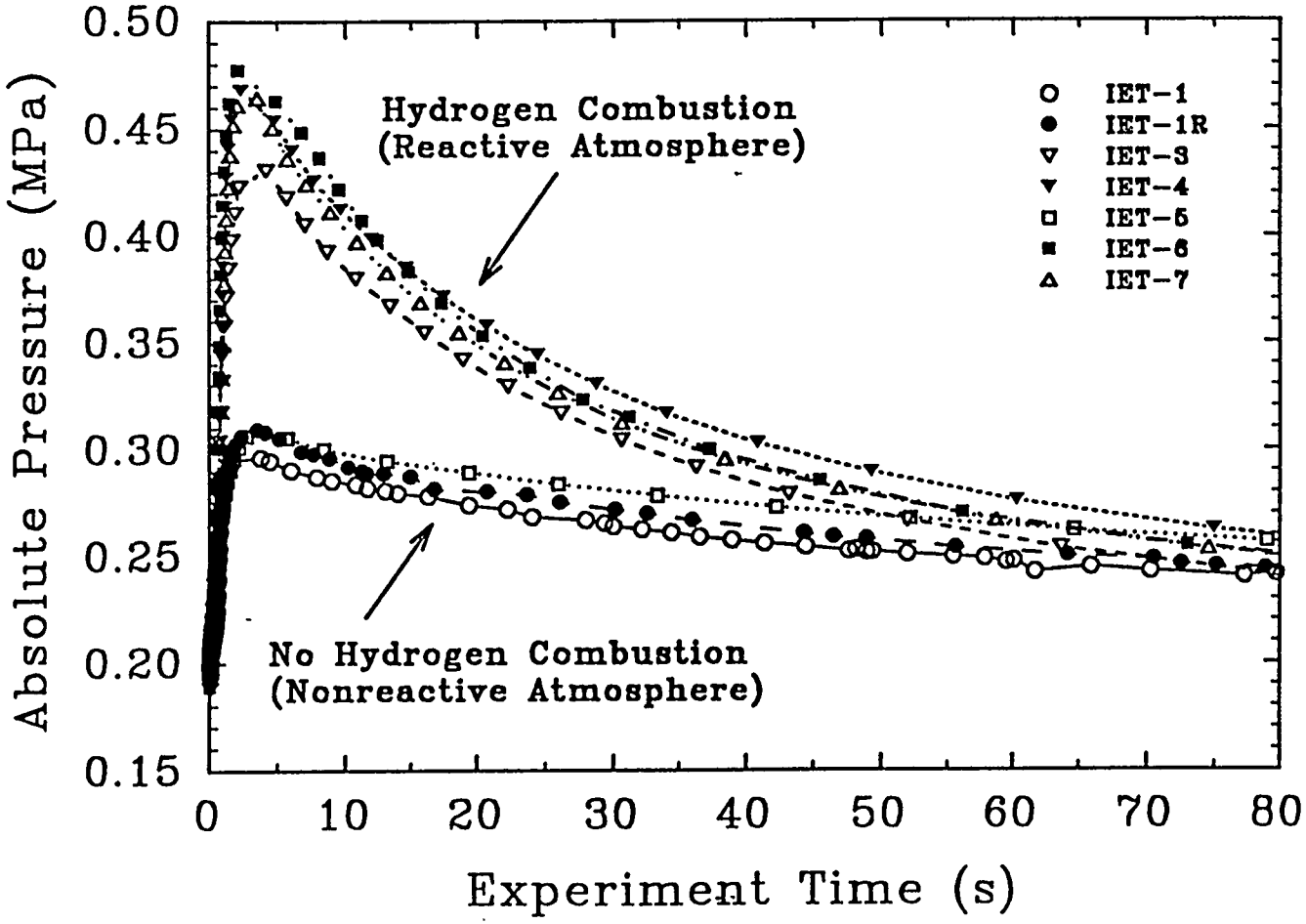

Figure E.3. Jet combustion in the SNL/IET tests.

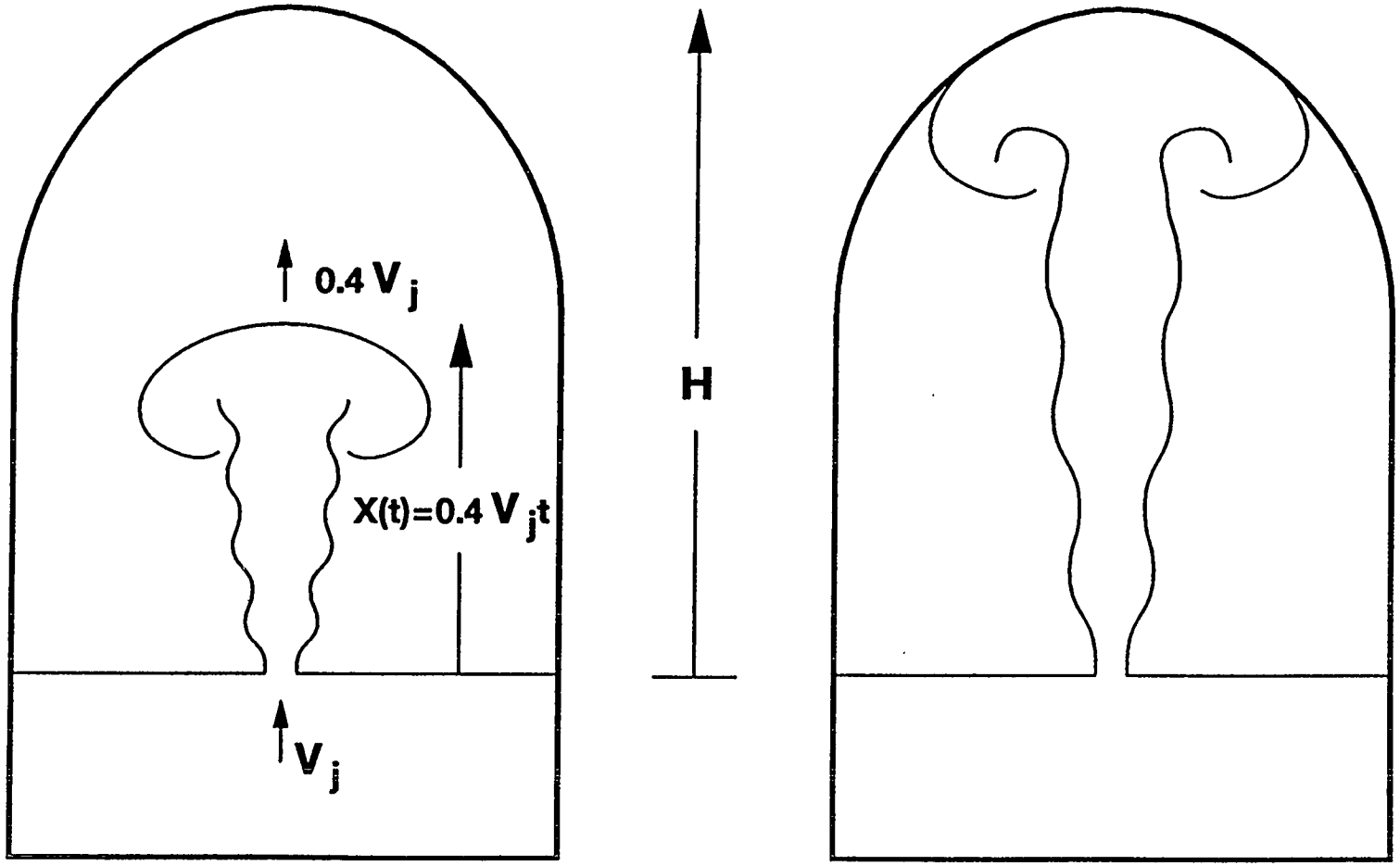

Figure E.4. Development of jets during DCH events.

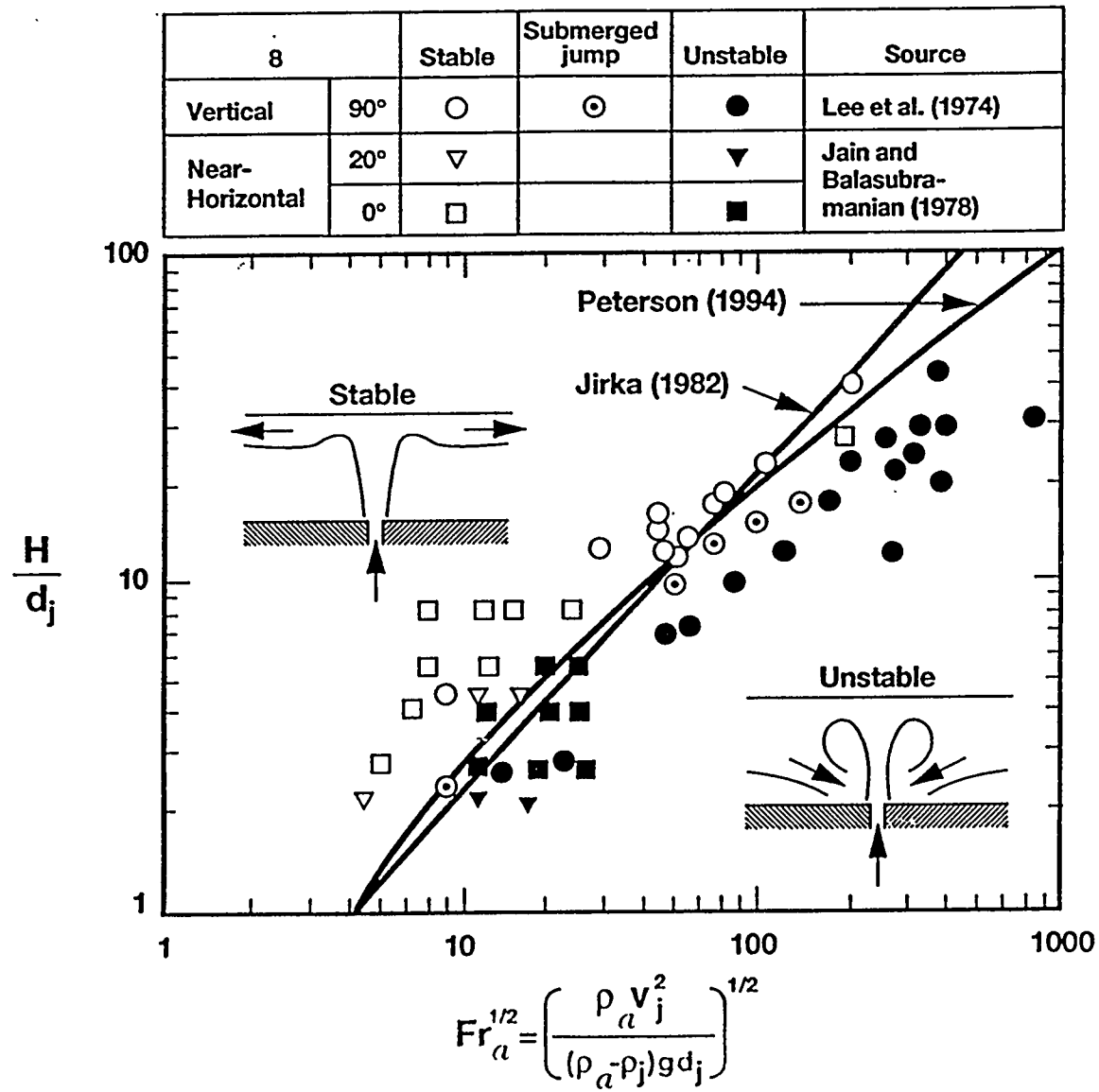

Figure E.5. Stability criterion for round, free, buoyant jets (from Peterson, 1994).

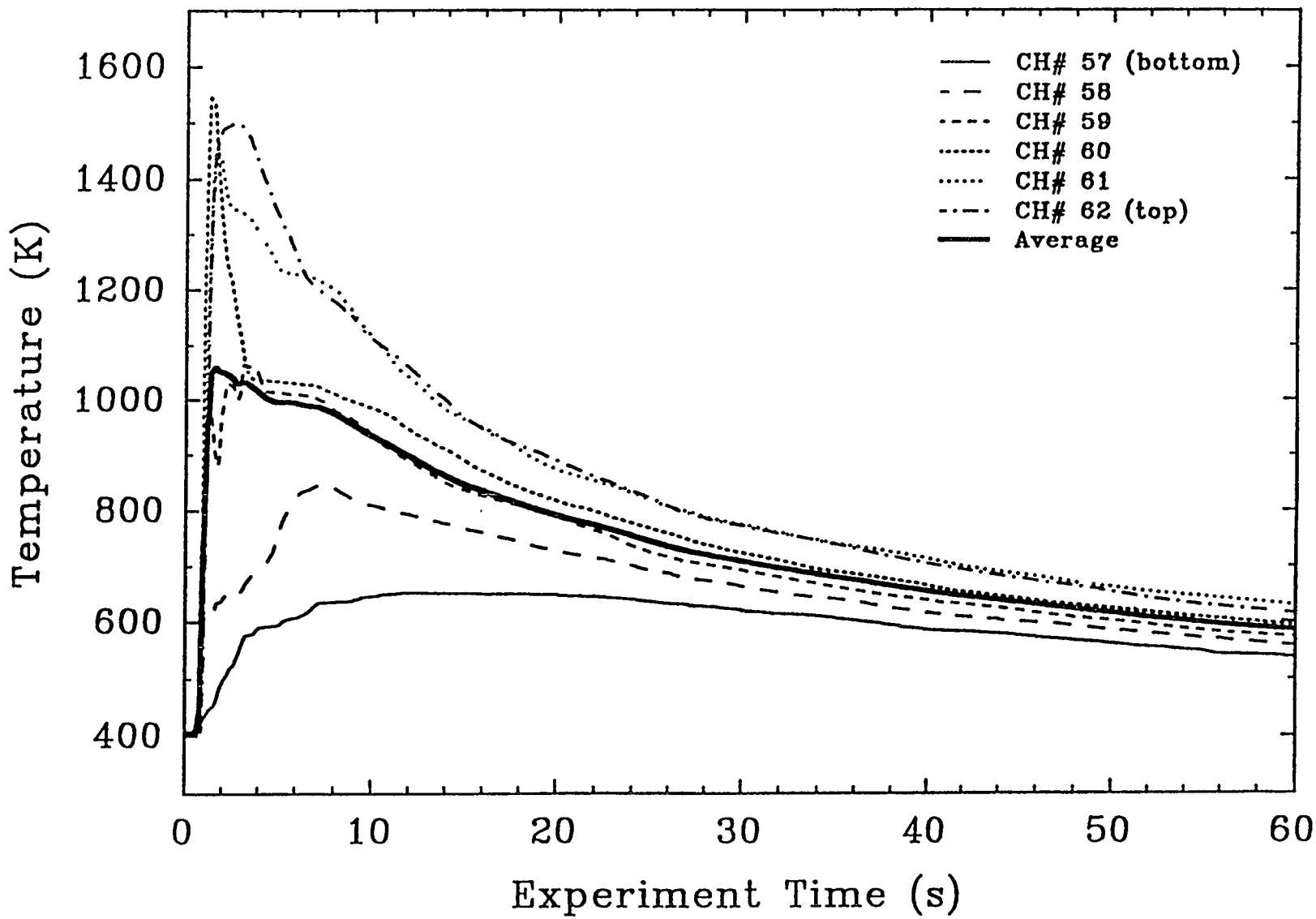

Figure E.6. Thermal stratification in the IET-11 experiment (from Blanchat, 1994).

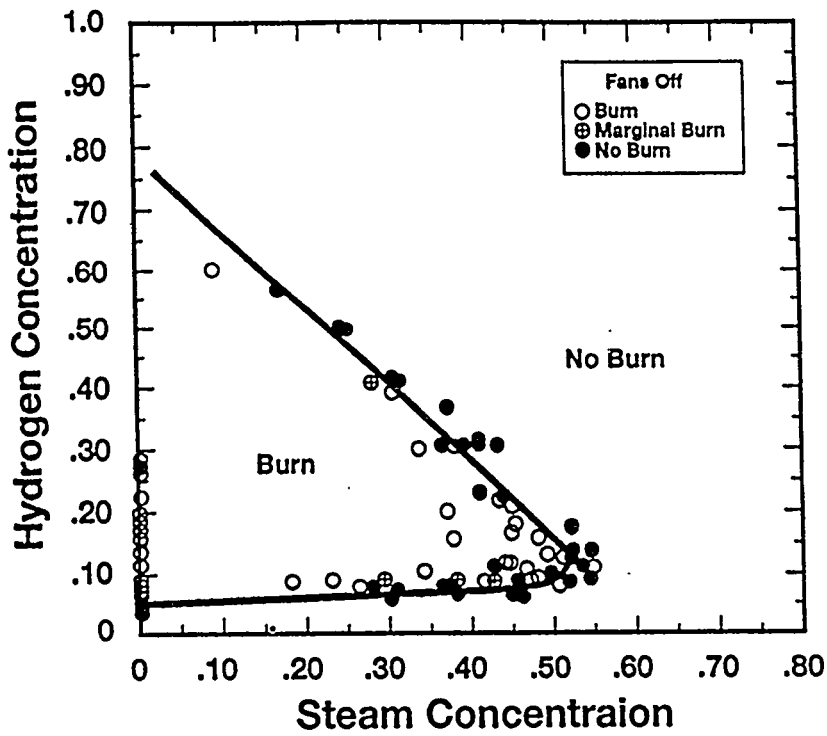

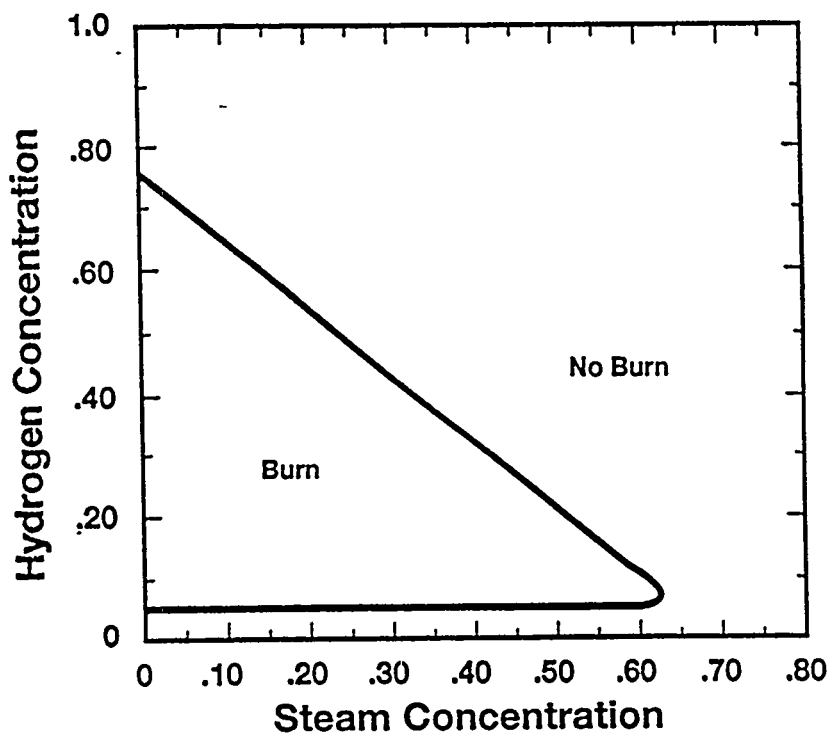

Figure E.7. Hydrogen/air/steam flammability charts from Marshall (1986) and Kumar (1985).

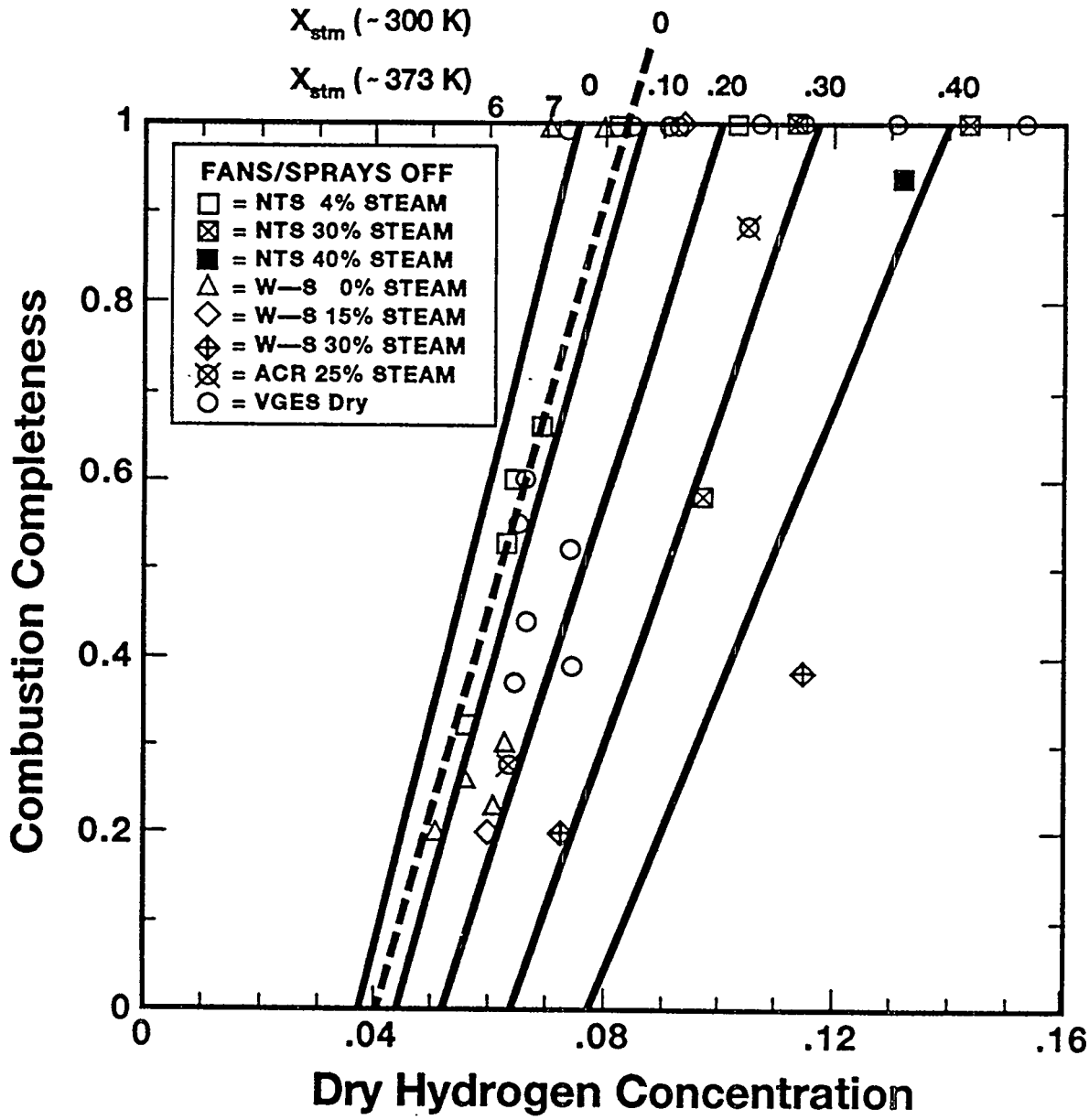

Figure E.8. Validation of combustion completeness model.

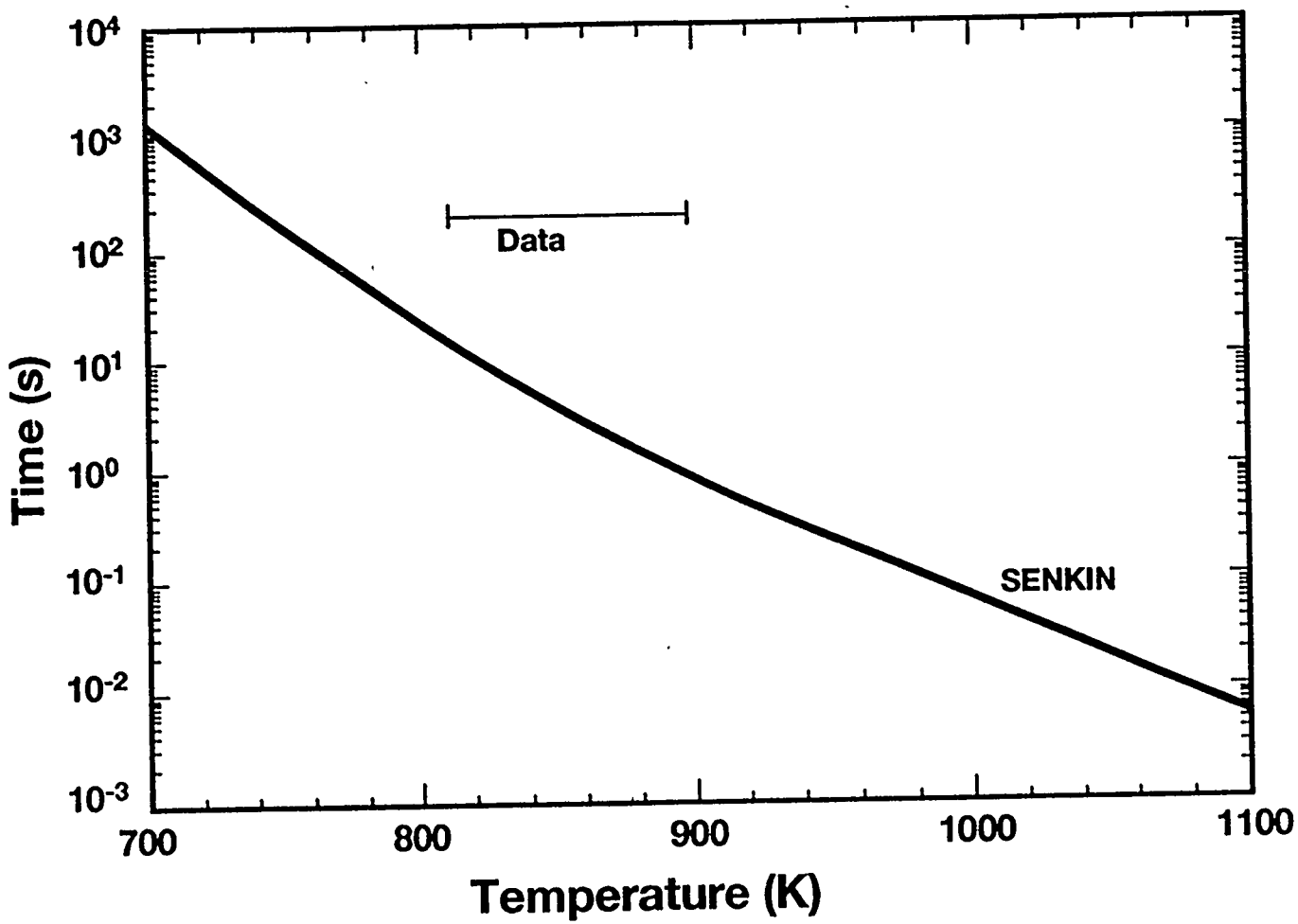

Figure E.9. SENKIN calculations for volumetric hydrogen combustion (X_{H2} = 0.048; X_{STM} = 0.38).

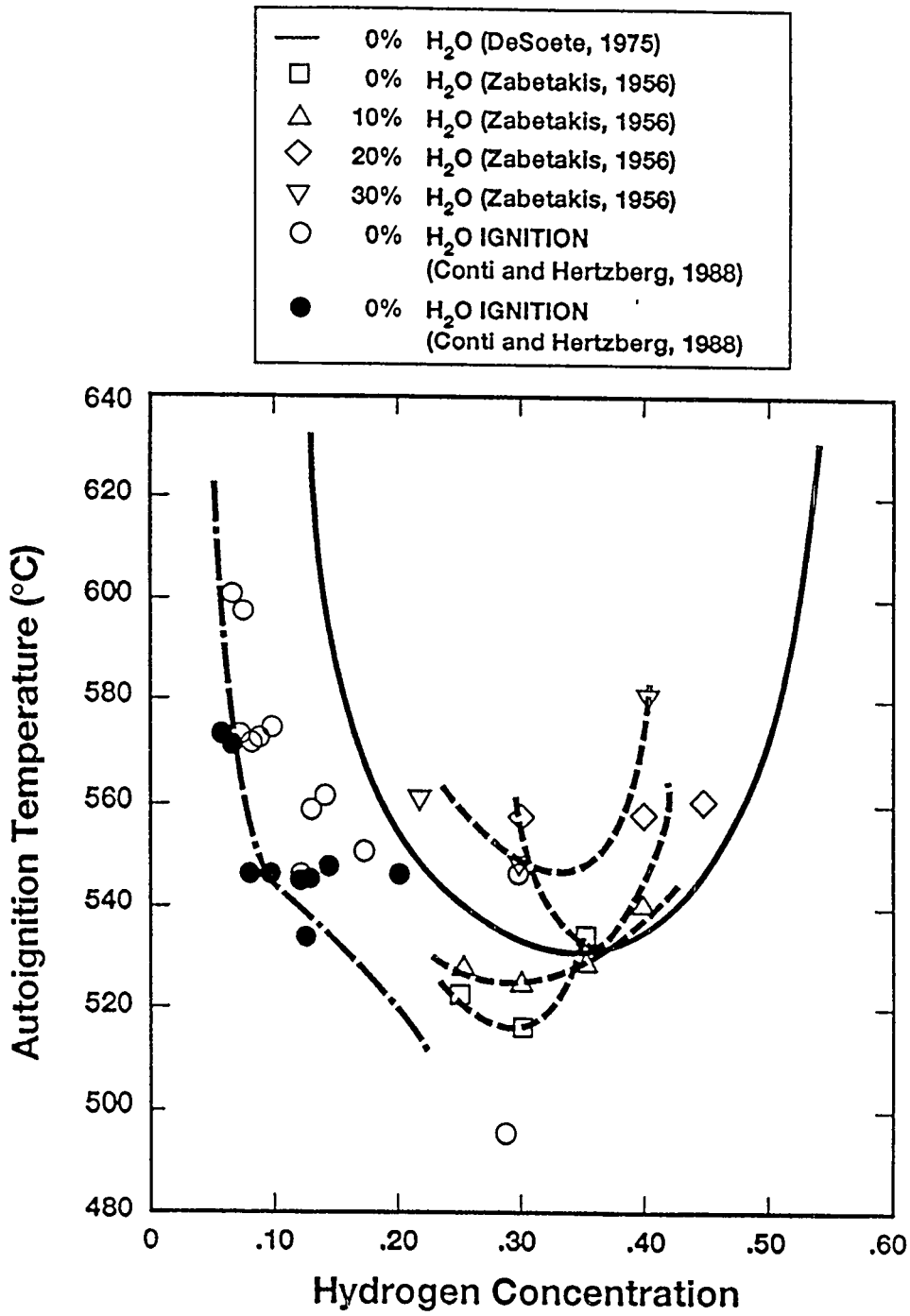

Figure E.10. Autoignition temperatures for hydrogen/air/steam mixtures (from Stamps, 1991).

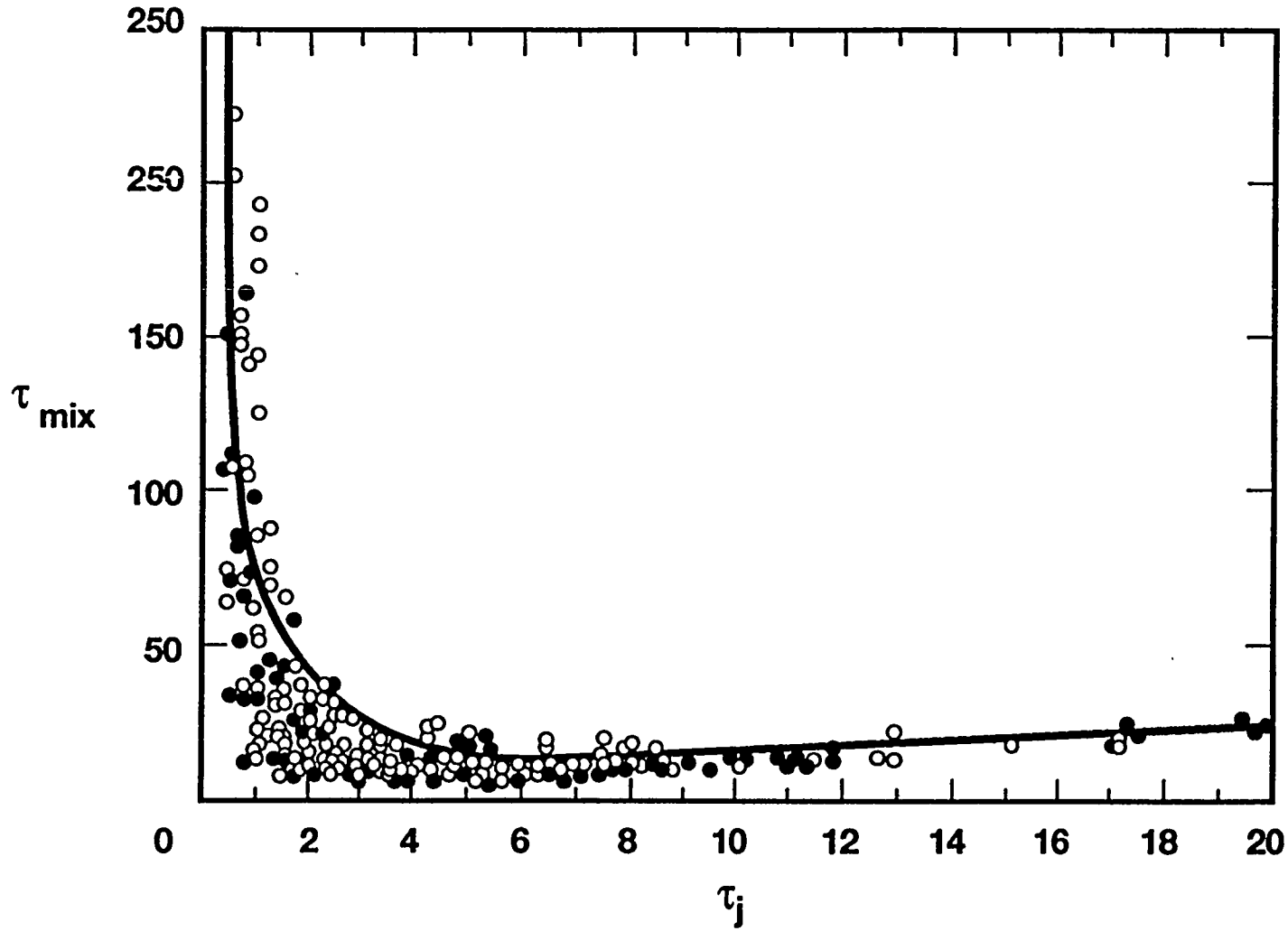

Figure E.11. Molecular mixing via jets in a confined volume (from Breidenthal et al. 1990).

DISTRIBUTION

U. S. Nuclear Regulatory Commission (6)
Office of Nuclear Regulatory Research
Attn: C. Tinkler, T-10-K-8
R. Lee, T-10-K-8
A. Rubin, T-10-K-8
F. Eltawila, T-10-K-8
W. Hodges, T-10-E-37
T. King, T-10-E-37
Washington, DC 20555-0001

U. S. Nuclear Regulatory Commission (2)
NRC/RES
Attn: E. Beckjord, MS: T-10-F-12
T. Speis, MS: T-10-F-12
Washington, DC 20555-0001

U.S. Nuclear Regulatory Commission (2)
Office of ACRS
Attn: M.D. Houston, T-2-E-26
T. Kress, T-2-E-26
Washington, DC 20555-0001

U. S. Department of Energy
Office of Nuclear Safety Coordination
Attn: R. W. Barber
Washington, DC 20545

U. S. Department of Energy (2)
Albuquerque Operations Office
Attn: C. E. Garcia, Director
For: C. B. Quinn
R. L. Holton
P. O. Box 5400
Albuquerque, NM 87185

Professor Theo G. Theofanous
Department of Chemical & Nuclear Engineering
Director, Center of Risk Studies & Safety
University of California
Santa Barbara, CA 93106

Electric Power Research Institute
Attn: A. Michaels
3412 Hillview Avenue
Palo Alto, CA 94303

UCLA
Nuclear Energy Laboratory
Attn: I. Catton
405 Hilgaard Avenue
Los Angeles, CA 90024

Brookhaven National Laboratory (3)
Attn: R. A. Bari
T. Pratt
N. Tutu
130 BNL
Upton, NY 11973

Argonne National Laboratory (4)
Attn: J. Binder
C. Johnson
L. Baker, Jr.
B. Spencer
9700 S. Cass Avenue
Argonne, IL 60439

Fauske and Associates, Inc.
Attn: R. Henry
16W070 West 83rd Street
Burr Ridge, IL 60952

General Electric Company
Nuclear Energy
Attn: F. J. Moody
175 Curtner Avenue
San Jose, CA 95125

Battelle Columbus Laboratory (2)
Attn: R. Denning
J. Gieseke
505 King Avenue
Columbus, OH 43201

Department of Energy
Scientific and Tech. Info. Center
P. O. Box 62
Oak Ridge, TN 37831

Distribution

Purdue University
School of Nuclear Engineering
Attn: M. Ishii
West Lafayette, IN 47907

University of Wisconsin
Nuclear Engineering Department
Attn: M. L. Corradini
1500 Johnson Drive
Madison, WI 53706

Richard R. Hobbins
2955 North Fish Creek Rd.
P.O. Box 971
Wilson, WY 83014

Battelle Pacific Northwest Laboratory
Attn: M. Freshley
P. O. Box 999
Richland, WA 99352

FOREIGN DISTRIBUTION:

AECL CANDU
Sheridan Park Research Community
2251 Speakman Avenue
Attn: V.J. Nath
Mississauga, Ontario L5K 1B2
CANADA

AECL Research (5)
Chalk River Research Laboratories
Attn: B.H. McDonald
L.N. Carlucci
D.S. Cox
L.W. Dickson
R.S. Dickson
Chalk River, Ontario KOJ 1JO
CANADA

AECL Research (2)
Whiteshell Laboratories
Attn: S.R. Mulpuru
L.A. Simpson
Pinawa, Manitoba R0E 1L0
CANADA

AERE Harwell (4)
Didcot
Attn: R.G.J. Ball
N.E. Beatham
M.A. Mignanelli
A.L. Nichols
Oxfordshire OX11 ORA
UNITED KINGDOM

Atomic Energy Council (2)
Attn: Yi-Bin Chen
S.J. Shieh
67, Lane 144
Keedling Road, Section 4
Taipei, Taiwan 106
REPUBLIC OF CHINA

Belgonucleaire SA (2)
Rue du Champ de Mars 25
Attn: H. Bairiot
J. Basselier
B-1050 Brussels
BELGIUM

Cadarache Center for Nuclear Studies (5)
Attn: B. Andre
P. Dumaz
M. Schwartz
A. Meyer-Heine
F. Serre
F-13108 Saint Paul-Lez-Durance Cedex
FRANCE

Com. Nacional de Seguridad Nucl. Salvag
Colonia Narvarte Delegation B. Juarez
Attn: M.M. Vaillard
Dr. Abrragan #779
C.P. 03020
MEXICO

Consejo de Seguridad Nuckan
SOR Angela de la Cruz No. 3
Attn: J. Bagues
28056 Madrid
SPAIN

Consejo de Seguridad Nuclear (2)
Justo Dorado 11
Attn: J.E. deCarlos
J.A. Martinez
28040 Madrid
SPAIN

Committee on the Use of Atomic Energy
for Peaceful Purposes
69 Shipchenski
Prokhod Blvd.
Attn: Y. Yanev
1574, Sofia
BULGARIA

Director Research, Science Education CEC (2)
Rue De La Loi 2000
Attn: W. Balz
B. Tolley
1049 Brussels
BELGIUM

E.T.S. Ingenieros Industriales
Attn: A. Alonso
Jost Gutierrez Abascal, 2
28006 Madrid
SPAIN

Finnish Centre for Radiation and
Nuclear Safety
Department of Nuclear Safety
P.O. Box 268
Attn: J.V. Sandberg
SF-00101 Helsinki
FINLAND

ENEL-CRTN
Via Monfalcone 15
Attn: E. Borioli
20132 Milan
ITALY

E.T.S. Ingenieros Industriales
Jost Gutierrez Abascal, 2
Attn: A. Alonso
28006 Madrid
SPAIN

Gesellschaft Fuer Reaktorsicherheit
Attn: M. Finnhaber
M. Sonnenkalb
K. Trambauer
Forschungsgelande
D-8046 Garching
GERMANY

Gesellschaft fur Reaktorsicherheit (GRS)
Postfach 101650
Glockengrasse 2
5000 Koeln 1
GERMANY

Hungarian Atomic Energy Commission
H-1374 Budapest, P.O. Box 565
Attn: S. Elo
Budapest
HUNGARY

Institut de Protection et de Surete Nucleaire (6)
CEN/FAR-B.P. No. 6
F-92265
Fontenay-aux-Roses
Attn: J. Bardelay
J. Duco
M. Gomolinski
M. LeComte
M. LiVolant
R. Pochard
Cedex
FRANCE

Institute of Nuclear Energy Research
P.O. Box 3
Attn: Sen-I Chang
Lung-Tan
TAIWAN 325

Insitute for Electric Power Research (2)
Division of Nuclear & Power Engineering
Attn: Z. Techy
L. Voross
POB 233
H-1368 Budapest
HUNGARY

Japan Atomic Energy Research Institute (4)
Tokai-mura
Naku-gun
Attn: K. Soda
J. Sugimoto
Y. Maruyama
N. Yamano
Ibaraki-ken, 319-11
JAPAN

JRC Ispra Establishment (5)
Thermodynamics and Radiation Physics
Attn: J. Capitao
Y. Drossinos
P. Fasoli-Stella
A.V. Jones
I. Shepherd
J-201020 Ispra (Varese)
ITALY

Jozef Stefan Institute
Jamova 39
Attn: B. Mavko
61111 Ljubljana
SLOVENIA

Kernforschungszentrum Karlsruhe (3)
P.O. Box 3640
Attn: S. Hagen
P. Hoffman
B. Kuczera
75 Karlsruhe
GERMANY

Korea Atomic Energy Research Institute
150 Dukjin-dong, Yoosung-gu
Attn: Hee-Dong Kim
Taejeon 305-353
KOREA

Korea Institute of Nuclear Safety
Safety Review and Assessment Division
P.O. Box 16, Daeduk-Danji
Attn: J.J. Lee
Taejon, 305-353
KOREA

Netherlands Energy Research Foundation (6)
P.O. Box 1
Attn: A.A. Booij
E. Cordfunke
M.E. Huntelaar
R. Konings
S. Spoelstra
P. Stoop
1755 ZG Petten (NH)
THE NETHERLANDS

Nuclear Power Engineering Center
Fujitakanko Building
17-1, 3-Chrome, Toranomon, Minato-Ku
Attn: Kenji Takumi
Tokyo, 105
JAPAN

Nuclear Electric (3)
Berkeley Nuclear Laboratory, Berkeley
Attn: C. Chapman
J. Eccles
J. Gwyther
Gloucestershire GL 13 9PB
UNITED KINGDOM

Nucleare e della Protezione Sanitaria (3)
(DISP)
Ente Nazionnle Energie Alternative (ENEA)
Viale Regina Margherita, 125
Cassella Postale M. 2358
Attn: G. Petrangeli
M. Pezzilli
G. Saponaro
1-00144 Roma A.D.
ITALY

Nuclear Regulatory Authority
Bajkalska 27
Attn: J. Misak
820 07 Bratislave
SLOVAK REPUBLIC

Nuclear Research Institute (2)
Attn: J. Kujal
F. Pazdera
250 68 Rez
CZECH REPUBLIC

Nuclear Safety Insitute (4)
Russian Research Center KI
I Kurchatov Square
Attn: V. Asmolov
E.G. Basanski
V. Demin
S.B. Dorofeev
123182 Moscow
RUSSIA

N.V. Kema
P.O. Box 9035
Attn: P. Kloeg
6800 ET Arnhem
THE NETHERLANDS

Ontario Hydro (2)
700 University Avenue
Attn: O. Akalin
F.C. Iglesias
Toronto, Ontario M5G 1X6
CANADA

Paul Scherrer Institute
Attn: P. Hosemann
CH-5232 Villigen, PSI
SWITZERLAND

Polytechnical University of Madrid
Nuclear Engineering Department
Jose Gutierrez Abascal, 2
Attn: A. Alonzo-Santos
28006 Madrid
SPAIN

Power Reactor Nuclear Fuel Development
Corporation (PNC)
9-13, 1-Chome
Akasaka
Attn: A. Watanabe
Minato-Ku, Tokyo
JAPAN

Reactor Centrum Nederland
Attn: K.J. Brinkman
1755 ZG Petten
THE NETHERLANDS

Research Centre Rossendorf, Inc.
Forschungszentrum Rossendorf
Postfach 19
Attn: Dr. H. Funke
DO-8051 Dresden
GERMANY

Royal Institute of Technology (2)
Department of Nuclear Reactor Engineering
Attn: K.M. Becker
B.R. Sehgal
S-10044 Stockholm
SWEDEN

Russian Academy of Sciences (3)
Nuclear Safety Institute
52, B. Tulskaya
Attn: L. Bolshov
V. Chudanov
V.F. Strizhov
113191 Moscow
RUSSIA

State Office for Nuclear Safety
Slezska 9
Attn: J. Stuller
120 00 Prague 2
CZECH REPUBLIC

Distribution

Statens Karnkraftinspektion (2)
P.O. Box 27106
Attn: W. Frid
L. Hammar
S-10252 Stockholm
SWEDEN

Studsvik Nuclear
S-611 82, Nykoping
Attn: K.O. Johansson
SWEDEN

Swiss Federal Nuclear Safety Inspectorate (2)
Attn: S. Chakraborty
U. Schmocker
Ch-5232 Villigen - HSK
SWITZERLAND

Technical Research Centre of Finland
Vuorimiehentie 5
Attn: L. Mattila
SF-02150 Espoo
FINLAND

Technische Universitat Munchen
Attn: H. Karwat
8046 Garching, Forschungagelande
Munich
GERMANY

Toshiba Corporation
8 Shinsugita-Cho, Isogo-Ku
Attn: M. Naito
Yokohama 235
JAPAN

UKAEA Culham Laboratory
Attn: B. D. Turland E5.157
Abingdon
Oxfordshire OX14 3DB
UNITED KINGDOM

UKAEA, Risley Nuclear Laboratories (4)
Risley, Warrington
Attn: A.T.D. Butland
I.H. Dunbar
G.F. Holford
C.D. Wheatley
Cheshire WA3-4NE
UNITED KINGDOM

UKAEA, Winfrith Technology Centre (7)
Attn: B.R. Bowsher
T.J. Haste
S.R. Kinnersly
J.N. Lillington
A. Mason
D. Sweet
D.A. Williams
Dorchester Dorset DT2 8DH
UNITED KINGDOM

Ruhr-University of Bochum
Dept. of Nuclear & New Energy System
Attn: U. Brockmeier
GERMANY

University of Stuttgart (2)
IKE
Pfaffenwaldring 31
Attn: U. Bieder
N. Kourti
D-7000 Stuttgart 80
GERMANY

VATESI (2)
Gediminis Prospect 36
Attn: A. Kaliatka
P. Vaisnys
Vilnius
LITHUANIA

SANDIA DISTRIBUTION: (30)

MS0100	Document Processing for DOE/OSTI, 7613-2 (10)
MS0619	Technical Publications, 7151
MS0736	N.R. Ortiz, 6400
MS0739	D.C. Williams, 6429
MS0742	J.E. Kelly, 6414
MS0744	W.A. von Riesemann, 6403
MS0744	D.A. Powers, 6404
MS0745	S.L. Thompson, 6418
MS0745	R.C. Smith, 6418
MS0745	T.J. Tautges, 6418
MS0899	Technical Library, 7141 (5)
MS1137	M.D. Allen, 6422
MS1137	T.K. Blanchat, 6422
MS1137	M.M. Pilch, 6422
MS1139	K.O. Reil, 6423
MS1139	R.C. Schmidt, 6423
MS9018	Central Technical Files, 8523-2

NRC FORM 335 (2-89) NRCM 1102, 3201, 3202

U.S. NUCLEAR REGULATORY COMMISSION

BIBLIOGRAPHIC DATA SHEET

(See instructions on the reverse)

1. REPORT NUMBER (Assigned by NRC, Add Vol., Supp., Rev., and Addendum Numbers, if any.)

NUREG/CR-6075
SAND93-1535
Supp. 1

2. TITLE AND SUBTITLE

The Probability of Containment Failure by Direct Containment Heating in Zion

3. DATE REPORT PUBLISHED

MONTH	YEAR
December	1994

4. FIN OR GRANT NUMBER

J6027

5. AUTHOR(S)

M. M. Pilch, M. D. Allen, D. L. Knudson,*
D. W. Stamps, E. L. Tadios

6. TYPE OF REPORT

Technical

7. PERIOD COVERED *(Inclusive Dates)*

8. PERFORMING ORGANIZATION – NAME AND ADDRESS *(If NRC, provide Division, Office or Region, U.S. Nuclear Regulatory Commission, and mailing address; if contractor, provide name and mailing address.)*

Sandia National Laboratories
Albuquerque, NM 87185-1137

*Idaho National Engineering Laboratory
Idaho Falls, ID 83415

9. SPONSORING ORGANIZATION – NAME AND ADDRESS *(If NRC, type "Same as above"; if contractor, provide NRC Division, Office or Region, U.S. Nuclear Regulatory Commission, and mailing address.)*

Division of Systems Research
Office of Nuclear Regulatory Research
U. S. Nuclear Regulatory Commission
Washington, D.C. 20555-0001

10. SUPPLEMENTARY NOTES

11. ABSTRACT *(200 words or less)*

Supplement 1 of NUREG/CR-6075 brings to closure the DCH issue for the Zion plant. It includes the documentation of the peer review process for NUREG/CR-6075, the assessments of four new splinter scenarios defined in working group meetings, and modeling enhancements recommended by the working groups. In the four new scenarios, consistency of the initial conditions has been implemented by using insights from systems-level codes. SCDAP/RELAP5 was used to analyze three short-term station blackout cases with different lead rates. In all three cases, the hot leg or surge line failed well before the lower head and thus the primary system depressurized to a point where DCH was no longer considered a threat. However, these calculations were continued to lower head failure in order to gain insights that were useful in establishing the initial and boundary conditions. The most useful insights are that the RCS pressure is low at vessel breach, metallic blockages in the core region do not melt and relocate into the lower plenum, and melting of upper plenum steel is correlated with hot leg failure. THE SCDAP/RELAP output was used as input to CONTAIN to assess the containment conditions at vessel breach. The containment-side conditions predicted by CONTAIN are similar to those originally specified in NUREG/CR-6075.

12. KEY WORDS/DESCRIPTORS *(List words or phrases that will assist researchers in locating the report.)*

Direct Containment Heating (DCH)
high pressure melt ejection
probabilistic framework
Zion nuclear power plant
severe accident
containment failure probability
pressurized water reactor

13. AVAILABILITY STATEMENT

Unlimited

14. SECURITY CLASSIFICATION

(This Page)

Unclassified

(This Report)

Unclassified

15. NUMBER OF PAGES

16. PRICE